Universidad de Valladolid

Facultad de Ciencias

Química Inorgánica / I. U. CINQUIMA

TESIS DOCTORAL

Polymerization of Norbornene and Alkenyl-Norbornenes Catalyzed by Palladium-Benzyl or Nickel-Aryl Complexes: Effects in Polymer Structure and Application as Catalyst Support

Presentada por Ignacio Pérez Ortega para optar al grado de doctor por la Universidad de Valladolid

Dirigida por:

Ana Carmen Albéniz Jiménez

AUTORIZACIÓN DE LA DIRECTORA DE TESIS

Ana Carmen Albéniz Jiménez, Catedrática de Química Inorgánica de la Universidad de Valladolid e investigadora del I. U. CINQUIMA

CERTIFICA:

Que la memoria titulada "Polymerization of Norbornene and Alkenyl-Norbornenes Catalyzed by Palladium-Benzyl or Nickel-Aryl Complexes: Effects in Polymer Structure and Application as Catalyst Support*"* ha sido realizada en el I. U. CINQUIMA y el Área de Química Inorgánica de la Facultad de Ciencias de la Universidad de Valladolid por Don Ignacio Pérez Ortega alumno del programa de doctorado "*Doctorado en Química: Química de Síntesis, Catálisis y Materiales Avanzados"* y autoriza su presentación para que sea calificada como Tesis Doctoral.

Valladolid, 08 de diciembre de 2020

La Directora de la Tesis

Fdo: Ana Carmen Albéniz Jiménez

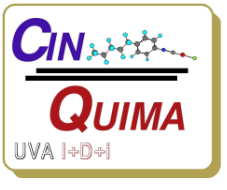

La Tesis Doctoral titulada "Polymerization of Norbornene and Alkenyl-Norbornenes Catalyzed by Palladium-Benzyl or Nickel-Aryl Complexes: Effects in Polymer Structure and Application as Catalyst Support" ha sido realizada gracias al apoyo económico de la Dirección General de Investigación del MINECO/Agencia Estatal de Investigación MICINN (proyectos CTQ2013-48406-P, CTQ2016-80913-P, PID2019-111406GB-I00), de la Junta de Castilla y León (proyectos VA051P17 y VA062G18), así como de un contrato del MINECO (ref: PEJ2018-003794-A) financiado por el Fondo Social Europeo y la Iniciativa de Empleo Juvenil.

Hasta el momento el trabajo presentado en esta Tesis está contenido en las siguientes publicaciones:

Capítulo 1

"Benzylic Complexes of Palladium(II): Bonding Modes and Pentacoordination for Steric Relief" Martín-Ruiz, B.; Pérez-Ortega, I.; Albéniz, A. C. *Organometallics* **2018**, *37*, 1074-1085. DOI: 10.1021/acs.organomet.8b00065

"α-Substituted Benzylic Complexes of Palladium(II) as Precursors of Palladium Hydrides" Martín-Ruiz, B.; Pérez-Ortega, I.; Albéniz, A. C. *Organometallics* **2018**, *37*, 1665-1670. DOI: 10.1021/acs.organomet.8b00066

Capítulo 4

"Trispyrazolylborate Ligands Supported on Vinyl Addition Polynorbornenes and Their Copper Derivatives as Recyclable Catalysts". Molina de la Torre, J. A.; Pérez-Ortega, I.; Beltrán, A.; Rodríguez, M. R.; Díaz-Requejo, M. M.; Pérez, P. J.; Albéniz, A. C. *Chem. Eur. J* **2019**, *25*, 556-563. DOI: 10.1002/chem.201803852

A mis padres, a mi hermano y a mi abuela

INDEX

Chapter 1

Chapter 2

Chapter 3

Chapter 4

Preface

Preface

The vinylic addition polymerization of norbornene produces a type of polymer (VA-PNB) which keeps the bicylic structure of norbornene and has a completely aliphatic skeleton. It has got attractive properties, such as thermal and chemical stability, ideal for some applications as materials or in the field of heterogenous catalysis as support. Our group has made in the past contributions to the synthesis of functionalized VA-PNBs and their use in catalysis. This thesis is a step further and collects the results obtained in the VA-polymerization of alkenyl-norbornenes, leading to substituted polymers with pendant double bonds that are very useful starting materials to introduce other functional groups in the polymer. The most representative catalysts for the synthesis of VA-PNBs are complexes of the late transition metals, such as Ni(II) and Pd(II). Among them, a special category are the complexes that can initiate the polymerization without the presence of an additional co-catalyst and therefore show in their structure a M-R bond where R = allyl, alkyl, aryl or H. In this thesis two types of complexes with M-R bonds were employed for the synthesis and mechanistic studies on the vinylic addition polymerization of norbornene and their derivatives. The goal was not only to develop new active catalysts for this reaction but also to understand certain unprecedented features of the polymerization mechanism.

i) *η^3-Benzylic complexes of palladium(II).* η^3-benzylic complexes of palladium(II) can be considered as weakly stabilized Pd-alkyls due to the formation of a π-interaction at the

expense of the aromaticity of the ring. They have a very rich chemistry and have been almost unexplored in the polymerization of norbornene. Following this line, in *Chapter 1* it is described the synthesis and study of the behavior in solution of a large variety of η^3-benzylic complexes of palladium(II) bearing an α-pentrafluorophenylmethyl substituent. In *Chapter 2*, the use of these η^3-benzylic complexes of palladium(II) in the vinylic addition polymerization of norbornene and alkenyl-norbornenes is described. Some of them show remarkable activity and a characteristic behavior in the initiation of the reaction.

ii) *Nickel(II) aryl complexes.* In *Chapter 3*, a new type of polynorbornene skeleton combining the vinylic addition polymerization (VA) and a ring opening of the norbornene (RO) by a β-C elimination is described with two different catalytic systems. The first one is the use of the well-known $[Ni(C_6F_5)_2L_2]$ where L = PPh_3, $AsPh_3$ or $SbPh_3$, extensively studied in our research group, in combination with coordinating solvents. The second one is a new type of cationic Ni(II) complexes bearing an aryl ring, a phosphine and a chelate ligand of moderate coordinating ability ($[Ni(Aryl)(MeCOCH_2C(XR)Me_2)(PPh_3)](BF_4)$ where Aryl = *o*-CF_3-C_6H_4 or *o*-CH_3-C_6H_4; and XR = OH, OMe or SMe). The study reveals the determining factors involved in the ring opening (RO) of the norbornene by a β-C elimination. The incorporation of the resulting ring-opened units in the polymer as we observed is unprecedented.

Finally, in *Chapter 4* a route to anchor trispyrazolylborate copper(I) complexes (Tp^xCu) is developed by hydroboration reaction of the starting VA-polynorbornenes with alkenyl pendant groups. These supported complexes have been tested as heterogenous recyclable catalysts in nitrene or carbene transfer reactions. This is a way of making these reactions more sustainable, combining the use a non-highly toxic metal as copper and the advantages of the heterogeneous catalysis.

The four chapters are subdivided in four sections: Introduction, Results and Discussion, Conclusions and Experimental Section. This dissertation includes an appendix with a list of abbreviations used and an index of the compounds described, numbered in order of appearance. The references are present as footnotes in every chapter without the tittle of the publication and are also collected in the appendix as a list with the tittle of the publication, to make the search of cross references easier. This thesis is presented to obtain the International Ph.D. degree, and, as part of the doctoral training, it was decided to write this dissertation in

English. To comply with the current regulations of the UVa, a brief summary of the results is presented in Spanish with its own bibliography and the general conclusions.

Chapter 1

1. Synthesis, Characterization and Behavior in Solution of α-Pentafluorophenylmethyl Benzylic Complexes of Palladium(II): Precursors of Palladium Hydrides

1.1. Introduction to benzylic complexes of transition metals

1.1.1. A general view of the benzylic ligands

The ability of transition metals to bind multiple atoms of a single ligand (hapticity) leads to interesting binding patterns in organometallic complexes. The allyl derivatives are very common ligands employed in organometallic chemistry that can coordinate to a metal center in two different fashions: the σ form or the η^3 form (Eq. 1.1).

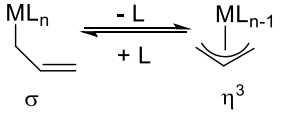

(1.1)

The benzylic moiety is a fragment that presents some similitudes but important differences with the allyl ligand. In contrast with the two coordination modes described for the allyl

fragment, the benzylic moiety can present up to four coordination modes represented in Figure 1.1. The adoption of one coordination mode is dependent of the nature of the ML_n fragment.

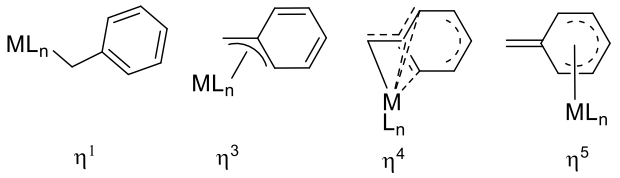

Figure 1.1. Representation of the coordination modes for the benzylic fragment.

The η^4 coordination mode is unusual and only a few reports with high-valent early transition metals and actinides can be found in the literature.[1] Some examples of this coordination mode for the benzylic fragment are represented in Figure 1.2. The analysis of the structures by X-ray diffraction showed the presence of a strong M-C^1 σ-interaction together with a secondary interaction involving the C^2, C^3 and C^7 of the π system.

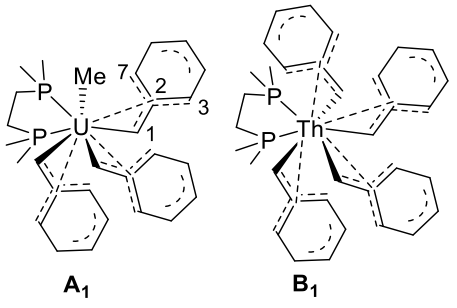

Figure 1.2. Examples of η^4 coordination mode for the benzylic fragment with uranium and thorium.

The η^5 coordination mode is also extremely unusual, and it was proposed as an excited state (**C$_1$***) to explain the dynamic behavior of [Rh(η^3-$CH_2C_6(CH_3)_5$)($P(O^iPr)_3)_2$] (**C$_1$**) and structurally characterized in the iron complex **D$_1$** (Figure 1.3).[2]

[1] a) Mintz, E. A.; Moloy, K. G.; Marks, T. J. *J. Am. Chem. Soc*. **1982**, *104*, 4692-4695. b) Edwards, P. G.; Andersen, R. A.; Zalkin, A. *Organometallics* **1984**, *3*, 293-298. c) Gwyneth, R. D.; Jarvis, A. J. Kilbour, B. T. *J. Chem. Soc. D: Chem. Comm.* **1971**, 1511-1512.
[2] a) Burch, R. R.; Muetterties, E. L.; Day, V. W. *Organometallics* **1982**, *1*, 188-197. b) Hamon, J. -H.; Astruc, D.; Roman, E. *J. Am. Chem. Soc*. **1981**, *103*, 2431-2433.

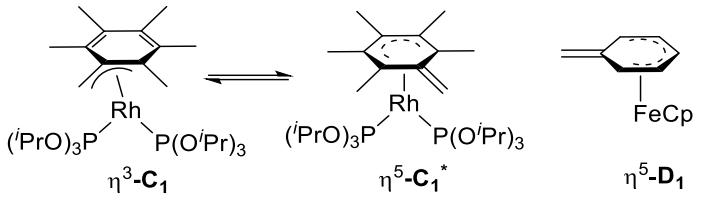

Figure 1.3. Representation of the two η^5-benzylic complexes reported in the literature.

Besides the rare η^4- and η^5-benzylic complexes reported, the most common coordination modes for the benzylic fragments are σ and η^3. In contrast with the allyl fragment, the formation of the η^3 mode is made at the expense of the aromaticity of the ring, so it requires an energy cost that it is not present in the allyl fragment (Eq. 1.2). Even with this energy cost, many η^3-benzylic complexes have been isolated for many metals over time. However, since the formation of the σ-benzyl regains the aromaticity of the ring, this is often an easy process and the benzylic fragment can be considered as a stabilized metal alkyl.

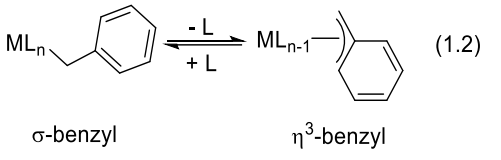

We will focus this introduction in the synthetic methodology and the dynamic behavior of the η^3- and σ-benzylic complexes of group 10 metals, specially palladium(II), used in this thesis work. For more details on the synthesis and the dynamic behavior of other benzylic complexes a complete review by Trost and Czabaniuk is available.[3]

1.1.2. Synthesis of benzylic complexes of nickel(II), palladium(II) and platinum(II)

In general terms, there are two methods for the synthesis of benzylic complexes. The first one is the oxidative addition of a benzylic derivative to a zerovalent complex. The second one is the insertion of a styrene derivative into a M-alkyl or M-H bond.

[3] Trost, B. M.; Czabaniuk, L. C. *Angew. Chem., Int. Ed*. **2014**, *53*, 2826-2851.

The first σ-benzylic complex of nickel(II) was synthesized by Jacob and co-workers in 1975.[4] Some years later, in 1987, the group of Poveda, Carmona and co-workers reported the isolation and characterization of a σ- and a η^3-benzylic complex of nickel(II) (Eq. 1.3).[5] The coordination mode of the benzylic fragment was controlled by the number of equivalents of the phosphine added. Oxidative addition of a benzyl chloride to the $Ni(COD)_2$ in the presence of two equivalents of PMe_3 afforded the complex **E_1** in 90% yield. The η^3-benzylic complex **F_1** was synthesized in the same way but in the presence of one equivalent of PMe_3 (70% yield).

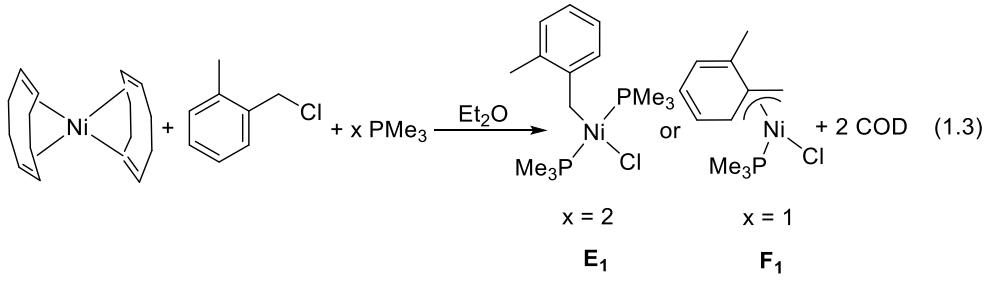

Following a related methodology but with a chelate ligand, Bazand and co-workers synthesized a binuclear and a mononuclear benzylic complexes.[6] Addition of $Ni(COD)_2$ to a mixture containing benzyl chloride and sodium 2-(diphenylphosphino)benzoate in THF afforded the binuclear complex $\{[Ni(\sigma\text{-}CH_2C_6H_5)(C_6H_5)_2P(C_6H_4)(\mu\text{-}CO_2)\text{-}\kappa^3P,O,O']\}_2$ (**G_1**) (Scheme 1.1). The mononuclear complex **H_1** was generated by opening a coordination site on Ni via the addition of $B(C_6F_5)_3$ in a ratio **G_1**:$B(C_6F_5)_3$ 1:2. In a similar fashion, in 2003, it was described the synthesis of two related complexes to **G_1** and **H_1** employing the ligand 2-(alkylideneamino)benzoate.[7] Some more η^3- and σ-benzylic nickel complexes have been described over the years.[8]

[4] Jacob, V. K.; Thiele, K. -H.; Keilberg, Ch. Niebuhr, R. *Anorg. Allg. Chem*. **1975**, *415*, 109-1144.
[5] Carmona, E.; Marin, J. M.; Paneque, M.; Poveda, M. L. *Organometallics* **1987**, *6*, 1757-1765.
[6] Komon, Z. J. A.; Bu, X.; Bazan, G. C. *J. Am. Chem. Soc.* **2000**, *122*, 12379-12380.
[7] Shim, C. B.; Kim, Y. H.; Lee, B. Y.; Dong, Y.; Yun, H. *Organometallics* **2003**, *22*, 4272-4280.
[8] a) Kim, Y. H.; Kim, T. H.; Lee, B. Y. *Organometallics* **2002**, *21*, 3082-3084. b) Kwon, H. Y.; Lee, S. Y.; Lee, B. Y.; Shin, D. M.; Chung, Y. K. *Dalton Trans.* **2004**, 921-928. c) Albers, I. Eleuterio, A.; Cámpora, J.; Maya, C. M.; Palma, P.; Sánchez, L. J.; Passaglia, E. *J. Organomet. Chem.* **2004**, *689*, 833-839. d) Sujith, S.; Noh, E. K.; Yeoul, B. L.; Han, J. W. *J. Organomet. Chem.* **2008**, *693*, 2171-2176.

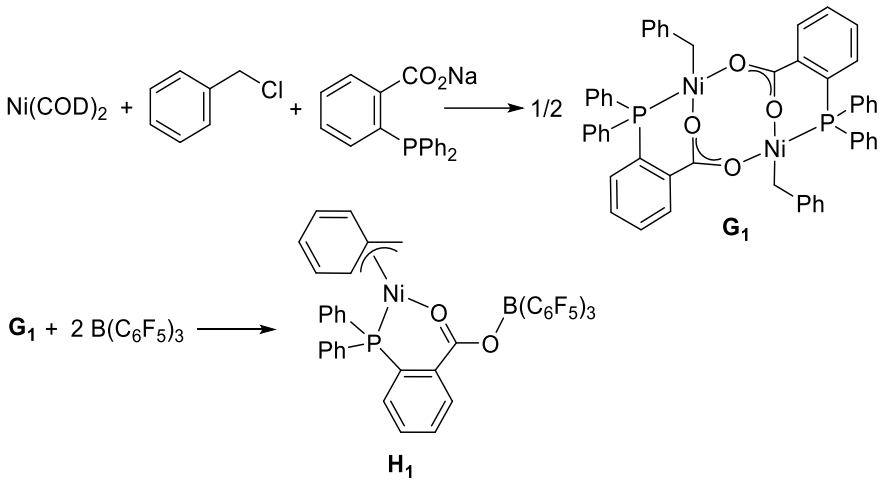

Scheme 1.1. Formation of the dimeric complex **G₁** and the mononuclear complex **H₁**.

Therefore, the general method for the synthesis of σ or η^3-benzylic complexes of nickel(II) is the oxidative addition of a benzylic reagent in the presence of the appropriate ligand and $Ni(COD)_2$, that is the most common source of nickel(0). In contrast, as shown below, the common route for the synthesis of benzylic complexes of platinum(II) is by insertion of a styrene derivative into a Pd-H bond.

η^3-benzylic complexes of platinum(II) have been less studied than the benzylic complexes of palladium(II) or nickel (II).[9,10] The first report of the synthesis of a benzylic complex of platinum(II) was published in 1990 by the group of Spencer and co-workers.[9] Complex **J₁** was synthesized, as represented in Eq. 1.4, by protonation of the Pt(0) complex [Pt(η^2-CH_2=CHC_6H_5)(dppb)] with $HBF_4 \cdot Et_2O$ yielding the corresponding cationic η^3-benzylic complex of platinum(II) (**J₁**). The behavior of the complex in solution was studied by the same group in a later report in 1992.[10]

[9] Crascall, L. E.; Lister, S. A.; Redhouse, A. D.; Spencer, J. L. *J. Organomet. Chem*. **1990**, *394*, C35 - C38.
[10] Crascall, L. E.; Spencer, J. L. *J. Chem. Soc. Dalton Trans*. **1992**, 3445-3452.

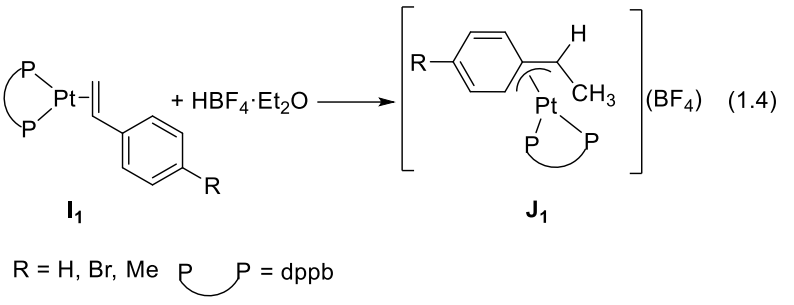

Some recent works described the synthesis of zwitterionic σ and η^3-benzylic complexes of platinum(II) with (P-S) chelate ligands (Figure 1.4).[11]

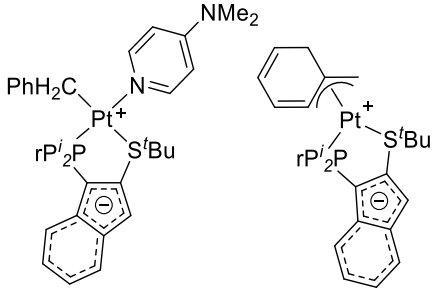

Figure 1.4. σ ad η^3 zwitterionic complexes of platinum(II) with (P-S) ligands.

The benzylic complexes of palladium(II) are, by far, the most studied class of benzylic compounds because of their involvement as intermediates in catalytic reactions of styrene derivatives or benzylic reagents.

In 1970 Stevens and Shier reported the synthesis of the first η^3-benzylic complex of palladium(II) with phosphine ligands represented in Scheme 1.2.[12] The addition of $AgBF_4$ to the σ-benzyl complex **K₁** (the complex **K₁** was synthesized by a previous reported method)[13] afforded the $[Pd(\eta^3\text{-}CH_2C_6H_5)(PEt_3)_2](BF_4)$ complex **L₁**.

[11] a) Hesp, K. D.; McDonald, R.; Ferguson, M. J.; Schattec, G. Stradiotto, M. *Chem. Commun.* **2008**, 5645-5647. b) Marx, T.; Wesemann, L.; Dehnen, S. A. *Organometallics* **2000**, *19*, 4653-4656.
[12] Stevens, R. R.; Shier, G. D. *J. Organomet. Chem.* **1970**, *21*, 495-499.
[13] Calvin; G.; Coates, G. E. *J. Chem. Soc*. **1960**, 2008-2016.

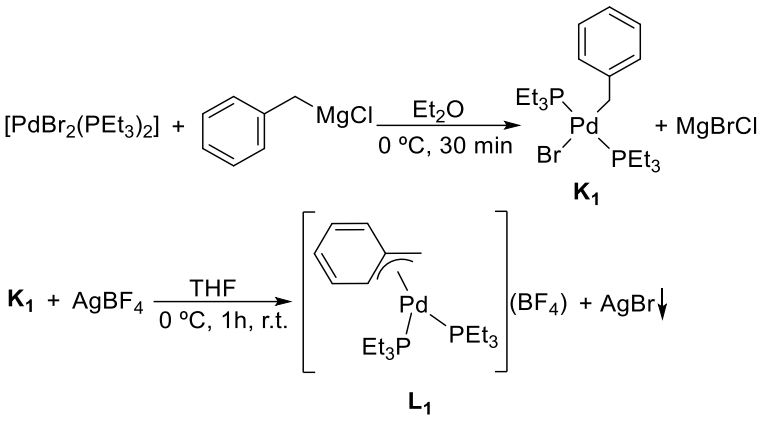

Scheme 1.2. Synthesis of a η^3-benzylic complex of palladium(II) by addition of $AgBF_4$ to the σ-complex **K_1**. The complex **K_1** was synthesized by addition of the benzyl Gringard reagent to $[PdBr_2(PEt_3)_2]$.

After this study, Klabunde reported the synthesis of the benzylic dimer **M_1** by co-condensation of benzyl chloride with palladium vapors.[14] The formation of some $[Pd(\sigma\text{-}CH_2Ph)ClL_2]$ from the dimer **M_1** was performed by addition of two equivalents per palladium of ligands such as pyridine or triethylphosphine. (Scheme 1.3).

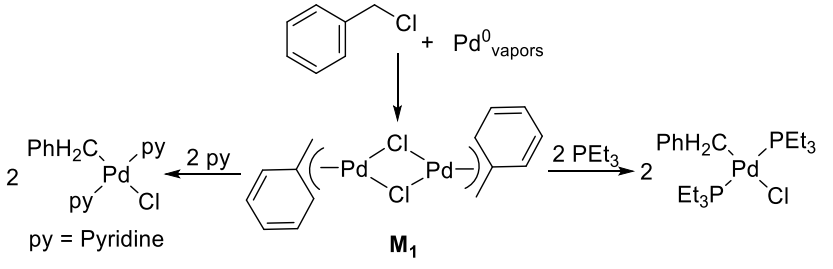

Scheme 1.3. Formation of two σ-complexes from the η^3-**M_1** complex by addition of some donor ligands

At this point, all the studies were made in solution but no crystallographic evidence for a η^3-benzylic complex of palladium(II) was reported. The first X-Ray molecular structure of a η^3-benzylic palladium(II) complex was determined in 1978 by Maitlis and co-workers.[15] The complex **N_1** was synthesized by oxidative addition of clorotriphenylmethane to $[Pd_2(dba)_3(s)]$ (s = solvent) giving an insoluble complex, converted in the complex **N_1** by addition of Tlacac. The X-Ray structure of **N_1** showed the coordination of the palladium center to the C^1, C^2 and

[14] Roberts, J. S.; Klabunde, K. *J. Am. Chem. Soc*. **1977**, *99*, 2509-2515.
[15] Sonoda, A.; Bailey, P. M.; Maitlis, P. M. *J. Chem. Soc. Dalton Trans*. **1979**, 346-350.

C^{α} with a very symmetrical η^3-benzylic fragment (similar Pd-C^{α} and Pd-C^2 bond lengths, Scheme 1.4).

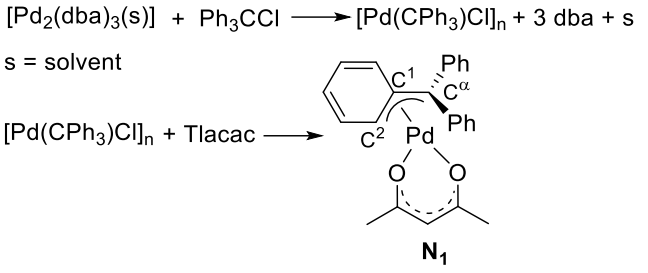

Scheme 1.4. Synthesis of the complex **N₁** which structure in solid state shows a very symmetrical η^3-benzylic moiety.

Besides oxidative addition as a synthetic method for the isolation of some η^3-benzylic palladium(II) complexes, insertion of styrene into an alkyl- or acyl-palladium fragment is another way employed for the synthesis of these complexes (Scheme 1.5-1.6).[16,17] The dimethyl palladium complex with bipy or TMEDA was treated with styrene in the presence of stoichiometric amounts of (tetrakis-3,5-bis(trifluoromethyl)phenyl)boric acid ($HBAr_4^f$) yielding the cationic benzylic complex **O₁** with TMEDA or a mixture of **P₁** and **P₁´** (1:1 ratio) with the bipyridine ligand and CH_4. The acid is essential to protonate one of the methyl ligands and create an available coordination site for the styrene. Complex **P₁´** is probably formed in situ by insertion of styrene in an intermediate hydride ``[PdH(bipy)(CH_2Cl_2)](BAr^f_4)´´ generated by β-hydrogen elimination from the complex **P₁**. *E*-β-methylstyrene was detected in the crude of the reaction. The TMEDA in the complex **O₁** was easily displaced by dppp in methylene chloride at room temperature to yield quantitatively **Q₁**.[16]

[16] Gatti, G.; Lopez, J. A.; Mealli, C.; Musco, A. *J. Organomet. Chem.* **1994**, *483*, 77-89.
[17] Brookhart, M.; Rix, F. C.; DeSimone, J. M. *J. Am Chem. Soc.* **1992**, *114*, 5894-5895.

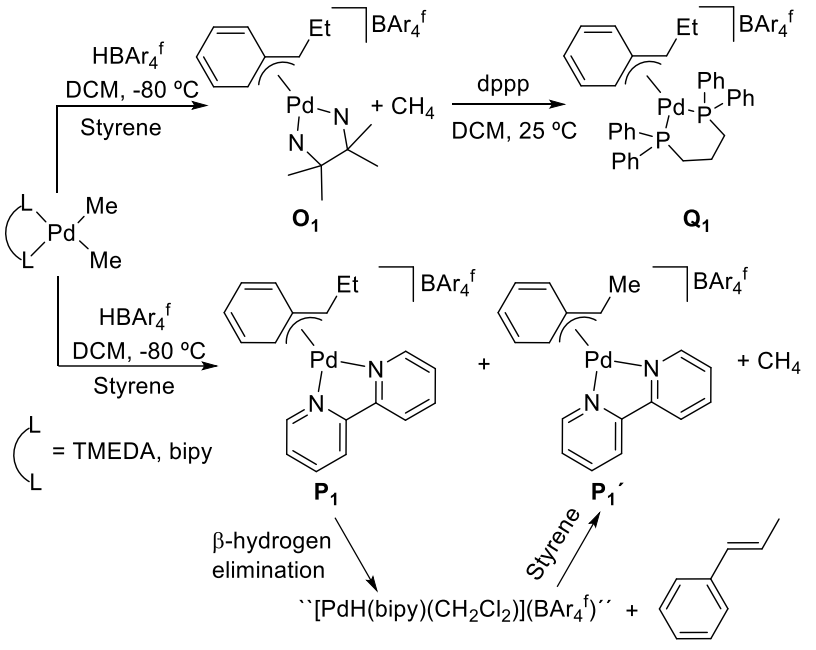

Scheme 1.5. Synthesis of η^3-benzylic complexes **O₁**, **Q₁** and the mixture **P₁** and **P₁´** by insertion of the starting alkyl-palladium complex into the styrene in the presence of an acid.

Brookhart and co-workers described the insertion of styrene into a Pd-acyl bond giving the Pd-benzylic complex σ-**T₁** (Scheme 1.6).[17] The solvated complex [Pd(CH_3)(N-N)($NCCH_3$)](BAr_4^f) (**R₁**) was synthesized by protonation of [Pd(CH_3)$_2$(N-N)] with $HBAr_4^f$. Now, the complex **R₁** in the presence of CO gave the corresponding carbonyl-acyl **S₁**. The insertion of a styrene derivative into the Pd-acyl bond gave the complex σ-**T₁**.

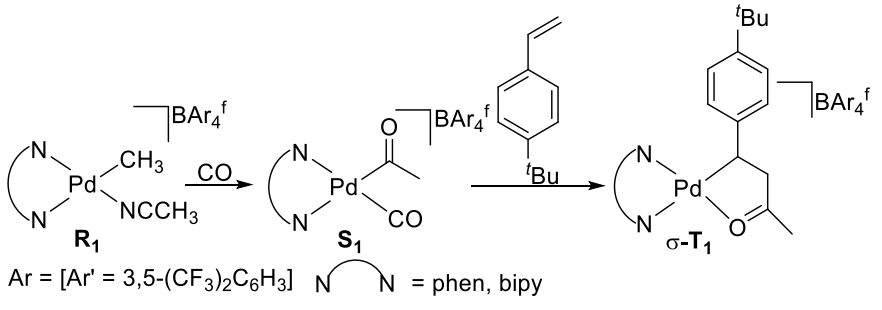

Scheme 1.6. Insertion of a styrene derivative into a Pd-acyl bond in the complex **S₁** to gives the σ-benzylic complex **T₁**.

Heteroaryl rings such as furans or indenyls have also been employed in the synthesis of some complexes of palladium(II) related to the η^3-benzylic compounds (Figure 1.5).[18]

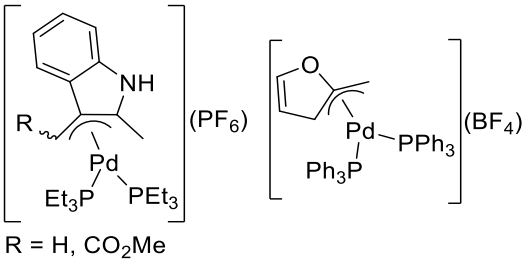

Figure 1.5. Representative related η^3-benzylic complexes of palladium(II) with heteroaryls.

1.1.3. Dynamic behavior of benzylic complexes of palladium(II) and nickel(II)

Most of the benzylic complexes reported exhibit a rich fluxionality in solution involving processes such as interconversion of the *ortho* protons of the aryl ring (η^3-σ-η^3 rearrangement),[10,16,18,19a] suprafacial sigmatropic rearrangement[15,19a,20] or ligand site exchange.[16]

The interconversion of the *ortho* protons in the aryl is a very common process in many η^3-benzylic complexes.[10,16,18,19a] In general terms, a static ^{1}H NMR for all the benzylic complexes gives two signals for H^2 and H^6 of the aryl ring (Scheme 1.7). The fast aryl rotation is deduced when only one peak for both protons is observed in the ^{1}H NMR. For example, the presence of this fluxional process in solution was observed previously in the complexes **P₁** or **P₁'** (Scheme 1.7).[16] The first equilibrium (K_1) is a η^3-σ rearrangement of the benzylic fragment with an aryl rotation around the C^{α}-C^{ipso}. This aryl rotation interchanges the position of H^2 and H^6. The η^3 to σ rearrangement is facile in benzylic derivatives, as well as the C-C rotation

[18] a) Oitsuka, K.; Yamamoto, M.; Suzuki, S.; Takahashi, S. *Organometallics* **2002**, *21*, 581-583. b) Dewhurst, R. D.; Müller, R.; Kaupp, M.; Radacki, K.; Götz, K. *Organometallics*, **2010**, *29*, 4431-4433.
[19] a) Becker, Y.; Stille, J. K. The *J. Am. Chem. Soc.* **1978**, *100*, 845-850. b) Brookhart, M.; Buck, R. C.; Danielson III, E. *J. Am. Chem. Soc.* **1989**, *111*, 567-574. c) Rix, F. C.; Brookhart, M.; White, P. S. *J. Am. Chem. Soc.* **1996**, *118*, 2436-2448.
[20] a) Stühler, H. -O. *Angew. Chem. Int. Ed. Engl.* **1980**, *19*, 468-469. b) Su, S.-C. H.; Wojcicki, A. *Organometalics* **1983**, *2*, 1296-1301. c) Carmona, E.; Paneque, M.; Poveda, M. L. *Polyhedron* **1989**, *8*, 285-291. d) Campora, J.; Gutierrez, E.; Poveda, M. L.; Ruiz, C.; Carmona, E. *J. Chem. Soc. Dalton Trans.* **1992**, 1769-1774.

so this is a quite common fluxional process even at low temperatures. The second equilibrium (K_2, Scheme 1.7) is an exchange of the positions of the 2-2´-pyridyl. The coordination site exchange takes place in the Y-shape intermediate that is generated by a topomerization process in the T-shape σ-benzylic intermediate. A Pd-C^{α} rotation in the Y shape σ-benzylic and recoordination into the η^3-benzylic form result in an exchange of the relative positions of the nitrogen atoms in the bipyridine ligand.

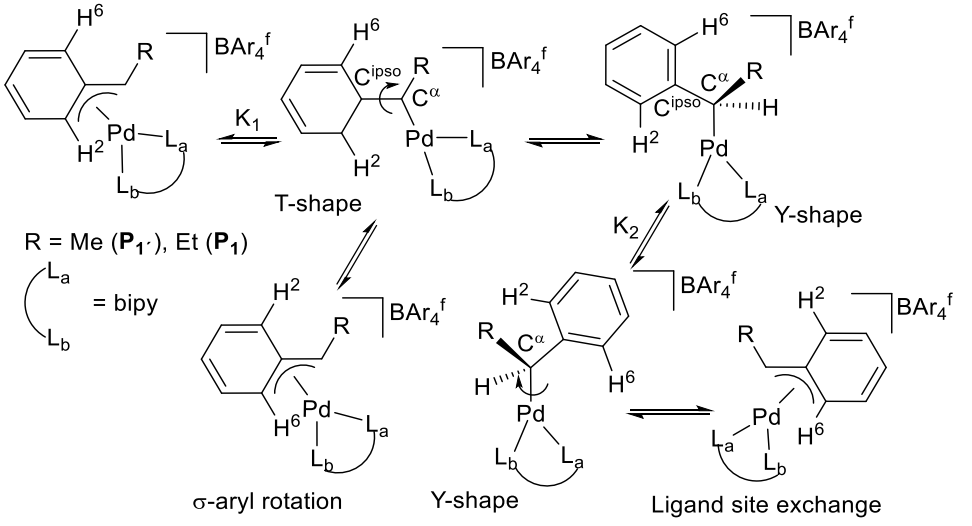

Scheme 1.7. σ-aryl rotation around the C^{α}-C^{ipso} that makes equivalents the H^2 and H^6 and ligand exchange site for the nitrogen atoms in the bipyridine.

The equilibrium between the σ- and η^3-benzyl species in solution is involved in many fluxional processes as shown above. In some cases, the exchange is slow and it is possible to observe this equilibrium as it was reported by Brookhart and co-workers (Eq. 1.5).[17] At room temperature, the chelate compound σ-**T1** is in a very fast equilibrium with the η^3-**T1** complex but it is possible to reach a static NMR spectrum at -100 ºC. The ratio of σ-**T1**:η^3-**T1** at -80 ºC is 3:1.

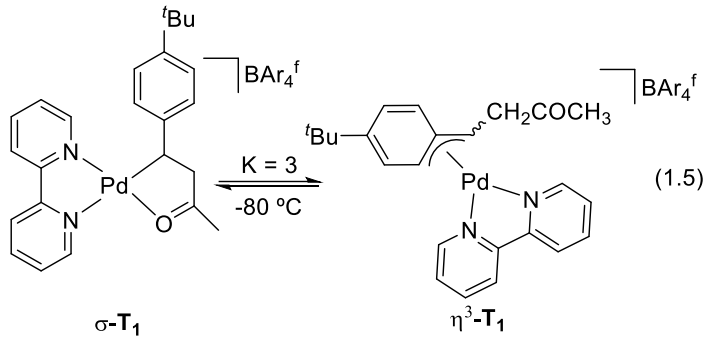

The η^3-σ rearrangement is also dependent on the solvent (Scheme 1.8).[19a] In a non-coordinating solvent the σ-complex is too high in energy and could not be detected in the experimental conditions. However, in the presence of deuterated acetonitrile the σ-benzylic complex was detected in the ^{1}H NMR. The coordination of the vacant site generated in the σ form by the acetonitrile gives the stabilization necessary to observe this coordination mode in solution.

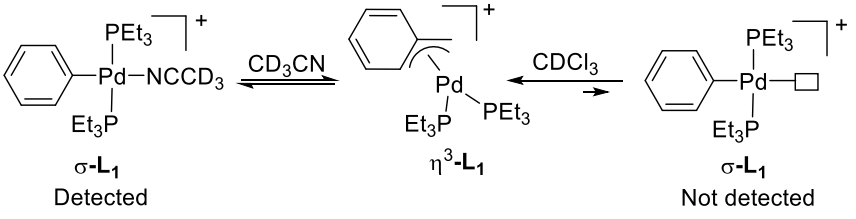

Scheme 1.8. Dependence of the η^3-σ equilibrium to the solvent.

Another important fluxional process observable in some η^3-benzylic complexes is the suprafacial sigmatropic rearrangement. In a non-α-substituted benzylic complex, when this process is fast, it makes the two methylene protons and the *ortho* and *meta* carbons equivalents in NMR (Scheme 1.9, (a)).[15,19a,20] The α-substituted benzylic complexes present, in addition to the σ and η^3 coordination modes, two different positions for the R substituent giving two isomers, *syn* or *anti*, in the η^3 coordination mode. The suprafacial sigmatropic rearrangement can interconvert these two isomers (Scheme 1.9, (b)).

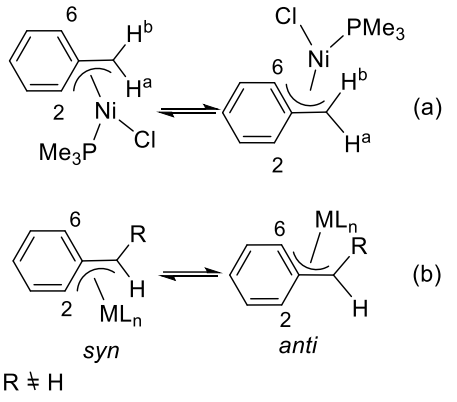

Scheme 1.9. (a) Suprafacial sigmatropic rearrangement in a non α-substituted benzylic complex of nickel(II) and (b) the interconversion of the two isomers (*syn* or *anti*) present in an α-substituted benzylic complex by suprafacial sigmatropic rearrangement.

1.1.4. Reactivity of benzyls: some examples of Pd-catalyzed transformations of benzylic reagents and of styrene derivatives

The study of the structure and the properties in solution of the benzylic complexes is important since they are intermediates in metal-catalyzed reactions involving benzylic reagents or styrene derivatives. Specifically, palladium catalyzed transformation of these type of compounds is a very common route to build new organic molecules.[21,22]

The initial reports of benzyl palladium intermediates proposed in a catalytic reaction started with the use of benzyl, aryl or styrene halides by Heck and co-workers (Scheme 1.10, (a)).[23] Later investigations in Heck reactions of benzylic substrates were reported including intramolecular Heck reactions,[24] and asymmetric Mizoroki-Heck reactions using phosphoramidites as chiral ligands.[25] Suzuki-Miyaura cross coupling reactions were also

[21] Recent review: a) Liégault, B.; Renaud, J.-L.; Bruneau, C. *Chem. Soc. Rev*. **2008**, *37*, 290-299. Recent examples: c) Hikawa, H.; Koike, T.; Izumi, K.; Kikkawa, S.; Azumaya, I. *Adv. Synth. Catal*. **2016**, *358*, 784-791; d) Yang, M. –H.; Hunt, J. R.; Sharifi, N.; Altman, R. A. *Angew. Chem. Int. Ed.* **2016**, *55*, 9080-9083. e) Najib, A.; Hirano, K.; Miura, M. *Org. Lett.* **2017**, *19*, 2438-2441.
[22] a) LaPointe, A. M.; Rix, F. C.; Brookhart, M. *J. Am. Chem. Soc*. **1997**, *119*, 906-917. b) Trzeciak, A. M.; Ciunik, Z.; Ziólkowski, J. J. *Organometallics* **2002**, *21*, 132-137. c) Johns, A. M.; Utsunomiya, M.; Incarvito, C. D.; Hartwig, J. F. *J. Am. Chem. Soc.* **2006**, *128*, 1828-1839. d) Narahashi, H.; Shimizu, I.; Yamamoto, A. *J. Organomet. Chem*. **2008**, *693*, 283-296.
[23] Heck, R. F.; Nolley, J. P. *J. Org. Chem.* **1972**, *37*, 2320-2322.
[24] a) Wu, G.-Z.; Lamaty, F.; Negishi, E.-I. *J. Org. Chem.*, **1989**, *54*, 2507-2508. b) Grigg, R.; Sukirthalingham, S.; Sridharan, V. *Tetrahedron Lett*.**1991**, *32*, 2545-2548.
[25] Yang, Z.; Zhou, J. S. *J. Am. Chem. Soc*. **2012**, *134*, 11833-11835.

studied with different benzyl reagents.[26,27] Yu and co-workers reported the synthesis of triarylmethanes by a Suzuki-Miyaura coupling of diarylmethyl carbonates with arylboronic acids (Scheme 1.10, (b)). Other well known example of the reactivity of benzylic reagents is the alkylation reaction reported by Fiuad and co-workers (Scheme 1.10, (c)).[28,29]

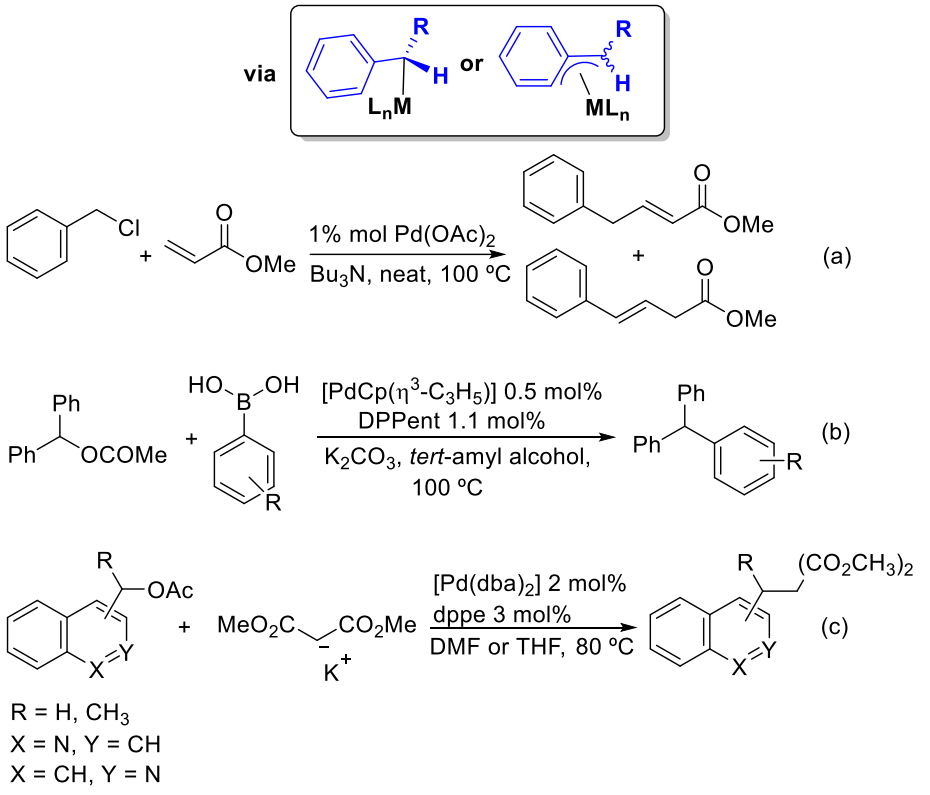

Scheme 1.10. Three reactions where is involved the formation of an intermediate benzylic complex.

The group of Brookhart and co-workers reported an elegant study about the Pd-catalyzed hydrosilation and dehydrogenative silation reaction of styrene.[22a] The catalytic cycle (Scheme 1.11) involves the formation of two η^3-benzylic complexes. In the hydrosilation pathway, after the insertion of the styrene into the Pd-SiR_3 bond, the σ-benzylic complex quickly rearranges into the η^3-benzylic complex (**U**$_1$) that is the resting state for the hydrosilation

[26] Suzuki-Miyaura *Org. Lett.*, **2008**, *10*, 973-976.
[27] Shimizu, M.; Tomioka, Y.; Nagao, I.; Hiyama, T. *Synlett* **2009**, 3147-3150.
[28] Legros, J. -Y.; Fiaud, J. -C. *Tetrahedron Lett.* **1992**, *33*, 2509-2510.
[29] Legros, J.-Y.; Primault, G.; Toffano, M.; Riviere, M.-A.; Fiaud, J.-C. *Org. Lett*. **2000**, *2*, 433-436.

reaction of styrene. In contrast, in the dehydrogenative silation, the σ-benzylic complex undergoes β-H elimination and the $PdHL_n$ intermediate can trap a new molecule of styrene (the coordination of the styrene is more favorable than of *trans*-$R_3SiCH{=}CHC_6H_5$) giving a new σ-benzylic complex that quickly rearranges into the η³-benzylic complex (**V₁**). In this catalytic cycle, the σ-benzylic complex, a Pd-alkyl, can be stabilized in its η³-benzylic form and that slows down the typical reactivity of the alkyl, the β-H elimination, allowing the hydrosilation cycle to operate.

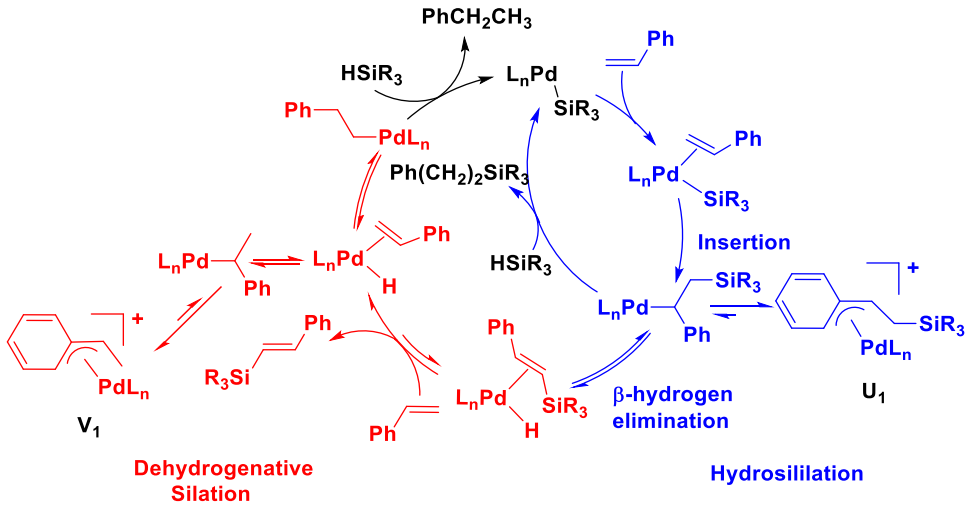

Scheme 1.11. Proposed catalytic cycle for the hydrosilation and dehydrogenative silation of styrene.

The occurrence of the η³-benzylic form has also been used by Sigman and co-workers to achieve the Pd-catalyzed diarylation of styrenes (Scheme 1.12).[30] The σ-**W₁** complex, generated by the insertion of a styrene derivative into the Pd-Ph bond, can lead directly to the Heck product by β-hydrogen elimination. In contrast, an additional stabilization provided by the formation of the η³-**W₁** complex slows down the β-hydrogen elimination and thus enable a second transmetalation (complex η³-**Y₁**) that by reductive elimination yields the diarylation product.

[30] Urkalan, K. B.; Sigman, M. S. *Angew. Chem. Int. Ed.* **2009**, *48*, 3146-3149.

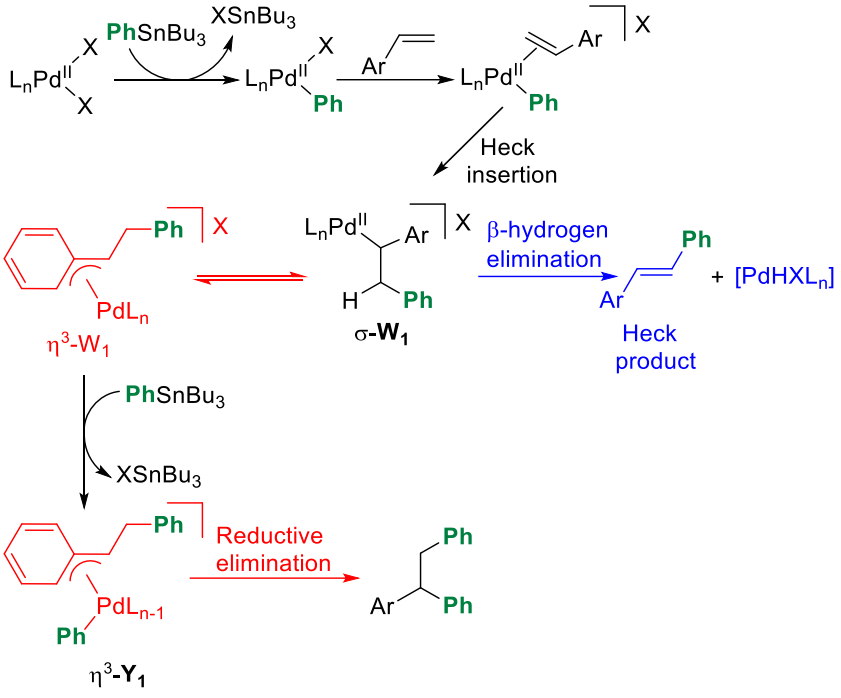

Scheme 1.12. Proposed mechanism for an oxidative heck (in blue) and difuncionalization of the σ-palladium complex by a second transmetalation in complex η^3-**W₁** (in red).

The possibility of β-H elimination in an α-substituted-benzylic palladium complex and the fact that this process can be slowed down by η^3-coordination of the benzylic fragment, has been used in our research group to study several aspects in the chemistry of a generated palladium hydride. An unprecedented hydrogen transfer between palladium atoms was studied with the η^3-benzylic dimer **1.**[31] The decomposition process by β-hydrogen elimination of **1** in $CDCl_3$ was followed by ^{19}F NMR. Organic compounds **2** and **3** were formed in a ratio of 1.4:1. A mixture of metallic Pd and $PdBr_2$ was also observed. The proposed mechanism for the hydride transfer is summarized in Scheme 1.13. A η^3-σ conversion gives the intermediate **I** which by β-hydrogen elimination gives the intermediate **II** containing the Pd-H moiety. Compound **2** is generated directly in this process, or a hydrogen transfer can occur between the Pd-atoms through an intermediate **III** containing a bridging hydrido ligand. **III** eventually undergoes reductive elimination of R-H (R = $PhCHCH_2Pf$) to form **3**, **2**, $PdBr_2$ and Pd black.

[31] Albéniz, A. C.; Espinet, P.; Lin, Y. -S. *Organometallics*, **1997**, *16*, 4030-4032

Most of the Pd-H generated is transferred to give **3** and the efficiency of the process, measured by the ratio **3**/**2**, is 0.72 (a maximum value of 1 is expected for a total transfer of the hydride).

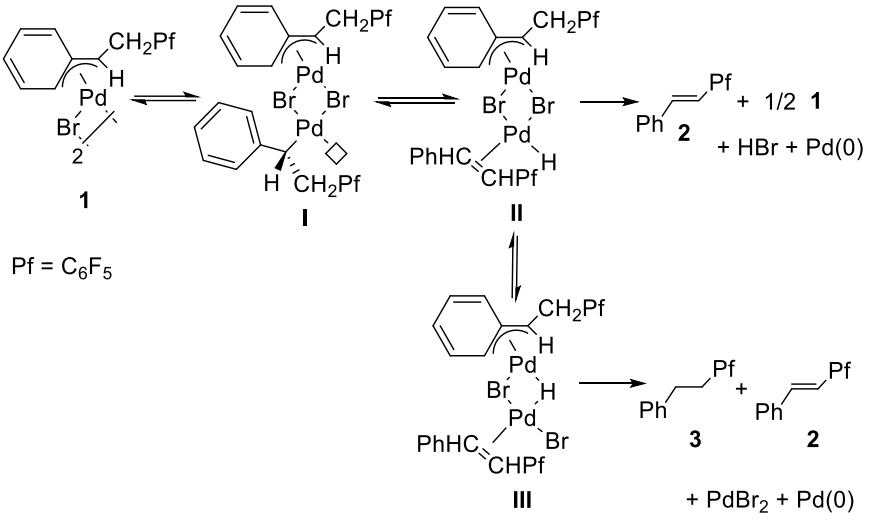

Scheme 1.13. Mechanism proposed by the formation of compounds **2** and **3**.

This H-transfer in complex **1** was used to study the effect of common radical traps on palladium hydride complexes.[32] As mentioned above, the efficiency of the process is E = **3**/**2** = 0.72 without the presence of any additives but in the presence of different radical traps the efficiency of the process changed as is shown in Table 1.1. These results show that common radical traps such as galvinoxyl, DPPH or TEMPO react with palladium hydrides and they should be used with caution in mechanistic studies: If their use as additives slow down a catalytic reaction, this effect can be due to the trap of a radical or just to the decomposition of a palladium hydride intermediate in a non-radical reaction.

[32] Albéniz, A. C.; Espinet, P.; López-Fernández, R.; Sen, A. *J. Am. Chem. Soc*. **2002**, *124*, 11278-11279.

Table 1.1. Efficiency of the H-Transfer with different radical traps. [a]

Entry	additive[b]	**3**/**2**
1	none	0.74
2	TBP	0.73
3	galvinoxyl	0.33
4	DPPH	0.18
5	TEMPO	0.11

a) Samples of **1** in $CDCl_3$ in a N_2 atmosphere were left to decompose for 10 days. b) Molar ratio **1**:additive = 1:2. TBP = 2,4,6-tri-tert-butylphenol; DPPH = di(phenyl)-(2,4,6-trinitrophenyl)iminoazanium; TEMPO = 2,2,6,6-tetramethyl-1-oxylpiperidine

The palladium hydride species **II** in Scheme 1.13 can be trapped by insertion of an alkene into the Pd-H bond and this can occur by substitution of **2** by a less substituted, more coordinating alkene. Therefore, the benzylic complex **1** can be used as a source of Pd-H as reagent. This has been carried out with R-(+)-limonene and the stereroselective *cis*-palladium migration occurs with retention of the original stereochemistry of R-(+)-limonene to give a chiral palladium allyl enantioselectively (Eq. 1.6).[33]

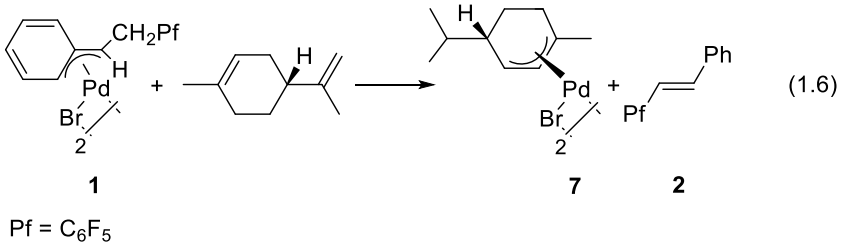

1 **7** **2**

Pf = C_6F_5

[33] Albéniz, A. C.; Espinet, P.; Lin, Y.-S.; Martín-Ruiz, B. *Organometallics* **1999**, *18*, 3359-3363.

1.1.5. Aim of the work in this chapter

The decomposition of an α-substituted palladium benzyl by β-H elimination and the fate of the resulting Pd-H species depends on the other ligands completing the coordination sphere of the metal. The ligands also influence the fluxional behavior of the complex, specially the η^3- to σ-benzylic coordination shift. In this chapter the synthesis and characterization of η^3-benzylic complexes of palladium(II) bearing an α-(pentafluorophenylmethyl) substituent with different ligands is described. The objective of the work collected here is to understand how the type and number of auxiliary ligands control the structure of the benzyl complex and its decomposition by β-hydrogen elimination. Also, how it can be used to access $PdHL_n$ fragments, as a source of Pd-H as reagent.

1.2. Results and Discussion

1.2.1. Synthesis and characterization of α-(pentafluorophenylmethyl)benzylic complexes of palladium(II)

The dimeric complex **1**, the starting point for the synthesis of all benzylic complexes, was synthesized by insertion of styrene into the Pd-C_6F_5 bond of [PdBr(C_6F_5)($NCMe)_2$] as described before (Eq. 1.7).[31]

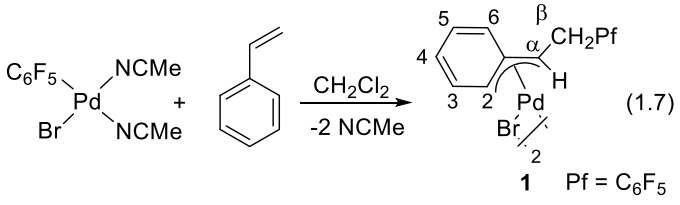

(1.7)

Upon addition of ligands to **1**, complexes with different coordination modes were found depending on the stoichiometric ratio [Pd]:ligand and the solvent used. Scheme 1.14 shows all the σ- and η^3-(pentafluorophenylmethyl)benzyl complexes that can be generated and characterized in solution,[34] but the work in this dissertation is centered on the η^3-benzylic complexes **4a-f**. The presence of the pentafluorophenyl group is most useful since the simplicity and wide chemical shift range in its ^{19}F NMR spectra allow to detect new species and the composition of mixtures of isomers. Most complexes are fluxional and display a dynamic behavior that was evident in their NMR spectra and it is described below. The stability of the complexes is very different but all of them eventually decompose by β-H elimination. For this reason, only some of the complexes could be isolated and most of them were characterized at low temperature to guarantee enough stability and static spectra.

[34] a) Martín-Ruiz, B.; Pérez-Ortega, I.; Albéniz, A. C. *Organometallics* **2018**, *37*, 1074-1085.

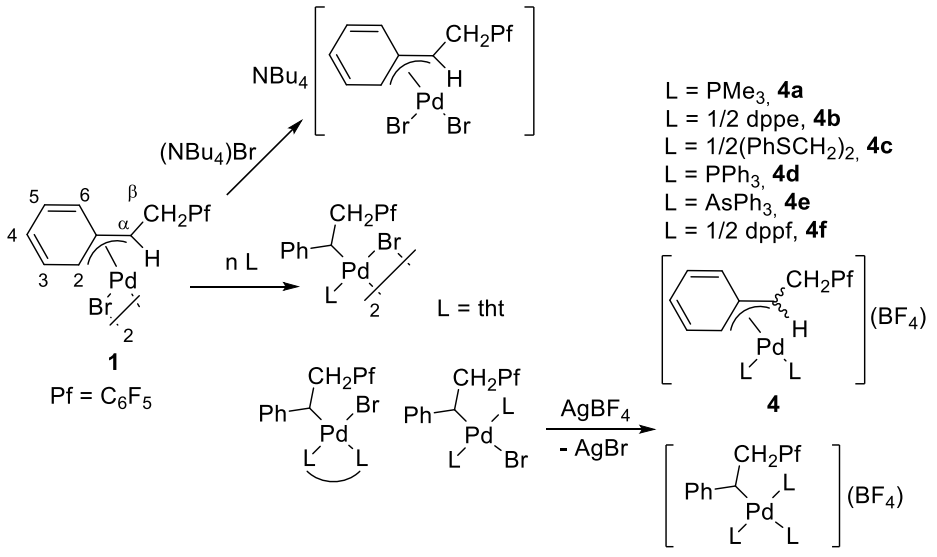

Scheme 1.14. Representation of all α-(pentafluorophenylmethyl)benzylic complexes of palladium(II).

The NMR data collected for the complexes depicted in Scheme 1.14 and those in the available literature, show characteristic spectroscopic features that allow to distinguish the σ-and η^3-benzylic coordination modes (Table 1.2).

Table 1.2. General features for σ and η^3-benzylic complexes of palladium(II).

Complex	δ C^{α}	$^1J_{C^{\alpha}\text{-}H}$	General δ trend aromatic protons
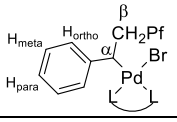	30-44 ppm	130-140 Hz	δ H_{para} < δ H_{meta} < δ H_{ortho}
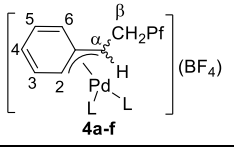 **4a-f**	around 60 ppm	155 Hz	δ H^2 < δ H^6 < δ H^3, H^5 < δ H^4

The salient feature for the σ-benzylic palladium(II) complexes is the chemical shift of C^{α} in the ^{13}C NMR spectra around 30-44 ppm and $^1J_{C^{\alpha}\text{-}H}$ = 130-140 Hz, in the range of $C(sp^3)$-H coupling. The ^1H NMR signals in the aromatic region generally follow the trend: δ H_{para} < δ H_{meta} < δ H_{ortho} with equivalent ortho hydrogens or meta hydrogens in a free rotating phenyl group (Table 1.2).

On the other hand, the η^3-coordination mode is characterized spectroscopically by the chemical shift for the C^{α} in the ^{13}C NMR spectra around 60 ppm and a value of $^1J_{C^{\alpha}\text{-}H}$ close to 155 Hz consistent with a sp^2 carbon atom. Both parameters have higher values than those of the σ-benzylic situation and allow to distinguish both coordination modes. In a static η^3-benzylic complex the ortho and meta protons of the phenyl ring are inequivalent and H^2 is clearly shifted upfield. The order in the aromatic signals in the ^1H NMR spectra usually follow the trend: $\delta\ H^2 < \delta\ H^6 < \delta\ H^3$, $H^5 < \delta\ H^4$ (Table 1.2).

1.2.1.1. Cationic η^3-benzylic complexes of palladium(II)

The η^3-(pentafluorophenylmethyl)benzylic complexes are generated by the addition to the starting dimer **1** of two equivalents of $AgBF_4$ and four equivalents of monodentate ligands (PMe_3, PPh_3, $AsPh_3$) or two equivalents of bidentate ligands (dppe, $(PhSCH_2)_2$, dppf) (Eq. 1.8, see Experimental Section for more details).

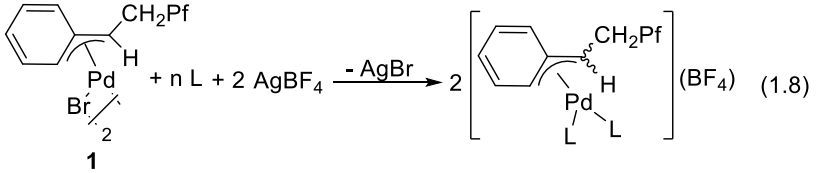

1

Pf = C_6F_5

n = 2, L = 1/2: dppe (*syn*-**4b**), 1/2 $(PhSCH_2)_2$ (**4c**), dppf (*anti*-**4f**)

n = 4, L = 2: PMe_3 (**4a**), PPh_3 (*anti*-**4d**), $AsPh_3$ (*anti*-**4e**)

The NMR data for the η^3-benzylic complexes synthesized in this work are collected in Table 1.5-1.8 (^{13}C, ^1H, ^{31}P and ^{19}F, respectively) in the Experimental Section. The characteristic chemical shift for the C^{α} (60 ppm) and value of $^1J_{C^{\alpha}\text{-}H}$ (150 Hz) of the η^3-coordination mode is observed for **4a-f**.

Only one of the two possible isomers (*syn* or *anti*) of the η^3-coordinated benzylic group is observed at any of the temperatures used for characterization of all the complexes prepared (Figure 1.6). A fast suprafacial sigmatropic rearrangement in solution can produce the transformation of the *syn* into the *anti* η^3-benzylic isomer, and it would lead to average spectra in the H^{α} and H^{β} region, which could be misinterpreted as the presence of only one species. However, the stability of both isomers is expected to be different as well as the chemical shift

of H^{α} in both situations. Thus, in a fast exchange scenario the variation of the equilibrium constant upon changing the temperature should be reflected in a significant change in the chemical shifts of H^{α}, which is not observed in any of the complexes studied.

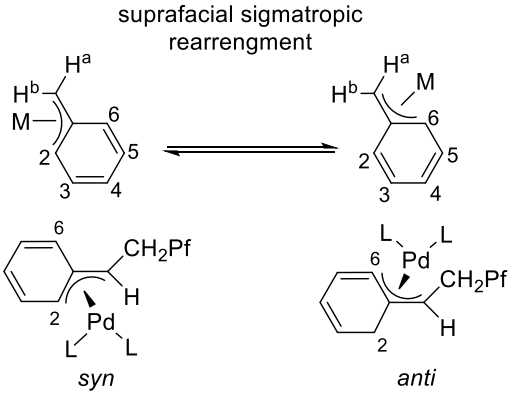

Figure 1.6. Suprafacial sigmatropic rearrengment in η^3-benzylic complexes which allow the transformation of the *syn* into the *anti* η^3-benzylic isomer.

In complex **1** the $-CH_2C_6F_5$ substituent is in the *syn* position, far from the metal center, and the presence of this isomer is confirmed by the NOE effect observed between H^{α} and H^2 in a ^1H 2D-ROESY experiment (Figure 1.7). This experiment was also carried out for the complex **4b** (L = 1/2 dppe, Figure 1.8). The analysis of the ^1H 2D-ROESY experiment at low temperature showed a high intensity NOE cross-peak between H^{α} and H^2, but a less intense NOE effect between H^{α} and H^6 is also present. In the phase sensitivity ROESY experiment a chemical exchange cross peak also appears. This indicates the presence of a slow H^2-H^6 exchange. A *syn* η^3-benzylic isomer where a slow shift to a σ-benzyl and aryl rotation occurs

explains the results obtained but does not rule out the sigmatropic shift (i.e. *syn-anti* exchange).

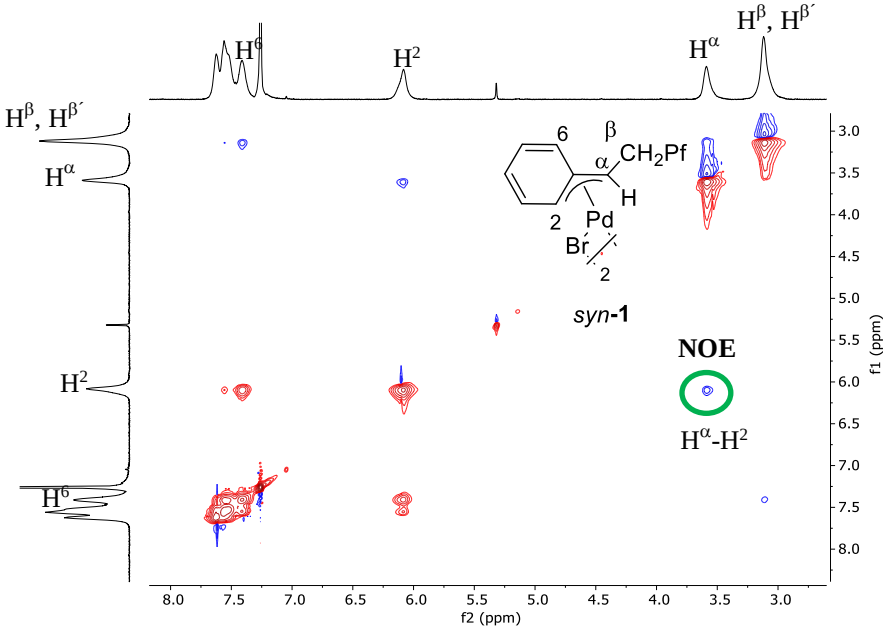

Figure 1.7. ROESY NMR at 298 K of the complex **1**. The correlation (green circle) between H^{α}-H^{2} indicates the presence of the *syn*-isomer.

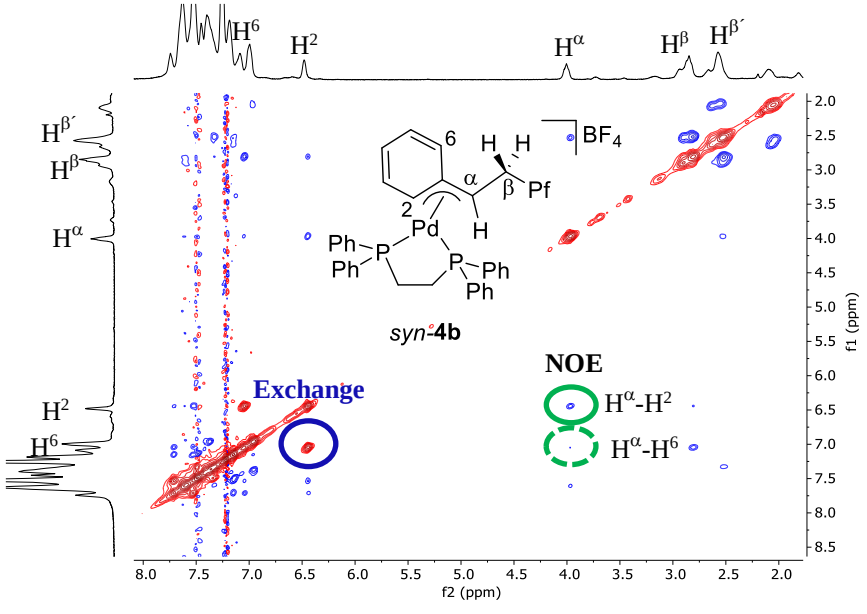

Figure 1.8. ROESY NMR at 233 K of the complex **4b**. The correlation (green circle) between H^{α}-H^{2} indicates the presence of the *syn*-isomer with a slow H^{2}-H^{6} exchange (blue circle).

The cationic complexes **4d** (L = PPh_3), **4e** (L = $AsPh_3$) and **4f** (L = 1/2 dppf) show static ^1H NMR spectra below 223 K and an *anti* configuration for the η^3-benzyl group. This is supported by the observation in solution of NOE effect between H^{α} and H^6 cross peak in the ^1H 2D-ROESY for the complex *anti*-**4f** (Figure 1.9) The complexes *anti*-**4d** and *anti*-**4e** present, in the ROESY NMR experiment, the same cross peak between H^{α}-H^6.

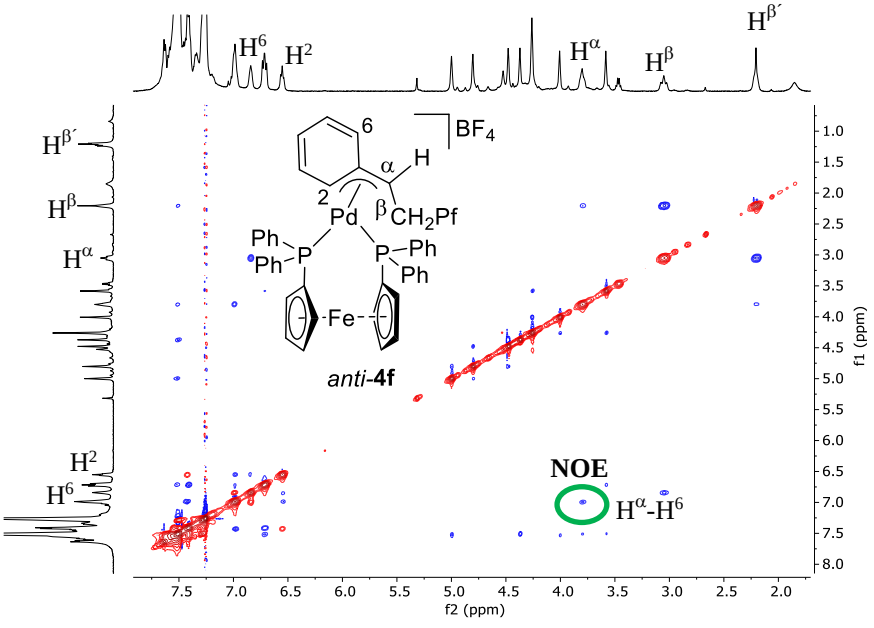

Figure 1.9. ROESY NMR at 223 K of the complex **4f**. The correlation (green circle) between H^{α}-H^6 indicates the presence of the *anti*-isomer.

A low quality crystal of the complex *anti*-**4f** was obtained by slow diffusion in a mixture of CH_2Cl_2/pentane (Figure 1.10). The structure of the complex shows the *anti* disposition of the η^3-benzylic group. Because the low quality of the crystals, the distances of the Pd-benzyl fragment cannot be discussed but an asymmetric benzyl fragment is expected (different Pd-C^{α} and Pd-C^2 bond lengths) as it is reported in the literature for other η^3-benzilic complexes.[9]

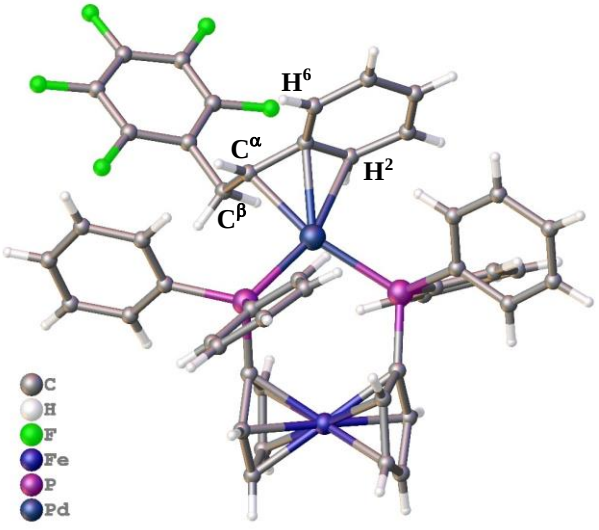

Figure 1.10. Molecular structure of **4f** determined on low quality crystals and incompletely refined (R = 12%). Only the cation is shown.[35]

This result contrasts with the complex **1** where the *syn* isomer was found, and to the η^3-benzylic complex **4b** (L = 1/2 dppe) where the *syn* isomer is also present. In general, the *anti* arrangement in the η^3-benzylic moiety is surprising since the *syn*-arrangement in allylic compounds generally results in less steric hindrance although there are some precedents in the literature with the η^3-benzylic fragment showing the *anti* disposition.[9] To try to elucidate the reasons for this isomer preference, density functional theory (DFT) calculations were carried out. We selected the M06 functional for both *syn* and *anti* isomers of complex **4d** (L = PPh_3) and also for both isomers of complex **4b** (L = 1/2 dppe). Geometries were initially optimized with a medium-sized basis set (LANL2DZ ECP for Br and SDD for Pd and 6-31+G(d) for all other atoms), including solvation (SMD, dichloromethane as solvent). The resultant free energies were then corrected with an extended basis set (LANL2DZ ECP again for Br and SDD def2-QZVP for Pd but 6-311++G** for all other atoms). As mentioned above ^{1}H 2D-ROESY experiments indicate that in solution **4d** adopts the *anti* configuration whereas a stronger cross peak between H^{α} and H^2 seems to indicate that **4b** corresponds to the *syn*

[35] As it was mentioned in the text, suitable crystals for a high quality X-ray crystal structural determination could not be obtained for **4f**. However, a disordered molecular structure (the disorder affecting mainly but not only to the anion and solvent molecules of crystallization) was obtained which could not be completely refined (R = 12%). It shows the structure of an *anti*-η^3-benzylic complex..

isomer. Both complexes are ionic and the optimized geometries were first calculated just considering the cation. However, since our experimental data were collected in dichloromethane, a low polarity, low dielectric constant solvent, the interaction with the tetrafluoroborate anion was also considered.[36] To compare the relative stability of the two isomers, we selected the structure where the BF_4 is placed as shown in Figure 1.11. There is a clear energy preference for the *anti* configuration in complex **4d** (4.97 kcal mol^{-1}). This isomer shows a less symmetrical benzylic moiety (Pd-C^{α}, Pd-C^{2} (Å): 2.123, 2.602 (*anti*-**2d**); 2.156, 2.426 (*syn*-**2d**)) and a wider P-Pd-P angle (P-Pd-P = 103.78˚ for anti-**2d** vs. 100.66˚ for *syn*-**2d**) which could help to accommodate the two sterically demanding *cis*-PPh_3.

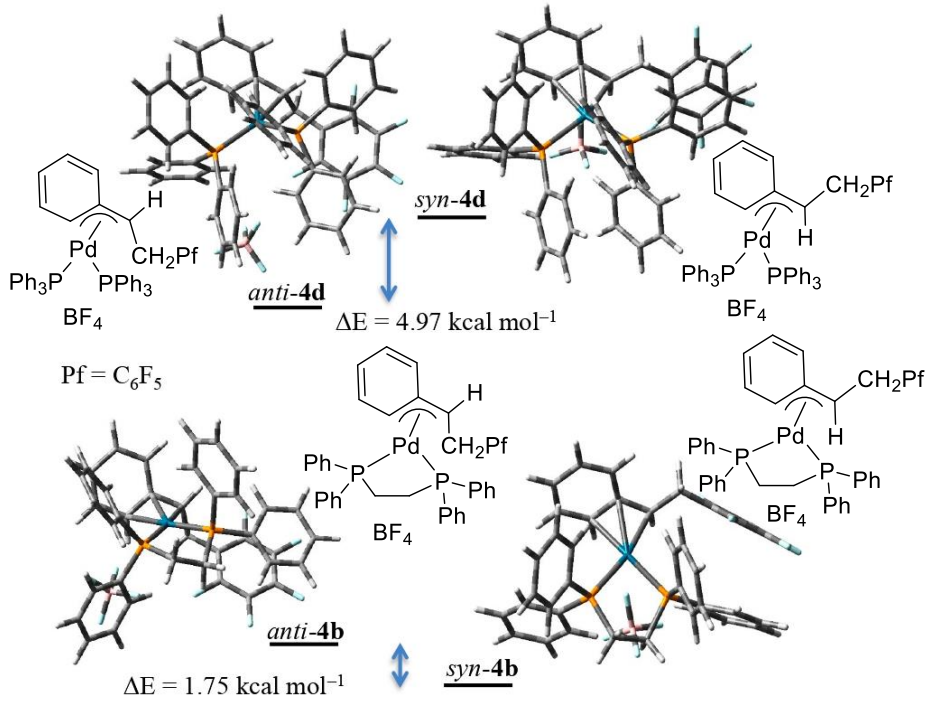

Figure 1.11. Energy difference in Kcal/mol between the two isomers (*syn* or *anti*) in the complexes **4b** and **4d**.

[36] Geometries were calculated for two different relative locations of the cation and anion, labeled up and down relative to the C^{ipso} benzylic carbon. There is no significant energy difference for the up or down BF_4^- structures for each isomer (less than 1 kcal/mol), but the down location being always more stable. Thus, the energy differences between the *syn* and *anti* isomers are given in Figure 1.11 for the down BF_4^- location.

In contrast, there is a very small energy difference for both isomers of **4b** and the *syn* isomer is slightly favored (1.75 kcal mol^{-1}). This difference is enough to observe just one isomer as a major species in solution (*syn*-**4b** ⇌ *anti*-**4b**, $K = 5\ 10^{-2}$). The geometrical parameters for both **4b** isomers are very similar. Given the lower steric demand of dppe and its lower bite angle, the adoption of an *anti* configuration, which allows a wider P-Pd-P angle as observed for **4d**, does not introduce any significant decrease in steric hindrance.

1.2.1.2. Neutral η^3-benzylic complexes of palladium(II) with PPh_3, $AsPh_3$ and dppf: Steric relief by pentacoordination

The behavior of these ligands, the bulkiest reacted with complex **1** (Scheme 1.15), is clearly different and shows surprising structural solutions to cope with the steric hindrance of L. The addition of one equivalent of triphenylphosphine per palladium to complex **1** brings about the formation of the η^3-benzylic complex **5** (Scheme 1.15). A static ^1H NMR spectrum is observed at 213 K with separated signals for H^2 (δ 6.97) and H^6. The arrangement of C^α and PPh_3 is *cis* according to the low value of $^3J_{P\text{-}H^\alpha}$ (< 6 Hz) and $^2J_{P\text{-}C^\alpha}$ (< 20 Hz).

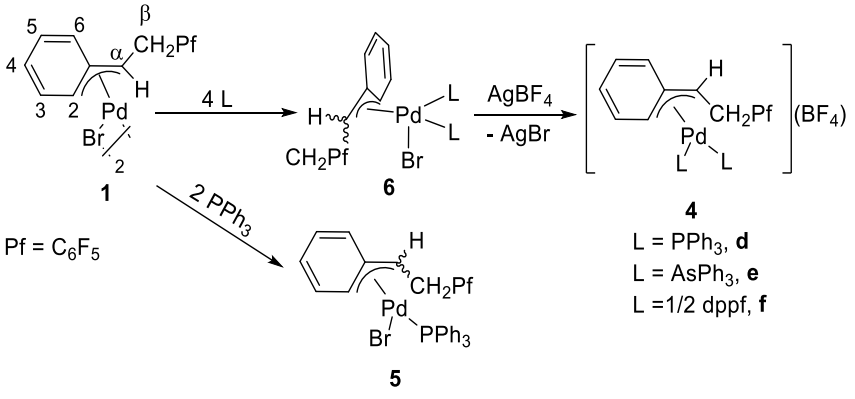

Scheme 1.15. Complexes formed upon addition different amounts of PPh_3, $AsPh_3$ or dppf to **1**.

On the other hand, when 2 equivalents of PPh_3 per palladium were added to a $CDCl_3$ suspension of **1** at 213 K a new complex was found in solution. An η^3-benzylic complex (**6d**) is formed (C^α, 60.63 ppm; $^1J_{C^\alpha\text{-}H}$ = 155 Hz; H^2 and H^6, 6.77 ppm), with two inequivalent phosphine ligands in a *cis* arrangement ($^2J_{P\text{-}P}$ = 51.9 Hz). The bromo ligand is not out of the coordination sphere of palladium, since the addition of $AgBF_4$ leads to a different species, the

cationic η^3-benzylic derivative **4d** (C^{α}, 70.5 ppm; $^1J_{C^{\alpha}\text{-}H}$ = 155 Hz; H^2, 6.72 ppm; H^6, 7.11 ppm; $^2J_{P\text{-}P}$ = 47 Hz). Thus, we propose that the complex **6d** must be the pentacoordinated species shown in the Scheme 1.15. Five is not the most common coordination number for Pd(II) but pentacoordinated palladium complexes have been reported before with three different structures: square pyramidal (spy), trigonal bipyramidal (tbp) or distorted square pyramidal.[37-40] The same behavior was found for L = $AsPh_3$ (**6e**) and L = 1/2 diphenylphosphinoferrocene (dppf, **6f**) and complete spectroscopic data for these complexes can be found in Table 1.5-1.8.

Some additional experiments were run to learn about the structure in solution of complexes **6**. Since **6d** is generated and characterized in a solvent of low polarity such as $CDCl_3$, it is possible that could form tight ionic pairs in solution, so the spectroscopic differences of **6d** and **4d** would be a result of a different interaction between the cation and either bromide or BF_4^-. A measure of the conductivity of a solution of **6d** in acetone at 223 K gave a non-electrolyte. The η^3-benzylic mode (C^{α}, 52.37 ppm) and the coordination sphere of palladium (two PPh_3 in a *cis* arrangement) are maintained in acetone, supporting the occurrence of a pentacoordinated species.

[37] Pentacoordinated palladium(II) complexes are not common but representative examples have been long known: Albéniz, A. C.; Espinet, P. Encyclopedia of Inorganic Chemistry, King, R. B. Ed.; England; 1994, 3018.

[38] Selected examples of trigonal bipyramidal Pd(II) compounds (other than those with specially designed tripod ligands): a) Konietzny, A.; Bailey, P. M.; Maitlis, P. M. *J. Chem. Soc. Chem. Commun*. **1975**, 78-79. b) Albano, V. G.; Castellar, C.; Cucciolino, M. E.; Panunzi, A.; Vitagliano, A. *Organometallics*, **1990**, *9*, 1269-1276. c) Burger, P. Baumeister, J. M. *J. Organomet. Chem*. **1999**, *575*, 214-222. d) López-Torres, M.; Fernández, A.; Fernández, J. J.; Suárez, A.; Pereira, M. T.; Ortigueira, J. M.; Adams, H. *Inorg. Chem.* **2001**, *40*, 4583-4587. e) Binotti, B.; Bellachioma, G.; Cardaci, G.; Macchioni, A.; Zuccaccia C.; Foresti, E.; Sabatino, P. *Organometallics* **2002**, *21*, 346-354. f) Bedford, R. B.; Betham, M.; Butts, C. P.; Coles, S. J.; Cutajar, M.; Gelbrich, T.; Hursthouse, M. B.; Scully, P. N.; Wimperis, S. *Dalton Trans*. **2007**, 459-466. g) Kirai, N.; Ta-kaya, J.; Iwasawa, N. *J. Am. Chem. Soc.* **2013**, *135*, 2493-2496.

[39] Square pyramidal Pd(II) derivatives: a) Collier, J. W.; Mann, F. G.; Watson, D. G.; Watson, H. R. 351. *J. Chem. Soc*. **1964**, 1803-1814. b) Chui, K. M.; Powell, H. M. *J. Chem. Soc. Dalton Trans.* **1974**, 1879-1889. c) Chui, K. M.; Powell, H. M. *J. Chem. Soc. Dalton Trans.* **1974**, 2117-2122. d) Louw, W. J.; de Waal, D. J. A. *J. Chem. Soc Dalton Trans.***1976**, 2364-2368. e) Hansson, S.; Norrby, P.-O.; Sjögren, M. P. T.; Åkermark, B.; Cucciolito, M. E.; Giordano, F.; Vitagliano, A. *Organometallics*, **1993**, *12*, 4940-4948. f) Bröring, M.; Brandt, C. D. *Chem. Commun*. **2003**. 2156-2157. g) Zhang, X.; Xia, Q.; Chen, W. *Dalton Trans.* **2009**, 7045-7054.

[40] Rülke, R. E.; Ernsting, J. M.; Spek, A. L.; Elsevier, C. J.; Van Leeuwen, P. W. N. M.; Vrieze, K. *Inorg. Chem.* **1993**, *32*, 5769-5778.

The distinct behavior of complexes **6d-f,** synthesized by addition of a two fold molar amount of PPh_3 or $AsPh_3$ per Pd or an equimolar amount of dppf, can be due to the steric features of these ligands rather than to electronic factors. We hypothesized that the large angle L-Pd-L in the complexes with the PPh_3, $AsPh_3$ and dppf is the responsible for the formation of pentacoordinated complexes. The average angle (P-Pd-P) in *cis*-$Pd(PPh_3)_2$ complexes is 98º and as it is expected, a larger angle is found for As-Pd-As (100.37˚).[41,42] The bite angle of dppf in related allylic complexes (101.2˚) is also large and shows a big difference with that of dppe (85.77˚), whose complex **4b** is a tetracoordinated σ-benzyl.[43]

As mentioned above, the analysis of **6d** at 213 K by NMR spectroscopy gives us some information about its structure in solution. We know that the complex is in the η^3-benzylic form (C^{α}, 60.63 ppm; $^1J_{C^{\alpha}\text{-}H}$ = 155 Hz; H^2 and H^6, 6.77 ppm) with *cis*-PPh_3 ($^2J_{P\text{-}P}$ = 51.9 Hz) and a *trans*-C^{α}-P ($^2J_{C^{\alpha}\text{-}P}$ = 50 Hz) arrangement. We considered three isomeric forms that meet those requirements and their structures were minimized using the same DFT methods described above (see also computational details in the Experimental Section. As shown in Figure 1.12, the geometries found correspond to square-pyramidal complexes with apical Br (**6d**-spy-apiBr) or apical PPh_3 (**6d**-spy-apiPPh_3) and a complex that could be described as a very distorted trigonal bipyramid with axial PPh_3 and C^{α} (**6d**-dist tbp). All three structures are favored when compared to the tetracoordinate σ-benzyl and both square pyramidal derivatives **6d**-spy-apiBr and **6d**-spy-apiPPh_3 are the most stable species, although the small energy difference found does not allow to favor one over the other (Figure 1.12). As observed before for **4d**, all the pentacoordinated η^3-benzylic structures show analogous and significant differences in the distances Pd-C^{α} (between 2.134-2.123 Å) and Pd-C^2 (between 2.604-2.575 Å).[10] The P-Pd-P angle is larger for the more stable **6d**-spy-apiBr (101˚) and **6d**-spy-apiPPh_3 (102˚) but smaller for **6d**-dist tbp (97.3˚). This angle is 99˚ for the σ-benzyl. However moderate in value, the larger P-Pd-P angle in the square pyramidal pentacoordinated structures can alleviate the steric constraints imposed by the bulkiest ligands in a *cis* arrangement, and, in contrast to what could be expected, favor an increase of the coordination number as a way

[41] Cambridge Structural Database System (CSD System, version 5.38, **2016**). Cambridge Crystallographic Data Centre, 12 Union Road, Cambridge CB2 1EZ, UK.
[42] Kemmitt, R. D. W.; McKenna, P.; Russell, D. R.; Sherry, L. J. S. *J. Chem. Soc. Dalton Trans.* **1985**, 259-268.
[43] Van Haaren, R. J.; Goubitz, K.; Fraanje, J.; van Strijdonck, G. P. F.; Oevering, H.; Coussens, B.; Reek, J. N. H.; Kamer, P. C. J.; van Leeuwen P. W. N. M. *Inorg. Chem.* **2001**, ***40***, 3363-3372.

to reach an overall less constrained geometry. Pentacoordination has also been observed in the solid state for η^3-allyl or alkyl-olefin derivatives bearing in-plane the sterically demanding phenantroline ligands (Figure 1.13).[38b,c,39e]

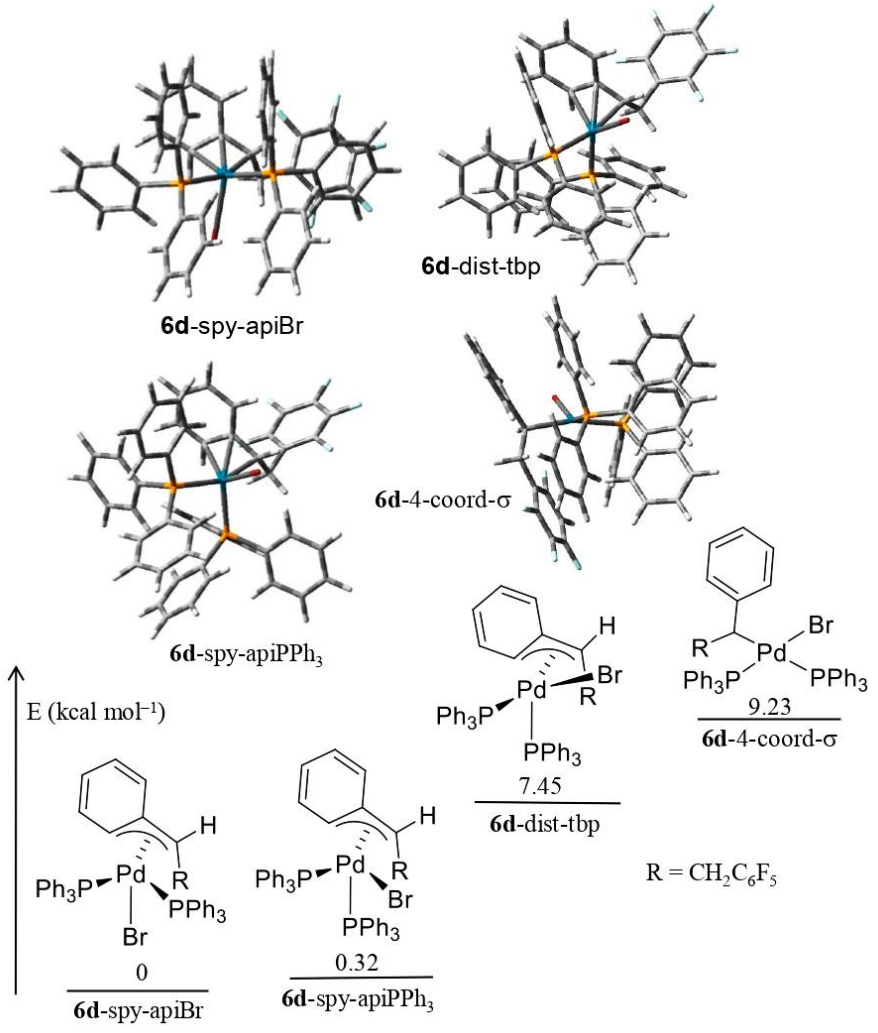

Figure 1.12. Representative energy diagram for the different calculated isomers for the pentacoordinated complex **6d**.

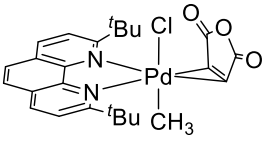

Figure 1.13. Pentacoordinated palladium(II) complex [PdCl(CH_3)($C_4H_2O_3$)($C_{14}H_{12}N_2$)].

1.2.2. Fluxional behavior of α-(pentafluorophenylmethyl)benzylic complexes of palladium(II)

The benzylic complexes synthesized in this chapter show a rich dynamic behavior in solution. A static η^3-benzylic complex shows in the ^{1}H NMR inequivalence for the ortho protons (H^2 and H^6). This behavior is observed for example for the complex **1** in $CDCl_3$ where the ortho protons (H^2 and H^6) have got different chemical shifts even at 298 K (Figure 1.15, a)). However, this is not always observed. A fast η^3-σ-η^3 equilibrium can exchange H^2 and H^6 by rotation of the phenyl ring, leading to one signal for both protons and depending on the ligand this process can occur at very different rates. For example, in the case of complex **4a** (L = PMe_3), only one signal for H^2 and H^6 is observed even at 223 K indicating a fast rotation around the C^{α}-C^{ipso} (Figure 1.14). This interconversion is already known for other η^3-benzylic complexes.[15-17]

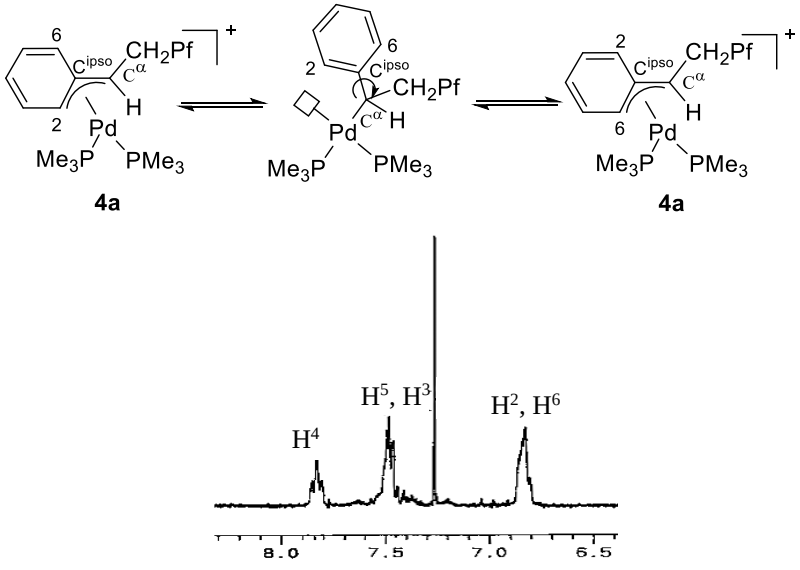

Figure 1.14. ^{1}H NMR spectrum at 223 K for the complex **4a** where it is observed the fast rotation around the C^{α}-C^{ipso} making H^2 and H^6 equivalents.

The aryl rotation (interconversion of H^2 and H^6) can be altered in the presence of coordinating solvents as the case of the complex **1**. The η^3-benzylic complex **1** shows a static ^{1}H NMR spectrum in $CDCl_3$ at room temperature (Figure 1.15, a)). Upon addition of two equivalents of acetonitrile per palladium, the coalescence of H^2 and H^6 signals is observed, which indicates

a fast η^3-σ-η^3 interconversion that allows, by rotation, the equivalence of both H_{ortho} aromatic protons (Figure 1.15, b)). A similar behavior was proposed before by Stille with [Pd(η^3-C_7H_7)(PEt_3)$_2$](BPh_4).[19a]

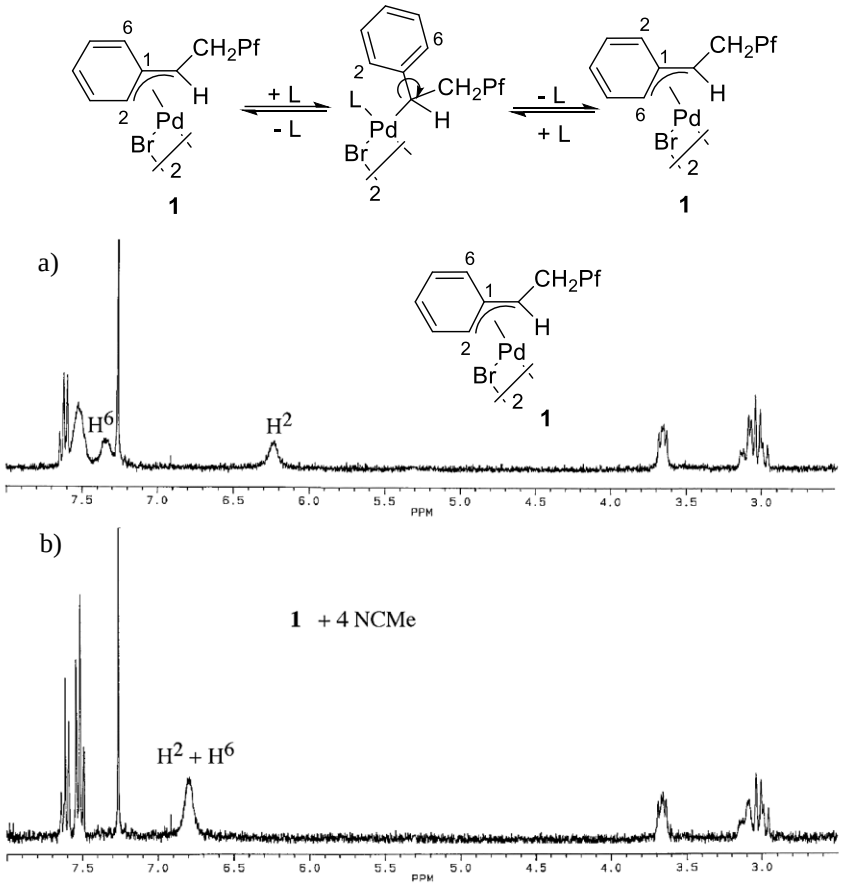

Figure 1.15. σ-aryl rotation in the complex **1** altered by the presence of NCMe in the solution. a) ^{1}H NMR spectrum of **1** in $CDCl_3$ and b) ^{1}H NMR spectrum of **1** in $CDCl_3$ + 4 NCMe.

The pentacoordinated complexes with two monodentate ligands (**6d**, **6e** and **6f**) undergo ligand exchange as the temperature is increased and the process is clearly observed in the $^{31}P\{^1H\}$ NMR for the phosphino derivative **6d**. The AX spin system at 213 K becomes a broad signal at 273 K (Figure 1.16). Upon addition of PPh_3 to **6d** at 233 K the broadening of the ^{31}P signal of free phosphine is also observed. Thus, a ligand dissociation to a tetracoordinated η^3 complex **5** and subsequent recoordination contribute to the exchange (Scheme 1.16). The calculated pentacoordinated complex **6d**-spy-apiBr is in fact the result of the reaction of **4d**

with bromide as the entering ligand, and **6d**-spy-apiPPh$_3$ forms when **5** reacts with PPh$_3$ as the entering ligand.

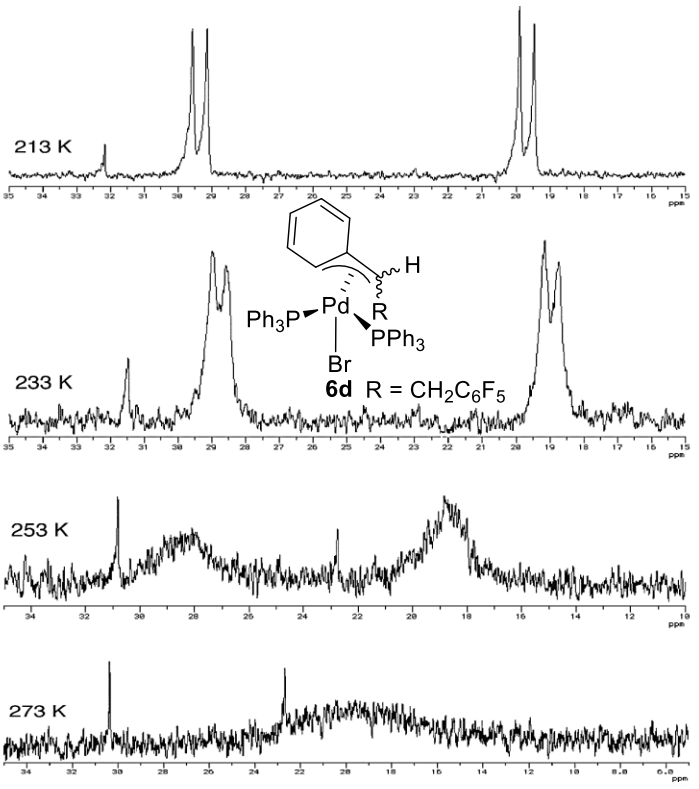

Figure 1.16. $^{31}P\{^1H\}$ NMR spectrum of **6d** at different temperatures showing a ligand exchange.

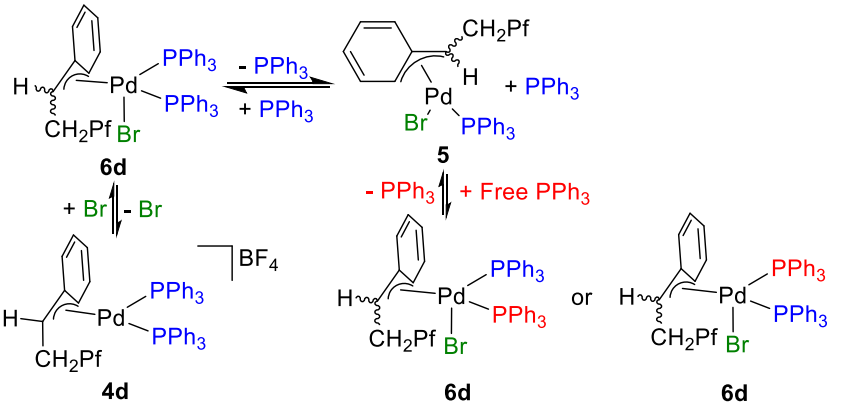

Scheme 1.16. Ligand exchange in pentacoordinated complex **6d** in the presence of an excess of PPh$_3$.

1.2.3. α-(pentafluorophenylmethyl)benzylic complexes of palladium(II) as hydride precursors

1.2.3.1. Decomposition of benzylic complexes

As mentioned in the last part of the introduction of this chapter, the benzylic complex **1** can be a source of the "Pd-H" fragment (Scheme 1.17). We have studied how the presence of additional ligands in several α-(pentafluorophenylmethyl)benzylic complexes of palladium (II) affect their decomposition and the hydride transfer between palladium atoms, i.e the ratio **2**/**3** which is a measure of the efficiency of the transfer.

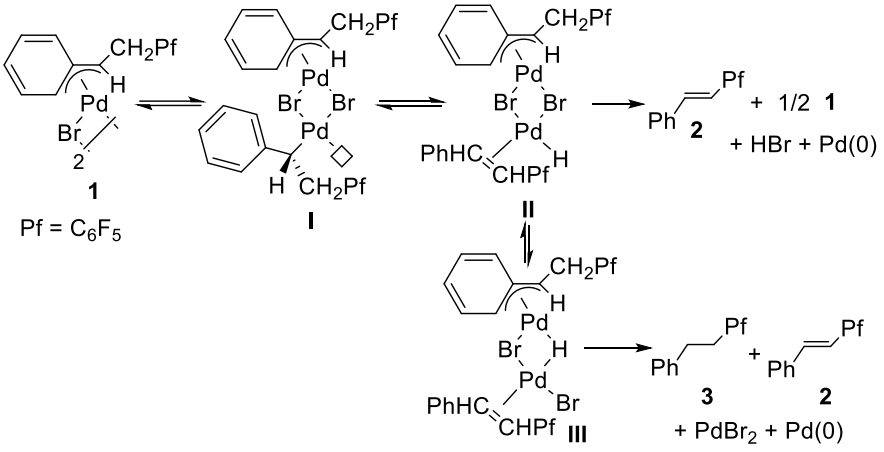

Scheme 1.17. Decomposition process for all benzylic complexes of palladium(II).

Indeed, all the complexes decompose, at different rates, by β-hydrogen elimination to form **2** and in some cases the reduction compound **3**. The data for the decomposition are collected in Table 1.3.[44] The times for complete decomposition are given and they show large differences in stability. The cationic derivatives are more stable than their neutral counterparts. The more electrophilic the metal the lower the tendency to lose a ligand and create a coordination vacant site (cf. decomposition times for entries 2, 4 and 5 and entries 3 and 6, Table 1.3). Furthermore, an electron deficient metal does not favor the cleavage of the C-H bond. The pentacoordinated complexes **6d** and **6e** decompose fast even at low temperature (entries 5 and 6, Table 1.3). Both are fluxional and the dynamic behavior of complex **6d** indicates a fast

[44] Martín-Ruiz, B; Pérez-Ortega, I; Albéniz, A. C. *Organometallics* **2018**, *37*, 1665-1670.

ligand exchange above 253 K (Scheme 1.16 and Figure 1.16). This increases the chances of creating a vacant coordination site for β-H elimination. For complexes **6d** and **6e** both products of β-H elimination, **2** and the corresponding [PdHBrL$_2$], could be detected by ^{1}H NMR: [PdBrH(PPh$_3$)$_2$] (δ = -11.82 t, $^2J_{P\text{-}H}$ = 9.5 Hz); [PdBrH(AsPh$_3$)$_2$] (δ = -14.37, s).[45] Also, [PdH(PPh$_3$)$_3$]$^+$ was detected in the decomposition of **4d** (see below).

Table 1.3. Decomposition details for different benzylic complexes.

Entry	[Pd]	L	Pd:L	T (K)	t[b]	*trans*-**2** (%)	**3** (%)	E[d]
1	**1**[c]	---	---	293	7 days	46	33	0.72
2	**4d**	PPh$_3$	1:2	293	6 h	100	---	0
3	**4e**	AsPh$_3$	1:2	293	2 days	100	---	0
4	**5**	PPh$_3$	1:1	293	10 min	68	31	0.45
5	**6d**	PPh$_3$	1:2	273	10 min	96	4	0.04
6	**6e**	AsPh$_3$	1:2	273	30 min	48.7	37.7	0.77

a) $CDCl_3$ as solvent. b) Time for complete decomposition. c) Complex **1** is only slightly soluble in $CDCl_3$ and this may decrease the decomposition rate. d) E = [**3**]/[**2**].

Besides the different stability discussed above, Table 1.3 also shows the occurrence of hydride transfer between palladium atoms for each particular complex, using the parameter of efficiency of the transfer E = [**3**]/[**2**] (last column). Previous studies in the group on the decomposition of complex **1** ruled out the protonation of a Pd-benzyl as a source of **3**.[31] It was also shown that no deuterium incorporation in **3** was observed in the decomposition of [PdBr(σ-(pentafluorophenylmethyl)benzyl)(PMe$_3$)$_2$] in the presence of D_2O, indicating that protonation of the benzylic-palladium moiety is not responsible of the formation of the saturated compound **3** even for a σ-benzylic complex with the strong donor ligand PMe$_3$.

The hydride transfer is clearly aided by the presence of bridging atoms. Bromide is playing that role for the complexes studied and in the absence of Br or other ligand capable of acting as a bridge, the hydride transfer observed is very small or non-existent (entries 2 and 3, Table

[45] Heaton, B. T.; Hébert, S. P. A.; Iggo, J. A.; Metz, F.; Whyman, R. *J. Chem. Soc., Dalton Trans.* **1993**, 3081-3084.

1.3). In the case of complexes of composition [PdRBrL2] (R = H, benzyl) three possible dimeric intermediates can be proposed for the exchange (**IV-VI**, Scheme 1.18). The triply bridged intermediate **IV** has been proposed in the exchange of aryl groups between palladium atoms where two of the bridging ligands are aryl groups.[46] In our case only the hydride is an electron deficient ligand and, generally, it forms a stronger bridge than an aryl ring. For this reason, a triple bridge is probably not necessary for an efficient transfer and presumably the doubly bridging species **V** or **VI** are stable enough to support the exchange. In any case, the dissociation of a ligand is required and strongly coordinating species may prevent the transfer. This is observed when comparing complexes **6d** (L = PPh_3, E = 0.04) and **6e** (L = $AsPh_3$, E = 0.77) where virtually no transfer occurs for the stronger phosphine ligand but the value of E is high for the less coordinating arsine (entries 5 and 6, Table 1.3). When the ratio L:Pd decreases, the hydride transfer is more effective (cf. entries 4 and 5, Table 1.3).

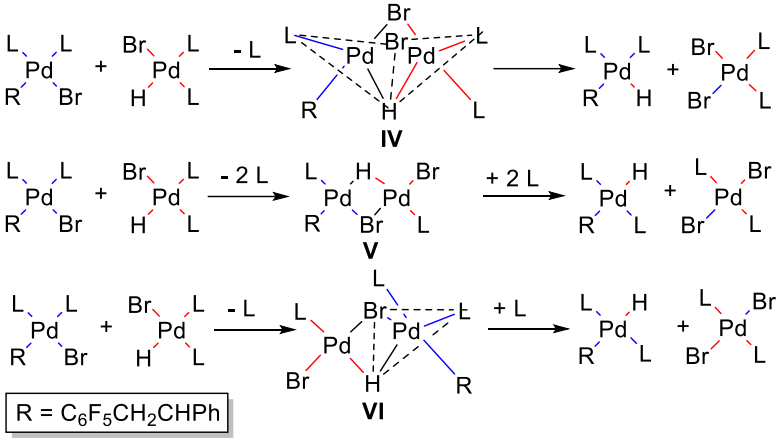

Scheme 1.18. Three possible dimeric intermediates for the hydride transfer.

As can be seen in Table 1.3, the hydride transfer mechanism can be quite efficient reaching high values of E (see for example entries 1 and 6, Table 1.3) which implies that almost all the Pd-H produced by β-H elimination is consumed in the reduction of the remaining Pd-R moieties. In a catalytic reaction, this means that if a substituted benzylic halide is used as reactant, a dehalogenation reaction can be a competing process. A Heck-type reaction with styrene can also produce a formal hydrogenation of the product through this mechanism; thus, this pathway could be responsible for the sometimes observed saturated byproducts, or play a

[46] Casado, A. L.; Casares, J.; Espinet, P. *Organometallics* **1997**, *16*, 5730-5736.

role in the mechanism of the reductive Heck-type reactions where palladium hydrides are formed in the presence of suitable hydrogen donors.[47] According to our results, this inter-palladium transfer can be minimized by avoiding the presence of halides in solution (i.e. by using a different benzylic precursor such as a diazonium salts) and using a higher L:Pd ratio and better coordinating ligands, provided the target catalytic reaction is not drastically slowed down by such a ligand choice.

1.2.3.2. Trap of the Pd-H generated from the benzylic complexes with dienes.

In the absence of other reagents in solution the palladium hydride species, formed by β-H elimination from the benzylic complexes either decompose or transfer to another palladium benzyl to give the reduction product **3** (Scheme 1.17). However, these species could be trapped by insertion of an alkene into the Pd-H bond and this could be a new starting point for the reincorporation of Pd(II) species in a catalytic cycle. Also, the Pd-H species thus generated can be used as reagents and this has been shown in the synthesis of enantiomerically pure allyls from R-(+)-limonene and complex **1** (see Introduction, Eq 5.1).[33] In this case the exocyclic, less substituted double bond of limonene, inserts into the Pd-H bond and the stereroselective *cis*-palladium migration occurs with retention of the original stereochemistry of R-(+)-limonene.

We have studied here how the presence of additional ligands can affect this H-transfer to R-(+)-limonene as a diene to give complexes **7** and **8** (Eq. 1.9). As can be seen in Table 1.4, entry 2, the presence of an equimolar amount of triphenylphosphine is enough to effectively block the coordination and insertion of a double bond of the diene into the Pd-H one. A higher amount of PPh_3 or $AsPh_3$ produces the same result (entries 3 and 4, Table 1.4). Complexes **5** and **6** decompose by β-H elimination but the transfer of hydride to the diene is null. Still, the presence of the diene significantly reduces the inter-palladium H-transfer to give **3** and the E

[47] a) Cacchi, S; Arcadi, A. *J. Org. Chem.* **1983**, *48*, 4236-4240. b) Friestad, G. K.; Branchaud, B. P. *Tetrahedron Lett.* **1995**, *36*, 7047-7050. c) Gligorich, K. M.; Cummins, S. A.; Sigman, M. S. *J. Am. Chem. Soc.* **2007**, *129*, 14193-14195. d) Gottumukkala, A. L.; de Vries, J. G.; Minnaard, A. J. *Chem. Eur. J.* **2011**, *17*, 3091-3095. d) Raoufmoghaddam, S.; Mannathan, S.; Minnaard, A. J.; de Vries, J. G.; Reek, J. N. H. *Chem. Eur. J.* **2015**, *21*, 18811-18820. e) Yue, G.; Lei, K.; Hirao, H.; Zhou, J. *Angew. Chem. Int. Ed.* **2015**, *54*, 6531-6535. f) Kong, W.; Wang, Q.; Zhu, J. *Angew. Chem. Int. Ed.* **2017**, *56*, 3987-3991.

factor is reduced to 0.27 and 0.04 for complexes **5** and **6e** (vs. 0.45 and 0.77 without diene, Table 1.3). This means that the formation of the required dimeric halogen-bridged species is disfavored in the presence of the diene.

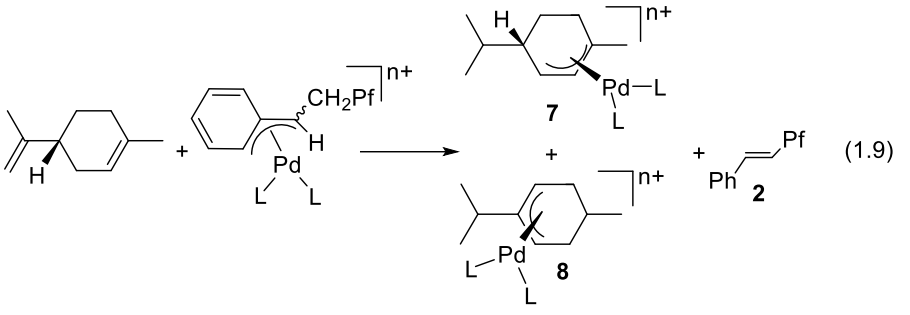

(1.9)

Table 1.4. Data for the formation of the allyls compounds represented in Eq. 1.9 with different benzylic complexes of palladium(II)

Entry	Complex	L, n	Ratio **7**:**8**	H-transfer to diene (%)[a]
1	**1**	Br, 0	1:0[b]	73
2	**5**	Br, PPh_3, 0		0
3	**6d**	Br, 2 PPh_3, 0	–	0
4	**6e**	Br, 2 $AsPh_3$, 0	–	0
5	**4d**	2 PPh_3, 1	1:3.8	58
6	**4e**	2 $AsPh_3$, 1	1.6:1	61

a) Calculated by integration in the crude ^{1}H NMR spectrum: %H-transfer to diene = (**7**+**8**)/**2** x 100. b) A small amount of an allyl complex resulting from insertion of the endocyclic is detected.

The cationic derivatives **4d**,**e** do form a mixture of allylic derivatives from R-(+)-limonene (**7** and **8**, Eq. 1.9) that result from insertion of the exocyclic, less substituted double bond into the Pd-H moiety. The presence of both isomeric complexes **7** and **8** is caused by differences in the Pd-migration process (Scheme 1.19). A straight Pd-migration to reach the endocyclic double bond of limonene leads to **7**. However, in the course of palladium migration a coordinated cyclohexadiene fragment (a terpinene) is formed: if a double bond coordination

switch from one to the other occurs, followed by insertion of the initial endocyclic bond into the Pd-H bond the Pd-migration changes its course and **8** is formed (Scheme 1.19). This is not observed for the neutral complex **1** where a fast, direct Pd-migration is observed and **7** is formed selectively. About 60% of the generated Pd-H generated from decomposition of the cationic complexes **4d**,**e** is trapped by R-(+)-limonene, a percentage that increases to 73% for the naked palladium hydride derived from **1**.

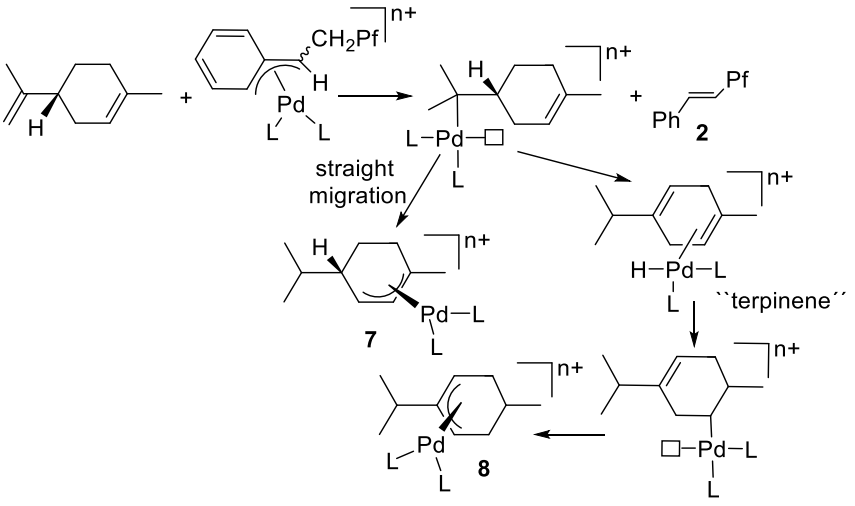

Scheme 1.19. Representation of the H-transfer from a benzylic complex to the R-(+)-limonene. The scheme represents the two possible ways for the formation of the allyls **7** and **8**.

1.2.3.3. Decomposition of the cationic η^3-benzylic complex 4d

Complex **4d** shows an interesting and clean decomposition process in CD_2Cl_2. After 6 h, the analysis of the ^1H NMR showed the complete disappearance of the initial complex with the formation of a new set of signals at 5.98 ppm, 4.80 ppm and 7.02 ppm (Figure 1.17, a)). In the ^{19}F NMR, we only observed the formation of the olefin **2** generated by β-hydrogen elimination so the new complex has not got any C_6F_5 in its structure. The ^{31}P NMR shows two inequivalent phosphines at 42.71 ppm and 8.95 ppm (Figure 1.17, b)). Furthermore, the solution color changes to the initial orange to red. All the data are indicative of the formation of a palladium cluster of type $[Pd_3(PPh_3)_4](BF_4)_2$ (**9**).

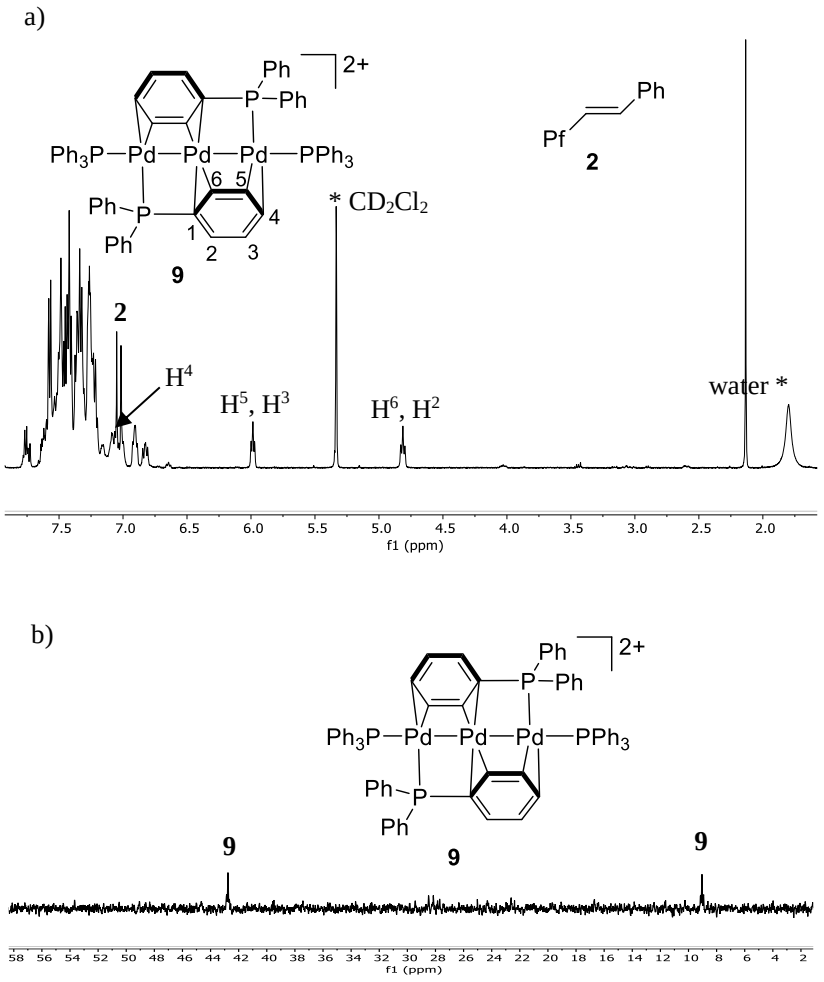

Figure 1.17. a) ^{1}H NMR of complex **4d** in CD_2Cl_2 at 25 ºC after 6 hours, where we can see the complete disappearance of the initial complex **4d** and the formation of the cluster **9**. b) ^{31}P NMR of complex **4d** in CD_2Cl_2 at 25 ºC after 6 hours, where we can see the complete disappearance of the initial complex **4d** and the formation of the cluster **9**.

Crystals of **9** were obtained from the solution and the molecular structure, determined by X-ray diffraction is shown in Figure 1.18. The complex has a linear Pd-Pd-Pd arrangement and can be considered as a Pd(0)-Pd(II) mixed valence derivative. The formation of this palladium cluster $[Pd_3(PPh_3)_4](BF_4)_2$ (**9**) was described before by two alternative synthetic routes: from $[Pd(\mu\text{-}OH)(PPh_3)_2]_2(BF_4)_2$ in a mixture of ethanol/CH_2Cl_2 or mixing $Pd(OAc)_2$:PPh_3 in a 1:2

ratio in MeOH with three equivalents of CF_3SO_3H.[48] All experimental evidences studied previously support the formation of this type of clusters by reduction of the initial Pd(II) complex by the alcohol. In our experiments no reductant was used since **4d** decomposes in a solution in CD_2Cl_2 by β-hydrogen elimination to form the olefin **2** and a $[PdHL_n]^+$ intermediate that undergoes evolution to complex **9**.

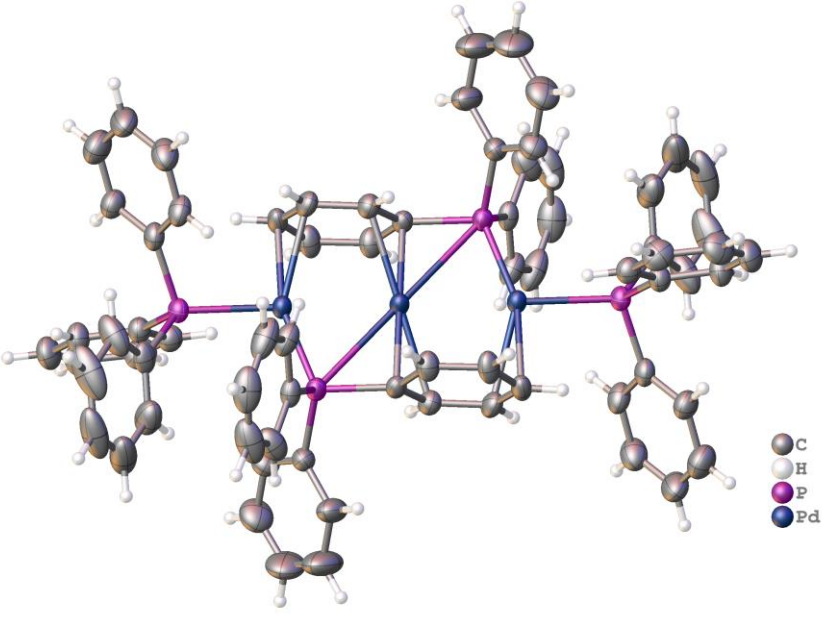

Figure 1.18. ORTEP representation of the complex **9** obtained by X-Ray analysis. The two BF_4^- anion were omitted to clarity.

A palladium hydride complex $[PdH(PPh_3)_3]^+$ (**10**) was detected in the decomposition process of **4d** (Figure 1.19, a)). The structure of the complex **10** has been described before and our spectroscopic data match with those reported before (see Experimental Section).[49] The complex **10** can be generated in solution by the addition to **4d** of one equivalent of phosphine and heating the solution at 45 ºC for 40 min (Figure 1.19, b)). The initial orange color rapidly changes to a yellow solution with the formation of a little amount of Pd^0 black. Because the presence of an excess of phosphine from this decomposition the doublet of triplets at -7 ppm

[48] a) Kannan, S.; James, A. J.; Sharp, P. R. $[Pd_3(PPh_3)_4]^{2+}$ *J. Am. Chem. Soc.* **1998**, *120*, 215-216. b) Omondi, B.; Shawb, M. L.; Holzapfel, C. W. *J. Organomet. Chem.* **2011**, *696*, 3091-3096.
[49] Zudin, V. N.; Chinakov, V. D.; Nekipelov, V. M.; Likholobov, V.A. Yermakov, Y. L. *J. Organomet. Chem.* **1985**, *289*, 425-430.

in the ^{1}H NMR become a broad doublet and the two phosphorus signals are also broad (Figure 1.20). These changes in the ^{1}H and ^{31}P NMR were described before and they are a consequence of the equilibrium between the coordinate phosphine and the free phosphine.[49] Complex **10** is not an intermediate in the formation of **9**, but rather a product of the trap of a bis-phosphino hydride "$PdH(PPh_3)_2^+$" by an additional phosphine. We can observe that in the decomposition of **4d** in the presence of phosphine along with formation of complex **10** a small amount of complex **9** appears in the solution (molar ratio **10**:**9** = 1:0.03, Figure 1.19, b)).

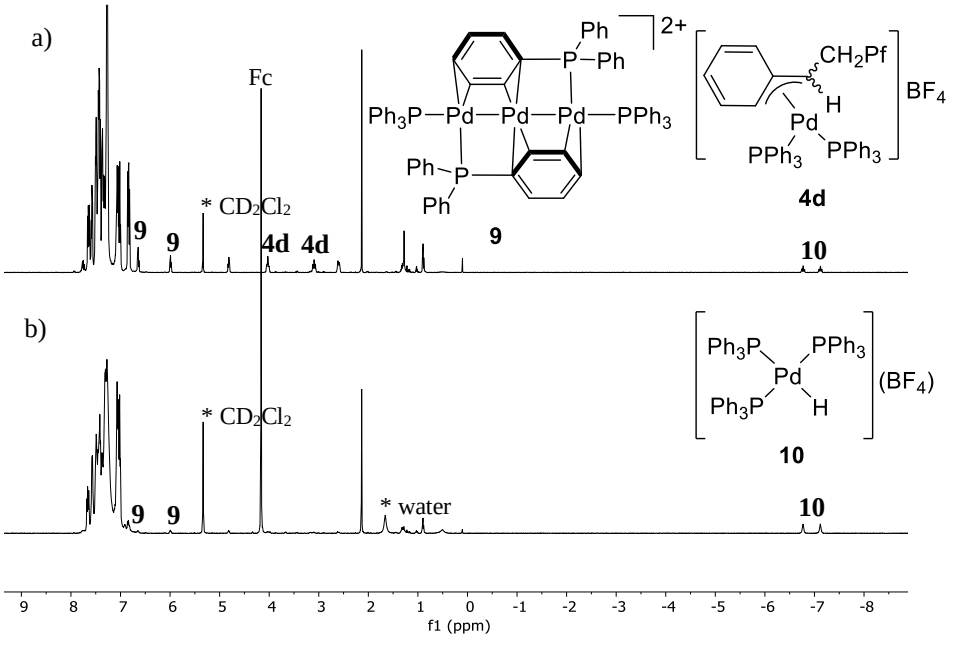

Figure 1.19. ^{1}H NMR (500.13 MHz, CD_2Cl_2) at 298 K of a) complex **4d** after 1 h at room temperature, where we can see the remaining complex **4d**, the formation of cluster **9** and **10**. b) a mixture of **4d** and 1 eq. of PPh_3 after heating the solution at 45 ºC for 40 min. *Signal corresponding to the solvent and water; Fc = ferrocene used as internal standard.

After 24 h at room temperature the complex **10** remains in solution as the major product but eventually converts to $[PdCl(PPh_3)_3](BF_4)$ as we can observe in the ^{31}P NMR (Figure 1.20, c)).[50]

[50] Urriolabeitia, E. P. *J. Chem. Edu.* **1997**, *74*, 325-327.

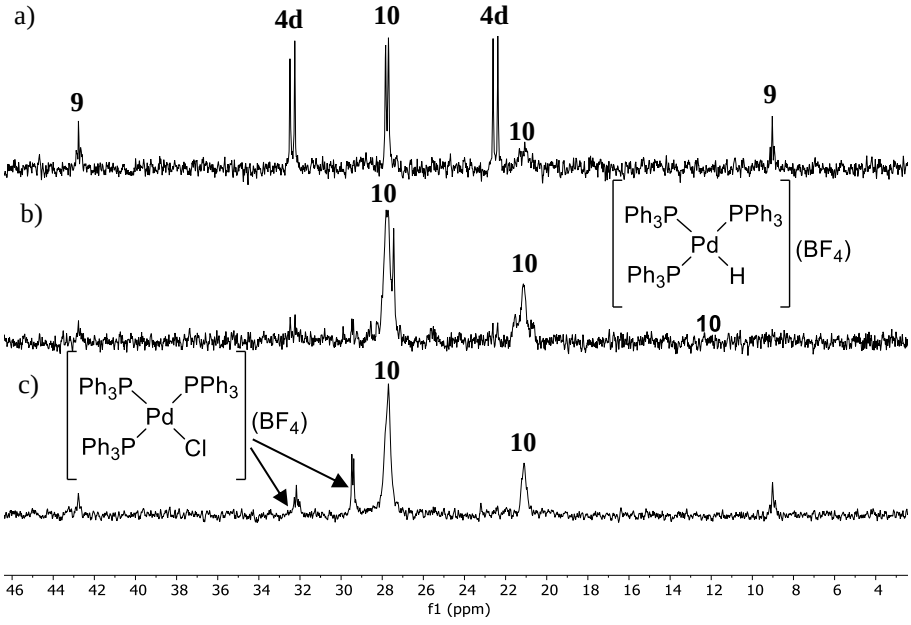

Figure 1.20. a) ^{31}P NMR (202.457 MHz, CD_2Cl_2) at 298 K of a) at 1 hour in the decomposition of the complex **4d** where we can see the remaining complex **4d**, the formation of the cluster $[Pd_3(PPh_3)_4](BF_4)_2$ (**9**) and the $[PdH(PPh_3)_3](BF_4)$ complex **10** at 298 K. b) a mixture of **4d** and 1 eq. of PPh_3 after heating the solution at 45 ºC for 40 min. c) complex **10** after 24h.

A plausible route for the formation of **9** is depicted in Scheme 1.20. The intermediate "$PdH(PPh_3)_2^+$" (**VII**) formed by β-H elimination can decompose in two ways: a) by elimination of HBF_4 to give the Pd^0 complex (**VIII**) or b) by H-exchange between two molecules of **VII** to give one molecule of **IX** and a putative dihydride which, by reductive elimination of H_2, leads to one molecule of **VIII**. Now a comproportionation reaction between one molecule of **VIII** and one molecule of **IX** gives the dimeric intermediate Pd^I-Pd^I complex **X**. And, finally, the dimeric complex **X** reacts with one molecule of **VIII** to give the Pd^I-Pd^0-Pd^I cluster complex **9**. The free phosphine generated in the formation of the cluster is trapped by the intermediate **VII** with the formation of the complex **10**. This complex it is not a competent intermediate in the reaction and it is limiting the decomposition process because its high stability in solution.

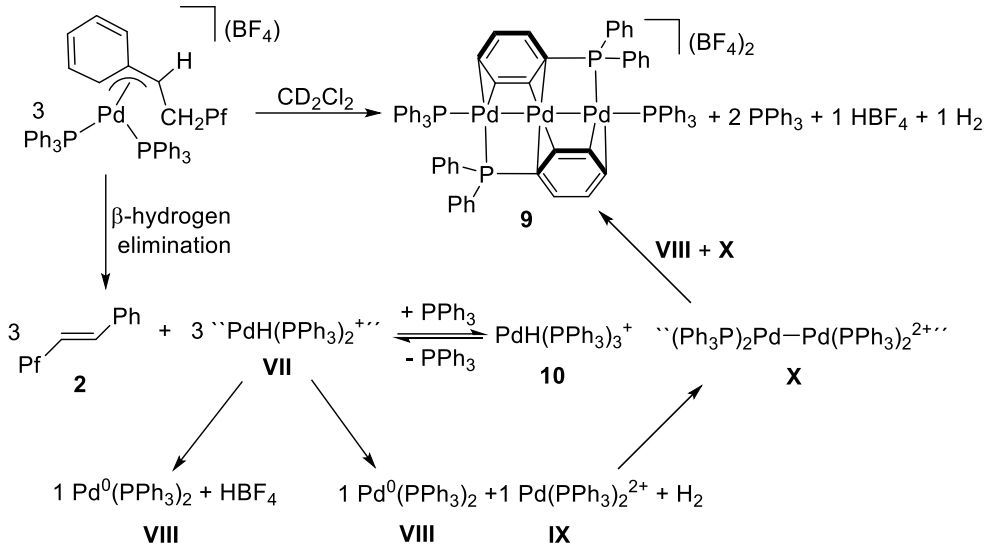

Scheme 1.20. Proposed route for the formation of the cluster **10.**

1.3. Conclusions

In conclusion, we have characterized several η^3-benzylic complexes of palladium(II) bearing a α-(pentafluorophenylmethyl)benzylic substituent with different ligands. The *anti* or *syn* isomer present in solution was distinguished by NMR ROESY experiments showing the presence of the *syn* isomer in complexes **1** and **4b** and the *anti* isomer in complexes **4d-f**. DFT calculations were performed to support our experimental evidence showing the preference for the *anti* isomer in the complex **4d**. The adoption of an *anti* isomeric form for the α-substituted η^3-benzyls is preferred for the complexes with the bulkiest ligands we tried ($AsPh_3$, PPh_3 and dppf) because it allows a wider L-Pd-L angle and a less congested geometry, and therefore a favorable situation. A steric relief by pentacoordination is proposed for the neutral η^3-benzylic complexes **6d-f** generated in situ mixing **1** and two equivalents per palladium of $AsPh_3$, PPh_3 or one equivalent of dppf. The experimental evidence was corroborated with some DFT calculations confirming the higher stability of two pentacoordinated square pyramidal geometries (**6d**-spy-apiBr and the **6d**-spy-apiPPh_3) than the σ-benzylic form.

All the η^3-benzylic complexes decompose eventually by β-hydrogen elimination to give **2** and a``$PdHL_n$´ intermediate. This hydride intermediate can be transferred to a palladium-benzyl complex to give the reduction product **3**. This process is proposed to occur in a dimeric intermediate and is aided by the presence of bridging ligands and low coordinating ligands. On the other hand, the ``$PdHL_n$´ intermediate can be trapped in the presence of dienes such as R-(+)-limonene to give the corresponding allyls **7** and **8**.

Finally, during the decomposition process of complex **4d** we found the formation of the mixed valence trimetallic palladium cluster **9**. We propose this cluster is generated in a clean reaction from $[PdH(PPh_3)_2]^+$ formed after the β-hydrogen elimination in **4d**. This intermediate can trap one molecule of free phosphine to give the detected hydride $[PdH(PPh_3)_3](BF_4)$ (**10**) which is a reservoir of hydride but it is not direct involved in the formation of the cluster **9**.

1.4. Experimental Section

1.4.1. General methods

^{1}H, ^{19}F, ^{13}C and ^{31}P NMR spectra were recorded on Bruker AC-300, ARX-300 and AV-400 as well as Agilent MR-500 instruments at the LTI-UVa. Chemical shifts (in δ units, ppm) were referenced to Me_4Si (^{1}H and ^{13}C), $CFCl_3$ (^{19}F) and H_3PO_4 (85%, ^{31}P). Signal assignments were made with the aid of heteronuclear ^{1}H-^{13}C HMQC and homonuclear ^{1}H COSY and ROESY experiments. NMR data for the complexes can be found in Table 1.5-1.8. Elemental analyses were carried out in a Carlo Erba 1108 microanalyser (at the Vigo University, Spain). Solvents were dried using a solvent purification system SPS PS-MD-5 or distilled from appropriate drying agents under nitrogen, prior to use. $[Pd_2(\mu\text{-}Br)_2(\eta^3\text{-}CHPhCH_2C_6F_5)_2]$ (**1**) was prepared as previously reported.[31]

1.4.2. Collected NMR spectroscopic data for the benzylic complexes discussed in this chapter

Table 1.5. ^{13}C NMR data for the η^3-benzylic complexes of palladium(II).[a]

Pd	T	C^{α}	$^{1}J\ C^{\alpha}$-H	C^{β}	$^{1}J\ C^{\beta}$-H	$^{2}J\ C^{\alpha}$-P	C^{1}	C^{2}/C^{6}	C^{3}/C^{5}	C^{4}
4a	223 K	62.05	160.2	22.21	137.3	43.6	118.08	103.04/127.60	129.81/132.09	133.66
4b	223 K	63.82	156.4	21.52	133.0	45.8	120.65	113.17/110.20	*	*
4c[b]	293 K	67.80	155.0	23.14	136.0	----	*	132.7		*
4d	223 K	70.48	156.0	21.19	132.5	53.0	118.46	107.03/126.3	133.02/*	132.3
4e	243 K	68.34	158.5	21.59	135.8	----	115.66	108.21/123.8	*	*
4f	223 K	68.94		20.60		70.0	*	105/	134.5	*
5	233 K	59.65	155.4	21.78	133.4	< 20	*	134/	*	*
6d	223 K	60.63	155.0	24.84	133.2	50.0	*	*	*	*
6e	243 K	54.68	*	23.27	136.0	----	*	118.56	*	*
6f	223 K	58.91	150.0	25.80	134	71.0	*	*	*	*

a) δ, 75.468 MHz; spectra recorded in $CDCl_3$ unless otherwise noted. The signals and coupling constants that could not be assigned due to signal overlap or low intensity resonances are marked with an asterisk. b) 125 MHz.

Table 1.6. ^{1}H NMR data for the η^3-benzylic complexes of palladium(II).[a]

Pd	H^{α} (J)	H^{β} (J)	$H^{\beta'}$ (J)	H^2 / H^6	Other
4a	3.60 m	3.09 m	3.09 m	6.82 m	1.20 (d, 9H, J = 9.8, Me), 1.72 (d, 9H, J = 8.8, Me), 7.46 (m, 2H, H^3,H^5), 7.83 (m, 1H, H^4)
4b	4.02 t (10.5)	2.95 m	2.66 m	6.53 b / 7.15 m	7.50 (m, 2H, H^3, H^5), 7-7.9 (m, 21H, H^4, Ph dppe)
4c	4.35 m	3.32 m	3.20 m	7.15 m	3.10 (m, 4H, CH_2S), 7.35, 7.4, 7.52 (m, 9H, H^3, H^4, H^5, $H_{meta, para}$ Ph, H_{ortho} Ph), 7.60 (m, 2H, H_{meta} Ph), 7.77, (m, 2H, H_{ortho} Ph)
4d	3.92 m	3.23 bt (12.9)	2.46 bd (12.9)	6.77 m/ 7.11 d	6.38 (t, J = 7.1, 1H, H^3) 6.71 (m, 6H, Ph PPh_3), 6.98 (bt, 1H, H^4), 7.15-7.5 (m, 24H, Ph PPh_3, H^5)
4e	4.27 dd (12, 4.2)	3.30 t (13.4)	2.58 bd (13.4)	6.89 d (8) / 7.09 d (8)	6.78 (t, J = 8.0, 1H, H^3) 6.87 (m, 6H, Ph $AsPh_3$), 7.18-7.43 (m, 26H, Ph PPh_3, H^5, H^4)
4f	3.81 m	3.02 m	2.19 m	6.76 / 7	3.64, 3.96, 4.25, 4.35, 4.47, 4.78, 4.95 (s, 8H, Cp), 6.52 (m, 1H, H^3), 6.67 (m, 2H, Ph dppf), 7 (m, 3H, H^6, Ph dppf), 7.15-7.75 (m, 18H, H^5, H^4, Ph dppf)
5	3.62 bd	2.90 bt	2.01 bd	6.97 b / 7.2-7.9 m	7.2-7.9 (m, 19H, H^3, H^4, H^5, H^6, PPh_3)
6d	3.54 bd (9.0) (9.5)	3.86 ta (13, 9)	2.94 bd (13.0) (12.0)	6.77 m	6.9-7.7 (m, 33H, H^3, H^4, H^5, PPh_3)
6e	3.82 m	2.93 t (12.3)	2.5 b	7.12 m	7.3-7.8 (a, 33H, $H^{3,4,5}$, $AsPh_3$)
6e	3.41 m	3.70 m	3.07 m	7.0-8.0 m	3.37, 3.44, 4.15, 4.32, 4.48, 4.51, 4.57 (s, 8H, Cp), 7.0-8.0 (m, 23H, H^3, H^5, H^4, Ph dppf)

a) δ, 300.130 MHz; spectra recorded in $CDCl_3$.

Table 1.7. ^{31}P NMR data for the η^3-benzylic complexes of palladium(II).[a]

Complex	T	P_A	P_B	J_{P-P} (Hz)
4a	223 K	-7.45 d	-24.97 d	49.9
4b	223 K	54.15 d	46.80 d	43.0
4d	213 K	32.75 d	23.30 d	47.0
4f	223 K	32.12	20.75	51.5
5	213 K	33.63	-----	-----
6c	213 K	29.35 d	19.68 d	51.9
6e	223 K	31.35 d	16.49 d	55.1

a) δ, 121.495 MHz; spectra recorded in $CDCl_3$.

Table 1.8. ^{19}F NMR data for the η^3-benzylic complexes of palladium(II).[a]

Complex	T	F_{meta}	F_{para}	F_{ortho}	Other
4a	223 K	-161.51m	-156.25t	-143.40m	-151.70m (BF_4)
4b	223 K	-161.31a	-155.97a	-143.19m	-153.51m (BF_4)
4c	293 K	-162.33a	-157.03a	-142.71m	-152.01m (BF_4)
2d	213 K	-161.59m	-156.22t	-142.60m	-152.86m (BF_4)
2e	243 K	-162.24m	-156.79t	-142.30m	-152.78m (BF_4)
2f	293 K	-162.40m	-157.17t	-142.57m	-153.19m (BF_4)
5	213 K	-161.69m	-156.36t	-143.10m	
6d	213 K	-162.39m	-157.54t	-142.75m	
6e	233 K	-161.75a	-156.62a	-142.70a	

a) δ, 282.405 MHz; spectra were recorded in $CDCl_3$.

1.4.3. Synthesis and isolation of cationic η^3-benzylic complexes 4b, 4c, 4d, 4e and 4f

1.4.3.1. Synthesis of [Pd(η^3-CHPhCH$_2$C$_6$F$_5$)(dppe)](BF$_4$) (4b)

Complex **1** (0.3 g, 0.33 mmol) was added to a solution of $AgBF_4$ (0.13 g, 0.65 mmol) and dppe (0.26 g, 0.66 mmol) in acetone (20 mL) at 233 K. The suspension was stirred for 30 min protected from light and then it was filtered through magnesium sulfate at 233 K. The filtrate was evaporated to dryness and the residue was triturated with pentane (15 mL). The yellow product was filtered, washed with pentane (2 x 5 mL) and air-dried (0.42 g, 74 % yield). The complex was stored at -20 ˚C. NMR data collected in Table 1.5-1.8. Analysis calc. for $C_{40}H_{32}BF_9P_2Pd$: C, 55.68; H, 3.74; found: C, 55.36; H, 3.80.

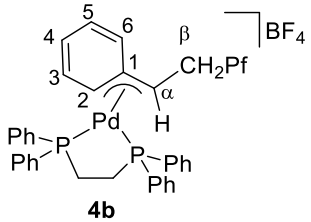

4b

1.4.3.2. Synthesis of [Pd(η^3-CHPhCH$_2$C$_6$F$_5$)(PhSCH$_2$)$_2$](BF$_4$) (4c)

Complex **1** (0.3 g, 0.33 mmol) was added to a solution of $AgBF_4$ (0.13 g, 0.65 mmol) and $(PhSCH_2)_2$ (0.16 g, 0,66 mmol) in acetone (20 mL) at 233 K. The suspension was stirred for 30 min protected from light and then it was filtered through magnesium sulfate at 233 K. The filtrate was evaporated to dryness and the residue was triturated with pentane (15 mL). The yellow product was filtered, washed with pentane (2 x 5 mL) and air-dried (0.25 g, 67 % yield). The complex was stored at -20 ˚C. NMR data collected in Table 1.5-1.8. Analysis calc. for $C_{28}H_{22}BF_9PdS_2$: C, 47.32; H, 3.12; found: C, 47.15; H, 3.18.

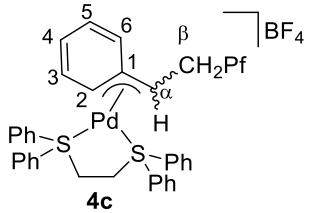

4c

1.4.3.3. Synthesis of [Pd(η^3-CHPhCH$_2$C$_6$F$_5$)(PPh$_3$)$_2$](BF$_4$) (4d)

Complex **1** (0.3 g, 0.33 mmol) was added to a solution of $AgBF_4$ (0.13 g, 0.65 mmol) and PPh_3 (0.34 g, 1.31 mmol) in acetone (20 mL) at 233 K. The suspension was stirred for 30 min

protected from light and then it was filtered through magnesium sulfate at 233 K. The filtrate was evaporated to dryness and the residue was triturated with pentane (15 mL). The orange product was filtered, washed with pentane (2 x 5 mL) and air-dried (0.37 g, 67 % yield). The complex was stored at -20 ˚C. NMR data collected in Table 1.5-1.8. Analysis calc. for $C_{40}H_{32}BF_9P_2Pd$: C, 60.72; H, 3.87; found: C, 60.19; H, 3.85.

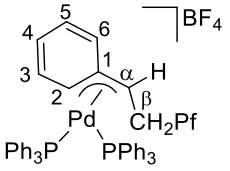

4d

1.4.3.4. Synthesis of [Pd(η^3-CHPhCH$_2$C$_6$F$_5$)(AsPh$_3$)$_2$](BF$_4$) (4e)

Complex **1** (0.3 g, 0.33 mmol) was added to a solution of $AgBF_4$ (0.13 g, 0.65 mmol) and $AsPh_3$ (0.40 g, 1.31 mmol) in acetone (20 mL) at 233 K. The suspension was stirred for 30 min protected from light and then it was filtered through magnesium sulfate at 233 K. The filtrate was evaporated to dryness and the residue was triturated with pentane (15 mL). The yellow product was filtered, washed with pentane (2 x 5 mL) and air-dried (0.5 g, 75 % yield). The complex was stored at -20 ˚C. NMR data collected in Table 1.5-1.8. Analysis calc. for $C_{50}H_{38}As_2BF_9Pd$: C, 55.77; H, 3.56; found: C, 55.99; H, 3.44.

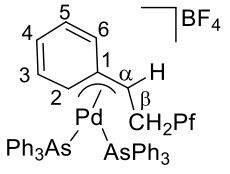

4e

1.4.3.5. Synthesis of [Pd(η^3-CHPhCH$_2$C$_6$F$_5$)(dppf)](BF$_4$) (4f)

Complex **1** (0.3 g, 0.33 mmol) was added to a solution of $AgBF_4$ (0.13 g, 0.65 mmol) and dppf (0.36 g, 0.66 mmol) in acetone (20 mL) at 233 K. The suspension was stirred for 30 min protected from light and then it was filtered through magnesium sulfate at 233 K. The filtrate was evaporated to dryness and the residue was triturated with pentane (15 mL). The red product was filtered, washed with pentane (2 x 5 mL) and air-dried (0.4 g, 78 % yield). The complex was stored at -20 ˚C. NMR data collected in Table 1.5-1.8. Analysis calc. for $C_{48}H_{36}BF_9FeP_2Pd$: C, 56.59; H, 3.56; found: C, 56.53; H, 3.52.

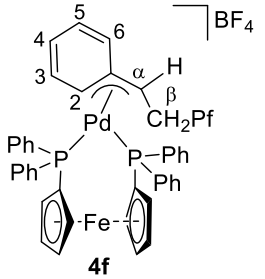

4f

1.4.4. Generation in situ of η^3-benzylic complexes 4a, 5, 6d, 6e and 6f

1.4.4.1. Generation of [Pd(η^3-CHPhCH$_2$C$_6$F$_5$)(PMe$_3$)$_2$)](BF$_4$) (4a)

Complex **1** (0.020 g, 0.022 mmol) was added to a solution of $AgBF_4$ (0.009 g, 0.044 mmol) and PMe_3 (0.007 g, 0.088 mmol) in acetone (5 mL) at 233 K. The suspension was stirred for 10 min protected from light and then it was filtered through magnesium sulfate at 233 K. The filtrate was evaporated to dryness and the residue was dissolved in $CDCl_3$ (0.6 mL) and the complex in solution was characterized by NMR. NMR data collected in Table 1.5-1.8.

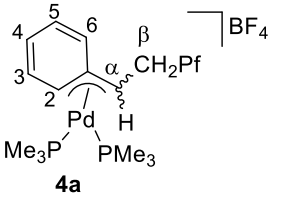

4a

1.4.4.2. Generation of [Pd(η^3-CHPhCH$_2$C$_6$F$_5$)Br(PPh$_3$))] (5)

Complex **1** (0.020 g, 0.022 mmol) was suspended in an NMR tube with 0.6 mL of $CDCl_3$ at 233 K. The PPh_3 (0.012 g, 0.044 mmol) was added generating an orange solution. The solution was checked by NMR spectroscopy at 233 K. NMR data collected in Table 1.5-1.8.

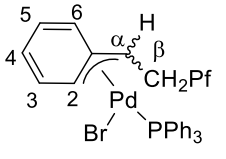

5

1.4.4.3. Generation of [Pd(η^3-CHPhCH$_2$C$_6$F$_5$)Br(PPh$_3$)$_2$)]) (6d)

Complex **1** (0.020 g, 0.022 mmol) was suspended in an NMR tube with 0.6 mL of $CDCl_3$ at 223 K. The PPh_3 (0.024 g, 0.088 mmol) was added generating an orange solution. The solution was checked by NMR spectroscopy at 243 K. NMR data collected in Table 1.5-1.8.

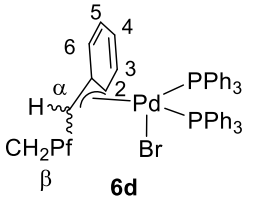

6d

1.4.4.4. Generation of [Pd(η^3-CHPhCH$_2$C$_6$F$_5$)Br(AsPh$_3$)] (6e)

Complex **1** (0.020 g, 0.022 mmol) was suspended in an NMR tube with 0.6 mL of $CDCl_3$ at 243 K. The $AsPh_3$ (0.027 g, 0.088 mmol) was added generating an orange solution. The solution was checked by NMR spectroscopy at 223 K. NMR data collected in Table 1.5-1.8.

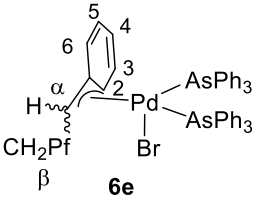

6e

1.4.4.5. Generation of [Pd(η^3-CHPhCH$_2$Pf)Br(dppf)] (6f)

Complex **1** (0.020 g, 0.021 mmol) was suspended in an NMR tube with 0.6 mL of $CDCl_3$ at 223 K. The dppf (0.049 g, 0.088 mmol) was added generating an orange solution. The solution was checked by NMR spectroscopy at 223 K. NMR data collected in Table 1.5-1.8.

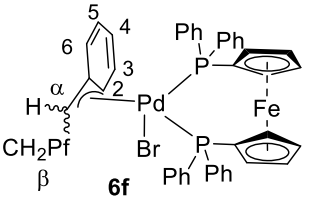

6f

1.4.5. Decomposition reactions

A solution of 0.02 mmol of the corresponding complex was prepared in $CDCl_3$ (0.6 mL). For the less stable derivatives, the complex was prepared in situ by addition of the appropriate

ligand to a suspension of **1** at 223 K and characterization of the mixture before the decomposition follow up. The evolution of the complexes was monitored by ^{19}F, ^{31}P and ^{1}H NMR until complete decomposition has occurred. The information is collected in Table 1.3.

1.4.6. Reactions with dienes. Reaction of complex 4e with R-(+)-limonene

Complex **4e** (15 mg, 0.0139 mmol) was placed in an NMR tube and dissolved in dry $CDCl_3$ (0.7 mL) at 233 K. R-(+)-Limonene (4.5 µL, 0.0278 mmol) was added and the reaction was followed by ^{19}F and ^{1}H NMR at room temperature. After 24 h, the ^{19}F NMR clearly shows the complete decomposition of the benzylic complex and the formation of stilbene **2**. The ^{1}H NMR of the crude mixture shows the formation of complexes **7e** (62%) and **8e** (38%). The ratio **7e**+**8e**/**2** indicates a hydride transfer efficiency of 61%. The dark mixture was treated with activated carbon and it was filtered through Kieselgur. The orange solution was evaporated to dryness and the orange residue was washed with 2 x 2 mL of hexane. The solid was dried and characterized by NMR.

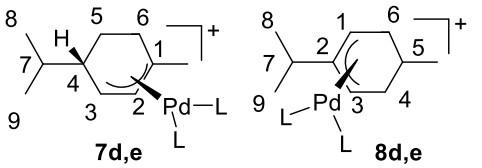

7e: ^{1}H NMR (400.13 MHz, δ, $CDCl_3$): 6.05 (d, J = 6.6 Hz, 1H, H^2), 4.94 (d, J = 6.6 Hz, 1H, H^3), 1.80 (m, 1H, H^6), 1.66 (m, 1H, $H^{6'}$), 1.64 (m, 1H, H^5), 1.39 (s, 3H, Me^1), 1.28 (m, 1H, H^4), 1.02 (m, 1H, H^7), 1.09 (m, 1H, $H^{5'}$), 0.57 (d, J = 5.8 Hz, 3H, H^8), 0.55 (d, J = 5.8 Hz, 3H, H^9).

8e: ^{1}H NMR (400.13 MHz, δ, $CDCl_3$): 5.03 (bm, 2H, H^1, H^3), 2.29 (m, 1H, H^7), 2.25 (m, 1H, H^5), 1.66 (m, 2H, H^4, H^6), 1.25 (m, 2H, $H^{4'}$, $H^{6'}$), 1.03 (d, J = 6.8 Hz, 6H, H^8, H^9), 0.75 (d, J = 6.3 Hz, 3H, Me^5).

The reaction of **4d** with R-(+)-limonene was carried out in the same way. The ratio of complexes in the crude mixture was **7d** (21%) and **8d** (79%).

7d: ^{1}H NMR (500.13 MHz, δ, $CDCl_3$): 6.01 (t, J = 7 Hz, 1H, H^2), 4.50 (t, J = 7 Hz, 1H, H^3), 1.73 (m, 1H, H^6), 1.51 (m, 1H, $H^{6'}$), 1.49 (s, 3H, Me^1), 1.19 (m, 1H, H^5), 1.03 (m, 1H, H^4), 0.95 (m, 1H, H^7), 0.99 (m, 1H, $H^{5'}$), 0.54 (d, J = 5.3 Hz, 3H, H^8), 0.52 (d, J = 5.3 Hz, 3H, H^9). $^{31}P\{^{1}H\}$ NMR (161.976 MHz, δ, $CDCl_3$): 26.29 (d, P_A, J = 40.5), 21.91 (d, P_B, J = 40.5).

8d: ^{1}H NMR (400.13 MHz, δ, $CDCl_3$): 4.6 (m, 2H, H^1, H^3), 2.33 (m, 1H, H^7), 2.05 (m, 1H, H^5), 1.2 (m, 2H, H^4, H^6), 1.07 (d, J = 6.8 Hz, 6H, H^8, H^9), 1.05 (m, 2H, $H^{4'}$, $H^{6'}$), 0.65 (d, J = 6.3 Hz, 3H, Me^5). $^{31}P\{^{1}H\}$ NMR (161.976 MHz, δ, $CDCl_3$): 22.54 (s).

1.4.7. Reaction of complex 6e with R-(+)-limonene

Complex **1** (15 mg, 0.0163 mmol) and $AsPh_3$ (20 mg, 0.0652 mmol) were placed in an NMR tube. The solids were dissolved in 0.7 mL of dry $CDCl_3$ at 213 K. R-(+)-Limonene (10.5 µL, 0.0652 mmol) was added to the orange solution. The reaction was followed by ^{1}H and ^{19}F NMR at room temperature. After 24 h the complete decomposition of **6e** to stilbene **2** was observed and no formation of any allyl-palladium complex.

1.4.8. Generation in situ of complex [PdH(PPh$_3$)$_3$](BF$_4$) (10)

Complex **4d** (0.016 g, 0.0189 mmol) was dissolved in 0.6 mL of CD_2Cl_2 in an NMR tube. To the orange solution was added the PPh_3 (0.0005 g, 0.0189 mmol) and the solution was heated for 40 min at 45 ºC. The solution color changes to yellow and the complex **10** generated in situ was characterized by NMR spectroscopy. ^{1}H NMR (500.13 MHz, δ, CD_2Cl_2): 7.6-7 (m, 45 H, Ph PPh_3), -6.95 (dt, $J_{Ptrans-H}$ = 174 Hz, J_{Pcis-H} = 12.9, 1H). ^{31}P NMR (202.457 MHz, δ, CD_2Cl_2): 27.75 (bd, 1P, P_{trans}), 21.15 (b, 2P, P_{cis}). ^{19}FNMR (470.592 MHz, δ, CD_2Cl_2): -153.20 BF_4.

1.4.9. X-ray structure determinations

The complex **4f** was crystalized by slow diffusion in a mixture of CH_2Cl_2/pentane at 233 K yielding orange crystals. The cluster complex **9** was crystalized by slow evaporation of a solution in CD_2Cl_2 of the reaction mixture yielding red prism crystals.

The crystals were mounted on the tip of a glass fibers. X-ray measurements were made using Bruker SMART CCD area-detector diffractometer with Mo Kα radiation (0.71073 Å). Reflections were collected, intensities integrated, and the structures were solved by direct methods procedure. Non-hydrogen atoms were refined anisotropically and hydrogen atoms were constrained to ideal geometries and refined with fixed isotropic displacement parameters. Data collection was performed at 298 K.

As it was mentioned in the text, the X-ray structure obtained for **4f** could not be completely refined due to the low-quality crystal (R = 12 %). The residuals of both crystals (**4f** and **9**) are shown in Table 1.9.

Table 1.9. Crystal data and structure refinement for complex **4f** and **9**.

	9	**4f**
Empirical formula	$C_{76}H_{64}B_4Cl_{12}F_{16}P_4Pd_3$	$C_{50}H_{40}BF_9P_2FePdCl_4$
Formula weight	219.30	1188.62
Temperature/K	298.15	149.9(3)
Crystal system	triclinic	triclinic
Space group	P-1	P-1
a/Å	12.2831(5)	11.0441(11)
b/Å	14.5092(6)	13.7161(9)
c/Å	14.5987(5)	16.0313(17)
α/°	81.124(3)	83.471(7)
β/°	65.758(3)	76.338(9)
γ/°	76.557(3)	84.545(7)
Volume/Å^3	2302.25(17)	2338.6(4)
Z	8	2
ρ_{calc}g/cm^3	1.582	1.688
μ/mm^{-1}	1.069	1.065
F(000)	1086.0	1192.0
Crystal size/mm^3	? × ? × ?	0.169 × 0.151 × 0.037
Radiation	MoKα (λ = 0.71073)	MoKα (λ = 0.71073)
2Θ range for data collection/°	6.608 to 59.248	6.768 to 59.214
Index ranges	-14 ≤ h ≤ 16, -18 ≤ k ≤ 20, -15 ≤ l ≤ 20	-12 ≤ h ≤ 15, -18 ≤ k ≤ 18, -20 ≤ l ≤ 22
Reflections collected	16375	17548
Independent reflections	10502 [Rint = 0.0292, Rsigma = 0.0658]	10852 [Rint = 0.1853, Rsigma = 0.6404]
Data/restraints/parameters	10502/0/520	10852/0/622
Goodness-of-fit on F^2	1.079	0.907
Final R indexes [I>=2σ (I)]	R1 = 0.0606, wR2 = 0.1596	R1 = 0.1208, wR2 = 0.2004
Final R indexes [all data]	R1 = 0.0921, wR2 = 0.1910	R1 = 0.3826, wR2 = 0.3206
Largest diff. peak/hole / e Å^{-3}	1.21/-0.89	1.27/-1.35

1.4.10. Computational details

All calculations were performed using the DFT approach with the M06 functional[51,52] using Gaussian09 as program package.[53] The selected basis set was 6-31+G(d) for C, P, F, H,[54,55]LANL2DZ ECP for the Br and SDD for Pd[56,57] (Basis set I). Solvation was introduced through the SMD model, where we applied dichloromethane as the solvent (ε= 9.1). All geometry optimizations were carried out in solution with no restrictions. Free energy corrections were calculated at 298.15 K and 10^5 Pa pressure, including zero point energy corrections (ZPE). Vibrational frequency calculations were performed to establish the stationary points were minima (without imaginary frequencies) or transition states (with one imaginary frequency). Final potential energies were refined by performing additional single-point energy calculations, Pd was described with SDD def2-QZVP, the Br atom was described with LANL2DZ ECP and the remaining atoms were treated with 6-311++G** basis set (Basis set II). All reported energies in the manuscript correspond to Gibbs energies in solution, obtained from potential energies (including solvation) with basis set II plus Gibbs energy corrections with basis set I. We are indebted to Prof. Agustí Lledós (Universidad Autónoma de Barcelona) for his help with the DFT calculations.

[51] Becke, A. D. *J. Chem. Phys.* **1993**, *98*, 5648-5652.
[52] Grimme, S.; Antony, J.; Ehrlich, S.; Krieg, H. H-Pu *J. Chem. Phys*. **2010**, *132*, 154104.
[53] Gaussian 09, Revision D.01. Frisch, M. J.; Trucks, G. W.; Schlegel, H. B.; Scuseria, G. E.; Robb, M. A.; Cheeseman, J. R.; Scalmani, G.; Barone, V.; Mennucci, B.; Petersson, G. A.; Nakatsuji, H.; Caricato, M.; Li, X.; Hratchian, H. P.; Izmaylov, A. F.; Bloino, J.; Zheng, G.; Sonnenberg, J. L.; Hada, M.; Ehara, M.; Toyota, K.; Fukuda, R.; Hasegawa, J.; Ishida, M.; Nakajima, T.; Honda, Y.; Kitao, O.; Nakai, H.; Vreven, T.; Montgomery, Jr., J. A.; Peralta, J. E.; Ogliaro, F.; Bearpark, M.; Heyd, J. J.; Brothers, E.; Kudin, K. N.; Staroverov, V. N.; Keith, T.; Kobayashi, R.; Normand, J.; Raghavachari, K.; Rendell, A.; Burant, J. C.; Iyengar, S. S.; Tomasi, J.; Cossi, M.; Rega, N.; Millam, J. M.; Klene, M.; Knox, J. E.; Cross, J. B.; Bakken, V.; Adamo, C.; Jaramillo, J.; Gomperts, R.; Stratmann, R. E.; Yazyev, O.; Austin, A. J.; Cammi, R.; Pomelli, C.; Ochterski, J. W.; Martin, R. L.; Morokuma, K.; Zakrzewski, V. G.; Voth, G. A.; Salvador, P.; Dannenberg, J. J.; Dapprich, S.; Daniels, A. D.; Farkas, O.; Foresman, J. B.; Ortiz, J. V.; Cioslowski, J.; Fox, D. J. Gaussian, Inc., Wallingford CT, **2013**.
[54] Francl, M. M.; Petro, W. J.; Hehre, W. J.; Binkley, J. S.; Gordon, M. S.; DeFrees, D. J.; Pople, J. A. *J. Chem. Phys*. **1982**, *77*, 3654-3665.
[55] Clark, T.; Li-F *J. Comput. Chem.* **1983**, *4*, 294-301.
[56] Ehlers, A. W.; Böhme, M.; Dapprich, S.; Gobbi, A.; Höllwarth, A.; Jonas, V.; Köhler, K. F.; Stegmann, R.; Veldkamp, A.; Frenking, G. *Chem. Phys. Lett*. **1993**, *208*, 111-114.
[57] Roy, L. E.; Hay, P. J.; Martin, R. L. *J. Chem. Theory Comput*. **2008**, *4*, 1029-1031.

Chapter 2

2. Homo- and Co-polymerization of Norbornene and Alkenyl Norbornenes Employing α-Pentafluorophenylmethyl Benzylic Complexes of Palladium(II)

2.1. Introduction to the polymerization of norbornene and their derivatives

Cyclic olefins have acquired an important role in the synthesis of new types of polymers with attractive properties. Norbornene is an interesting monomer because it can be polymerized to give polymers with different structures and properties. Moreover, norbornene derivatives are easily prepared by a [4π + 2π]-Diels-Alder cycloaddition of cyclopentadiene and a dienophile that can incorporate a wide range of functional groups (Eq. 2.1).[58-60]

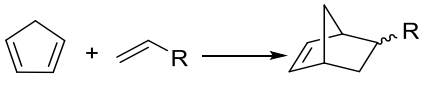

(2.1)

[58] Bauld, L. N. *Tetrahedron* **1989**, *45*, 5307-5363.
[59] Wynne, J. H.; Lloyd, C. T.; Cozzens, R. F. *Chem. Lett.* **2002**, *31*, 926-927.
[60] Liaw, D. J.; Huang, C. C.; Hong, S. M.; Chen, W. H.; Lee, K. R.; Lai, J. Y. *Polymer* **2006**, *47*, 4613-4621.

Up to now, four different principal methodologies for the synthesis of polynorbornenes have been developed, that occur by different mechanisms: radical polymerization, ionic polymerizations (cationic), ring opening metathesis polymerization (ROMP) and vinylic addition polymerization (VA). The goal of the work described in this chapter is to develop an active catalyst for the vinylic polymerization of norbornene derivatives, in particular 5-alkenyl-2-norbornenes (Eq. 2.1, R = $-(CH_2)_n-CH=CH_2$). Vinylic addition polynorbornenes (VA-PNBs) are interesting materials for the support of catalysts, reagents, etc. The introduction of pendant functional groups in this type of polymers, such as a double bond when alkenyl norbornenes are polymerized, can be useful to synthesize a variety of other functionalized VA-PNBs, as it will also be shown in this chapter. This introduction contains an account of the different methods of polymerization of norbornene with selected examples of the polymerization of the target alkenyl-norbornenes.

2.1.1. Radical polymerization of norbornene

The free radical polymerizations of vinyl monomers is an important synthetic method to produce a high range of polymeric materials. A general simplified mechanism for the free radical polymerization is represented in Scheme 2.1.[61] After the formation of the free radical, the initiation of the polymerization starts by the attack of the free radical to the vinyl monomer (*Initiation Step*). The polymer chain is generated by subsequent radical additions to n molecules of the vinyl monomer (*Propagation Step*). Mutual annihilation of the propagating radical is a common termination of the polymerization (*Termination Step*). Other radical decomposition pathways such as the transfer of the radical to the solvent or radical disproportionation can also terminate the polymerization, but they that are not depicted in Scheme 2.1.

[61] Rudin, A.; Choi, P. The Elements of Polymer Science & Engineering. *In Free-Radical Polymerization;* Academic Press*;* 2013; pp. 341-389.

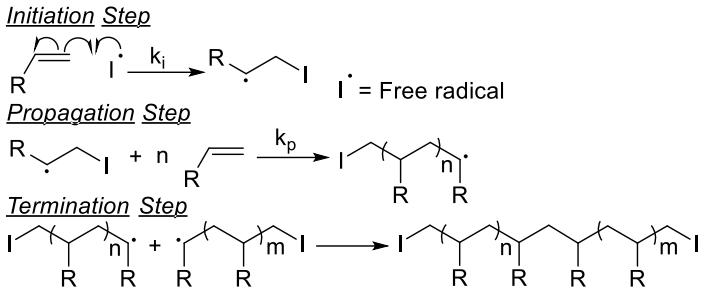

Scheme 2.1. Mechanism for the radical polymerization.

The first early study in the radical polymerization of norbornene was reported by Gaylord and co-workers in 1976.[62] Two types of enchainment in the structure of the polynorbornene were determined by analysis of ^{1}H and ^{13}C NMR of the polymer: the 2,3-enchainment and the 2,7-enchainment (Scheme 2.2).[63] The 2,3-connectivity is generated by the attack of the free radical into the endocyclic double bond and propagation. However, the radical can undergo a transposition into the bridging carbon atom of the ring (the C^{7} carbon) generating a new propagating radical and, consequently, the 2,7-enchainment. In general, the norbornene presents low activity in the radical polymerization (modest yields and low glass transition temperature (T_g)). Efforts have been made to study how to improve the radical polymerization of norbornene and norbornadiene derivatives.[64-68]

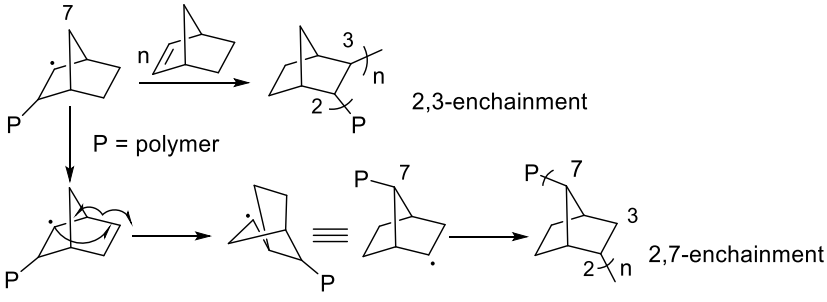

Scheme 2.2. Representation of the two enchainments generated in the radical polymerization of norbornene.

[62] Gaylord, N. G; Mandal, B. M.; Martan, M. *J. Polym. Sci. Polym. Lett. Ed.* **1976**, *14*, 555-559.
[63] Yeh, A. -C. *J. Chin. Chem. Soc.* **2003**, *50*, 959-964.
[64] Graham, P. J.; Buhle, E. L.; Pappas, N. *J. Org. Chem.* **1961**, *26*, 4658-4662.
[65] Niu, Q. J.; Frechet, J. M. Polymers for 193-nm *Angew. Chem., Int. Ed.* **1998**, *37*, 667-670.
[66] Shiotsuki, M.; Kai, H.; Endo, T. *J. Polym. Sci., Part A: Polym. Chem.* **2014**, *52*, 2528-2536.
[67] Pasquale, A. J.; Allen, R. D.; Long, T. E. *Macromolecules* **2001**, *34*, 8064-8071.
[68] Kanao, M.; Otake, A.; Tsuchiya, K.; Ogino, K. *J. Photopolym. Sci. Tec.* **2009**, *22*, 365-370.

2.1.2. Cationic polymerization of norbornene and alkenyl-norbornenes

Ionic polymerization is another synthetic method to build polymers employing olefins as the starting material.[69] The cationic polymerization is generally initiated by Lewis or Bronsted acids. The general connectivity shown in Scheme 2.2 for the radical polymerization can be applied for the cationic polymerization. As in the case of the radical mechanism, the polymerization of norbornene or alkenyl-norbornenes gives polymers with low to modest yields and low molecular weights. Furthermore, the many possible transpositions of the intermediate carbocation generated in the case of alkenyl-norbornenes results in a non-very controllable polymerization, and as a consequence, the structure of the skeleton is hard to predict. For example, the cationic polymerization of alkenyl-norbornenes was studied by the group of Finkelshtein and co-workers in the presence of borane derivatives.[69d] The cationic polymerization of 5-vinyl-2-norbornene proceeded with low yield and molecular weight. The ^{1}H NMR showed the presence of only 12% of olefinic protons, whereas a polymerization exclusively through the endocyclic double bond would generate a polymer with 25% of olefinic protons. This observation implies the participation of the exocyclic double bond. The proposed structure for the polymer is presented in Eq. 2.2.

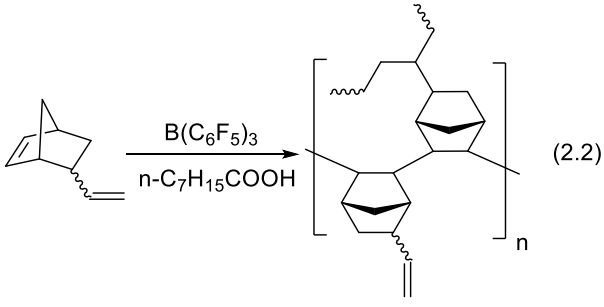

(2.2)

[69] a) Kennedy J. P., Hinlicky, J. A. *Polymer* **1965**, *6,* 133-141. b) Kennedy, I. P.; Makowski, H. S. *J. Polym. Sci., Part C* **1968**, *22*, 247-265. c) Gaylord, N. G.; Deshpande, A. B.; Mandal, B. M.; Martan, M. *J. Macromol. Sci. Chem. A* **1977**, 11/5, 1053-1070. d) Bermeshev, M. V.; Bulgakov, B. A; Genaev, A. M.; Kostina, J. V.; Bondarenko, G. N.; Finkelshtein, E. S. *Macromolecules* **2014**, *47,* 5470-5483.

2.1.3. ROMP (Ring Opening Metathesis Polymerization) of norbornene and alkenyl-norbornenes

The ROMP (Ring Opening Metathesis Polymerization) of norbornene or its derivatives has been extensively studied.[70] The accepted mechanism was described firstly by Chauvin in 1970 (Scheme 2.3).[71] The polymerization starts with the coordination of the cyclic olefin to the metal alkylidene center. Subsequently, a [2+2] cycloaddition gives a metalacyclobutane followed by a cycloreversion to afford a new metal-alkylidene (*Initiation Step*). This step occurs many times until all the monomer is consumed (*Propagation Step*). ROMP is normally quenched with the addition of ethyl vinyl ether (X=Y: CH_2CH-OEt, Scheme 2.3) which reacts with the carbene in the polymer chain to remove the metal from the polymer (*Termination Step*).

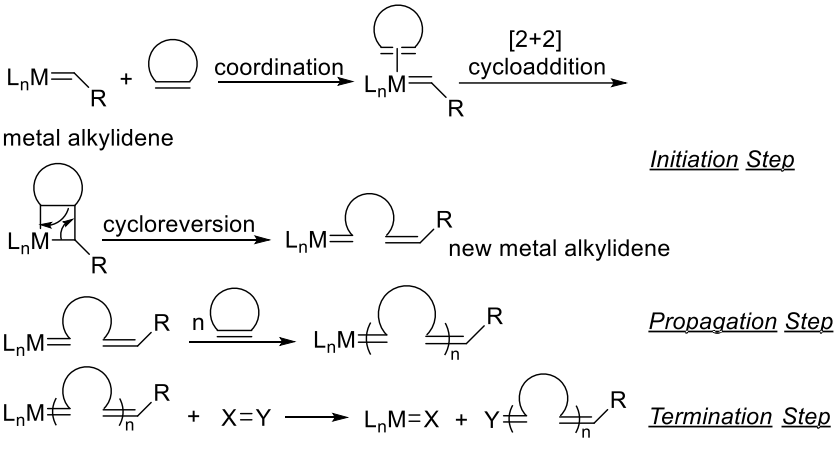

Scheme 2.3. General accepted mechanism for ROMP polymerization of cyclic olefins.

In ROMP, the driving force is the energy release corresponding to the strain in the ring of the cyclic olefin (ΔH^o negative) compensating the decrease of the entropy. Thus, strained olefins such as cyclobutene, cyclopentene, *cis*-cyclooctene and norbornene readily polymerize by ROMP. Scheme 2.4 shows the polynorbornene skeleton when synthesized by ROMP. The first homogenous catalysts for ROMP were the titanacyclobutane complexes developed by

[70] a) Grubbs, R. H.; Tumas, W. *Science*, **1989**, 243, 90-915. b) Bielawski, C. W.; Hillmyer, M. A. Handbook of Metathesis. *In Synthesis of Ruthenium Carbene Complexes;* Eds. Grubbs, R. H.; Wiley-VCH: Winham, Germany 2003; pp 86-94. b) Sutthasupa, R.; Masashi, S. Sanda, F. *Polym. J.* **2010**, *42*, 905-915. c) Choinopoulos, I. *Polymers* **2019**, *11*, 298-329.
[71] Hérisson, P. J. -L.; Chauvin, Y. Y. *Makromol. Chem.* **1970**, *141*, 161-176.

Grubbs and co-workers and the well-defined W-carbenes by Schrock and co-workers (Figure 2.1).[72,73] Despite all the chemistry developed with Ti, W or Mo for the ROMP polymerization of norbornene derivatives, the high oxophilicity of all these carbene complexes limited their application. A very important improvement in this area was the development of the ruthenium carbene chemistry for ROMP since ruthenium(II) is a metal center with low oxophilicity so the tolerance to many functional groups is high. The first contribution in the ruthenium carbene chemistry for this type of polymerization was in 1975,[74] but the first well-defined single-component Ru complex was reported by Grubbs and co-workers in 1992.[75,76] Later, new generation of Ru complexes were developed (Figure 2.1).

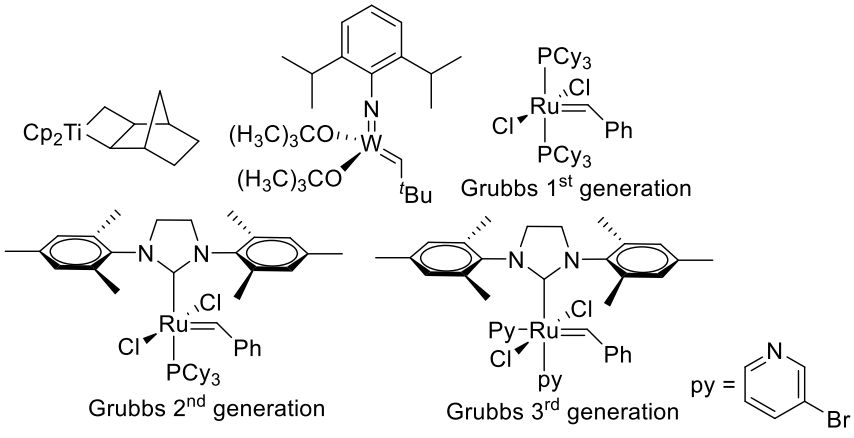

Figure 2.1. Representative examples of titanium, tungsten and ruthenium carbenes employed in ROMP.

Other metal complexes such as vanadium and niobium carbenes were developed in the following years. In the particular case of alkenyl-norbornenes, the group of Nomura and co-workers studied the polymerization of norbornene, 5-vinyl-2-norbornene and 5-ethylidene-2-norbornene with (arylimido)vanadium(V)-alkylidenes and (imido)niobium(V)-alkylidene

[72] a) Gilliom, L. R.; Grubbs, R. H. J. *Am. Chem. Soc*. **1986**, *108*, 733-742. b) Cannizzo, L. F.; Grubbs, R. H. *Macromolecules* **1988**, *21*, 1961-1967.
[73] a) Schrock, R. R.; Feldman, J.; Cannizzo, L. F; Grubbs, R. H. *Macromolecules* **1987**, *20*, 1169-1172. b) Ivin, K. J.; Kress, J; Osborn, J. A. *Makromol. Chem.* **1992**, *193*, 1695-1707.
[74] Porri, L.; Diversi, P.; Lucherimi, A.; Rossi, R. *Makromol. Chem.* **1975**, *176*, 3121-3125.
[75] Nguyen, S. T.; Johnson, L. K.; Grubbs, R. H; Ziller, J. W. *J. Am. Chem. Soc*. **1992**, *114*, 3974-3975.
[76] a) Scholl, M.; Ding, S.; Lee, C. W.; Grubbs, R. H. *Org. Lett.* **1999**, *1*, 953-956. b) Love, J. A.; Morgan, J. P.; Trnka, T. M.; Grubbs, R. H. *Angew. Chem. Int. Ed*. **2002**, *41*, 4035-4037. c) Garber, S. B.; Kingsbury, J. S.; Gray, B. L.; Hoveyda, A. H. *J. Am. Chem. Soc*. **2000**, *12*, 8168-8179.

complexes (Scheme 2.4, b)).[77,78] Some other studies with tungsten carbenes were reported for the polymerization of 5-vinyl-2-norbornene.[79]

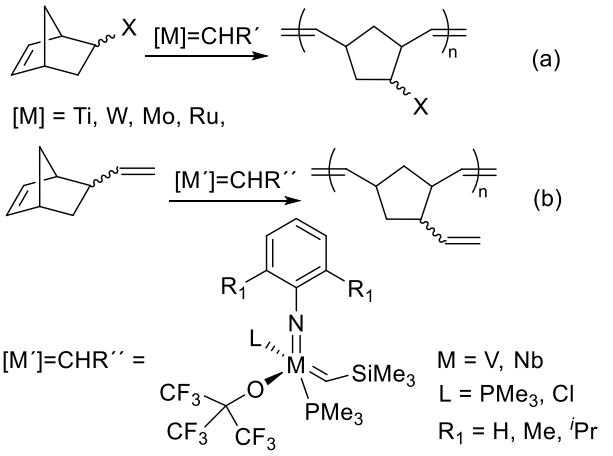

Scheme 2.4. ROMP polymerization of substituted norbornenes and 5-vinyl-2-norbornene.

Many of the reported metal catalysts, especially Grubbs' ruthenium carbenes, show a high activity in the polymerization of norbornene or norbornene derivatives with a large variety of functional groups (Scheme 2.4, a)). However, the presence of double bonds in the structure of the polymer can be disadvantageous, since the unsaturation increase the reactivity of the polymer and makes it less suitable for its use in, for example, supported catalysis. In many cases, a subsequent hydrogenation is necessary for some applications, but this is not possible for X = alkenyl since it would also eliminate this functional group (Scheme 2.5).[80] In contrast, vinylic addition polynorbornenes (VA-PNBs) present a completely robust aliphatic skeleton, as will be shown below, and very good thermal stability making them ideal for supported catalysis.

[77] a) Hou, X.; Nomura, K. *J. Am. Chem. Soc.* **2016**, *138*, 11840-11849. b) Wised, K.; Nomura, K *Organometallics*, **2017**, *36*, 4103-4106. c) *J. Polym. Sci., A: Polym. Chem.* **2017**, *55*, 3067-3074.
[78] Wised, K.; Nomura, K. *Organometallics*, **2016**, *35*, 2773-2777.
[79] Górski, M.; Szymánska-Buzar, T. *J. Mol. Catal. A: Chem.* **2006**, *257*, 41-47.
[80] García-Loma, R.; Albéniz, A. C. *RSC Adv.* **2015**, *5*, 70244-70254.

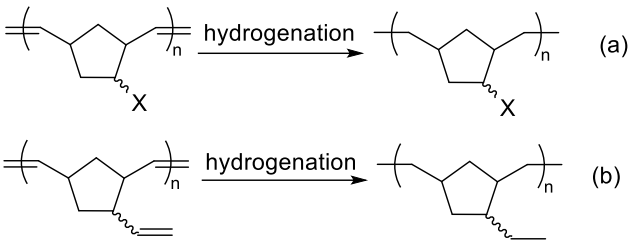

Scheme 2.5. Necessary posterior hydrogenation of ROMP polymers for supported catalysis that can hydrogenate also the vinyl pendant double bond in the ROMP polymer with 5-vinyl-2-norbornene.

2.1.4. Vinylic addition polymerization of norbornene and their derivatives

The vinylic addition (VA) polymerization of norbornene generates a polymer skeleton with a formal linear chain of norbornanediyl units generated by a *cis*-2,3-*exo* insertion of the norbornene (Figure 2.2). This is an efficient method for the synthesis of completely aliphatic polymers with good yields, high molecular weights and attractive properties such as optical transparency, high Tg and low dielectric constant.[81-84] The VA polynorbornenes are conventionally represented in two ways ($\mathbf{A_2}$ and $\mathbf{B_2}$, Figure 2.2) which are equivalent and accepted.

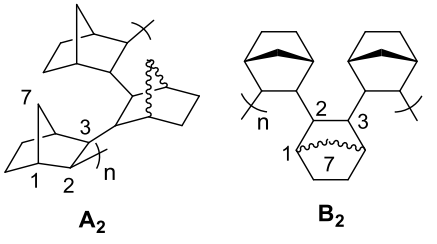

Figure 2.2. Two types of representation for the skeleton of VA-PNB.

[81] Park, K. H.; Twieg, R. J.; Ravikiran, R.; Rhodes, L. F.; Shick, R. A. Yankelevich, D.; Knoesen, A. *Macromolecules* **2004**, *37*, *14*, 5163-5178.
[82] Varanasi, P. R.; Mewherter, A. M.; Lawson, M. C.; Jordhamo, G.; Allen, R.; Optiz, J.; Ito, H.; Wallow, T.; Hofer, D. IBM 193nm *J. Photopolym. Sci. Technol*. **1999**, *12*, 493-500.
[83] Grave, N. R.; Kohl, P. A.; Bidstrup-Allen, S. A.; Jayaraman, S.; Shick, R. A. *J. Polym. Sci., Part B: Polym. Phys*. **1999**, *37*, 3003-3010.
[84] Kohl, P. A.; Zhao, Q.; Patel, K.; Schmidt, D.; Bidstrup-Allen, S. A.; Shick, R. A.; Jayaraman, S. *Electrochem. Solid-State Lett.* **1998**, *1*, 49-51.

The general accepted mechanism for the vinylic addition polymerization can be separated in three different steps. The first step is the coordination of the norbornene to the metal center by the displacement of a ligand if it is necessary. Following the coordination, the *cis*-2,3-*exo* insertion into the M-R bond (where R = H, alkyl or aryl) generates a new M-norbornenyl bond. These two steps are commonly called initiation step (Scheme 2.6, *Initiation Step*). The propagation step consists in the coordination and insertion of n molecules of norbornene generating the polymer chain (Scheme 2.6, *Propagation Step*). The termination of the polymerization is not well known and it will be discussed in detail in *Chapter 3*.

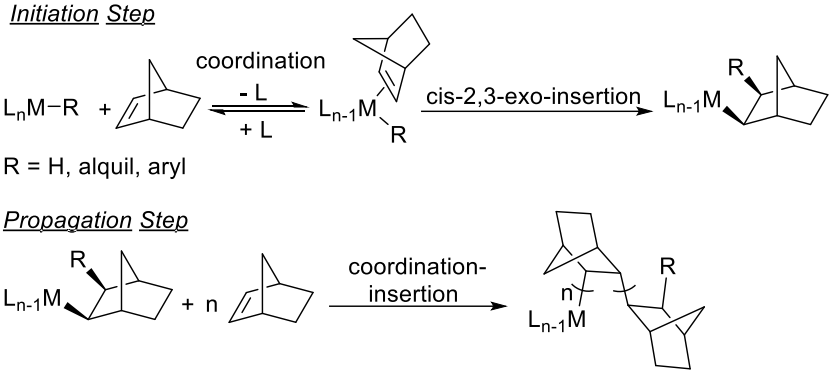

Scheme 2.6. General mechanism for the vinylic addition polymerization of norbornene.

The insertion of the norbornene into the M-R bond that initiates the polymerization and subsequent insertions into the M-norbornenyl bond are always *cis*, and *exo* because this is the less sterically hindered face of the norbornene ring. As depicted in Figure 2.3, the hydrogens atoms on the ring are closer to the M-R bond in the *endo* approach. Several studies reported the stoichiometric insertion of the norbornene or norbornadiene ring by the *exo* face using Pd(II)-acyl complexes.[85]

[85] a) Brumbaugh, J. S.; Whittle, R. R.; Parvez, M.; Sen, A. *Organometallics* **1990**, *9*, 1735-1747. b) Markies, B. A.; Kruis, J. D.; Marco, J.; Rietveld, H. P.; Kai, J.; Verkerk, A. N.; Boersma, J.; Kooijman, H.; Lakin, M. T.; Spek, A. L.; van Koten, G. *J. Am. Chem. Soc.* **1995**, *117*, 5263-5274.

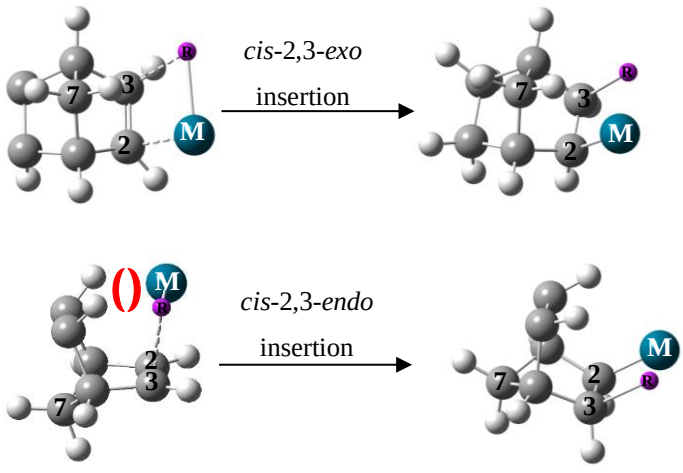

Figure 2.3. Schematic representation of the insertion on the *exo* or *endo* face of the norbornene.

The tacticity of a polymer, the relative disposition of the substituents in the space, is also important in the VA-polynorbornenes and influences in the properties of the polymer.[86-88] Two types of stereoregular polymer can be generated attendant to the disposition of the bringing C^7 atom (Figure 2.4): if all the bridging C^7 atoms are in the same disposition the polymer is 2,3-*erythro*-di-isotactic. On the other hand, if the bridging C^7 atoms are alternated, the polymer is 2,3-*erythro*-di-syndiotactic. An additional complication related with the microstructure of the VA-PNBs can be found in the VA-polymerization of substituted norbornenes. Normally these monomers are generated by a Diels-Alder reaction that affords a mixture of *exo* and *endo* isomers in a ratio *exo*:*endo* = 1:3-1:4 and both isomers can be polymerized. Therefore, to the additional complexity of the stereochemistry in VA-PNBs is added the fact that two stereochemical configurations are possible for the C-R bond in the norbornenyl units (from the *endo* and *exo* isomers) in substituted norbornenes. As a result, the microstructure of the polynorbornenes is very complex making their characterization difficult.

[86] Wilks, B R; Chung, W. J.; Ludovice, P. J.; Rezac, M. R.; Meakin, Hill, P. A. J. *J. Polym. Sci: Part B* **2003**, *41*, 2185-2199.
[87] Arndt, M.; Engehausen, R.; Kaminsky, W.; Konstantin, Z. *J. Mol. Cat. A: Chem.* **1995**, *101* 171-178.
[88] a) Boggioni, L.; Losio, S.; Tritto, I. *Polymers* **2018**, *10*, 647-671. b) Ahmed, S.; Ludovice. P. J.; Kohl, P. *Comput. Theor. Polym. Sci.* **2000**, *10*, 221-233.

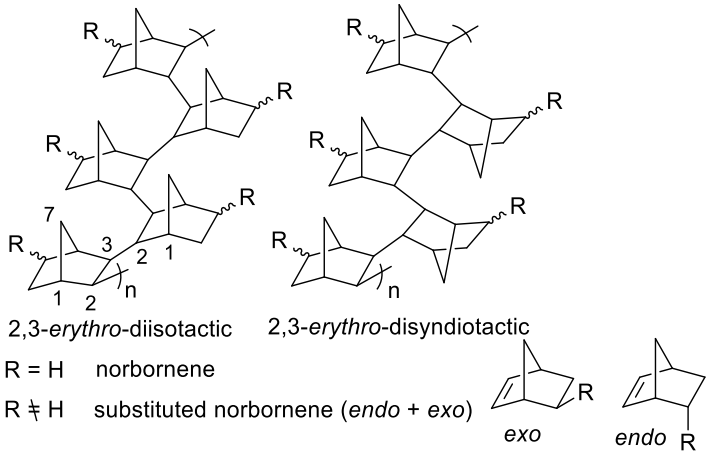

Figure 2.4. Tacticity of the VA polynorbornene and the additional complexity of the skeleton generated by the presence of *exo* and *endo* isomers.

The VA polymerization is energetically less favorable than the ROMP polymerization, and the tolerance to different substituted norbornenes is much lower.[89] This is an important difference that makes the number of very active catalyst for the VA-polymerization of substituted norbornenes very scarce when compared to those for the VA-polymerization of the parent norbornene.

2.1.4.1. Vinylic addition polymerization of norbornene and alkenyl-norbornenes with early transition metals

In the early 1980s, well-defined single site Zr or Ti complexes started to emerge as important catalysts in the vinylic addition polymerization of norbornene.[87,90-92] The group of Kaminsky and co-workers reported the polymerization of cyclic olefins with the chiral metallocenes [$ZrCl_2$Et(indenyl)$_2$] and [$ZrCl_2Me_2$Si(indenyl)$_2$].[92a] By comparison of the chemical shifts of

[89] Finkelshtein, E. S.; Bermeshev, M. V.; Gringolts, M. L.; Starannikova, L. E.; Yampolskii, Y. P *Russ. Chem. Rev*. **2011**, *80*, 341-361

[90] Hasan, T.; Nishii, K.; Shiono, T.; Ikeda, T. *Macromolecules* **2002**, *35*, 8933-8935.

[91] a) Yoshida, Y.; Mohri, J. -I.; Ishii S. -I.; Mitani, M.; Saito, J.; Matsui, S.; Makio, H.; Nakano, T.; Tanaka, H.; Onda, M.; Yamamoto, Y.; Mizuno, A.; Fujita, T. *J. Am. Chem. Soc.* **2004**, *126*, 12023-12032. b) Tang, L. -M.; Hu, T.; Bo, Y. -J.; Li, Y. -S.; Hu, N. -H *J. Organomet. Chem.* **2005**, *690*, 3125-3133. c) Ravasio, A.; Boggioni, L.; Scalcione, G.; Bertini, F.; Piovani, D.; Tritto, I. *J. Polym. Sci. A: Polym. Chem.* **2012**, 50, 3867-3874. d) Ochedzan-Siodłak, W.; Siodłak, D.; Piontek, A.; Doležal, K. *Catalysts* **2019**, *9*, 1041-1052.

[92] a) Kaminsky, W.; Bark, A.; Arndt, M. *Makromol. Chem., Macromol. Symp*. **1991**, *47*, 83-93. b) Lasarov, H.; Mönkkönen, K.; Pakkanen, T. T. *Macromol. Chem. Phys*. **1998**, *199*, 1939-1942. c) Tschage, M.; Jung, S.; Spaniol, T. P.; Okuda, J. *Macromol. Rapid Commun*. **2015**, *36*, 219-223.

the polymer signals in the ^{13}C NMR with some norbornene models, a selective insertion by the *exo*-face of the norbornene was deduced (signals below 22 ppm in the ^{13}C NMR would be indicative for a insertion by the *endo*-face (Figure 2.5)).

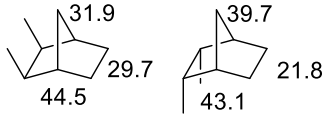

Figure 2.5. ^{13}C NMR chemical shifts for model units simulating the insertion of the norbornene by the *exo*-face (left) or the *endo*-face (right).

Depending on the catalytic system employed, the polymerization of 5-alkenyl-2-norbornenes with early transition metal complexes can selectivity occurs through to the exocyclic double bond[93] or through the endocyclic bond.[94] The group of Otsu and co-workers reported a polymerization of 5-vinyl-2-norbornene (VNB) through the external double bond in the presence of $TiCl_3$ and a trialkylaluminum as the co-catalyst (Eq. 2.3).[93b] The IR spectrum shows the absence of the absortions for the exocyclic double bond at 910 and 990 cm^{-1} (δ-C=C-H) but the presence of the vinylene band due to the bicyclic ring at 680 cm^{-1} (δ-C=C-H). All the IR data agree with a vinylic addition polymerization through the exocyclic double bond and the polymer structure is represented in Eq. 2.3.

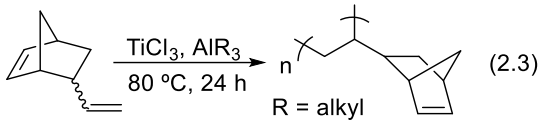

On the other hand, the vinylic addition polymerization of alkenyl-norbornenes through the endocyclic double bond is the most common pathway. The higher reactivity of the cyclic double bond towards addition polymerization is a result of the ring strain release in the process. Copolymerization of 5-vinyl-2-norbornene through the endocyclic double bond with ethylene and norbornene was studied by Pakkanen and co-workers with zirconium and titanium complexes (Eq. 2.4).[94c,d]

[93] Endo, K.; Fuji, K.; Otsu, T. *Makromol. Chem. Rapid Commun.* **1991**, *12*, 409-412. b) Endo, K.; Fuji, K.; Otsu, T. *Macromol. Chem. Phys.* **1996**, *197*, 97-104.
[94] Lohse, D. J.; Datta, S.; Kresge, E. N. *Macromolecules* **1991**, *24*, 561-566. b) Marathe, S.; Sivaram, S. *Macromolecules* **1994**, *27*, 1083-1086. c) Lasarov, H.; Pakkanen, T. T. *Macromol. Chem. Phys*. **2000**, *201*, 1780-1786. d) Lasarov, H.; Pakkanen, T. T. *Macromol. Rapid Commun.* **2001**, *22*, 434-438.

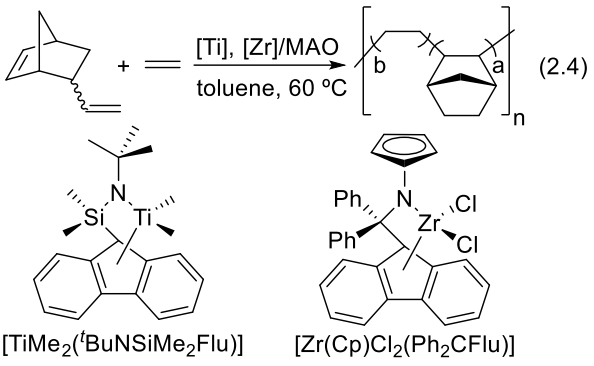

2.1.4.2. Vinylic addition polymerization of norbornene and alkenyl-norbornenes with late transition metals

Despite the fact that there are many catalytic systems developed with early transition metals, the late transition metals are the most common metals for the vinylic addition polymerization of norbornene and their derivatives. There are some reports with cobalt,[95] iron[96] and copper[97] (Figure 2.6), but most catalytic systems are based on nickel(II) and palladium(II).[89,98] The lower oxophilicity of the late transition metals (usually softer metal centers) when compared to early transition metals is an attractive feature to achieve the polymerization of monomers with polar groups. However, although some active catalyst have been developed, the polymerization of norbornene derivatives is also difficult with Ni- or Pd-complexes.[98b,c]

[95] a) Sato, Y.; Nakayama, Y.; Yasuda, H. *J. Organomet. Chem.* **2004**, *689* 744-750. b) Leone, G.; Boglia, A.; Boccia, A. C.; Scafati, S. T.; Bertini, F.; Ricci, G. *Macromolecules* **2009**, *42*, 9231-9237.

[96] a) Lassahn, P.-G.; Lozan, V.; Timco, G. A.; Christian, P.; Janiak, C.: Winpenny, R. E. P *J. Catal*. **2004**, *222*, 260-267. b) Chen, Y. J.; Huang, Z. L.; Zhang, C. Z.; Wie, T.; Zhang, L. W. *J. Mol. Catal. A: Chem.* **2006**, *259*, 133-141. c) Benade, L. L.; Ojwach, S. O.; Obuah, C.; Guzei, I. A.; Darkwa. J. *Polyhedron*, **2011**, *30*, 2878-2883.

[97] a) Carlini, C.; Giaiacopi, S.; Marchetti, F.; Pinzino, C.; Galletti, A. M. R.; Sbrana, G. *Organometallics* **2006**, *25*, 3659-3664. b) Pei, L.; Gao, H. *J. Mol. Cat. A: Chem.* **2011**,*336*, 94-99. c) Tian, J.; He, X.; Liu, J.; Denga, X.; Chen, D. *RSC Adv.* **2016**, *6*, 22908-22916.

[98] a) Blank, F.; Janiak, C. *Coord. Chem. Rev*. **2009**, *253*, 827-861. b) Finkelshtein, E. S.; Gringolts, M.; Bermeshev, M. V.; Chapala, P.; Yulia, R. Membrane Materials for Gas and Vapor Separation: Synthesis and Application of Silicon-Containing Polymers. *In Polynorbornenes***.** John Wiley & Sons Ltd. 2017; pp 143-221. c) García-Loma, R.; Albéniz, A. C. *Asian J. Org. Chem*. **2019**, *8*, 304-315.

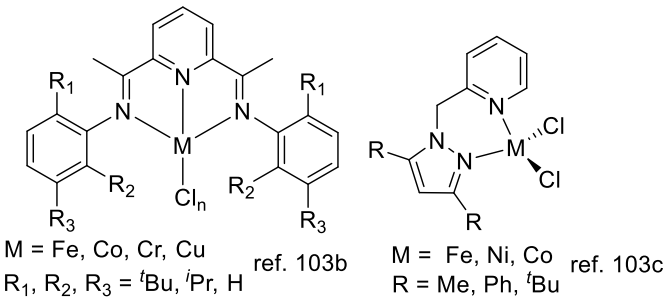

Figure 2.6. Some representative complexes with iron, cobalt and copper for the vinylic addition polymerization of norbornene.

Many of the metal complexes of Ni(II) and Pd(II) used in the vinylic addition polymerization require the presence of an additional co-catalyst to initiate the polymerization. Most frequently, methylaluminoxane derivatives (MAO) are used as cocatalyst followed by Lewis acid boron derivatives and borate compounds.[99,100] Representative examples of palladium(II) and nickel (II) complexes that need MAO or boron derivatives as additives are depicted in Figure 2.7.

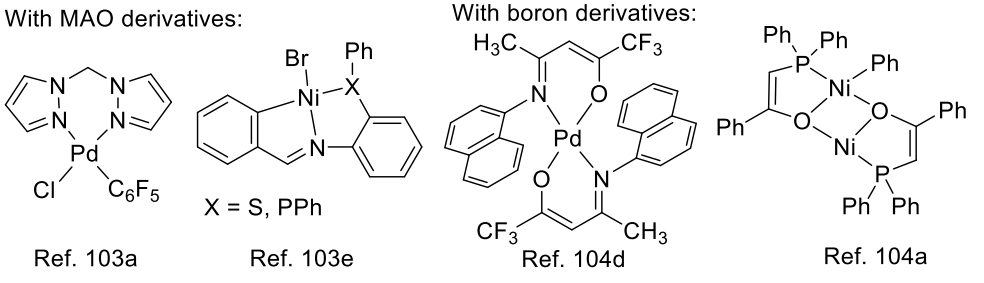

Figure 2.7. Some representative examples of Ni(II) and Pd(II) precatalysts activated by MAO and boron derivatives.

[99] a) Zhao, C. T.; Ribeiro, M. D.; Portela; M. F.; Pereira, S.; *Eur. Polym. J.* **2001**, *37*, 45-54. b) Sachse, A.; Demeshko, S.; Dechert, S. Daebel, V.; Langeb, A.; Meyer. F *Dalton Trans.* **2010**, 39, 3903-3914. c) Blank, F.; Scherer, H.; Ruiz, J.; Rodríguez, V.; Janiak, C. *Dalton Trans.* **2010**, *39*, 3609-3619. d) Blank, F.; Vieth, J. K.; Ruiz, J.; Rodríguez, R.; Janiak, C. *J. Organomet. Chem.*, **2011**, *696*, 473-487. e) Qiao, Y. -L.; Jin. G. -X. *Organometallics* **2013**, *32*, 1932-1937. f) Hao, Z.; Yang, N.; Gao, W.; Xin, L.; Luo, X.; Mu, Y. *J. Organomet. Chem.* **2014**, *749*, 350-355. g) Zhuang, R.; Liu, H.; Guo, J.; Dong, B.; Zhao, W.; Hu, Y.; Zhang, X. *Eur. Polym. J.* **2017**, *93*, 358-367. h) Youa, F.; Liua, H.; Luo, G.; Shi, X. Tridentate *Dalton Trans.* **2019**, *48*, 12219-12227. f) Liu, H.; Yuan, H.; Shi, X. *Dalton Trans.* **2019**, *48*, 609-617.

[100] a) Barnes, D. A.; Benedikt, G. M.; Goodall, B. L.; Huang, S.S.; Kalamarides, H. A.; Lenhard, S.; McIntosh, L. H.; Selvy, K. T.; Shick, R. A.; Rhodes, L. F. *Macromolecules* **2003**, *36*, 2623-2632. b) Saito, T.; Wakatsuki, Y. *Polymer*, **2012**, *53*, 308-315. c) He, X.; Liu, Y.; Chen, L; Yiwang, C.; Chen, D. Ni(II) and Pd(II) *J. Pol. Sci. Part A: Pol. Chem.* **2012**, *50*, 4695-4704. d) Tiana, J.; Zhua, H.; Liua, J.; Chenb, D.; Hea, X. *Appl. Organometal. Chem.* **2014**, *28*, 702-711.

On the other hand, the use of a well-defined precatalyst is an important methodology that helps to investigate the mechanism involved in the vinylic addition polymerization. In all cases, it is necessary the presence of a M-R bond to initiate the polymerization (where R = alkyl, aryl, allyl or H; M = Ni, Pd). A variety of palladium and nickel complexes that present a M-R bond that can initiate the vinylic addition polymerization of norbornene and their derivatives have been studied over the years (Figure 2.8).[101]

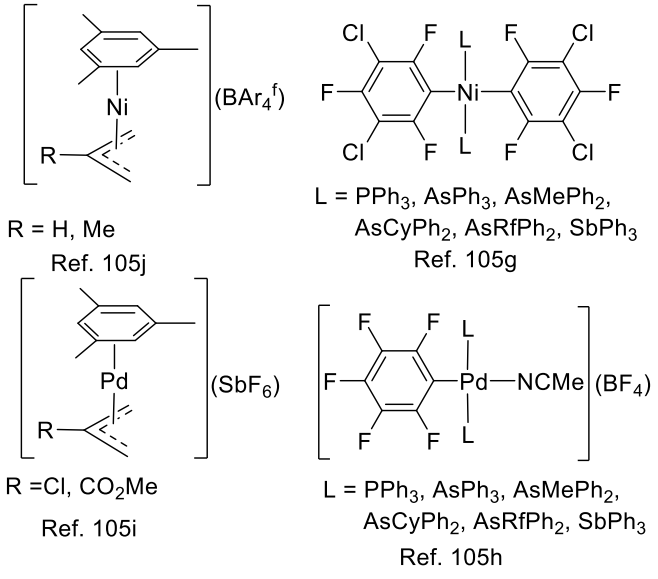

Figure 2.8. Representative examples of nickel(II) and palladium(II) complexes for the vinylic addition polymerization of norbornene without co-catalyst.

There is ample experimental proof of the occurrence of the insertion of the norbornene into the M-R bond of the catalyst (M = Ni, Pd). For example, the group of Brookhart and co-workers reported the characterization of the first insertion product (**C**$_2$) of norbornene into a cationic allyl palladium complex (Scheme 2.7). The second insertion product (**C**$_2$) where the

[101] a) Sen, A.; Lal, T. -W. *Organometallics* **1982**, *1*, 415-418. b) Mehler, C.; Risse, W. *Makromol. Chem., Rapid Commun.* **1991**, *12*, 255-259. c) Mehler, C.; Risse, W. **1992**, *25*, 4226-4228. d) Safir, A. L.; Novak, B. M. *Macromolecules* **1995**, *28*, 5396-5398. e) Hennis, A. D.; Polley, J. D.; Long, G. S.; Yandulov, A. S.; D.; Lipian, J.; Benedikt, G. M.; Rhodes L. F. *Organometallics* **2001**, *20*, 2802-2812. f) Lipian, J.; Mimna, R. A.; Fondran, J. C.; Yandulov, D.; Shick, R. A.; Goodall, B. L.; Rhodes, L. F.; Huffman, J. C. *Macromolecules* **2002**, *35*, 8969-8977. g) Casares, J. A.; Espinet, E.; Martín-Alvarez, J. M.; Martínez-Ilarduya, J. M.; Gorka, S. *Eur. J. Inorg. Chem.* **2005**, 3825-3831. h) Casares, J. A.; Espinet, E.; Gorka, S. *Organometallics* **2008**, *27*, 3761-3769. i) Walter, M. D.; Moorhouse, R. A.; Urbin, S. A.; White, P. S.; Brookhart, M. *J. Am. Chem. Soc.* **2009**, *131*, 9055-9069. j) Walter, M. C.; Moorhouse, R. A.; White, P. S.; Brookhart, M. *J. Pol. Sci. Part A: Pol. Chem.* **2009**, *47*, 2560-2573.

norbornene is acting as a chelate is the real limiting step of the initiation (coordination of the double bond to the palladium and a γ-agostic interaction with the *syn*-H^7 hydrogen). In principle, this limitation might be overcome by introducing electron-withdrawing or sterically demanding groups on the allyl fragment.

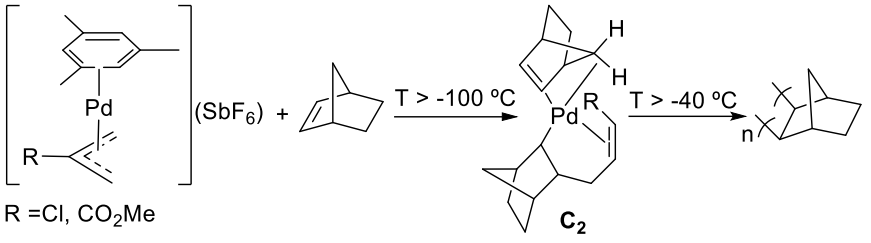

Scheme 2.7. First insertion product (**C_2**) where the norbornene is acting as a chelate.

Nickel(II) or palladium(II) complexes bearing fluorinated ligands such as pentafluorophenyl groups (R = C_6F_5) are very useful complexes since ^{19}F NMR can be used as a tool, with the simplicity and wide chemical shift range of these spectra. The C_6F_5 group has been detected anchored to several VA-polynorbornenes synthesized using [$Ni(C_6F_5)_2L_2$] (L = toluene, $SbPh_3$) complexes as catalysts, indicating an initiation step by insertion of norbornene into the Ni-C_6F_5 bond.[100a,101g,h]

The incorporation of functional groups into the polymer chains is an important point to modify specific properties of the material.[102] In addition to the physical properties induced by the presence of functional groups in the polymer, there is also an interest in functionalize polymers related to support transition-metal catalyst or reagents.[103] Many active catalysts in the vinylic addition polymerization of norbornene present low activities towards vinylic addition polymerization of alkenyl-norbornenes.[100d] Two factors explain the difference in the reactivity between both monomers. First, the more difficult coordination of the endocyclic

[102] Cowie, J. M. G.; Arrighi, V. Polymers: Chemistry and Physics of Modern Materials. *In Polymer for the Electronic Industry*; 3rd edition; Chapman & Hall: New York, 1991, pp. 455-487.
[103] Stannylates reagents: a) Carrera, N.; Gutiérrez, E.; Benavente, R.; Villavieja, M. M.; Albéniz, A. C.; Espinet, P. *Chem. Eur. J.* **2008**, *14*, 10141-10148. b) Meana, I.; Albéniz, A. C.; Espinet, P. *Adv. Synth. Catal*. **2010**, *352*, 2887-2891. c) Martínez-Arranz, S.; Carrera, N.; Albéniz, A. C.; Espinet, P.; Vidal-Moya, A. *Adv. Synth. Catal*. **2012**, *354*, 3551-3560. NHCs: d) Molina de la Torre, J. A.; Albéniz, A. C. Organocatalyst *ChemCatChem* **2014**, *6*, 3547-3552. e) Molina de la Torre, J. A.; Albéniz, A. C. *ChemCatChem* **2016**, *8*, 2241-2248. Organocatalysis: f). Sagamanova, I. K.; Sayalero, S.; Martínez-Arranz, S.; Albéniz, A. C.; Pericàs, M. A. *Catal. Sci. Technol*. **2015**, *5*, 754-764. Diimines: g) Molina de la Torre, J. A.; Albéniz, A. C. *Eur. J. Inorg. Chem.* **2017**, 2911-2919. Radical reactions: h) García-Loma, R.; Albéniz, A. C. Stannylated *Eur. J. Org. Chem.* **2017**, 4247-4254.

double bond in alkenyl-norbornenes because of the increase in the steric hindrance when the hydrogen atom is substituted for a pendant double bond. The second factor is the formation of stable intermediates that can also explain the difference in the reactivities for the *endo* and *exo* isomers, the later more reactive.[104] The initial proposal to explain this difference is the formation of a σ-bond or π-bond (for vinyl pendant groups) between the metal center and the functional group that is only possible in the *endo* isomer (Figure 2.9). This coordination mode slows the polymerization down.

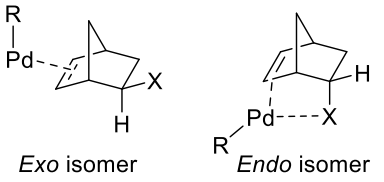

Figure 2.9. Coordination of the endocyclic double bond of a substituted norbornene to a palladium catalyst through the *exo* face (left) and the *endo* face (right). The coordination by the *endo* face allows the formation of a ``chelate´´ intermediate.

As we discussed above, the insertion of the endocyclic double bond is the most common way in the polymerization of alkenyl-norbornenes because it implies a ring strain release. However, with some catalyst such as $[Pd(NCMe)_4](BF_4)_2$ the exocyclic double bond of the 5-vinyl-2-norbornene can participate in the polymerization.[99d,105] The preference for the polymerization through the endocyclic double bond is clear but the insertion into the exocyclic double bond opens a new way for the termination of the polymerization by β-hydrogen elimination as it is shown in Scheme 2.8.

[104] a) Kang, M.; Sen, A. *Organometallics* **2004**, *23*, 5396-5398. b) Funk, J. K.; Andes, C. E.; Sen, A. *Organometallics* **2004**, *23*, 1680-1683. c) Potier, J.; Commarieu, B.; Soldera, A.; Claverie, J. P. *ACS Catal*. **2018**, *8*, 6047-6054.
[105] Blank, F.; Scherer, H.; Janiak, C. *J. Mol. Cat. A: Chem.* **2010**, *330*, 1-9.

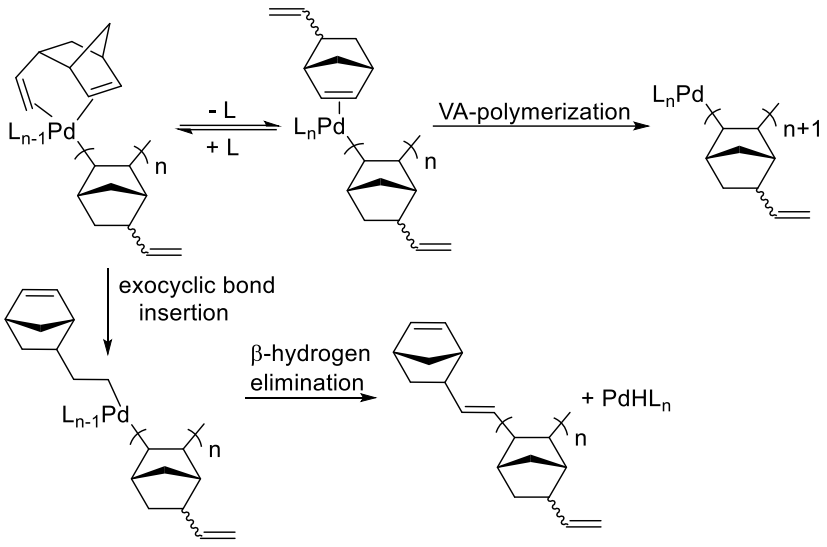

Scheme 2.8. Formation of a stable chelate olefin with 5-vinyl-2-norbornene and the termination step proposed by β-hydrogen elimination.

Two very recent reports about the vinylic addition polymerization of alkenyl-norbornenes were disclosed by Miller and Brookhart, and Bermeshev in 2020.[106] Brookhart et al studied the vinylic addition polymerization of 5-ethylidene-2-norbornene with nickel and palladium allyl cationic complexes in the presence of phosphines as ligands (Scheme 2.9 (a)). In general, the palladium complexes, in the same conditions, showed better activities and polymers with higher molecular weights than the nickel complexes.[106a] The group of Bermeshev reported excellent activities for the vinylic addition polymerization of 5-ethylidene-2-norbornene with a combination of a palladium cynnamaldehyde allyl precatalyst, sodium tetrakis[3,5-bis(trifluoromethyl)phenyl]borate ($NaBAr_4^f$) and PCy_3 (Scheme 2.9, (b)). However, the catalyst showed only modest results when used for the polymerization of 5-vinyl-2-norbornene, the least reactive isomer of the alkenyl-norbornenes

[106] a) Farquhar, A. H.; Brookhart, M.; Miller, A. J. M. *Polym. Chem*. **2020**, *11*, 2576-2484. b) Bermesheva, E. V.; Wozniak, A. I.; Fedor A. Andreyanov, F. A.; Karpov, G. O.; Nechaev, M. S.; Asachenko, A. F.; Topchiy, M. A.; Melnikova, E. K.; Nelyubina, Y. V.; Gribanov, P. S.; Bermeshev, M. V. *ACS Catal*. **2020**, *10*, 1663-1678.

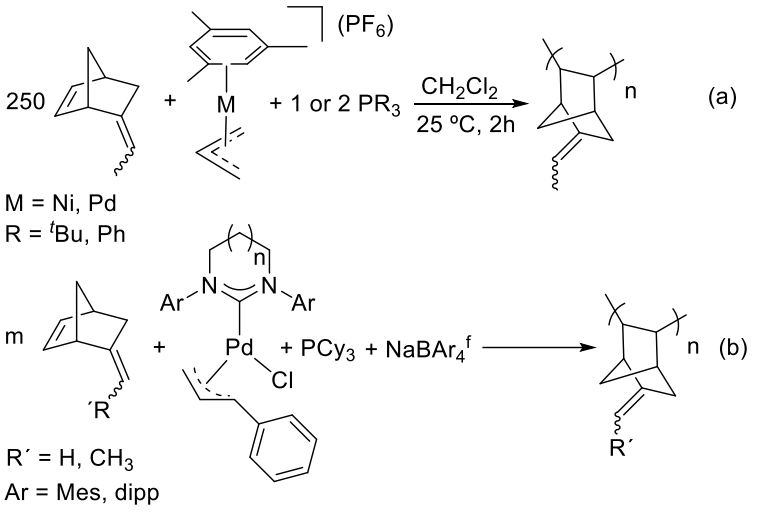

Scheme 2.9. Polymerization of alkenyl-norbornenes with nickel(II) and palladium(II) complexes.

Some of the most common ligands employed in the polymerization of norbornene and their derivatives are phosphine ligands, because of the wide range of the electronic and steric properties,[107] that can enhance the activity of the catalyst in the polymerization of norbornene. The ligands normally need to meet two requirements for a good activity: they have to stabilize the intermediate complex in solution enough to keep it on as an active metal center, but they need to be weakly coordinated to allow the access of the norbornene to the metal center. The activity in the polymerization is also dependent of the ratio Pd:L.[101e,f,104a,b,108,] In this way, the use of bulky phosphines in palladium-catalyzed reactions have been acquired an important relevance in the last years.[109] Bulky monophosphine-ligated alkyl or arylpalladium complexes are presented as very good candidates for the polymerization of norbornene and substituted norbornenes. Its structure presents a T-shape geometry with a vacant coordination site that is crucial for high activities in the polymerization of norbornene.[110] Some representative

[107] a) Strohmeier, W.; Müller, F. -J. *Chem. Ber*. **1967**, 2812-2821. b) Tolman, C. A.; Seidel, W. C.; Gosser, L. W. *J. Am. Chem. Soc*. **1974**, 96, 53-60. c) Tolman, C. A. **1977**, *3*, 313-347.
[108] Breunig, S.; Risse, W. *Makromol. Chem.* **1992**, *193*, 2915-2927
[109] a) Torraca, K. E.; Huang, X. H.; Parrish, C. A.; Buchwald, S. L. *J. Am. Chem. Soc*. **2001**, *123*, 10770-10771. b) Lee, S.; Beare, N. A.; Hartwig, J. F. *J. Am. Chem. Soc.* **2001**, *123*, 8410-8411. c) Littke, A. F.; Schwarz, L.; Fu, G. C. *J. Am. Chem. Soc*. **2002**, *124*, 6343-6348. d) Littke, A. F.; Fu, G. C. *Angew. Chem., Int. Ed*. **2002**, *41*, 4176-4121. e) Strieter, E. R.; Blackmond, D. G.; Buchwald, S. L. *J. Am. Chem. Soc*. **2003**, *125*, 13978-13980. f) Anderson, K. W.; Buchwald, S. L. *Angew. Chem., Int. Ed*. **2005**, *44*, 6173-6177.
[110] a) Yamashita, M.; Takamiya, I.; Jin, K.; Nozaki, K. *Organometallics* **2006**, *25*, 4588-4595. b) Yamashita, M.; Takamiya, I.; Jin, K.; Nozaki, K. *Organometallics* **2008**, *27*, 5347-5352 c) Kim, D. -G.; Bell, A.; Register, R. A. *ACS Macro Lett*. **2015**, *4*, 327-330

examples of these type of complexes for the polymerization of substituted norbornenes are collected in Scheme 2.10.

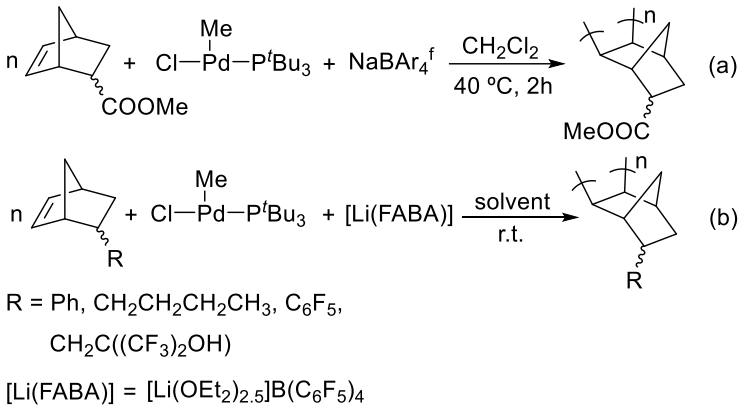

Scheme 2.10. Some representative examples for the polymerization of substituted norbornenes with a palladium complex with low Pd:phosphine ratio (1:1) reported by Nozaki et al. (a) [110a,b] and Register et al. (b).[110d]

2.1.4.3. Functionalization of VA-PNBs: Direct polymerization of substituted norbornenes or functionalization post-polymerization

The direct polymerization of functionalized norbornenes or their copolymerization with norbornene gives, in general, bad or modest results, as mentioned before. The early transition metal complexes do not tolerate functionalized norbornenes with polar groups which produce the deactivation of the catalyst.[111] On other hand, complexes of late transition metals such as palladium(II) or nickel(II) are more tolerant to the presence of polar groups.[110] However, also for these metals, the reactivity of the substituted norbornene is low in comparison with the norbornene. Consequently, in copolymerization reactions of norbornene and substituted norbornenes, is hard to control the amount of functionalization in the copolymers. The control of this functionalization can affect to the properties of the polymers and for the support of reagents or catalysts is crucial: the functionalization incorporated determines the amount of the catalyst or reagent anchored to the skeleton.

One alternative methodology to incorporate functional groups in the backbone of VA-PNB is a functionalization post-polymerization. In our research group, ω-bromoalkyl VA-PNBs were

[111] Wendt, A. R.; Fink, G. *Macromol. Chem. Phys.* **2000**, *201*, 1365-1373.

synthesized by copolymerization of norbornene and ω-bromoalkyl norbornenes (Eq. 2.5).[112] Copolymers containing percentages of incorporation of the halogenated monomer in the range between 59% (a/b = 0.7) and 26% (a/b = 2.8) could be obtained by tuning the composition of the feed.

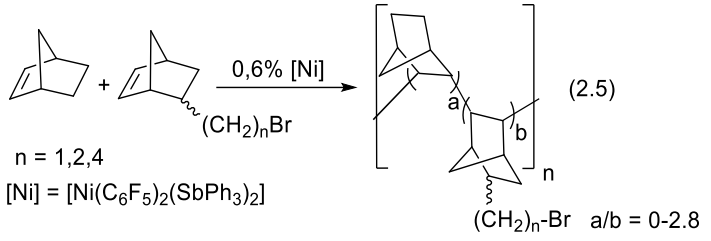

(2.5)

With these types of copolymers it is possible incorporate pendant polar functional groups by nucleophilic substitution of the bromine atom. In this way, it is possible to anchor functional groups such as -N_3, -CN, Me-COO- y -SR (Eq. 2.6). For instance, it has been reported that the polymer with cyano groups could not be synthesized by direct vinylic addition polymerization or copolymerization with norbornene because the presence of the cyano group produces the deactivation of the nickel catalyst.[113]

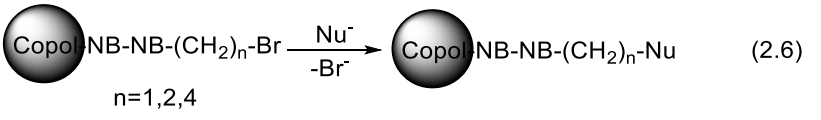

(2.6)

The main problem in this route is the competitive reaction between the nucleophilic substitution and the HBr elimination reaction, which occurs preferentially when nucleophiles with a strong basic character such as OH^- are used. So, following this approach, the synthesis of alcohols cannot be realized. The hydroboration followed by oxidation,[114] or epoxidation of double bonds are two convenient methods for this purpose.[94b,115] Therefore, alkenyl substituted VA-PNBs can be a good starting material to introduce functional groups in the polymer that cannot be synthesized from the available materials.

[112] Martínez-Arranz, S.; Albéniz, A. C.; Espinet, P. *Macromolecules* **2010**, *43*, 7482-7487.
[113] Park, K. H.; Twieg, R. J.; Ravikiran, R.; Rhodes, L. F.; Shick, R. A.; Yankelevich, D.; Knoesen, A. *Macromolecules* **2004**, *37*, 5163-5178.
[114] Nomura, K.; Liu, J.; Fujiki, M.; Takemoto, A. *J. Am. Chem. Soc.* **2007**, *129*, 14170-14171.
[115] Commarieu, B.; Potier, J.; Compaore, M.; Dessureault, S.; Goodall, B. L.; Li, X.; Claverie, J. P. *Macromolecules*, **2016**, *49*, 920-925.

2.1.4.4. Vinylic addition polymerization of olefins in the presence of benzylic complexes of nickel(II) and palladium(II)

As discussed above (section 2.1.4.2), the presence of a vacant coordination site in the polymerization of olefins is crucial to ensure good activities. The η^3-benzylic complexes of nickel(II) and palladium(II) are, in fact, a very good candidates because the easy accommodation of a new ligand thanks to the equilibrium η^3-σ (Eq. 2.7).

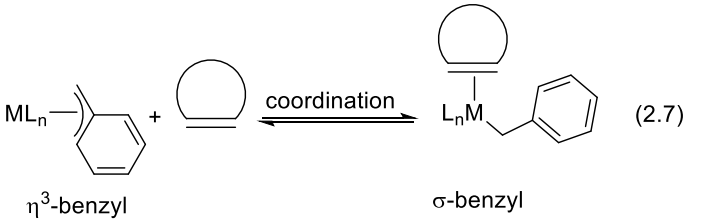

Some η^3-benzylic nickel(II) complexes for ethylene oligomerization were developed over the years (Figure 2.10).[6-8] Furthermore, there is only one precedent of a η^3-benzylic complex of nickel(II) bearing NHC ligands with an application in the vinylic addition polymerization of norbornene.[8d] Palladium benzylic complexes have also been employed in the copolymerization of styrene and carbon monoxide in 1992 and 2001 by Brookhart and Nozaki, respectively.[17,116]

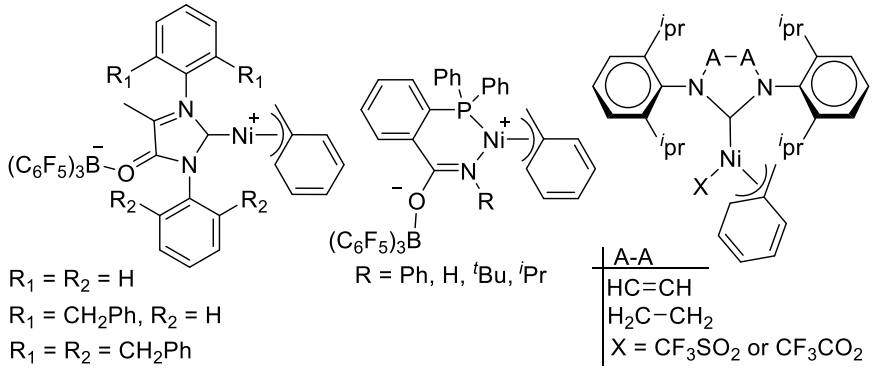

Figure 2.10. Representative η^3-benzylic complexes of nickel(II) for ethylene oligomerization and norbornene vinylic addition polymerization

[116] Nozaki, K.; Komaki, H.; Kawashima, Y.; Hiyama, T.; Matsubara, T. *J. Am. Chem. Soc.* **2001**, *123*, 534-544.

2.1.5. Aim of the work in this chapter

This chapter study the polymerization of norbornene and substituted norbornenes, in particular alkenyl-norbornenes, with some of the α-methylpentafluorophenyl benzylic complexes of palladium(II) described in *Chapter 1*. The main objectives of the work are the following: a) to develop efficient catalysts for the VA-polymerization of norbornenes based on palladium benzylic complexes; b) to find out and understand how the initiation of the polymerization occurs and how this relates to the decomposition pathways of palladium α-substituted benzyls; c) to synthesize useful VA-PNBs as starting materials for the introduction of interesting functional groups.

2.2. Results and Discussion

2.2.1. Activity of benzylic complexes of palladium(II) in the homopolymerization of norbornene

We started exploring the activity in the homopolymerization of norbornene of a selection of the benzylic complexes of palladium(II) discussed in *Chapter 1* (Scheme 1.14-1.15). We selected four complexes with different electrophilicity of the metal center (neutral or cationic) and with a different ligand environment. There are many catalysts for the polymerization of norbornene but this reaction will allow the selection of the best type of η^3-benzylic palladium complex for the polymerization of more challenging norbornene derivatives. The polymerization experiments were performed following the Eq. 2.8 and the results are summarized in Table 2.1.

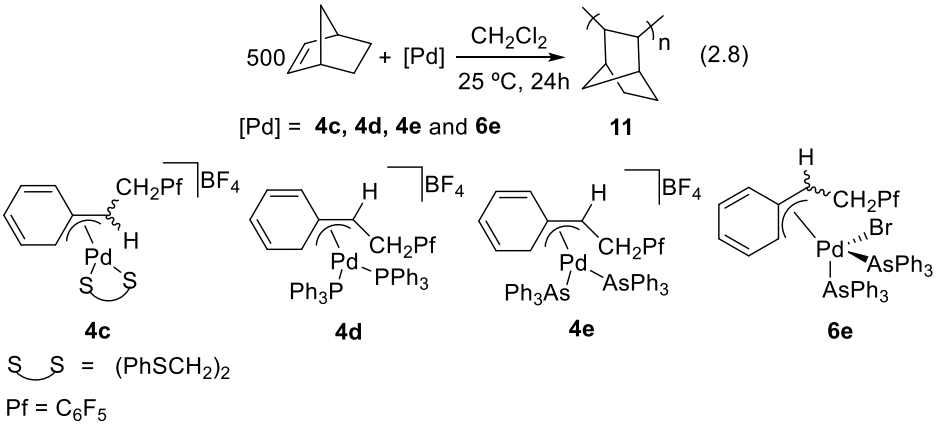

Complex **6e**, a pentacoordinated neutral complex gave no polymer after 24 h of reaction (entry 1, Table 2.1). A neutral complex with a less electrophilic metal does not favor the coordination and subsequent insertion of norbornene.[117,118] In contrast, the three cationic complexes (with a more electrophilic palladium center) showed some activity with an important effect of the ligand environment. The complex **4c** with a quelating ligand has less tendency to generate a coordination vacant site so the yield in the homopolimerization is worse than its counterparts with monodentate ligands (compare entries 2, 3 and 4, Table 2.1). Comparing the two

[117] Sen, A.; Lai, T. W.; Thomas, R. R. *J. Organomet. Chem.* **1988**, *358*, 567-588.
[118] Sen, A. *Acc. Chem. Res.* **1988**, *21*, 421-428.

complexes with monodentate ligands (entries 3 and 4, Table 2.1), the complex with the more labile $AsPh_3$ (**4e**) gave the best result. Better yields in the polymerization of norbornene for complexes with more labile ligands has been observed before by Janiak and co-workers for $[Pd(C_5H_5)(C_6F_5)L]$ where L = $SbPh_3$, $AsPh_3$ and PPh_3,[99d] or the nickel complexes $[Ni(C_6Cl_2F_3)_2L_2]$ reported by Espinet and Casares where the order for the yield in the vinylic addition polymerization of norbornene follow the trend: $SbPh_3$ > $AsPh_3$ >> PPh_3.[101g] Therefore, complex **4e**, the one with a highly electrophilic palladium center and the labile ligand $AsPh_3$ in its coordination sphere is the best choice for a vinylic addition polymerization catalyst.

Table 2.1. Activity of the η^3-benzylic complexes of in Pd(II) the homopolymerization of NB.[a]

Entry	Catalyst	Yield (%)[b]
1	**6e**	0%
2	**4c**	25 %
3	**4d**	40 %
4	**4e**	95 %

a) The reactions were carried out using CH_2Cl_2 as solvent ($[NB]_o$ = 1.2 M), 25 ºC, 24 h, under N_2, molar ratio monomer/Pd = 500:1. b) Yields are referred to the total monomer mass.

2.2.2. Activity of complex 4e in the homopolymerization of substituted norbornenes

The complex **4e**, the best of the benzylic complexes of palladium(II) for the polymerization of norbornene, was also tested in the polymerization of substituted norbornenes with polar groups and alkenyl-norbornenes. The results are summarized in Table 2.2.

Table 2.2. Results for the polymerization of alkenyl-norbornenes in the presence of catalyst **4e**.[a]

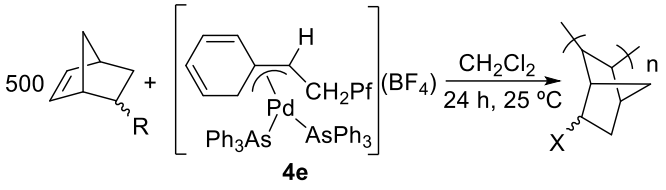

4e

X: -CH=CH_2 (VNB), -C=CH-CH_3 (ENB), -$(CH_2)_2$-CH=CH_2 (BNB), -COOH, -CH_2OH

X = -CH=CH_2 **12**
X = -C=CH-CH3 **13**
X = -$(CH_2)_2$-CH=CH_2 **14**

Entry	Monomer	Yield (%)[b]	M_w[c]	M_n[c]	M_{ntheo}[d]
1	 VNB	16.6%	7161	5994	9.975
2	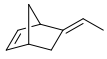 ENB	32.0%	16.404	10.434	19.951
3	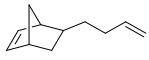 BNB	23.2%	17.287	11.296	17.186

a) The reactions were carried out using CH_2Cl_2 as solvent ([Monomer]$_o$ = 1.2 M), 25 ºC, 24 h, under N_2, molar ratio monomer/Pd = 500:1. b) Yields are referred to the total monomer mass. c) M_n and M_w determined by GPC in $CHCl_3$ using polystyrene standards and given in Daltons. d) Mn_{theo} calculated following the next equation: (monomer/Pd mol ratio) x $M_w$monomer x (yield/100)

The homopolymerization experiments with NBCOOH and NBCH_2OH did not give any polymer. In the analysis of the reaction crude mixture we observe the presence of the unreacted monomer and no oligomer formation. The introduction of a less polar group such as a pendant double bond affords homopolymers with low yields (Table 2.2). The better yield in the polymerization with ENB comparison with the yield in the VNB experiment (entries 1 and 2, Table 2.2) is consistent with the higher reactivity of ENB toward the vinylic addition polymerization reported in the literature.[106b] The molecular weight is also higher for the monomers ENB and BNB than for the VNB indicating that the propagation step is more efficient for these two monomers (Table 2.2). Furthermore, the large difference in the M_n obtained by GPC and the M_{ntheo} calculated is indicative that some chain transfer mechanism

is operating in the polymerization. The yield in the homopolymerization of alkenyl-norbornenes is not high but the characterization of these homopolymers can give us an idea about the structure of the VA polymers generated with the catalyst **4e**, which will be similar in the copolymerization process with norbornene whose copolymers are more difficult to characterize.

All the isolated polymers are soluble in common organic solvents and they were characterized by IR, NMR and GPC. The analysis of the unreacted monomer after the polymerization reaction in the homopolymerization of VNB indicates a change in the ratio *endo/exo*. The initial ratio of the monomer is 80:20 but after the polymerization experiment the ratio changes to 86:14. This change is indicative of a preference in the polymerization of the *exo* isomer as we commented before in the introduction. The IR spectrum of the polymer **12** agrees with a preferential polymerization through the endocyclic double bond. The remaining exocyclic double bond is characterized by bands at 1636 cm^{-1} (ν-C=C-) and at 905 cm^{-1} (δ-C=C-H) (Figure 2.11). No appreciable band at 680 cm^{-1} for the bending (δ-C=C-H) of the endocyclic double bond is presented in the polymer **12**.[93b] Furthermore, all the VA-PNBs, in general, are characterized by a band for the skeleton around 1450 cm^{-1}.

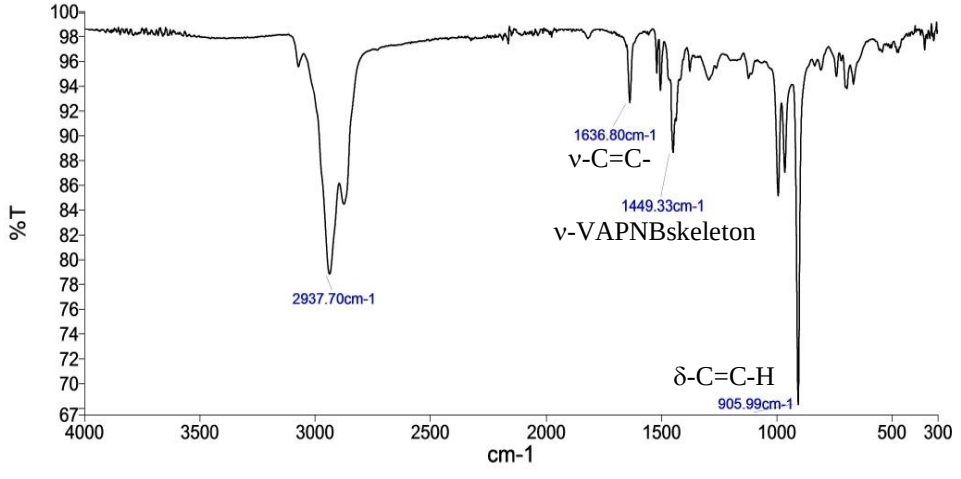

Figure 2.11. IR spectrum of VA-PVNB (**12**) (VNB:Pd = 500:1)

The exocyclic double bond can be distinguished by the presence of resonances at 6.1-5.7 ppm (H^8) and 5.1-4.5 ppm (H^9) in the ^1H NMR (green rectangles, Figure 2.12) and resonances at 144-140.5 ppm (C^8) and 115.4-111.6 ppm (C^9) in the ^{13}C NMR (Figure 2.13). The *exo* and

endo arrangements of the alkenyl group in the bicycle are visible in the ^{13}C NMR of the polymer **12** (Figure 2.13). The *cis*-2,3-*exo* insertion, the common way for the coordination-insertion of all norbornene derivatives is also presented in the polymer **12** because the absence of resonances around 20 ppm in the ^{13}C NMR.[92a] The resonance below of 20 ppm in the ^{13}C NMR (13.8 ppm) in the polymer **12** is assigned to a terminal CH_3. Similar resonance at high field is found in the polymer VA-PENB (**13**) where a CH_3 is present in the monomer ENB (see below). This indicates that the partial isomerization of the vinyl group occurs. In the polymer **12** this signal at 13.8 ppm in the ^{13}C NMR is correlated by 2D ^{1}H-^{13}C HSQC with a broad signal at 1.56 ppm in the ^{1}H NMR. And, in the ^{1}H-^{1}H COSY the signal at 1.56 ppm is correlated with the broad signal between 5.45-5.55 ppm (blue box, Figure 2.12). The polymer **13** also presents the same correlation and same chemical shifts in the ^{1}H NMR and ^{13}C NMR for the CH_3 group. So, we can conclude that the polymer **12** is formed by a mixture of two different double bonds: -CH=CH_2 as a major component and -C=CH-CH_3, as it is represented in Figure 2.12-2.13. The amount of the double bond isomerized can be calculated by integration in the ^{1}H NMR of the olefin protons of the -CH=CH_2 (H^8) and the -C=CH-CH_3 ($H^{8'}$) (Figure 2.12). The molar percentage for the isomerized double bond presents in the polymer **12** is 17%.

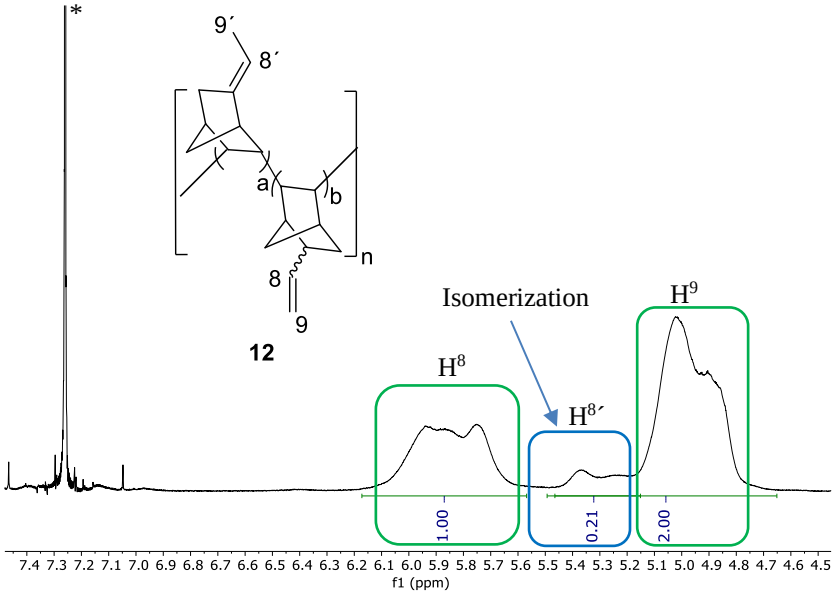

Figure 2.12. ^{1}H NMR spectra in $CDCl_3$ of the polymer VA-PVNB (**12**) (VNB:Pd = 500:1). *Signal corresponding to the solvent.

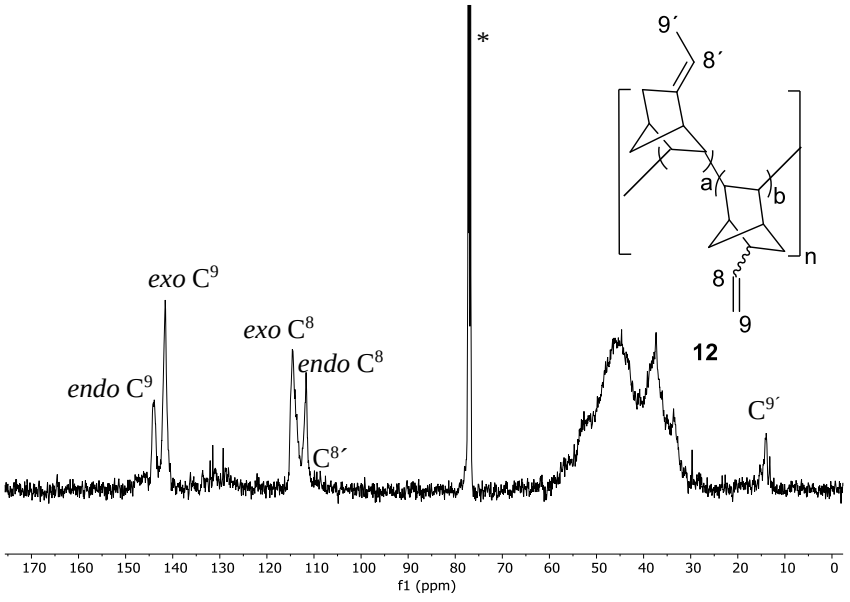

Figure 2.13. ^{13}C NMR spectrum of the polymer VA-PVNB (**12**) (VNB:Pd = 500:1) in $CDCl_3$. *Signal corresponding to the solvent.

The polymer VA-PBNB (**14**) presents a similar structure than the polymer **12**. The IR absorptions for the exocyclic double bond are present at 1650 cm^{-1} (ν-C=C-) and at 963 cm^{-1} and 907 cm^{-1} (δ-C=C-H). No band at 680 cm^{-1} for the bending (δ-C=C-H) of the endocyclic double bond is observed in the polymer **14**. The *cis*-2,3-*exo* insertion can be deduced also in this polymer because there are no skeletal resonances around 20 ppm in the ^{13}C NMR spectrum (Figure 2.14, b)).[91a] However, the isomerization of the terminal double bond also occurs and it is more important and complicated in the polymer **14**. Two signals at 17 ppm and 13.1 ppm are observed in the ^{13}C NMR that are assigned to two different CH_3 groups (Figure 2.14, b)). Both signals are correlated by 2D ^{1}H-^{13}C HSQC with a signal at 1.63 ppm in the ^{1}H NMR. By comparison with the expected chemical shifts of model structures (Figure 2.15) a mixture of *trans* and *cis*-2-butenyl groups (**14b** in Figure 2.15) as a result of the isomerization are tentatively assigned. The amount of isomerized double bond can be calculated in a similar way than for polymer **12**, leading to a molar percentage of 37% in polymer **14**.

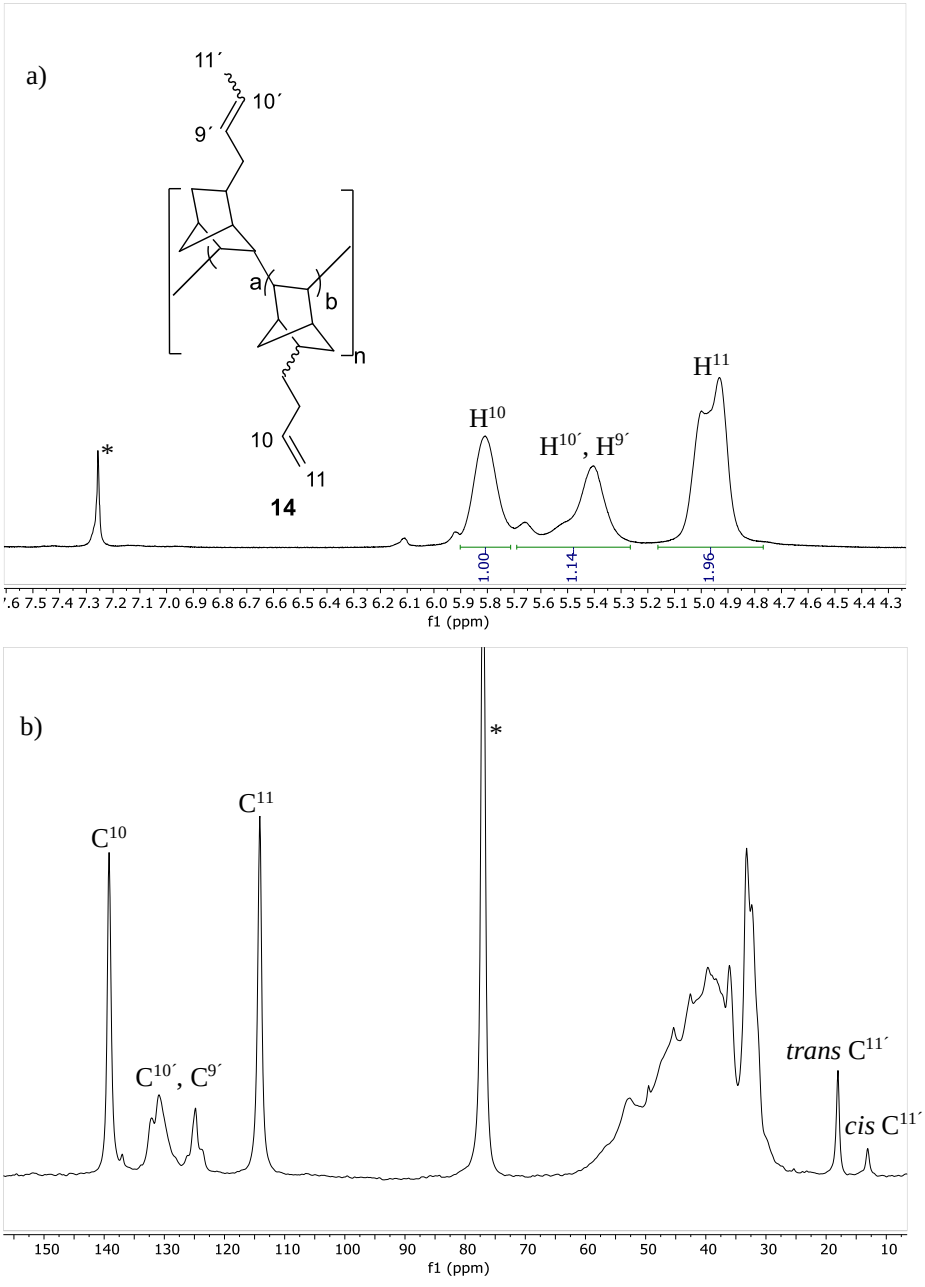

Figure 2.14. a) ^{1}H NMR and b) ^{13}C NMR spectra in $CDCl_3$ of polymer VA-PBNB (**14**).*Signal corresponding to the solvent.

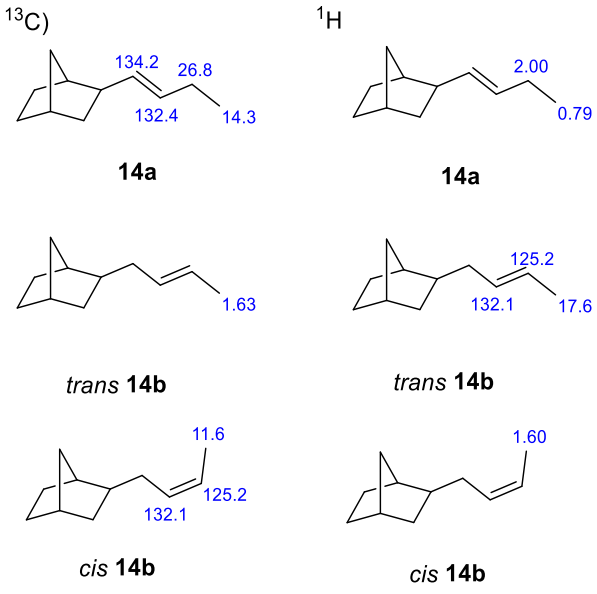

Figure 2.15. Representative models of the three possible isomers that can be formed in the skeleton of VA-PBNB (**14**).

The isomerization process is highly dependent on the ratio Pd:monomer and an increase of this ratio also increases the occurrence of the isomerization process. When polymerization experiments were performed with a ratio monomer:Pd = 25:1, short polymers could be isolated, short-**12** (M_w = 5043 Da) and short-**14** (M_w = 6718 Da). The short-**12** presents a slight increase in the isomerization process (25% in comparison with 17%) but the isomerization becomes very important in the short-**14** (78% in comparison with 37%). The parent benzylic complex **1** is an active isomerization catalyst of terminal olefins such as 1-hexene via the formation of a Pd-H, and this was described before by our research group.[32] The results here indicate that **4e** is also highly efficient for this process.

The isomerization process can take place in the monomer before it starts to polymerize or it can happen in the double bond of the formed polymer. No isomerized monomer was found in the mother liquors of the short-**14**. We cannot confirm if some monomer is isomerized before the polymerization starts because the reactivity of the isomer 5-(but-2-en-4-yl)-2-norbornene could be higher than the 5-(but-1-en-4-yl)-2-norbornene (the reactivity of the isomer ENB is higher than the VNB). However, the isomerization of the terminal double bond incorporated to the skeleton of VA-PBNB (**14**) in the presence of 10% mol of the catalyst **4e** is very fast

(see Experimental Section, polymer **14b**). After 30 min almost all the terminal double bonds are isomerized.

The polymer VA-PENB (**13**) presents, in contrast to **12** and **14**, a broad signal around 5.9-6.2 ppm that matches with the resonance for the endocyclic double bond in the monomer ENB (Figure 2.16, red rectangle). The amount of this double bond is low (6.1 % molar ratio) in comparison with the exocyclic double bond indicating a preferential polymerization through the endocyclic double bond but not exclusively. The 2D ^{1}H-^{13}C HSQC of the polymer **13** shows a correlation peak between the signal at 6.2-5.9 with a signal in the ^{13}C NMR at 131 ppm that is the typical chemical shift for the endocyclic double bond of the norbornenes. The broad signal between 5.75-5.6 ppm (green rectangle, Figure 2.16) has got a similar chemical shift to the fragments resulting from a ring opening of the norbornene that we will discuss in more detail in *Chapter 3*.

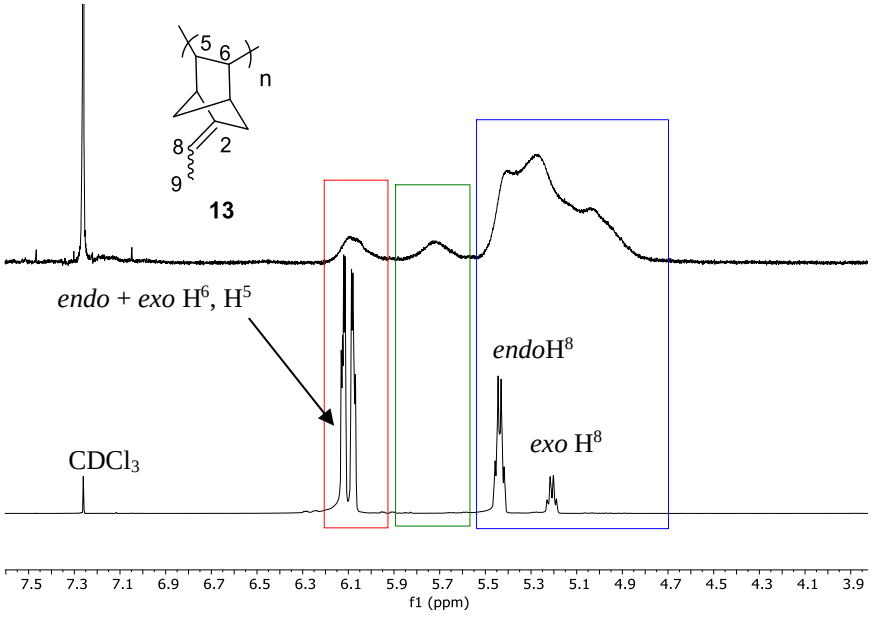

Figure 2.16. Comparison of the ^{1}H NMR of the monomer ENB and the isolated polymer VA-PENB (**13**) in $CDCl_3$. The ^{1}H NMR only shows the part for the olefinic protons.

All the homopolymers synthesized in this section present broad signals corresponding to the pentafluorophenyl group bound to carbon in the ^{19}F NMR (Figure 2.17), indicating an initiation step by insertion of the alkenyl-norbornene into the Pd-CHPh($CH_2C_6F_5$) bond. We

will discuss in section 2.2.5 the possible pathways for the initiation step in all the polymerization and copolymerization reactions with catalyst **4e**.

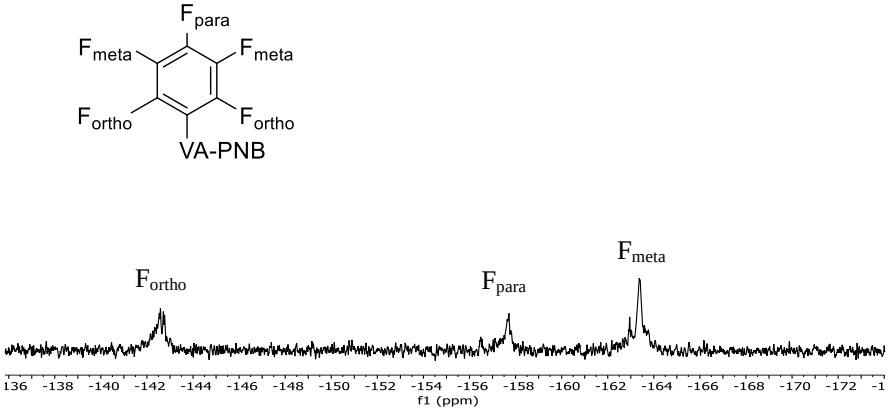

Figure 2.17. ^{19}F NMR spectrum in $CDCl_3$ of polymer VA-PVNB (**12**).

In summary, the homopolymerization of alkenyl-norbornenes with catalyst **4e** generates polymers with moderate-low molecular weights and low yields. Furthermore, an isomerization process of the terminal double bond can be observed with the monomers VNB and BNB, responsible for the formation of internal double bonds in the skeleton of the alkenyl VA-PNBs.

2.2.3. Activity of complex 4e in the copolymerization of substituted norbornenes with norbornene

The copolymerization process is more interesting than the homopolymerization for the post-functionalization of the polymer because it is possible the control the degree of functionalization in the VA-PNBs by the initial composition feed of the monomers. The results for the copolymerization experiments are summarized in Table 2.3.

Table 2.3. Copolymerization of substituted norbornenes with norbornene in the presence of catalyst **4e**.[a]

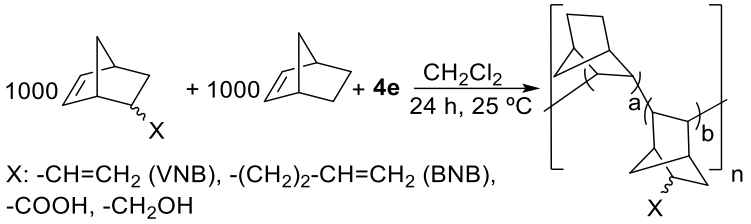

X: -CH=CH_2 (VNB), -$(CH_2)_2$-CH=CH_2 (BNB), -COOH, -CH_2OH

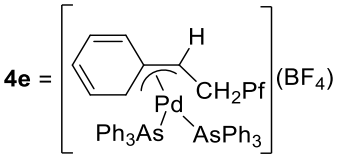

X: -CH=CH_2 **15**; -$(CH_2)_2$-CH=CH_2 **16**; -COOH **17**;-CH_2OH **18**

Entry	Monomers	Yield (%)[b]	a/b[c]	mmol FNB/gr[d]	M_w[e]	M_w/M_n[e]
1	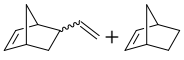	64%	1.8/1	3.5	56465	2.4
2	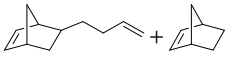	57.3%	2.1/1	2.3	29875	1.85
3	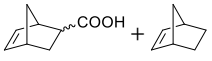	34%	---	---	---	---
4	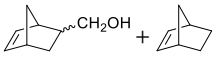	14%	---	---	---	---

a) The reactions were carried out using CH_2Cl_2 as solvent ($[Monomer]_o$ = 1.2 M), 25 ºC, 24 h, under N_2, molar ratio NB/FNB/Pd = 500:500:1. b) Yields are referred to the total monomer mass. c) a/b was determined by integration in the ^{1}H NMR (see Experimental Section). d) mmol functionalized monomer/g pol. calculated from the ratio a/b: [1/[((a/b) x (M_{wNB})) + (M_{wFNB})]] x 1000 where M_{wNB} is the molecular weight of the monomer norbornene (94.16) and M_{wFNB} is the molecular weight of the VNB (120.19) or BNB (177.16). e) Determined by GPC in $CHCl_3$ using polystyrene standards; M_w in Daltons.

The copolymers **17** and **18** were obtained with low yields and they are insoluble in common organic solvents. The IR spectra confirm the presence of carboxylic groups anchored to the skeleton of the VA-PNBs in the copolymer **17** (1750 cm^{-1}, ν-C=O) and hydroxyl groups in the copolymer **18** (3450 cm^{-1} ν-OH and 1046 cm^{-1} ν-C-O). These bad results are not surprising because the presence of the COOH groups or OH produce the deactivation of the catalyst as we observed before in the homopolymerization experiments where no polymer or oligomer were isolated.

In contrast, good yields were obtained for the copolymerization of NB with VNB (VA-Co-PNB-VNB, **15**) and NB with BNB (VA-Co-PNB-BNB, **16**). The two copolymers in entries 1 and 2, Table 2.3 are soluble in common organic solvents, so they can be characterized by NMR techniques and GPC. The GPC chromatograms show a unimodal distribution indicating the presence of one copolymer and not a mixture of two homopolymers. An analogous structure to the homopolymers can be deduced for the copolymers: A *cis*-2,3-*exo* insertion of the endocyclic double bond (no signals around 20 ppm in the ^{13}C NMR) with the presence of the two arrangements (*endo* and *exo*) of the alkenyl substituent in the copolymer **15**.[92a] In contrast with the homopolymerization process, the isomerized double bond is not present in the isolated copolymer **15** but it is still visible in the copolymer **16** but less abundant (13% in the copolymer **16** versus 37% in the homopolymer **14**). The composition, ratio mmol NB/mmol FNB (FNB = functionalized norbornene = VNB or BNB) incorporated in the isolated polymers presented in Table 2.3 was determined by comparison of the integral values of the olefinic and aliphatic regions in the ^{1}H NMR (see Experimental Section for details).

We choose the 5-vinyl-2-norbornene for the screening of the polymerization conditions because it is commercial and the presence of a terminal double bond is very convenient for organic transformations that we will discuss latter. The incorporation of the VNB monomer in the copolymer can be roughly controlled by the monomer ratio in the feed, as shown in Table 2.4 for the copolymerization of NB and VNB (entries 2, 3 and 4, Table 2.4). The NB content in the copolymer is always higher than in the initial monomer feed showing the higher reactivity expected for the norbornene: even when the initial monomer feed is NB:VNB = 1:2 (entry 2, Table 2.4), the norbornene is present in higher amount than the VNB. This higher reactivity is also patent in the values of the reactivity ratios of NB (r_{NB}) and VNB (r_{VNB}), i.e. the ratio of rate constants for reaction of one monomer with the same or a different monomer: $r_{NB} = k_{NBNB}/k_{NBVNB}$ and $r_{VNB} = k_{VNBVNB}/k_{VNBNB}$. They can be determined using the Fineman-Ross method that is based in the copolymerization equation (see Experimental Section for more details),[119] and the values for the copolymerization with catalyst **4e** are: $r_{NB} = 1.97$ and $r_{VNB} = 0.0048$. The reactivity ratios of the two monomers give us an idea of the structure of the polymer. Because the product $r_{NB}r_{VNB}$ is close to 0, we expect an alternating copolymer.[120]

[119] Fineman, R.; Ross, S. D. *J. Polym. Sci*. **1950**, *5*, 259-269.
[120] Rudin, A.; Choi, P. The Elements of Polymer Science & Engineering. *In Copolymerization*; Academic Press; 2013; pp. 391-425.

The ratio of the monomers in the initial feed has got an important influence in the molecular weight: when the relative amount of NB in the initial feed is higher, the molecular weight of the polymer increases (compare entries 1 and 2, Table 2.4). In fact, when the ratio NB:VNB is 2:1 (entry 3, Table 2.4) the isolated polymer is insoluble. In this case the composition of the polymer was calculated using FT-IR spectroscopy (see Experimental Section).

The polymers present high PDI indicating a not very controllable vinylic addition polymerization. The amount of catalyst has not got any influence in the composition of the polymer since the composition of the polymers is determined by the reactivity ratios of the monomers which are independent of the amount of the catalyst in the feed. However, there is a significant decrease of the yield for a molar amount of **4e** below 0.05% (entries 1, 4 and 5, Table 2.4).

Table 2.4. Screening of the reaction conditions for the copolymerization of NB and VNB with catalyst **4e**.[a]

Entry	NB:VNB:**4e**[b]	Yield(%)[c]	a/b[d]	mmol VNB/g[e]	M_w[f]	M_w/M_n[f]
1	500:500:1	62.6%	1.8/1	3.5	56.464	2.4
2	500:1000:1	53.6%	1.4/1	4.0	30.620	3.4
3[g]	1000:500:1	80.5%	3.9/1	2.07	---	---
4	1000:1000:1	64.0%	2.1/1	3.1	63.915	2.1
5	2000:2000:1	43.0%	2.3/1	3.0	---	---

a) The reactions were carried out using CH_2Cl_2 as solvent ($[VNB]_o$ = 1.2 M), 25 ºC, 24 h under N_2. b) initial composition feed in the copolymerization. c) Yields are referred to the total monomer mass. d) a/b was determined by integration in the ^{1}H NMR. e) mmol of VNB/g copolymer calculated from the ratio a/b: [1/[((a/b) x (M_w NB)) + (M_w VNB)]] x 1000. f) Determined by GPC in $CHCl_3$ using polystyrene standards; M_w in Daltons. g) mmol of VNB/gr copolymer determined by FT-IR spectroscopy

2.2.4. New catalytic system with high activity in the polymerization of alkenyl-norbornenes

The modest results obtained in the homopolymerization of alkenyl-norbornenes with the catalyst **4e** encouraged us to search for a better η^3-benzylic palladium catalyst for vinylic

addition polymerization. We concluded before that a cationic complex with monodentate ligands is necessary to obtain good yields in the polymerization of norbornene (Table 2.1). A more electrophilic metal favors the coordination-insertion of the olefin into the Pd-R bond.[117,118] On the other hand, it is known the ratio ligand:Pd has got a very important influence in the results of the polymerization, since the monomer competes with the auxiliary ligands for coordination to the metal.[110] All of our isolated η^3-benzylic complexes studied in the polymerization of norbornene have got a ratio ligand:Pd 2:1. Checking our previous studies in the synthesis of benzylic complexes, we know the existence in solution of a neutral complex with a ratio Pd:L 1:1, the complex **5**. This complex **5** is generated in situ adding two equivalents of PPh_3 to dimer **1** (Eq. 2.9). So, it is reasonable to assume that the addition of a bromide scavenger would lead to a cationic benzylic complex with a ratio Pd:L = 1:1, useful as polymerization catalyst.

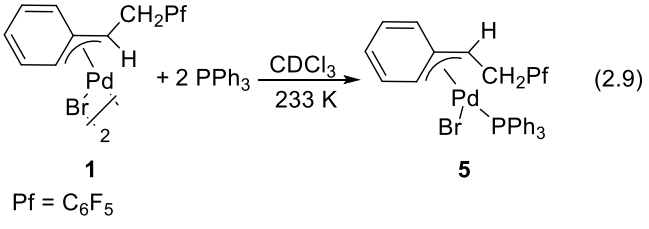

1 **5** (2.9)

Pf = C_6F_5

Following this methodology, we tested, in the polymerization of 5-vinyl-2-norbornene (VNB), the formation in situ of a cationic complex adding two equivalents of phosphine and two equivalents of $AgBF_4$ or $NaBAr_4^f$ to the dimeric complex **1** (Eq 2.10). The results are summarized in Table 2.5.

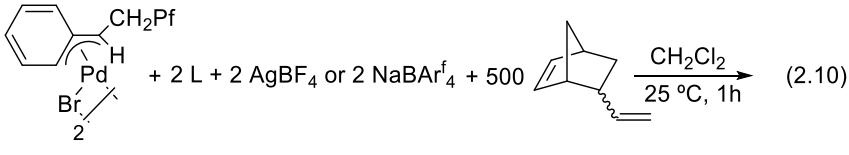

1 (2.10)

Table 2.5. Vinylic addition polymerization of VNB according to Eq. 2.10.[a]

Entry	Phosphine	MBR_4	Yield (%)[b]
1	PPh_3	$AgBF_4$	5%
2	P^tBu_3	$AgBF_4$	13%
3	PPh_3	$NaBAr_4^f$	99%
4	P^tBu_3	$NaBAr_4^f$	99%

a) The reactions were carried out using CH_2Cl_2, $[VNB]_o$ = 3.7 M), 25 ºC, 1 h, under N_2, molar ratio VNB/Pd = 500:1. b) Yields are referred to the total monomer mass.

The combination of PPh_3 or P^tBu_3 and $AgBF_4$ does not afford good yields in both cases (entries 1 and 2, Table 2.5). During the generation of the complex in situ, we observed the formation of Pd black after the addition of $AgBF_4$ indicating that the catalytic active species is not stable in the reaction conditions. In contrast, the addition of the $NaBAr_4^f$ produces excellent yields with both phosphines (entries 3 and 4, Table 2.5) and no Pd black was observed. The higher efficiency of $NaBAr^f_4$ in comparison with $AgBF_4$ cannot be explained because of the insolubility of the salt generated after the abstraction of the bromine atom (AgBr for the $AgBF_4$ and NaBr for the $NaBAr^f_4$). There are some precedents in the literature explaining the role of the counterions in different catalytic applications.[121] We believe that the high difference in the activity is a consequence of the stabilization of the naked complex generated in solution. In some way, the bulky BAr_4^{f-} is shielding the palladium more efficiently stabilizing the complex enough to avoid the decomposition but without interfering in the activity of the catalyst.

After these initial results, we performed a study with different phosphines fixing the ratio VNB:Pd 25000:1. All the results are summarized in Table 2.6, along with Tolman's electronic parameter (ν-CO in the IR spectrum of $Ni(CO)_3PR_3$, a higher value of ν-CO indicates a more electronwithdrawing phosphine) and the phosphine cone angle (θ).[107]

[121] a) Krossing, I. Raabe, I. *Angew. Chem. Int. Ed.* **2004**, *43*, 2066-2090. b) BÖing, C.; Franciò, G.; Leitner, W. *Adv. Synth. Catal.* **2005**, *347*, 1537-1541. c). Brownie, J. H.; Baird, M. C. *Organometallics* **2003**, *22*, 33-41.

The less donating phosphine ($P(C_6F_5)_3$, ν_{CO} = 2091) gives a polymer with low yield (entry 5, Table 2.6). It is clear that at least a moderately good donor is needed most probably to stabilize the naked palladium(II) complex generated in situ. Comparing two phosphines with the same electronic effect, the PPh_3 and the P(*o*-tolyl)$_3$, we can observe a decrease in the yield with the bulkiest phosphine (entries 3 and 4, Table 2.6). The same is observed for the trialkylphosphines and modest results were obtained with the bulky P^tBu_3 whereas the PCy_3, a phosphine with the same electronic character but lower cone angle, is giving the best results in the polymerization on VNB with the catalytic system **1**/phosphine/$NaBAr_4^f$ (entries 1 and 2, Table 2.6). The P(*o*-tolyl)$_3$ with a high cone angle is hindering more efficiently the palladium center and therefore, the coordination of the VNB to the palladium center is worst traduced in a decrease in the yield. The steric hindrance of a bulkier phosphine could disfavor the coordination of the VNB to the palladium center and result in a decrease in the yield. It has to be noted that in the case of P^tBu_3 it is known that this phosphine can undergo metalation processes, and therefore, this can open a catalysts decomposition pathway.[122]

Table 2.6. Scope of the phosphines with the system **1**/phosphine/$NaBAr_4^f$ in the polymerization of VNB.[a]

Entry	Phosphine	Cone angle (º)[107]	υ_{CO} (cm^{-1})[107]	Yield (%)[b]
1	P^tBu_3	182	2056	50%
2	PCy_3	170	2056	90%
3	P(*o*-tolyl)$_3$	194	2066	40%
4	PPh_3	145	2069	62%
5	$P(C_6F_5)_3$	184	2091	5%

a) The reactions were carried out using CH_2Cl_2 as solvent ($[VNB]_o$ = 3.7 M), 25 ºC, 5 h, ratio VNB:Pd = 25.000:1, 2 equivalents of phosphine and $NaBAr_4^f$ per palladium. b) Yields are referred to the total monomer mass.

In summary, the best phosphine for the vinylic addition polymerization of VNB with the combination of **1**/phosphine/$NaBAr_4^f$ is the use of the PCy_3 that is a good donor to stabilize the active species and not too bulky to disfavor the coordination of the VNB. With the best

[122] Goel A. B.; Goel S. *Inorg. Chim. Acta* **1985**, *98*, 67-70.

catalytic system selected (**1**/PCy_3/$NaBAr_4^f$) we studied the effect of the reaction conditions in the polymerization. (Table 2.7-2.8). The yield of the polymerization is not affected by an excess of the phosphine or the initial concentration of monomer when a ratio VNB:Pd 25000:1 was used (entries 1-4, Table 2.7). Increasing the ratio VNB:Pd to 50000:1 (0.02% or 20 ppm of Pd), the yield of the polymerization is more sensitive to the equivalents of phosphine added, solvent, temperature and initial concentration of VNB (entries 5-11, Table 2.7). When four equivalents of phosphine are used instead of two, there is a sightly increase in the yield (48% to 64%, respectively; entries 5 and 6, Table 2.7). The choice of the solvent is crucial in the polymerization reaction, and the more polar CH_2Cl_2 is a better solvent than toluene (compare entries 5, 7 and 8, Table 2.7). A similar behavior was reported before in the polymerization of ENB with a mixed N-Heterocyclic carbene/phosphine palladium(II) complex.[101n] A cationic complex is generated in situ in this reaction so the polarity of the solvents is important in its stabilization and in the catalytic activity. An increase in the yield from 48 % to 85% is observed when the temperature of the reaction increases from 25 ºC to 45 ºC, respectively (entries 5 and 9, Table 2.7). The increase of the activity of a catalyst with the temperature it is well known and it is a consequence of the increase of the initiation and propagation rate constants.

The last factor we checked is the initial concentration of the monomer in solution (entries 5, 10 and 11, Table 2.7). There is a slight increase in the yield of the polymerization when the reaction was performed in a lower concentration of VNB ($[VNB]_o$ = 1.85 M (entries 5 and 9, Table 2.7)), but an important decrease when the initial concentration of VNB is high ($[VNB]_o$ = 5.55 M (entries 5 and 10, Table 2.7)). The concentration is a crucial factor in this polymerization because the viscosity of the solution. If the $[VNB]_o$ is high, the solution quickly becomes very viscous. This means that the polymerization stops to be controlled by thermodynamic factors and starts to be controlled by diffusion factors (c.f in a high viscosity mixture the diffusion of the reagents is low) affecting the final yield.[99d] On the other hand, if the solution is not very concentrated, the viscosity of the mixture is lower just increasing towards the end of the polymerization.

Table 2.7 Screening of reaction conditions with the system **1**/PCy_3/$NaBAr_4^f$ in the polymerization of VNB.[a]

Entry	T (ºC)	eq. PCy_3	VNB:Pd	Solvent	$[VNB]_o$	Yield (%)[b]
1	25	2	25000:1	CH_2Cl_2	3.7	90%
2	25	4	25000:1	CH_2Cl_2	3.7	90%
3	25	2	25000:1	CH_2Cl_2	1.85	95%
4	25	2	25000:1	CH_2Cl_2	5.55	90%
5	25	2	50000:1	CH_2Cl_2	3.7	48%
6	25	4	50000:1	CH_2Cl_2	3.7	64%
7	25	2	50000:1	Toluene	3.7	25%
8	25	2	50000:1	CH_2Cl_2/Toluene (1:3)	3.7	50%
9	45	2	50000:1	CH_2Cl_2	3.7	85%
10	25	2	50000:1	CH_2Cl_2	1.85	60%
11	25	2	50000:1	CH_2Cl_2	5.55	28%

a) The reactions were carried out using CH_2Cl_2, 5h, under N_2. b) Yields are referred to the total monomer mass.

We extended the study of our catalytic system employing very low loadings of catalyst and including the polymerization of 5-ethylidene-2-norbornene (ENB). The results are summarized in Table 2.8. When the ratio of VNB:Pd increases from 50000:1 to 100000:1 (10 ppm of Pd) at 45 ºC the yield of the polymerization is 35% (entry 3, Table 2.8). To ensure good yields in the polymerization with low catalyst loadings, we need to use higher temperatures. It is therefore necessary the use another solvent with very similar polarity than the CH_2Cl_2 but with higher boiling point such as 1,2-dicloroethane. The yield with the ratio of VNB:Pd 100000:1 at 75 ºC after 5 hours increases to 85% (entry 4, Table 2.8). When the ratio FNB:Pd increases to 500000:1 (2 ppm of Pd) where FNB = VNB or ENB, it is necessary to increase the reaction time to 24 h to get good yields (62 % for VNB and 65 % for ENB, entries 5 and 7, Table 2.8). The addition of 4 equivalents of PCy_3 instead of 2 (entries 6 and 8, Table 2.8) increases the yield of the reaction to 92-95 % for both monomers.

Table 2.8. Effect of the amount of catalyst with the system **1**/PCy_3/$NaBAr_4^f$ in the polymerization of VNB and ENB.[a]

Entry	T (ºC)	eq. phos.	VNB:Pd	Solvent	Time	Yield (%)[b]
1	25	2	50000:1	CH_2Cl_2	5 h	48%
2	45	2	50000:1	CH_2Cl_2	5 h	85%
3	45	2	100000:1	CH_2Cl_2	5 h	35%
4	75	2	100000:1	1,2-dicloroethane	5 h	85%
5	75	2	500000:1	1,2-dicloroethane	24 h	62%
6	75	4	500000:1	1,2-dicloroethane	24 h	92%
7[c]	75	2	500000:1	1,2-dicloroethane	24 h	65%
8[c]	75	4	500000:1	1,2-dicloroethane	24 h	95%

a) The reactions were carried out using CH_2Cl_2 or 1,2-dicloroethane, $[VNB]_o$ = 3.7 M, under N_2. b) Yields are referred to the total monomer mass. c) ENB instead of VNB.

Only some of the polymers synthesized in this section are soluble in $CHCl_3$ when freshly prepared and can be characterized by NMR. However, they become insoluble upon standing in an aging process that has already been described for other polynorbornenes.[123] Also, because of the high monomer:Pd ratios used, they are expected to have high molecular weights. As we observed before for the homopolymers generated with the catalyst **4e** some important structural characterization such as the initiation pathway of the polymerization or undesired reactions such as isomerization of the double bond can be deduced when the chains of the polymers are not long. So, to try to elucidate better the structure of these polymers, we generated short soluble polymers with a ratio FNB:Pd = 250:1 (FNB = VNB or ENB). In the ^{1}H NMR of the VA-PVNB (**12**) obtained, the ratio olefinic signals to aliphatic protons (1:2:9) is the expected one for a vinylic addition polymerization exclusively by the endocyclic double bond (Figure 2.18, a)). In contrast with the isomerization process visible in the vinylic addition polymerization of VNB with the catalyst **4e** (see section 2.2.2), no isomerized double bond is found in the skeleton of the VA-PVNB generated with the precatalyst system **1**/PCy_3/$NaBAr_4^f$

[123] Chu, P. P.; Huang, W.-J.; Chang, F.-C.; Fan, S. Y. *Polymer* **2000**, *41*, 401-404

(no signal at 13.8 ppm in the ^{13}C NMR, red rectangle in Figure 2.18 b)). The high yields reported in all this section are indicative of a fast initiation and propagation steps, so the isomerization of the olefin is not a competitive reaction in this process. The *cis*-2,3-*exo* insertion, the common way for the coordination-insertion of all norbornene derivatives is also presented in these polymers (no resonances around 20 ppm are visible in the ^{13}C NMR (Figure 2.18 b)). *Endo* and *exo* arrangements of the alkenyl substituent in the bicycle are also visible in the ^{13}C NMR spectrum with a ratio that do not reproduce the initial ratio of the isomers in the monomer as is expected for the higher reactivity of the *exo* isomer.[104] No signals of the C_6F_5 anchored to the skeleton of the VA-PVNB are visible in the ^{19}F NMR indicating a different initiation step that the proposed for the cationic benzylic complex **4e** through the insertion of VNB into the Pd-$C^{\alpha}HPhCH_2C_6F_5$ bond. We will discuss this point later in this chapter.

A similar structure is deduced for the VA-PENB (**13**) synthesized with the same methodology (ratio ENB:Pd = 250:1). The analysis of the ratio olefinic protons:aliphatic protons (1:11) in the ^1H NMR spectrum reproduce the theoretical ratio (1:11) considering an exclusively insertion of the endocyclic double bond (Figure 2.19, a)). We do not observe the presence of residual signals corresponding to the endocyclic double bond around 6.1 ppm so the exocyclic double bond is not participating in the polymerization. As we mentioned for the polymerization of VNB with this system (**1**/PCy_3/$NaBAr_4^f$), both the initiation and the propagation step through the endocyclic double bond are very fast and no competing reactions are observed. As for VA-PVNB, no signals are detected in the ^{19}F NMR for a C_6F_5 group anchored to the polymer skeleton.

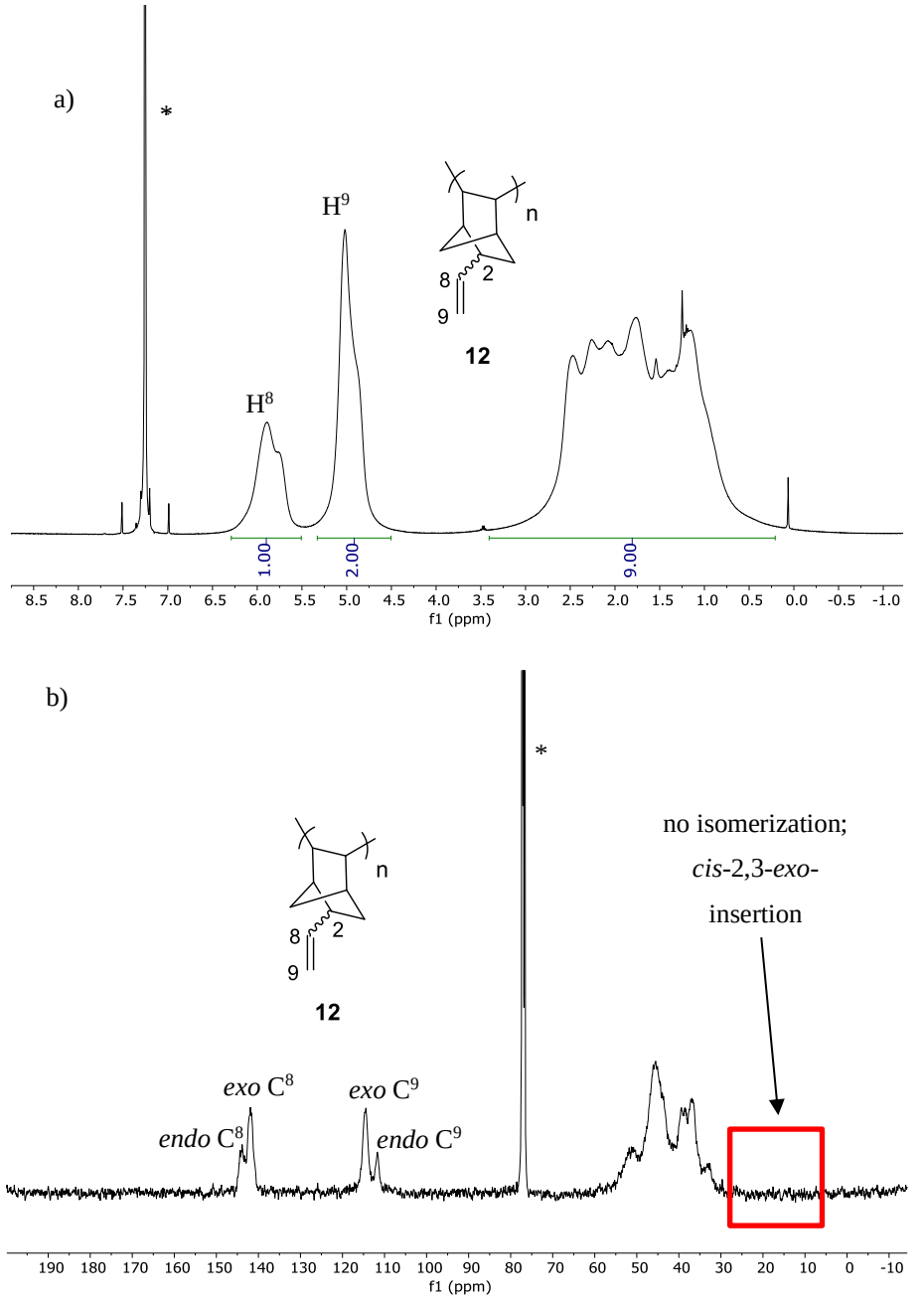

Figure 2.18. a) ^{1}H NMR (500.13 MHz, dry $CDCl_3$) and b) ^{13}C NMR (125.758 MHz, dry $CDCl_3$) of a polymer VA-PVNB (**12**) generated with the system **1**/PCy_3/$NaBAr_4^f$ (ratio VNB:Pd = 250:1) at 298 K. *Signal corresponding to the solvent.

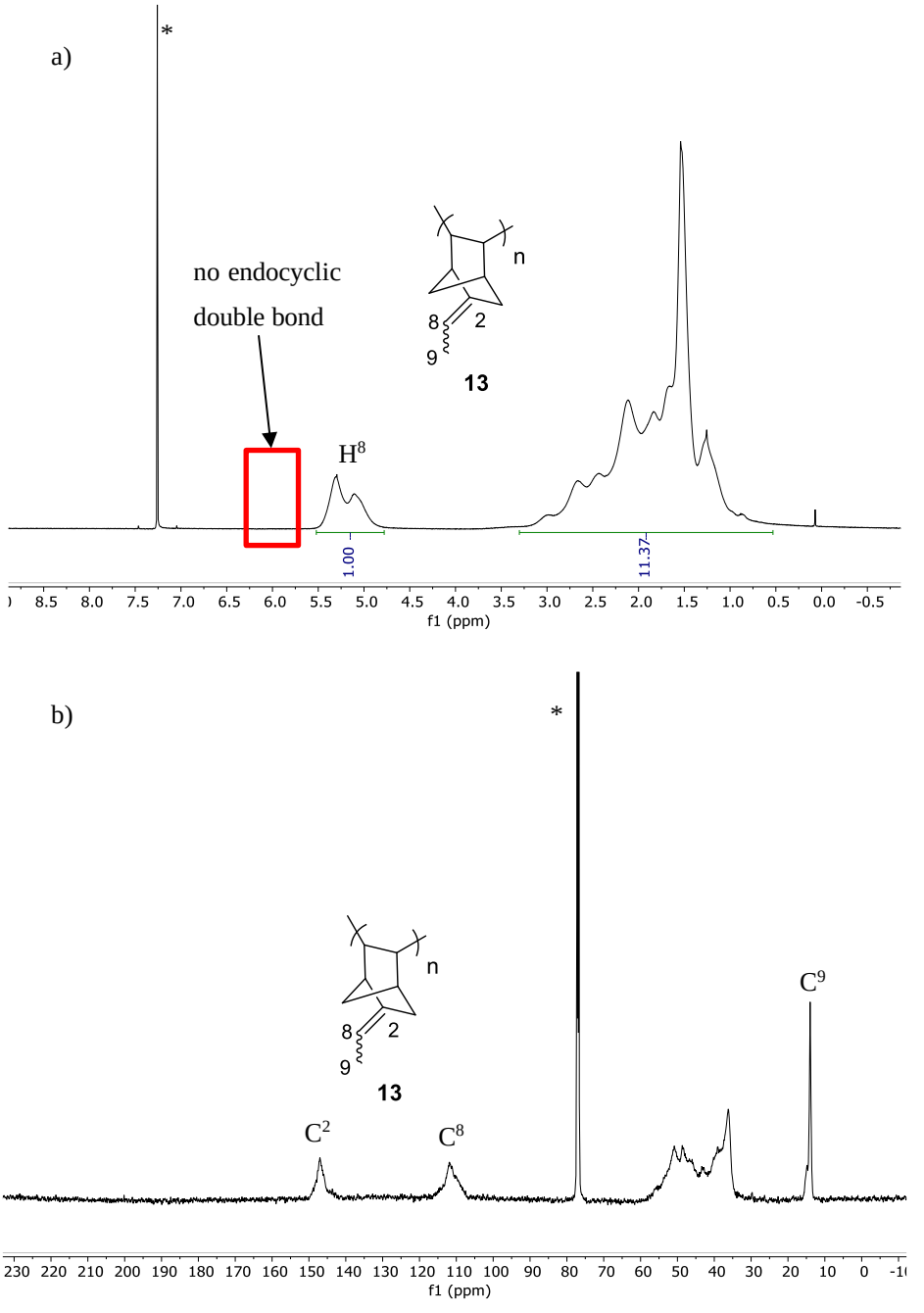

Figure 2.19. a) ^{1}H NMR (500.13 MHz, dry $CDCl_3$) and b) ^{13}C NMR (125.758 MHz, dry $CDCl_3$) of the polymer VA-PENB (**13**) generated with the system **1**/PCy_3/$NaBAr_4^f$ (ratio ENB:Pd = 250:1) at 298 K. * Signal corresponding to the solvent.

In summary, we developed a highly efficient catalytic system for the vinylic addition polymerization of VNB and ENB employing an in-situ benzylic complex with a low ratio Pd:L (1:1) generated mixing the η^3-benzylic dimer **1**, 2 equivalents of PCy_3 and $NaBAr_4^f$ per palladium. The catalytic system shows excellent results even with very low loadings of catalyst (0.0002% mol, 92-95%).

2.2.5. Mechanistic information for the vinylic addition polymerization of norbornene and 5-vinyl-2-norbornene with the catalyst 4e and the system 1/PCy_3/$NaBAr_4^f$

2.2.5.1. Initiation step in the vinylic addition polymerization of norbornene and 5-vinyl-2-norbornene wih the catalyst 4e

The study of the behavior of the palladium benzylic complexes as precursors of Pd-H and the trap of these species in the presence of olefins was studied before in *Chapter 1* (section 1.2.3.2).[44]

The initiation step for the vinylic addition polymerization of norbornene and their derivatives with the benzylic complex **4e** is a particular case of the interaction of this complex with olefins and can follow two different pathways summarized in Scheme 2.11. In *Path a),* the polymerization starts by insertion of the endocyclic double bond into the Pd-H bond of the intermediate $[PdHL_n]^+$ generated by β-hydrogen elimination. On the other hand, in *Path b)*, the insertion of NB into the Pd-$CHPhCH_2C_6F_5$ bond starts the polymerization. It is possible to measure the amount of Pd-H generated in solution by quantifying the amount of *trans*-$PhCH{=}CH_2C_6F_5$ (**2**) formed by ^{19}F NMR. Figure 2.20 shows the amount of **2** generated as a function of the concentration of norbornene after 1 h of reaction.

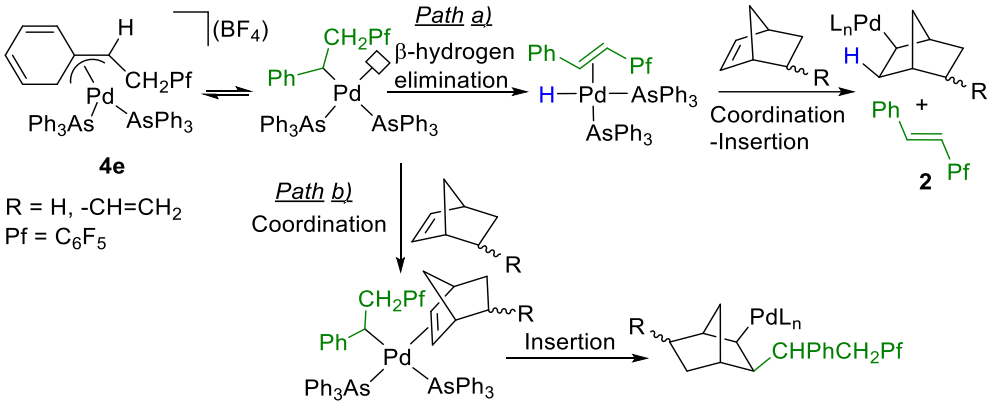

Scheme 2.11. Two possible pathways for the initiation step in the vinylic addition polymerization of norbornene and their derivatives in the presence of the catalyst **4e**.

At low concentration of norbornene (or low ratio [NB]/[**4e**]), the amount of Pd-H generated is high so the initiation step through insertion of NB into the Pd-H bond could be more important. However, at high concentration of norbornene (or high ratio [NB]/[**4e**], closer to the conditions for the polymerization) the amount of Pd-H is low so the initiation step through insertion of the NB into the Pd-CHPhCH$_2$C$_6$F$_5$ will be preferred.

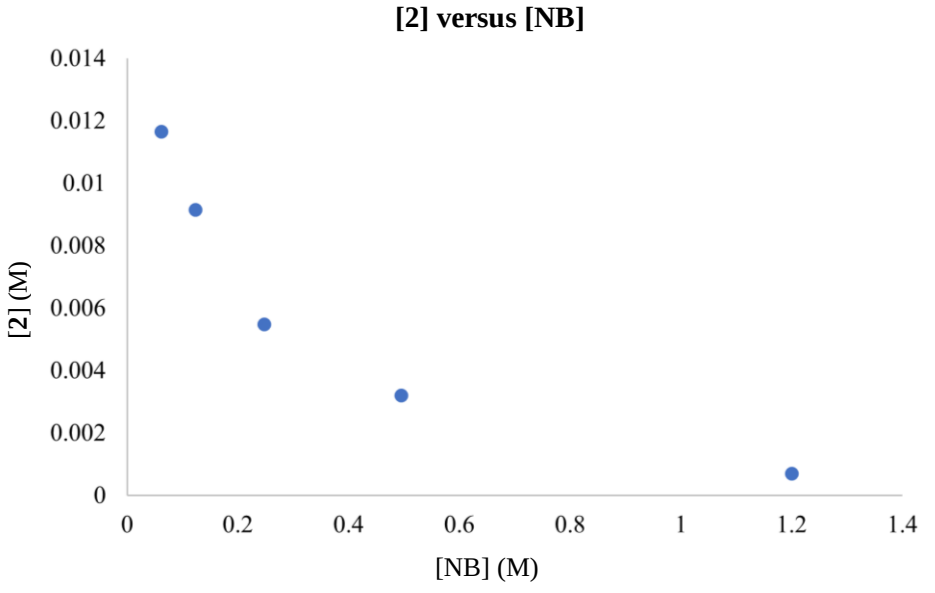

Figure 2.20. Plot of the concentration of *trans*-PhCH=CH$_2$C$_6$F$_5$ (**2**) versus the concentration of NB after 1 hour of reaction.

The initiation step through insertion into the Pd-C^{α} bond can also be confirmed in the homopolymerization of VNB by the analysis of the reaction mixture after 24 h in the ^{19}F NMR (ratio VNB:Pd = 25:1, Figure 2.21). The insertion into the Pd-C^{α} is the main initiation pathway and this is shown by comparing the integral of the broad signal observed for the C_6F_5 group bound to the polymer, VA-PVNB-CHPh(CH_2)C_6F_5, with that of **2**, which represent the maximum amount of $[PdHL_n]^+$ generated in solution. As can be seen in Figure 2.21, 90% of the benzylic group-CHPh$CH_2C_6F_5$ is anchored to the skeleton (insertion into the Pd-C^{α} bond) and only 10 % of *trans*-PhCH=$CH_2C_6F_5$ (**2**) is generated (maximum insertion into the Pd-H bond). Furthermore, the C_6F_5 groups anchored to the skeleton are visible in the ^{19}F NMR of all isolated homopolymers and soluble copolymers generated with the catalyst **4e**.

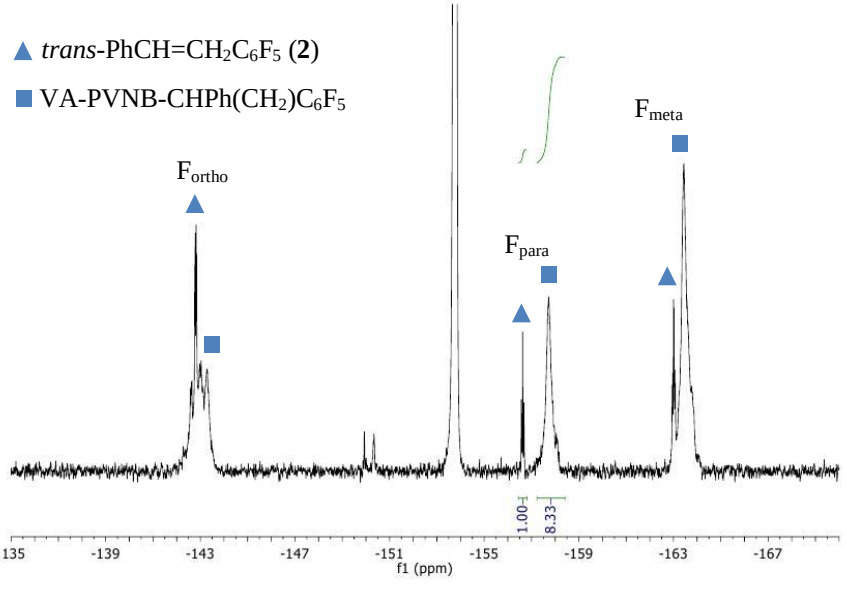

Figure 2.21. ^{19}F NMR spectrum for the polymerization of VNB with the catalyst **4e** after 24h (ratio VNB:Pd = 25:1).

2.2.5.2. Initiation for the vinylic addition polymerization of 5-vinyl-2-norbornene with the precatalyst system 1/PCy_3/$NaBAr_4^f$

As discussed in *Chapter 1*, complex **5** is generated in solution by the addition of 1 equivalent of the PPh_3 per palladium to the dimer **1**. This complex is characterized by a static ^1H NMR

spectrum at 213 K with separated signals for H^2 (δ 6.97) and H^6. The cis arrangement of C^α and PPh_3 is proposed according to the low value of $^3J_{P\text{-}H^\alpha}$ (< 6 Hz) and $^2J_{P\text{-}C^\alpha}$ (< 20 Hz) (Figure 2.22).

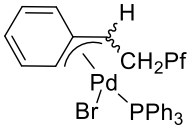

5

Figure 2.22. Structure in solution of complex **5**.

In a similar way, the highly active catalyst for vinylic addition polymerization of VNB and ENB is generated in situ from the dimer **1** and 1 equivalent of PCy_3 per palladium, so it is interesting to get some NMR spectral information about the species formed in solution. First, we checked the complex generated by the addition of one equivalent of PCy_3 per palladium to complex **1** in CD_2Cl_2 or in a mixture of CD_2Cl_2/CD_3CN (85:1 v/v, molar ratio **1**: CD_3CN = 0.02:1) at 195 K (Eq. 2.11 and Figure 2.23).

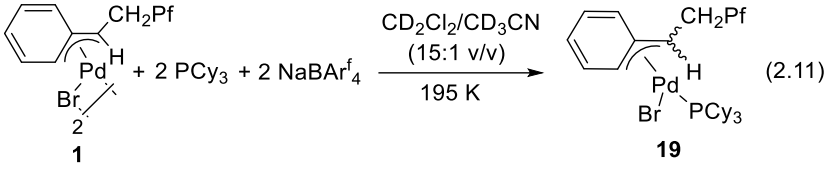

(2.11)

1 **19**

A new complex was formed that shows a new set of signals for the C_6F_5 group in the ^{19}F NMR as well as a little amount of decomposition products: the olefin **2** (9 %) and **3** (3%). In addition, the ^{31}P NMR shows only a broad signal at 48.5 ppm (Figure 2.24, a)). We could not determine the *cis* or *trans* stereochemistry of the complex, but by analogy to complex **5**, the *cis* arrangement of C^α and PCy_3 is depicted.

The η^3 coordination mode of the benzylic fragment is also presents in this complex with a C^α at 53.48 ppm that is in the range of the values that we reported before (Table 1.2). All the aryl carbons are inequivalent and their signals well separated in the ^{13}C NMR spectrum. The ^1H NMR spectrum at 195 K shows one signal for H^2 and H^6 but the inequivalence of H^3 and H^5 (Figure 2.23, a)). This is not consistent with the η^3-σ-η^3 interconversion and fast aryl rotation observed for other fluxional η^3-benzyls, since this would exchange both *ortho*

hydrogens and both *meta* hydrogens. It is difficult to think in a fluxional process that would affect differently to the *ortho* and the *meta* aryl hydrogens, so the coincidental almost equal chemical shifts for H^2 and H^6 cannot be ruled out. The amount of CD_3CN added to the solution will be crucial for the stabilization of the cationic species generated in the next step and has got no effect in spectral pattern of complex **19** (Figure 2.23, b)).

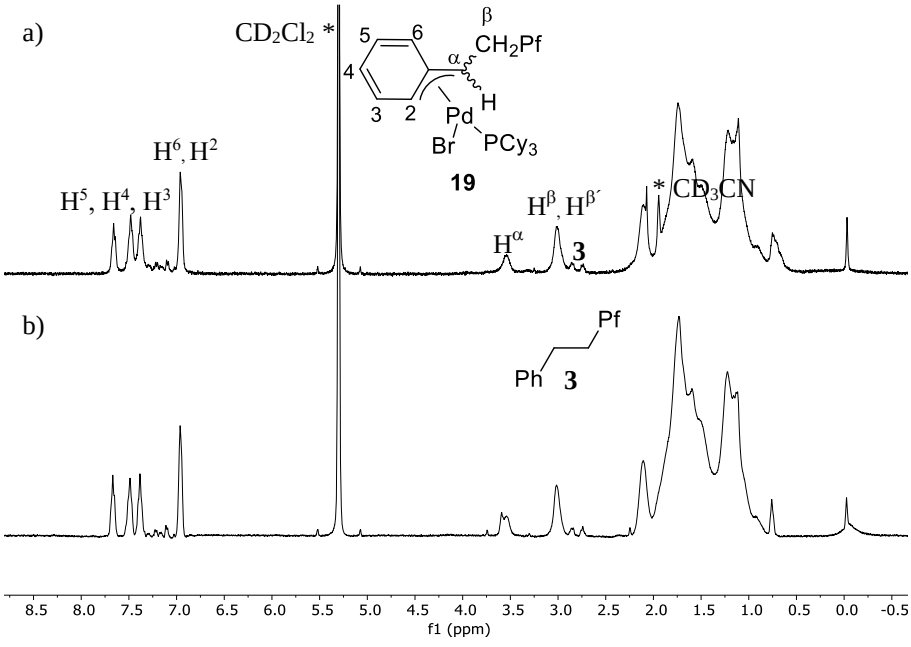

Figure 2.23 ^{1}H NMR spectra of complex **19**: a) in a mixture of CD_2Cl_2/CD_3CN (85:1, v/v) at 195 K. b) in CD_2Cl_2 at 195 K. *Signal corresponding to the solvent.

When in same conditions (CD_2Cl_2/CD_3CN = 85:1 v/v, molar ratio **1**: CD_3CN = 0.02:1) 2.2 equivalents of PCy_3 per palladium were added to complex **1** we did not observe any changes in the spectroscopic data. The ^{31}P NMR shows the signal of complex **19** (48.5 ppm) and free PCy_3 (Figure 2.24, b)). The second molecule of PCy_3 is not coordinating to the palladium center in contrast with the reaction with PPh_3 that led to the pentacoordinated complex **6d** (*Chapter 1*). The high cone angle of the PCy_3 in contrast with the PPh_3 (170˚ vs 145˚) is preventing the coordination of an additional ligand.[107]

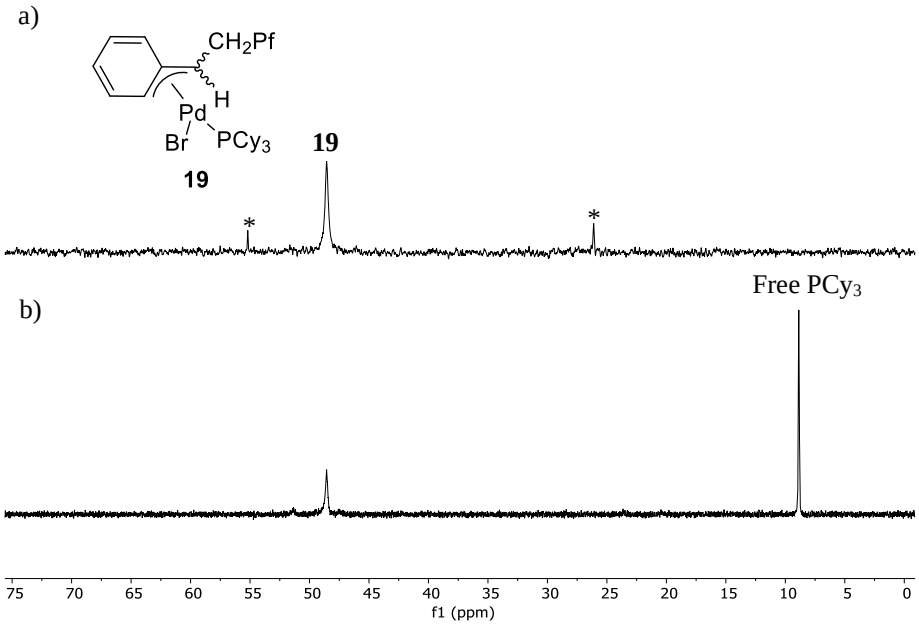

Figure 2.24. a) ^{31}P NMR spectra of complex **19** in a mixture of CD_2Cl_2/CD_3CN (85:1 v/v) at 195 K generated from **1** and 1 equivalent of PCy_3 per palladium. b) ^{31}P NMR spectra of complex **19** in a mixture of CD_2Cl_2/CD_3CN (85:1 v/v)) at 195 K generated from **1** and 2.2 equivalents of PCy_3 per palladium. *unidentified compounds.

When a solution of complex **19** in a mixture of CD_2Cl_2/CD_3CN (85:1 v/v, mol ratio **1**:CD_3CN = 0.02:1) at 195 K was mixed with 2.3 equivalents of $NaBAr_4^f$ the expected cationic complex **20** is generated in situ in solution. Complex **20** shows similar spectroscopy features in the ^1H NMR than complex **19** but we can observe some changes in the chemical shifts in the ^{19}F NMR (Figure 2.25) and in the ^{31}P NMR (48.5 ppm for **19** and 46.2 ppm for **20**). It is important to note that in the absence of the amount of CD_3CN added to the solution complex **19** decomposes very fast in the presence of $NaBAr_4^f$ by β-hydrogen elimination to form **2** and several unidentified compounds. The role of the weakly coordinating acetonitrile is to stabilize the naked complex generating in solution upon removal of the bromide. In the polymerization experiments the catalyst is generated in situ always in the presence of the VNB or ENB.

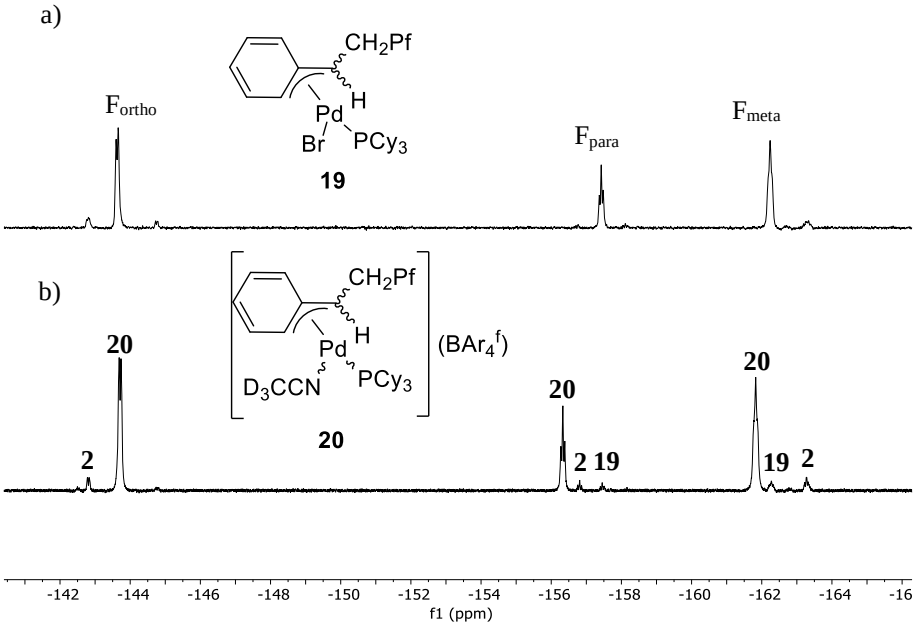

Figure 2.25. a) ^{19}F NMR spectra in a mixture of CD_2Cl_2/CD_3CN (85:1 v/v) at 195 K of: a) complex **19**; b) complex **20** (a residual amount of complex **19** is still visible in the ^{19}F NMR, as well as the olefin **2**).

Once we have the information of the species generated in solution from the precatalyst mixture, we studied the initiation step of the synthesis of VA-PVNB with this catalytic system in conditions that resemble the polymerization reaction. As we mentioned before, we did not find any evidence of a C_6F_5 anchored to the polymer, even in a short polymer (ratio VNB:Pd = 250:1), indicating that the initiation step via insertion into the Pd-C^{α} bond is not the main route. The polymerization experiments with this catalytic system were always carried out by mixing first the complex **1** in CH_2Cl_2 and VNB followed by the addition of the PCy_3 and the $NaBAr_4^f$ (Method a, see Experimental Section). While we mixed complex **1** and VNB we observed a change in the color of the solution, indicative of a reaction between the VNB and the complex **1**. So, we performed an experiment mixing the yellow suspension of **1** in $CDCl_3$ and five equivalents of VNB per palladium. Instantly, the suspension turns to a clear yellow solution. All the signals of complex **1** disappear in the ^{19}F NMR and we only observe the formation of the olefin **2** (Figure 2.26). Therefore, a $PdHL_n$ intermediate is generated by β-hydrogen elimination and the insertion of the VNB must occur into the Pd-H bond. This observation is crucial to understand why we do not observe any signal for the C_6F_5 group in the polymer.

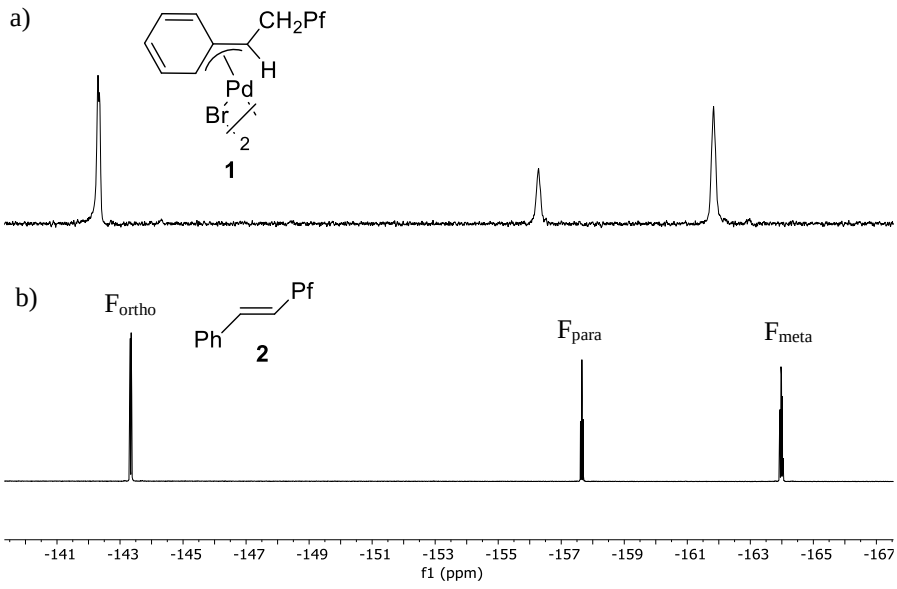

Figure 2.26. a) ^{19}F NMR in $CDCl_3$ of dimer **1** at 298 K. b) ^{19}F NMR in $CDCl_3$ after the reaction of dimer **1** in the presence of five equivalents of VNB per palladium at 298 K.

Scheme 2.12 represents the plausible steps in this initiation process. The first step is the trap of the palladium hydride species generated from **1** by insertion of the endocyclic double bond of VNB, as observed before for R-(+)-limonene (*Chapter 1*). From the insertion product, a cationic complex with the coordinated phosphine is the most probable active compound for the vinylic addition polymerization of VNB with this catalytic system.

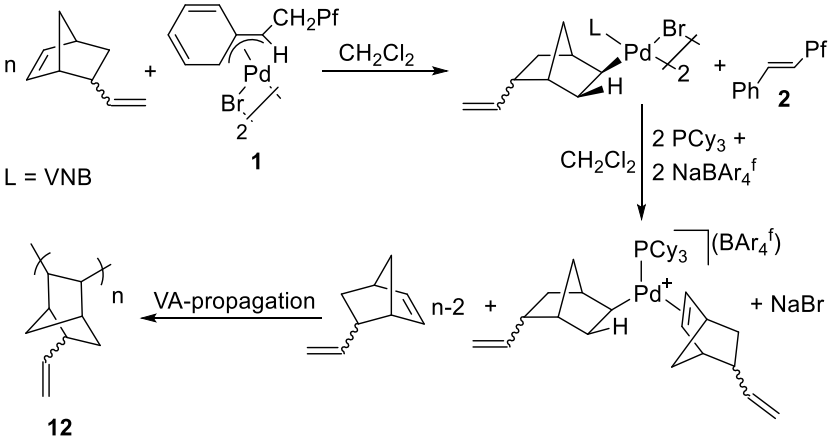

Scheme 2.12. Possible initiation pathway in the vinylic addition polymerization of VNB with the system **1**/PCy_3/$NaBAr_4^f$ when mixing the precatalyst component in the presence of VNB (Method a).

At this point we wondered if complex **20**, generated at low temperature by mixing complex **1**, PCy_3 and $NaBAr_4^f$ could be active in the vinylic addition polymerization of VNB. Thus, we generated the complex **19** at low temperature without the presence of additional amount of CD_3CN and immediately we added the $NaBAr_4^f$ followed by the VNB (Method b, Scheme 2.13, Experimental Section for more details). The conditions were the same reported for entry 5, Table 2.7, except for the mixing procedure of the precatalyst components.

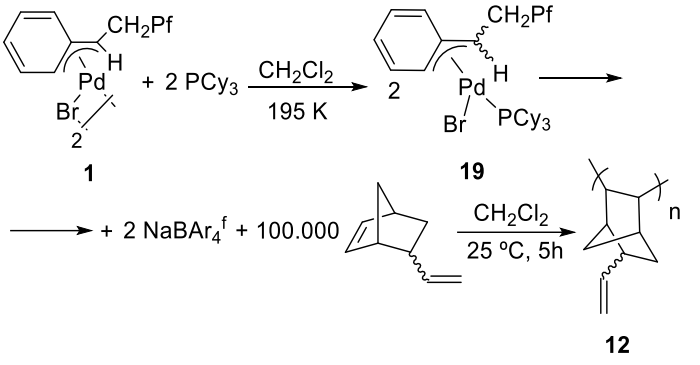

Scheme 2.13. Polymerization of VNB following the conditions in entry 5, Table 2.7 but previously mixing the precatalyst component at low temperature in the absence of VNB (Method b).

The yield of the polymerization (53 %) is very similar to the one reported in entry 5, Table 2.7 (48 %) confirming that the cationic complex resulting fromm **19** and $NaBAr_4^f$ is also active in the vinylic addition polymerization of VNB. The initiation step in this case is also the insertion of the VNB into the $PdHL_n$ generated from β-H elimination in the benzylic group. As we can see in the ^{19}F NMR of a reaction performed following the Method b (ratio **1**:PCy_3:$NaBAr_4^f$:VNB = 1:2:2:125), the benzylic fragment undergoes β-H elimination (Figure 2.27). Minor signals of unidentified compounds also appear but they do not match those corresponding to the insertion of the VNB into the Pd-$CHPhCH_2C_6F_5$ bond. This behavior contrasts with the initiation observed for the vinylic addition polymerization of VNB with the catalyst **4e** where the insertion of VNB occurs into the Pd-$CHPhCH_2C_6F_5$ bond preferentially (90% of $CHPhCH_2Pf$ anchored to the skeleton versus 10 % that undergoes β-H elimination, Figure 2.21).

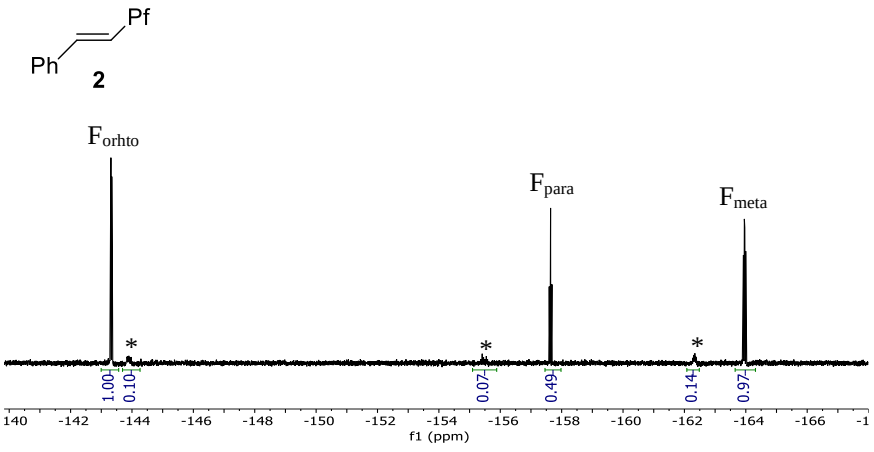

Figure 2.27. ^{19}F NMR in $CDCl_3$ of the reaction mixture of **1**:PCy_3:$NaBAr_4^f$:VNB = 1:2:2:125 at 298 K. *minor signals of unknown compounds.

2.2.6. Functionalization post-polymerization of VA-Co-PNB-VNB (15) and VA-Co-PNB-BNB (16)

The direct functionalization of VA-PNBs by copolymerization of NB and substituted norbornenes with polar functional groups such as CH_2OH or COOH generates insoluble polymer with low yields (Table 2.3). So, this route is not a convenient way to incorporate polar groups in the skeleton of VA-PNBs. In contrast, the copolymers of NB and alkenyl-norbornenes can be synthesized with good yields, are soluble in common organic solvents as $CHCl_3$ and it is possible to control their degree of functionalization by the ratio NB:VNB in the monomer feed, a crucial feature for the application in the field of supported catalysis. We selected the skeleton of VA-Co-PNB-VNB (**15**) and VA-Co-PNB-BNB (**16**) with pendant terminal double bonds as a starting materials for the synthesis of new functional groups in the polymers. In this section we describe the use of two well-known reactions for the incorporation of some functional groups: the hydroboration and the hydrosylilation of olefins. The regioselective hydroboration of the polymer **15** in the presence of $HBBr_2 \cdot SMe_2$ leads the formation of an intermediate alkyldibromoborane. This intermediate was not isolated but easily reacts with H_2O to generate the polymeric boronic acid **21** or with a mixture of H_2O_2/NaOH to afford the hydroxyl polymer **22** (Scheme 2.14). All the functionalized polymers are insoluble in common organic solvents, so they were characterized by solid state

CP-MAS NMR and IR spectroscopy. The dramatic changes in the solubility of these VA-PNB polymers upon functionalization is known and it was reported before for other functional groups, such as imidazolium fragments, by our research group.[103d,e,112] In addition to the structural changes introduced by the new substituent, a modification of the conformational behavior of the rigid bicyclic units in the polymer backbone during the hydroboration/oxidation processes could also contribute to this change in solubility behavior.[123]

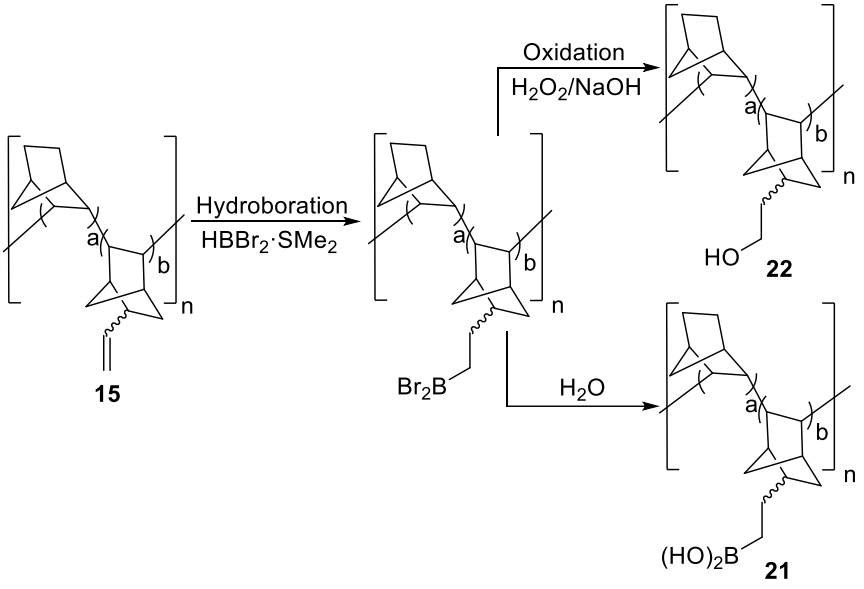

Scheme 2.14. Synthetic route for the formation of polymers **21** and **22** by hydroboration.

The complete hydroboration of the polymer **15** can be observed in the IR spectrum of the boronic acid **21** (Figure 2.28). It shows the complete disappearance of the bands for the pendant double bonds (905 cm^{-1}, δ-C=C-H, Figure 2.28, a)) and the formation of new bands assigned to the boronic acid (3382 cm^{-1}, ν-OH; 1348 cm^{-1}, ν-B-O; 1632 cm^{-1}, δ-OH, Figure 2.28, b)).

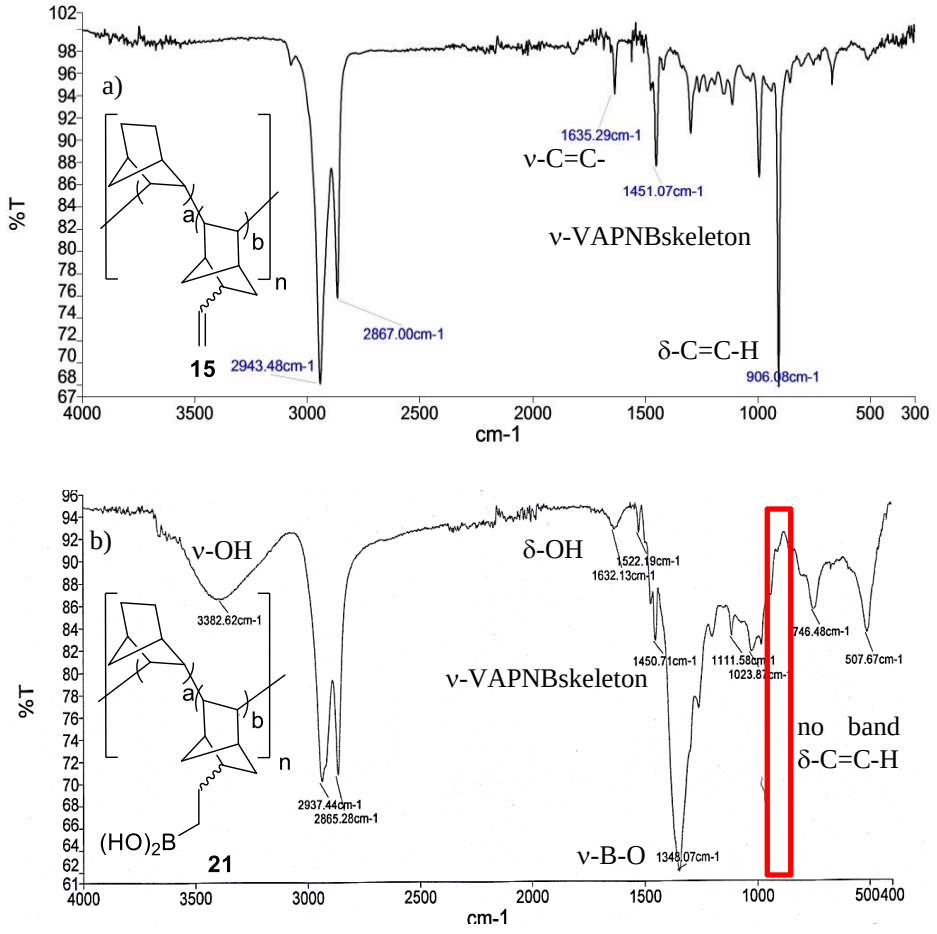

Figure 2.28. IR spectra of: a) VA-Co-PNB-VNB (**15**) and b) boronic acid VA-Co-PNB-NB$(CH_2)_2B(OH)_2$ (**21**).

The disappearance of the olefinic resonances is clear in the ^{13}C solid state NMR of the hydroxyl polymer **22**. The IR spectrum clearly indicates the formation of the alcohol by some representative absorptions for this group present in the polymer **22** (3354 cm^{-1} ν-OH and 1047 cm^{-1} ν-C-O, Figure 2.29).

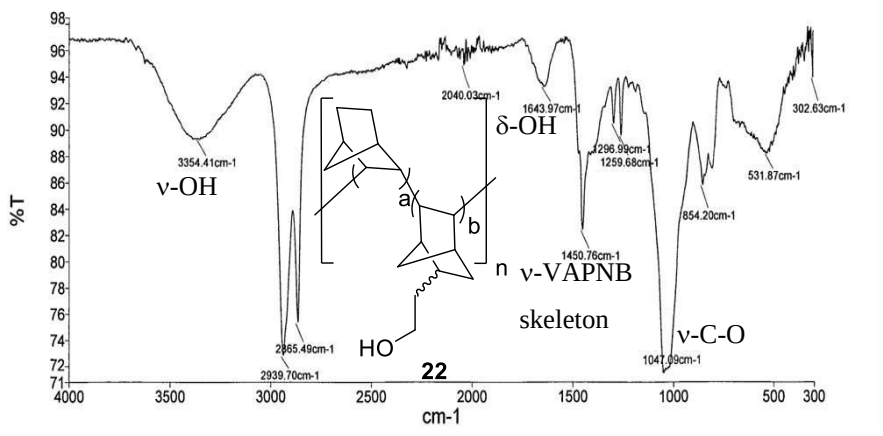

Figure 2.29. IR spectrum of the functional polymer VA-Co-PNB-NB$(CH_2)_2$OH (**22**) with hydroxyl groups.

The hydroxyl group can be a good starting point for the synthesis of new functional groups. For example, in the course of a collaboration to develop new supported phosphite ligands with the group of Prof. Pericás at the ICIQ, we synthesized a 1,3,2-tetramethylethylene phosphite anchored to VA-PNBs (Eq. 2.12).[124] The copolymer **22** reacts with two equivalents of NEt_3 and 1,3,2-tetramethylethylene chlorophosphite to obtain the pinacolyl phosphite anchored to the skeleton of VA-PNB (**23**). The ammonium salts generated can be easily washed with MeOH.

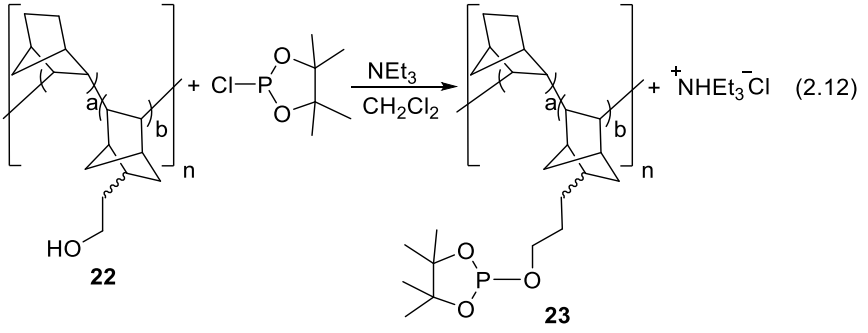

[124] a) Raducan, M.; Rodríguez-Escrich, C.; Cambeiro, X. C.; Escudero-Adán, E. C: Pericás, E. C.; Echavarren, A. M. A *Chem. Commun*., **2011**, *47*, 4893-4895. b) Swennenhuis, B. H. G.; Chen, R.; Van Leeuwen, P. W. N. M.; Vries, J. G.; Kamer, P. C. J. *Eur. J. Org. Chem*. **2009**, 5796-5803.

The polymer was characterized by solid state CP-MAS NMR and IR spectroscopy. The ^{31}P CP-MAS NMR clearly shows a signal at 147.7 ppm typical of phosphite compounds. The presence of P-O band (963 cm^{-1}) in the IR spectrum is also significative.[125]

The hydrosililation of olefins is another route to functionalize double bonds with silane groups, that are versatile synthetic fragments.[126] Well-stablished metal-catalyzed methods are available, in particular using platinum catalysts. Because of the high efficiency (very low amounts of Pt(0) are necessary) and commercial availability, we selected the Karstedt catalyst for our hydrosylilation reaction. In this case, we selected the copolymer with the longer chain (Va-Co-PNB-BNB, **16**) to demonstrate that this polymer can also be functionalized. The hydrosylilation of the pendant double bond of the VA-Co-PNB-BNB (**16**) in the presence of an excess of $SiHClMe_2$ and the Karstedt catalyst gave a white polymer which was isolated with good yield (81.1 %) and it was insoluble in common organic solvents (Eq. 2.13).

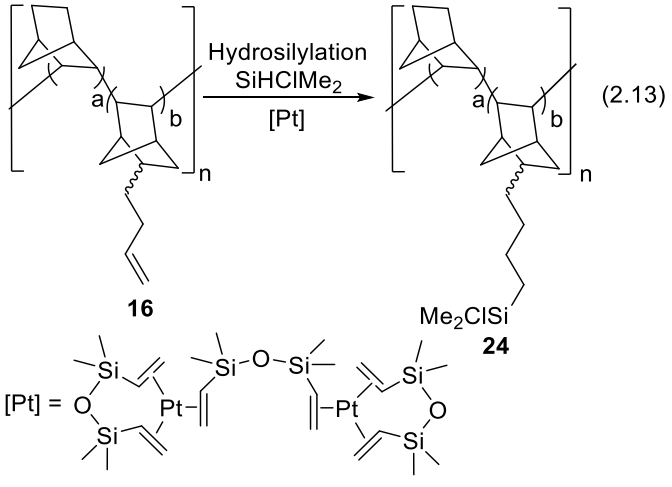

(2.13)

The characterization of the polymer **24** was made using the IR spectroscopy. New bands for the ν-Si-C (846 cm^{-1}, 809 $cm^{-1}$and 789 cm^{-1}) and ν-Si-Cl (475 cm^{-1}) can be assigned to the polymer **24** (Figure 2.30, b)).[127] Also in this case, the disappearance of the band for the ν-

[125] Williams, B. D. G.; Netshiozwi, T. E. *Tetrahedron*, **2009**, *65*, 9973-9982.
[126] a) Pandarus, V.; Ciriminna, R.; Gingras, G.; Béland, F.; Kaliaguine, S., Pagliaro, M. *Green Chem*. **2019**, *21*, 129-140. b) Nakajimaa, Y.; Shimada, S. *RSC advances* **2015**, 20603-20616. c) Chungkyun, K., Kyungmi, A. *J. Orgrnomet. Chem.* **1997**, *547*, 55-63. d) Sommer, L. H.; Pietrusza, E. W.; Whitmore, F. C. *J. Am. Chem. Soc*. **1947**, *69*, 188-188. e) Speier, J. L. Webster, J. A. G.: Barnes, H. *J. Am. Chem. Soc*. **1957**, *79*, 974-979.
[127] Niemiec, W.; Szczygiel, P.; Jelén, P.; Handke, M. *J. Mol. Struct.* **2018**, *1164*, 217-226.

C=C- bond (1640 cm^{-1}) and the band for the δ-C=C-H (963 cm^{-1} and 907 cm^{-1}) is clear in the IR spectrum (Figure 2.30, a)). A small amount of the hydrolysis of the Si-Cl bond is observed in all of silane polymers by the presence of a Si-O band at 1047 cm^{-1} in the IR spectrum (Figure 2.30 b)).

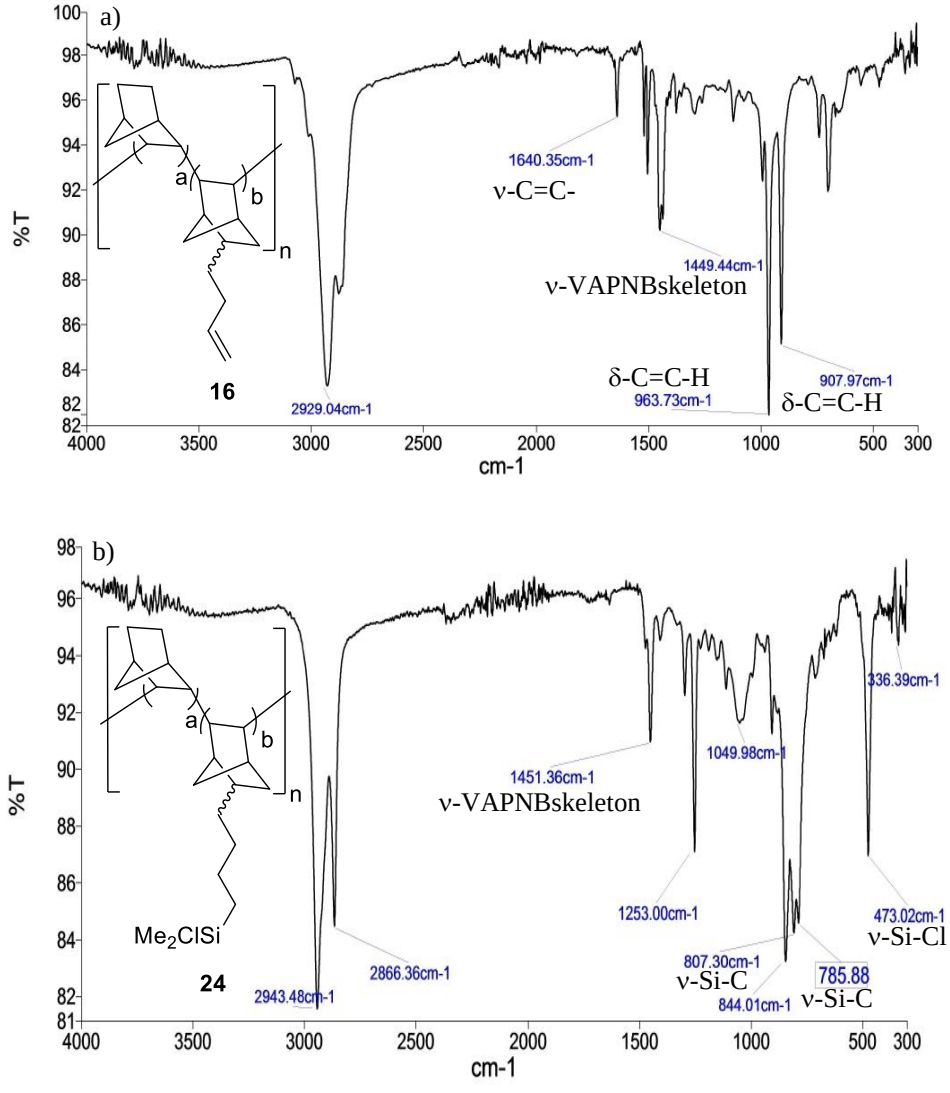

Figure 2.30. IR spectra of: a) VA-Co-PNB-BNB (**16**) and b) VA-Co-PNB-NB$(CH_2)_4SiClMe_2$ (**24**).

The presence of the Si-Cl bond in the skeleton of the polymer is a good way for the formation of new silicon bonds such as Si-H or Si-allyl as represented in Scheme 2.15. The allyl substituent is easily incorporate to the polymer by the addition of a little excess of the corresponding Gringard reagent prepared in situ. The IR spectrum of the polymer **25** reflects the disappearance of the Si-Cl band and the formation of new bands typical for a terminal double bond (1634 cm^{-1}, ν-C=C-). On the other hand, the Si-H is generated by the addition of an excess of $LiAlH_4$ in Et_2O to the polymer **24**. The formation of Si-H groups in the polymer **26** is very clear in the IR spectrum with an intense band at 2108 cm^{-1} associated with the ν-Si-H.

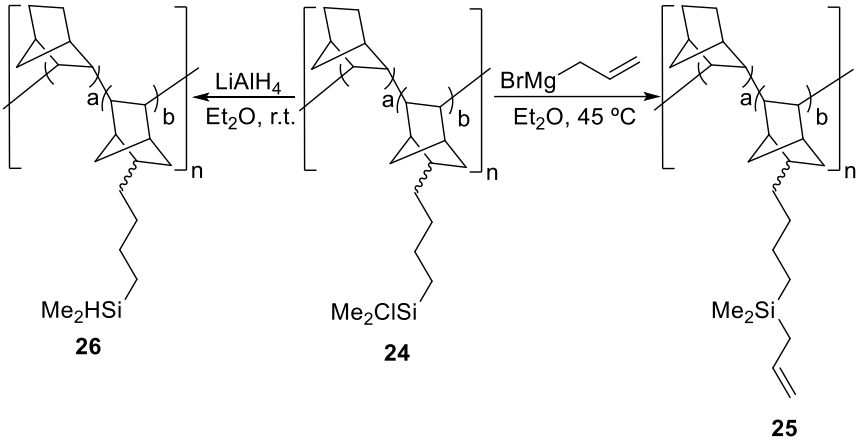

Scheme 2.15. Synthetic route for the formation of the new Si-allyl in the polymer **25** and Si-H in the polymer **26**.

2.3. Conclusions

η^3-benzylic complexes of palladium(II) are useful catalyst for the vinylic addition (VA) polymerization of norbornene and norbornene derivatives. The catalyst showing the best results for the synthesis of VA-PNB is $[Pd(\eta^3\text{-}CHPhCH_2C_6F_5)(AsPh_3)_2](BF_4)$ (**4e**), a cationic complex with labile ligands. It shows low activity in the VA-homopolymerization of alkenyl-norbornenes, but it is efficient in the copolymerization of alkenyl norbornenes with norbornene generating copolymers with good yields and a functionalization range that depends on the monomer feed ratio. The direct incorporation of polar functional groups as COOH and CH_2OH by direct copolymerization is not possible with the catalyst **4e**.

A highly active catalyst for the vinylic addition polymerization of VNB was developed by the combination of the dimer η^3-benzylic complex **1**, PCy_3 and the crucial counteranion BAr_4^{f-}. The homopolymerization of 5-vinyl-2-norbornene (VNB) can be quantitatively carried out using a molar amount of Pd as low as 0.01% (10 ppm). This is the highest activity reported for the VA-polymerization of this monomer. The use of the BAr_4^{f-} counterion is crucial as well as a donating, bulky phosphine such as PCy_3.

The study of the initiation step with the catalyst **4e** showed a preferential insertion of the norbornene or the VNB into the Pd-$CHPhCH_2C_6F_5$ bond. In contrast, in the VA-polymerization of VNB with the precatalyst system **1**/PCy_3/$NaBAr_4^f$ the initiation step occurs exclusively by the insertion of the monomer into a Pd-H bond generated in situ by β-hydrogen elimination.

The copolymers VA-Co-PNB-VNB (**15**) and VA-Co-PNB-BNB (**16**) are excellent starting materials for the incorporation of functional groups by functionalization post-polymerization of their alkenyl pendant groups employing well-known reactions such as the hydroboration and the hydrosilylation. With these methods it is possible the incorporation of hydroxyl group (**22**), a phosphite compound (**23**) and different silane derivatives (**24**, **25** and **26**) in VA-PNBs. This is important due to the difficult direct polymerization of norbornene derivatives with these functional groups.

2.4. Experimental Section

2.4.1. Materials and general considerations

All the reagents were purchased from commercial sources without any further purification. The 5-vinyl-2-norbornene, 5-ethylidene-2-norbornene, 5-methanol-2-norbornene and 5-carboxylic acid-2-norbornene are a mixture of *endo*/*exo* isomers in a ratio 80:20. The 5-(but-1-en-4-yl)-2-norbornene was synthesized by a Diels-Alder reaction between DCP (dicyclopentadiene) and 1,6-hexadiene following a reported method and also is a mixture of *endo*/*exo* isomers in ratio 80:20.[128] A solution of norbornene in CH_2Cl_2 was used for all the polymerization experiments whose concentration was determined by titration by ^{1}H NMR. The internal standard employed was $C_6H_3Br_3$. A solution of PCy_3 was prepared by weighing with a high precision instrument and dissolved under N_2 in dry toluene (M = 0.038). All solvents were used without any purification except the CH_2Cl_2 that was dried using an SPS PS-MD-5 solvent purification system and the toluene that was dried using Na. $CDCl_3$ was dried using neutral activated aluminum oxide and CD_2Cl_2 was dried with CaH_2. The platinum(0)-1,3-divinyl-1,1,3,3-tetramethyldisiloxane complex (Karstedt catalyst) is commercial available and consist in a solution in xylene with an approximate amount of Pt of 2%. The synthesis of the complexes $[Pd_2(\mu\text{-}Br)_2(\eta^3\text{-}CHPhCH_2C_6F_5)_2]$ (**1**), $[Pd(\eta^3\text{-}CHPhCH_2C_6F_5)(AsPh_3)_2](BF_4)$ (**4e**), $[Pd(\eta^3\text{-}CHPhCH_2C_6F_5)(PPh_3)_2](BF_4)$ (**4d**) and $[Pd(\eta^3\text{-}CHPhCH_2C_6F_5)(PhSCH_2)_2](BF_4)$ (**4c**) was described in *Chapter 1*. All polymerizations were carried out under N_2 by standard Schlenks techniques. The 1,3,2-tetramethylethylene chlorophosphite (PClpin) was synthesized using a reported method.[129] The $HBBr_2{\cdot}SMe$ is a commercial solution in CH_2Cl_2 with a molar concentration of 1 M.

NMR spectra in solution were recorded at 298 K unless note using Bruker AV-400, Agilent MR-500 and MR-400 instruments. Chemical shifts (δ) are reported in ppm and referenced to $SiMe_4$ (^{1}H and ^{13}C), $CFCl_3$ (^{19}F) and 85% H_3PO_4 (^{31}P). The solid state NMR spectra were recorded at 293 K under magic angle spinning (MAS) in a Bruker AV-400 spectrometer using a Bruker BL-4 probe with 4mm diameter zirconia rotors spinning at 8 kHz. ^{13}C CP MAS NMR spectra were measured at 100.61 MHz and recorded with proton decoupling (tppm), with a 90º pulse length of 4.5 µs and a contact time of 3 ms and recycle delay of 3 s. The ^{13}C NMR spectra were referred to glycine (CO signal at 176.1 ppm). IR spectra were collected on the solid samples using a Perkin-Elmer FT/IR SPECTRUM FRONTIER spectrophotometer with CsI + ATR diamond accessory. Size exclusion chromatography (SEC, also gel permeation chromatography, GPC) was carried out using a WatersSEC system on a three-column bed (Styragel 7.8_300 mm columns: 50-100000, 5000-500000 and 2000-4000000 Da)

[128] H. G. G. Dekking, *J. Pol. Sci.* **1961**, *55*, 525-530.
[129] A. Zwierzak, *Can. J. Chem.* **1967**, *45*, 2501-2512.

and a Waters 410 differential refractometer. SEC samples were run in $CHCl_3$ at 313 K and calibrated to polystyrene standards.

2.4.2. Homopolymerization and oligomerization experiments

2.4.2.1. Synthesis of VA-PNB (11)

In a Schlenk tube a solution of norbornene in CH_2Cl_2 (0.64 mL, 5 mmol; 7.84 M) was diluted with 3.5 mL of dry CH_2Cl_2 under N_2 ($[NB]_o$ = 1.2 M). Subsequently, the catalyst **4e** (10.73 mg, 0.01 mmol) was added generating a yellow solution. After 15 min, a white precipitate appeared in the solution and the suspension was stirred 24 h at 25 ºC. MeOH (15 mL) were added to the suspension, and the mixture was stirred for 30 min at room temperature and filtered off. The white solid was washed with MeOH (2 x 20 mL) and air dried for 6 h and in a vacuum stove (60 mbar) at 40 ºC for 12 h (0.45 g, 95.7% yield). IR (neat, cm^{-1}): 2943 (ν-CH asym.), 2866 (ν-CH sym.), 1449 (ν-VAPNBskeleton).

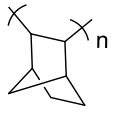

11

2.4.2.2. Synthesis of VA-PVNB (12)

In a Schlenk tube 5-vinyl-2-norbornene (0.71 mL, 5 mmol) was diluted in 3.5 mL of dry CH_2Cl_2 under N_2 ($[VNB]_o$ = 1.2 M). Subsequently, the catalyst **4e** was added (10.76 mg, 0.01 mmol) and the yellow solution was stirred 24 h at 25 ºC. MeOH (15 mL) was added to the solution inducing the precipitation of the polymer. The suspension was stirred for 30 min at room temperature and filtered off. The white solid was washed with MeOH (2 x 20 mL) and air dried for 6 h and in a vacuum stove (60 mbar) at 40 ºC for 12 h (0.07 g, 16.6% yield). ^{1}H RMN (500.13 MHz, δ, $CDCl_3$): 6.07-5.63 (b, 1H, H^8), 5.5-5.15 (b, 1H, $H^{8'}$), 5.16-4.77 (b, 2H, H^9), 2.80-0.76 (20H, $H^{9'}$, H^7, $H^{7'}$, H^6, $H^{6'}$, $H^{5'}$, H^5, H^4, $H^{4'}$, H^3, $H^{3'}$, H^2, H^1, $H^{1'}$). ^{13}C (125.66 MHz, δ, $CDCl_3$): 150-145 ($C^{2'}$), 146-145 (*endo* C^8), 145-141.6 (*exo* C^8), 114.5-112.5 (*exo* C^9), 114.5-112.5 (*endo* C^9), 113-108 ($C^{8'}$), 58.6-30 (C^7, $C^{7'}$ C^6, $C^{6'}$, C^5, $C^{5'}$, C^4, $C^{4'}$, C^3, $C^{3'}$, C^2, C^1, $C^{1'}$), 14.0 ($C^{9'}$).^{19}F NMR (470.592 MHz, δ, $CDCl_3$): -142 (b, F_{ortho}), -157.9 (b, F_{para}), -163 (b, F_{meta}). IR (neat, cm^{-1}): 2941 (ν-CH asym.), 2873 (ν-CH sym.), 1635 (ν-C=C-), 1449 (ν-VAPNBskeleton), 904 (δ-C=C-H). M_w (Da) = 7161. M_w/M_n = 1.09.

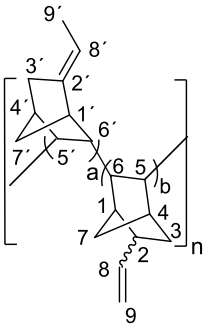

12

2.4.2.3. Synthesis of VA-PENB (13)

In a Schlenk tube 5-ethylidene-2-norbornene (0.67 mL, 5 mmol) was diluted in 3.5 mL of dry CH_2Cl_2 under N_2 ($[ENB]_0$ = 1.2 M). Subsequently, the catalyst **4e** was added (10.76 mg, 0.01 mmol) and the yellow solution was stirred 24 h at 25 ºC. MeOH (15 mL) was added to the solution inducing the precipitation of the polymer. The suspension was stirred for 30 min at room temperature and filtered off. The white solid was washed with MeOH (2 x 20 mL) and air dried for 6 h and in a vacuum stove (60 mbar) at 40 ºC for 12 h (0.19 g, 32% yield). ^{1}H RMN (500.13 MHz, δ, $CDCl_3$): 5.5-4.8 (b, 1H, H^8), 3.5-0.8 (b, 11H, H^9 H^7, H^6, H^5, H^4, H^3, H^1). ^{13}C (125.66 MHz, δ, $CDCl_3$): 149.8-141.1 (C^2), 117-107 (C^8), 58.6-32 (C^7, C^6, C^5, C^4, C^3, C^1), 14.0 (C^9). ^{19}F NMR (470.592 MHz, δ, $CDCl_3$): -140-144 (b, F_{ortho}), -157.9 (b, F_{para}), -163 (b, F_{meta}). IR (neat, cm^{-1}): 2944 (ν-CH asym.), 2913 (ν-CH sym.), 1690 (ν-C=C-), 1434 (ν-VAPNBskeleton), 808 (δ-C=C-H). M_w (Da) = 16404. M_w/M_n = 1.57.

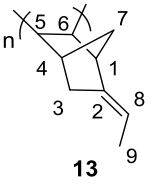

13

2.4.2.4. Synthesis of VA-PBNB (14)

In a Schlenk tube 5-(but-1-en-4-yl)-2-norbornene (0.44 g, 2.5 mmol) was diluted in 1.6 mL of dry CH_2Cl_2 under N_2 ($[BNB]_0$ = 1.2 M). The catalyst **4e** was added (5.38 mg, 0.005 mmol) and the yellow mixture was stirred 24 h at 25 ºC. MeOH (15 mL) was added to the solution inducing the precipitation of the polymer. The suspension was stirred for 30 min at room temperature and filtered off. The white solid was washed with MeOH (2 x 20 mL) and air dried for 6 h and in a vacuum stove (60 mbar) at 40 ºC for 12 h (0.102 g, 23.2% yield). ^{1}H RMN (500.13 MHz, δ, $CDCl_3$): 5.9-5.7 (b, 1H, H^{10}), 5.6-5.3 (b, 2H, $H^{10´}$, $H^{9´}$), 5.10-4.9 (b,

2H, H^{11}), 3-0.5 (b, 27H, $H^{11´}$, H^9, H^8, $H^{8´}$, H^7, $H^{7´}$, H^6, $H^{6´}$, H^5, $H^{5´}$, H^4, $H^{4´}$, H^3, $H^{3´}$, H^2, $H^{2´}$, H^1, $H^{1´}$). ^{13}C (125.66 MHz, δ, $CDCl_3$): 140-138.5 (C^{10}), 133-124 ($C^{10´}$, $C^{9´}$), 115-113 (C^{11}), 60-30 (C^9, C^8, $C^{8´}$, C^7, $C^{7´}$, C^6, $C^{6´}$, C^5, $C^{5´}$, C^4, $C^{4´}$, C^3, $C^{3´}$, C^2, $C^{2´}$, C^1, $C^{1´}$), 17.0 (*trans* $C^{11´}$), 13.1 (*cis* $C^{11´}$). ^{19}F NMR (470.592 MHz, δ, $CDCl_3$): -142-144.5 (b, F_{ortho}), -157 (b, F_{para}), -163 (b, F_{meta}). IR (neat, cm^{-1}): 2941 (ν-CH asym.), 2873 (ν-CH sym.), 1635 (ν-C=C-), 1449 (ν-VAPNBskeleton), 904 (δ-C=C-H). M_w (Da) = 17287. M_w/M_n = 1.53.

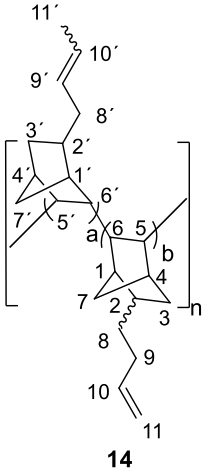

14

2.4.2.5. Polymerization of VNB (short-12, VNB:Pd = 25:1)

The catalyst **4e** (60 mg, 0.055 mmol) was placed in a Schlenk tube under N_2 and it was diluted in 1 mL of dry CH_2Cl_2. To the yellow solution was added the VNB (0.2 mL, 1.4 mmol) and the mixture was stirred 24 h at 25 ºC. After this time, the solution was evaporated to dryness and the residue was dissolved in 5 mL of Et_2O. MeOH (10 mL) was added to the solution inducing the precipitation of the polymer as a white solid. The suspension was stirred for 30 min at room temperature, the solid was filtered off and washed with MeOH (2 x 10 mL). The white solid was air dried for 6 h (0.09 g, 54% yield). ^{1}H RMN (500.13 MHz, δ, $CDCl_3$): 6.1-5.5 (b, 1H, H^8), 5.5-5.15 (b, 1H, $H^{8´}$), 5.16-4.67 (b, 2H, H^9), 3.4-0.76 (20H, $H^{9´}$, H^7, $H^{7´}$, H^6, $H^{6´}$, $H^{5´}$, H^5, H^4, $H^{4´}$, H^3, $H^{3´}$, H^2, H^1, $H^{1´}$). ^{13}C (125.66 MHz, δ, $CDCl_3$): 150-145 ($C^{2´}$), 146-145 (*endo* C^8), 145-141.6 (*exo* C^8), 114.5-112.5 (*exo* C^9), 114.5-112.5 (*endo* C^9), 113-108 ($C^{8´}$), 58.6-30 (C^7, $C^{7´}$ C^6, $C^{6´}$, C^5, $C^{5´}$, C^4, $C^{4´}$, C^3, $C^{3´}$, C^2, C^1, $C^{1´}$), 14.0 ($C^{9´}$).^{19}F NMR (470.592 MHz, δ, $CDCl_3$): -140-144 (b, F_{ortho}), -157.9 (b, F_{para}), -163 (b, F_{meta}). IR (neat, cm^{-1}): 2941 (ν-CH asym.), 2873 (ν-CH sym.), 1635 (ν-C=C-), 1449 (ν-VAPNBskeleton), 904 (δ-C=C-H). M_w (Da) = 5043. M_w/M_n = 1.1.

2.4.2.6. Polymerization of BNB (short-14, BNB:Pd = 25:1)

The catalyst **4e** (60 mg, 0.055 mmol) was placed in a Schlenk tube under N_2 and it was diluted in 1 mL of dry CH_2Cl_2. To the yellow solution was added the BNB (0.25 g, 1.4 mmol) and the mixture was stirred 24 h at 25 ºC. After this time, the solution was evaporated to dryness and the residue was dissolved in 5 mL of Et_2O. MeOH (10 mL) was added to the solution inducing the precipitation of the polymer as a white solid. The suspension was stirred for 30 min at room temperature, the solid was filtered off and washed with MeOH (2 x 10 mL). The white solid was air dried for 6 h (0.11 g, 69% yield). ^{1}H RMN (500.13 MHz, δ, $CDCl_3$): 5.9-5.7 (b, 1H, H^{10}), 5.6-5.3 (b, 2H, $H^{9´}$, $H^{10´}$) 5.10-4.9 (b, 2H, H^{11}), 3-0.5 (b, 27H, $H^{11´}$, H^9, H^8, $H^{8´}$, H^7, $H^{7´}$, H^6, $H^{6´}$, H^5, $H^{5´}$, H^4, $H^{4´}$, H^3, $H^{3´}$, H^2, $H^{2´}$, H^1, $H^{1´}$). ^{13}C (125.66 MHz, δ, $CDCl_3$): 140-138.5 (C^{10}), 133-124 ($C^{10´}$, $C^{9´}$) 115-113 (C^{11}), 60-30 (C^9, C^8, $C^{8´}$, C^7, $C^{7´}$, C^6, $C^{6´}$, C^5, $C^{5´}$, C^4, $C^{4´}$, C^3, $C^{3´}$, C^2, $C^{2´}$, C^1, $C^{1´}$), 17 (*trans* $C^{11´}$), 13.1 (*cis* $C^{11´}$). ^{19}F NMR (470.592 MHz, δ, $CDCl_3$): -140-144 (b, F_{ortho}), -157.9 (b, F_{para}), -163 (b, F_{meta}). IR (neat, cm^{-1}): 2929 (ν-CH asym.), 2888 (ν-CH sym.), 1640 (ν-C=C-), 1449 (ν-VAPNBskeleton), 907 (δ-C=C-H). M_w (Da) = 6718. M_w/M_n = 1.13.

2.4.2.7. Isomerization of VA-PBNB (14) in the presence of catalyst 4e (14b)

In an NMR tube the polymer **14** (28 mg, 0.196 mmol, 7 mmol -C=C-/g pol.) was dissolved in 0.6 mL of dry $CDCl_3$. To the solution was added the catalyst **4e** (21 mg, 0.0196 mmol) and the reaction was followed by ^{1}H NMR. After 30 min of reaction, the orange solution was transfer to a 50 mL bottom flask and 5 mL of MeOH were added. The white solid was filtered off, washed with MeOH (2 x 5 mL) and air dried for 6 h (0.025 g, 90% yield). ^{1}H RMN (500.13 MHz, δ, $CDCl_3$): 5.6-5.1 (b, 2H, H^{10}, H^9), 3.3-0.5 (b, 14H, H^{11}, H^8, H^7, H^6, H^5, H^4, H^3, H^2, H^1). ^{13}C (125.66 MHz, δ, $CDCl_3$): 135-123 (C^{10}, C^9), 56-27 (C^8, C^7, C^6, C^5, C^4, C^3, C^2, C^1), 17.1 (*trans*-C^{11}), 13.1 (*cis*-C^{11}).

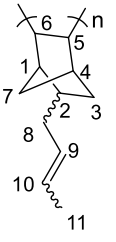

14b

2.4.3. Copolymerization Experiments

2.4.3.1. Synthesis of VA-Co-PNB-VNB (15) (a/b = 1.8/1)

In a Schlenk tube a solution of norbornene in CH_2Cl_2 (0.63 mL, 5 mmol; 7.84 M) and 5-vinyl-2-norbornene (0.71 mL, 5 mmol) were placed under N_2. The two monomers were diluted in 2.8 mL of dry CH_2Cl_2 ($[VNB]_o$ = 1.2 M, $[NB]_o$ = 1.2 M) and the catalyst **4e** (10.73 mg, 0.01 mmol) was added. After 1 h, a white precipitate appeared in the solution and the suspension was stirred 24 h at 25 ºC. MeOH (15 mL) were added to the suspension, the mixture was stirred for 30 min at room temperature and filtered off. The white solid was washed with MeOH (2 x 20 mL) and dried under air 6 h and in a vacuum stove (60 mbar) at 40 ºC for 12 h (0.68 g, 63.5% yield). ^{1}H RMN (500.13 MHz, δ, $CDCl_3$): 6.07-5.63 (b, 1H, H^8), 5.16-4.77 (b, 2H, H^9), 2.80-0.76 (b, 18H, H^7, $H^{7'}$, H^6, $H^{6'}$, H^5, $H^{5'}$, H^4, $H^{4'}$, H^3, $H^{3'}$, H^2, $H^{2'}$, H^1, $H^{1'}$). ^{13}C (125.66 MHz, δ, $CDCl_3$): 146-145 (*endo* C^8), 145-141.6 (*exo* C^8), 114.5-112.5 (*exo* C^9), 114.5-112.5 (*endo* C^9), 60-21 (C^7, $C^{7'}$, C^6, $C^{6'}$, C^5, $C^{5'}$, C^4, $C^{4'}$, C^3, $C^{3'}$, C^2, $C^{2'}$, C^1, $C^{1'}$). ^{19}F NMR (470.592 MHz, δ, $CDCl_3$): -140-144 (b, F_{ortho}), -157.9 (b, F_{para}), -163 (b, F_{meta}). IR (neat, cm^{-1}): 2943 (ν-CH asym.), 2867 (ν-CH sym.), 1635 (ν-C=C-), 1451 (ν-VAPNBskeleton), 906 (δ-C=C-H). M_w (Da) = 54464. M_w/M_n = 2.4.

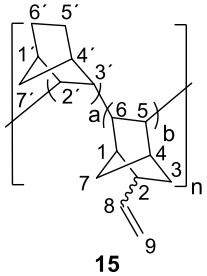

15

2.4.3.2. Synthesis of VA-Co-PNB-VNB (15) (a/b = 21.5/1)

In a Schlenk tube were added a solution of NB in CH_2Cl_2 (19.5 mL, 100 mmol; 5.11 M) and the VNB (1.8 mL, 12.5 mmol). After, 61.8 mL of dry CH_2Cl_2 ($[VNB]_o$ = 0.2 M, $[NB]_o$ = 4.7 M) were added followed by the catalyst **4e** (0.107 g, 0.1 mmol). After 20 min, a white precipitate appeared in the solution and the suspension was stirred 24 h at 25 ºC. MeOH (40 mL) were added to the suspension, the mixture was stirred for 1 h at room temperature and filtered off. The white solid was washed with MeOH (2 x 60 mL) and dried under air 12 h and in a vacuum stove (60 mbar) at 40 ºC for 18 h (7.8 g, 71.5% yield).

2.4.3.3. Synthesis of VA-Co-PNB-BNB (16) (a/b = 2.1/1)

In a Schlenk tube a solution of norbornene in CH_2Cl_2 (0.63 mL, 5 mmol; 7.84 M) and 5-(but-1-en-4-yl)-2-norbornene (0.74 g, 5 mmol) were added under N_2. The two monomers were

diluted in 2.8 mL of dry CH_2Cl_2 ($[BNB]_o$ = 1.2 M, $[NB]_o$ = 1.2 M) and the catalyst **4e** (10.73 mg, 0.01 mmol) was added. After 1 h, a white precipitate appeared in the solution and the suspension was stirred 24 h at 25 ºC. MeOH (15 mL) were added to the suspension, the mixture was stirred for 30 min at room temperature and filtered off. The white solid was washed with MeOH (2 x 20 mL) and dried under air 6 h and in a vacuum stove (60 mbar) at 40 ºC for 12 h (0.68 g, 63.5% yield). ^{1}H RMN (500.13 MHz, δ, $CDCl_3$): 5.9-5.7 (b, 1H, H^{10}), 5.6-5.3 (b, 2H, $H^{10'}$, $H^{9'}$) 5.10-4.9 (b, 2H, H^{11}), 3-0.5 (b, 27H, $H^{11'}$, H^9, H^8, $H^{8'}$, H^7, $H^{7'}$, H^6, $H^{6'}$, H^5, $H^{5'}$, H^4, $H^{4'}$, H^3, $H^{3'}$, H^2, $H^{2'}$, H^1, $H^{1'}$). ^{13}C (125.66 MHz, δ, $CDCl_3$): 140-138.5 (C^{10}), 133-124 (2C, $C^{10'}$, $C^{9'}$), 115-113 (C^{11}), 60-30 (C^9, C^8, $C^{8'}$, C^7, $C^{7'}$, C^6, $C^{6'}$, C^5, $C^{5'}$, C^4, $C^{4'}$, C^3, $C^{3'}$, C^2, $C^{2'}$, C^1, $C^{1'}$,), 17.0 (*trans* $C^{11'}$), 13.1 (*cis* $C^{11'}$). ^{19}F NMR (470.592 MHz, δ, $CDCl_3$): -142-143 (b, F_{ortho}), -157.9 (b, F_{para}), -163.5 (b, F_{meta}). IR (neat, cm^{-1}): 2941 (ν-CH asym.), 2873 (ν-CH sym.), 1635 (ν-C=C-), 1449 (ν-VAPNBskeleton), 904 (δ-C=C-H). M_w (Da) = 29875. M_w/M_n = 1.85.

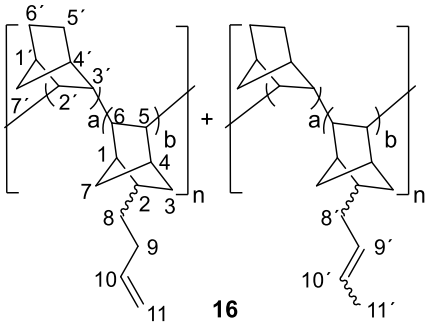

16

2.4.3.4. Synthesis of VA-Co-PNB-NBCOOH (17)

In a Schlenk tube a solution of norbornene in CH_2Cl_2 (0.63 mL, 5 mmol; 7.84 M) and 5-norbornene-2-carboxilic acid (0.71 mL, 5 mmol) were diluted in 3 mL of dry CH_2Cl_2 under N_2 ($[NBCOOH]_o$ = 1.2 M, $[NB]_o$ = 1.2 M). Finally, the catalyst **4e** (10.76 mg, 0.01 mmol) was added. After 1 h, a white precipitate appeared in the solution and the suspension was stirred 24 h at 25 ºC. To the suspension were added 15 mL of MeOH, the mixture was stirred for 30 min at room temperature and filtered off. The white solid was washed with MeOH (2 x 20 mL) and dried under air 6 h and in a vacuum stove (60 mbar) at 40 ºC for 12 h (0,61 g, 34,2% yield). IR (neat, cm^{-1}): 3500 (ν-OH), 2942 (ν-CH asym.), 2866 (ν-CH sym.), 1452 (ν-VAPNBskeleton), 1750 (ν-C=O), 1701 (ν-C=O), 1028 (ν-C-O).

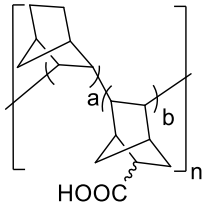

17

2.4.3.5. Synthesis of VA-Co-PNB-NBCH$_2$OH (18)

In a Schlenk tube a solution of norbornene in CH_2Cl_2 (0.63 mL, 5 mmol; 7.84 M) and 5-norbornene-2-methanol (0.6 mL, 5 mmol) were diluted in 2.9 mL of dry CH_2Cl_2 under N_2. Finally, the catalyst **4e** (10.76 mg, 0.01 mmol) was added($[NBCH_2OH]_o$ = 1.2 M, $[NB]_o$ = 1.2 M). After 1 h, a white precipitate appeared in the solution and the suspension was stirred 24 h at 25 ºC. MeOH (15 mL) were added to the suspension, the mixture was stirred for 30 min at room temperature and filtered off. The white solid was washed with MeOH (2 x 20 mL) and dried under air 6 h and in a vacuum stove (60 mbar) at 40 ºC for 12 h (0.16 g, 14.4% yield). IR (neat, cm^{-1}): 3359 (ν-OH), 2940 (ν-CH asym.), 2864 (ν-CH sym.), 1449 (ν-VAPNBskeleton), 1028 (ν-C-O).

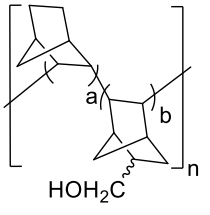

18

2.4.4. Homopolymerization experiments of VNB and ENB with the precatalyst mixture 1/AgBF$_4$ or NaBAr$_4^f$/phosphine

2.4.4.1. General procedure for the polymerization of VNB with the precatalyst mixture 1/phosphine/AgBF$_4$/VNB (1:2:2:500) (entry 1, Table 2.5)

The catalyst **1** (0.005 g, 0.00546 mmol) was placed in a Schlenk tube under N_2 and it was suspended in 0.7 mL of dry CH_2Cl_2. The VNB was added (0.78 mL, 5.46 mmol; $[VNB]_0$ = 3.7 M) and the suspension turned into a colourless solution. Subsequently, the PPh_3 (0.00285 g, 0.0109 mmol) and $AgBF_4$ (0.0021 g, 0.0109 mmol) were added. Immediately, some Pd^0 black were generated in the solution. The suspension was stirred 1 h at 25 ºC. After this time, 20 mL of MeOH were added inducing the precipitation of the polymer as a white solid. The

solid was filtered off and washed with MeOH (2 x 20 mL) and Et_2O (2 x 10 mL). Finally, the white solid was air dried for 12 h and in a stove at 60 ºC to constant weight (33 mg. 5% yield).

2.4.4.2. General procedure for the polymerization of VNB with the precatalyst mixture 1/phosphine/$NaBAr_4^f$/VNB (1:2:2:500) (entry 3, Table 2.5)

The catalyst **1** (0.005 g, 0.00546 mmol) was placed in a Schlenk tube under N_2 and it was suspended in 0.7 mL of dry CH_2Cl_2. The VNB was added (0.78 mL, 5.46 mmol; $[VNB]_0$ = 3.7 M) and the suspension turned into a colourless solution. Subsequently, the PPh_3 (0.00285 g, 0.0109 mmol) and $NaBAr_4^f$ (0.00964 mg, 0.0109 mmol) were added. Instantly, the colourless solution changed to an intense yellow solution. The solution was stirred 1 h at 25 ºC giving a viscous mixture quickly. After this time, 10 mL of $CHCl_3$ were added to the viscous mixture and it was stirred for 15 min. The polymer was precipitated by adding 15 mL of MeOH. The solid was filtered off and washed with MeOH (2 x 15 mL) and Et_2O (2 x 10 ml). Finally, the white solid was air dried for 6 h and in a stove at 70 ºC to constant weight (0.6 g, 99% yield).

2.4.4.3. General procedure for the polymerization of VNB or ENB with the precatalyst mixture 1/PCy_3/$NaBAr_4^f$/VNB (1:2:2:250)

The catalyst **1** (0.0025 g, 0.00273 mmol) was placed in a Schlenk tube under N_2 and it was suspended with 2 mL of dry CH_2Cl_2. The VNB was added (0.19 mL, 1.368 mmol) and the suspension turns to a colourless solution. Subsequently, the PCy_3 in a toluene solution (0.14 mL, 0.00546 mmol; 0.038 M) and $NaBAr_4^f$ (0.0048 mg, 0.00546 mmol) were added($[VNB]_0$ = 0.5 M). Instantly, the colourless solution changes to an intense yellow solution. The solution was stirred 1 h at 25 ºC. The polymer was precipitated by adding 20 mL of MeOH. The solid was filtered off and washed with MeOH (2 x 20 mL) and Et_2O (2 x 10 ml). Finally, the white solid was air dried for 12 h and in a stove at 70 ºC to constant weight (0.15 g, 97% yield). ^{1}H RMN (500.13 MHz, δ, $CDCl_3$): 6.1-5.6 (b, 1H, H^8), 5.25-4.6 (b, 2H, H^9), 3-0.5 (b, 9H, H^7, H^6, H^5, H^4, H^3, H^2, H^1). ^{13}C (125.66 MHz, δ, $CDCl_3$): 145-144 (*endo* C^8), 144-140 (*exo* C^8), 116-114 (*exo* C^9), 114-112.5 (*endo* C^9), 55-30 (C^7, C^6, C^5, C^4, C^3, C^2, C^1).

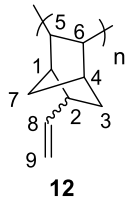

12

The polymerization of ENB was carried out in the same way than VNB: (0.155 g, 98% yield). ^{1}H RMN (500.13 MHz, δ, $CDCl_3$): 5.5-4.7 (b, 1H, H^8), 3.25-0.5 (b, 11H, H^9, H^7, H^6, H^5, H^4, H^3, H^1). ^{13}C (125.66 MHz, δ, $CDCl_3$): 150-142 (C^2), 115-105 (C^8), 60-30 (C^7, C^6, C^5, C^4, C^3, C^1), 15 (C^9).

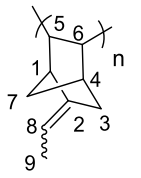

13

2.4.4.4. General procedure for the polymerization of VNB with the precatalyst mixture 1/PCy_3/$NaBAr_4^f$/VNB (1:2:2:50000) by the Method a (entry 5, Table 2.7)

The catalyst **1** (0.56 mg, $6.1x10^{-4}$ mmol) was placed under N_2 in a Schlenk tube and it was dissolved in 7.8 mL of dry CH_2Cl_2 generating a yellow solution. The VNB was added (8.7 mL, 61 mmol; $[VNB]_0$ = 3.7 M) and the solution changed to a colourless solution. Immediately, the PCy_3 in a toluene solution (32 μl, $1.22x10^{-3}$ mmol; 0.038 M) and the $NaBAr_4^f$ (0.0011 g, $1.22x10^{-3}$ mmol) were added. Instantly, the colourless solution changed to an intense yellow solution. The solution was stirred 5 h at 25 ºC giving a viscous mixture after 1 h. After this time, 20 mL of $CHCl_3$ were added to the viscous mixture and it was stirred for 15 min. The polymer was precipitated by adding 15 mL of MeOH. The solid was filtered off and washed with MeOH (2 x 30 mL) and Et_2O (2 x 10 ml). Finally, the white solid was air dried for 6 h and in a stove at 70 ºC to constant weight (3.5 g, 48% yield).

All the polymerizations presented in Table 2.6-2.8 were carried out following this general procedure (Method a) changing the appropriate reaction condition: phosphine, solvent, concentration, temperature or amount of catalyst. The amount of catalyst **1** was weighed in a high precision scale.

2.4.4.5. Procedure for the polymerization of VNB with the precatalyst mixture 1/PCy_3/$NaBAr_4^f$/VNB (1:2:2:50000) by the Method b (entry 5, Table 2.7)

The catalyst **1** (0.56 mg, $6.1x10^{-4}$ mmol) was placed in a Schlenk tube under N_2 and it was dissolved in 7.8 mL of dry CH_2Cl_2 generating a yellow solution. The yellow solution was cooled to 195 K in a 2-propanol bath and after 10 min in the cool bath to ensure a constant temperature, the PCy_3 in a toluene solution (32 μl, $1.22x10^{-3}$ mmol; 0.038 M) was added. A clear yellow solution was formed and the $NaBAr_4^f$ (0.0011 g, $1.22x10^{-3}$ mmol) and VNB (8.7 mL, 61 mmol; $[VNB]_0$ = 3.7 M) were added at 195 K. The intense yellow solution was allowed to reach room temperature (30 min) and then the solution was stirred 5 h at 25 ºC giving a viscous mixture quickly. After this time, 20 mL of $CHCl_3$ were added to the viscous mixture and it was stirred for 15 min. The polymer was precipitated by adding 15 mL of MeOH. The solid was filtered off and washed with MeOH (2 x 30 mL) and Et_2O (2 x 10 ml). Finally, the white solid was air dried for 6 h and in a stove at 70 ºC to constant weight (3.8, 53% yield).

2.4.4.6. Formation in situ of complex 19

In an NMR tube under N_2 was placed the PCy_3 (0.0015 g, 0.00546 mmol) and it was dissolved in 0.6 mL of CD_2Cl_2. The solution was cooled at 195 K in a 2-propanol bath and CD_3CN (7 μL, 0.1365 mmol) was added. After 10 min in the cool bath to ensure a constant temperature, the complex **1** was added (0.0025 g, 0.00273 mmol) and the yellow solution generated was checked by NMR spectroscopy. ^1H RMN (500.13 MHz, δ, 195 K, CD_2Cl_2 + CD_3CN (85:1 v/v)): 7.69-7.40 (3H, H^5, H^4, H^3), 7.00 (bs, 2H, H^6, H^2), 3.58 (bs, 1H, H^α), 3.01 (bs, 2H, H^β, $H^{\beta'}$), 2-1 (PCy_3). ^{13}C (125.66 MHz, δ, 195 K, CD_2Cl_2 + CD_3CN (85:1 1 v/v)):133-129 (C^5, C^4, C^3), 129.25 (C^6), 107.7 (C^2), 53.48 (C^α), 23.94 (C^β), 26.5 (PCy_3). ^{19}F (470.592 MHz, δ, 195 K, CD_2Cl_2 + CD_3CN (85:1 1 v/v)): -143.6 (m, F_{ortho}), -157.4 (t, F_{para}), -162.18 (m, F_{meta}). ^{31}P (202.497 MHz, δ, 195 K, CD_2Cl_2 + CD_3CN (85:1 1 v/v)): 48.5.

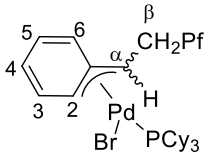

19

2.4.4.7. Formation in situ of complex 20

In an NMR tube under N_2 was placed the PCy_3 (0.0015 g, 0.00546 mmol) and it was dissolved in 0.6 mL of CD_2Cl_2. The solution was cooled at 195 K in a 2-propanol bath and CD_3CN (7 μL, 0.1365 mmol) was added. After 10 min in the cool bath to ensure a constant temperature, the complex **1** was added (0.0025 g, 0.00273 mmol) generating a yellow solution. To this solution was added the $NaBAr_4^f$ (0.0058 g, 0.006552 mmol) and the yellow solution was checked by NMR spectroscopy. ^1H RMN (500.13 MHz, δ, 195 K, CD_2Cl_2 + CD_3CN (85:1, 1 v/v)): 7.7-7.3 (m, 18H, H^5, H^4, H^3, Ph BAr_4^f), 7.00 (bs, 2H, H^6, H^2), 3.66 (bs, 1H, H^α), 2.97 (bs, 2H, H^β, $H^{\beta'}$), 2-1 (PCy_3). ^{19}F NMR (470.592 MHz, δ, 195 K, CD_2Cl_2 + CD_3CN (85:1 1 v/v)): -143.65 (m, F_{ortho}), -156.3 (t, F_{para}), -161.80 (m, F_{meta}). ^{31}P (202.497 MHz, δ, 195 K, CD_2Cl_2 + CD_3CN (85:1 v/v)): 46.2.

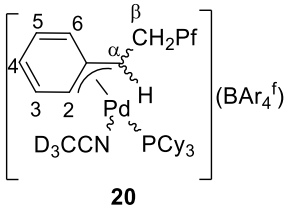

20

2.4.5. Functionalization post-polymerization of VA-Co-PNB-VNB (15) and VA-Co-PNB-BNB (16)

Note: The functionalization of all the polymers (mmol functional group/g pol.) and the polymer composition given as a ratio of monomers (a/b = NB/NB functionalized (FNB)) are related by the equation: $[1/[((a/b) \times (M_{wNB})) + (M_{wFNB})]] \times 1000$ where M_{wNB} is the molecular weight of the monomer norbornene (94.16) and M_{wFNB} is the molecular weight of the FNB.

2.4.5.1. Synthesis of VA-Co-PNB-NB$(CH_2)_2B(OH)_2$ (21) (a/b = 2.7/1)

In a 100 mL Schlenk tube the polymer **15** (0.10 g, 0.31 mmol; 3.1 mmol-CH=CH_2/g pol.) was dissolved in 10 mL of dry CH_2Cl_2 under N_2. The polymer was stirred for 10 min until completely dissolution. The $HBBr_2 \cdot SMe_2$ (0.31 mL, 0.31 mmol; 1 M in CH_2Cl_2) was added and the mixture was stirred for 5 h at reflux. The suspension was allowed to reach room temperature and then, a mixture of MeOH/H_2O (20 mL, 1:1 v/v) was added. The suspension was stirred at room temperature for 30 min. The white solid was filtered off and washed with MeOH (2 x 10 mL). The solid was air dried for 12 h (0.1 g, 88% yield). IR (neat, cm^{-1}): 3354 (ν-OH), 2940 (ν-CH asym.), 2864 (ν-CH sym.), 1450 (ν-VAPNBskeleton), 1348 (ν-B-O).

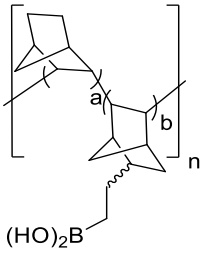

21

2.4.5.2. Synthesis of VA-Co-PNB-NB$(CH_2)_2OH$ (22) (a/b = 2.9/1)

In a 100 mL Schlenk tube was dissolved the polymer **15** (0.10 g, 0.31 mmol; 3.1 mmol-CH=CH_2/g pol.) in 10 mL of dry CH_2Cl_2 under N_2. The polymer was stirred 10 minutes until completely dissolution. The $HBBr_2 \cdot SMe_2$ (0.31 mL, 0.31 mmol; 1 M in CH_2Cl_2) was added and the mixture was stirred 5 h at reflux. The suspension was allowed to reach room temperature and then, MeOH (10 mL) were added followed by a solution of $NaOH_{(aq)}$ (0.66 mL, 4 mmol; 6M) and $H_2O_{2(aq)}$ (0.72 mL, 7 mmol; 33%). The suspension was stirred at room temperature for 2 h. The white solid was filtered off and washed with MeOH (2 x 10 mL), with a mixture of MeOH/H_2O (2 x 20 mL, 1:1 v/v) and finally with MeOH (10 mL). The solid was air dried for 12 h and in a vacuum stove (60 mb) at 70 ºC for 12 hours (0.1 g, 95 % yield).[13]C CP-MAS: 74-25 ppm. IR (neat, cm^{-1}): 3354 (ν-OH), 2940 (ν-CH asym.), 2864 (ν-CH sym.), 1450 (ν-VAPNBskeleton), 1047 (ν-C-O).

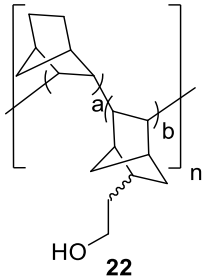

22

2.4.5.3. Synthesis of VA-Co-PNB-NB(CH_2)$_2$OH (22) (a/b = 16.9/1)

In a 500 mL Schlenk tube was added the polymer **15** (7.8 g, 3.63 mmol; 0.46 mmol-CH=CH_2/g pol.) under N_2. After, 200 mL of dry CH_2Cl_2 were added and the polymer was stirred 20 min at room temperature. After this time, $HBBr_2 \cdot SMe_2$ was added (3.63 mmol, 3.63 mL; 1 M in CH_2Cl_2) and the suspension was stirred 5h at reflux. The suspension was allowed to reach room temperature and then, 100 mL of MeOH were added followed by a 6 M solution of $NaOH_{(aq)}$ (1.8 mL, 10.89 mmol) and $H_2O_{2(aq)}$ (0.6 mL, 5.81 mmol; 33%). The suspension was stirred at room temperature for 2 h. The white solid was filtered off and washed with MeOH (2 x 10 mL), with a mixture of MeOH/H_2O (2 x 20 mL, 1:1 v/v) and finally with MeOH (10 mL). The solid was air dried for 12 h and in a vacuum stove (60 mb) at 70 ºC for 12 hours (7.5 g, 96.5% yield).

2.4.5.4. Synthesis of VA-Co-PNB-NB(CH_2)$_2$O($C_6H_{12}PO_2$) (23) (a/b = 21.7/1)

In a 250 mL Schlenk tube was placed the VA-Co-PNB-NB(CH_2)$_2$OH (**22**) (3.8 g, 2.2 mmol; 0.57 mmol OH/g pol.) under N_2. The polymer was suspended in 80 mL of dry CH_2Cl_2 and the suspension was stirred for 20 min at 263 K. The NEt_3 (0.61 mL, 4.4 mmol) was added and the suspension was stirred 1 h more at 263 K. After this time, a solution of PClpin (0.88 mL, 5.5 mmol) in 20 mL of dry CH_2Cl_2 was added very slowly at 263 K. The suspension was stirred for 12 h at room temperature. The white solid was filtered under N_2 and washed with dry CH_2Cl_2 (3 x 50 mL), dry MeOH (3 x 50 mL), dry THF (3 x 50 mL) and dry Et_2O (3 x 50 mL). The white solid was vacuum dried (3.74 g, 98% yield). ^{31}P NMR MAS (400.13 MHz, δ): 147.72. ^{13}C NMR MAS: 95-90 (C_{pin}), 76-20 (VA-PNB carbons and methyl's of the phosphite). IR (neat, cm^{-1}): 2942 (ν-CH asym), 2865 (ν-CH sym), 1451 (ν-VAPNBskeleton), 963 (ν-P-O).

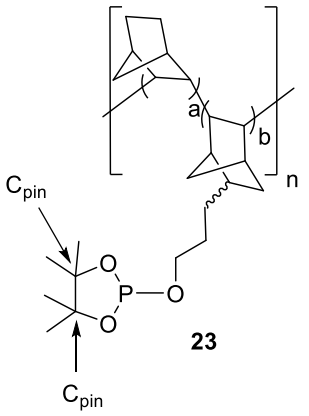

23

2.4.5.5. Synthesis of VA-Co-PNB-NB(CH$_2$)$_4$SiClMe$_2$ (24) (a/b = 2.12/1)

In a 250 mL Schlenk under N_2 the VA-Co-PNB-BNB (**15**) (1.5 g, 4 mmol; 2.66 mmol-CH=CH$_2$/g pol.) was dissolved in 30 mL of dry CH_2Cl_2. After complete dissolution, the $HSiClMe_2$ (2.15 g, 22.32 mmol) and the Karstedt′s Catalyst (0.128 g, 2% in Pt, $6.6x10^{-4}$ mmol) were added. The colorless solution was stirred at reflux for 16 h. Then, 40 mL of dry MeCN were added inducing the precipitation of a white solid that was decanted. The gray solution was cannulated, and the solid was washed with MeCN (2 x 40 mL). The white solid was vacuum dried for 3 h and stored in the freezer under N_2 (1.5 g, 81.1% yield). IR (neat, cm^{-1}): 1450 cm^{-1} (ν-VAPNBskeleton), 846 cm^{-1} (ν-Si-C), 809 cm^{-1} (ν-Si-C), 789 cm^{-1} (ν-Si-C), 475 cm^{-1} (ν-Si-Cl). Note: The polymer needs to be kept in anhydrous conditions, since the Si-Cl bond hydrolizes easily.

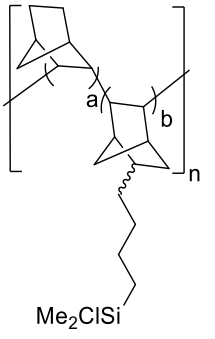

24

2.4.5.6. Synthesis of VA-Co-NB-NB(CH$_2$)$_4$Si(C$_3$H$_5$)Me$_2$ (25) (a/b = 2.07/1)

In a 50 mL Schlenk under N_2 the VA-Co-PNB-NB$(CH_2)_4SiClMe_2$ (**24**) (0.8 g, 1.7 mmol; 2.1 mmol Si-Cl/g pol.) was suspended in 20 mL of dry THF. A freshly prepared solution of allylmagnesiumbromide in Et_2O (3.8 mL, 2.41 mmol; 0.62 M) was added. The suspension

was stirred at reflux for 5 h. Then, 30 mL of MeOH were added and the mixture was stirred for 30 min at room temperature. The white solid was filtered off and washed with a solution of $HCl_{(aq}$ (3 x 20 mL, 10%), a solution of $KOH_{(aq)}$ (2 x 20 mL, 12 M), MeOH (1 x 20 mL) and Et_2O (1 x 20 mL). The white solid was vacuum dried and stored in the freezer (0.65 g, 80.8%). IR (neat, cm^{-1}): 1634 cm^{-1} (ν-C=C-), 1450 cm^{-1} (ν-VAPNBskeleton), 837 cm^{-1} (ν-Si-C), 783 cm^{-1} (ν-Si-C).

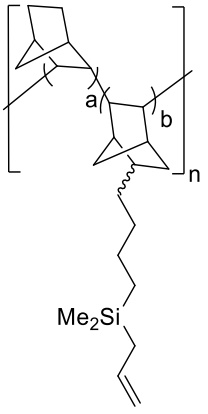

25

2.4.5.6.1. Preparation of the allylmagnesiumbromide solution

In a 50 mL Schlenk under N_2, Mg turnings (85 mg, 3.5 mmol) were placed together with a I_2 crystal. The mixture was heated until the complete consumption of the I_2. The Mg was suspended in 2 mL of dry Et_2O and a solution of allylbromide (0.3 ml, 3.5 mmol) in 2 mL of dry Et_2O was added. The suspension was stirred 3 h at 25 ºC. The resultant grey solution was titrated by ^1H NMR using biphenyl as an internal standard.

2.4.5.7. Synthesis of VA-Co-PNB-NB(CH₂)₄SiHMe₂ (26) (a/b = 2.26/1)

In a 50 mL Schlenk under N_2 the VA-Co-PNB-NB$(CH_2)_4$SiClMe$_2$ (**25**) (0.5 g, 1.05 mmol; 2.1 mmol Si-Cl/g pol.) was suspended in 15 mL of dry Et_2O. The suspension was cooled at 273 K and $LiAlH_4$ (0.1g, 2.6 mmol) was added. The suspension was stirred for 12 h at room temperature. Then, 20 mL of MeOH were added and the grey solid was filtered off. The solid was washed with a solution of $HCl_{(aq)}$ (3 x 20 mL, 10%), a solution of $KOH_{(aq)}$ (2 x 20 mL, 12 M), MeOH (1 x 20 mL) and Et_2O (1 x 20 mL). The white solid was vacuum dried and stored in the freezer (0.4 g, 87% yield). IR (neat, cm^{-1}): 2108 cm^{-1} (ν-Si-H), 1450 cm^{-1} (ν-VAPNBskeleton), 884 cm^{-1} (ν-Si-C), 834 cm^{-1} (ν-Si-C), 787 cm^{-1} (ν-Si-C).

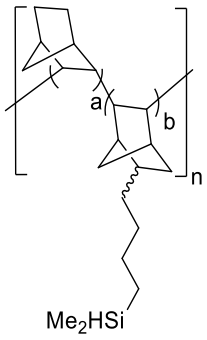

26

2.4.6. Determination of the composition of the copolymers VA-Co-PNB-VNB (15) and VA-Co-PNB-BNB (16)

2.4.6.1. Soluble copolymers by ^{1}H NMR spectroscopy

The calculation of the composition of the copolymers VA-Co-PNB-VNB (**15**) was made following this general equation: a/b = {(IntA-3IntB)/10}/(IntB/3) where IntA = total integral value of the aliphatic region, IntB = total integral value of the alkene region and the numeric coefficients take into account the number of protons in norbornene and 5-vinyl-2-norbornene). As an example, for the polymer **15** presented in the Figure 2.31 the result is: a/b = {(30.59 - 3 x 3.08)/10}/{3.08/3} = 2.1.

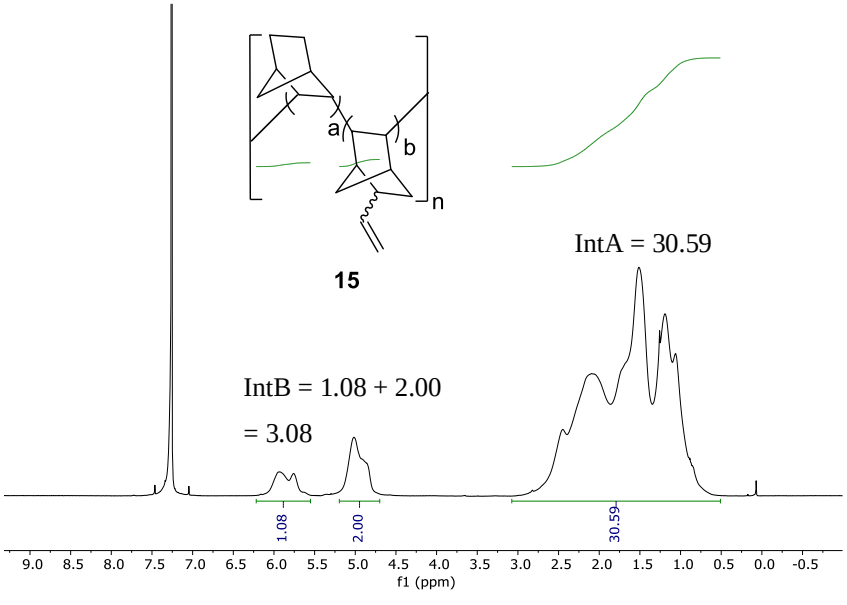

Figure 2.31. ^{1}H NMR (500.13 MHz, dry $CDCl_3$) for the VA-Co-PNB-VNB (**15**) with a ratio a/b = 2.1/1 (entry 4, Table 2.4).

The equation for the calculation of the composition of VA-Co-PNB-BNB (**16**) is different because we have the presence of two different double bonds due to isomerization during the polymerization, where the ratio of olefinc protons:aliphatic protons is different. The final equation is the following: (a/b = {(IntA-(13IntB/3)-(14IntC/2)/10}/{(IntB/3)+IntC/2} where IntA = total integral value of the aliphatic region, IntB = total integral value of the alkene region for the terminal double bond and IntC = total integral value of the alkene region for the internal pendant double bond and the numeric coefficients take into account the number of protons in norbornene, 5-(but-1-en-4-yl)-2-norbornene (BNB) and 5-(but-2-en-4-yl)-2-norbornene. So, for the copolymer presented in the ^{1}H NMR of the Figure 2.32 the result is: a/b = {(37.95-(13x2.91/3)-(14x0.3/2)/10}/{(2.91/3)+0.3/2} = 2.1

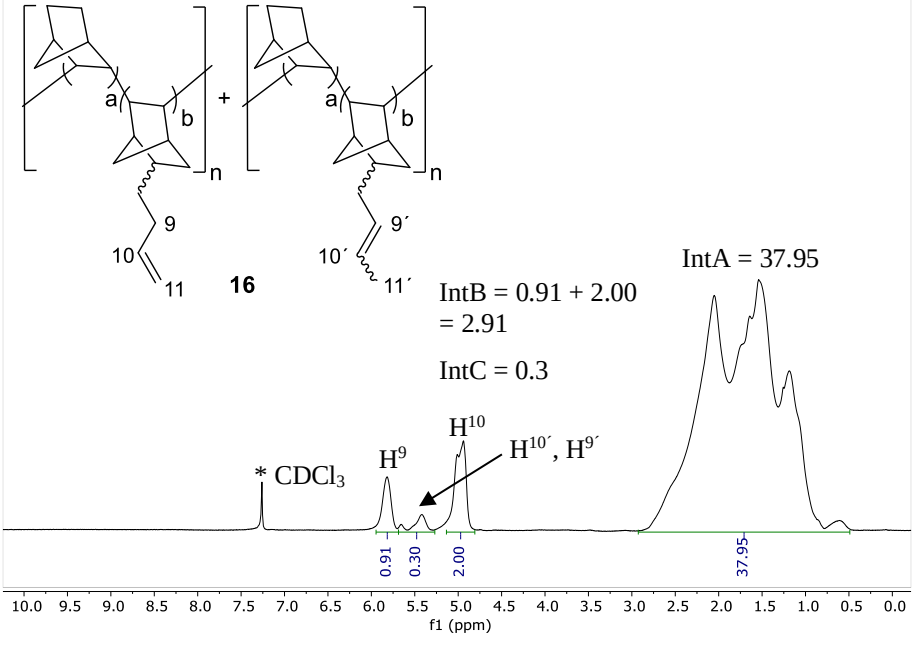

Figure 2.32. ^{1}H NMR (500.13 MHz, dry $CDCl_3$) for the VA-Co-PNB-BNB (**16**) a/b = 2.1, where we still can see the presence of isomerized double bond.

2.4.6.2. Insoluble copolymers by FT-IR spectroscopy

The composition of the insoluble copolymers can be determined using FT-IR spectroscopy. The use of FT-IR spectroscopy in pharmaceutical industry is gaining much popularity as a quantitative tool due to its rapid and non-destructive nature, simple sample preparation, ease use and less or no solvent consumption for monitoring quality.[130] For the quantification of the

[130] a) Salari, A.; Young, R. E. *Int. J. Pharm.* **1998**, *163*, 157-166. b) Hua, Y.; Erxlebena, A.; Rydera, A. G.; McArdle, P. *J. Pharm. Biomed. Anal.* **2010**, *53*, 412-420. c) Mallah, M. A.; Sherazi, S. T. H.; Bhanger, M. I.; Mahesar, S. A. Bajeer, M. A. *Spectrochim. Acta A Mol. Biomol. Spectrosc Spectroscopy* **2015**, *141*, 64-70.

composition of our insoluble copolymers **15** we elaborated a calibration line. The calibration line correlates the composition of some soluble copolymers, where the composition is known by ^{1}H NMR spectroscopy, with the area of a selected band of the copolymer **15**. We chose the band at 1634 cm^{-1} that correspond with the stretching of the terminal ν-C=C- double bond because is it in a very clean part of the spectrum. The standard samples include the homopolymer VA-PVNB (maximum composition, entry 1, Table 2.9), some soluble copolymers VA-Co-PNB-VNB (**15**) where the composition is known by ^{1}H NMR spectroscopy (entries 2 and 3, Table 2.9) and some standards with low composition generated by mixing known amounts of VA-PNB and VA-Co-PNB-VNB (**15**) (entries 4, 5 and 6, Table 2.9). The plot of the area versus the composition gives us the calibration line that is represented in Figure 2.33. With this calibration line is easy to calculate the composition of an insoluble polymer by interpolation.

Table 2.9. Area calculated for the band at 1634 cm^{-1} with different standards.

Entry	Area[a]	mmol VNB/g polymer
1	137.4	8.32[b]
2	75.2	4.04[b]
3	40.94	1.97[b]
4	31.97	1.42[c]
5	23.19	0.75[c]
6	16.57	0.52[c]

a) Area calculated by FTIR spectroscopy. b) composition of the homopolymer VA-PVNB, copolymer VA-Co-PNB-VNB (ratio NB:VNB = 500:1000) and VA-Co-PNB-VNB (ratio NB:VNB = 1000:1000 calculated by ^{1}H NMR spectroscopy. c) the standards with low composition were obtained by mixing a known amount of VA-PNB and known amount of VA-Co-PNB-VNB.

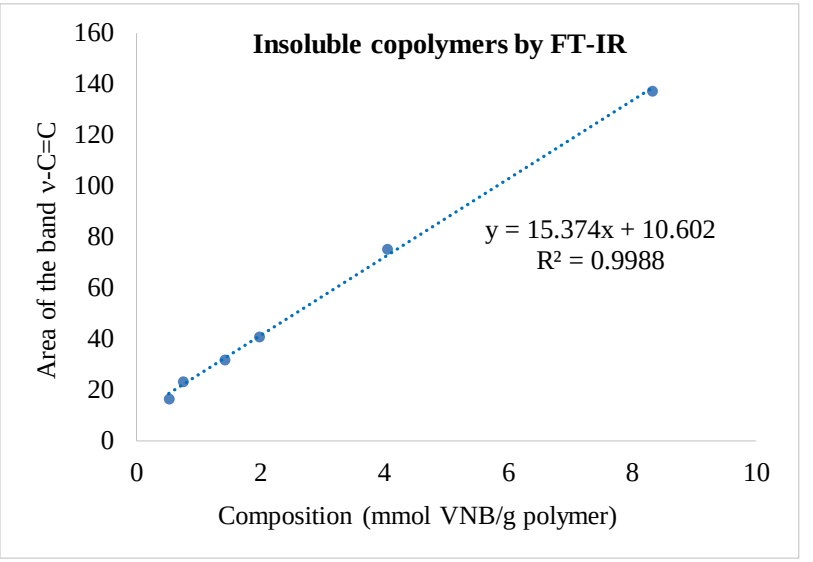

Figure 2.33. Plot of the area of the band ν-C=C- versus the composition (mmol VNB/g polymer).

2.4.7. Determination of the reactivity ratios for the copolymerization of NB and VNB with catalyst 4e

The kinetics of the copolymerization between two monomers was studied by Mayo and Lewis in 1944.[131] The Mayo-Lewis equation or the copolymer equation considers the mix of two monomers, M_{NB} and M_{VNB} in our case, and the four possible equations for the reaction of each monomer with the end terminated group of a propagating chain (M_{NB}* and M_{VNB}*). The equation and the constants can be written as follows:

$$M^*_{NB} + M_{NB} \xrightarrow{k_{NBNB}} M_{NB}M^*_{NB}$$
$$M^*_{NB} + M_{VNB} \xrightarrow{k_{NBVNB}} M_{NB}M^*_{VNB}$$
$$M^*_{VNB} + M_{VNB} \xrightarrow{k_{VNBVNB}} M_{VNB}M^*_{VNB}$$
$$M^*_{VNB} + M_{NB} \xrightarrow{k_{VNBNB}} MV_{NB}M^*_{NB}$$

The monomer reactivities ratio are given by $r_{NB} = k_{NB\text{-}NB}/k_{NB\text{-}VNB}$ and $r_{VNB} = k_{VNB\text{-}VNB}/k_{VNB\text{-}NB}$ and the copolymer composition equation which relates the polymer composition to the monomer composition is given by

[131] Mayo, F. R.; Lewis, F. M. *J. Am. Chem. Soc.* **1944**, *66*, 1594-1601.

$$\frac{d[M_{NB}]}{d[M_{VNB}]} = \frac{[M_{NB}]}{[M_{VNB}]} \times \frac{(r_{NB}[M_{NB}] + [M_{VNB}])}{(r_{VNB}[M_{VNB}] + [M_{NB}])}$$

Fineman and Ross developed a simple method to obtain good accuracy in the reactivity ratios.[119] This method can only be applied at very low conversion where the composition of the monomer in the polymer can be approximated to the composition of the monomer in the feed. With some rearrangement in the equation above and rewriting it in terms of mole fractions, where f_{NB} and f_{VNB} are the mole fraction of the monomer in the feed and F_{NB} and F_{VNB} the mole fraction of the monomers in the copolymer, it is possible to obtain the following equation:

$$G = Hr_{NB} - r_{VNB}$$

$$\text{where } G = \frac{f_{NB}(2F_{NB}-1)}{(1-f_{NB})F_{NB}}$$

$$\text{and } H = \frac{f_{NB}^2(1-F_{NB})}{(1-f_{NB})^2F_{NB}}$$

A plot of G versus H gives a straight line where the slope is r_{NB} and the intercept is $-r_{VNB}$. Copolymerizations of norbornene and vinylnorbornene were carried out at the monomer feed ratios f_{NB} summarized in Table 2.10. The copolymerizations were quenched by precipitation of the polymer by adding 10 mL of MeOH (4-14 % conversions). The plot of G versus H is represented in Figure 2.34. The slope of the line gives the r_{NB} = 1.97 and the intercept the r_{VNB} = 0.0048.

Table 2.10. Experimental data obtained employing different initial molar fractions in the feed of NB.[a]

Entry	F_{NB}	f_{NB}	G	H
1	0.873	0.75	2.56	1.31
2	0.833	0.666	1.59	0.79
3	0.743	0.5	0.65	0.34
4	0.666	0.334	0.25	0.12

a) All the reactions were carried out in a Schlenk tube under N_2 in CH_2Cl_2 stopping the polymerization by the addition of 10 ml of MeOH when the conversion is between 4-14%.

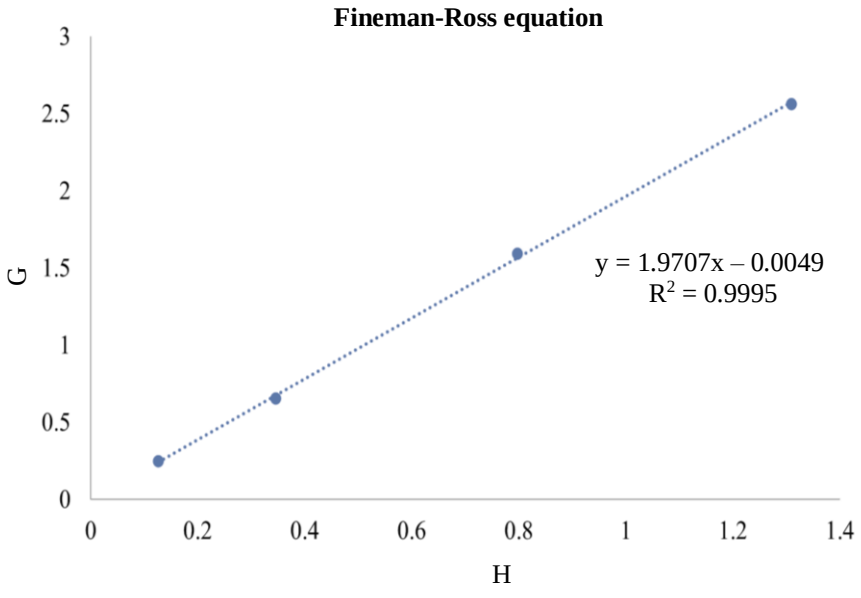

Figure 2.34. Representation of G vs H for the calculation of r_{NB} and r_{VNB} for the copolymerization of NB and VNB with the catalyst **4e**.

Chapter 3

3. Study of the Vinylic Addition Polymerization of Norbornene: A New Propagation Pathway by β-Carbon Elimination

3.1. Introduction

In the course of former studies in the group on the vinylic addition (VA) polymerization of norbornene derivatives with polar groups, some alterations in the polymer structure were found that led us to study some aspects of the vinylic addition polymerization of norbornene in more detail. The results of this study are collected in this Chapter, as well as an introduction that gives the relevant information on the main mechanistic aspects of the VA-polymerization of norbornene and related processes that are interesting precedents for this work. In particular, the goal was to find out the origin of the polymer backbone alterations, that involved the formation of double bonds in the structure, and to determine the factors that trigger their formation. This is important to control the polymer structure of the VA-PNBs.

3.1.1. Polynorbornene skeleton types

Norbornene can be polymerized in different ways and depending on the polymerization mechanism polymers with distinct structures can be synthesized. This was discussed in

Chapter 2 and Scheme 3.1 summarizes the main polyborbornene structures. The radical and cationic polymerizations of NB usually give polymers with low molecular weights and low yields. Therefore, the ROMP and VA polymerization of norbornene, with their respective unsaturated or all-aliphatic 2,3-*exo*-enchained bicyclic backbones, are the most important polymerization procedures. Few exceptions to the polymer structures shown in Scheme 3.1 (VA-PNBs (**A**$_3$), ROMP-PNBs (**B**$_3$) and cationic or radical-PNB (**C**$_3$)) have been described.

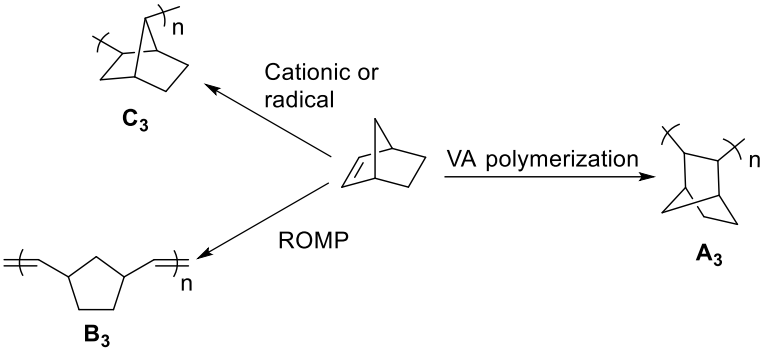

Scheme 3.1 Principal methods for the norbornene polymerization.

Using zirconium metallocenes in the vinylic oligomerization of norbornene, Fink and co-workers reported a new propagation way based in σ-bond metathesis.[132] The oligomers synthesized using the combination of [$ZrCl_2$^{i}Pr$(Ind)_2$]/MAO presented in their structure the *cis*-2,3-*exo* linkages but also the unexpected 2-*exo*,7´-*syn* linkage (Scheme 3.2). In a hydrooligomerization, the reaction starts with the insertion of the first norbornene into the Zr-H or Zr-D bond. The three first norbornenes are inserted in a *cis*-2,3-*exo* mode and subsequently, a conformational rearrangement occurs and the *syn*-hydrogen atom on C^7 of the penultimate monomer inserted interacts with the zirconium atom. A σ-bond metathesis follows with the transposition of the zirconium atom to the C^7 carbon. After this metathesis, the same cycle starts again: a triple *cis*-2,3-*exo* insertion followed by σ-bond metathesis. The mechanism for the formation 2-*exo*-7´-*syn* linkage is not exclusive for zirconium

[132] a) Karafilidis, C.; Hermann, H.; Rufínska, A.; Gabor, B.; Mynott, R. J.; Breitenbruch, G.; Weidenthaler, C.; Rust, J.; Joppek, W.; Brookhart, M. S.; Thiel, W.; Fink, G. *Angew. Chem. Int. Ed.* **2004**, *43*, 2444-2446. b) Karafilidis, C.; Angermund, K.; Gabor, B.; Rufínska, A.; Mynott, R. J.; Breitenbruch, G.; Thiel, W.; Fink, G. *Angew. Chem. Int. Ed.* **2007**, *46*, 3745-3749.

metallocenes. A similar behavior was found with a palladium(II) complex bearing an imine-N-Heterocyclic carbene ligand.[133]

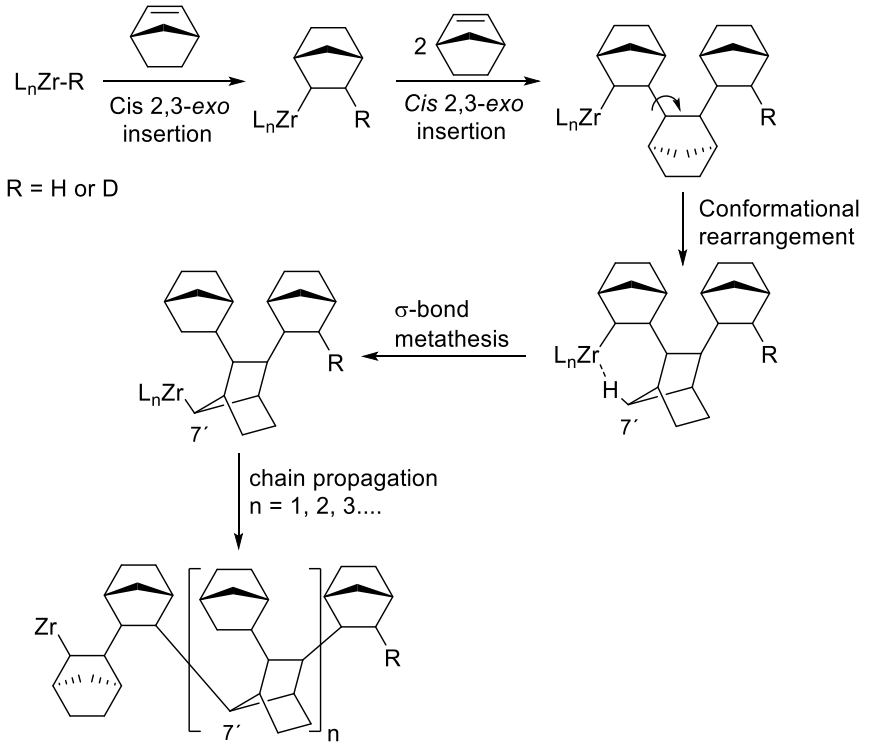

Scheme 3.2. Vinylic addition polymerization of norbornene with Zr complexes involving a σ-bond metathesis.

The ROMP polymerization and the vinylic addition polymerization of cyclic olefins have been simultaneously observed for the same metal center. In these cases an α-elimination process converts the VA-catalyst (a metal alkyl) to a ROMP-catalyst (a metal carbene, Scheme 3.3). This interconversion can generate a new skeleton, intermediate between the ROMP and VA-PNBs. The initial studies in this area was elaborated with cyclobutenes in combination with a Ziegler-Nata catalyst.[134] However, the first evidence for the operation of the two mechanisms with the same catalyst in the polymerization of norbornene was reported

[133] Deng, J.; Gao, H.; Zhu, F.; Wu, Q. *Organometallics* **2013**, *32*, 4507-4515.
[134] a) Dall'asta, G.; Motroni, G. *J. Polym. Sci. A: Pol. Chem* **1968**, *6*, 2405-2413. b) Dall'asta, G. *J. Polym. Sci. A: Pol. Chem* **1968**, *6*, 2397-2404.

by Farona and co-workers.[135] In the course of the years, several groups reported this methodology to make the combination of ROMP and VA polymerization of norbornene with a single catalyst.[136]

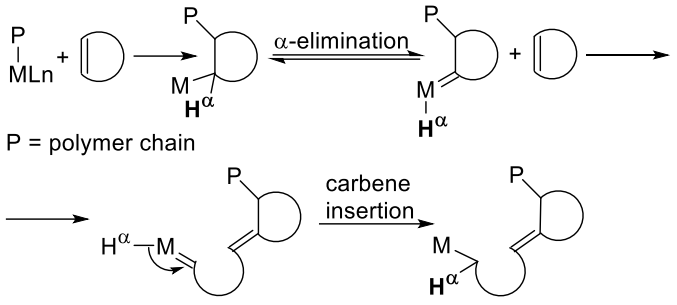

Scheme 3.3. Interconversion between a VA-polymerization and ROMP polymerization with the same catalyst by an α-elimination.

A way to switch between the two mechanisms is the use of an auxiliary ligand that can reversibly abstract a proton from the cationic species to make the alkylidene (ROMP polymerization) and re-add a proton to the metal alkylidene to regenerate the cationic species (VA polymerization). A recent work in this chemistry was developed by the group of Buchmeiser and co-workers.[137] They synthesized some Ti and Zr complexes with pyridine-borane ligands where the pyridine is capable to abstract/re-add a proton to the α-carbon of the inserted norbornenyl. An overview of the mechanism is represented in the Scheme 3.4. After the vinylic insertion of the norbornene, the pyridine abstracts one of the α-protons (**H**$^{\alpha}$) to make the Ti-alkylidene complex. Subsequently coordination-insertion of n molecules of norbornene by ROMP polymerization generates the ROMP skeleton. Now, at some point of the polymerization the re-addition of the α-proton (**H**$^{\alpha}$) to the Ti-alkylidene regenerates the Ti-alkyl and restarts the propagation of the norbornene by vinylic addition polymerization (VA polymerization).

[135] Johnston, J. A.; Tokles, M.; Hatvany, G. S.; Rinaldi, P. L.; Farona, M. F. *Macromolecules* **1991**, *24*, 5532-5534.
[136] a) Hartner, F. M.; Schwartz, J.; Clift, S. M. *J. Am. Chem. Soc.* **1983**, *105*, 640-641. b) Tritto, I.; Sacchi, M. C.; Grubbs, R. H. *J. Mol. Catal.* **1993**, *82*, 103-111. c) Manivannan, R.; Sundararajan, G.; Kaminsky, W. *Macromol. Rapid Commun.* **2000**, *21*, 968-972. d) Manivannan, R.; Sundararajan, G.; Kaminsky, W. *J. Mol. Catal. A: Chem.* **2000**, *160*, 85-95.
[137] a) Zou, Y.; Wang, D.; Wurst, K.; Kühnel, C.; Reinhardt, I.; Decker, U.; Gurram, V.; Camadanli, S.; Buchmeiser, M. R. *Chem. Eur. J.* **2011**, *17*, 13832-13846. b) Buchmeiser, M. R.; Camadanli, S.; Wang, D.; Zou, Y.; Decker, U.; Kühnel, C.; Reinhardt, I. *Angew. Chem. Int. Ed.* **2011**, *50*, 3566-3571.

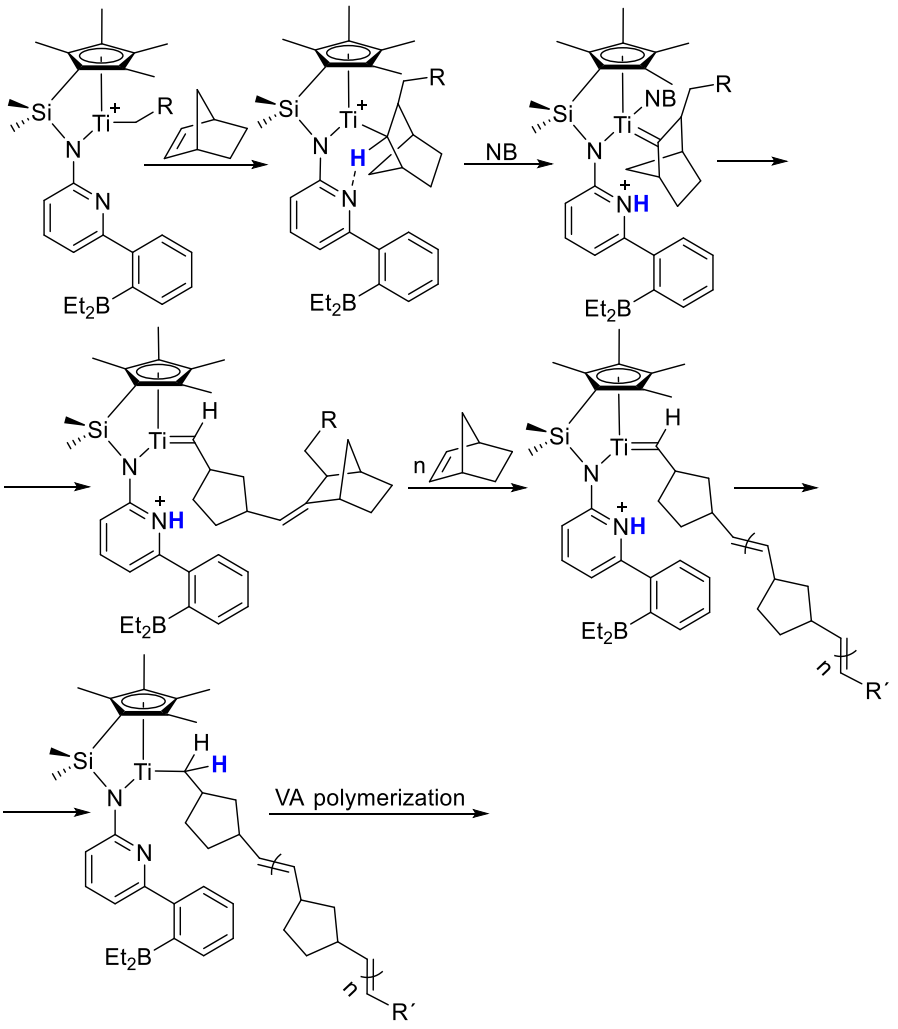

Scheme 3.4. An overview of the mechanism proposed for the formation of mixed skeleton ROMP-VA-PNB by Ti-based pyridine-borane ligands.

Although, in general, each catalyst follows a specific pathway for the polymerization of norbornene, it is interesting to know the factors that may deviate a catalyst from its expected polymerization mechanism. This is important to detect the potential structural errors introduced in a specific polymer backbone since it may also lead to a completely different polymer skeleton, as shown above.

3.1.2. The mechanism for the vinylic addition polymerization of norbornene: A puzzling termination step

As mentioned in the introduction of *Chapter 2*, the most general accepted mechanism for the vinylic addition polymerization can be separated in three different steps. The first step (*Initiation Step*) is the coordination of the norbornene followed by *cis*-2,3-*exo* insertion into the M-R bond (where R = H, alkyl or aryl) generating a new M-norbornenyl bond (Scheme 3.5).

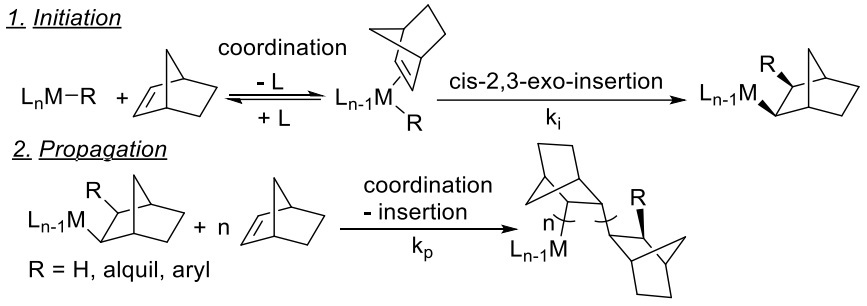

Scheme 3.5. Initiation and propagation step for the vinylic addition polymerization of norbornene.

The second step (*Propagation Step*) involves the coordination-insertion of n molecules of norbornene to generate the propagating chain. In many catalytic systems, in particular those based on Ni or Pd, the initiation step is slow in comparison with the propagation step, which is fast ($k_i < k_p$, Scheme 3.5). This affects the ratio M_w/M_n, the polydispersity index or PDI. A high value indicates a non-very controllable mechanism: if the PDI is high, the M_w (molecular weight averaged in weight) is higher than the M_n (molecular weight averaged in number) and this is indicative of the formation of few initial active centers that grow very fast giving long polymer chains. As more active centers form with time, the decrease of the monomer concentration lead to shorter polymer chains. On the other hand, a low PDI (similar M_w and M_n) is indicative of a situation where a fast initiation takes place and all the catalytic centers grow at a similar rate ($k_i > k_p$, Scheme 3.5). A low PDI is also found for a living polymerization (with some exceptions).[138] The main feature in a living polymerization is that the termination step of the polymerization is suppressed and the catalyst remains attached to the polymer chain ready to start a new polymerization upon addition of a new batch of monomer.

[138] Gold, L. *J. Chem. Phys*. **1958**, *28*, 91-99.

The nature of the termination step for the vinylic addition polymerization of norbornene is not clear. Different termination or chain transfer reactions have been proposed for the polymerization of α-olefins but they cannot operate in the same mode for bicyclic olefins. The different processes for the termination step with α-olefins were studied by T. Ziegler and co-workers using theoretical methods on a metallocene ethylene system.[139-141] They studied three types of processes: β-hydrogen elimination to generate a metal hydride, vinylic C-H bond activation and β-hydrogen transfer to a molecule of monomer (Scheme 3.6). Since β-hydrogen elimination is so thermodynamically unfavored (ΔH = 176 kJ/mol) it seems to be an unlikely chain termination mechanism in the vinylic addition polymerization of α-olefins with metalocenes, although it can be a most plausible route for Pd or Ni catalysts (Scheme 3.6, a)).[142] The C-H activation is a mechanism that can operate for the termination step generating a terminated alkane chain and a vinylzirconocene (Scheme 3.6, b)). However, the preferred mechanism is the β-H transfer to a molecule of monomer (Scheme 3.6, c)).

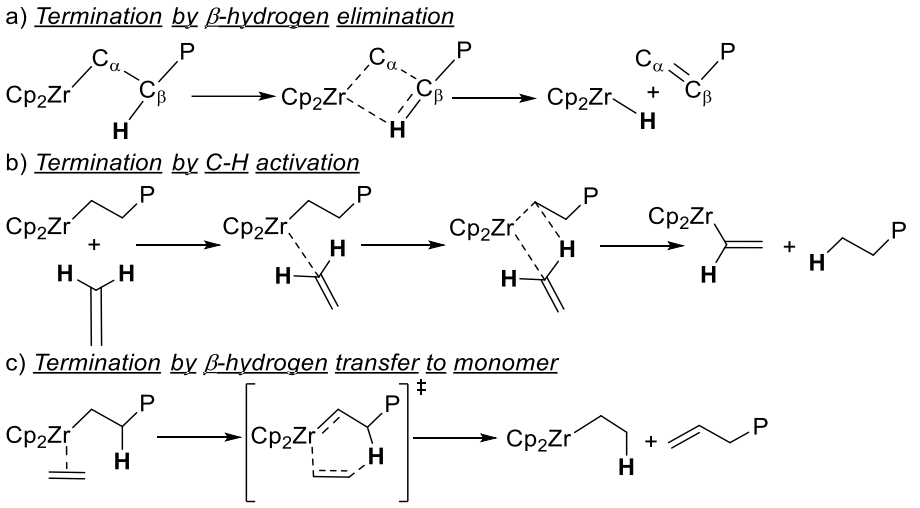

Scheme 3.6. Termination step by a) β-hydrogen elimination, b) C-H activation and c) β-hydrogen transfer to monomer in the vinylic addition polymerization of olefins.

[139] Woo, T. K.; Fan, L.; Ziegler, T. *Organometallics* **1994**, 13, 2252-2261.
[140] Lohrenz, J. C. W.; Woo, T. K. Fan, L.; *J. Organomet. Chem.* **1995**, *497*, 91-104.
[141] Margl, P.; Deng, L.; Ziegler, T. Chain *J. Am. Chem. Soc.* **1999**, *121*, 154-162.
[142] O'Connor, K. S.; Lamb, J. R.; Vaidya, T.; Keresztes, I.; Klimovica, K.; LaPointe, A. M.; Daugulis, O.; Coates, G. W. *Macromolecules* **2017**, *50*, 7010-7027.

None of these pathways are favored for norbornene. The β-H elimination involving the hydrogen atom at the bridgehead carbon of the norbornene (blue H atom), is impossible because of Bredt's rule: A carbon-carbon double bond cannot be placed at the bridgehead of a bicyclic ring system, unless the rings are large enough (Scheme 3.7, a)). In addition, a basic requirement for the β-H elimination is the coplanarity of the metal-carbon bond and the β-H atom implicated which is not possible in the norbornene ring (orange H atom) (Scheme 3.7, b)). The other possibility, that is the β-H transfer to another molecule of norbornene is forbidden in the polymerization of norbornene because of the lack of coplanarity between the metal atom, C^{β}, C^{α} and the β-H atom (Scheme 3.7, c)). The hydrogen transfer of the β-H atom leads to a product that does not comply with the Bredt's rule.

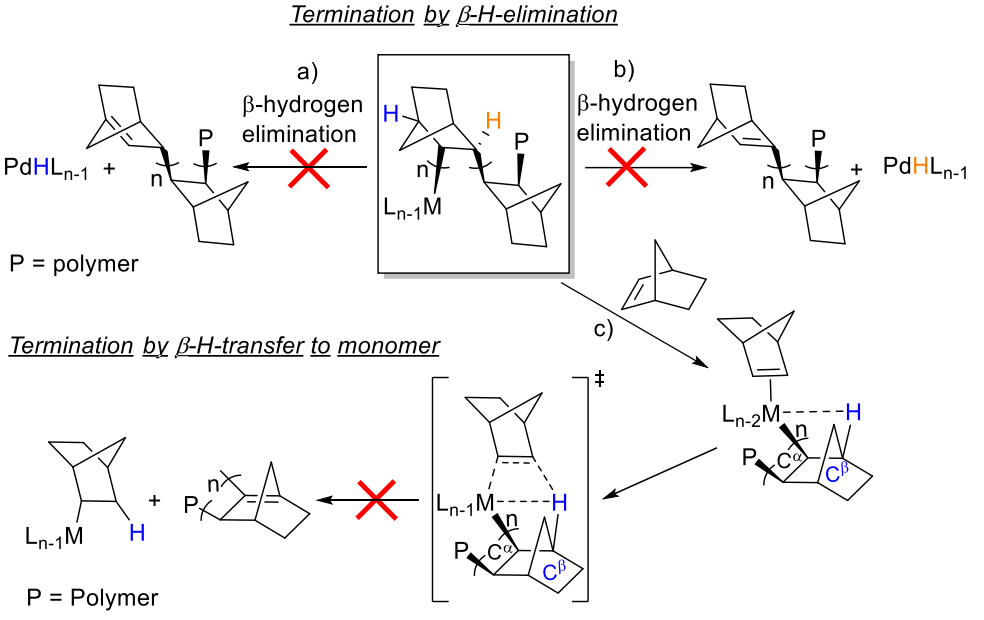

Scheme 3.7. Forbidden routes by β-hydrogen elimination and β-hydrogen transfer to monomer for the termination in the vinylic addition polymerization of norbornene.

Some reports in the literature on the norbornene polymerization with palladium complexes described that the Pd-C bond remains attached to the polynorbornene after the vinylic addition polymerization finishes. This Pd-C bond can be destroyed by insertion of carbon monoxide and subsequent addition of methanol. Pd(0) precipitates, and the VA-PNB was isolated with methyl ester end groups.[101c] The chain termination in the norbornene polymerization has been induced by the use of certain additives that allow a termination pathway. For example, the

addition of a linear olefin RCH=CH_2 gives, by insertion in the M-polynorbornenyl bond, a M-CH_2-CHR-polynorbornenyl fragment where the β-H elimination can occur. This has been used in Pd-based catalytic systems.[143] In the case of alkenyl-norbornenes, the insertion of the metal center into the exocyclic double bond followed by β-H elimination was proposed as a termination pathway by Janiak and co-workers (Scheme 3.8).[99d,105]

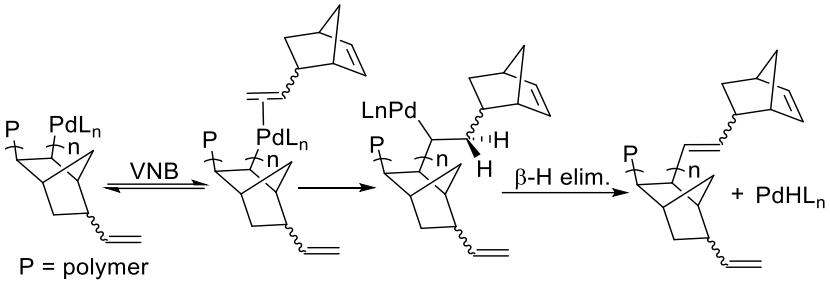

Scheme 3.8. Proposed termination pathway for alkenyl-norbornenes.

The addition of formic acid also produces the termination of the polynorbornene chain and occurs via formation of Pd-H species and reductive elimination of H-polynorbornenyl polymer chains.[144]

Rhodes and co-workers proposed a mechanism for the termination pathway in the vinylic addition polymerization of an ester-functionalized norbornene with the catalyst $[Pd(NCMe)_4](BF_4)_2$ in absence of any chain transfer additive.[145] The VA-polymerization of 2-acetoxymethyl-5-norbornene with $[[Pd(NCMe)_4](BF_4)_2$ as catalyst (ratio monomer/Pd = 1000:1) proceeded with low yield (34 %) and gave polymers with low molecular weight (M_n = 1130 Da). This M_n is much lower than the one expected in those conditions for a living polymerization where each metal center initiates a polymer chain and the termination is not favored. If the polymerization is living, the theorical M_n is related to the ratio of monomer and catalyst and can be calculated considering the molecular weight of the monomer and the yield. In this case the theorical M_n is ≈ 56000 (i.e 1000 x 0.34 x $M_w$monomer). The difference in the values indicates that some type of chain termination is operating in the polymerization and

[143] Benedikt, G. M.; Elce, E.; Goodall, B. L.; Kalamarides, H. A.; McIntosh, L. H.; Rhodes, L. F.; Selvy, K. T.; Andes, C.; Oyler, K.; Sen, A. *Macromolecules* **2002**, *35*, 8978-8988.
[144] Kandanarachchi, P.; Chang, C.; Simth, S.; Bradley, P.; Rhodes, L. F.; Lattimer, R. P.; Benedikt, G. M. *J. Photopolym. Sci. Thecnol*. **2013**, *26*, 431-439.
[145] McDermott, J.; Chang, C.; L. Martín, F.; Rhodes, L. F. *Macromolecules* **2008**, *41*, 2984-2986.

therefore, the Pd-C bond of the growing polymer chain does not remain intact. By the study of some oligomers and its characterization by MALDI-TOF MS and NMR spectroscopy, they concluded a possible formation of end groups such as **D₃**. It was proposed that **D₃** is formed by a β-γ-C-C cleavage of the ring followed by β-hydrogen elimination, which leads to an *exo*-methylene cyclohexenyl ring. This mechanism is controlling the grown of the chain (Scheme 3.9).

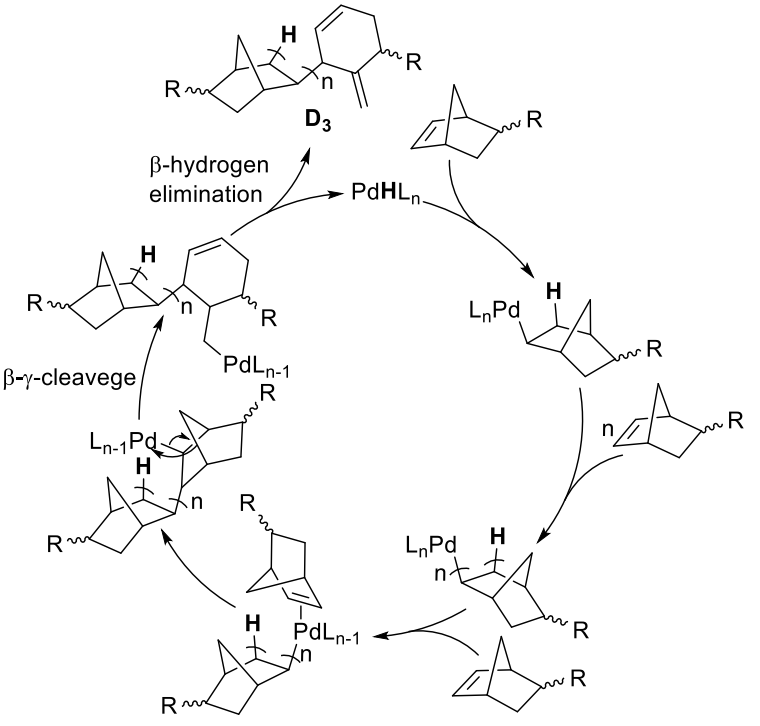

Scheme 3.9. Proposed mechanism for the termination step in the vinylic addition polymerization of substituted norbornenes with palladium catalyst.

3.1.3. β-C elimination in the norbornene ring with palladium and nickel complexes

β-carbon elimination mediated by transition metals is a well-known process.[146] Although more common for early transition metals, there are examples of β-γ-C-C cleavage by group 10 metals, in particular palladium and platinum and more rarely nickel. Early work in this area was reported by the groups of Noyori and Maitlis.[146a,c] Noyori described the opening of the cyclopropyl ring by β-C elimination to give a palladium allyl (Scheme 3.10),[146a] a transformation that is involved in skeletal rearrangements in palladium chemistry,[147] as well other processes.[148] The ring opening of cyclobutanes via β-C elimination is also well known.[146h,i,j]

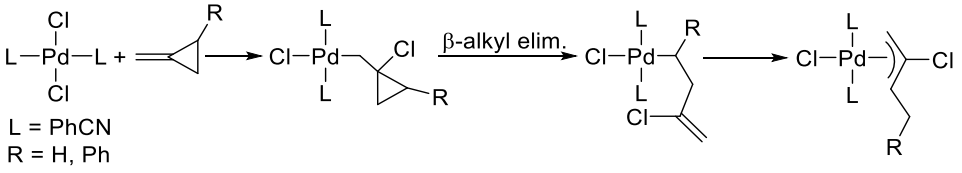

Scheme 3.10. β-alkyl elimination from palladium(methycyclopropyl) complexes.

Maitis et al. described the reactivity of complex **E**$_3$ in the presence of HCl.[146c] The formation of dichloro(pentamethylcycopentadiene)palladium(II) (**G**$_3$) and styrene could be explained by protonation of the starting complex **E**$_3$ and a β-γ-C-C cleavage in the intermediate **F**$_3$ (Scheme

[146] a) Noyori, R.; Takaya, H. *J. Chem. Soc. D*, **1969**, 525-525. b) Miller, R. G.; Golden, H. J.; Baker, D. J.; Stauffer, R. D. *J. Am. Chem. Soc.* **1971**, *93*, 6308-6309. c) Calvo, C.; Hosokawa, T.; Reinheimer, H.; Maitlis, P. M. *J. Am. Chem. Soc.* **1972**, *94*, 3238-3240. d) Nishimura, T.; Uemura, S. *J. Am. Chem. Soc.* **2000**, 122, 12049-12050. e) Zhang, Z.; Lu, X.; Xu, Z.; Zhang, Q.; Han, X. *Organometallics* **2001,** *20*, 3724-3728. f) Satoh, T.; Miura, M.; *Top Organomet. Chem*. **2005**, *14*, 1-20. g) Matsuda, T.; Ashida, S.; Murakami, M. *J. Am. Chem. Soc*. **2006**, *128*, 2166-2167. h) O'Reilly, M. E.; Dutta, S.; Veige A. S. *Chem. Rev.* **2016**, *116*, 8105-8145. i) Fumagalli, G.; Stanton, S.; Bower, J. F. *Chem. Rev.* **2017**, *117*, 9404-9432. j) Song, F.; T Gou, T.; Wanga, B. -Q.; Shi, Z. -J. *Chem. Soc. Rev.* **2018**,*47*, 7078-7115. k) Cao, J.; Chen, J.; Sun, F. -N.; Sun, Y. -L.; Jiang, K. -Z.; Yang, K. -F.; Xu, Z.; Xu, L.-W. *Angew. Chem. Int. Ed.* **2019**, *58*, 897-901.

[147] Albéniz, A. C.; Espinet, P.; Lin, Y. -S. *J. Am. Chem. Soc*. **1996**, *118*, 7145-7152

[148] a) Green, M.; Hughes, R. P. *J. Chem. Soc., Dalton Trans*. **1976**, 1880-1889. b) Larock, R. C.; Varaprath, S. *J. Org. Chem*. **1984**, *49*, 3432-3435 c) Fischetti, W.; Heck, R. F. *J. Organomet. Chem.* **1985**, *293*, 391-405. d) Owczarczyk, Z.; Lamaty, F.; Vawter, E. J.; Negishi, E. *J. Am. Chem. Soc.* **1992**, *114*, 10091-10092.

3.11).[146b] This is one of the few examples where β-C elimination does not involve in a ring opening process.[149]

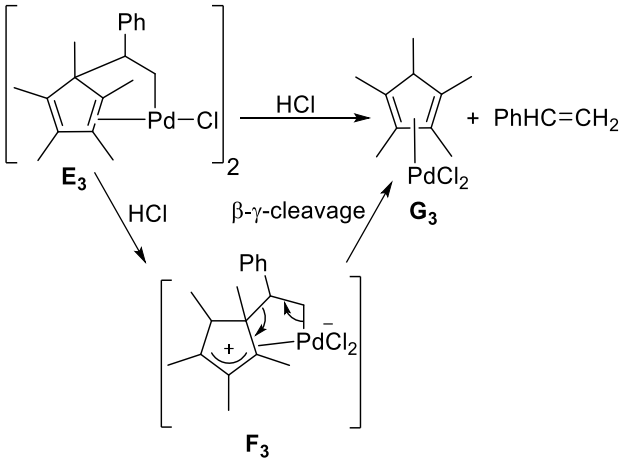

Scheme 3.11. β-carbon elimination in a palladium complex in the presence of HCl.

β-carbon elimination or β-γ-C-C cleavage of the norbornene ring in the presence nickel or palladium complexes is a well-established process. Following the seminal work of Catellani et al,[150] many palladium catalyzed coupling processes have been developed that are mediated by norbornene leading to the selective functionalization of arenes.[151] As shown in the example of Scheme 3.12, the NB mediation involves a β-C elimination with no alteration of the bicyclic structure. Insertion of norbornene into the ``PdArI´´ generated in situ and the ortho C-H cleavage assisted by base generates the intermediate **H3**. In the intermediate **I3**, formed by oxidative addition of the R^2X to **H3** followed by reductive elimination, the β-C elimination regenerates the norbornene and **J3**. Further reaction of the Pd-C bond of **J3** gives the final product **K3**.

[149] Campora, J.; Gutierrez-Puebla, E.; Lopez, J. A.; Monge, A.; Palma, P.; del Rio, D.; Carmona, E. *Angew. Chem., Int. Ed*. **2001**, *40*, 3641.
[150] a) Catellani, M.; Chiusoli, G. P. *J. Organomet. Chem.* **1982**, *239*, C35-C37. b) Catellani, M.; Chiusoli, G. P. *J. Organomet. Chem.* **1985**, *286*, C13-C16. c) Catellani, M.; Chiusoli, G. P.; Ricotti, S. *J. Organomet. Chem.* **1985**, *296*, C11-C15.
[151] a) Wang, J.; Dong, G. *Chem. Rev*. **2019**, *119*, 7478-7528. b) Della Ca', N.; Fontana, M.; Motti, E.; Catellani, M. *Acc. Chem. Res*. **2016**, *49*, 1389-1400

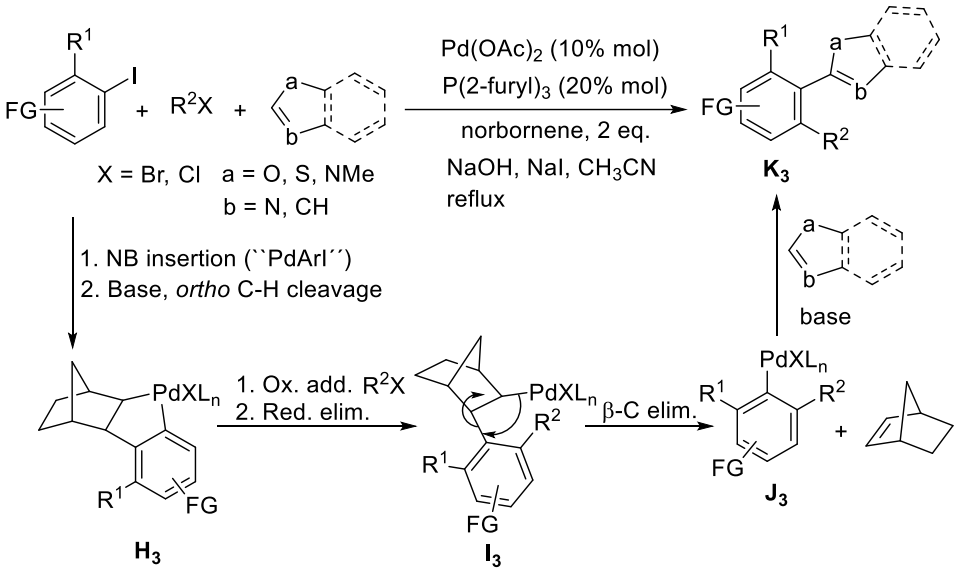

Scheme 3.12. Direct arylation of aryl iodides mediated by norbornene.

There are a few examples in the literature where the opening of the norbornene ring occurs.[152-155] Catellani and co-workers reported, in 1983, a β-γ-C-C cleavage after two sequential insertions of norbornene into a Pd-Ar bond generated by oxidative addition of an ArBr to $[Pd(PR_3)_4]$ (R = Aryl) (Scheme 3.13).[152b] The mechanism proposed involves the formation of a "PdArX" (X = Br, carboxylate) complex followed by the insertion of two norbornene units. The β-hydrogen elimination is not accessible as we mentioned before in this introduction (Scheme 3.7), so an alternative β-γ-C-C cleavage occurs, followed by a now easy β-H elimination to generate the compound **L3**. The authors suggested that the formation of **M3** resulted from a C-H activation of the arene and reductive elimination.

[152] a) Catellani, M.; Chiusoli, G. P.; Sgarabotto, P. *J. Organomet. Chem.* **1982**, *240*, 311-319. b) Catellani, M.; Chiusoli, G. P *J. Organomet. Chem.* **1983**, 247, C59-C62. c) Bocelli, G.; Catellani, M.; Chiusoli, G. P. *J. Organomet. Chem.* **1984**, *219*, 225-232. d) Catellani, M. *Synlett* **2003**, *3*, 298-313.
[153] Dzhemilev, U. M.; Khusnutdinov, R. I.; Galeev, D. K.; Tolstikov, G. A. *Izvestiya Akademii Nauk SSSR*, **1979**, *28*, 854-856.
[154] Tenaglia, A.; Terranova, A.; Waegell, B. *J. Mol. Cat.* **1987**, *40*, 281-287
[155] Portnoy, M.; Ben-David, Y.; Rousso, I.; Milstein, D. *Organometallics* **1994**, *13*, 3465-3479.

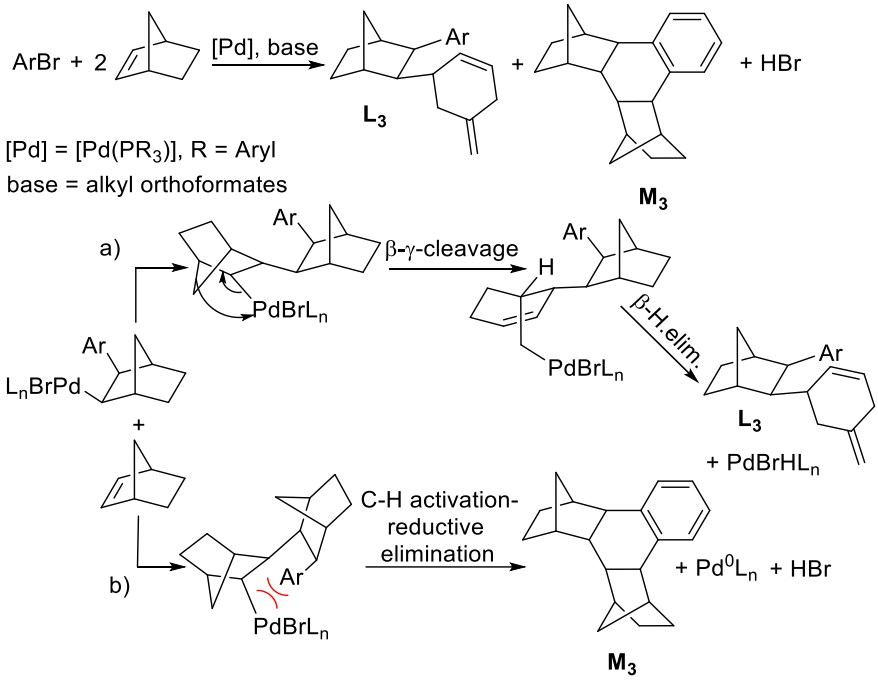

Scheme 3.13. Schematic representation of the competition between the β-γ-C-C cleavage and the C-H activation-reductive elimination with norbornene and a Pd-Aryl complex.

Another β-γ-C-C cleavage was reported in the dimerization of norbornene in the presence of nickel-phosphine complexes (Eq. 3.1).[154] When L = dppe, the exclusive formation of product **N3** was observed.

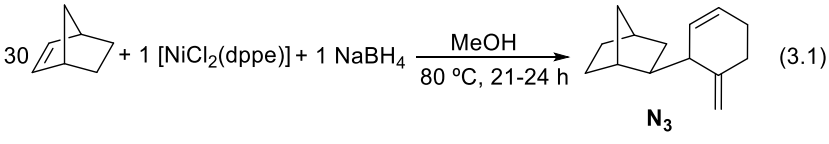

(3.1)

The mechanism proposed for the dimerization starts with the formation of a $NiClHL_2$ complex and subsequent decomposition to generate a Ni(0) complex that is the real active species. The interaction between the norbornene and the Ni(0) complex generates a nickelacyclopentane **I** intermediate that via protonolysis of one of the Ni-C bonds, β-γ-C-C cleavage and finally β-H elimination leads to **N3** (Scheme 3.14).

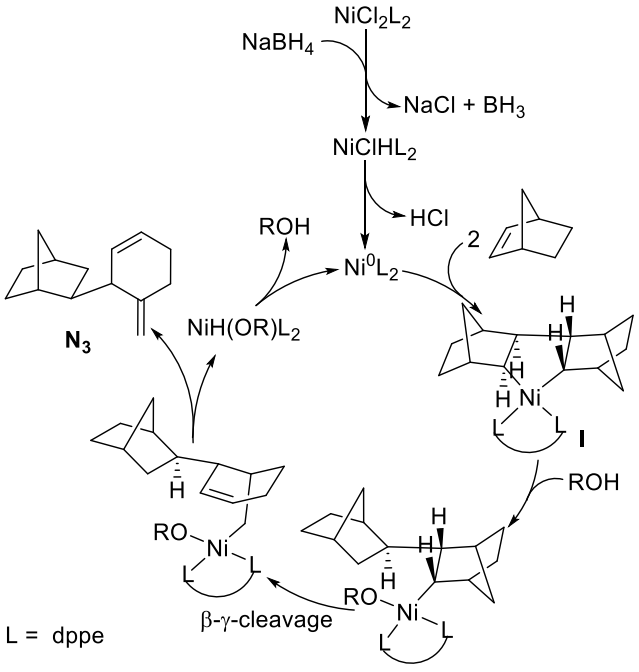

Scheme 3.14. Proposed mechanism for the formation of the product **N₃** by a metalacycle intermediate.

In the course of a study of the effect of chelating ligands in the Heck reaction, Milstein and co-workers reported a similar β-carbon elimination of the norbornene ring by palladium-Aryl complexes (Scheme 3.15).[155] Heating the phenyl palladium complex in DMF at 100 ºC in the presence of an excess of norbornene resulted in the isolation of the isomers **O₃**-**Q₃**. The most probable pathway for this reaction is the insertion of the norbornene into the Pd-Ph bond followed by β-carbon elimination and subsequently β-hydrogen elimination to produce the compound **O₃**. After the β-hydrogen elimination, the Pd-H species generated in the reaction mixture can catalyze the isomerization of the internal double bond in the cyclohexene generating the other isomers (**P₃** and **Q₃**).

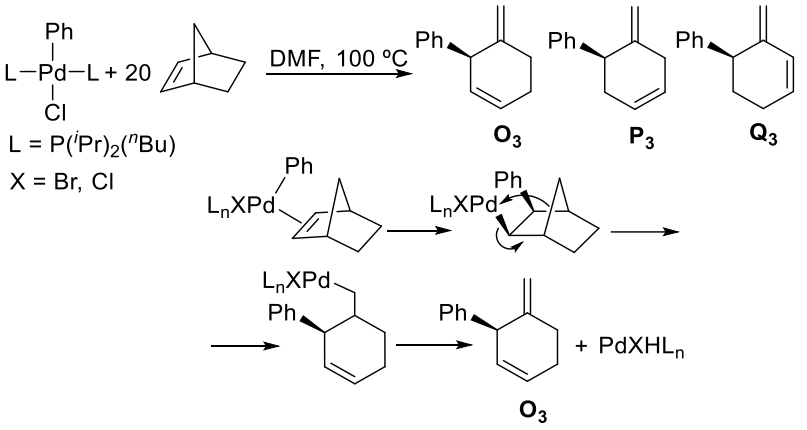

Scheme 3.15. Formation of the cyclohexene ring by β-carbon elimination.

3.1.4. Aim of the work in this chapter

In this chapter, we will describe the formation of a new type of skeleton for the polynorbornene that combines the normal propagation step of a vinylic addition polymerization (VA) with the β-γ-C-C cleavage of the norbornenyl ring (RO). The aim of the work is to characterize the new polynorbornene backbone and to understand the factors that favor the ring opening as well as to develop suitable catalysts to obtain the new VA/RO-PNBs. We have studied the behavior of different nickel complexes to determine how the opening of the ring by β-γ-C-C cleavage in the vinylic addition polymerization of norbornene can be influenced by the presence of amounts of coordinating solvents or the ligands in the coordination sphere of the nickel.

3.2. Results and Discussion

3.2.1. Study of the formation of new type of skeleton in the vinylic addition polymerization of norbornene with [Ni(C_6F_5)L_2] complexes

The complex *trans*-[Ni(C_6F_5)($SbPh_3$)$_2$] (**27**) has been employed before in our research group in the vinylic addition polymerization of norbornene and the copolymerization of norbornene with ω-bromoalkyl substituted norbornenes.[112] Analogous *trans*-[Ni($C_6F_3Cl_2$)L_2] (L = AsR_3) have been also used in the polymerization of norbornene.[101g] The polymers obtained in these reactions were isolated with good to excellent yields and high M_{ws}. All the NMR data of the isolated polymers indicated a vinylic addition type polymerization with a very fast propagation, i.e the ligand, $SbPh_3$ in most cases, is not competing with the norbornene for the coordination. On the other hand, when the same catalyst **27**, was employed in our research group for the copolymerization of norbornene and norbornenyl carbonate (Eq 3.2) the polymer showed additional olefinic signals in the ^{1}H NMR unexpected for an aliphatic VA-skeleton of the copolymers (Figure 3.1).[103g] The aliphatic protons of the skeleton are present between 3-0.9 ppm and the signal at 5.1-4.8 is associated with the protons H^2 and H^3. The new broad signal appears between 5.8-5.6 ppm (Figure 3.1) and we can discard a ROMP polymerization type because the signals for the double bond in the skeleton of the ROMP polynorbornene have lower chemical shifts, about 5.3-5.2 ppm.[77] The NMR data matches with the formation of a cyclohexene ring by a β-γ-C-C cleavage (or β-carbon elimination) in the norbornene, as proposed before by Rhodes and co-workers,[144,145] and by Catellani and co-workers in the Pd-catalyzed dimerization of norbornene, as mentioned in the Introduction.[152-154] However, as far as we know, a ring-opened norbornene by β-γ-C-C cleavage has never been observed as a constituent fragment of a polymer backbone.

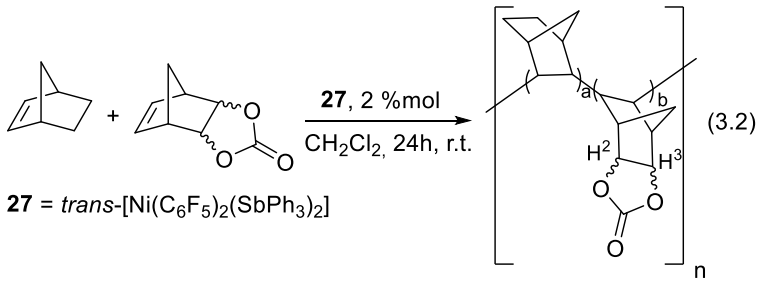

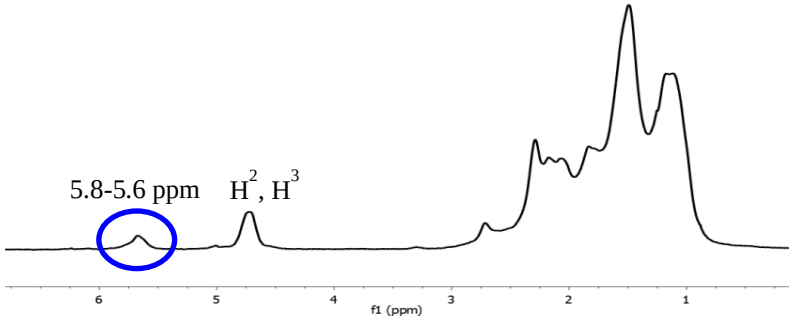

Figure 3.1. ^{1}H NMR of the isolated copolymer of norbornene and norbornenyl carbonate synthesized with the catalyst *trans*-[Ni(C_6F_5)($SbPh_3$)$_2$] (**27**).

The difference between the polymerization of norbornene and the copolymerization of norbornene with norbornenyl carbonate is the presence of a substituted norbornene which bear a polar, coordinating group and its polymerization is slower than that of the norbornene.[110,111] We hypothesized that the β-γ-C-C cleavage is a process dependent of the rate of the propagation step and this idea is summarized in Scheme 3.16. During the growth of the polymer, one molecule of the norbornenyl carbonate can coordinate through the oxygen stopping the propagation. At this moment, it is possible that the ring of the norbornene opens by a β-γ-C-C-cleavage to generate a Ni-cyclohexenyl bond. In the work of Rhodes with palladium catalysts (Scheme 3.9) this opening is a way to finish the polymerization by β-hydrogen elimination. But this Ni-cyclohexenyl is still active in the polymerization and now the norbornenyl carbonate can decoordinate and re-coordinate through the endocyclic double bond restarting the propagation of the polymerization. In this way the ring-opened norbornene is incorporated in the polymer structure.

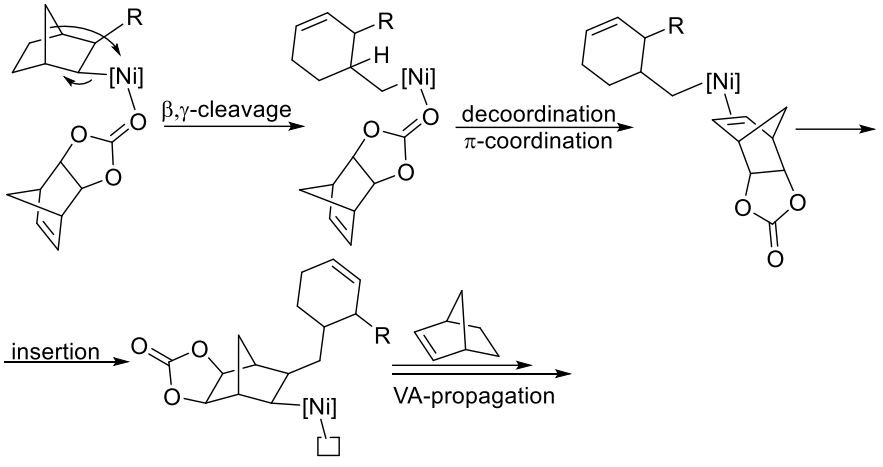

Scheme 3.16. Mechanism proposed for the formation of the cyclohexene ring by β-γ-C-C cleavage of the norbornene ring in the copolymerization of norbornene and norbornenyl carbonate.

Considering the idea that upon slowing down the propagation step we are increasing the possibility of the β-γ-C-C cleavage and therefore introducing a modification in the polymer backbone, we studied the formation of these structural ``errors´´ in the vinylic addition polymerization of norbornene and the factors that favor it using several nickel complexes. In all this chapter, we will name the polynorbornene whose skeleton is a mixture of a vinylic addition polymerization and a ring opening of the NB bicycle by β-γ-C-C cleavage as VA/RO-PNB (vinylic addition/ring opening polynorbornene). The bicyclic NB units in the polymer will be labeled VA (NB_{VA}) and the methylcyclohexeneyl units will be referred to as RO (NB_{RO}) or, occasionally, as structural errors.

We first studied the effect of the ligands coordinated to the nickel center in the complexes *trans*-[Ni(C_6F_5)$_2$$L_2$], as well as the initial concentration of the reagents in the polymerization of norbornene (Table 3.1). All the polymers were characterized by NMR spectroscopy and some of them by GPC. The structure of the polymers as well as some mechanistic considerations will be discussed in the next section, but all of them present the same basic structure: an aliphatic skeleton with variable amounts of RO norbornene units (signals at 5.8-5.4 ppm in ^{1}H NMR). The amount of NB_{ROs} or structural errors was quantified by ^{1}H NMR using the following equation for the ratio between NB_{VA} and NB_{RO} units: NB_{VA}/NB_{RO}= [IntA-(IntB/2) x 8]/10(IntB/2) where IntA = integral value of the aliphatic region and IntB = integral value of the 5.8-5.4 region (cyclohexene double bond). An example is shown in Figure 3.2

and the equation is: NB_{VA}/NB_{RO}= [115.62-(2/2) x 8]/10(2/2) = 14.3/1. From this ratio the percentage of NB_{RO} units can be deduced.

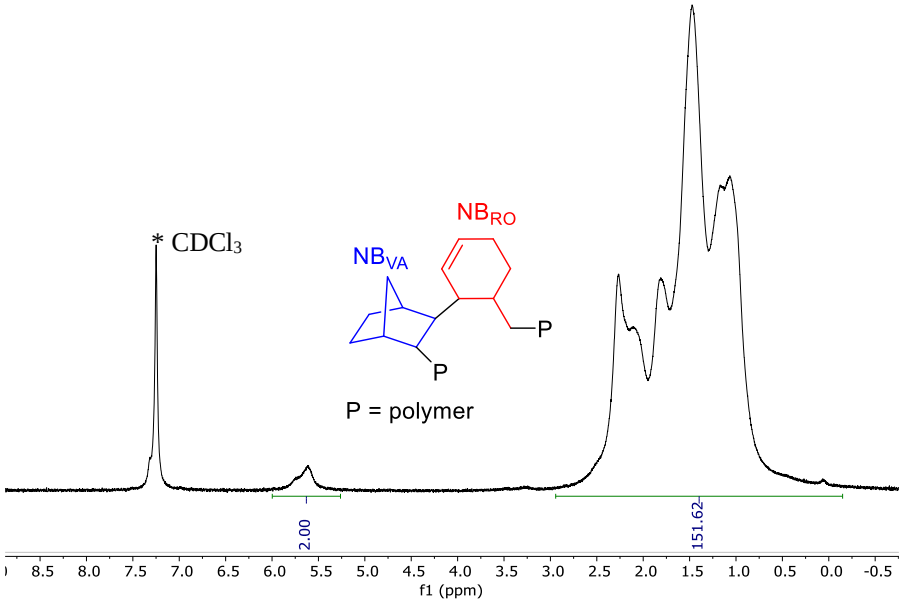

Figure 3.2. Example of ^{1}H NMR in dry $CDCl_3$ of VA/RO-PNB (vinylic addition/ring opening polynorbornene) for the calculation of the ratio NB_{VA}/NB_{RO} (entry 4, Table 3.1)

We can observe an important influence of the concentration of the reagents in the formation of NB_{RO} units with the catalyst **28** (L = $AsPh_3$). At high concentration (entry 3, Table 3.1), no structural errors are found in the skeleton of the isolated polymer. However, at low concentration (entry 4, Table 3.1), the formation of NB_{RO} units (6.4%) is significant in the skeleton of VA/RO-PNB with a decrease in the yield of the polymerization. The influence of the concentration in the rate of the propagation step is crucial: when decreasing the concentration of the monomers, the rate of the propagation step decreases and therefore, the β-γ-C-C cleavage starts to compete with the propagation step increasing the formation of ring opening units (NB_{RO}).

The ligands coordinated to the nickel center also have an effect. Comparing catalysts **27** and **28** at low monomer concentration (entries 2 and 4, Table 3.1), we can observe that the catalyst with the most labile ligand (complex **27**) generates a very little number of NB_{RO} units (1.5%). In contrast, the catalyst with $AsPh_3$ (**28**) affords a polymer with a higher percentage of NB_{RO}

units (6.4%). Furthermore, catalyst **29** where L = PPh_3, the best ligand of the series, generates bad results in the polymerization of norbornene with the formation of just oligomers (entry 6, Table 3.1). It is obvious that a ligand that competes better with the norbornene for the coordination to the nickel center ($AsPh_3$ vs $SbPh_3$) leads to a lower propagation rate and a higher probability for the formation of units.

Table 3.1. Study of the formation of errors with the catalysts **27**, **28** and **29**.[a]

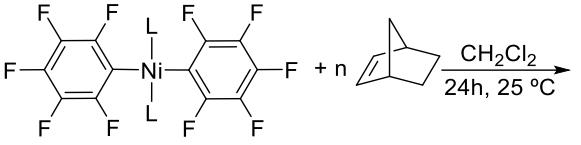

L = $SbPh_3$, **27**; $AsPh_3$, **28**; PPh_3, **29**

Entry	Catalyst	NB:Ni	$[NB]_o$[b]	NB_{VA}/NB_{RO}[c]	% NB_{RO}[d]	Yield (%)[e]
1	**27**	75:1	0.34	no NB_{RO}	0%	90%
2	**27**	75:1	0.061	67/1	1.5%	75%
3	**28**	75:1	0.34	no NB_{RO}	0%	95%
4	**28**	75:1	0.061	14.3/1	6.4%	67%
5	**28**	225:1	0.061	no NB_{RO}	0%	74%
6	**29**	75:1	0.34	---	---	---

a) The reactions were carried out using CH_2Cl_2, 25 ºC, 24 hours, under N_2. b) Initial molar concentration of NB. c) The ratio NB_{VA}/NB_{RO} was calculated by integration in the ^1H NMR of a solution of the polymer in dry $CDCl_3$ (see above, Figure 3.2). d) The molar % was calculated with the ratio NB_{VA}/NB_{RO} by the equation: $NB_{RO}/(NB_{VA} + NB_{RO})*100$. e) Yields are referred to the total monomer mass.

Finally, we checked the effect of the ratio NB/Ni using complex **28** and the same NB initial concentration (entries 4 and 5, Table 3.1). No NB_{RO} units in the polymerization of norbornene were observed when the ratio increased from 75/1 to 225/1 at low initial concentration of NB. A lower concentration of the catalyst in the conditions of entry 5 (Table 3.1) influences the rate of the initiation and propagation steps but also determines that the concentration of free ligand is lower. This makes the competition of the ligand and NB for coordination to Ni advantageous for NB and the propagation step faster.

We also studied the influence of the presence of coordinating solvents. Many catalysts that are active in VA-polymerization of norbornene in CH_2Cl_2 or toluene do not work in coordinating solvents such as acetone, and this has been shown before for $[NiAr_2L_2]$.[101g] However, mixtures of CH_2Cl_2 with a small amount of a co-solvent lead to VA/RO-PNB with moderate yields. We tested four coordinating solvents as additives in the polymerization of NB with complex **28**: acetone, acetophenone, DMA and acetonitrile (Table 3.2).

At high initial concentration of NB (0.34 M), and in the presence of 160 equivalents of acetone, we observed the formation of a 6% of NB_{RO} in the skeleton of VA/RO-PNB. Thus, this percentage is very similar to the percentage observed at low concentration without a coordinating solvent (see entries 1 and 3, Table 3.2). At the same ratio NB/catalyst/solvent (75/1/160) and the same initial NB concentration, 0.061 M, the use of DMA or MeCN as co-solvent does not afford any polymer whereas acetone or acetophenone lead to polymers in good yields (entries 4, 7, 11 and 12, Table 3.2). When using DMA, it is necessary to decrease the amount of solvent to a ratio 75/1/20 or 40 to isolate polymers with good to modest yields (entries 8-10, Table 3.2). The effect of the solvent in the polymerization and the percentage of NB_{RO} in the polymer is consistent with the coordination ability of these solvents: MeCN > DMA > PhCOMe > MeCOMe. Increasing the ratio solvent:Ni, an increase of the number of NB_{RO} units is observed (compare entries 4-6 or 9-10, Table 3.2). In general, the higher the number of NB_{RO} units in the VA/RO-PNB, the lower the yield of the polymerization and the lower the molecular weight of the polymer obtained (entries 7-10, Table 2.3).

Table 3.2. Study of the formation of VA/RO-PNBs with the catalysts **28** in the presence of coordinating solvents.[a]

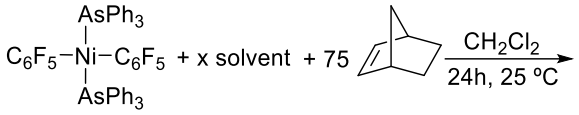

28

Entry	$[NB]_o$[b]	x solvent	NB_{VA}/NB_{RO}[c]	% NB_{RO}[d]	Yield (%)[e]	M_w[f]	M_w/M_n[f]
1	0.061	none	14.6/1	6.4%	67%	---	---
2	0.34	none	no NB_{RO}	0%	95%	---	---
3	0.34	160 acetone	15.7/1	6.0%	70%	---	---
4	0.061	160 acetone	12.1/1	7.6%	65%	---	---
5	0.061	320 acetone	9.4/1	9.6%	63%	---	---
6	0.061	640 acetone	8.5/1	10.2%	50%	---	---
7	0.061	160 acetophenone	7.6/1	11.6%	64%	17.391	1.5
8	0.061	20 DMA	7.0/1	12.5%	34%	12.570	1.4
9	0.34	20 DMA	13.9/1	6.7%	74%	33.605	1.6
10	0.34	40 DMA	8.4/1	10.5%	55%	22.366	1.7
11	0.061	160 DMA	---	---	0%	---	---
12	0.34	20 MeCN	---	---	0%	---	---

a) The reactions were carried out using the catalyst **28**, ratio NB:**28** = 75:1, CH_2Cl_2 as solvent, 25 ºC, 24 h, under N_2. b) Initial molar concentration. c) The ratio NB_{VA}/NB_{RO} was calculated by integration in the ^1H NMR of a solution of the polymer in dry $CDCl_3$ (see above, Figure 3.2). d) the molar % was calculated with the ratio NB_{VA}/NB_{RO} by the next equation: $NB_{RO}/(NB_{VA} + NB_{RO})$*100. e) Yields are referred to the total monomer mass. f) M_w in Daltons determined by GPC in $CHCl_3$ using polystyrene standards.

All the effects discussed before for the formation of a VA-PNB skeleton or a VA/RO-PNB are summarized in Figure 3.3. The change from a conventional mechanism for the vinylic addition polymerization (VA) to a VA/RO polymerization is dependent on the propagation rate: upon decreasing the propagation rate, the β-γ-C-C cleavage is more important leading to a VA/RO-PNB. Controlling the different factors at play (low ratio NB/Ni and low $[NB]_o$, modestly-coordinating ligands or co-solvents of intermediate coordination ability) a VA/RO-

polynorbornene with a range of 6-11% of ring-opened NB units (NB_{RO}) and a good yield can be obtained with complex **28**. The effect of the solvents in the vinylic addition polymerization of norbornene is very interesting because they can play a similar role to the polar groups in substituted norbornenes as we commented in the initial part of this section for the copolymerization of norbornene with norbornenyl carbonate. On the other hand, when a high k_p is ensured (high ratio NB/Ni and high $[NB]_o$, weakly-coordinating ligands) the formation of VA-PNB without NB_{RO} units occurs.

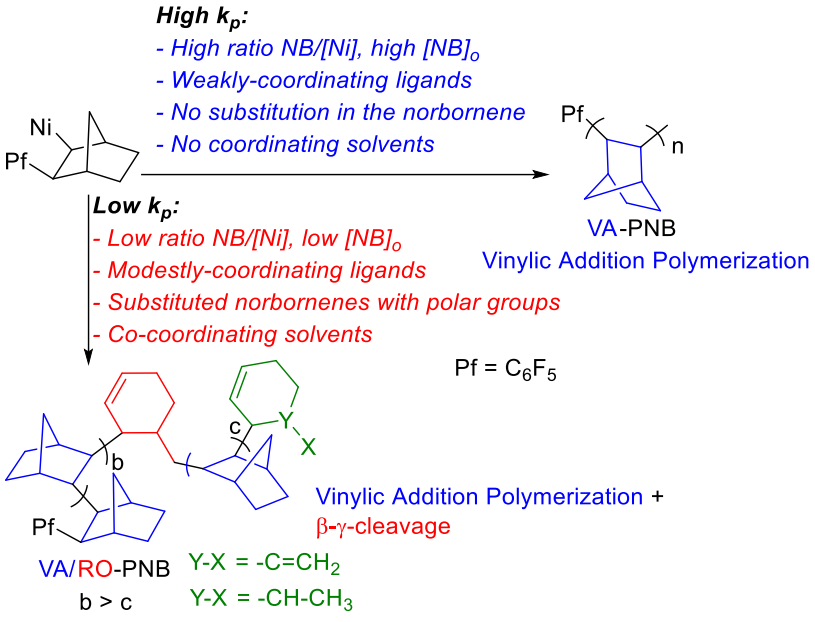

Figure 3.3. Conditions that affect the change from a VA-polymerization to a VA/RO-polymerization.

3.2.2. Study of the structure of VA/RO-PNB and some mechanistic considerations in the polymerization of NB with catalyst 28

The polymers collected in Table 3.1-3.2 were isolated as white solids soluble in solvents such as $CHCl_3$, THF and CH_2Cl_2. All the GPC collected show unimodal distributions indicating the presence of only one polymer. Figure 3.4-3.5 show the solution ^1H and ^{13}C spectra of two analogous polymers with different molecular weights and different percentage of NB_{RO} units. A comparative analysis of both VA/RO-PNBs will help to characterize their structure and identify the terminal groups in the polymer. As expected for these macromolecules, broad

signals appear. The ^{1}H NMR shows the presence of the aliphatic protons typical for the vinylic addition polymerization mechanism (2.5-0.45 ppm). The ^{13}C NMR of the aliphatic region (54.7-22.9 ppm) does not show signals below 20 ppm indicating a coordination-insertion of the norbornene exclusively by the *exo*-face.

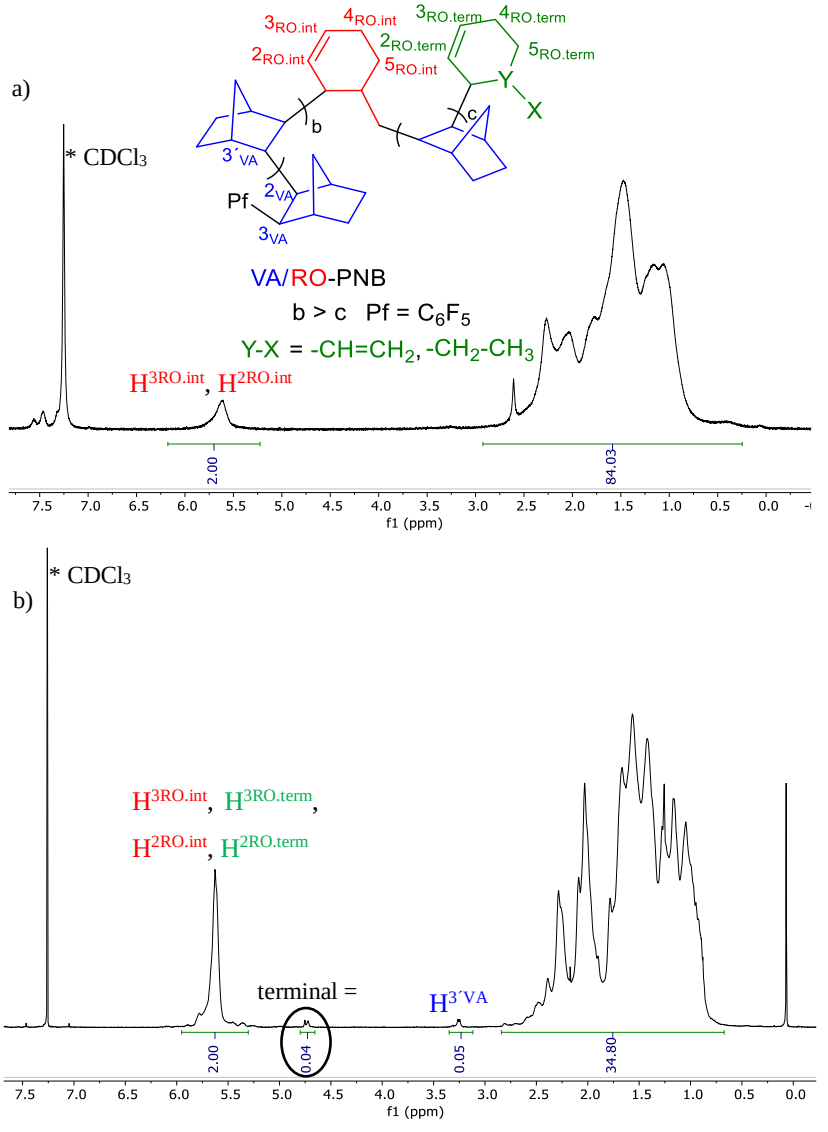

Figure 3.4. a) ^{1}H NMR in $CDCl_3$ of a polymer VA/RO-PNB with a ratio NB_{VA}/NB_{RO} = 7.6/1 (entry 7, Table 3.2); M_w = 17.391. b) ^{1}H NMR for a short polymer VA/RO-PNB in $CDCl_3$ with a ratio NB_{VA}/NB_{RO} = 2.7/1.

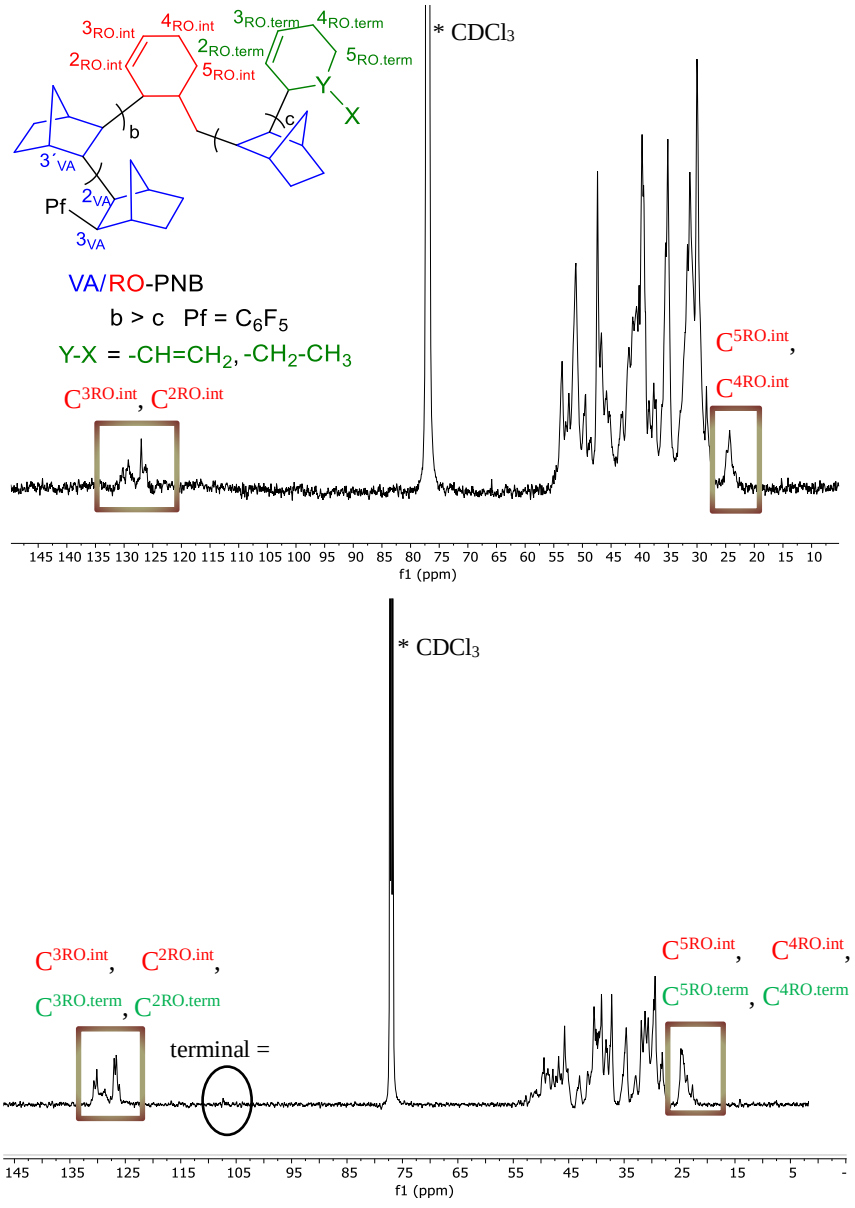

Figure 3.5. a) ^{13}C NMR in $CDCl_3$ of a polymer VA/RO-PNB with a ratio NB_{VA}/NB_{RO} = 7.6/1 (entry 7, Table 3.2); M_w = 17.391. b) ^{13}C NMR in $CDCl_3$ of a short polymer VA/RO-PNB in $CDCl_3$ with a ratio NB_{VA}/NB_{RO} = 2.7/1.

A broad signal at 5.8-5.4 ppm appears in the ^{1}H NMR and the corresponding carbon atoms can be assigned in the ^{13}C NMR by 2D ^{1}H-^{13}C HSQC to the resonances at 132-125 ppm. The comparison of the spectroscopic data of the cyclohexene ring between the dimer **30**, that we synthesized independently,[154] and our polymer is consistent with the presence of the

cyclohexene ring in the skeleton of our VA/RO-PNB: cyclohexene double bond at 5.69 ppm in ^{1}H NMR and 129.65, 127.55 ppm in the ^{13}C NMR for **30** (Figure 3.6) vs 5.8-5.4 ppm in ^{1}H NMR and 132-125 ppm in ^{13}C NMR in the polymer VA/RO-PNB (Figure 3.4-3.5). The assignment of the other ^{1}H and ^{13}C signals in the VA/RO-PNB is collected in the Experimental Section.

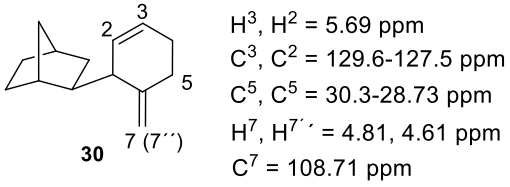

Figure 3.6. Some representative chemical shifts for the dimer **30**.

The initiation step through the Pd-C_6F_5 bond is clear in the ^{19}F NMR where we can observe the presence of the C_6F_5 groups bound to the polymer. The presence of multiple signals indicates the presence of different environments for the C_6F_5 group or even slow rotation of the ring around the C_{NB}-C_6F_5 bond (Figure 3.7).

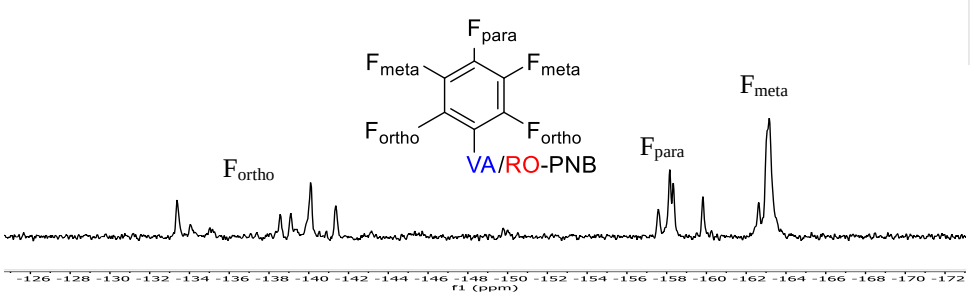

Figure 3.7. ^{19}F NMR in $CDCl_3$ of VA/RO-PNB with NB_{VA}/NB_{RO} ratio = 7.6/1 (rati NB:Ni:acetophenone = 75:1:160; entry 7, Table 3.2) at 298 K.

After the β-γ-C-C cleavage there is a possible termination pathway by β-hydrogen elimination with the formation of a cyclohexene ring with a terminal double bond.[144,145] We do not observe the presence of terminal double bonds in the NMR spectra of the VA/RO polymer shown in Figure 3.4 a) (no signals around 4.8-4.6 ppm). However, in the short polymer where the ratio of terminal groups to the atoms in the polymer main chain is higher, a small signal is visible at 4.7 ppm that is associated with a ^{13}C NMR resonance at 107.46 ppm. These chemical shifts are very similar than the signals observed for the terminal double bond in the dimer **30** (Figure

3.6). Therefore, the termination step by β-hydrogen elimination is observable for small polymers obtained at low NB/**28** ratio but it is not the dominant process after the β-γ-C-C cleavage occurs since only 2% of the NB_{RO} units undergo β-hydrogen elimination (the ratio NB_{RO} in the polymer main chain to the terminal NB_{RO} ($NB_{RO.term}$) calculated by ^{1}H NMR is 1/0.02)

The broad NMR signals in the polymer spectra, due to the complex morphology of these polymers and their high molecular weight, does not allow to make a complete assignment. 2D ^{1}H-^{13}C short and long range correlations, including phase sensitive experiments that allow to distinguish secondary and tertiary carbons (gHSQCAD and gHMBCAD), were very helpful to see additional features. For example, the initiation of the polymerization (C_6F_5-norbornenyl) is visible in the ^{1}H NMR of the short polymer by the presence of the $H^{3'VA}$ at 3.26 ppm (Figure 3.4, b)). This proton has a higher chemical shift than the other aliphatic protons because of the presence of the C_6F_5 group and correspond to a CH group as we can observe in the phase sensitive gHSQCAD NMR. The broad signal between 25-22 ppm, separated from the rest of the aliphatic signals of the polymer in the ^{13}C NMR, correlates in the long range ^{1}H-^{13}C with the ^{1}H signal of the internal double bond of the cyclohexene ring. We assigned this part of the ^{13}C NMR to the $C^{4RO.int}$, $C^{5RO.int}$ and $C^{4RO.term}$, $C^{5RO.term}$ (for the short polymer). The other signals in the ^{13}C NMR cannot be distinguished completely but we can see in the phase sensitive gHSQCAD which regions correspond to the CH_2 and the CH of the skeleton.

A general view for the mechanism is represented in Scheme 3.17. The polymerization starts with the insertion of the norbornene into the Ni-C_6F_5 bond. After subsequent-coordination-insertion of b molecules of norbornene (the normal propagation way for a vinylic addition polymerization), a β-γ-C-C cleavage can occur leading to a cyclohexenylmethyl-nickel ring. Now the polymerization continues through the Ni-alkyl bond with the insertion of c molecules of norbornene until another β-γ-C-C cleavage occurs. It is reasonable to assume that as the polymerization proceeds and the concentration of the norbornene deceases, the propagation rate slows down and the probability of a β-carbon elimination increases, so c will be lower than b in Scheme 3.17. We propose an alternating structure for the polymer with long chains of bicyclic norbornene units (NB_{VA}) intercalated with ring-opened norbornene units (NB_{RO}) that are more concentrated at the end of the polymerization, i.e the polymer presents a composition drift. To test this, we determined the number of NB_{RO} units as the polymerization

proceeds which will tell us if it is the distribution of these structural errors is regular in all the polymer.

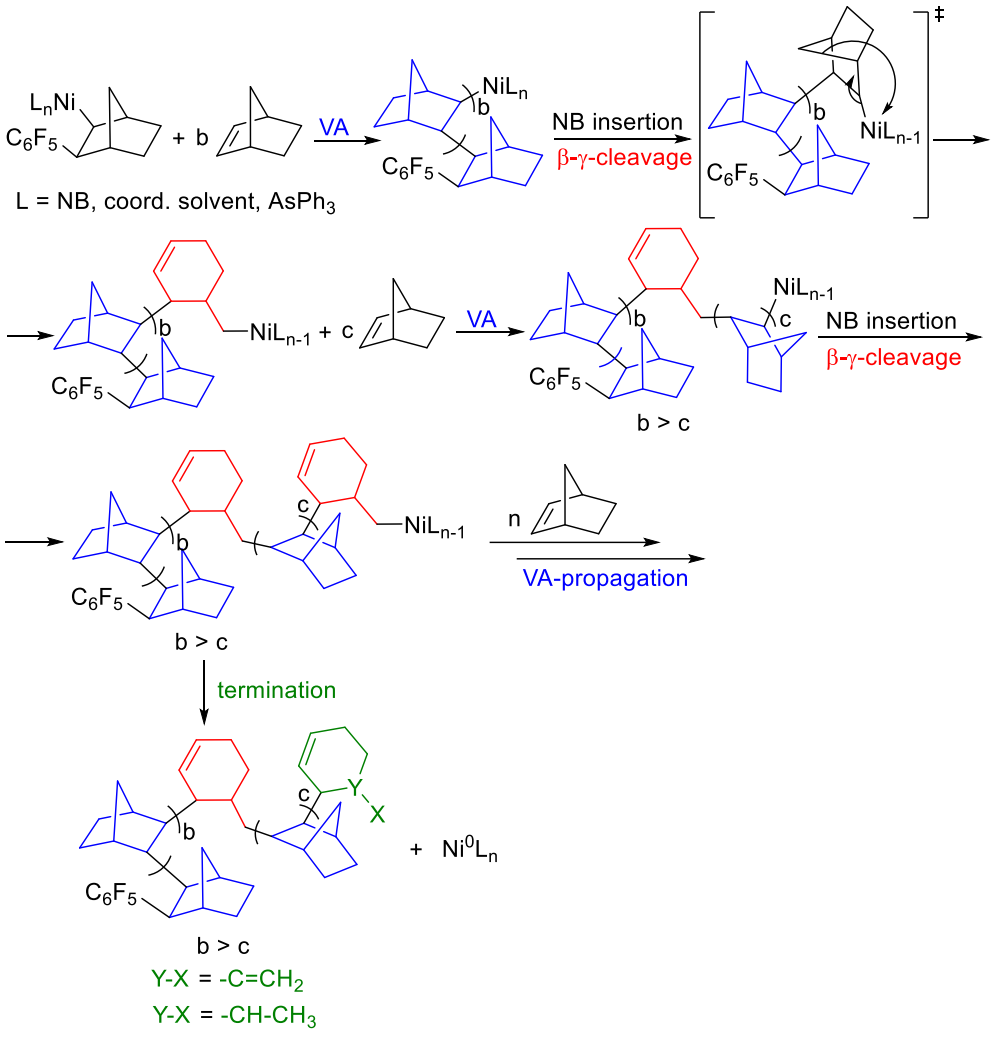

Scheme 3.17. Proposed mechanism for the vinylic addition polymerization of norbornene with the catalyst **28**.

In the same conditions (NB:Ni:acetophenone = 75:1:160), we performed several experiments stopping the polymerization at different times by the addition of MeOH. All the data obtained are collected in Table 3.3. As the polymerization proceeds with the time, the molecular weight of the polymer obtained increases as well as the yield.

Table 3.3. Polymerization of norbornene with the combination NB:Ni:acetophenone = 75:1:160 at different times with the complex **28**.[a]

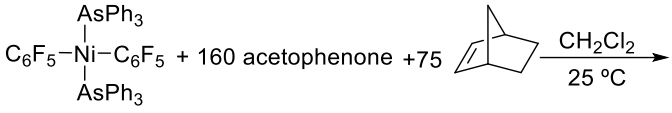

28

Entry	Time (min)	NB_{VA}/NB_{RO}[b]	% NB_{RO}[c]	Yield (%)[d]	M_n[e]	M_w[e]
1	5	32.3/1	3.0%	3.5%	5788	6688
2	10	15.7/1	6.0%	10.6%	6044	7261
3	20	12.7/1	7.3%	19.8%	6242	7398
4	40	10.0/1	9.1%	38.6%	6949	8457
5	120	7.5/1	11.8%	60.9%	8827	11829

a) The reactions were carried out using 12 ml of CH_2Cl_2 ($[NB]_o$ = 0.061 M), ratio NB:Ni:acetophenone = 75:1:160, 25 ºC, under N_2. b) The molar ratio NB_{VA}/NB_{RO} was calculated by integration in the ^1H NMR of a solution of the polymer in dry $CDCl_3$ (see above, Figure 3.2). c) the molar % was calculated with the ratio NB_{VA}/NB_{RO} by the next equation: $NB_{RO}/(NB_{VA} + NB_{RO})$*100. d) Yields are referred to the total monomer mass. e) M_n and M_w in Daltons determined by GPC in $CHCl_3$ using polystyrene standards.

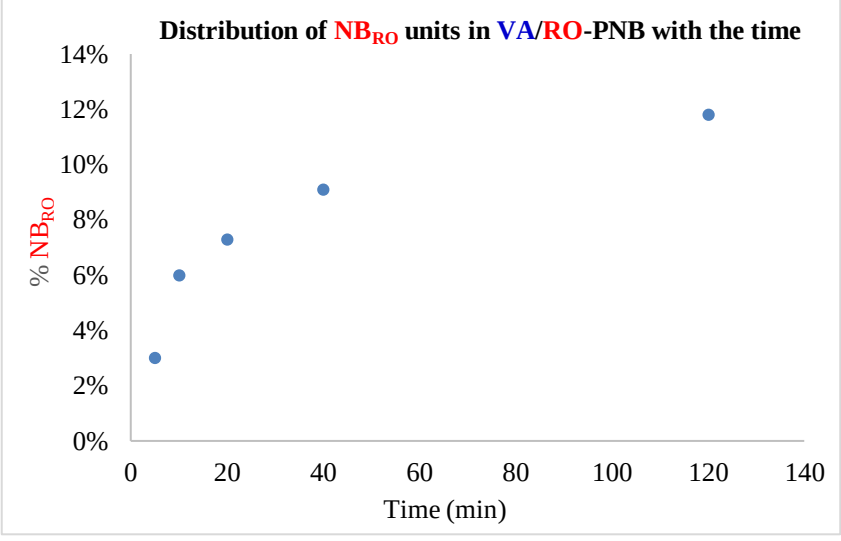

Figure 3.8. Distribution of NB_{RO} units with the time for the polymerization of norbornene with the catalyst **28** in the presence of acetophenone (ratio NB:Ni:acetophenone = 75:1:160).

A representation of the percentage of NB_{RO} in the polymer versus the time shows that the distribution of the NB_{RO} units is not regular (Figure 3.8). The number of ring opened NB_{RO} in a polymer obtained at the beginning of the polymerization is low, since the concentration of the norbornene and the rate of the propagation are high. As the monomer is consumed, the polymer grows at a slower rate and the ring opening occurs more often: the result is a polynorbornene with a higher percentage of NB_{RO} units, which will be unevenly distributed in the polymer chain (more concentrated at the end of the growth). The termination step is still not very clear in this system but we know the β-hydrogen elimination can operate. Only in the short polymer the termination by β-hydrogen elimination (Y-X = $-C=CH_2$) is visible (Figure 3.4, b)) but it is possible that the same mechanism can operate in the long polymer where the observation of the chain termination group is more difficult (higher molecular weight, lower percentage of termination group in the polymer chain). On the other hand, if some of nickel remains attached to the polymer after the polymerization finishes, it is possible that the addition of MeOH can terminate the polymerization transferring a H via a ``$NiHL_n$´´ intermediate (Y-X = $CH-CH_3$).

3.2.3. Study of the formation of ring-opened norbornene by β-C elimination in the polymerization of norbornene with [NiArXL$_2$] and [NiArL$_3$]$^+$ complexes.

3.2.3.1. Polymerization of norbornene using the [NiArCl(PPh$_3$)$_2$]/AgBF$_4$ precatalyst mixture

The complexes [NiArCl(PPh_3)$_2$] (Ar = *o*-CF_3-C_6H_4, **31**; *o*-CH_3-C_6H_4, **32**) were synthesized following the methodology developed by Jamison and co-workers (Eq. 3.3).[156] Complex **31** was synthesized before by and oxidative addition of *o*-CF_3-C_6H_4I to a Ni(0) source but it was not characterized by NMR spectroscopy.[157] All the spectroscopic data obtained by NMR agree with square planar complexes with two phosphines in *trans*-disposition (see Experimental Section).

[156] Standley, E. A.; Smith, S. J.; Müller, P.; Jamison, T. F. Complexes *Organometallics* **2014**, 33, 2012-2018.
[157] SennŌ, M.; Tsuchiya, S.; Hidai, M.; Uchida, Y. X-Ray *Bull. Chem. Soc. Japan*, **1976**, *49*, 1184-1186.

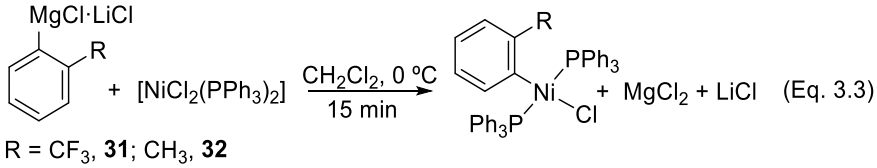

The complexes **31** and **32** were tested in the polymerization of norbornene but as expected, neither polymer nor oligomers were detected. A better polymerization catalyst can be obtained by abstraction of the Cl atom with, for example, a silver salt, which provides an available coordination site for the monomer and also increases the electrophilicity of the metal center. Also, the presence of a CF_3 group in complex **31**, gives some additional spectroscopic information for mechanistic studies and some structural information of the skeleton of VA-PNB and VA/RO-PNB.

We started exploring the polymerization of norbornene generating in situ a cationic complex using $AgBF_4$ and the complex [Ni(*o*-CF_3-C_6H_4)Cl(PPh_3)$_2$] (**31**) in a 1:1 (v/v) mixture CH_2Cl_2/toluene, where the starting silver salt is completely soluble. After filtration of the solid AgCl, the formed the solution was evaporated to dryness and a solution of NB in CH_2Cl_2 was added to the residue containing the Ni species (Scheme 3.18).

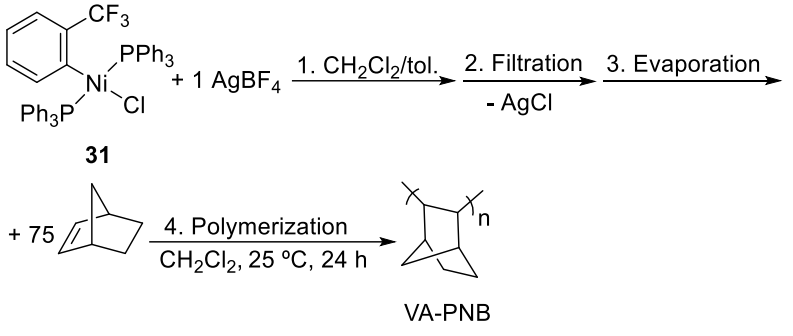

Scheme 3.18. Synthetic methodology for the polymerization of NB with a catalyst generated in situ by the combination of **31**/$AgBF_4$ (ratio 1:1) in CH_2Cl_2/toluene.

A polymer was isolated after 24 h with very good yield (86 %) and no structural errors were found in the structure of the polymer that conforms to a typical VA-PNB (Figure 3.9). The initiation step through the Ni-(*o*-CF_3-C_6H_4) bond is confirmed by the presence in the ^{19}F NMR spectrum of a signal at -58.05 ppm for the *o*-CF_3-C_6H_4 anchored to the VA-PNB.

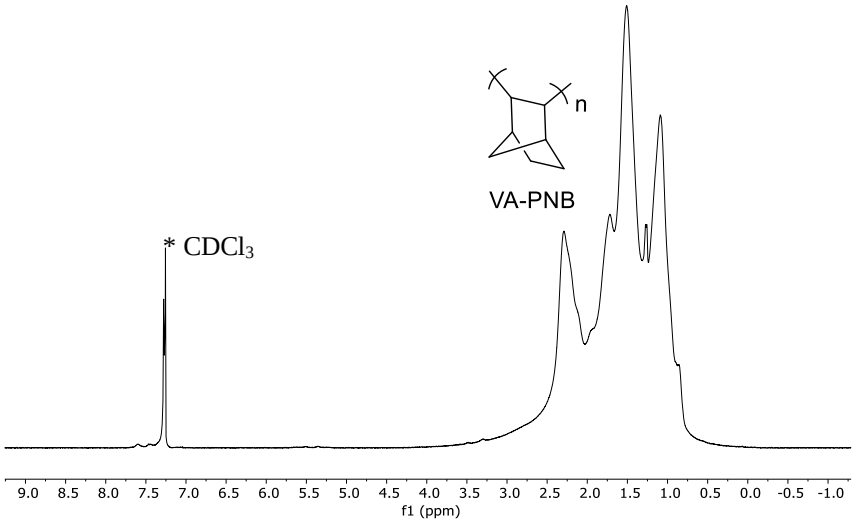

Figure 3.9. ^{1}H NMR (500.13 MHz, dry $CDCl_3$) for the VA-PNB generated with the system **31**/$AgBF_4$ in CH_2Cl_2/toluene (ratio NB:**31**/$AgBF_4$ = 75:1:1) at 298 K.

We also tested the polymerization of norbornene by the formation of a cationic complex in situ from **31** and $AgBF_4$ in acetone, where both reagents are soluble (Scheme 3.19).

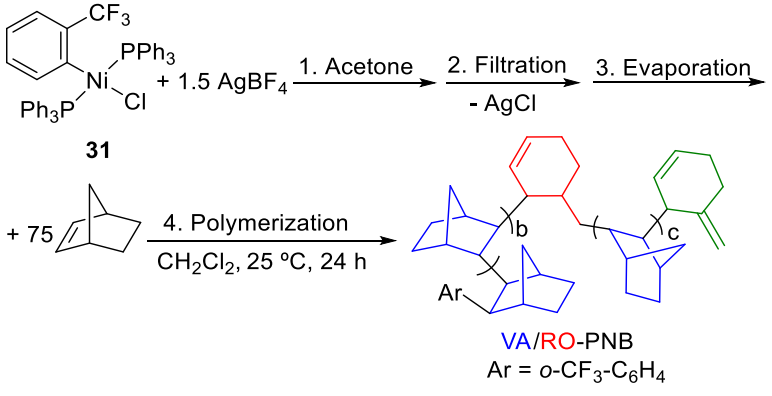

Scheme 3.19. Synthetic methodology for the polymerization of NB with a catalyst generated in situ by the combination of **31**/$AgBF_4$ (ratio 1:1.5) in acetone.

After 24 h a white polymer was isolated in 65% yield. The polymer is soluble in common organic solvents and it was characterized by NMR spectroscopy and GPC. The GPC shows a unimodal distribution with a low molecular weight (M_w = 4200 Da) and low PDI (1.3). Two

broad signals between 5.85-5.25 ppm and 4.8-4.6 ppm are observed in the ^{1}H NMR and the corresponding signals in the olefinic region in the ^{13}C NMR at 133-125 ppm and at 108 ppm, indicative of a VA/RO-PNB (Figure 3.10, a) and b)). The initiation of the polymerization through the Pd-aryl bond is clear in the ^{19}F NMR where we observe the presence of the CF_3 anchored to the skeleton (-58.37 ppm) (Figure 3.10, c)). All the collected data indicate the presence of only one polymer with some ring-opened NB units in their structure (NB_{RO}, signals for the cyclohexene ring between 5.85-5.25 ppm in the ^{1}H NMR and 133-123 ppm in the ^{13}C NMR) in a similar fashion that the polymers generated with the system *trans*-$[Ni(C_6F_5)_2(AsPh_3)_2]$ (**28**)/co-solvent. The main difference between them is the presence of a higher amount of the terminal double bond (signals at 4.8-4.6 ppm in the ^{1}H NMR and 108 ppm in the ^{13}C NMR) that is generated by β-hydrogen elimination from a Ni-methylcyclohexenyl fragment and leads to a chain termination process (NB_{ROterm} units).[144,145] The ratio NB_{VA}/NB_{RO} where NB_{RO} = total ring opening = (NB_{ROint} + NB_{ROterm}) can be calculated by the following equation: NB_{VA}/NB_{RO} = [IntA-((IntB-IntC)x8/2)-IntCx5/2]/10(IntB/2) where IntA = integral value of the aliphatic region and IntB = integral value of the 5.8-5.4 region (cyclohexene double bond) and IntC = integral value of the 4.8-4.6 region (terminal double bond).[158] For example, in the polymer presented in Figure 3.10 a), the ratio NB_{VA}/NB_{RO} is 7.5/1. The ratio of the ring-opened norbornene that gets incorporated into the polymer main chain (NB_{ROint}) and that undergoing β-H elimination and chain termination (NB_{ROterm}) can be calculated by the following equation NB_{ROint}/NB_{ROterm} = (IntC/IntB-IntC) where, as above, IntB = integral value of the 5.8-5.4 region (cyclohexene double bond) and IntC = integral value of the 4.8-4.6 region (terminal double bond). So, in for polymer depicted in Figure 3.10 a), the ratio is 1/0.21. This ratio is important because indicates that not all the norbornene that undergo a ring opening by β-C elimination, leads to the termination of the polymerization and the polymer is genuine VA/RO-PNB.

[158] 8 is the number of protons of the cyclohexene ring of NB_{ROint}; 5 are the protons of the cyclohexene ring of NB_{ROterm};10 are the protons of the norbornene.

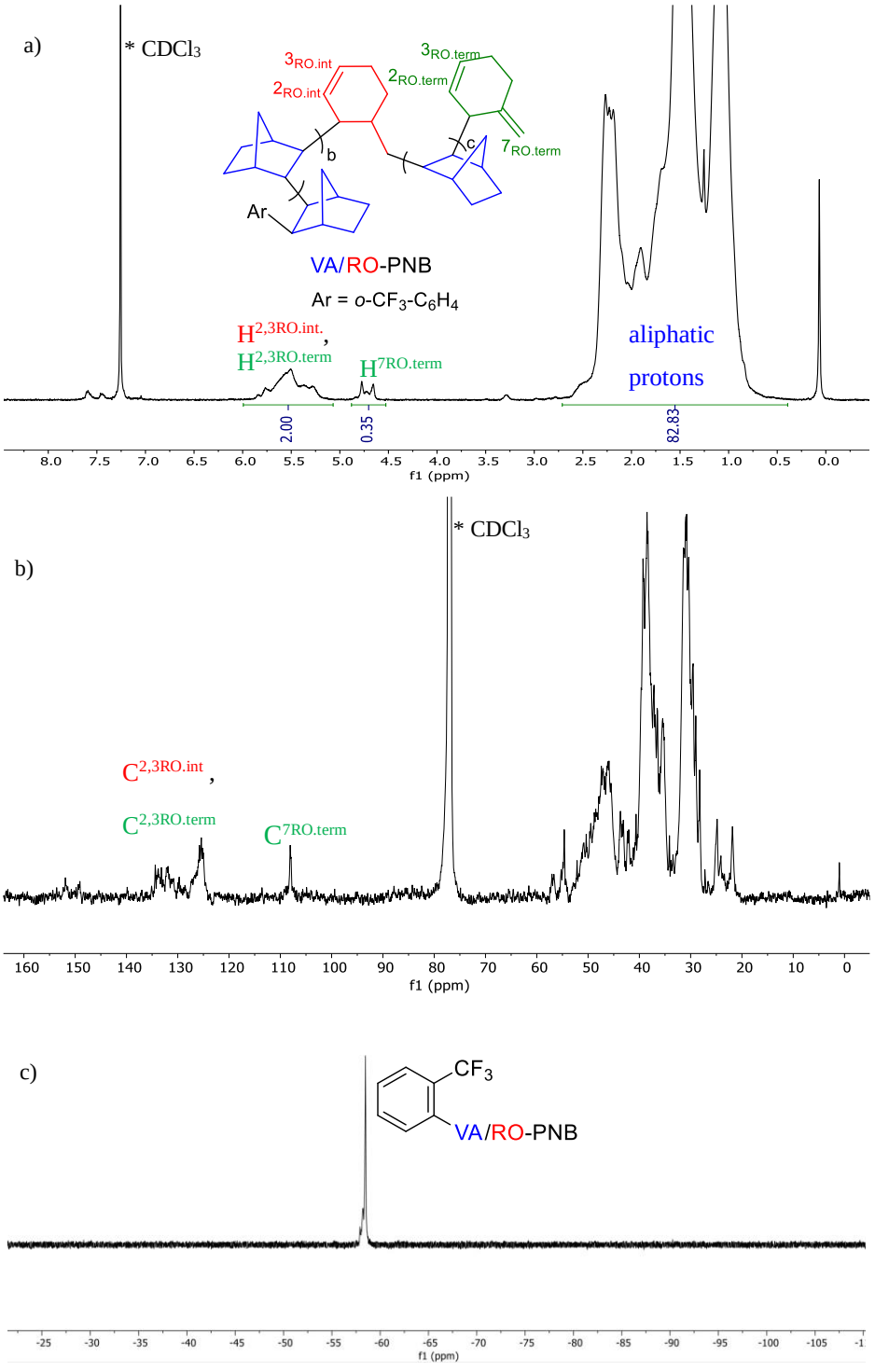

Figure 3.10. a) ^{1}H NMR, b) ^{13}C NMR and c) ^{19}F NMR in $CDCl_3$ at 298 K for the VA/RO-PNB obtained with a catalyst generated form **31**/$AgBF_4$ in acetone (ratio NB:Ni = 75:1).

The different structures of the polymers obtained upon changing the catalyst preparation procedure is a strong indication that the active nickel species in both experiments are also different. First, we studied by NMR spectroscopy the reaction of **31** and $AgBF_4$ in the mixture CH_2Cl_2/toluene (Scheme 3.20).

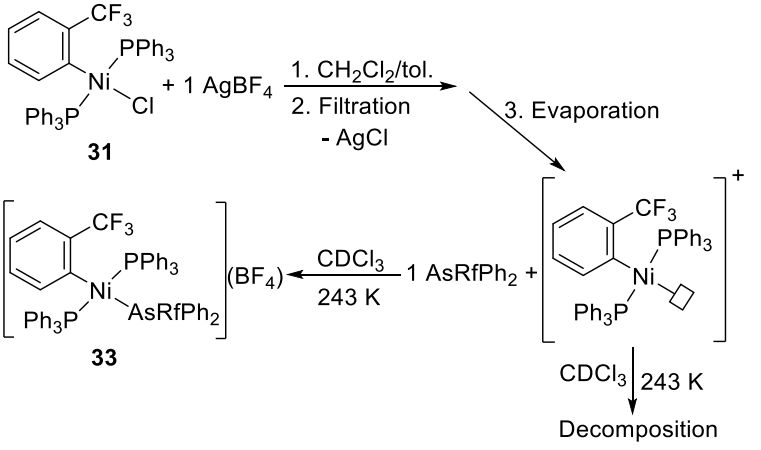

Scheme 3.20. Formation of complex **33** in the presence of 1 equivalent of $AsRfPh_2$ by the abstraction of the Cl atom in the complex **31** in the mixture CH_2Cl_2/toluene.

After the chloride abstraction, we observed that the solution evolves with time, even at low temperature, into a complex mixture of species that could not be characterized. However, the species formed can be trapped by addition of 1 equivalent of $AsRfPh_2$ (Rf = $C_6Cl_2F_3$) to stabilize the cationic complex generated in situ as complex **33** (Figure 3.11, a) and b)). The ^{19}F NMR shows the presence of the *o*-CF_3-C_6H_4 group at -58.3 ppm as a broad triplet indicating that the two phosphines are coordinated to the nickel center in a *trans* disposition. Although broad, the signal in the ^{31}P NMR also shows the coupling to the CF_3 group (broad quartet). The $AsRfPh_2$ is coordinated to the nickel center as shown by ^{19}F NMR where the F_{ortho} and F_{para} of the Rf group appear at -97.8 ppm and at -103.1, respectively, clearly different from the free $AsRfPh_2$ (-98.51 and -108.29 ppm).

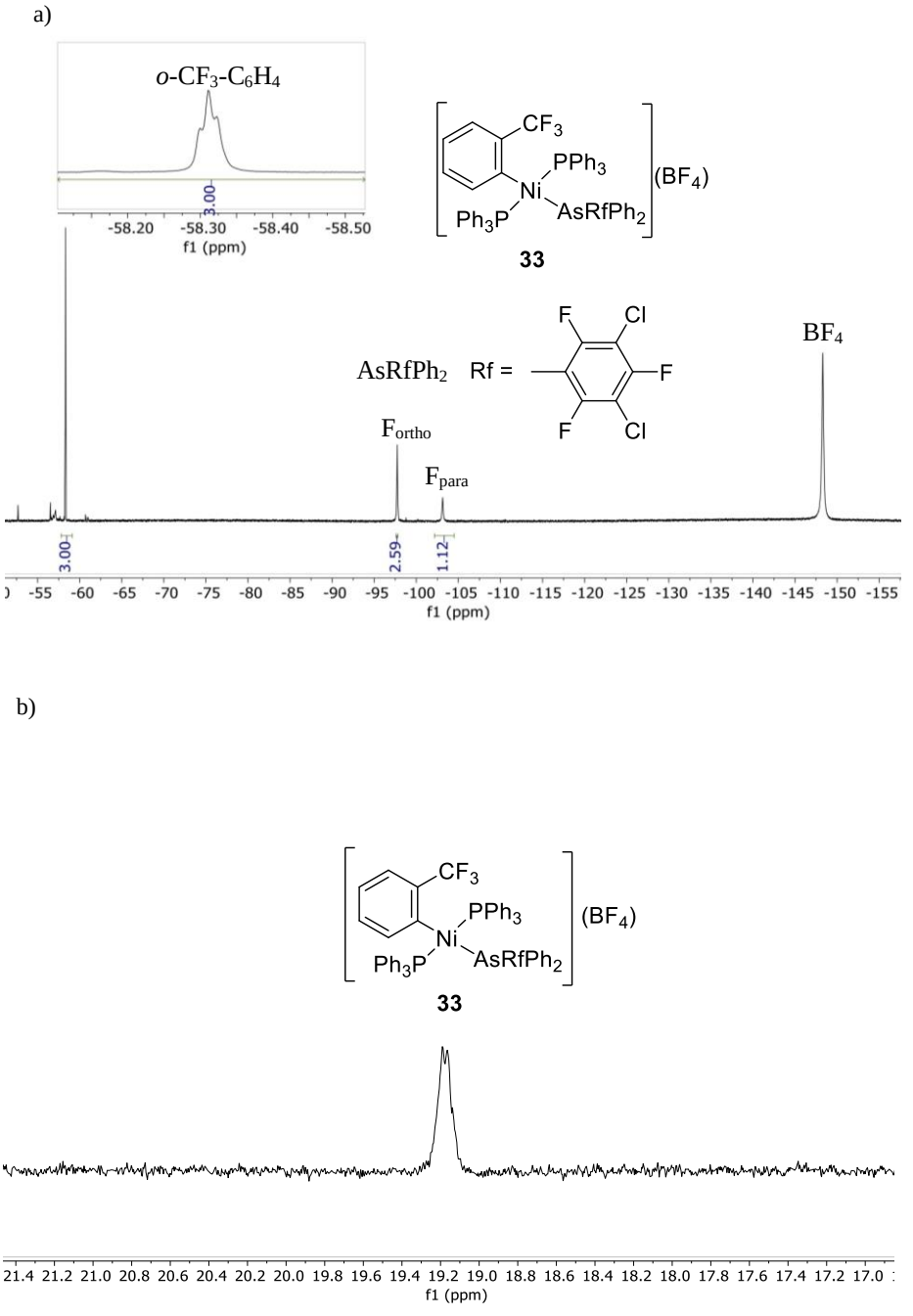

Figure 3.11. a) ^{19}F NMR and b) ^{31}P NMR of complex **33** generated in situ with the complex **31**, 1 equivalent of $AgBF_4$ and 1 equivalent of $AsRfPh_2$ in CH_2Cl_2/toluene at 243 K.

Table 3.4 shows the results of the polymerization of norbornene using the catalyst generated in-situ from **31**/$AgBF_4$ in CH_2Cl_2//toluene or the complexes formed in the presence of an additional ligand: [Ni(*o*-CF_3-C_6H_4)(PPh_3)$_2$L] (L = $AsRfPh_2$, **33**; $SbPh_3$) which could have a critical effect in the formation of structural errors in the vinylic addition polymerization of norbornene.

Table 3.4. Polymerization of NB with the mixture **31**/$AgBF_4$ in CH_2Cl_2/toluene with or without the presence of additional ligands.[a]

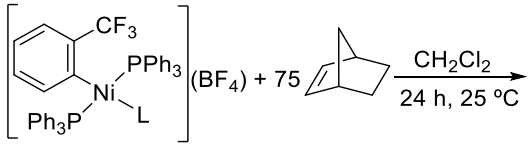

L = none
L = $SbPh_3$
L = $AsRfPh_2$, **34**

Rf = 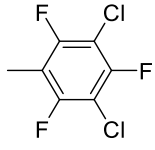

Entry	[Ni]	Ligand	NB_{VA}/NB_{RO}[b]	% NB_{RO}[c]	Yield (%)[d]
1	**31**	---	---	---	91%
2	**31**	$SbPh_3$	65.5/1	1.5%	94%
3	**33**	$AsRfPh_2$	34.3/1	2.8%	77%

a) The reactions were carried out using CH_2Cl_2, $[NB]_o$ = 0.3 M, ratio NB:Ni: = 75:1, 25 ºC, 24 h, under N_2. b) The molar ratio NB_{VA}/NB_{RO} was calculated by integration in the ^{1}H NMR of a solution of the polymer in dry $CDCl_3$ (see above, Figure 3.2). c) the molar % was calculated with the ratio NB_{VA}/NB_{RO}: $NB_{RO}/(NB_{VA} + NB_{RO})$*100. d) Yields are referred to the total monomer mass.

All the polynorbornenes present in Table 3.4 are almost complete aliphatic (VA-PNBs) and only very little percentage of structural errors by ring opening can be found. In the absence of ligands (entry 1, Table 3.4) the polynorbornene does not show the presence of NB_{RO}, indicating the propagation of the polymerization is fast enough with only one easily available coordination site on Ni. When an additional ligand is added, some NB_{RO} units appear in the skeleton of the polynorbornene (entries 2 and 3, Table 3.4). The percentage increases with the coordination ability of the ligand: the $AsRfPh_2$ is competing better than the $SbPh_3$ for the coordination of the norbornene and therefore, the propagation is slower.

The catalyst preparation carried out by reacting complex **31** with $AgBF_4$ in acetone gives a complex in solution with a completely unexpected structure (Scheme 3.21). Complex **34** is a cationic nickel(II) complex bearing a chelating ligand generated in situ from the aldol condensation of acetone.

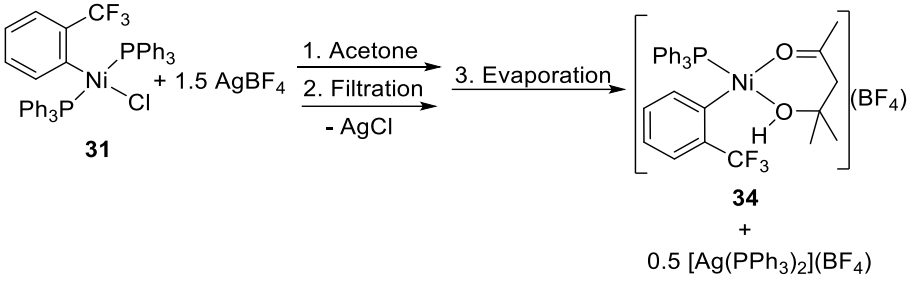

Scheme 3.21. Formation of complex **34** in the presence of 1.5 equivalents of $AgBF_4$ in acetone.

The orange solution generated after the catalyst preparation was characterized at 233 K by NMR spectroscopy in $CDCl_3$, since the complex generated in situ slowly decomposes at room temperature. A new resonance at -58.1 ppm (doublet, $J_{P\text{-}F}$ = 6 Hz, Figure 3.12, a)) appears in the ^{19}F NMR with the complete disappearance of the starting complex at -58.95 ppm (triplet, $J_{P\text{-}F}$ = 6 Hz, Figure 3.12, c)). The change in the multiplicity from triplet to doublet in the ^{19}F NMR indicates only one phosphine remains coordinated to the nickel center in the new complex. It is necessary use an excess of $AgBF_4$ (1.5 equivalents) to achieve a complete conversion of **31** into **34** (Figure 3.12, a), b)).

In the ^{31}P NMR spectrum, two different set of resonances are observed: a singlet at 25.41 ppm and additional signals in the 14.7-11.3 ppm region (Figure 3.13, a)). The singlet corresponds to complex **34** and, by comparison with some previous reports, the two doublets upfield can be assigned to silver phosphine complexes of type $[Ag(PPh_3)_n](X)$.[159-161] In particular the signal is a doublet of doublets at 13 ppm and correspond to the silver complex $[Ag(PPh_3)_2](BF_4)$ ($J_{Ag^{109}\text{-}P}$ = 584 Hz and $J_{Ag^{107}\text{-}P}$ = 510.8 according to the ratio of $J_{Ag^{109}\text{-}P}/J_{Ag^{107}\text{-}P}$ = 1.14, that is the same ratio for the gyromagnetic constants).

[159] Muetterties, E. L.; Alegranti, C. W. System *J. Am. Chem. Soc.* **1972**, 94, 6386-6391.
[160] Bachman, R. E.; Andretta, D. F. *Inorg. Chem.* **1998**, *37*, 5657-5663.
[161] a) Aalyea, E. C.; Dia, S. A. Stevens, S. *Inorganica Chim. Acta* **1980**, 44, L203-L204. b) Camalli, M.; Caruso, F. *Inorganica Chim. Acta* **1987**, *127*, 209-213.

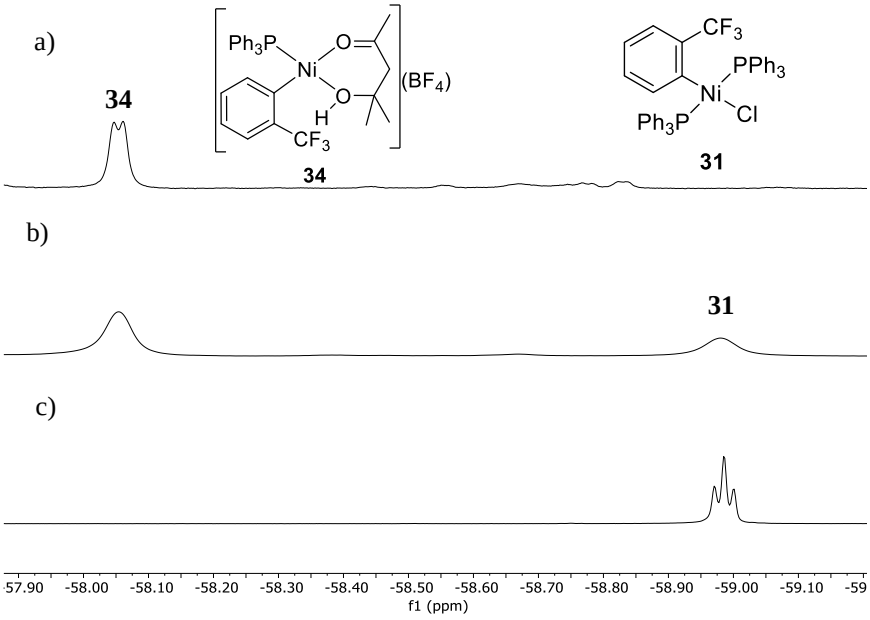

Figure 3.12. ^{19}F NMR (CF_3 region) in $CDCl_3$ at 233 K for: a) the residue of the reaction of **31** and 1.5 equivalents of $AgBF_4$; b) the residue of the reaction of **31** and 1 equivalent of $AgBF_4$; c) complex **31**.

Many reports over the years have shown the relationship between the coupling constant $J_{Ag\text{-}P}$ and the coordination number of silver(I) phosphino complexes.[159-161] The coupling constant decreases as the coordination number in the silver(I) complex increases,[162] and the values of the coupling constants we observe are in the range of the values for complexes with coordination number two ($J_{Ag^{107}\text{-}P}$ $[Ag(PPh_3)_2](BF_4)$ = 530 Hz;[159] $J_{Ag^{107}\text{-}P}$ $[Ag(Mes_3P)_2](PF_6)$ = 552 Hz and $J_{Ag^{107}\text{-}P}$ $[Ag(CH_3\text{-}p\text{-}C_6H_4P)_2](PF_6)$ = 496 Hz.[160,162a] Therefore, we can confirm the presence of the silver complex $[Ag(PPh_3)_2](BF_4)$. The molar ratio of **34** to $[Ag(PPh_3)_2](BF_4)$ determined by ^{31}P NMR is around 1:0.5 (Figure 3.13, a)). This ratio confirms that the excess of the $AgBF_4$ is trapping the phosphine liberated to the solution upon formation of **34**. The excess of $AgBF_4$ (1.5 equiv. referred to the complex **31**) is crucial to ensure the complete reaction. When we carried out the same reaction but adding only 1 equivalent of $AgBF_4$ (Figure 3.12-3.13, b)), we observed the formation of **34** but some of the starting complex **31** remains in the solution. The now broad signal for the silver(I) phosphine complex changes its the chemical shift (13 ppm with 1.5 eq. of $AgBF_4$ (Figure 3.13, a)) and 11 ppm with 1 eq. of $AgBF_4$ and average coupling constant of $^1J_{Ag\text{-}P}$ = 330 Hz (Figure 3.13,

[162] Barron, P. F.; Dyason, J. C.; Healy, P. C.; Engelhardt, L. M.; Skelton, B. W.; White, A. H. *J. Chem. Soc., Dalton Trans.* **1986**, 1965-1970.

b)), which indicates the presence of a different $[Ag(PPh_3)_n](BF_4)$ complex with n > 2 or even a fast interconverting mixture. Therefore, the role of the silver is bifunctional: one equivalent is employed to remove the chlorine atom in the complex **31** with the formation of AgCl that is visible as a white solid removed by filtration, and the other 0.5 equivalents are used to take out the free phosphine displaced from the nickel complex by the chelating ligand to give **34.**

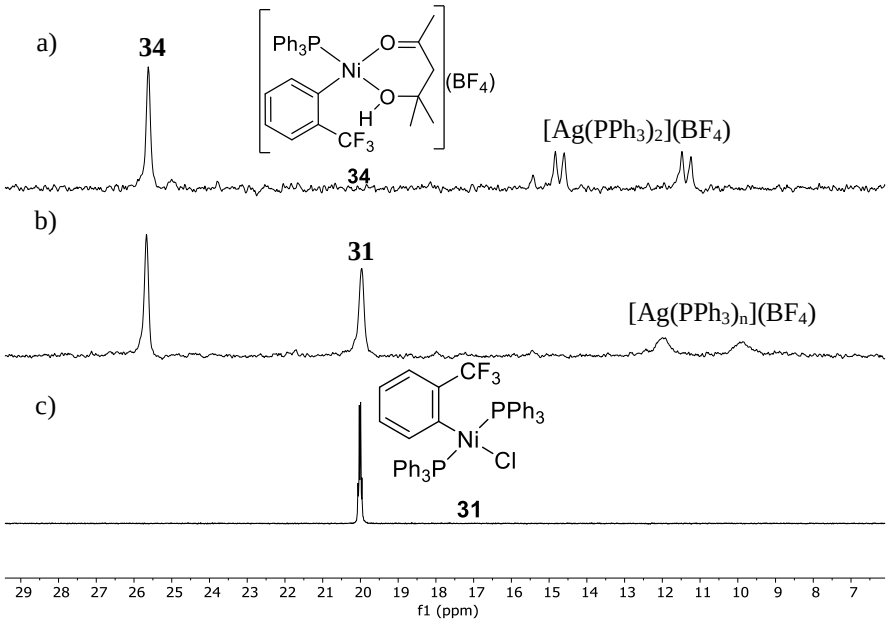

Figure 3.13. ^{31}P NMR in $CDCl_3$ at 233 K for: a) the residue of the reaction of **31** and 1.5 equivalents of $AgBF_4$; b) the residue of the reaction of **31** and 1 equivalent of $AgBF_4$; c) complex **31**

The chelating ligand ($CH_3CO(CH_2)C(CH_3)_2OH$) coordinated to the nickel center is visible in the ^1H NMR (Figure 3.14, a)) and ^{13}C NMR (Figure 3.14, b)) spectra. The most salient features of the ligand are the presence of the OH group at 4.93 ppm and the presence of the of the two diastereoisotopic protons bound to C^{10} (H^{10} at 3.3 ppm and $H^{10'}$ at 2.74 ppm). Furthermore, in the ^{13}C NMR we can observe the presence of the carbonyl signal at 220 ppm and the quaternary carbon C^{11}.

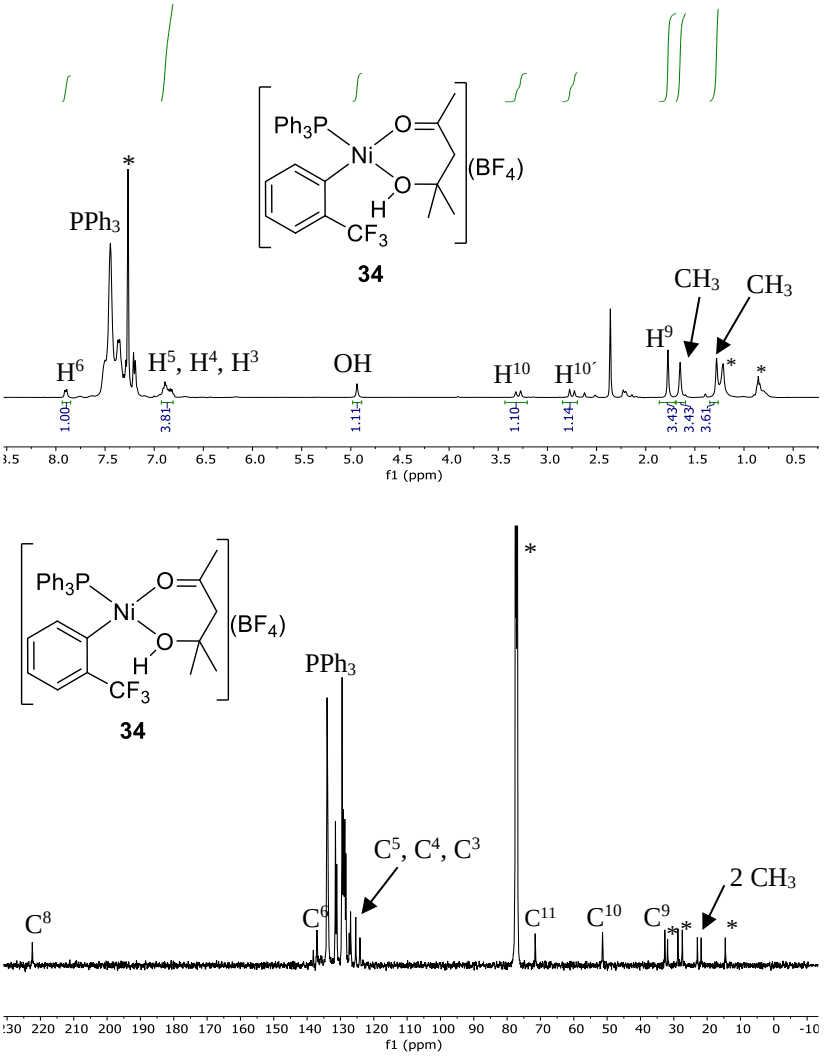

Figure 3.14. NMR in $CDCl_3$ at 233 K for complex **34** generated in situ: a) ^{1}H NMR; b) ^{13}C NMR. *Signals corresponding to the solvent and hexane.

Complex **34** can be generated in situ by an alternative route using the dimeric hydroxo complex **35**. Complex **35** was synthesized from **31** following an analogous preparation to that reported before (Eq. 3.4).[163] It is a mixture of isomers in solution, in a ratio that is dependent on the solvent and Eq. 3.4 shows the isomers present in a $CDCl_3$ solution. More information

[163] a) Klein, H. F.; Karsch, H. K. *Chem. Rer.* **1973**, *106*, 1433-1452. b) Christian, A. H.; Müller, P.; Monfette, S. *Organometallics* **2014**, *33*, 2134-2137. c) Carmona, E.; Pilar Palma, J. M. M; Paneque, M.; Poveda, M. L. *Inor. Chem.*, **1989**, *28*, 1895-1900.

on the characterization of these isomers and the molecular structure of *cis-anti*-**35** is collected in the Experimental section.

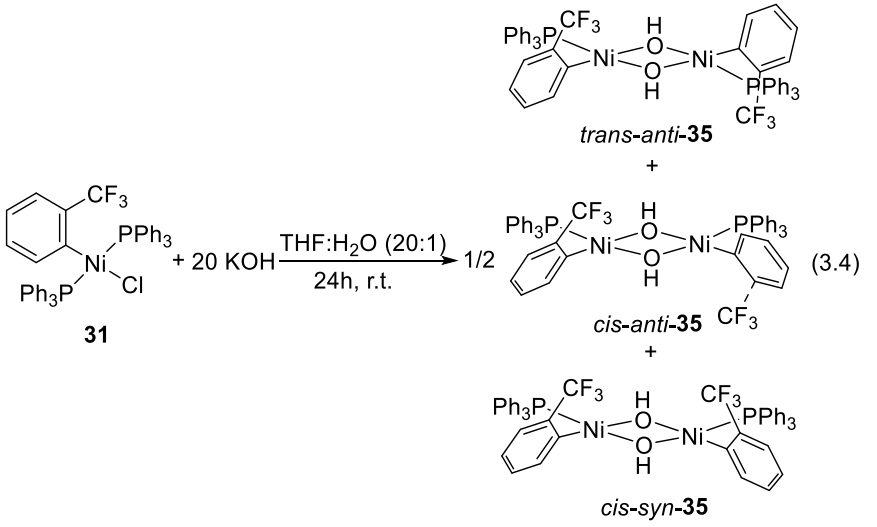

The addition of HBF_4 to complex **35** opens two sites in the Ni coordination sphere that can be occupied by the keto-alcohol added to the solution (Eq. 3.5). The formation of **35** can be observed in the ^{1}H NMR spectrum of the reaction mixture by the presence of the two diastereotopic protons (H^{10} and $H^{10'}$) that are typical for the ligand coordinated to the nickel center as discussed before (Figure 3.15). Also, we can see in the ^{19}F NMR and ^{31}P NMR the characteristic signals for the complex **34** (-58.1 ppm in the ^{19}F NMR and at 25.4 ppm in the ^{31}P NMR as the major signal).

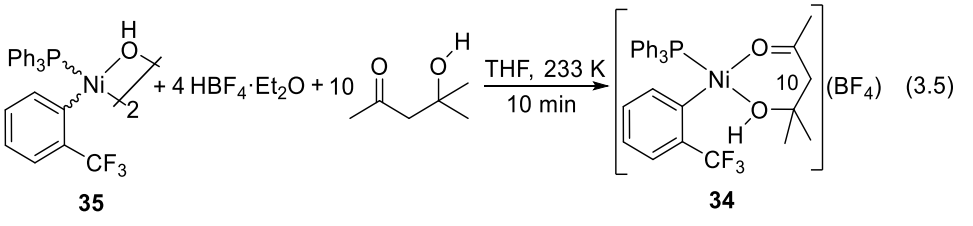

This is a convenient route to get the fragment "$NiArPPh_3$" in a clean way, just generating two molecules of water as byproduct. However, the reaction needs a large excess of the ligand to form complex **34** as the sole product. When the stoichiometric amount of the ligand is used, we generate a mixture of complexes. This is in contrast with the formation of **34** from **31** and $AgBF_4$, where no excess of the aldol condensation product is observed in solution (Figure

3.13 a). This indicates that the formation of the chelating ligand may occur in the nickel coordination sphere, the metal acting as a template and promoting the reaction. All the attempts to isolate the complex **34** by either route failed due to the easy decomposition upon handling its solutions.

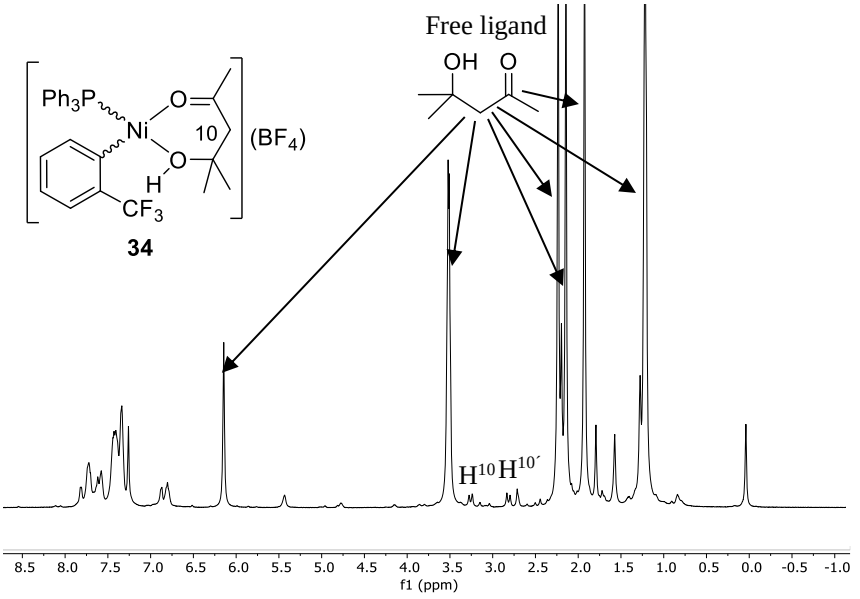

Figure 3.15. a) ^{1}H NMR spectra at 233 K for the reaction crude between the hydroxo dimer **35**, $HBF_4 \cdot Et_2O$ and the ligand $MeCOCH_2C(OH)Me_2$.

In conclusion, the active species in the polymerization of norbornene when the precatalyst mixture of **31** and $AgBF_4$ is prepared in acetone is the complex **34**, responsible for the formation of NB_{RO} units in the skeleton of the polymer VA/RO-PNB.

3.2.3.2. Polymerization of norbornene in the presence of [NiAr(L-L)(PPh3)](BF4)

As described above, the polymerization of norbornene in the presence of [Ni(*o*-CF_3-C_6H_4)($MeCOCH_2C(OH)Me_2$)(PPh_3)](BF_4) (**34**), generated in situ, leads to a VA/RO-PNB with a substantial percentage or ring opened NB by β-C elimination. Therefore, we explored the behavior of other analogous [NiAr(L-L)(PPh_3)](BF_4) and [NiAr(L-X)(PPh_3)] complexes as potential catalyst in the synthesis of this new polynorbornene skeleton. The complexes used and their preparation routes are shown in Scheme 3.22.

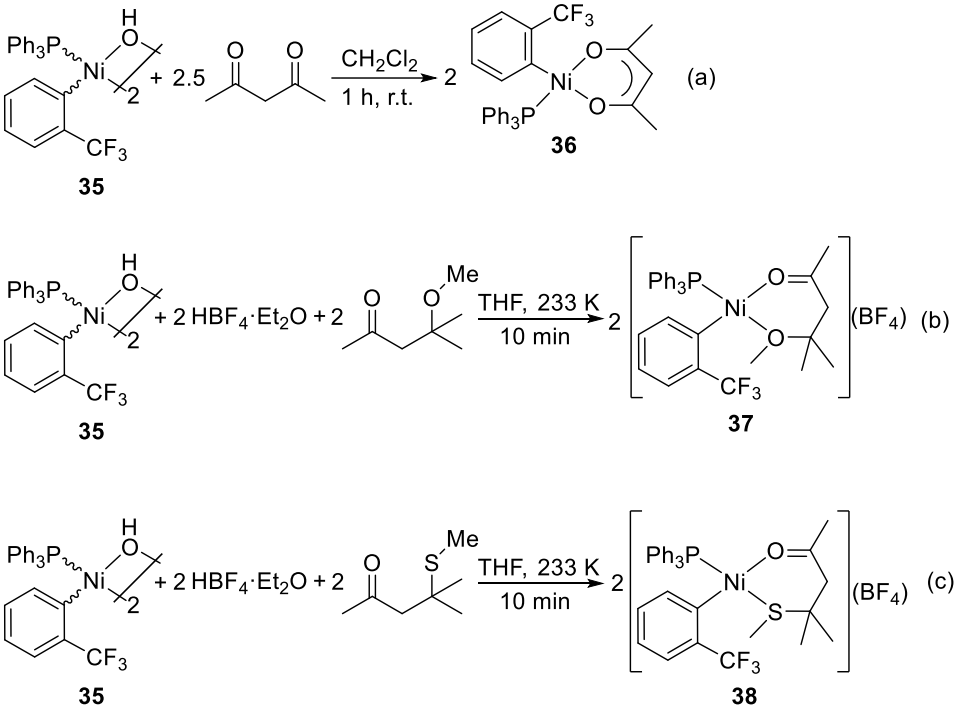

Scheme 3.22. Synthesis of quelate complexes **36**, **37** and **38** from the starting hydroxo dimer **35**.

Complex **36** was synthesized by the addition of Hacac to the hydroxo dimer **35** (Scheme 3.22, a)). The basicity of the OH group is enough to deprotonate the acidic proton of the Hacac without the addition of an external base. The X-ray structure of **36** shows the expected square planar Ni(II) complex (Figure 3.16 and Table 3.5). All the bond distances and angles are very similar to other reported nickel structures with the acac and PPh_3 ligands.[164]

[164] Cotton, A. F.; Frenz, B. A.; Hunter, D. L. *J. Am. Chem. Soc* **1974**, *96*, 4820-4825.

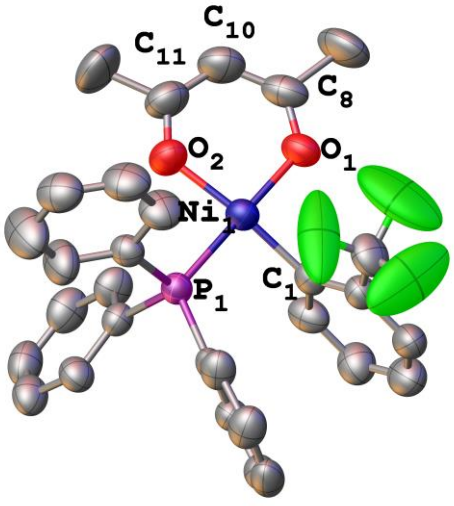

Figure 3.16. ORTEP representation of complex **36** (40% of probability). The hydrogen atoms were omitted to clarity.

Table 3.5. Selected distances (Å) and angles (º) for complex **36**.

Ni1-P1	2.164(11)	C4-C5	1.518(8)
Ni1-O1	1.882(4)	C8-C10	1.379(8)
Ni1-O2	1.884(4)	O2-Ni1-P1	86.79(11)
Ni1-C1	1.880(4)	O1-Ni1-C1	88.96(15)
O1-C8	1.269(6)	C1-Ni1-P1	90.74(12)
O2-C11	1.264(6)	O2-Ni1-O1	93.81(14)

Complexes **37** and **38** were prepared by the addition of HBF_4 and the stoichiometric amount of the chelating ligand. This is the same procedure used for the generation of complex **34** but, in contrast with the the keto-alcohol in the later complex, the keto-ether or keto-thiother derivatives are more coordinating and an excess of the ligand is not required (Scheme 3.22).

Only complex **38** could be isolated and its molecular structure determined by X-ray diffraction. It shows the *trans* disposition of the PPh_3 and the SMe group (Figure 3.17 and Table 3.6). Complex **38** shows only one isomer in solution, both when the bulk sample or the crystals used for X-ray diffraction were dissolved, which was assigned the same stereochemistry observed in the solid state. Complexes **37** and **34** could not be isolated in a

pure form. They were characterized in solution and, by analogy to **38**, the *trans* PPh_3-OR stereochemistry was tentatively assigned.

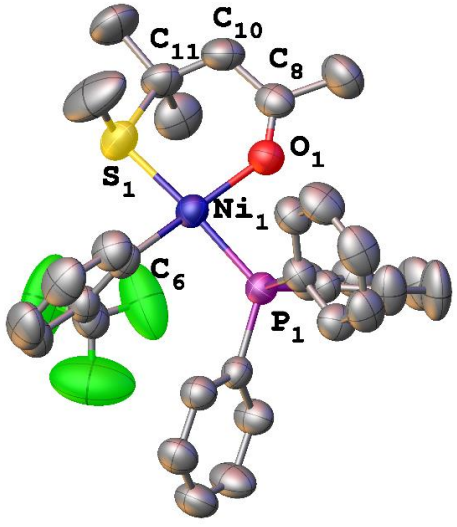

Figure 3.17. ORTEP representation of complex **38** (40% of probability). The hydrogen atoms were omitted to clarity.

Table 3.6. Selected distances (Å) and angles (º) for complex **38**.

Ni1-P1	2.2037(14)	C10-C11	1.533(10)
Ni1-S1	2.2042(17)	O1-Ni1-P1	87.47(12)
Ni1-O1	1.945(4)	S1-Ni1-C1	87.99(16)
Ni1-C1	1.891(5)	C1-Ni1-P1	90.15(16)
O1-C8	1.229(6)	S1-Ni1-O1	95.25(12)
S1-C11	1.841(6)		
C8-C10	1.466(9)		

All the complexes either isolated (**36**, **38**) or generated in situ (**34**, **37**) were tested in the polymerization of norbornene and the results are collected in Table 16.3. The neutral complex [Ni(*o*-CF_3-C_6H_4)(acac)(PPh_3)] (**36**) did not afford any polymer (entry 1, Table 3.7) and only a mixture of oligomers was distinguished in the ^{1}H NMR spectrum of the oily residue after

the reaction. The very low activity of complex **36** in the polymerization of norbornene is associated to two factors: the low electrophilicity of the metal (the coordination-insertion is less favorable than in a cationic complex),[117,118] and the low ability of the complex to generate a vacant coordination site.

Table 3.7. Control of the number of NB_{RO} units in the skeleton of VA/RO-PNB.[a]

Entry	Catalyst	NB:Ni[b]	NB_{VA}/ NB_{RO}[c]	$\%NB_{RO}$[d]	NB_{ROint}/ NB_{ROterm}[e]	Yield (%)[f]	M_w[g]	PDI[g]
1	**36**	75:1	---	---	---	oligo.	---	---
2[h]	**31**/$AgBF_4$ (**34**)	75:1	7.5/1	11.7%	1/0.21	55%	4200	1.3
3[h,i]	**31**/$AgBF_4$ (**34**)	75:1	5.7/1	14.9%	1/0.14	45%	3122	1.18
4[h]	**32**/$AgBF_4$	75:1	4.9/1	16.9%	1/0.22	67%	3118	1.2
5[h]	**32**/$AgBF_4$	125:1	8.3/1	12%	1/0.17	60%	4722	1.3
6[h]	**32**/$AgBF_4$	250:1	10.3/1	8.8%	1/0.34	65%	5169	1.5
7[h]	**32**/$AgBF_4$	500:1	13.9/1	6.7%	1/0.24	34%	14462	1.8
8[h]	**37**	75:1	5.7/1	14.9%	1/0.12	50%	---	---
9	**38**	75:1	---	---	---	dimer	---	---

a) The reactions were carried out using CH_2Cl_2 as solvent, $[NB]_o$ = 0.3 M unless noted, 25 ºC, 24 h, under N_2. b) molar ratio NB:Ni. c) The ratio NB_{VA}/NB_{RO} was calculated by integration in the ^1H NMR of a solution of the polymer in dry $CDCl_3$ (see section 3.2.2.1 and Figure 3.10 a)). d) The molar % was calculated using the ratio NB_{VA}/NB_{ROint} as (NB_{RO}/NB_{VA} + NB_{RO}) x 100. e) The ratio NB_{RO}/NB_{ROterm} was calculated by integration of ^1H NMR signals as shown in section 3.2.2.1 and Figure 3.10 a). f) Yields are referred to the total monomer mass. g) M_w in Daltons determined by GPC in $CHCl_3$ using polystyrene standards. h) The polymerization was carried out with the catalyst generated in situ (see Experimental Section). i) $[NB]_0$ = 0.061 M

Complex **34** was generated in situ from the mixture **31**/$AgBF_4$/acetone, as described in detail in the preceding section and shown in Scheme 3.22, and used in the polymerization experiments. The analogous combination [Ni(*o*-CH_3-C_6H_4)Cl(PPh_3)$_2$] (**32**)/$AgBF_4$/acetone was also used. Since [Ag(PPh_3)$_2$](BF_4) is present in these reaction mixtures, we independently tested that the polymerization of norbornene with this complex does not occur (see Experimental Section). As we discussed in the formation of VA/RO-PNBs with the system

trans-[Ni(C_6F_5)$_2$$L_2$]/solvent, the percentage of ring opening by β-C elimination (NB_{RO}) in the polymerization increases when the initial concentration of norbornene is low (entries 2 and 3, Table 3.7). Also a lower initial NB:Ni molar ratio leads to polymers with a higher amount of NB_{RO} units (entries 4-7, Table 3.7) and lower molecular weights. In an extreme situation, the use of a NB:Ni = 2:1 molar ratio makes complex **34** a dimerization catalysts, and the dimers **39** and **40** were obtained using this NB:Ni molar ratio and the **31**/$AgBF_4$/acetone or **32**/$AgBF_4$/acetone precatalyst mixture, respectively (Figure 3.18).

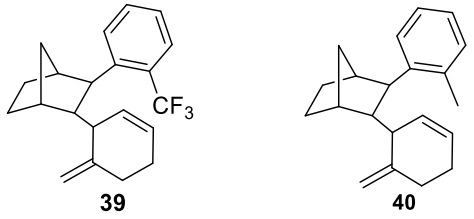

39 **40**

Figure 3.18. Dimers of norbornene formed with the catalytic system **31** or **32**/$AgBF_4$ in acetone in the presence of 2 equivalents of norbornene.

Complex **37**, bearing a keto-ether chelating ligand and generated in situ as shown in Scheme 3.22, behaves in a similar way than complex **34** generated in situ and produces a VA/RO-PNB with a slightly higher percentage of NB_{RO} at the same concentration (entries 2 and 8, Table 3.7). Probably this effect is a consequence of the better coordination ability of the OMe donor fragment in contrast with the OH group in **34**. However, when the coordination ability of the ligand is high, as in complex **38** with the SMe group, only some dimers were detected after 24 h of reaction. Interestingly, the major compound isolated in this reaction is the dimer **30** where the insertion of NB occurs into the Ni-H of a ``[$NiHL_n$]$^{+}$´´ intermediate. The coordination ability of the chelating $MeCOCH_2C(OR)Me_2$ ligand modulated by changing the OR group is crucial in the vinylic addition polymerization of norbornene and this effect tells us that the ligand is playing a role in the propagation of the polymerization.

According to the ratio of ring-opened norbornene in the polymer chain and in the termination NB_{ROint}/NB_{ROterm} (Table 3.7), we can say that after the β-γ-C-C cleavage of the norbornene ring happens, the possibility for a β-hydrogen elimination to occur is between 10-25%. In terms of the possibilities, an increase of the amount of NB_{RO} in the polymers, increases the β-hydrogen elimination and the chances for chain termination. Indeed, the molecular weight of the polymers decrease with the percentage of NB_{RO} (see entries 1-4, Table 3.7). However the

effect in the molecular weight is not linear and it seems that other factors are also controlling the molecular weights which could be associated with some changes in the propagation constant when the β-γ-C-C cleavage is operating more frequently.

3.2.4. Structure of the polymers VA/RO-PNB synthesized using [Ni(o-CF$_3$-C$_6$H$_4$)(MeCOCH$_2$C(OHMe$_2$)(PPh$_3$)](BF$_4$) (34) as catalyst

As we discussed before in section 3.2.2.1, the structure of the polymers obtained using catalyst **34** (and also all those collected in Table 3.7) correspond to VA/RO-PNBs that contain cyclohexene rings generated by β-carbon elimination (NB_{RO}, signals between 5.8-5.2 ppm) alternated with bicyclic units (NB_{VA}) in the skeleton of the polymer. The termination of the polymerization by β-hydrogen elimination generating a terminal methylenecyclohexene (signals between 4.8-4.6 ppm for the exocyclic double bond) is also clearly visible in these polymers. The structure proposed for the polymer and the structure of the dimer **30** for comparison are depicted in Figure 3.19. The blue protons in the polymer are the corresponding protons with a prime in the dimer (i.e $7^{VA} = 7'$) and the green protons in the polymer are the protons in the dimer without prime (i.e $7^{RO.term} = 7$). ^{1}H-^{13}C correlation NMR experiments were very helpful in the structural analysis.

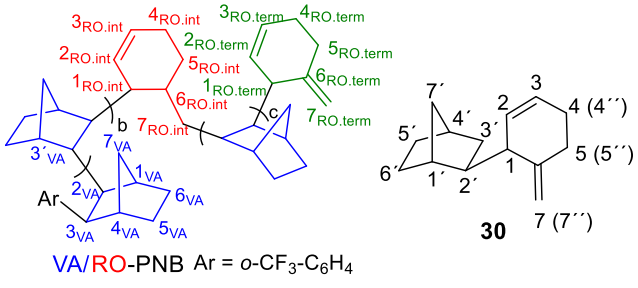

Figure 3.19. Proposed structure for the VA/RO-PNBs synthesized in entry 2, Table 16.3 showing the NB_{VA} units and the ring-opened norbornenes in the polymer main chain (NB_{RO}.int) and as terminal groups (NB_{RO}.term), as well as the structure of the dimer **30**.

The central part of the internal double bond between 5.7-5.45 in the ^{1}H NMR correlates with a well-defined region in the ^{13}C NMR between 127.5-123 ppm (Figure 3.20 a), red rectangle). Interestingly, the proton signal between 5.7-5.45 shows a cross peak in the long range ^{1}H-^{13}C correlation (gHMBCAD NMR) with carbon signals between 25.30-21.6 ppm. This part of the spectrum is associated with the $C^{5RO.int}$ and $C^{4RO.int}$ and it is not present in the dimer **30**, since

the presence of the terminal double bond close to the C^4 and C^5 increases their chemical shifts (31-29 ppm). The associated $H^{5RO.int}$ and $H^{4RO.int}$ are easily assigned employing the ^1H-^{13}C gHSQCAD (2-1.9 ppm, red rectangle in Figure 3.20, b)) This signal pattern and chemical shifts are also present in a very similar range for the VA/RO-PNB generated with complex **28** in the presence of coordinating solvents (Figure 3.5, a) and b)). In contrast to these polymers, the VA/RO-PNBs synthesized with complex **34**, show a higher amount of terminal methylene cyclohexene fragments. The terminal methylenecyclohexene ring in the polymer and in the dimer **30** are comparable so the NMR signals need to be similar. The terminal double bond in the dimer **30** shows two signals for H^7 and $H^{7´´}$ at 4.81 and 4.61 ppm in the ^1H NMR. These signals are also visible in the same chemical shifts in the isolated polymer ($H^{7RO.term}$ = 4.8-4.6 ppm). The ^{13}C associated to the terminal double bond in the dimer **30** is at 108.7 ppm (C^7) and at 108 ppm in the polymer ($C^{7RO.term}$).

The initiation step, as we commented before, is observable in the ^{19}F NMR (Figure 3.10, c)) with a signal for the *o*-CF_3-C_6H_4-VA/RO-PNB at -58.37 ppm. Furthermore, the signal for the corresponding benzylic proton (H^{3VA}) is observable in the ^1H NMR at 3.25 ppm that is in the same range of chemical shift of the dimer **39**, synthesized with the same catalyst (3.19 ppm, see Experimental Section).

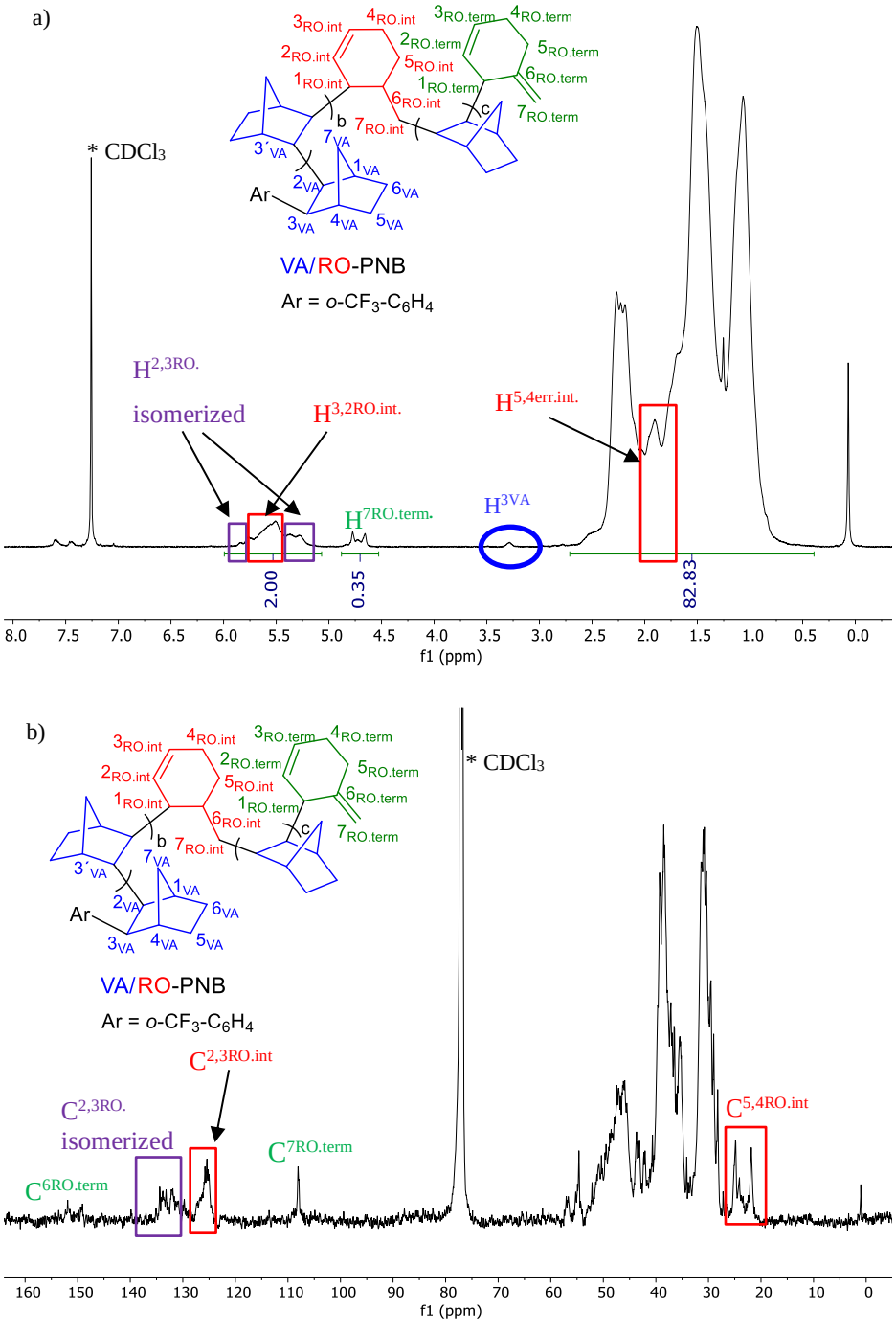

Figure 3.20. a) ^{1}H NMR and b) ^{13}C NMR in dry $CDCl_3$ of the polymer VA/RO-PNB generated with the combination of **31**/$AgBF_4$ (ratio NB:**31**/$AgBF_4$ = 75:1:1.5 in acetone, entry 2, Table 3.7; M_w = 4200).

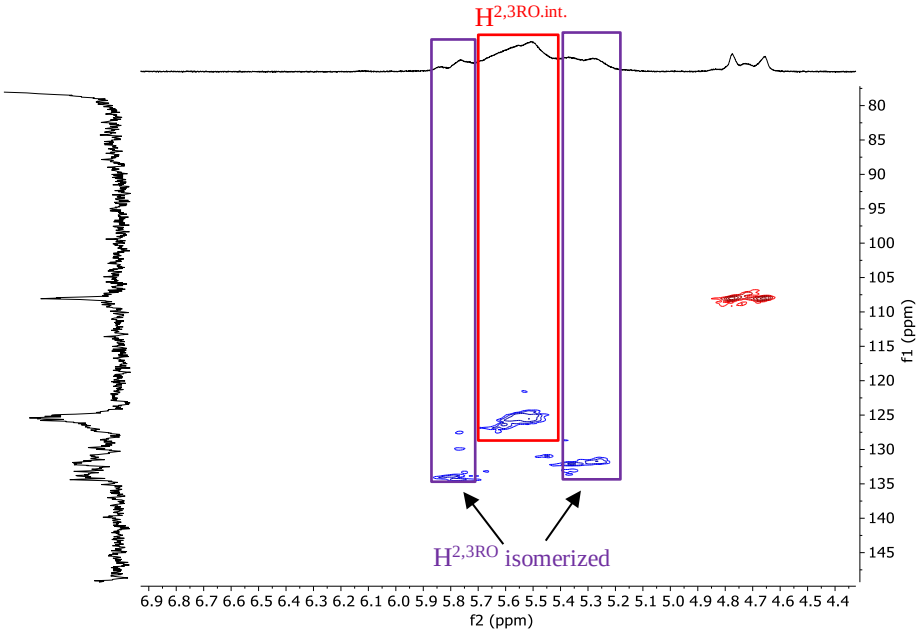

Figure 3.21. Enlarged ^{1}H-^{13}C gHSQCAD of the polymer VA/RO-PNB corresponding to the broad region between 5.85-5.25 ppm. generated with the combination of **31**/AgBF$_4$ (ratio NB:**31**/AgBF$_4$ = 75:1:1.5 in acetone, entry 2, Table 3.7; M_w = 4200).

The regions of the broad olefinic signal between 5.85-5.7 and 5.45-5.25 in the ^{1}H NMR and their associated ^{13}C NMR signals shown in Figure 3.20-3.21 (purple rectangles) can be the result of an isomerization process of the endocyclic double bond of the cyclohexene ring by the ``NiHL$_n$´´ generated after the β-hydrogen elimination (Scheme 3.22). A related isomerization process was reported before by Milstein and co-workers in a β-γ-C-C cleavage of the norbornene ring by palladium complexes (see Scheme 3.15 in the Introduction, section 3.1.3).[155] They reported isomers with similar chemical shifts than those we observe in the polymer. The major one they detected has got chemical shifts for the protons of the endocyclic double bond at 5.85 ppm and at 5.72 ppm in the ^{1}H NMR, probably corresponding to the conjugated diene (Scheme 3.23). We could not determine if the double bond isomerization process affects both internal and terminal NB$_{RO}$ units. We assume that it will be more accused in the terminal methylenecyclohexene ring because it is sterically more accessible, as it has been represented in Scheme 3.23. This isomerization was not observed in the VA/RO-PNBs synthesized with complex **28**, since in this case the termination by β-H elimination is less important and therefore the amount of ``NiHL$_n$´´ species that can carry out the isomerization is lower.

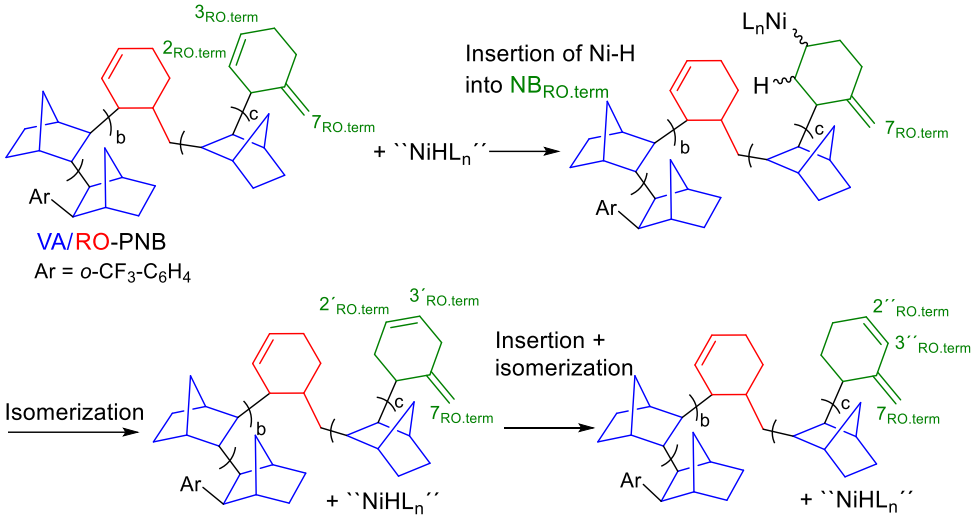

Scheme 3.23. Formation of different isomers in the methylenecyclohexene ring of the VA/RO-PNB.

The other NMR signals can be assigned by comparison with the chemical shifts of the dimer **30**. The phase sensitive ^{1}H-^{13}C gHSQCAD correlation allows to identify the secondary and tertiary carbons and their corresponding protons. Table 3.8-3.9 collect the chemical shift ranges for the polymer VA/RO-PNB as well as a comparison with the dimer **30**.

Table 3.8. Chemical shifts range in the ^{1}H NMR for the VA/RO-PNB and the dimer **30**.[a]

	$H^{3,2ROisom}$ $H^{3,2RO.int}$ / H^{3},H^{2}	$H^{7RO.term}$/ H^{7}	H^{3Va}	$H^{6,5,4,1RO.int.}$, $H^{5,4,1RO.term}$, $H^{4,3,2,1VA}$ / $H^{5,4´,4,2´,1,1´}$	$H^{7,6,5Va}$, $H^{7RO.int}$ / $H^{7´,6´,5´,5´´,4´´,3´}$
VA/RO-PNB[b]	$H^{3,2ROisom}$: 5.85-5.7; 5.45-5.25 $H^{3,2RO}$: 5.7-5.45	4.8-4.6	3.25	2.5-1.55	1.55-0.5
30	5.69	4.81, 4.61	---	2.29-2.11	1.45-1.04

a) δ, 500.13 MHz; spectra recorded in $CDCl_3$. b) Obtained in the conditions of entry 2, Table 3.7 and shown in Figure 3.20.

Table 3.9. Chemical shift ranges in the ^{13}C NMR for the VA/RO-PNB and the dimer **30**.[a]

	$C^{6RO.term}$ /C^{6}	$C^{3,2RO.isom}$ $C^{3,2RO.}$/ $C^{3,2}$	$C^{7RO.term}$ / C^{7}	$C^{6,1RO.int}$, $C^{VA4,3,3',2,1,}$ $C^{1RO.term}$ / $C^{7',4',3,2',1,1'}$	$C^{7,6,5VA}$, $C^{7RO.int}$, $C^{5,4RO.term}$ / $C^{6',5',5,4}$	$C^{5,4RO.int}$
VA/RO-PNB[b]	155-149	$C^{3,2RO.isom}$: 133-127.5; $C^{3,2RO}$: 127.5-123	108	57.17-36.8	36.8-28.7	25-21
30	149.25	129.6-127.5	108.71	48.5-35.2	30.3-28.73	---

a) δ, 125.758 MHz; spectra recorded in $CDCl_3$. b) Obtained in the conditions of entry 2, Table 3.7 and shown in Figure 3.20.

3.2.5. Mechanistic proposal for the formation of VA/RO-PNB with the complexes [Ni(Ar)(MeCOCH$_2$C(XR)Me$_2$)(PPh$_3$)](BF$_4$) where XR = OH, OMe, SMe; and Ar = o-CF$_3$-C$_6$H$_4$, o-CH$_3$-C$_6$H$_4$

With all the information collected, we can draw a plausible mechanism for the formation of the VA/RO-PNBs presented in this section (Scheme 3.24). The polymerization starts with the coordination of one molecule of norbornene and the insertion into the Ni-Ar bond: the presence of the *o*-CF_3-C_6H_4 group attached to the polymer confirms this initiation. The coordination of the norbornene requires the displacement of one ligand coordinated to the nickel center. We can consider that the phosphine is exercising this role, but complex **38** shows no activity in the polymerization of norbornene even if the decoordination of the PPh_3 should be faster than in the complex **37** because the SMe has a higher *trans* effect than the OMe. Therefore, the chelating ligand needs to decoordinate one of its donor atoms to allow the coordination of the norbornene. The deccordination of the thioether in **38** is required to generate a coordination vacant site *cis* to the aryl group necessary for the insertion. Presumably, assuming the same complex stereochemistry for **34** and **37** (Figure 3.22) the decoordination of the dialkyl ether or the alcohol is much faster and the initiation takes place efficiently.

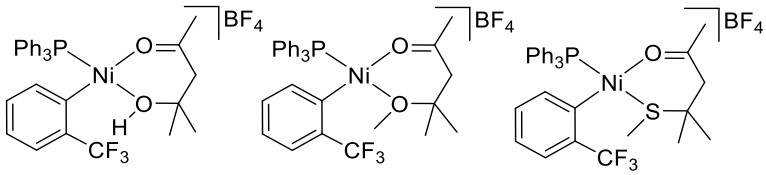

Figure 3.22. Representation of the isomer in complex **38** and the tentative assignation of the isomers in **34** and **37**.

After the first insertion, the coordination vacant site can be occupied by another molecule of norbornene or the ligand can recoordinate to the nickel center. So, the chelate ligand, by decoordination-recoordination of one of the donor atoms, is controlling the propagation rate of the polymerization. The skeleton of the vinylic addition chain (NB_{VA}) is generated by successive coordination-insertion of b molecules of norbornene. At some point, when the ligand is coordinated as a chelate, the rate of the propagation step slows down, and the β-γ-C-C cleavage can operate to open the norbornene ring and form the internal methylcyclohexene ring (NB_{RO}). After this β-γ-C-C cleavage, the Ni-methylcyclohexenyl bond restarts the VA-polymerization by coordination-insertion of c molecules of norbornene. The ring-opened norbornene is therefore incorporated into the main polymer chain ($NB_{RO.int}$ units). Eventually, after the β-γ-C-C cleavage, the Ni-methylcyclohexenyl group can undergo β-hydrogen elimination to finish the polymerization ($NB_{RO.term}$). The probability of the β-hydrogen elimination after a β-γ-C-C cleavage is about 10-25%. The ``$NiHL_n$`` generated can now isomerize the endocyclic double bond as observed in the ^1H NMR of the isolated polymers with signals outside the 5.7-5.4 ppm range.

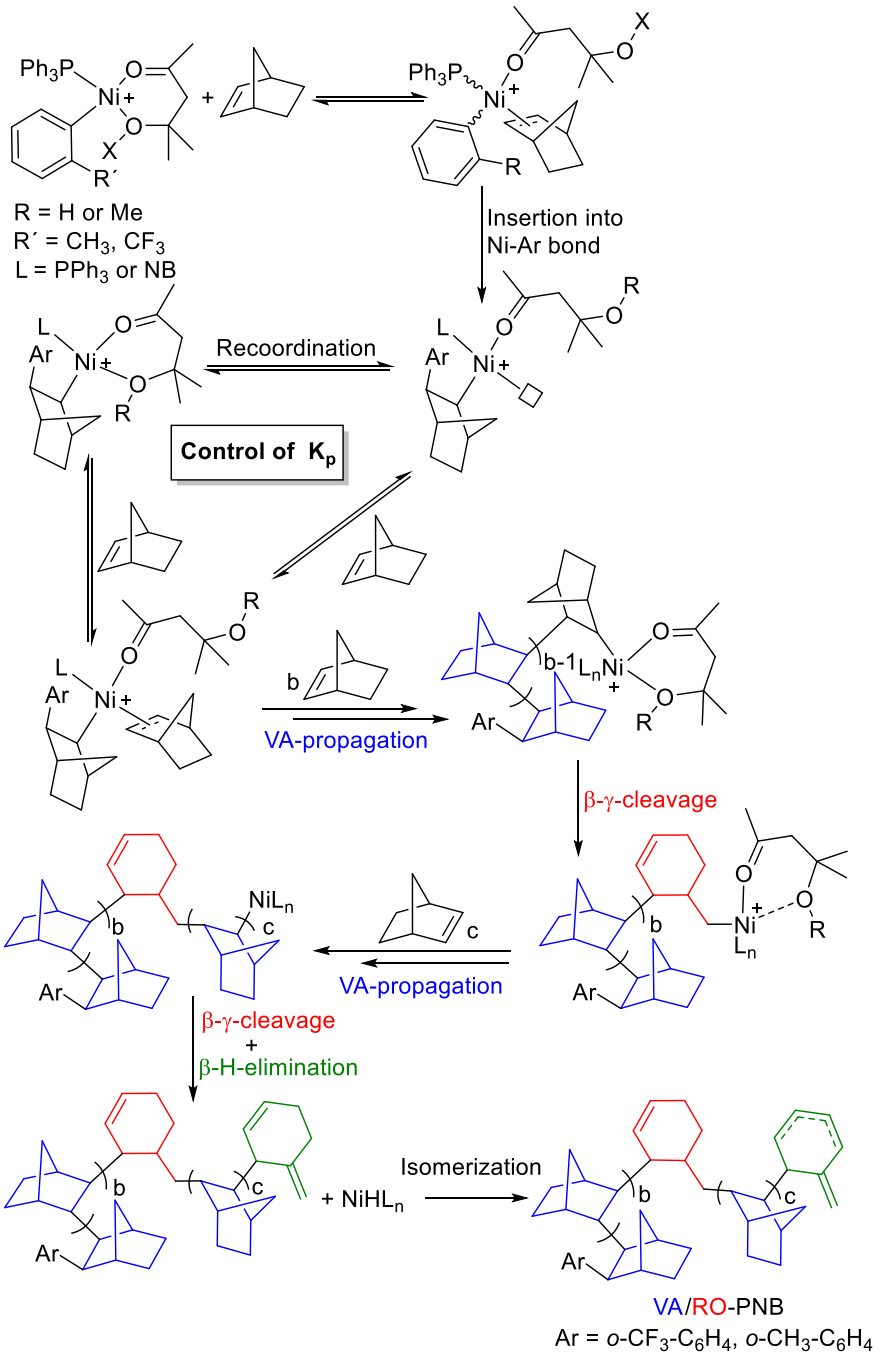

Scheme 3.24. Proposed mechanism for the formation of the VA/RO-PNBs with the type of catalysts [Ni(Ar)(MeCOCH$_2$C(XR)Me$_2$)(PPh$_3$)](BF$_4$) where XR = OH, OMe and SMe and Ar = *o*-CF$_3$-C$_6$H$_4$- or *o*-CH$_3$-C$_6$H$_4$.

3.3. Conclusions

A new type of polynorbornene skeleton VA/RO-PNB has been found by combination of two different processes with the same catalyst: the vinylic addition polymerization (VA) and the ring opening of the norbornene by a β- elimination (RO). The structures of these VA/RO-PNB are consistent with the presence of two different units in the skeleton: bicylic norbornenyl structures, as a results of the vinylic addition of norbornene (NB_{VA}), and cyclohexenylmethyl groups formed by internal ring opening of the norbornene by β-C elimination(NB_{RO}). The formation of VA/RO-polynorbornenes can be achieved by tunning different factors in order to decrease the propagation rate of the polymerization while still ensuring the growth of the polymer chain.

Among the catalysts $[Ni(C_6F_5)_2L_2]$ where L = PPh_3 (**29**), $AsPh_3$ (**28**) and $SbPh_3$ (**27**), complex **28** is the most convenient one to give a VA/RO-PNB. Stronger coordinating ligands make inactive catalysts (i.e. **29**) and those with easily substituted ligands lead to the conventional VA-PNBs (i.e **27**). The reaction conditions can be changed to control the number of ring-opened NB units in the polymer using complex **28**: An increase of the number of NB_{RO} units can be induced by lowering the initial monomer concentration or the NB:Ni ratio. A combination of complex $[Ni(C_6F_5)_2(AsPh_3)_2]$ (**28**) with controlled amounts of coordinating solvents is a useful catalytic system for the synthesis of VA/RO-PNBs. The coordination ability of the solvents is directly correlated with the amount of ring opening in the skeleton of VA/RO-PNB following the trend: MeCN > DMA > PhCOMe > MeCOMe. The structure of the VA/RO-PNBs was studied by NMR spectroscopy and agrees with the incorporation of cyclohexane rings (generated by the β-γ-C-C cleavage) in the structure of the skeleton.

We also discovered a new type of cationic complexes of niquel(II) bearing quelate ligands $[Ni(o\text{-}CF_3\text{-}C_6H_4)(MeCOCH_2C(XR)Me_2)(PPh_3)](BF_4)$ (XR = OH, **34**; OMe, **37**; or SMe, **38**) with a direct application in the formation of the skeleton VA/RO-PNB. The coordination ability of this ligand is crucial for the formation of the NB_{RO} units and whereas only dimers are generated with the SMe ligand, VA/RO-PNBs are obtained for the O,O-donors and a higher amount of NB_{RO} structures were found with the OR = OMe ligand than with the OR = OH one. The termination of the polymerization is clear in this type of catalytic system and it is happening by a β-hydrogen elimination after the β-γ-C-C cleavage of the norbornene in a

maximum of 25% of the ring opening events. It is interesting to note that the chain termination by β-hydrogen elimination is more important in the VA/RO-PNBs obtained with complexes **34** and **37** than with $[Ni(C_6F_5)_2(AsPh_3)_2]$ **(28)**/co-solvent. As a result, for a similar percentage of NB_{RO} units, the polymers obtained with the latter system are larger. A balance of open coordination sites and electron density on the metal account for these differences that lead to polymers with the new VA/RO-PNB backbone but different properties.

3.4. Experimental Section

3.4.1. Materials and General Considerations.

All the reagents were purchased from commercial sources and used as received unless noted. A solution of norbornene in CH_2Cl_2 was used for all the polymerization experiments whose concentration was determined by titration in ^1H NMR with $C_6H_3Br_3$ as internal standard. The CH_2Cl_2, THF, Et_2O and hexane were dried using an SPS PS-MD-5 solvent purification system. The acetone was dried with $CaSO_4$. $CDCl_3$ was dried using neutral activated aluminum oxide. The acetophenone and DMA were used without further purification. The *trans*-[Ni(C_6F_5)$_2$($SbPh_3$)$_2$] (**27**), *trans*-[Ni(C_6F_5)$_2$($AsPh_3$)$_2$] (**28**), *trans*-[Ni(C_6F_5)$_2$(PPh_3)$_2$] (**29**), *trans*-[Ni(*o*-CH_3-C_6H_4)Cl(PPh_3)$_2$] (**32**) were synthesized following reported methods.[101g,156]

NMR spectra in solution were recorded at 298 K using Bruker AV-400, Agilent MR-500 and MR-400 instruments. Chemical shifts (δ) are reported in ppm and referenced to $SiMe_4$ (^1H and ^{13}C), $CFCl_3$ (^{19}F) and 25% H_3PO_4 (^{31}P). IR spectra were collected on the solid samples using a Perkin-Elmer FT/IR SPECTRUM FRONTIER spectrophotometer with CsI + ATR diamond accessory. Elemental analyses were carried out in a Carlo Erba 1108 microanalyser (at the Vigo University, Spain). Size exclusion chromatography (SEC, also gel permeation chromatography, GPC) was carried out using a WatersSEC system on a three-column bed (Styragel 7.8_300 mm columns: 50-100000, 5000-500000 and 2000-4000000 Da) and a Waters 410 differential refractometer. SEC samples were run in $CHCl_3$ at 313 K and calibrated to polystyrene standards.

3.4.2. Polymerization experiments

3.4.2.1. Polymerization experiments with the catalysts 27, 28 and 29

A representative example for the polymerization experiment in entry 4, Table 3.1 is given. The other polymerizations were carried out following the same procedure changing the catalyst or the appropriate reaction condition.

[Ni(C_6F_5)$_2$($AsPh_3$)$_2$] (**28**) (0.010 g, 0.00994 mmol) was placed in a Schlenk tube under N_2. The yellow solid was dissolved in 12.1 mL of dry CH_2Cl_2 and a solution of norbornene in CH_2Cl_2 (0.2 mL, 0.75 mmol; 3.8 M, $[NB]_o$ = 0.061 M) was added to the mixture. After 20 min, a white solid appeared in the yellow solution. The suspension was stirred 24 h at 25 ºC. MeOH (10 mL) was added to the suspension inducing the complete precipitation of the polymer and the suspension was stirred 30 min at room temperature. The white solid was filtered off and washed with MeOH (2 x 10 mL) and Et_2O (5 mL). The white powder solid was air dried for 6 h (45 mg, 64% yield). NB_{VA}/NB_{RO} = 14.3. Characterization for polymers

entries 1, 3 and 5 in Table 3.1: ^{1}H RMN (500.13 MHz, δ, $CDCl_3$): 3-0.75 (b, 7H, H^7, H^6, H^5, H^4, H^3, H^2, H^1).

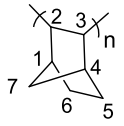

VA-PNB

For the characterization of VA/RO-PNB, see below.

3.4.2.2 Polymerization experiments with catalyst 28 in the presence of a coordinating solvent

Representative procedure for the polymerization experiment in entry 7, Table 3.2. The other polymerizations were carried out with the same procedure changing the catalyst or the appropriate reaction condition.

$[Ni(C_6F_5)_2(AsPh_3)_2]$ (**28**) (0.010 g, 0.00994 mmol) was placed in a Schlenk tube under N_2. The yellow solid was dissolved in 12 mL of dry CH_2Cl_2 followed by the addition of acetophenone (0.185 mL, 1.6 mmol). The solution was stirred for 5 min at room temperature. A solution of norbornene in CH_2Cl_2 (0.2 mL, 0.75 mmol; 3.8 M, $[NB]_o$ = 0.061 M) was added to the mixture and after 20 min a small amount of white solid appeared in the yellow solution. The suspension was stirred for 24 h at 25 ºC. MeOH (10 mL) was added to the suspension inducing the complete precipitation of the polymer and the suspension was stirred 30 min at room temperature. The white solid was filtered off, washed with MeOH (2 x 10 mL) and Et_2O (1 x 5 mL). The white powder solid was air dried for 6 h (47 mg, 67% yield). NB_{VA}/NB_{RO} = 7.6/1. M_w =17.391, M_w/M_n = 1.5. ^{1}H RMN (500.13 MHz, δ, $CDCl_3$): 5.8-5.4 (b, $H^{3RO.int}$, $H^{2RO.int}$), 2.5-1.57 (b, $H^{6RO.int}$, $H^{5RO.int}$, $H^{4RO.int}$, H^{4VA}, H^{3VA}, $H^{3'VA}$, H^{2VA}, H^{1VA}, $H^{1RO.int}$), 1.57-0.55 (b, $H^{7RO.int}$, H^{7VA}, H^{6VA}, H^{5VA}). ^{13}C (125.66 MHz, δ, $CDCl_3$): 132-125 ($C^{3RO.int}$, $C^{2RO.int}$,), 54.3-36.6 ($C^{6RO.int}$, C^{4VA}, C^{3VA}, $C^{3'VA}$, C^{2VA}, C^{1VA}, $C^{1RO.int}$), 36.3-28 (C^{7VA}, $C^{7RO.int}$, C^{6VA}, C^{5VA}), 25.4-22.6 ($C^{5RO.int}$, $C^{4RO.int}$). ^{19}F NMR (500,13 MHz, δ, $CDCl_3$): -133-143 (multiple signals, F_{ortho}), -157-158.5 (b, F_{para}), -162-163.5 (b, F_{meta}).

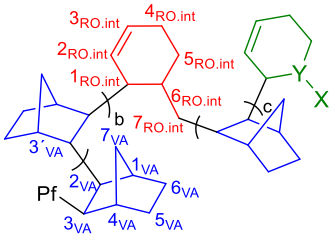

VA/RO-PNB

b > c Pf = C_6F_5

Y-X = -CH=CH_2, -CH_2-CH_3

3.4.2.3 Synthesis of a short VA/RO-PNB (NB_{VA}/NB_{RO} = 2.7/1, ratio NB:Ni:acetophenone = 10:1:30)

$[Ni(C_6F_5)_2(AsPh_3)_2]$ (**28**) (50 mg, 0.0497 mmol) was placed in a Schlenk tube under N_2. The yellow solid was dissolved in 2 mL of dry CH_2Cl_2 followed by the addition of acetophenone (0.17 mL, 1.5 mmol). The yellow solution was stirred for 5 min. A solution of norbornene (0.13 mL, 0.497 mmol; 3.8 M) was added to the mixture and the solution was stirred 24 h at 25 ºC. The solution was evaporated to dryness and the residue was purified by a preparative TLC in silica gel using Et_2O as eluent. The component with $R_f \approx 0$ was extracted with 10 mL of CH_2Cl_2 and the solution was evaporated to dryness. The residue was dissolved in 0.6 mL of dry $CDCl_3$ and analyzed by NMR spectroscopy. NB_{VA}/NB_{RO} = 2.7. ^{1}H RMN (500.13 MHz, δ, $CDCl_3$): 5.8-5.4 (b, $H^{3RO.int}$, $H^{3RO.term}$, $H^{2RO.int}$, $H^{2RO.term}$), 4.73 ($H^{7RO.term}$). 3.25 ($H^{3´VA}$), 2.5-1.57 (b, $H^{6RO.int}$, $H^{5RO.int}$, $H^{5RO.term}$, $H^{4RO.int}$, $H^{4RO.term}$, H^{4VA}, H^{3VA}, H^{2VA}, H^{1VA}, $H^{1RO.int}$), 1.57-0.55 (b, H^{7VA}, H^{6VA}, H^{5VA}, $H^{7RO.int}$). ^{13}C (125.66 MHz, δ, $CDCl_3$): 132-125 ($C^{3RO.int}$, $C^{3RO.term}$, $C^{2RO.int}$, $C^{2RO.term}$), 107.2 ($C^{7RO.term}$), 54.3-36.6 ($C^{6RO.int}$, C^{4VA}, C^{3VA}, $C^{3´VA}$, C^{2VA}, C^{1VA}, $C^{1RO.int}$), 36.6-26.6 ($C^{7RO.int}$, C^{6VA}, C^{5VA}), 25.4-22.6 ($C^{5RO.int}$, $C^{5RO.term}$, $C^{4RO.int}$, $C^{4RO.term}$). ^{19}F NMR (500,13 MHz, δ, $CDCl_3$): -132-140 (multiple signals, F_{ortho}), -157-158.5 (b, F_{para}), -162-163.5 (b, F_{meta}).

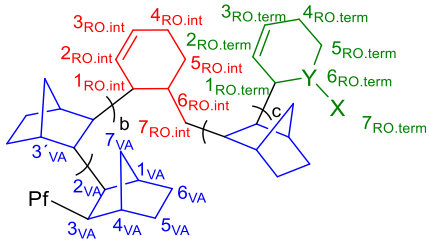

3.4.2.4. Polymerization of norbornene in the presence of the catalyst generated from 31/$AgBF_4$/ligand in CH_2Cl_2/Toluene

Representative procedure for the polymerization experiment in entry 1, Table 3.4. The other polymerizations in Table 3.4 were carried out with the same procedure adding 1 equivalent per nickel of $AsRfPh_2$ or $SbPh_3$.

In a 10 mL Schlenk tube was dissolved the $AgBF_4$ (0.005 g, 0.026 mmol) in 2 mL of dry toluene under N_2. In another 10 mL Schlenk tube was dissolved the complex **31** (0.020 g, 0.026 mmol) in 2 mL of dry CH_2Cl_2 under N_2. The solution of $AgBF_4$ was added to the solution of complex **31** and the mixture was stirred for 2 min at room temperature with the fast formation of a white solid (AgCl). The AgCl was removed using a PTFE filter and the

yellow solution was evaporated to dryness. The residue was redissolved in 3 mL of dry CH_2Cl_2 and a solution of norbornene was added (0.5 mL, 1.95 mmol; 3.8 M, $[NB]_o$ = 0.3 M). Instantly some white solid appeared in the yellow solution. The suspension was stirred 24 h at 25 ºC. MeOH (10 mL) was added to the suspension inducing the complete precipitation of the polymer and the suspension was stirred for 30 min at room temperature. The white solid was filtered off and washed with MeOH (2 x 10 mL) and Et_2O (5 mL). The white powder solid was air dried for 6 h (0.167 g, 91 % yield). ^{1}H RMN (500.13 MHz, δ, $CDCl_3$): 3-0.75 (b, 7H, H^7, H^6, H^5, H^4, H^3, H^2, H^1).

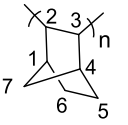

VA-PNB

3.4.2.5. Test polymerization of norbornene in the presence of $AgBF_4$/2PPh_3.

In a 10 mL Schlenk tube was dissolved the $AgBF_4$ (0.008 g, 0.039 mmol) in 2 mL of dry toluene under N_2. PPh_3 (0.020, 0.078 mmol) and 2 ml of dry CH_2Cl_2 were added to the solution. The mixture was stirred 5 min at room temperature and after this time, it was evaporated to dryness. The white solid was redissolved in 8.8 mL of dry CH_2Cl_2 and a solution of norbornene was added (0.8 mL, 2.9 mmol; 3.8 M, $[NB]_o$ = 0.3 M). The solution was stirred for 24 h at 25 ºC. After this time, 20 mL of MeOH were added but no solid (polymer) appeared in the solution. The solution was evaporated to dryness and the residue was checked by NMR spectroscopy in $CDCl_3$. Neither oligomers nor dimers were detected in the residue.

3.4.2.6. Polymerization of norbornene in the presence of the catalyst generated from 31 or 32/$AgBF_4$ in acetone

Representative procedure for the polymerization experiment in entry 2, Table 3.7. The other polymerizations in Table 3.7 were carried out with the same procedure changing the catalyst or the appropriate reaction condition.

In a 10 mL Schlenk tube was dissolved the $AgBF_4$ (0.008 g, 0.039 mmol) in 3 mL of dry acetone under N_2. In another 10 mL Schlenk tube was dissolved the complex **31** (0.020 g, 0.026 mmol) in 2 mL of dry CH_2Cl_2 under N_2. The solution of $AgBF_4$ was added to the solution of complex **31** and the mixture was stirred for 2 min at room temperature with the fast formation of a white solid (AgCl). The AgCl was removed using a PTFE filter and the orange solution was evaporated to dryness. The residue was redissolved in 6 mL of dry CH_2Cl_2 and a solution of norbornene was added (0.5 mL, 1.95 mmol; 3.8 M, $[NB]_o$ = 0.3 M). The solution was stirred for 24 h at 25 ºC. MeOH (10 mL) was added to the suspension inducing the complete precipitation of the polymer and the suspension was stirred 30 min at room temperature. The white solid was filtered off and washed with MeOH (2 x 10 mL) and Et_2O (5 mL). The white powder solid was air dried for 6 h (0.1 g, 55% yield). NB_{VA}/NB_{RO} = 7.5/1.

M_w = 4200; M_w/M_n = 1.3. Spectroscopy data for the VA/RO-PNB isolated are collected in Table 3.8-3.9.

3.4.2.7. Polymerization of norbornene in the presence of [Ni(o-CF_3-C_6H_4)(acac)(PPh_3)] (36)

The catalyst **36** (0.01 g, 0.0176 mmol) was placed in a Schlenk tube under N_2 and it was dissolved in 4 mL of dry CH_2Cl_2 followed by the addition of a solution of norbornene (0.35 mL, 1.32 mmol; 3.8 M, $[NB]_o$ = 0.3 M). The yellow solution was stirred at 24 h 25 ºC. After this time, 20 mL of MeOH was added but no solid (polymer) appeared in the solution. The solution was evaporated to dryness and the yellow residue was dissolved in 1 mL of $CHCl_3$. A preparative TLC in silica gel using Et_2O as eluent was performed. The component with Rf ≈ 0.6 was extracted with 15 mL of CH_2Cl_2. The suspension was filtered off and the solution was evaporated to dryness. The residue was dissolved in 1 ml of $CHCl_3$ and a new preparative TLC chromatography in silica gel using hexane as eluent was performed. Now, the component with Rf ≈ 0 was extracted with 15 mL of CH_2Cl_2 filtered off and the solution was evaporated to dryness. The colorless oil was analyzed by NMR spectroscopy. The ^{1}H NMR shows the formation of some oligomers with the opening of the ring by β-γ-C-C cleavage with visible signals for the internal RO units between 5.95-5.25 and multiple signals for the terminal RO units between 4.2-4.7. The initiation step through the *o*-CF_3-C_6H_4 is also visible in the ^{19}F NMR with a major signal at -58.75 ppm. The spectroscopy data are related those of the dimer **39** (see below).

3.4.2.8. Polymerization of norbornene in the presence of the catalyst 37 generated in situ

The complex **35** (0.015 g, 0.0155 mmol) was placed in a Schlenk tube under N_2 and it was dissolved in 6.8 mL of dry CH_2Cl_2. To the orange solution were added the $HBF_4 \cdot Et_2O$ (4.3 µl, 0.031 mmol) and the ligand $MeCOCH_2C(OMe)Me_2$ (4.5 µl, 0.031 mmol). The solution was stirred for 5 min at room temperature and a solution of norbornene was added (0.6 mL, 2.23 mmol; 3.8 M, $[NB]_0$ = 0.3 M). The orange solution was stirred 24 h at 25 ºC. MeOH (10 mL) was added to the suspension inducing the complete precipitation of the polymer and the suspension was stirred 30 min at room temperature. The white solid was filtered off and washed with MeOH (2 x 10 mL) and Et_2O (5 mL). The white powder solid was air dried for 6 h (0.094 g, 45% yield). Spectroscopy data for the VA/RO-PNB isolated are collected in Table 3.8-3.9.

3.4.2.9. Polymerization of norbornene in the presence of the catalyst 38

The catalyst **38** (0.020 g, 0.0286 mmol) was dissolved in a 10 mL Schlenk tube in 6.8 mL of dry CH_2Cl_2 under N_2. Immediately, a solution of norbornene in CH_2Cl_2 (0.55 mL, 2.1 mmol; 3.8 M, $[NB]_0$ = 0.3 M) was added. The yellow solution was stirred 24 h at 25 ºC. After this time, 20 mL of MeOH was added but no solid (polymer) appeared in the solution. The solution was evaporated to dryness and the yellow residue was dissolved in 1 mL of $CHCl_3$. A preparative TLC in silica gel using Et_2O as eluent was performed. The component with Rf ≈

0.6 was extracted with 15 mL of CH_2Cl_2. The suspension was filtered off and the solution was evaporated to dryness. The residue was checked by NMR spectroscopy in $CDCl_3$. The spectroscopy data matches those of the dimer **30** (see below).

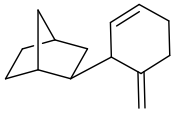

30

3.4.3. Formation in situ of complexes 33, 34 and 37

3.4.3.1. Complex 33

$AgBF_4$ (0.008 g, 0.0392 mmol) and $AsRfPh_2$ (0.017 g, 0.0392 mmol) were placed in a Sclenck tube under N_2 and dissolved in 2 mL of dry toluene at 243 K. A solution of complex **31** (0.030 g, 0.0392 mmol) in 2 mL of CH_2Cl_2 was added under N_2 and the mixture was stirred for 10 min at 243 K. After this time, a white solid (AgCl) appeared in the reddish solution. The AgCl was removed using a PTFE filter and the reddish solution was evaporated to dryness. The residue was redissolved in dry $CDCl_3$ and characterized in situ by NMR spectroscopy. ^{19}F NMR (470.592 MHz, δ, $CDCl_3$, 233 K): -58.3 (bt, J_{P-F} = 6 Hz, CF_3), -97.8 (F_{ortho}, $AsRfPh_2$), -103.1 (F_{para}, $AsRfPh_2$), -147.5 (BF_4). ^{31}P NMR (202.457 MHz, δ, $CDCl_3$, 233 K): 19.2 (m, 1P).

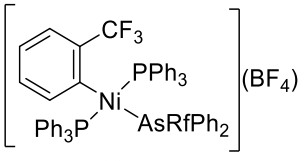

33

3.4.3.2. Complex 34, Method A: using complex 31 and $AgBF_4$ in acetone.

In a 10 mL Schlenk tube $AgBF_4$ (0.016 g, 0.078 mmol) was dissolved in 6 mL of dry acetone under N_2. Complex **31** (0.040 g, 0.052 mmol) was added to the solution and the mixture was stirred for 5 min at room temperature with the fast formation of a white solid (AgCl) and an orange solution. The AgCl was removed using a PTFE filter and the orange solution was evaporated to dryness. The orange oil was redissolved at 233 K in $CDCl_3$ and characterized in situ by NMR spectroscopy. The mixture contained **34** as well as $[Ag(PPh_3)_2]BF_4$ in a molar ratio 1:0.5. **34**. ^1H RMN (500.13 MHz, δ, $CDCl_3$, 233 K): 7.88 (d, 1H, $^1J_{H-H}$ = 6.9 Hz, H^6), 7.5-7.12 (m, PPh_3), 6.9-6.7 (m, 3H, H^5, H^4, H^3), 5.05 (bs, 1H, OH), 3.22 (d, 1H, $^1J_{H-H}$ = 19.7 Hz, H^{10}), 2.73 (d, 1H, $^1J_{H-H}$ = 19.7 Hz, $H^{10'}$), 1.75 (s, 3H, H^9), 1.65 (s, 3H, CH_3) 1.29 (s, 3H, CH_3). ^{13}C (125.758 MHz, δ, $CDCl_3$, 233 K): 222.2 (C^8), 137.07 (C^6), 133.9, 129.7, 127.7

(PPh_3), 128.5, 126.7, 124.1 (C^5, C^4, C^3), 71.6 (C^{11}), 51.35 (C^{10}), 32.13 (C^9), 27.8 (CH_3), 27.17 (CH_3).^{19}F NMR (470.592 MHz, δ, $CDCl_3$, 233 K): -58.12 (d, J_{P-F} = 6 Hz, CF_3), -150.2 (BF_4). ^{31}P NMR (202.457 MHz, δ, $CDCl_3$, 233 K): 25.41 (bs, 1P). $[Ag(PPh_3)_2]BF_4$: ^{31}P NMR (202.457 MHz, δ, $CDCl_3$, 233 K): 13 (dd, $J_{Ag^{109}-P}$ = 584 Hz; $J_{Ag^{107}-P}$ = 510.8).

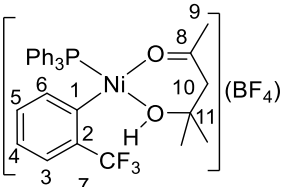

34

3.4.3.3. Complex 34, Method B: using the complex 35, $HBF_4{\cdot}Et_2O$ and the ligand $COCH_2(C(CH_3)_2)OH$

The complex **35** (30 mg, 0.031 mmol) was placed in a Schlenk tube under N_2 and dissolved in 3 mL of dry THF. The orange solution was cooled at 233 K in an acetone bath and the $HBF_4{\cdot}Et_2O$ (0.017 mL, 0.124 mmol) was added. The solution immediately changes to a red solution and after 5 min the ligand $MeCOCH_2C(OH)Me_2$ (0.038 mL, 0.31 mmol) was added. The solution changes again to orange and after 10 min at 233 K, the solution was evaporated to dryness. The orange residue was redissolved in dry $CDCl_3$ and the mixture was checked by NMR spectroscopy at 233 K. It contains complex **34** as the major product.

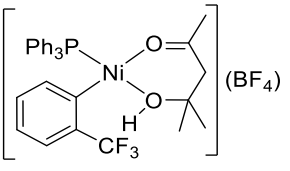

34

3.4.3.4. Characterization of $[Ni(o\text{-}CF_3\text{-}C_6H_4)(MeCOCH_2C(OMe)Me_2)(PPh_3)](BF_4)$ (37)

The complex **35** (0.021 g, 0.022 mmol) was dissolved in 2 mL of dry CH_2Cl_2. The orange solution was cooled in an acetone batch at 233 K and $HBF_4{\cdot}Et_2O$ was added (6 μL, 0.044 mmol). The orange solution changes to red solution. Immediately, the ligand $MeCOCH_2C(OMe)Me_2$ (7 μL, 0.044 mmol) was added to the mixture with the formation of a yellow solution. The mixture was stirred 10 min at 233 K. After this time, the solution was evaporated to dryness and the oil was dissolved in $CDCl_3$ at 233 K. The complex **37** was characterized in situ by NMR spectroscopy at 233 K. ^{1}H RMN (500.13 MHz, δ, $CDCl_3$, 233 K): 7.9 (bd, 1H, H^6), 7.7-7.25 (PPh_3), 7-6.7 (m, 3H, H^5, H^4, H^3), 3.53 (d, 1H, $^1J_{H-H}$ = 17.9 Hz, H^{10}), 3.12 (s, 3H, OMe), 2.98 (d, 1H, $^1J_{H-H}$ = 17.9 Hz, $H^{10'}$), 1.86 (s, 3H, H^9), 1.81 (CH_3), 1.25 (CH_3). ^{13}C (125.758 MHz, δ, $CDCl_3$): 137.5 (C^6), 133.7, 131, 128 (PPh_3), 128, 126, 124 (C^5,

C^4, C^3), 54.2 (C^{10}), 49 (OMe), 32.8 (C^9), 26.6 (CH_3), 24.6 (CH_3). ^{19}F NMR (470.592 MHz, δ, $CDCl_3$): -58.5 (bd, J_{P-F} = 6 Hz, CF_3), -152 (BF_4). ^{31}P NMR (202.457 MHz, δ, $CDCl_3$): 23 (m, 1P).

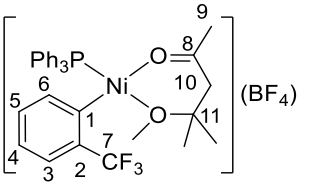

37

3.4.4. Synthesis of nickel(II) complexes

3.4.4.1. Synthesis of [Ni(o-CF_3-C_6H_4)Cl(PPh_3)$_2$] (31)

A solution of 1-iodo-2-(trifluoromethyl)benzene (0.47 mL, 3.4 mmol) in 3 mL of dry THF was placed in a 10 mL Schlenk tube under N_2 and cooled at 253 K. A THF solution of ^{i}Pr-MgCl·LiCl (2.6 mL, 3.4 mmol; 1.3 M in THF) was added to the cooled mixture and stirred at 253 K for 1 hour. $NiCl_2(PPh_3)_2$ (2 g, 3.1 mmol) was suspended in 20 mL of dry CH_2Cl_2 under N_2. The suspension was cooled at 273 K in an ice bath and the freshly prepared solution of *o*-CF_3-C_6H_4MgCl·LiCl was added. The suspension turns to an orange solution and it was stirred for 15 min at 273 K. The solution was evaporated to dryness and 10 mL of MeOH were added. The yellow solid generated was stirred for 10 min at 273 K. The solid was filtered off, washed with cold MeOH (2 x 5 mL) and air dried for 6 h (2 g, 84% Rdo.). ^1H RMN (500.13 MHz, δ, $CDCl_3$): 7.58-7.48 (m, 12H, H_{meta}, H_{ortho} Ph PPh_3), 7.38 (d, $^1J_{H-H}$ = 7.6, 1H, H^6), 7.33 (m, 6H, H_{para} Ph PPh_3), 7.24 (m, 12H, H_{meta}, H_{ortho} Ph PPh_3), 6.60 (d, $^1J_{H-H}$ = 7.6, 1H, H^3), 6.45 (d, $^1J_{H-H}$ = 7.6, 1H, H^4), 6.38 (t, $^1J_{H-H}$ = 7.6, 1H, H^5). ^{13}C (125.66 MHz, δ, $CDCl_3$): 151.09 (t, J_{C-P} = 34 Hz, C^1), 138.1 (t, $^4J_{C-F}$ = 4 Hz, C^6), 135.7 (q, $^2J_{C-F}$ = 29 Hz, C^2), 134.5, 127.7 (C_{meta}, C_{ortho} Ph PPh_3), 132 (t, J_{C-P} = 27 Hz, C^{ipso} PPh_3), 129.5 (C_{para} Ph PPh_3), 127.3 (C^5), 125.18 (q, $^1J_{C-F}$ = 273 Hz, C^7), 126.9 (C^3), 121.23 (t, $^4J_{C-F}$ = 1.8 Hz C^4). ^{19}F NMR (470.592 MHz, δ, $CDCl_3$): -58.9 (t, J_{P-F} = 6 Hz, CF_3). ^{31}P (202.457 MHz, δ, $CDCl_3$): 19.56 (q, J_{P-F} = 6 Hz, 2P). Analysis calc. for $C_{43}H_{34}ClF_3P_2Ni·CH_4O$: C, 66.40; H, 4.81; found: C, 66.79; H, 4.37.

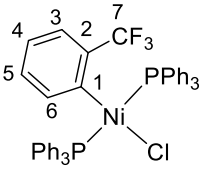

31

3.4.4.2. Synthesis and characterization of [Ni(o-CF_3-C_6H_4)(μ-OH)(PPh_3)]$_2$ (35)

Complex **35** was synthesized following a reported method for analogous complexes.[163]

In a 100 mL round-bottom flask complex **31** (1.76 g, 2.30 mmol) was dissolved in 28.5 mL of THF. KOH (2.6 g, 47 mmol) in pellets was grounded and added to the orange solution. In addition, 1 mL of H_2O (ratio THF:H_2O = 30:1) was added and the mixture was stirred vigorously for 24 h at room temperature. The color of the suspension changed from yellow to orange. After this time, the aqueous phase was removed and the organic solution was evaporated to dryness. The residue was redissolved in the minimal amount of THF and filtered off through celite. The orange solution was evaporated to dryness. The residue was triturated with 5 mL of pentane and stirred for 30 min at room temperature inducing the formation of an orange solid. The solid was filtered off, washed with pentante (2 x 5 mL) and air dried for 6 h (0.95 g, 89% yield).

In a solution of $CDCl_3$, complex **35** is a mixture of three isomers, resulting from the different dispositions of the phosphine (*cis* or *trans*) and CF_3 group (*syn* or anti) (Figure 3.23). The three isomers detected show in the ^{1}H NMR the presence of two inequivalent hydroxyl bridges (Figure 3.24). Only in the *trans-syn*-**35** isomer the two protons for the OH groups are equivalents and only one signal would be observed in the ^{1}H NMR. So, we can discard the presence of the isomer *trans-syn*-**35** in the $CDCl_3$ solution.

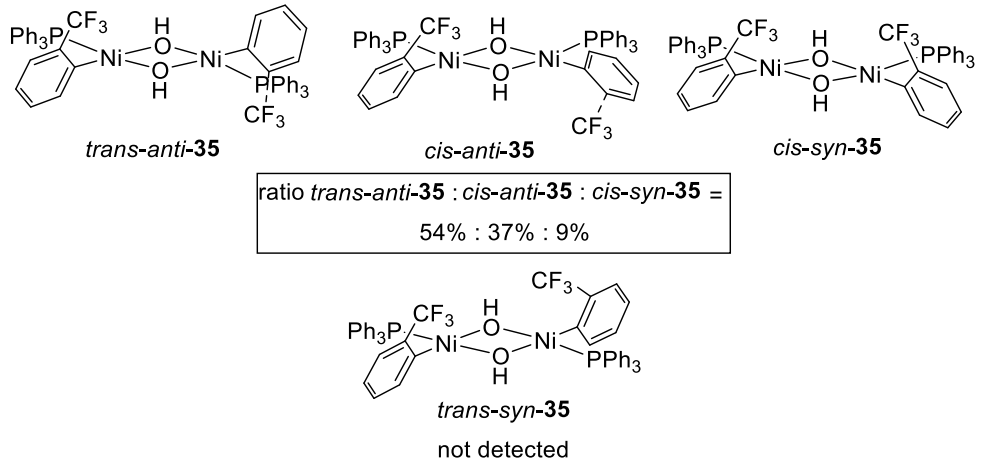

Figure 3.23. Three isomers for complex **35** detected in $CDCl_3$ at 298 K and the fourth isomer that was not detected.

By analogy to other hydroxo dimers, the complex with the two OH with similar chemical shifts (-4.0 ppm and -4.2 ppm in the ^{1}H NMR, Figure 3.24) is assigned to the isomer *trans-anti*-**35**. The two other *syn* isomers are conformed by two OH groups with very different chemical shifts but a priory is not possible assigned to which isomer (*cis-anti*-**35** or *cis-syn*-**35**) correspond each OH signal.

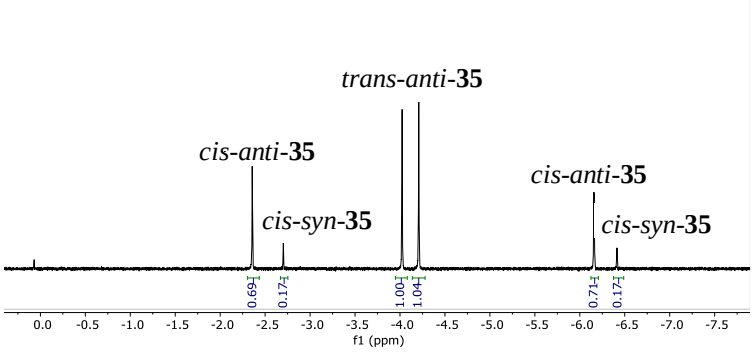

Figure 3.24. ^{1}H NMR of complex **35** in $CDCl_3$ at 298 K showing only the part of the OH groups.

We expected that the isomer with the two CF_3 in a *syn* disposition in the isomer *cis-syn*-**35** will be the minor compound because the steric hindrance between the two CF_3 is high. In addition, the NOESY experiment (Figure 3.25) shows that the minor isomer has got only one NOE peak (orange circle) between the *ortho* protons (H^6, $H^{6'}$) and one of the OH. This situation is expected for the isomer *cis-syn*-**35** where one of the OH is close to the *ortho* protons but the other is far away. A suitable crystal for X-Ray analysis can be obtained by a slow evaporation at 0 ºC of a solution of the complex **35** in pentane (Figure 3.26). The structure for the *cis-anti*-**35** agrees with the NOESY experiment where the two *ortho* protons have NOE interaction with the OH protons (green circles).

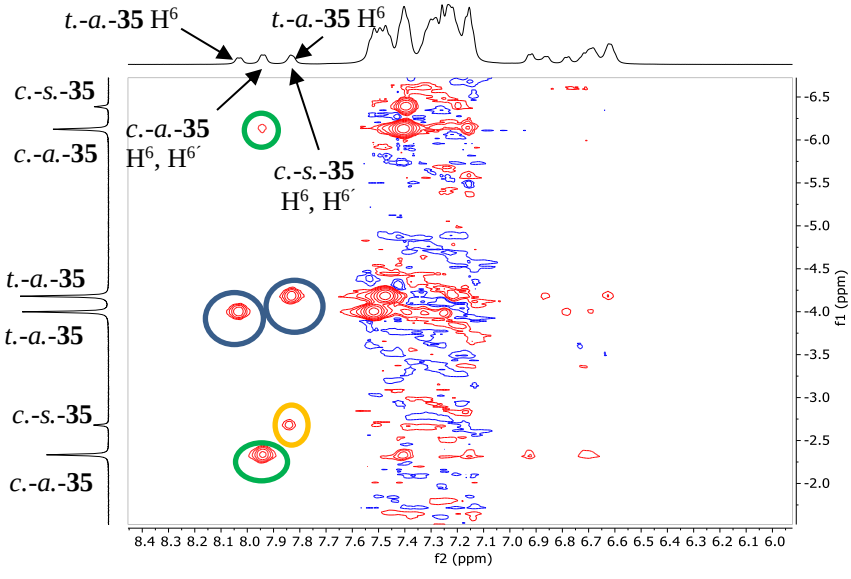

Figure 3.25. ^{1}H-^{1}H NOESY NMR of the complex **34** at 298 K. *t.-a.*-**35** = *trans-anti*-**35**; *c.-a.*-**35** = *cis-anti*-**35**; *c.-s.*-**35** = *cis-syn*-**35** at 298 K.

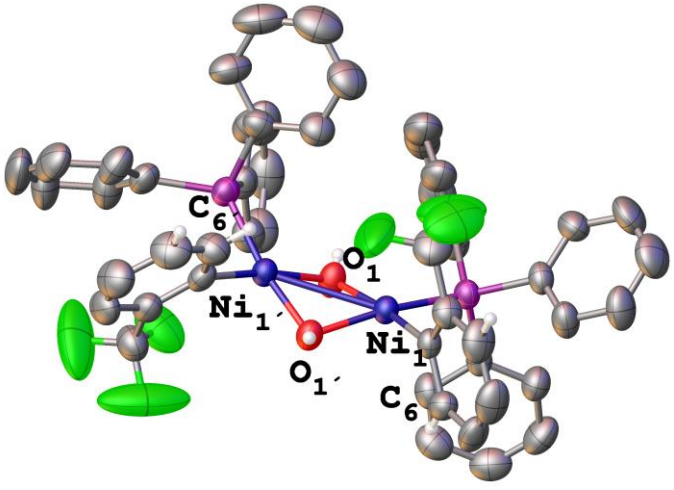

Figure 3.26. ORTEP representation of the complex *cis-anti*-**35** (40% of probability). Some of the hydrogen atoms were omitted for clarity.

The NMR data for compound **35** are the following: ^{1}H RMN (500.13 MHz, δ, $CDCl_3$): 8.03 (m, H^6 *trans-anti*-**35**), 7.94 (m, H^6, $H^{6´}$ *cis-anti*-**35**), 7.83 (m, $H^{6´}$ *trans-anti*-**35**; m 2H, H^6, $H^{6´}$ *cis-syn*-**35**), 7.56-7.19 (m, PPh_3), 6.92-6.58 (m, H^5, $H^{5´}$, H^4, $H^{4´}$, H^3, $H^{3´}$ *trans-anti*-**35**, *cis-anti*-**35**, *cis-syn*-**35**), -2.33 (s, 1H, OH , *cis-anti*-**35**), -2.68 (s, 1H, OH, *cis-syn*-**35**), -4 (s, 1H, OH, *trans-anti*-**35**), -4.19 (m, 1H, OH´, *trans-anti*-**35**), -6.13 (m, 1H, OH´, *cis-anti*-**35**), -6.39 (m, 1H, OH´, *cis-syn*-**35**). ^{13}C (125.66 MHz, δ, $CDCl_3$):146.5 (C^1, $C^{1´}$ *trans-anti*-**35**, *cis-anti*-**35**, *cis-syn*-**35**), 138.8 (C^6, $C^{6´}$, *cis-anti*-**35**), 138.3 (C^6, $C^{6´}$, *trans-anti*-**35**, *cis-syn*-**35**), 136.9 (C^2, $C^{2´}$ *trans-anti*-**35**, *cis-anti*-**35**, *cis-syn*-**35**), 133,9, 128 (C_{ortho}, C_{meta} Ph PPh_3), 129.91(C_{para}, C_{ipso} Ph PPh_3), 125.4 (q, $^{1}J_{C-F}$ = 273 Hz, C^7, $C^{7´}$), 126.27, 121.77, 125.9 (C^5, $C^{5´}$, C^4, $C^{4´}$, C^3, $C^{3´}$, *trans-anti*-**35**, *cis-anti*-**35**, *cis-syn*-**35**). ^{19}F NMR (470.592 MHz, δ, $CDCl_3$): -57.5 (d, J_{P-F} = 5.3 Hz, CF_3 *trans-anti*-**35**,), -57.8 (d, J_{P-F} = 5.3 Hz, CF_3´ *trans-anti*-**35**,), -57.9 (d, J_{P-F} = 5.3 Hz, CF_3, CF_3´ *cis-anti*-**35**, *cis-syn*-**35**), ^{31}P NMR (202.457 MHz, δ, $CDCl_3$): 28.29 (m, 2P, *trans-anti*-**35**), 28 (m, 2P, *cis-anti*-**35**), 27.66 (m, 2P, *cis-syn*-**35**). Analysis calc. for $C_{50}H_{40}F_6O_2P_2Ni_2 \cdot C_4H_8O$: C, 62.46; H, 4.60; found: C, 62.67; H, 4.19.

3.4.4.3. Synthesis of [Ni(o-CF_3-C_6H_4)(acac)(PPh_3)] (36)

The hydroxo dimer **35** (0.15 g, 0.155 mmol) was placed in a 50 mL round-bottom flask and it was dissolved in 10 mL of CH_2Cl_2. The Hacac was added (0.04 mL, 0.388 mmol) and the solution was stirred for 1 h at 25 ºC. The initial orange solution turned to yellow. The yellow solution was evaporated to dryness and 5 mL of pentane were added. The yellow solid was filtered off, washed with pentane (2 x 5 mL) and air dried for 3 h (0.12 g, 67% yield). ^{1}H RMN (500.13 MHz, δ, $CDCl_3$): 7.75 (bs, 1H, H^6), 7.46 (m, 3H, H_{para}, PPh_3), 7.46, 7.26 (m, 12H, H_{meta}, H_{ortho}, Ph PPh_3), 6.96 (bs, 1H, H^3), 6.72 (m, 2H, H^5, H^4), 5.34 (bs, 1H, H^9), 1.80 (bs, 3H,

CH_3), 1.36 (bs, 3H, CH_3). ^{13}C (125.66 MHz, δ, $CDCl_3$): 187, 185 (C^{10}, C^8), 150.3 (C^1), 137.16 (d, $^4J_{C-F}$ = 4 Hz, C^6), 136.2 (C^2), 134.10, 127.5 (C_{meta}, C_{ortho}, Ph PPh_3), 129.85(C_{para}, C_{ipso}, Ph PPh_3), 126.7 (C^4), 122.05 (C^5), 125.5 (C^3), 100 (C^9), 26.8 (CH_3), 26.0 (CH_3). ^{19}F NMR (470.592 MHz, δ, $CDCl_3$): -58.36 (d, J_{P-F} = 4.6 Hz, CF_3). ^{31}P NMR (202.457 MHz, δ, $CDCl_3$): 27.84 (q, J_{P-F} = 4.6 Hz).

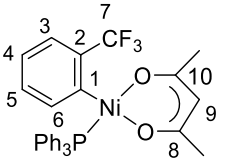

36

3.4.4.4. Synthesis of [Ni(o-CF_3-C_6H_4)($MeCOCH_2C(SMe)Me_2$)(PPh_3)](BF_4) (38)

The complex **35** (0.08 g, 0.083 mmol) was dissolved in 5 mL of dry THF. The orange solution was cooled in an acetone batch at 233 K and $HBF_4 \cdot Et_2O$ was added (0.023 mL, 0.166 mmol). The orange solution changes to a red solution. Immediately, the ligand $MeCOCH_2C(SMe)Me_2$ (0.032 mL, 0.21 mmol) was added to the mixture with the formation of a yellow solution. The mixture was stirred 10 min at 233 K. After this time, the solution was evaporated to dryness and the oil was triturated with 10 mL of hexane. The solution was separated from the yellow solid using a canula and the solid was washed with dry Et_2O (2 x 5 mL) and dry hexane (2 x 5 mL). The yellow solid was vacuum dried (0.046 g, 40% Yield). ^1H RMN (500.13 MHz, δ, $CDCl_3$): 7.6 (d, 1H, $^1J_{H-H}$ = 8 Hz, H^6), 7.46 (m, 3H, H_{para} PPh_3), 7.37 (m, 12H, H_{meta}, H_{ortho} PPh_3), 6.99 (d, 1H, $^1J_{H-H}$ = 8 Hz, H^3), 6.85 (m, 2H, H^5, H^4), 3.53 (d, 1H, $^1J_{H-H}$ = 21 Hz, H^{10}), 2.89 (d, 1H, $^1J_{H-H}$ = 21 Hz, $H^{10'}$), 2.18 (s, 3H, SMe), 1.77 (s, 3H, H^9). 1.5 (CH_3), 1.41 (CH_3). ^{13}C (125.758 MHz, δ, $CDCl_3$): 223.06 (C^8), 135.45 (C^6), 136.2 (C^2), 133.7, 128.8, (C_{ortho}, C_{meta}, PPh_3), 131 (C_{para}, C^{ipso}, PPh_3), 128.8, 123.8 (C^5, C^4), 49.7 (C^{10}), 40 (C^{11}), 32.98 (C^9), 27.17 (CH_3), 27.8 (CH_3), 12.43 (SMe). ^{19}F NMR (470.592 MHz, δ, $CDCl_3$): -58.4 (d, J_{P-F} = 5.7 Hz, CF_3), -152 (BF_4). ^{31}P NMR (202.457 MHz, δ, $CDCl_3$): 19.5 (m, 1P).

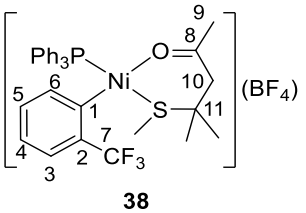

38

3.4.5. Synthesis of dimers of norbornene

3.4.5.1. Synthesis of dimer 30

The dimer **30** was synthesized following a previous reported method.[154] In a 100 mL Schlenk tube was placed [$NiCl_2$dppe] (0.58 g, 1 mmol) under N_2. 50 mL of dry MeOH and norbornene (2.82 g, 30 mmol) were added. Finally, the $NaBH_4$ (0.038 g, 1 mmol) was added and the brown suspension was heated 23 h at 80 ºC. After this time, the suspension was evaporated to dryness and 5 mL of CH_2Cl_2 were added to the residue. Water was added (20 mL) and after stirring the aqueous phase was discarded. This process was repeated twice and then the organic phase was washed with $NH_4Cl_{(aq)}$ (2 x 20 mL). The organic phase was dried with $MgSO_4$ and filtered off. The yellow solution was evaporated to dryness and 5 mL of Et_2O were added. The solid was removed by filtration and the solution was evaporated to dryness to yield a yellow oil.* ^{1}H RMN (500.13 MHz, δ, $CDCl_3$): 5.69 (m, 2H, H^3, H^2), 4.81 (m, 1H, H^7), 4.61 (m, 1H, $H^{7´´}$), 2.29-2.11 (m, 5H, H^5, H^4, $H^{4´}$, $H^{2´}$, $H^{1´}$,H^1), 1.45-1.04 (m, 10H , $H^{7´}$, $H^{6´}$, $H^{5´}$, $H^{5´´}$, $H^{4´´}$, $H^{3´}$), ^{13}C (125.66 MHz, δ, $CDCl_3$): 149.25 (C^6), 129.65, 127.55 (C^3, C^2), 108.71 (C^7), 48.55 ($C^{2´}$), 47.6 (C^1), 39.21 ($C^{1´}$), 36.35 ($C^{4´}$), 36.20 ($C^{7´}$), 35.20 ($C^{3´}$), 30.3-28.73 ($C^{6´}$, $C^{5´}$, C^5, C^4). (MS (EI, 70 eV): m/z (%) 188.14 (20), 95.08 (100), 77.03 (92), 67.05 (100).

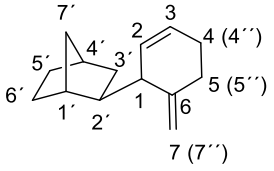

30

*Minor signals for other oligomers are detected in the ^{1}H NMR.

3.4.5.2. Synthesis of dimer 39

In a 10 mL Schlenk tube was dissolved $AgBF_4$ (0.012 g, 0.059 mmol) in 5 mL of dry acetone under N_2. Complex **31** (0.030 g, 0.040 mmol) was added to the solution and the mixture was stirred for 5 min at room temperature with the fast formation of a white solid (AgCl) and an orange solution. The AgCl was removed used a PTFE filter and the orange solution was evaporated to dryness. The residue was redissolved in 1 mL of CH_2Cl_2 and a solution of norbornene was added (0.021 mL, 0.08 mmol; 3.8 M). The solution was stirred 24 h at 25 ºC. Then, 5 mL of Et_2O were added and the yellow solid was filtered off. A preparative TLC in silica gel using Et_2O as eluent was performed to the residue. The component with Rf ≈ 0.6 was extracted with 15 mL of CH_2Cl_2. The suspension was filtered off and the solution was evaporated to dryness. The colorless residue was analyzed by NMR spectroscopy and MS.* ^{1}H RMN (500.13 MHz, δ, $CDCl_3$): 7.5-7.4 (m, 4H, $H_{arom.}$ Ar-CF_3), 5.59 (m, 1H, H^3), 5.50 (m, 1H, H^2), 4.2 (s, 1H, H^7), 3.4 (s, 1H, $H^{7´´}$), 3.19 (d, $^1J_{H\text{-}H}$ = 8.7 Hz, 1H, $H^{3´}$), 2.45 (m, 1H, $H^{4´}$),

2.37 (m, 1H, H^1), 2.35-2.02 (m, 4H, H^5, H^4, $H^{1´}$), 2.11 (m, 1H, $H^{2´}$), 1,93 (m, 1H, *syn* $H^{7´}$), 1.35 (m, 1H, *anti* $H^{7´}$), 1.6-1.3 (m, 4H, H^6, $H^{6´}$, $H^{5´´}$, $H^{4´´}$). ^{13}C (125.66 MHz, δ, $CDCl_3$): 150.6 (C^6), 131-125 (Ar-CF_3), 127.09 (C^3), 129.68 (C^2), 107,2 (C^7), 55.2 ($C^{2´}$), 48.04 ($C^{3´}$), 44.22 ($C^{1´}$), 42.15 (C^1), 38.99 ($C^{4´}$), 37.03 ($C^{7´}$), 31.96-28.35 ($C^{6´}$, C^5, $C^{5´}$, C^4). ^{19}F NMR (470.92 MHz, δ, $CDCl_3$): -58.71. MS (EI, 70 eV): m/z (%) 332.51 (1), 239 (30), 258 (30), 91 (40), 76 (40), 67 (100).

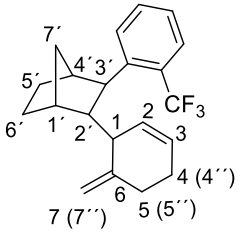

39

*Minor signals for other oligomers are detected in the ^1H NMR.

3.4.5.3. Synthesis of dimer 40

In a 10 mL Schlenk tube was dissolved $AgBF_4$ (0.012 g, 0.063 mmol) in 5 mL of dry acetone under N_2. Complex **32** (0.030 g, 0.042 mmol) was added to the solution and the mixture was stirred for 5 min at room temperature with the fast formation of a white solid (AgCl) and an orange solution. The AgCl was removed used a PTFE filter and the orange solution was evaporated to dryness. The residue was redissolved in 1 mL of CH_2Cl_2 and a solution of norbornene was added (0.022 mL, 0.084 mmol; 3.8 M). The solution was stirred 24 h at 25 ºC. Then, 5 mL of Et_2O were added and the yellow solid was filtered off. A preparative TLC in silica gel using Et_2O as eluent was performed to the residue. The component with Rf ≈ 0.6 was extracted with 15 mL of CH_2Cl_2. The suspension was filtered off and the solution was evaporated to dryness. The colorless residue was analyzed by NMR spectroscopy and MS.* ^1H RMN (500.13 MHz, δ, $CDCl_3$): 7.36, 7.15, 7.09 (m, 4H, $H_{arom.}$ Ar-CH_3), 5.55 (m, 1H, H^3), 5.25 (m, 1H, H^2), 4.5 (s, 1H, H^7), 4.04 (s, 1H, $H^{7´´}$), 3.02 (d, $^1J_{H-H}$ = 9 Hz, 1H, $H^{3´}$), 2.46 (m, 1H, $H^{4´}$), 2.38 (m, 1H, H^1), 2.35-1.9 (m, 3H, $H^{1´}$, H^5, H^4), 2.28 (s, 3H, CH_3), 2.09 (m, 1H, $H^{2´}$), 1,84 (m, 1H, *syn* $H^{7´}$), 1.29 (m, 1H, *anti* $H^{7´}$), 1.6-1.3 (m, 4H, $H^{6´}$, $H^{5´}$, $H^{5´´}$,$H^{4´´}$). ^{13}C (125.66 MHz, δ, $CDCl_3$): 150.9 (C^6), 129-126 (Ar-CH_3), 127.09 (C^3), 126.4 (C^2), 108,01 (C^7), 53.9 ($C^{2´}$), 49.3 ($C^{3´}$), 42.4 ($C^{4´}$), 41.96 ($C^{1´}$), 39.6 (C^1), 36.6 ($C^{7´}$), 31.96-27.9 ($C^{6´}$, C^5, $C^{5´}$, C^4). MS (EI, 70 eV): m/z (%) 278 (16), 250 (16), 185 (32); 129 (66); 115 (83), 105 (100), 67 (100).

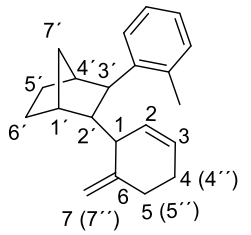

40

*Minor signals for other oligomers are detected in the ^{1}H NMR.

3.4.6. Data for X-Ray structure determinations

Crystals suitable for X-ray analyses were obtained by slow evaporation at 298 K of a solution of the complex [Ni(CF_3-*o*-C_6H_4)(μ-OH)(PPh_3)]$_2$ (**35**) in pentane, by slow vapor-diffusion of pentane to a solution of complex [Ni(acac)(CF_3-*o*-C_6H_4)(PPh_3)] (**36**) in CH_2Cl_2 at 273 K and by slow vapor-diffusion of pentane to a solution of complex [Ni(*o*-CF_3-C_6H_4)($MeCOCH_2C(SMe)Me_2$)(PPh_3)](BF_4) (**38**) in CH_2Cl_2 at 233 K.

The crystals were mounted on the tip of glass fibers. X-ray measurements were made using Bruker SMART CCD area-detector diffractometer with Mo Kα radiation (0.71073 Å). Reflections were collected, intensities integrated, and the structures were solved by direct methods procedure. Non-hydrogen atoms were refined anisotropically and hydrogen atoms were constrained to ideal geometries and refined with fixed isotropic displacement parameters. Data collection was performed at 298 K. Refinement proceeded smoothly to give the residuals shown in Table 3.10.

Table 3.10. Crystal data and structure refinement for complex **35**, **36** and **38**.

	35	**36**	**38**
Empirical formula	$C_{50}H_{40}F_6Ni_2O_2P_2$	$C_{30}H_{13}F_3NiO_2P$	$C_{32}H_{30}BF_7NiOPS$
Formula weight	966.18	552.08	682.09
Temperature/K	293(2)	293(2)	293(2)
Crystal system	triclinic	monoclinic	orthorhombic
Space group	P-1	$P2_1/c$	Pbcn
a/Å	13.0312(11)	18.5059(8)	16.7171(6)
b/Å	13.1540(13)	9.2157(4)	14.3676(6)
c/Å	14.7181(6)	35.3303(17)	37.0248(11)
α/°	81.840(5)	90	90
β/°	86.385(5)	96.492(4)	90
γ/°	63.640(9)	90	90
Volume/Å^3	2237.7(3)	5986.8(5)	8892.7(5)
Z	2	8	11
ρ_{calc}g/cm^3	1.434	1.225	1.401
μ/mm^{-1}	0.977	0.742	0.935
F(000)	992.0	2232.0	3808.0
Crystal size/mm^3	? × ? × ?	0.322 × 0.265 × 0.265	0.524 × 0.524 × 0.319
Radiation	Mo Kα (λ = 0.71073)	Mo Kα (λ = 0.71073)	Mo Kα (λ = 0.71073)
2Θ range for data collection/°	6.592 to 59.332	6.772 to 59.498	6.534 to 59.616
Index ranges	-18 ≤ h ≤ 16, -13 ≤ k ≤ 16, -14 ≤ l ≤ 18	-24 ≤ h ≤ 15, -7 ≤ k ≤ 12, -44 ≤ l ≤ 48	-15 ≤ h ≤ 22, -17 ≤ k ≤ 10, -50 ≤ l ≤ 35
Reflections collected	19757	25243	24643
Independent reflections	10477 [Rint = 0.0501, Rsigma = 0.1094]	13894 [R_{int} = 0.0374, R_{sigma} = 0.0694]	10307 [Rint = 0.0376, Rsigma = 0.0589]
Data/restraints/parameters	10477/0/567	13894/0/669	10307/0/473
Goodness-of-fit on F^2	1.011	1.156	1.033
Final R indexes [I>=2σ (I)]	R1 = 0.0621, wR2 = 0.0999	R_1 = 0.0737, wR_2 = 0.1880	R1 = 0.0896, wR2 = 0.2417
Final R indexes [all data]	R1 = 0.1396, wR2 = 0.1323	R_1 = 0.1202, wR_2 = 0.2152	R1 = 0.1476, wR2 = 0.2850
Largest diff. peak/hole / e Å^{-3}	0.61/-0.45	0.94/-0.51	0.68/-0.69

Chapter 4

4. Synthesis of Supported Trispyrazolylborate Copper(I) Complexes on VA-PNBs

4.1. Introduction

4.1.1. Copper supported catalysis: An approach to green chemistry

The development of environmentally friendly processes is an important goal in current chemistry research and this is referred to as Green Chemistry.[165] Research efforts have been made to use of benign solvents in chemical reactions, such as aqueous media,[166] or to increase the efficiency of the processes in terms of atom and step economy.[167] The support of a catalyst or a reagent in an organic or inorganic solid has rised great interest both in research labs and in the chemical industry, as a way to achieve greener synthesis. When molecular catalysts are supported, they retain the characteristics of the homogeneous catalysts but gain additional advantages. The main benefits are due to the easy physical separation of the catalyst from the reaction mixture by filtration, the easy recycling of the catalyst (especially important with expensive catalysts and ligands) and the microenvironment generated by the support (often a

[165] Horváthm, I. T.; Anastas, P. T. *Chem. Rev.* **2007**, *107*, 2169-2173.
[166] Li, C. J. *Chem. Rev.* **2005**, *105*, 3095-3165.
[167] Trost, B. *Acc. Chem. Res.* **2002**, *35*, 695-705.

polymer) that in some cases offers additional benefits.[168-170] For example, an increase in the stereoselectivity epoxidation of α-β-unsaturated ketones was reported in 1999 employing a binaphthyl polymer combined with diethylzinc. The authors proposed a cooperative effect between the neighboring catalytic sites in the polymer chain, which greatly increased the enantioselectivity of the catalyst from 37% to 88% ee.[169]

The use of copper complexes supported on a polymer matrix has increased in the last years because of the advantages of the heterogeneous catalysis (easy recover, recyclability...) in addition to the use of copper, that is a non-highly toxic metal.[171,172] Derivatives of polystyrenes such as Merrifield resin™ and JandaJel resin™ are the most common polymers for heteregeneous catalysis with supported copper complexes.[173] Other supports such as biodegradable polymers[174] or ROMP polymers[175] can be found in the literature but less frequently. Scheme 4.1 shows two examples of useful Cu-supported catalysts on polymeric matrixes.

---

[168] Hodge, P. *Chem. Soc. Rev*. **1997**, *26*, 417-423.
[169] Yu, H.; Zheng, X.; Lin, Z.; Hu, Q.; Huang, W.; Pu, L. *J. Org. Chem*. **1999**, *64*, 8149-8155.
[170] Harrison, C. R.; Hodge, P.; Hunt, B. J.; Khoshdel, E.; Richardson, G. *J. Org. Chem*. **1983**, *48*, 3721-3728.
[171] Egorova, K. S.; Ananikov, V. P. T *Organometallics* **2017**, *36*, 4071-4090.
[172] For reviews about polymer-supported catalysts, see: a) Clark, J. H.; Mcquarrie, D. Handbook of Green Chemistry & Technology; Blackwell Publ., London, 2002. b) Leadbeater, N. E.; Marco, M. *Chem. Rev*. **2002**, *102*, 3217-3274. c) McNamara, C. A.; Dixon, M. J.; Bradley, M. *Chem. Rev*. **2002**, 102, 3275-3300. d) Buchmeiser, M. R. Polymeric materials in organic synthesis and catalysis, Wiley-VCH, Weinheim, 2003. e) Benaglia, M.; Puglisi A.; Cozzi, F. *Chem. Rev*. **2003**, *103*, 3401-3430. f) Dioos, B. M. L.; Vankelecom, I. F. J.; Jacobs, P. A. *Adv. Synth. Catal*. **2006**, *348*, 1413-1446. g) Itsuno, S.; Haraguchi, N. Handbook of Asymmetric Heterogeneous Catalysis. *In Heterogeneous Enantioselective Catalysis Using Organic Polymeric Supports* eds. Ding K.; Uozumi, Y.; WileyVCH, Weinheim, 2008, pp. 73-129. h) Benaglia, M. Recoverable and Recyclable Catalysts; John Wiley & Sons, Chichester, 2009.
[173] a) Orlandi, S.; Mandoli, A.; Pini, D.; Salvadori, P. *Angew. Chem., Int. Ed.*, **2001**, *40*, 2519-2521. b) Mandoli, A.; Orlandi, S.; Pini, D.; Salvadori, P. *Chem. Commun*. **2003,** 2466-2467. c) Valodkar, V. B.; Tembeb, G. L.; Ravindranathan, M.; Rama, R. N; Ramaa H. S. *J. Mol. Cat. A: Chem*. **2004**, *208*, 21-32. d) Chiang, G. C. H.; Olsson, T. *Org. Lett*. **2004**, *6*, 3080-3082. e) Werner, H.; Herrerías, C. I.; Glos, M.; Gissibl, A.; Fraile, J. M.; Péres, I.; Mayoral, J. A.; Reiser, O. *Adv. Synth. Catal*. **2006**, *348*, 125-132. f) Drabina, P.; Svoboda, J.; Sedlák, M. *Molecules* **2017**, *22*, 865-883. g) Yan, S.; Pan, S.; Osako, T.; Uozumi, Y. *ACS Sustainable Chem. Eng*. **2019**, *7*, 9097-9102.
[174] a) Chtchigrovsky, M.; Primo, A.; Gonzalez, P.; Molvinger, K.; Robitzer, M.; Quignard, F.; Taran, F. *Angew. Chem. Int. Ed.* **2009**, *48*, 5916-5920. b) Pourjavadi, A.; Habibi, Z. *RSC Adv*. **2015**, 99498-99501. c) Mandala, B. H.; Rahman, L.; Hasbi, Rahim M. H.; Sarkar, S.M. *ChemistrySelect* **2016**, *1*, 2750-2756. d) Mandala, B. H.; Rahman, L. Yusoffa, M. M.; Chonga, K. F.; Sarkara, S. M. *ChemistrySelect* **2016**, *1*, 2750-2756. e) Sarkar, S. M.; Rahman, L. *J. Clean. Prod*. **2017**, *141*, 683-692.
[175] a) Sun, Z.; Unruean, P.; Aoki, H.; Kitiyanan, B.; Nomura, K. *Organometallics 2020*, **39**, *16*, 2998-3009. b) Vidal, F.; McQuade, J.; Lalancette, R.; Jäkle, F. *J. Am. Chem. Soc*. **2020**, *142*, 14427-14431. c) Kröll, R. M.; Schuler, N.; Lubbad, S.; Buchmeiser, M. R. *Chem. Commun*., **2003**, 2742-2743.

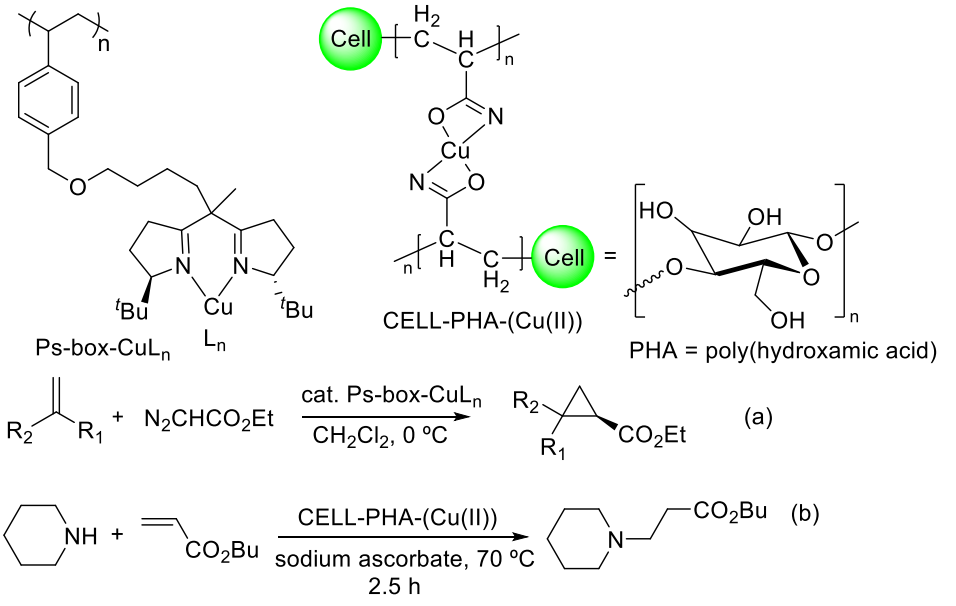

Scheme 4.1. Two examples of Cu-supported catalysts on polymeric matrixes such as polystyrene or a biodegradable polymer with application in cyclopropanation reaction (a) and Aza-Michael reaction (b).

Even though polystyrene supports are extensively used, some uncontrolled side reactions can occur in their skeleton as, for example the reaction of benzylic positions in the polystyrenes in radical processes (Figure 4.1). The double bonds in the ROMP polymers are also reactive centers that may interfere and limit their applicability. The double bond in the ROMP polymer can be hydrogenated but this is an additional step in the synthesis of the support.[80]

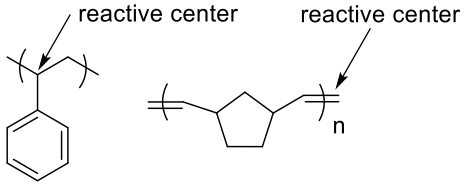

Figure 4.1. Reactive centers in polystyrene and ROMP polymers that can perform unwanted side reactions.

In contrast, the all-aliphatic skeleton of the vinylic addition polynorbornenes (VA-PNBs) gives a high thermal and chemical stability to these materials and make them ideal for some catalysis applications. In our research group, the VA-PNB support was employed for heterogeneous catalysis with good recyclability in reactions such as the Stille reaction with

polymeric stannylated VA-PNBs, giving very low tin contamination in the final product (Figure 4.2, a)).[103a,b,c] Stannylated VA-PNBs were also used as catalyst in radical reactions.[103h] Recyclable VA-PNB organocatalysts have been used in asymmetric aldol reactions in water (Figure 4.2, b) and d)),[103f] or supported N-heterocyclic carbenes for the synthesis of γ-butyrolactones (Figure 4.2, c)).[103d,e] The application of supported palladium(II) complexes bearing a polymeric N-heterocyclic carbene or α-diimine ligands in cross-coupling reactions could also been achieved.[103g]

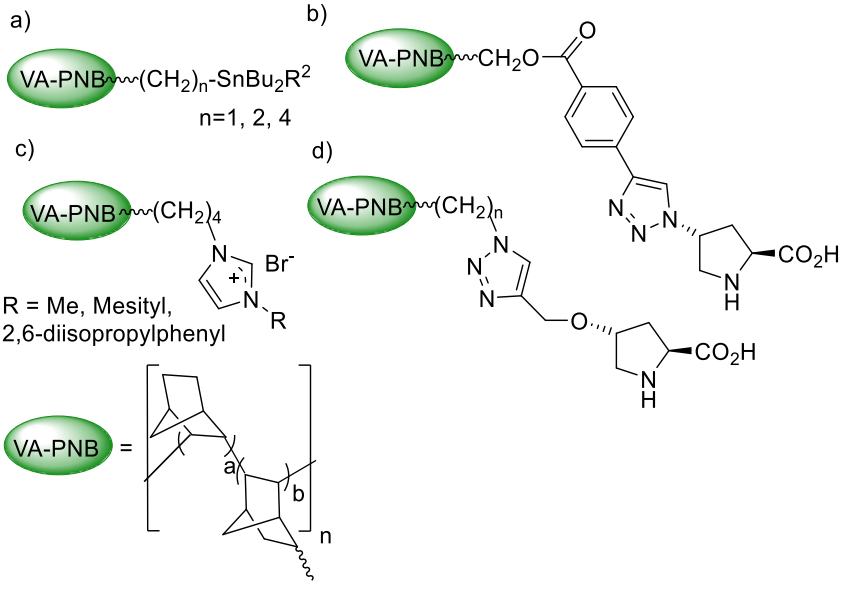

Figure 4.2. Some examples of catalysts and reagents anchored to the skeleton of VA-PNB.

4.1.2. Trispyrazolylborates (Tp^x) as convenient ligands to support Cu(I) complexes

4.1.3.1. Trispyrazolylborate ligands (Tp^x)

Trispyrazolylborates (Tp^x), have been extensively studied after their discovery by Trofimenko in 1966.[176] The Tp^x are a type of ligands included in a very large class of ligands called

[176] a) Trofimenko, S. *J. Am. Chem. Soc*. **1966**, *88*, 1842-1844. b) Trofimenko, S. *Chem. Rev*. **1993**, *93*, 943-980. c) Trofimenko, S. Scorpionates: The Coordination Chemistry of Polypyrazolylborate Ligands, Imperial College Press, London, 1999. d) C. Pettinari, Scorpionates II: Chelating Borate Ligands, Imperial College Press, London, 2008. e) Pettinari, C.; Santini, C. Comprehensive Coordination Chemistry II. *In Polypyrazolylborate and Scorpionate Ligands*. Eds.: Mc Claverty J. A.; Meyer T. J. Elsevier, Oxford, 2004, pp. 159-210.

scorpionates. The term scorpionate is a general name applied to many tridentate ligands because the coordination of the three arms resembles the tweezers of a scorpion (Figure 4.3).

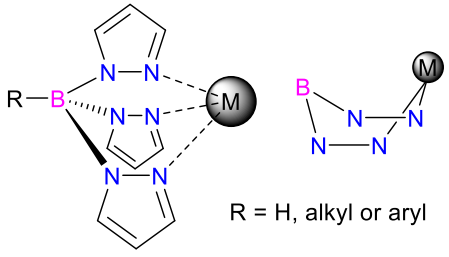

Figure 4.3. Representation of the general structure for trispyrazolylborates ligands (Tp^x).

The trispyrazolylborates are characterized by a six-member ring formed by the boron atom, two pyrazoles rings and the metal center (Figure 4.3). The third ring of pyrazole is in a pseudoaxial plane. The $6e^-$ Tp^x is a σ-N donor ligand occupying a *fac* position in complexes with a C_{3v} symmetry. Their extensive use in catalysis is derived from the large steric and electronic modifications that can be made in the pyrazole rings leading to an exhaustive control of the properties in each ligand in contrast with the limited tuning possible for the common and analogous Cp ligands (also anionic tridentate). The Tp^x where the B-H bond is substituted for a new B-R bond where R = alkyl or aryl, are the most interesting of this class of ligands but the least studied.

Some synthetic methodologies for the isolation of MTp^x were developed over the years. The initial route for the synthesis of Tp^x ligands was developed by Trofimenko and co-workers (Eq. 4.1).[177] The reaction of an alkali borohydride with an excess of pyrazole at very high temperatures afforded the correspond MTp^x where M = Li, Na, K. This synthetic route has got some limitations because it requires the use of high temperature and some pyrazole rings are not stable in these conditions.[178] Some modifications in this general synthetic method have been made over the years improving the yields and using a large variety of pyrazole rings.[179]

[177] Trofimenko, S. *Inorg. Synth.* **1970**, *12*, 99-109.
[178] Janiak, C.; Esser, L.; Teil B, *Z. Naturforsch.***1993**, *48*, 394-396.
[179] a) S. Trofimenko, *J. Am. Chem. Soc*. **1967**, *89*, 3170-3177. b) Kitamura, M.; Takenaka, Y.; Okuno, T.; Holl, R.; Wünsch, B. *Eur. J. Inorg. Chem.* **2008**, 1188-1192.

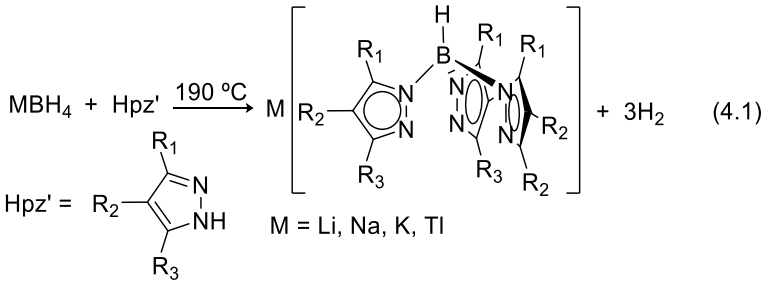

The hydrotrispyrazolylborates represented in Eq. 4.1 are the most common Tp^x ligands and fewer examples can be found in the litereature for RTp^x derivatives. There are two main routes for the synthesis of aryl-Tp^xs (Scheme 4.2, (a) and (b)).[180] $Li[B(Ph)(pz)_3]$ was prepared by a substitution reaction of the B-H bond in the starting phenylborohydride $Li[PhBH_3]$ in the presence of excess of pyrazole (Scheme 4.2, (a)).[183i] However, the main route for the synthesis of aryl-Tps^x was developed by Wagner and co-workers (Scheme 4.2, (b)).[180c]

Alkyl-Tps^x are not very common and only few synthetic procedures are available.[181] Alkyl boronic acids are starting materials for the synthesis of some RTp^xM ligands (Scheme 4.2). The initial borane $B(OMe)_3$ in the presence of a Grignard reagent generates the corresponding boronic acid *n*-$BuB(OH)_2$ that in the presence of a mixture or Napz and Hpz afforded the corresponding $Na[B(n\text{-}Bu)(pz)_3]$ with good yield (Scheme 4.2, (c)).[181a] Janiak and co-workers reported the synthesis of an Tl(alkyl-Tp^x) from the starting $MeBBr_2$ following a similar route employed for the synthesis of aryl-Tp^x (Scheme 4.2, (d)).[181b]

[180] a) Cotton, F. A.; Murillo, C. A.; Stults, B. R. *Inorg. Chim. Acta* **1977**, 22, 75-80. b) White, D. L.; Falle, J. W. *J. Am. Chem. Soc.* **1982**, *104*, 1548-1552. c) Jäkle, F.; Polborn, K.; Wagner, M. *Chem. Ber.* **1996**, *129*, 603-606. d) Biani, F. F.; Jäkle, F.; Spiegler, M.; Wagner, M.; Zanello, P. *Inorg. Chem.* **1997**, *36*, 2103-2111. e) Kisko, J. L.; Hascall, T.; Kimblin, C.; Parkin, G. *J. Chem. Soc., Dalton Trans.* **1999**, 1929-1935. f) Zhang, F.; Bolte, M.; Lerner, H. -W.; Wagner, M. *Organometallics* **2004**, *23*, 5075-5080. g) Reger, D. L.; Gardinier, J. R.; Smith, M. D.; Shahin, A. M.; Long, G. J.; Rebbouh, L.; Grandjean, F. *Inorg. Chem.* **2005**, *44*, 1852-1866. h) Reger, D. L.; Gardinier, J. R.; Gemmill, W. R.; Smith, M. D.; Shahin, A. M.; Long, G. J.; Rebbouh, L.; Grandjean, F *J. Am. Chem. Soc*. **2005**, *127*, 2303-2316. i) Graziani, O.; Hamon, P.; Thépot, J. -Y.; Toupet, L.; Szilágyi, P. A.; Molnár, G.; Bousseksou, A.; Tilset, M.; Hamon, J. -R. *Inorg. Chem.* **2006**, *45*, 5661-5674.

[181] a) Reger, D. L.; Tarquini, M. E. *Inorg. Chem.* **1982**, *21*, 840-842. b) Janiak, C.; Braun, L.; Girgsdies, F. *J. Chem. Soc., Dalton Trans.* **1999**, 3133-3136.

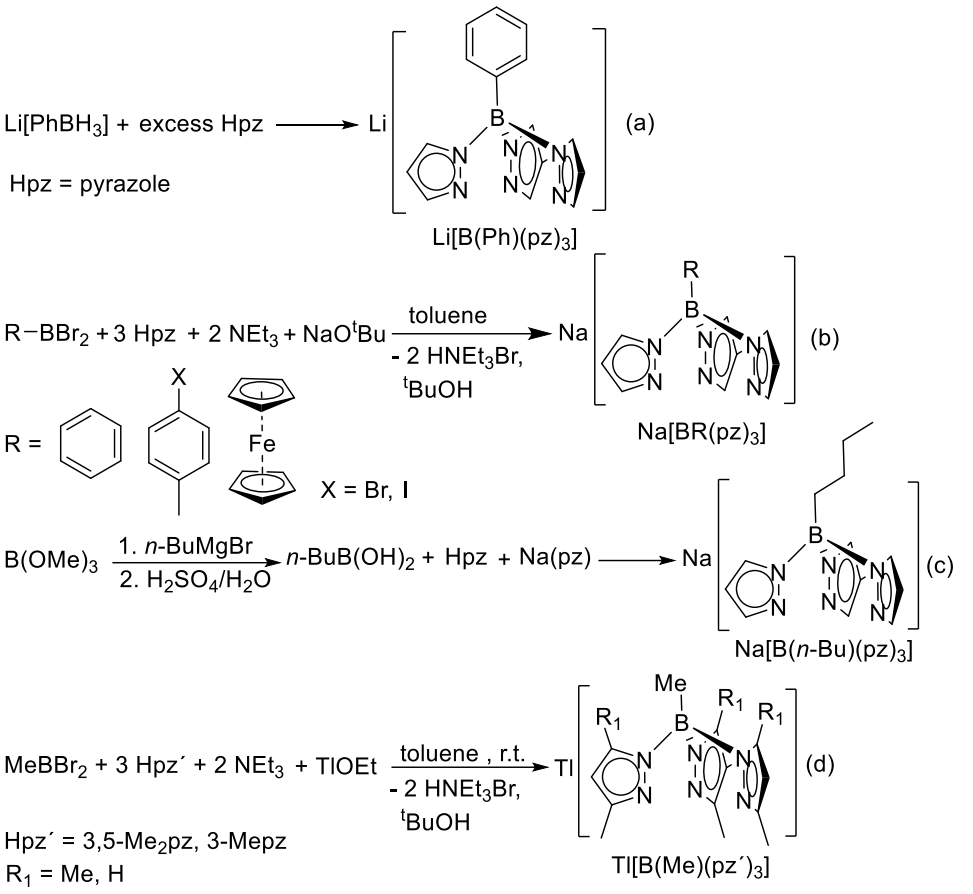

Scheme 4.2. Synthesis of some M[RTp^x] complexes starting from different boron sources.

The wide variety of Tp^x-metal complexes reported in the literature make these ligands ideal for many applications. Tp^x-metal complexes have been used in many catalytic transformations,[182] including the more challenging functionalization of unreactive C-H bonds.[183] Also, they have been used in the synthesis of model complexes that mimic the active

[182] a) Díaz-Requejo, M. M.; Pérez, P. J. *Chem. Rev*. **2008**, *108*, 3379-3394. b) Caballero, A.; Pérez, P. J.; *J. Organomet. Chem.* **2015**, *793*, 108-113. C) Caballero, A.; Díaz-Requejo, M. M.; M. R. Fructos, J. Urbano, Pérez P. J. Ligand Design in Metal Chemistry. *In Modern Applications of Trispyrazolylborate Ligands in Coinage Metal Catalysis*. Eds. Stradiotto, M.; Lundgren R. J. John Wiley & Sons, 2016, pp. 308-329.

[183] a) Caballero, A.; Díaz-Requejo, M. M.; Fructos, M. R.; Olmos, A.; Urbano, J.; Pérez, P. J. *Dalton Trans.* **2015**, *44*, 20295-20307. b) McKeown, B. A.; Lee, J. P.; Mei, J.; Cundari, T. R.; Gunnoe, T. B. *Eur. J. Inorg. Chem.* **2016**, 2296-2311.

site of some metaloenzymes,[184] and to generate materials with interesting magnetic properties.[185]

Because of their versatility, some efforts have been made to support the Tp^x ligand onto solid matrixes. This is an important goal for sustainability reasons in view that a recyclable catalyst is more efficient as far as cumulative TON is concerned and allows to decrease the extra waste resulting when the catalyst is discarded after each reaction. In the area of trispyrazolylborate-containing metal-based catalysts, very few reports have appeared regarding this issue. Some work in this area was developed by Pedro Pérez and co-workers (Figure 4.4).[186] They reported a $CuTp^x$ anchored to silica gel by classical and no classical hydrogen bonding and their application in the cyclopropanation reaction. The supported complex works with a similar activity than the homogenous counterparts for the cyclopropanation of styrene, *cis*-cyclooctene and 1-hexene but some leaching was observed after several cycles.

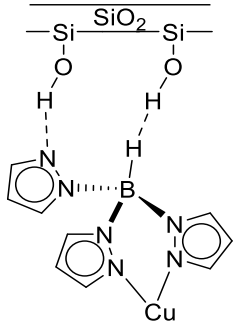

Figure 4.4. Synthesis of Cu^ITp^x anchored in a silica support.

On the other hand, the group of Ciriano, Casado and co-workers described the attachment of a trispyrazolylborate to carbosilane dendrimers.[187] The synthetic route is summarized in Scheme 4.3. The dendrimer with the borate-containing fragment **D_4** was synthesized by a hydrosilation reaction of the initial allyl borane **A_4** in the presence of the Karstedt´s catalyst and the dendrimer $Si[(CH_2)_3SiMe\{(CH_2)_3\text{-}SiMe_2H\}_2]_4$ **B_4**. The borane dendrimer **C_4** was

[184] Sallmann, M.; Limberg, C. *Acc. Chem. Res*. **2015**, *48*, 2734-2743.
[185] Hamon, P.; Thépot, J. -Y.; Le Floch, M.; Boulon, M. -E.; Cador, O.; Golhen, S.; Ouahab, L.; Fadel, L.; Saillard, J. -Y.; Hamon, J.-R *Angew. Chem. Int. Ed*. **2008**, *47*, 8687-8691.
[186] M. M. Díaz-Requejo, T. R. Belderrain, M. C. Nicasio, P. J. Pérez *Organometallics* **2000**, *19*, 285-289.
[187] Camerano, J. A.; Casado, M. A.; Ciriano, M. A.; Oro, L. A. *Dalton Trans*. **2006**, 5287-5293.

reacted with a fourfold molar amount of potassium pyrazolate and pyrazole in excess to give the dendrimer **D4** with the Tp^x moiety.

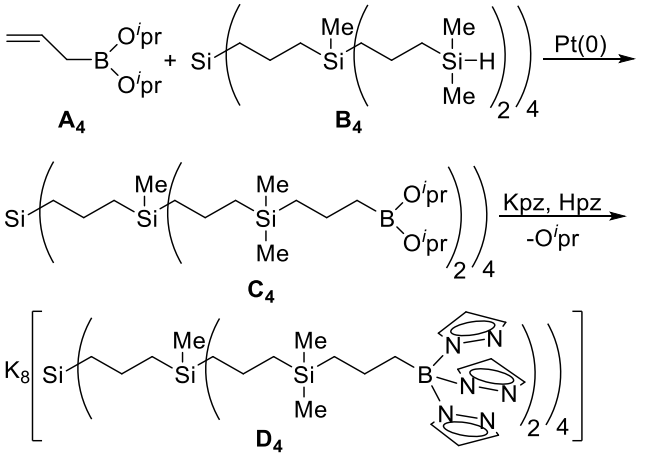

Scheme 4.3. Synthetic route for the formation of a Tp^x anchored in a dendrimer.

There are also some reports describing the attachement of Tp^x to polypeptides and other resins[188] and few examples of supported Tp^x ligands in polymers.[189-191] Scheme 4.4 shows the example reported by Jäkle and co-workers who followed the methodology developed in the homogenous media for the synthesis of aryl-Tp^xM to anchor a Tp^x in a polystyrene resin.[189a] The poly(4-trimethylsilyl)styrene **E4** was treated with BBr_3 to randomly replace the $SiMe_3$ group for BBr_2 groups (**F4**). In-situ treatment of the polymer-BBr_2 **F4** with a little excess of Me_3SiNMe_2 yields the $B(NMe_2)_2$-functionalized copolymer **G4**. The polymer containing the Tp^x fragment **H4** was synthesized adding two equivalents of Hpz and one equivalent of Napz in toluene at 100 ºC for 6 hours. A large upfield shift of the ^{11}B NMR signal to δ = 1 ppm confirms the formation the tetracoordinate borate anchored to the polymer (the ^{11}B NMR in

[188] a) Kuchta, M. C.; Gross, A.; Pinto, A.; Metzler-Nolte, N. *Inorg. Chem.* **2007**, *46*, 9400-9404. b) Desrochers, P. J.; Pearce, A. J.; Rogers, T. R.; Rodman, J. S.; *Eur. J. Inorg. Chem.* **2016**, 2465-2473. c) Desrochers, P. J.; Corken, A. L.; Tarkka, R. M.; Besel, B. M.; Mangum, E. E.; Linz, T. N. A *Inorg. Chem.* **2009**, *48*, 3535-3541.

[189] a) Qin, Y.; Cui, C.; Jäkle, F. *Macromolecules* **2008**, *41*, 2972-2974. b) Qin, Y.; Shipman, P. O.; Jäkle, F. *Macromol. Rapid Commun.* **2012**, *33*, 562-567.

[190] Shipman, P. O.; Cui, C.; Lupinska, P.; Lalancette, R. A.; Sheridan, J. B.; Jäkle, F. *ACS Macro Lett.* **2013**, *2*, 1056-1060.

[191] Desrochers, P. J.; Besel, B. M.; Corken, A. L.; Evanov, J. R.; Hamilton, A. L.; Nutt, D. L.; Tarkka, R. M. *Inorg. Chem.* **2011**, *50*, 1931-1941.

the polymer with $B(NMe)_2$ groups is at δ = 32 ppm). None of the few reported polymer-supported Tp^x derivatives were used in catalysis.

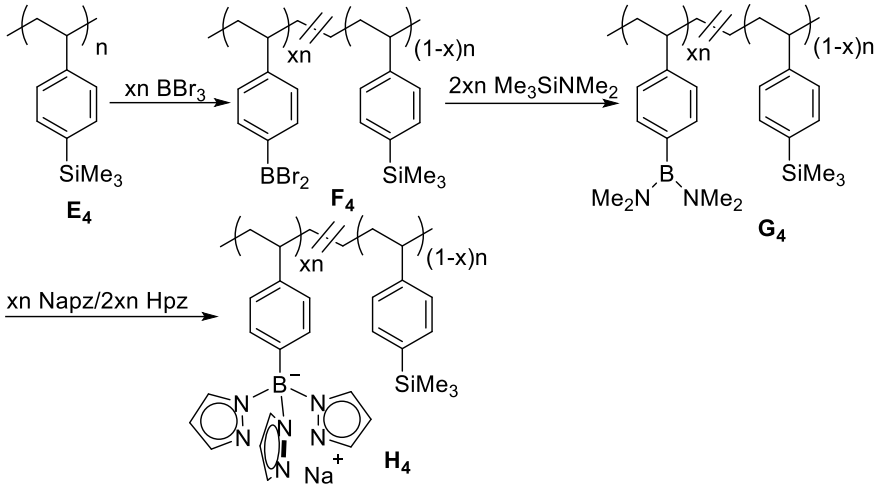

Scheme 4.4. Synthetic route for the immobilization of a $NaTp^x$ in a polystyrene.

4.1.3. Aim of the work in this chapter.

Since the robustness of the VA-PNB makes it an attractive support and no-polymer bound Tp^x has been use in catalysis, the main objective of this chapter is the design of proper methodologies to synthesize Tp-functionalized VA-polynorbornenes that can act as ligands for metal centers and show that they are useful as catalysts. To achieve that we have made use of the alkenyl-functionalized VA-PNBs we have developed as starting materials. As a catalytic test platform, we chose the VA-PNB-Tp^xCu(I) complexes and, in collaboration with the group of Prof. Pérez at the University of Huelva who have the experience on the behavior of Tp^xCu derivatives in homogenous catalytic processes, we tested their activity and recyclability.

4.2. Results and Discussion

4.2.1. Synthesis of the Tp-functionalized VA-polynorbornenes

The synthetic route developed to prepare the polymer-containing trispyrazolylborate (Tp^x) ligands involves the post-polymerization functionalization of vinylic addition polynorbornenes with pendant alkenyl groups (Eq. 4.2 and Scheme 4.5). The synthesis of the polymers **15** and **16** was carried out by a copolymerization of 5-vinyl-2-norbornene (VNB) or 5-(but-1-en-4-yl)-2-norbornene (BNB) with norbornene. Both the benzylic palladium complex [Pd(η^3-PhCHCH$_2$C$_6$F$_5$)(AsPh$_3$)$_2$](BF$_4$) (**4e**) or [Ni(C$_6$F$_5$)$_2$(SbPh$_3$)$_2$] (**27**) can be used as catalyts. However, as discussed in *Chapter 2*, the homo- and copolymers derived from BNB undergo a small but significant isomerization of the terminal double bond to an internal position when the palladium complex is used. This isomerization does not occur with the Ni complex and, in order to avoid this complication, the latter was used. The use of a copolymer is more convenient than a homopolymer since the functionalization degree of the former is lower, and therefore the reactive centers in the final supported catalyst are less concentrated. This minimizes the occurrence of possible decomposition pathways by bimolecular processes.

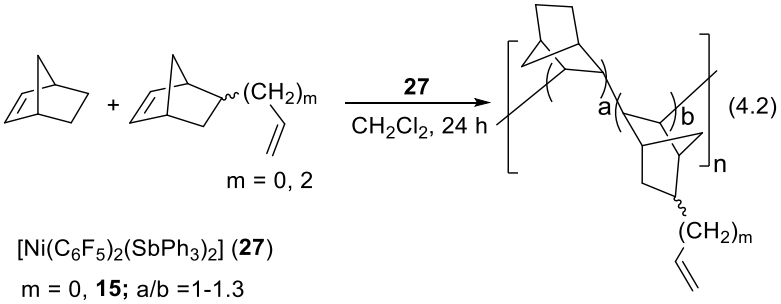

Copolymers of norbornene and VNB (m = 0, Eq. 4.2) or norbornene and BNB (m = 2, Eq. 4.2) were obtained. In both cases, the polymers were white solids with moderate yields and molecular weights in the range 35-45 x 10^3 Da and polydispersities (PDI) of ca. 2. The ^{1}H NMR spectra of the polymers assess the presence of the terminal double bond and the disappearance of the endocyclic norbornene double bond indicating the participation of the enodocylic double bond in the polymerization. Integration of the alkene vs the aliphatic resonances allows determining the composition of the copolymer (a/b ratio) and therefore the

degree of functionalization of the material (Figure 4.5). The determination was made using the ^{1}H NMR with the equation described in *Chapter 2* (a/b = {(IntA-3IntB)/10}/{IntB/3} where IntA = total integral value of the aliphatic region, IntB = total integral value of the alkene region and the numeric coefficients take into account the number of protons in norbornene and 5-vinyl-2-norbornene). So, in the polymer **15** presented in Figure 4.5 the composition is: a/b = {(21.30-3x 3.03)/10}/{3.03/3} = 1.17.

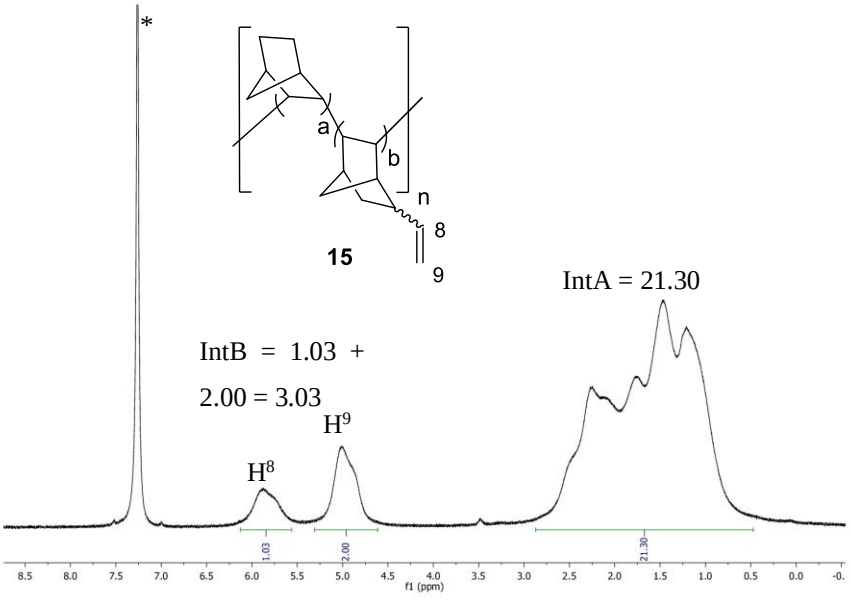

Figure 4.5. ^{1}H NMR in $CDCl_3$ of the polymer **15**. * Signal corresponding to the solvent.

As it has been observed before for the copolymerization reactions described in *Chapter 2*, the copolymers present a higher amount of norbornene (a/b >1) even when an equimolar amount of monomers were used in the feed. *Endo* and *exo* arrangements of the alkenyl substituent in the bicycle are visible in the ^{13}C NMR spectra of polymer **15** (Figure 4.6), in a ratio that does not reproduce the diastereoisomeric ratio in the starting alkenyl norbornene monomer (endo:exo = 80:20). This is expected since the minor *exo* isomer polymerizes faster than the *endo* one, leading to a more similar distribution of both isomers in the VA-PNB.[104] Nonetheless, the presence of both arrangements has no further influence in the post-polymerization functionalization reactions leading to the supported Tp^{x}. As usual, no signals around 20 ppm associated with an *endo* insertion are visible in the ^{13}C NMR (Figure 4.6) indicating a *cis*-2,3-*exo* insertion.

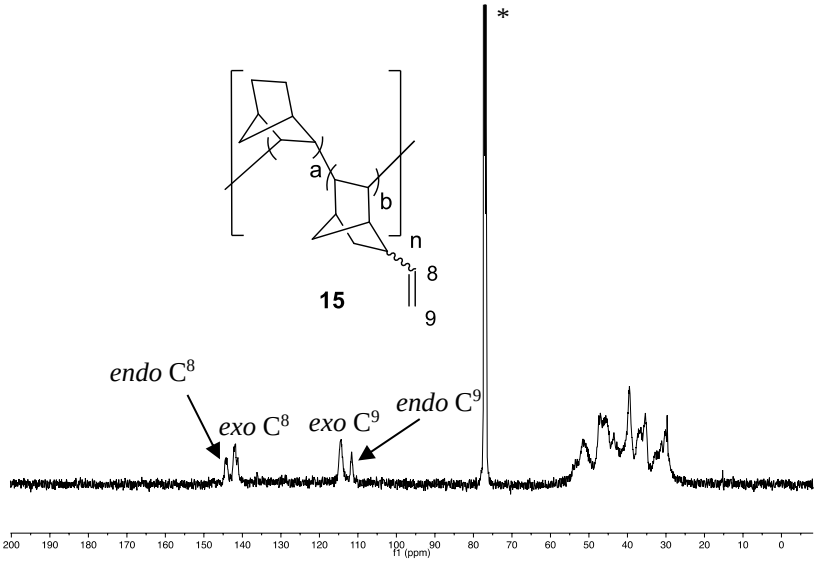

Figure 4.6. ^{13}C NMR spectra of the polymer **15** in $CDCl_3$ where it is visible the *exo* and *endo* arrangement. * Signal corresponding to the solvent

These VA-Co-PNB-VNB copolymers were used to synthesize the supported Tp^x ligands, a work carried out in collaboration with Jesús Ángel Molina de la Torre in our group. The hydroboration of the terminal double bonds of **15** with commercial $BHBr_2{\cdot}SMe_2$ leads to the polymeric alkyldibromoborane as we described for the copolymers **21** and **22** in *Chapter 2*. It was not isolated but reacted in situ with an excess of the corresponding pyrazole (Scheme 4.5). Slightly stronger reaction conditions (refluxing CH_2Cl_2 instead of room temperature) and longer reaction times were used for the bulkier 3,5-dimethyl-4-bromo pyrazole or 3-mesityl pyrazole. The subsequent addition of three equivalents of the strong base $Li(N^iPr_2)$ (LDA) induces the neutralization of the acid produced in the reaction and provides the alkali counterion. The polymer becomes insoluble upon functionalization and can be easily isolated by filtration and repeated washing with acetonitrile. Being insoluble, polymers **41**-**44** were characterized by solid state NMR. All of them showed characteristic signals of the pyrazole moieties in the ^{13}C CP-MAS spectrum as well as the typical ^{11}B resonance for tetracoordinated borates about 0-2 ppm. A specific cross linking process by formation of pyrazabole units, where two pyrazole rings are bridging two different boron atoms, could be possible but it is

disfavored by the use of an excess of pyrazole in the synthesis of polymers **41**-**44**.[192] The synthetic route proposed here is a very convenient way to access to the $RBBr_2$ fragment using a conventional organic reaction with high atomic efficiency. Furthermore, the Tp^x is attached to the polymer by a more flexible alkyl tether rather than the aryl linkage used in the few examples of polymer-containing Tp^x reported so far (Figure 4.4).

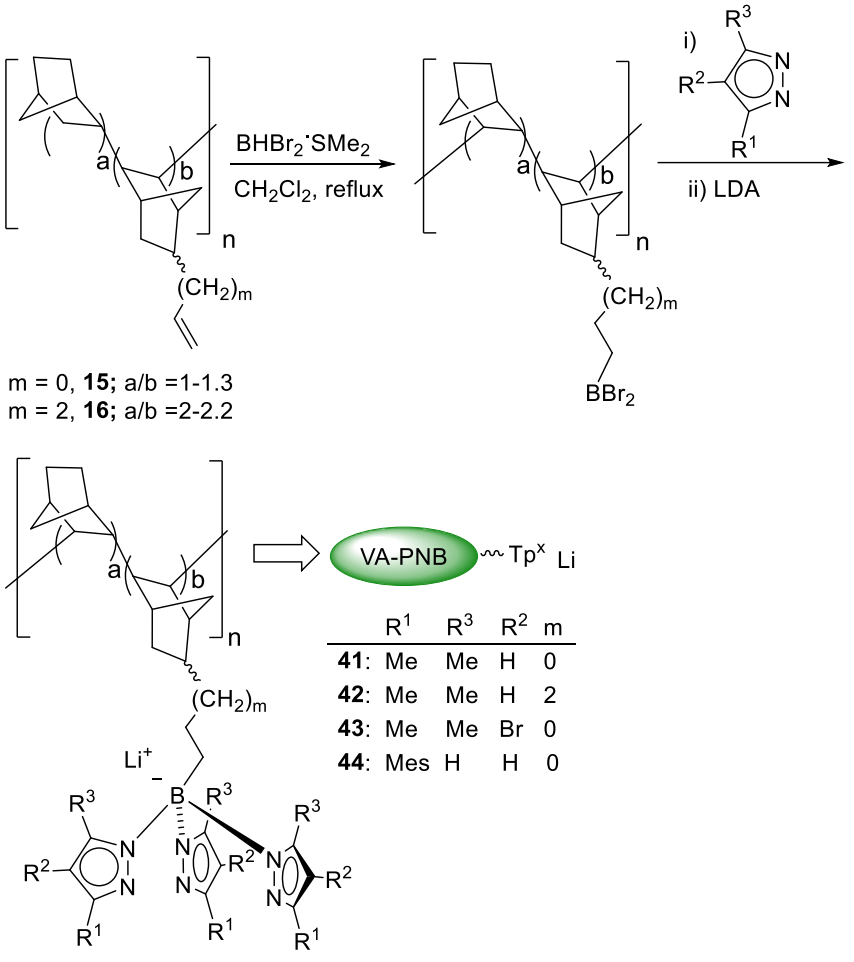

Scheme 4.5. Synthetic route developed for the synthesis of VA-PNB polymer-containing Tp^x ligands.

[192] We cannot discard the formation of pyrazabole units in this process. Spectroscopic data would not differentiate between pyrazaboles and the targeted pyrazolylborates, albeit the former would not be useful toward the formation of pyrazolyl-bonded metal complexes.

4.2.2. Synthesis of the CuTp^x VA-polynorbornenes

The formation of the supported CuTp^x complexes can be readily accomplished by addition of a solution of CuI in acetonitrile to a suspension of polymers **41**-**44** in the same solvent (Scheme 4.6). The metal loading of the polymers was determined by ICP-MS analysis of the copper content and it was found within a range of 40-90 mg Cu per gram of polymer, ensuring enough amount for its further use in catalysis. The incorporation of the copper to the polymer is quite efficient when compared to the maximum amount that can be loaded, according to the initial functionalization of the specific polymer used. For example, for an initial functionalization of the starting **15** a/b = 1.25 and complete transformation in all the synthetic steps, the maximum amount of Cu in **41-Cu** is 99.359 mg Cu/g polymer. The experimental value is 90.485 mg Cu/g polymer, i.e 91% of the maximum incorporation. The amount of copper loaded in the polymers is between 68% in the case of the bulkier ligand in **44** to 90-100% for polymers **41** and **42**. However, quantification of copper in the solid does not guarantee that it is coordinated by the N-donors of the ligand, a feature that is crucial for its catalytic behavior. The differences in the chemical shifts in the Tp^x fragment, that arise from coordination to the metal, cannot be seen in the low resolution solid state ^{13}C CP-MAS NMR spectra of these polymers. Thus, a different approach was taken based on the generation of carbonyl adducts VA-PNB-Tp^{x}Cu(CO) upon bubbling carbon monoxide through a suspension of the polymers (Scheme 4.6).

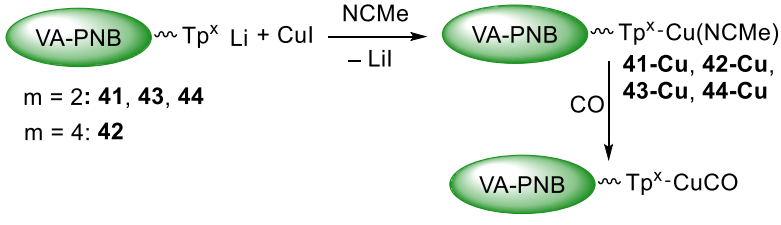

Scheme 4.6. Synthesis of Cu^{I}Tp^x-funcionalized VA-polynorbornenes.

FTIR studies on the VA-PNBTp^{x}CuCO showed bands for the stretching of the carbonyl group (ν(CO)) in a close proximity to those observed for the well-defined mononuclear complexes,[193] assessing the presence of tetracoordinated [Cu(CO)Tp^x] moieties as well as the

[193] a) Caballero, A.; Pérez, P. J. *J. Organomet. Chem.* **2015**, *793*, 108-113. b) Mairena, M. A.; Urbano, J.; Carbajo, J.; Maraver, J. J.; Álvarez, E.; Díaz-Requejo, M. M.; Pérez, P. J. *Inorg. Chem.* **2007**, *46*, 7428-7435.

corresponding [Cu(NCMe)Tp^x] in the parent Cu-containing polymers (Figure 4.7 and Table 4.1).

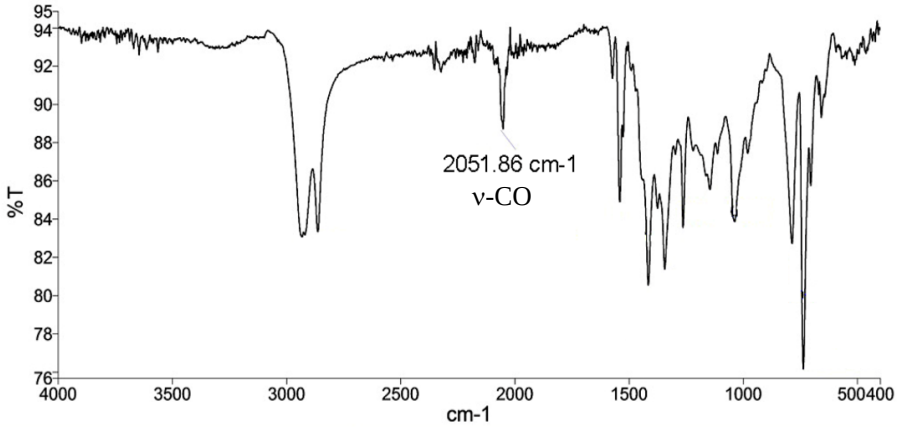

Figure 4.7. FTIR spectra of the polymer **41-Cu(CO)** where we can see the presence of the carbonyl band in a tetrahedral environment.

Table 4.1. ν-CO absorptions (cm^{-1}) for the VA-PNB supported copper complexes and their discrete analogues.

Entry	Tp^x	VA-PNB-Tp^x Cu(CO)	[CuTp^x(CO)]
1	Tp*, $R^1 = R^3$ = Me; R^2 = H	**41-Cu**(CO), 2052	2056
2	Tp*^{,Br}, $R^1 = R^3$ = Me; R^2 = Br	**43-Cu**(CO), 2066	2073
3	Tp^{Ms}, R^1 = Mes $R^2 = R^3$ = H	**44-Cu**(CO), 2089	2079

4.2.3. Application of the Tp^x-functionalized VA-polynorbornenes in some selected catalytic reactions

As we know by previous studies that the skeleton of the VA-PNBs is robust enough to be used in catalysis and it is resistant, for example, to high temperature conditions or radical processes that could compromise the performance of other types of polymeric supports.[103] Given the well-known capabilities of discrete Tp^{x}Cu(L) complexes to induce the catalytic transfer of carbene and nitrene units,[182] we have evaluated two of the new VA-PNB-Tp^{x}Cu(NCMe) in the well-known styrene cyclopropanation and aziridination reactions (Scheme 4.7 and Table

4.2). This work was carried out by the group of Prof. Pedro Pérez at the University of Huelva that has successfully developed the homogeneous catalytic systems and has long experience in these reactions. We have chosen **41-Cu** and **43-Cu** as representative examples since both of them are known to promote reactions **A** and **B**, at variance of **44-Cu**, with limited activity in nitrene transfer. Additionally, since the catalytic performance is due to the Tp^xCu core, **41-Cu** (m = 0) and **42-Cu** (m = 2) are identical from that point of view and the synthesis of **41-Cu** has the additional advantage of using a commercial monomer in the preparation of the precursor **15.**

Under standard conditions, **41-Cu** induced 90-99% yields (entries 2, 4 and 5, Table 4.2) in these three experiments, whereas the bromide-containing **43-Cu** behaved similarly for the cyclopropanation reaction but the nitrene transfer to styrene was less effective (50%, entry 3, Table 4.2). This lower yield corresponds to the formation of $TsNH_2$ as byproduct, due to the presence of adventitious water.

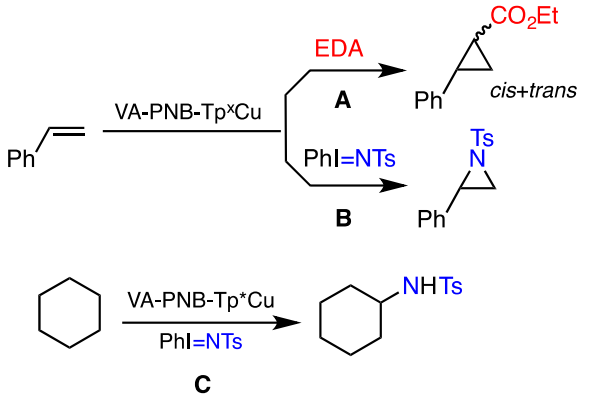

Scheme 4.7. Application of the VA-PNB-Tp^xCu in styrene cyclopropanation (reaction **A**), aziridination (reaction **B**) and amination of cyclohexane (reaction **C**).

Since these results are in line with those previously reported in the homogenous phase, the potential recycling of the heterogeneous materials was investigated with two reactions. Figure 4.8 shows the variation of the yields for the styrene cyclopropanation reaction using **41-Cu** as the catalyst, showing an excellent degree of recovery and reuse with no effect on those values up to five times. It is also worth mentioning that the *cis:trans* diastereoselectivity was maintained along those cycles. For the nitrene transfer reaction, also with **41-Cu**, recycling was performed three times (Figure 4.8), with a slight decrease of activity of ca. 10% after each

cycle in both the styrene aziridination and cyclohexane amination. This can be the result of partial degradation of the catalytic site due to the oxidant nature of the nitrene source, PhI=NTs.

Table 4.2. Catalytic activity VA-PNB-Tp^{x}Cu complexes toward the styrene cyclopropanation,[a] aziridination reactions[b] and amination of cyclohexane.[b] See Scheme 4.7 for reaction notation

Entry	Rxn	Catalyst	Yield(%)	*cis:trans*
1	A	VA-PNB-Tp*,^{Br}Cu(L)[d] (**43-Cu**)	85[a]	48:52
2	A	VA-PNB-Tp*Cu(L)[e] (**41-Cu**)	90[a]	45:55
3	B	VA-PNB-Tp*,^{Br}Cu(L) (**43-Cu**)	50[b]	---
4	B	VA-PNB-Tp*Cu(L) (**41-Cu**)	99[c]	---
5	C	VA-PNB-Tp*Cu(L) (**41-Cu**)	90[d]	---

a) [M]/[EDA]/[styrene] = 1:5:50, at room temperature; Yields and selectivity (*cis:trans*) were determined by GC (diethyl fumarate and maleate accounted until 100% of EDA). b) [M]/[PhINTs]/[styrene] = 1:5:25, at room temperature; Yields were determined by ^{1}H NMR ($TsNH_2$ accounted until 100% of PhINTs). c) [M]/[PhINTs] = 1:25 in 5 mL of cyclohexane at t = 60 ºC. Yields were determined by ^{1}H NMR ($TsNH_2$ accounted until 100% of PhINTs). d) mg Cu/g polymer = 64.96; L = NCMe. e) mg Cu/g polymer = 90.42; L = NCMe.

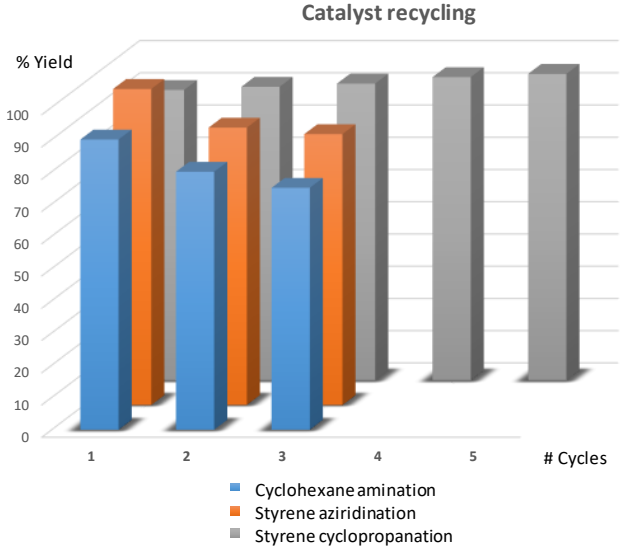

Figure 4.8. Recycling of **41-Cu** in the heterogeneous styrene cyclopropanation, aziridination reaction and cyclohexane amination.

4.3. Conclusions

We have developed a new synthetic route to anchor trispyrazolylborate ligands (Tp^x) to the skeleton of the VA-polynorbornene (VA-PNB-Tp^xLi). The route uses the hydroboration, a conventional and efficient reaction with alkenes, of the alkenyl-copolymers **15** or **16** for the introduction of the boron group in one step. The complexation of the copper is very efficient leading to VA-PNB-Tp^xCu with good yields and incorporations of copper between 40-90 mg Cu per gram of polymer. The tetrahedral environment of the Cu(I) was demonstrated by the similar stretching absortion of the CO in the VA-PNB-Tp^xCuCO complexes and the discrete Tp^xCuCO complexes.

The catalytic activity of the polymer-supported Cu(I) complexes was tested in catalytic carbene or nitrene transfer reactions by the group of Prof. Pedro Pérez at the University of Huelva showing a similar behavior than those found under homogeneous conditions. Moreover, the solids can be separated by simple filtration and reused with a high activity being maintained along the cycles.

4.4. Experimental Section

4.4.1. Materials and General considerations

The compounds $[Ni(C_6F_5)_2(SbPh_3)_2]$,[101g] 5-(but-1-en-4-yl)-2-norbornene,[128] 3,5-dimethyl,4-bromopyrazole,[194] and 3-(2,4,6-trimethylphenyl)pyrazole[195] were prepared according to the literature procedures. 5-Vinyl-2-norbornene (mixture of *exo* and *endo* isomers), 3,5-dimethylpyrazol and $BHBr_2{\cdot}SMe_2$, were purchased from Sigma-Aldrich or Acros. EDA, styrene and reagents for catalytic experiments were purchased from Sigma-Aldrich and used without previous purification. PhINTs was prepared according to the literature procedure.[196]

Solvents such as THF and CH_2Cl_2 were dried using a Solvent Purification System (SPS); acetonitrile was dried over CaH_2, distilled and deoxygenated prior to use.

NMR spectra were recorded at 293 K using Bruker AV-400 and Agilent MR-500 instruments. Chemical shifts (δ) are reported in ppm and referenced to $SiMe_4$ (^1H, ^{13}C). The solid state NMR spectra were recorded at room temperature under magic angle spinning (MAS) in a Bruker AV-400 spectrometer using a Bruker BL-4 probe with 4 mm diameter zirconia rotors spinning at 10 kHz. ^{13}C CP MAS NMR spectra were measured at 100.61 MHz and recorded with proton decoupling (tppm), with 90º pulse length of 4.5 μs and a contact time of 3 ms. Chemical shifts were calibrated indirectly through the glycine CO signal recorded at 176.0 ppm relative to $SiMe_4$. ^{11}B MAS NMR spectra were recorded at 128.38 MHz with proton decoupling, with a 90º pulse length of 7.5 μs. ^{11}B NMR chemical shifts are in ppm and were calibrated using powdered $NaBH_4$, which has a chemical shift of -42.06 ppm relative to the primary standard, liquid $BF_3{\cdot}O(C_2H_5)_2$ (where $\delta(^{11}B) = 0.00$ ppm).[197] IR spectra were recorded on neat samples using a Perkin-Elmer FT/IR SPECTRUM FRONTIER spectrophotometer with CsI + ATR diamond accessory in the range 200-4000 cm^{-1}. The catalytic reactions were monitored by GC analyses performed on Agilent Technologies model 6890N gas chromatography instrument with a FID detector using 30 m x 0.25 mm HP-5 capillary column.

Size exclusion chromatography (SEC) was carried out using a Waters SEC system on a three-column bed (Styragel 7.8x300 mm columns: $50\text{-}10^5$, $5x10^3\text{-}5x10^5$ and $2x10^3\text{-}4x10^6$ Da) and a Waters 410 differential refractometer. SEC samples were run in $CHCl_3$ at 313 K and calibrated to polystyrene standards. The copper content of the polymers was determined by ICP–MS, using Agilent 7500i equipment; the samples were dissolved in HNO_3 (65%) using an ETHOS SEL Milestone microwave oven. Each analysis is the average of two independent determinations for each sample. The maximum amount of copper in the polymers was

[194] Morgan, G. T.; Ackerman, I. *J. Chem. Soc. Trans* **1923**, *123*, 1308-1318.
[195] Rheingold, A. L.; White, C. B.; Trofimenko, S. *Inorg. Chem.* **1993**, 32, 3471-3477.
[196] Yamada, Y.; Yamamoto, T.; Okawara, M. *Chem. Lett*. **1975**, *4*, 361-362.
[197] Weiss, J. W. E.; Bryce, D. L. A *J. Phys. Chem. A* **2010**, *114*, 5119-5131.

calculated taking into account the initial functionalization of the starting polymer **44** and **43** (a/b ratio) and assuming a quantitative transformation in the reactions shown in Eq. 4.2.

4.4.2. Synthesis of polymer VA-Co-PNB-VNB (15)

In a 250 mL two-necked round-bottom flask, under nitrogen atmosphere, 5-vinyl-2-norbornene (4.373 g, 36.39 mmol) and norbornene (5.77 mL, 36.39 mmol; 6.31 M in CH_2Cl_2,) were dissolved in CH_2Cl_2 (110 mL). In another Schlenk flask $[Ni(C_6F_5)_2(SbPh_3)_2]$ (**27**) (0.8 g, 0.73 mmol) and $SbPh_3$ (0.10 g, 0.3 mmol) were dissolved in CH_2Cl_2 (20 mL). This solution was added to the mixture of monomers dropwise and allowed to react at 25 ºC for 24 hours. After this time the dark solution was poured onto MeOH (250 mL) resulting in the appearance of a grey powder. The solid was filtered and re-dissolved in CH_2Cl_2 (100 mL). Activated carbon was added and the mixture was filtered through diatomaceous earth affording a colorless solution, which was poured onto MeOH (250 mL) and stirred for 3 hours. The polymer was filtered, washed with MeOH (3 x 15 mL) and air-dried. A white solid was obtained (3.930 g, 50% yield). The integration of the alkene resonances in the ^{1}H NMR spectrum vs the aliphatic region gave a composition a/b = 1.17 (a/b = {(IntA-3IntB)/10}/{IntB/3} where IntA = total integral value of the aliphatic region and IntB = total integral value of the alkene region and the numeric coefficients take into account the number of protons in norbornene and 5-vinyl-2-norbornene). M_w (Daltons) = 43741. M_w /M_n = 2.32. IR (neat, cm^{-1}) 1635 (ν-C=C-), 992 (δ-C=C-H), 906 (δ-C=C-H). ^{1}H NMR (400.15 MHz, δ, $CDCl_3$): 6.1-5.6 (b, 1H, H^8), 5.2-4.6 (b, 2H, H^9), 2.8-0.2 (b, 19H). ^{13}C NMR (100.61 MHz, δ, $CDCl_3$): 145-143 (b, C^8 *exo*), 143-140 (b, C^8 *endo*), 116-113 (b, C^9 *endo*), 113-111 (b, C^9 *exo*), 55-45 (b, C^6, C^5, $C^{2´}$, $C^{3´}$), 44-39 (b, 4C, C^4, $C^{4´}$, C^1, $C^{1´}$), 41-39 (b, 1C, C^2), 38-34 (b, C^7, $C^{7´}$), 34-28 (b, C^6, $C^{6´}$, C^3).

This polymer can also be prepared in a larger scale starting from a seven-fold amount of monomers to obtain about 25 g of polymer (43% yield): White solid, a/b = 1.25, M_w (Daltons) = 45663. M_w /M_n = 2.34.

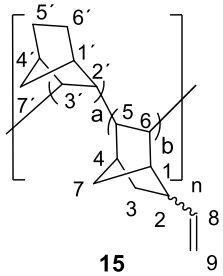

15

Polymer VA-Co-PNB-BNB (**16**) was prepared in the same way but using 5-(but-1-en-4-yl)-2-norbornene instead of 5-vinyl-2-norbornene: White solid, 32% yield a/b = 2.12, M_w (Daltons) = 34261. M_w /M_n = 1.77. ^{1}H NMR (400.15 MHz, δ, $CDCl_3$): 5.9-5.7 (b, 1H, H^8), 5.1-4.8 (b, 2H, H^9), 2.7-0.2 (b, 23H). ^{13}C NMR (100.61 MHz, δ, $CDCl_3$): 139 (b, C^{10}), 114 (b,

C^{11}), 55-45 (b, C^6, C^5, $C^{3'}$, $C^{2'}$), 44-39 (b, C^4, $C^{4'}$, C^1, $C^{1'}$,), 41-39 (b, C^2), 38-28 (b, C^9, C^8, C^7, $C^{7'}$,$C^{6'}$,C^5,C^3). IR (neat, cm^{-1}) 1639 (ν-C=C), 991 (δ-C=C-H), 908 (δ-C=C-H).

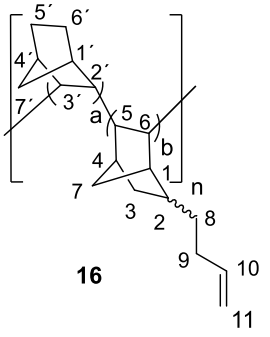

16

4.4.3. Synthesis of polymer VA-Co-PNB-NB(CH₂)₂(B(pzMe2)₃Li) (41)

Polymer VA-Co-PNB-VNB (5 g, 21.02 mmol of -CH=CH2; a/b = 1.25,) was dissolved in CH_2Cl_2 (350 mL) under nitrogen.[198] Dibromoborane-dimethyl sulfide adduct (21 mL, 21 mmol; 1.0 M solution in CH_2Cl_2) was added dropwise and the mixture was stirred for 5 hours at reflux. The reaction was then cooled to room temperature and 3,5-dimethylpyrazole (8.083 g, 81.08 mmol) was added. After stirring for 16 hours at room temperature the reaction was cooled to -78 ºC. A freshly prepared solution of lithium diisopropylamide (63.06 mmol), by mixing Li^nBu (1.6 M solution in hexanes, 39.4 mL, 63.04 mmol) and NH^iPr_2 (9 mL, 63.03 mmol) in THF (50 mL) at -78 ºC, was added dropwise. The mixture was stirred overnight while the suspension slowly warmed to room temperature. Volatiles were then removed under vacuum and the residue was thoroughly washed with CH_3CN (6 x 50 mL). The solid was filtered under a nitrogen atmosphere, washed with CH_3CN (6 x 30 mL) and dried under vacuum. The product was obtained as an orange solid (10.62 g, 93% yield). ^{13}C CP-MAS NMR (100.61 MHz): 155-140 (b, C^1, C^3), 113-102 (b, C^2), 72-20 (b, C^7, C^6, polyNB), 20-10 (b, C^4, C^5). ^{11}B MAS NMR (128.38 MHz): 0.9 (b). IR (neat, cm^{-1}): 1541, 1415, 1344, 1165, 1034, 781.

[198] The alkene content of the polymer **15** (z = mmol $CH=CH_2$/g) and the polymer composition given as a ratio of monomers incorporated (a/b = NB/NB-$CH=CH_2$) are related by the equation: z = 1000/(94.16(x/y)+120.194), where 94.16 and 120.194 are the molecular weights of norbornene and 5-vinyl-2-norbornene respectively.

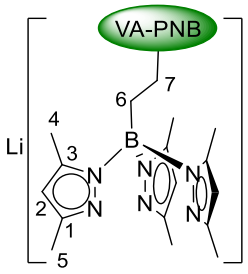

4.4.3.1. Synthesis of polymer VA-Co-PNB-NB(CH$_2$)$_4$(B(pz^{Me2})$_3$Li) (42)

The same procedure described for VA-PNB-VNB(B(pz^{Me2})$_3$Li) was used in this case, but using polymer VA-Co-PNB-BNB (a/b = 2.12, 2.87 mmol of -CH=CH$_2$/g pol). Yield 95%. ^{13}C CP-MAS NMR (100.61 MHz): 155-145 (b, C^3, C^1), 112-105 (b, C^2), 65-20 (b, C^8, C^9, C^7, C6, polyNB), 19-10 (b, C^5, C^4). ^{11}B MAS NMR (128.38 MHz): -0.5 (b). IR (neat, cm^{-1}): 1539, 1416, 1344, 1166, 1034, 774, 646, 452.

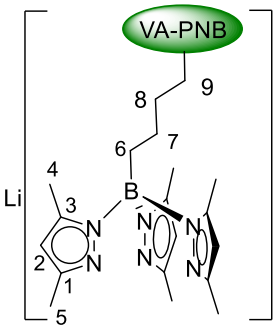

4.4.3.2. Synthesis of polymer VA-Co-PNB-NB(CH$_2$)$_2$(B(pzBr^{Me2})$_3$Li) (43)

VA-Co-PNB-VNB (5 g, 21.02 mmol of -CH=CH2, a/b = 1.25) was dissolved in CH_2Cl_2 (350 mL) under nitrogen. Dibromoborane-dimethyl sulfide adduct (21 mL, 21 mmol; 1.0 M solution in CH_2Cl_2,) was added dropwise and the mixture was stirred for 5 hours at reflux. The reaction was then cooled to room temperature and 3,5-dimethyl, 4-bromopyrazole (18.4 g, 105.1 mmol) was added. After stirring for 48 hours at reflux the yellowish reaction mixture was cooled to -78 ºC. A freshly prepared solution of lithium diisopropylamide (63.04 mmol), by mixing Li^{n}Bu (39.4 mL, 63.04 mmol;1.6 M solution in hexanes) and NH^{i}Pr$_2$ (9 mL, 63.2 mmol) in THF (50 mL) at -78 ºC, was added dropwise. The mixture was stirred overnight while the suspension slowly warmed to room temperature. Volatiles were then removed under vacuum and the residue was thoroughly washed with CH_3CN (6 x 50 mL). The solid was filtered under a nitrogen atmosphere, washed with CH_3CN (6 x 30 mL) and dried under vacuum. The product was obtained as a light brown solid (15.69 g, 96% yield). ^{13}C CP-MAS NMR (100.61 MHz): 153-142 (b, C^3, C^1), 101-94 (b, C^2), 70-18 (b, C^7, C^6, polyNB), 18-9 (b,

C^5, C^4). ^{11}B MAS NMR (128.38 MHz): 2.1 (br). IR (neat, cm^{-1}): 1526, 1416, 1339, 1160, 1082, 1036, 836, 760, 508.

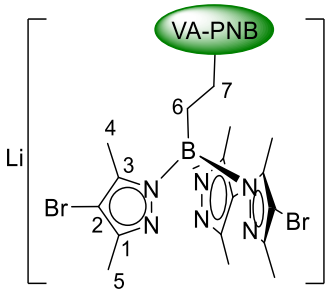

4.4.3.3. Synthesis of polymer VA-Co-PNB-NB(CH_2)$_2$(B(pz^{Mes})$_3$Li) (44)

Polymer VA-Co-PNB-VNB (0.3 g, 1.31 mmol of -CH=CH_2, a/b = 1.15) was dissolved in CH_2Cl_2 (30 mL) under nitrogen. Dibromoborane-dimethyl sulfide adducts (1.3 mL, 1.3 mmol; 1.0 M solution in CH_2Cl_2) was added dropwise and the mixture was stirred for 5 hours at reflux. The reaction was then cooled to room temperature and 3-(2,4,6-trimethylphenyl)-pyrazole (0.976 g, 5.24 mmol) was added. After stirring for 40 hours at reflux the yellowish reaction mixture was cooled to -78 ºC. A freshly prepared solution of lithium diisopropylamide (3.93 mmol), by mixing Li^{n}Bu (2.46 mL, 3.93 mmol;1.6 M solution in hexanes,) and NH^{i}Pr$_2$ (0.56 mL, 3.93 mmol) in THF (7 mL) at -78 ºC, was added dropwise. The mixture was stirred for 30 min at -78 ºC and 90 min at room temperature. Volatiles were then removed under vacuum and the residue was triturated with CH_3CN (20 mL). The solid was filtered under a nitrogen atmosphere, washed with CH_3CN (5 x 10 mL) and dried under vacuum. The product was obtained as a light brown solid (0.7025 g, 67% yield). ^{13}C CP-MAS NMR (100.61 MHz): 154-148 (b, C^1), 145-136 (b, C^7, C^9,C^5, C^3), 136-132 (b, C^4), 132-124 (b, C^8, C^6), 112-100 (b, C^2), 65-25 (b, C^{14}, C^{13}, polyNB), 25-17 (b, C^{12}, C^{11},C^{10},). ^{11}B MAS NMR (128.38 MHz): 3 (b). IR (neat, cm^{-1}): 1449, 1100, 849, 770, 441.

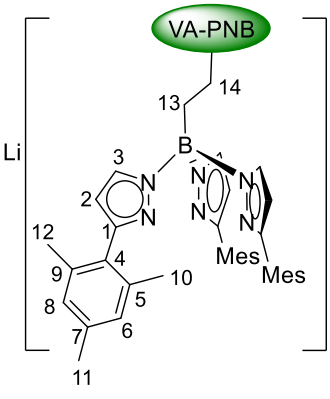

4.4.4. Synthesis of polymer VA-Co-PNB-$(CH_2)_2$(B(pz^{Me2})$_3$Cu(NCMe)) (41-Cu)

To VA-PNB-NB$(CH_2)_2$B(pz^{Me2})$_3$Li (10.2 g, 18.9 mmol) suspended in CH_3CN (40 mL) was added a solution of CuI (3.6 g, 18.9 mmol) in CH_3CN (120 mL). The mixture was stirred at room temperature for 3 hours. The solid was filtered under a nitrogen atmosphere, washed with CH_3CN (6 x 50 mL) and dried in vacuo (11.7 g, 97% yield). ICP-MS Cu: 90.485 mg Cu/g polymer; calculated maximum amount (for the initial functionalization of **15** a/b = 1.25 and complete transformation in previous steps): 99.359 mg Cu/g polymer. ^{13}C CP-MAS NMR (100.61 MHz): 153-141 (b, C^3, C^1), 114-100 (b, C^2), 60-19 (b, C^7, C^6, polyNB), 19-9 (b, C^5, C^4), 3 (NCMe).[199] ^{11}B MAS NMR (128.38 MHz): -1.5 (b). All the polymers with the -Cu(NCMe) fragment were synthesized following the same procedure.

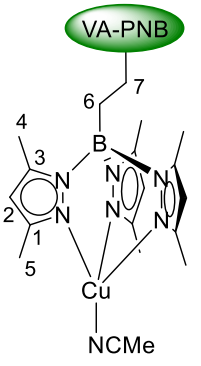

4.4.4.1. VA-Co-PNB-NB$(CH_2)_2$B(pz^{BrMe2})$_3$Cu(NCMe) (43-Cu)

96% yield. ICP-MS Cu: 65.007 mg Cu/g; calculated maximum amount (for the initial functionalization of **15** a/b = 1.25): 72.521 mg Cu/g polymer. ^{13}C CP-MAS NMR (100.61 MHz): 153-141 (b, C^3, C^1), 101-95 (b, C^2), 60-20 (b, C^7, C^6, polyNB), 19-8 (b, C^5, C^4), 2.9 (NCMe). ^{11}B MAS NMR (128.38 MHz): -1.1 (b).

[199] Acetonitrile is visible in the spectrum but due to the expected small chemical shift difference, it is not possible to tell if it is coordinated to the metal or it is free solvent embedded in the polymer.

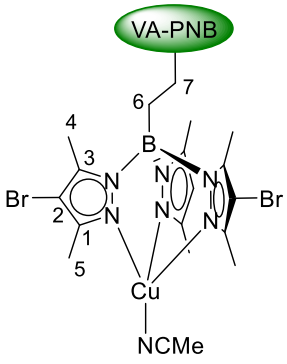

4.4.4.2. VA-Co-PNB-$(CH_2)_2$(B(pz^{Mes})$_3$Cu(NCMe)) (44-Cu)

97% yield. ICP-MS Cu: 48.032 mg Cu/g polymer; calculated maximum amount (for the initial functionalization of **15** a/b = 1.15): 70.545 mg Cu/g polymer. ^{13}C CP-MAS NMR (100.61 MHz): 157-153 (br, C^1), 146-136 (b, C^9, C^7, C^5, C^4, C^3), 134-126 (b, C^8, C^6), 117 (b, N*C*Me), 110-106 (b, C^2), 65-25 (b, C^{14}, C^{13}, polyNB), 25-18 (b, C^{12}, C^{11}, C^{10}), 3.2 (NC*Me*). ^{11}B MAS NMR (128.38 MHz): -2.6 (b).

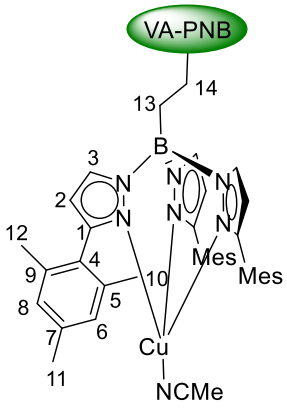

4.4.4.3. VA-Co-PNB-NB$(CH_2)_4$B(pz^{Me2})$_3$Cu(NCMe) (42-Cu)

95% yield. ICP-MS Cu: 85.083 mg Cu/g; calculated maximum amount (for the initial functionalization of **15** a/b = 2.12): 84.766 mg Cu/g polymer. ^{13}C CP-MAS NMR (100.61 MHz): 154-144 (b, C^3, C^1), 119 (b, N*C*Me), 112-106 (b, C^2), 63-20 (b, C^9, C^8, C^6, C^7, polyNB), 19-9 (b, C^5C^4,), 2.9 (NCMe).

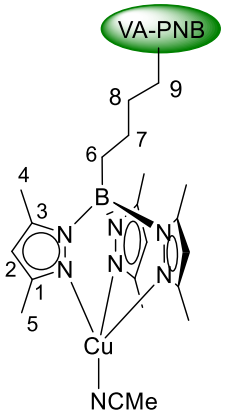

4.4.5. Synthesis of polymer VA-Co-PNB-NB(CH₂)₂B(pz^{Me2})₃Cu(CO)

A small amount of polymer VA-PNB-NBCH$_2$CH$_2$B(pz^{Me2})$_3$Cu(NCMe) and CH_2Cl_2 (5 mL) were placed in a Schlenk tube. CO was bubbled through the suspension for 2 hours at room temperature. The polymer was filtered and dried with a small flow of CO. IR (Neat): 2051 cm^{-1}(ν-CO).

All the polymers with the -Cu(CO) fragment were synthesized following the same procedure.

VA-Co-PNB-NB(CH$_2$)$_2$B(pz^{Mes})$_3$Cu(CO): IR (Neat): 2087 cm^{-1} (ν-CO)

VA-Co-PNB-NB(CH$_2$)$_2$B(pz^{BrMe2})$_3$Cu(CO): IR (Neat): 2066 cm^{-1} (ν -CO).

VA-Co-PNB-NB(CH$_2$)4B(pz^{Me2})$_3$Cu(CO): IR (Neat): 2052 cm^{-1} (ν-CO).

4.4.6. Catalytic reactions employing the VA-Co-PNB-(CH₂)₂(B(pz^{R2})₃Cu(NCMe)) complexes (41-Cu R = Me; 43-Cu R = Me, Br)

4.4.6.1. Catalytic cyclopropanation reaction

Dry and deoxygenated CH_2Cl_2 (5 mL) was added to a Schlenk flask containing VA-PNB-TpxCu(NCMe) (70 mg, ca. 0.1 mmol of Cu in **41-Cu** or **43-Cu**) and 5 mmol of styrene (50 equiv). A solution of EDA (0.5 mmol) in CH_2Cl_2 (5 mL) was slowly added for 12 h with the aid of a syringe pump, at room temperature. The mixture was then filtered, the solid washed with CH_2Cl_2 (2 x 5 mL), dried under vacuum and loaded again with solvent and reactants. The filtrate from the reaction mixture was analyzed by GC, identifying exclusively the product derived from styrene cyclopropanation and some diethyl fumarate and maleate from the formal dimerization of the CHCO$_2$Et units from EDA. The filtrate was taken to dryness and the residue was dissolved in $CDCl_3$. The ^{1}H NMR spectrum verified the results of the GC studies.

4.4.6.2. Catalytic aziridination reaction

Dry and deoxygenated CH_2Cl_2 (5 mL) was added to a Schlenk flask containing VA-PNB-TpxCu(NCMe) (70 mg, ca. 0.1 mmol of Cu in **41-Cu** or **43-Cu**). Styrene (2.5 mmol, 25 equiv.) and PhINTs were introduced in one portion (0.5 mmol), and the mixture was stirred for 12 h at room temperature. The mixture was then filtered, the solid washed with CH_2Cl_2 (2 x 5 mL), dried under vacuum and loaded again with solvent and reactants. Volatiles from the filtrated were removed under vacuum, the resulting aziridine and $TsNH_2$ (from the reaction of PhINTs with adventitious water) were identified by ^{1}H NMR spectroscopy of the reaction crude in $CDCl_3$.

4.4.6.3. Catalytic amination of cyclohexane

Dry and deoxygenated cyclohexane (5 mL) was added to an ampule containing VA-PNB-TpxCu(NCMe) (70 mg, ca. 0.1 mmol of Cu in **41-Cu** or **43-Cu**) and PhINTs (0.5 mmol). The mixture was stirred for 12 h at 60 ºC. After this, the mixture was filtered, the solid washed with CH_2Cl_2 (2 x 5 mL), dried under vacuum and loaded again with solvent and reactants. Volatiles from the filtrated were removed under vacuum, and the N-cyclohexyl-4-methylbenzenesulfonamide and $TsNH_2$ (from the reaction of PhINTs with adventitious water) were identified by ^{1}H NMR spectroscopy of the reaction crude in $CDCl_3$.

General Conclusions

We have characterized several η^3-benzylic complexes of palladium(II) bearing an α-(pentafluorophenylmethyl)benzylic substituent with different ligands. The *anti* or *syn* isomer present in solution was distinguished by NMR ROESY experiments showing the presence of the *syn* isomer in complexes **1** and **4b** and the *anti* isomer in complexes **4d-f**. DFT calculations were performed to support our experimental evidence showing the preference for the *anti* isomer in the complex **4d**. A steric relief by pentacoordination is proposed for the neutral η^3-benzylic complexes **6d-f** generated in situ mixing **1** and two equivalents per palladium of $AsPh_3$, PPh_3 and dppf. The experimental evidence was corroborated with some DFT calculations confirming the higher stability of two pentacoordinated square pyramidal geometries (**6d**-spy-apiBr and the **6d**-spy-apiPPh_3) than the σ-benzylic form.

All the η^3-benzylic complexes decompose eventually by β-hydrogen elimination to give **2** and a``$PdHL_n$´ intermediate. This hydride intermediate can be transferred to a palladium-benzyl complex to give the reduction product **3**. On the other hand, the ``$PdHL_n$´ intermediate can be trapped in the presence of dienes such as R-(+)-limonene to give the corresponding allyls **7** and **8**. A special decomposition pathway was found for the complex **4d** with the formation of the palladium cluster $[Pd_3(PPh_3)_4](BF_4)_2$ (**9**).

We have tested the η^3 benzylic complexes of palladium(II) in the vinylic addition (VA) polymerization of norbornene and norbornene derivatives. The catalyst showing the best results for the synthesis of VA-PNB is [Pd(η^3-$CHPhCH_2Pf$)($AsPh_3$)$_2$](BF_4) (**4e**), a cationic complex with labile ligands. It shows low activity in the VA-homopolymerization of alkenyl-norbornenes, but it is efficient in the copolymerization of alkenyl norbornenes with norbornene generating copolymers with good yields. A highly active catalyst for the vinylic addition polymerization of VNB was developed by the combination of the dimer η^3-benzylic complex **1**, PCy_3 and the crucial counteranion BAr_4^{f-}. The homopolymerization of 5-vinyl-2-norbornene (VNB) can be quantitatively carried out using a molar amount of Pd as low as 0.01 mol% (10 ppm).

The study of the initiation step with the catalyst **4e** showed a preferential insertion of the norbornene or the VNB into the Pd-$CHPhCH_2C_6F_5$ bond. In contrast, in the VA-polymerization of VNB with the precatalyst system **1**/PCy_3/$NaBAr_4^f$ the initiation step occurs exclusively by the insertion of the monomer into a Pd-H bond generated in situ by β-hydrogen

elimination. The copolymers VA-Co-PNB-VNB (**15**) and VA-Co-PNB-BNB (**16**) are excellent starting materials for the incorporation of functional groups by functionalization post-polymerization of their alkenyl pendant groups employing well-known reactions such as the hydroboration and the hydrosilylation.

A new type of polynorbornene skeleton VA/RO-PNB has been found by combination of two different processes with the same catalyst: the vinylic addition polymerization (VA) and the ring opening of the norbornene by a β-C elimination (RO). The structures of these VA/RO-PNBs are consistent with the presence of two different units in the skeleton: bicylic norbornenyl structures, as a results of the vinylic addition of norbornenes (NB_{VA}), and cyclohexenylmethyl groups formed by internal ring opening of the norbornene by β-C elimination. The formation of VA/RO-polynorbornenes can be achieved by tunning different factors in order to decrease the propagation rate of the polymerization while still ensuring the growth of the polymer chain.

Among the catalysts $[Ni(C_6F_5)_2L_2]$ where L = PPh_3 (**29**), $AsPh_3$ (**28**) and $SbPh_3$ (**27**), complex **28** is the most convenient one to give a VA/RO-PNB. The reaction conditions can be changed to control the number of ring-opened NB units in the polymer using complex **28**: An increase of the number of NB_{RO} units can be induced by lowering the initial monomer concentration or the NB:Ni ratio. A combination of complex $[Ni(C_6F_5)_2(AsPh_3)_2]$ (**28**) with controlled amounts of coordinating solvents is a useful catalytic system for the synthesis of VA/RO-PNBs. The coordination ability of the solvents is directly correlated with the amount of ring opening units in the skeleton of VA/RO-PNB following the trend: MeCN > DMA > PhCOMe > MeCOMe.

We also discovered a new type of cationic complexes of niquel(II) bearing quelate ligands $[Ni(o\text{-}CF_3\text{-}C_6H_4)(MeCOCH_2C(XR)Me_2)(PPh_3)]$ (XR = OH, **34**; OMe, **37**; or SMe, **38**) with a direct application in the formation of the skeleton VA/RO-PNB. The coordination ability of this ligand is crucial for the formation of the NB_{RO} units and whereas only dimers are generated with the SMe ligand, VA/RO-PNBs are obtained for the O,O-donors and a higher amount of NB_{RO} structures were found with the OR = OMe ligand than with the OR = OH one. The termination of the polymerization is clear in this type of catalytic system and it is happening by a β-hydrogen elimination after the β-γ-C-C cleavage of the norbornene in a maximum of 25% of the ring opening events. It is interesting to note that the chain termination

by β-hydrogen elimination is more important in the VA/RO-PNBs obtained with complexes **34** and **37** than with $[Ni(C_6F_5)_2(AsPh_3)_2]$ (**28**)/co-solvent.

Finally, we have developed a new synthetic route to anchor the trispyrazolylborate (Tp^xLi) to the skeleton of the VA-polynorbornene (VA-PNB-Tp^xLi), by functionalization of the alkenyl-copolymers **15** or **16**. The complexation of the copper to the VA-PNB-Tp^xLi affords the polymeric VA-PNB-$Tp^xCu(NCMe)$ with good yields and incorporations of copper between 40-90 mg Cu per gram of polymer. The coordination environment of the Cu(I) was checked by comparison of the CO IR absorption in VA-PNB-Tp^xCuCO with the discrete Tp^xCuCO complexes. The catalytic activity of VA-PNB-$Tp^xCu(NCMe)$ was tested in the group of Prof. Pedro Pérez at the University of Huelva showing a similar behavior than those found in homogeneous conditions. Moreover, the polymeric catalysts can be recycled.

Resumen

Resumen En Español

Prefacio

La polimerización vinílica de norborneno produce un tipo de polímero (VA-PNB) donde la estructura del biciclo se mantiene intacta y presenta un esqueleto completamente alifático. Presentan propiedades interesantes que los hace ideales para algunas aplicaciones como materiales o para aplicaciones en el ámbito de la catálisis heterogénea. Nuestro grupo ha contribuido con anterioridad a la síntesis de VA-PNBs funcionalizados y a su uso en catálisis. Esta tesis recoge los resultados obtenidos en la polimerización-VA de alquenil norbornenos generando esqueletos polímericos con dobles enlaces colgantes que son grupos de partida para la introducción de otros grupos funcionales. Los complejos metálicos más representativos como catalizadores para la síntesis de este tipo de polímeros son complejos de la derecha de las series de transición y en concreto, Ni(II) y Pd(II). Entre los catalizadores más utilizados, son especialmente interesantes aquellos que presentan un enlace M-R donde R = alilo, arilo, alquilo o H que pueden iniciar la polimerización sin presencia de un co-catalizador. En esta tesis se han empleado dos tipos de complejos que presentan enlace un M-R para la síntesis y estudios mecanísticos de la polimerización por adicción vinílica de norborneno y sus derivados. El objetivo es no solo desarrollar nuevos catalizadores si no también entender algunas características del mecanismo no descritas con anterioridad.

i) Complejos η^3-bencílicos de paladio(II): Los complejos η^3-bencílicos de paladio(II) pueden ser considerados como alquilos estabilizados debido a la formación de una interacción π a

expensas de la aromaticidad del anillo. Estos complejos presentan una química muy rica y casi no han sido utilizados en la polimerización por adicción vinílica de norborneno. Por ello, en el *Capítulo 1* se han sintetizado una amplia variedad de η^3 complejos bencílicos de paladio(II) sustituidos en alfa con un grupo pentafluorofenilmetilo y se ha estudiado su comportamiento en disolución. En el *Capítulo 2*, estos complejos han sido empleados en reacciones de polimerización por adición vinílica de norborneno y alquenil norbornenos. Algunos de ellos presentan una excelente actividad y un comportamiento interesante en la etapa de iniciación de la polimerización.

ii) Complejos arilo de niquel(II): En el *Capítulo 3*, se describe la formación de un nuevo esqueleto de polinorborneno no descrito con anterioridad que combina la adicción vinílica (VA) con la apertura del anillo por medio de un proceso de β-C eliminación (RO). Este tipo de esqueleto nuevo se ha estudiado con dos grupos de complejos de Ni(II) distintos. En primer lugar, los complejos $[Ni(C_6F_5)_2L_2]$ donde L = PPh_3, $AsPh_3$ o $SbPh_3$ en combinación con disolventes coordinantes. En segundo lugar, una nueva clase de complejos catiónicos de Ni(II) que poseen un grupo arilo, una fosfina y un ligando quelato ($[Ni(Aril)(MeCOCH_2C(XR)Me_2)(PPh_3)](BF_4)$ donde Aril = *o*-CF_3-C_6H_4 o *o*-CH_3-C_6H_4; y XR = OH, OMe o SMe). Los estudios realizados revelan los factores determinantes en la apertura del anillo de norborneno (RO) mediante eliminación de β-C. La incorporación de las unidades por apertura del anillo al esqueleto del polímero no tiene precedentes.

Finalmente, se han empleado los polímeros con grupos alquenilo descritos en esta tesis para el soporte de complejos trispirazolilborato de cobre(I) mediante una ruta sintética que incluye una reacción de hidroboración. Estos complejos fueron empleados como catalizadores heterogéneos en reacciones transferencia de los grupos nitreno o carbeno. Este método permite hacer este tipo de reacciones más sostenibles, combinando el uso de un metal no muy tóxico como el cobre y las ventajas de la catálisis heterogénea.

Los cuatro capítulos que se presentan en esta tesis están subdivididos en cuatro secciones: Introducción, Resultados y Discusión, Conclusiones y Parte Experimental. Se incluye además un apéndice con un listado de las abreviaturas usadas y un índice con los compuestos descritos, numerados por orden de aparición. Esta tesis se presenta para la obtención del Doctorado Internacional. Como parte de la formación del doctorando se ha decidido escribirla en inglés. De acuerdo con la regulación vigente en la UVa, se incorpora un breve resumen de los

resultados en español con su propia bibliografía, así como un prefacio y unas conclusiones generales.

Resumen de los Resultados

Capítulo 1: Síntesis, Caracterización y Comportamiento en Disolución de Complejos α-Pentafluorofenilmetil Bencílicos de Paladio(II): Precursores de Hidruros de Paladio

Los complejos bencílicos son una clase de complejos que presentan ciertas similitudes con los complejos alilo. A diferencia de estos, el paso a la forma σ-bencilo es fácil y se pueden considerar como alquilos estabilizados. Esto se debe a que en su forma η^3 se pierde la aromaticidad del anillo lo que implica un coste adicional de energía que no está presente en los alilos (Ecuación I).

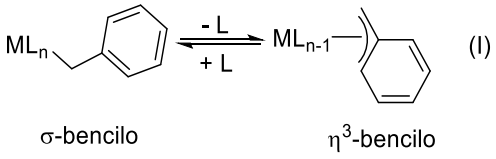

A lo largo de los años se han sintetizado una amplia variedad de complejos de este tipo con distintos metales de transición,[I] pero los complejos bencílicos de paladio(II) tienen especial interés por ser intermedios en reacciones catalizadas por este metal de derivados bencílicos halogenados o con derivados de estireno.[II] En nuestro grupo de investigación se han estudiado con anterioridad algunos complejos bencílicos de paladio(II) (Esquema I).[III] El *Capítulo 1* se ha centrado en el estudio y síntesis de derivados catiónicos η^3-bencílicos de paladio(II) por reacción del complejo dímero **1** en presencia de la cantidad apropiada de ligando y $AgBF_4$ (**4**, Esquema I).

[I] Trost, B. M.; Czabaniuk, L. C. *Angew. Chem., Int. Ed*. **2014**, *53*, 2826-2851.
[II] a) Legros, J. -Y.; Fiaud, J. -C. *Tetrahedron Lett.* **1992**, *33*, 2509-2510. b) LaPointe, A. M.; Rix, F. C.; Brookhart, M. *J. Am. Chem. Soc.* **1997**, *119*, 906-917. c) Legros, J.-Y.; Primault, G.; Toffano, M.; Riviere, M.-A.; Fiaud, J.-C. *Org. Lett.* **2000**, *2*, 433-436. d) Urkalan, K. B.; Sigman, M. S. Angew. Chem. Int. Ed. 2009, 48, 3146-3149. Suzuki-Miyaura *Org. Lett.* **2008**, *10*, 973-976. e) Shimizu, M.; Tomioka, Y.; Nagao, I.; Hiyama, T. *Synlett* **2009**, 3147-3150.
[III] a) Albéniz, A. C.; Espinet, P.; Lin, Y. -S. Alkyls *Organometallics*, **1997**, *16*, 4030-4032. b) Martín-Ruiz, B.; Pérez-Ortega, I.; Albéniz, A. C. *Organometallics* **2018**, *37*, 1074-1085.

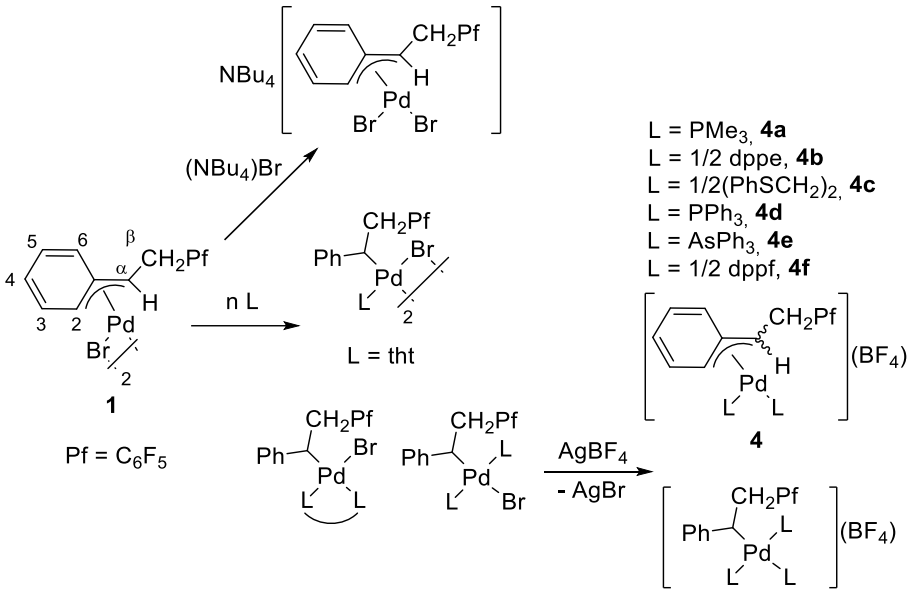

Esquema I. Complejos bencílicos estudiados en el grupo de investigación. El *Capitulo 1* se centrará en el estudio de los complejos **4a-f**.

El estudio en disolución de estos complejos por espectroscopia de RMN permitió deducir la presencia del modo de coordinación η^3 (60 ppm C^{α} y $^{1}J_{C^{\alpha}\text{-}H}$ = 155 Hz en RMN de ^{13}C) y la estereoquímica (*syn* o *anti*) de alguno de los complejos (Figura I). La presencia del isómero *syn*-**4b** y del *anti*-**4d** en disolución fue determinada mediante un experimento bidimensional ^{1}H-^{1}H ROESY de RMN y apoyada además por cálculos DFT que muestran la mayor estabilidad de estos derivados.

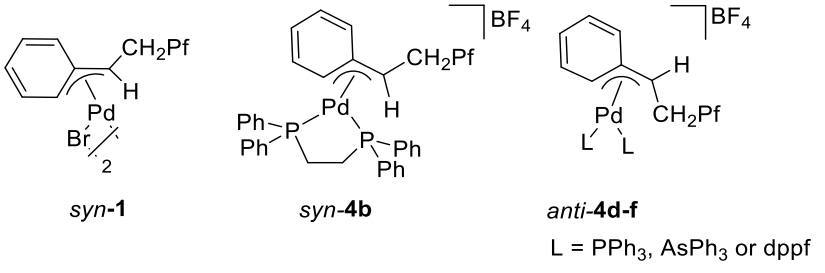

Figura I. Isómero *syn* presente en los complejos **1** y **4b** e isómero *anti* presente en los complejos **4d-f.**

Un comportamiento especial se encontró cuando el complejo dímero **1** se hizo reaccionar con 4 equivalentes de los ligandos PPh_3, $AsPh_3$ y dppf (Ecuación II). Las evidencias experimentales, así como los cálculos DFT, apuntan a la presencia en disolución de una

especie pentacoordinada. Los parámetros geométricos obtenidos por DFT predicen que la pentacoordinación en estos casos supone un alivio en la congestión de la estructura de forma más eficaz que la formación de la especie σ-bencílica, que es la obtenida con los ligandos menos voluminosos.

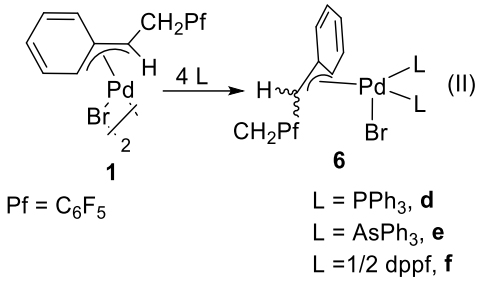

Todos los complejos preparados se descomponen a distintas velocidades mediante β-eliminación de hidrogeno. El intermedio hidruro de paladio generado fue empleado como fuente de hidruro estequiométrica para obtener alilos usando como sustrato de partida el R-(+)-limoneno (Ecuación III). Una mezcla de dos alilos (**7** y **8**) se obtuvo con los complejos bencílicos catiónicos **4d** y **4e**, resultado de procesos de migración de paladio distintos dentro del anillo.

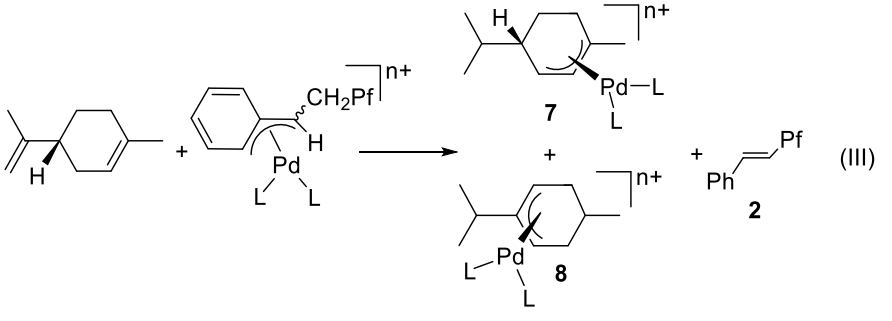

Capítulo 2: Homo- y Copolimerización de Norborneno y Alquenil Norbornenos Empleando Complejos α-Pentafluorofenilmetil Bencílicos de Paladio(II)

La polimerización de norborneno o sus derivados por adicción vinílica (VA) es un método de polimerización que permite la obtención de polinorbornenos (VA-PNBs) con un esqueleto robusto y alifático que lo hace ideal para aplicaciones de catálisis.[IV] Los complejos más empleados y que mejores resultados generan como catalizadores son los complejos de Ni(II) y Pd(II), que son metales más blandos que los de la izquierda de la series de transición y por lo tanto más tolerantes a la presencia de grupos funcionales en el monómero.[V] De especial interés son los complejos que presentan en su estructura un enlace M-R (donde R = alilo, alquilo, arilo o H) que pueda iniciar la polimerización sin presencia externa de un co-catalizador.

Es el *Capítulo 2* de esta tesis se describe el empleo de los complejos α-pentafluorofenilmetil η^3-bencílicos de paladio(II) estudiados en el *Capítulo 1* como catalizadores en la polimerización de norborneno y sus derivados. El complejo que presenta mayor actividad es catiónico, donde la coordinación-inserción del norborneno esta favorecida, y presenta ligandos lábiles que compiten peor con el norborneno por la coordinación al centro metálico. El complejo **4e** que es catiónico y presenta $AsPh_3$ como ligando es el que mejor resultados generó (Tabla I).

A pesar de los buenos resultados obtenidos para la polimerización por adición vinílica de norborneno, la polimerización de alquenil norbornenos generó resultados modestos y polímeros con pesos moleculares bajos (Tabla I). Sin embargo, la copolimerización de norborneno con alquenil norbornenos generó polímeros con rendimientos buenos y pesos

[IV] Reactivos estannilados: a) Carrera, N.; Gutiérrez, E.; Benavente, R.; Villavieja, M. M.; Albéniz, A. C.; Espinet, P. *Chem. Eur. J.* **2008**, *14*, 10141-10148. b) Meana, I.; Albéniz, A. C.; Espinet, P. *Adv. Synth. Catal*. **2010**, *352*, 2887-2891. c) Martínez-Arranz, S.; Carrera, N.; Albéniz, A. C.; Espinet, P.; Vidal-Moya, A. *Adv. Synth. Catal*. **2012**, *354*, 3551-3560. NHCs: d) Molina de la Torre, J. A.; Albéniz, A. C. Organocatalyst *ChemCatChem* **2014**, *6*, 3547-3552. e) Molina de la Torre, J. A.; Albéniz, A. C. *ChemCatChem* **2016**, *8*, 2241-2248. Organocatálisis: f). Sagamanova, I. K.; Sayalero, S.; Martínez-Arranz, S.; Albéniz, A. C.; Pericàs, M. A. *Catal. Sci. Technol*. **2015**, *5*, 754-764. Diiminas: g) Molina de la Torre, J. A.; Albéniz, A. C. *Eur. J. Inorg. Chem*. **2017**, 2911-2919. Reacciones Radicalarias: h) García-Loma, R.; Albéniz, A. C. Stannylated *Eur. J. Org. Chem*. **2017**, 4247-4254.

[V] a) Yamashita, M.; Takamiya, I.; Jin, K.; Nozaki, K. *Organometallics* **2006**, *25*, 4588-4595. b) Yamashita, M.; Takamiya, I.; Jin, K.; Nozaki, K. *Organometallics* **2008**, *27*, 5347-5352 c) Kim, D. -G.; Bell, A.; Register, R. A. *ACS Macro Lett*. **2015**, *4*, 327-330. C) Wendt, A. R.; Fink, G. *Macromol. Chem. Phys.* **2000**, *201*, 1365-1373.

moleculares más altos (M_w = 20.000-60.000 Da, VA-Co-PNB-NBV (**15**) y VA-Co-PNB-NBB (**16**)).

Tabla I. polimerización de NB, NBV, NBE y NBB con el catalizador **4e**.

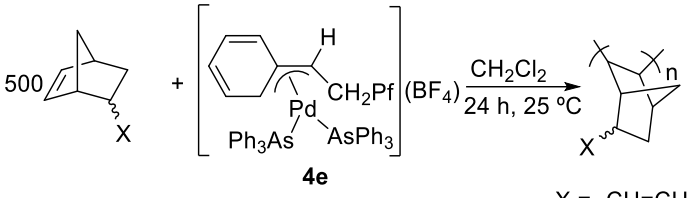

X: H (NB), -CH=CH_2 (NBV),
-C=CH-CH_3 (NBE), -$(CH_2)_2$-CH=CH_2 (NBB)

X = -CH=CH_2 **12**
X = -C=CH-CH3 **13**
X = -$(CH_2)_2$-CH=CH_2 **14**

Entrada	Monómero	Rdto. (%)	M_w[c]	M_n[c]
1	 NB	95%	---	---
2	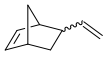 NBV	16.6%	7161	5994
3	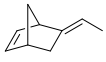 NBE	32.0%	16.404	10.434
4	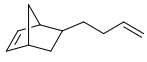 NBB	23.2%	17.287	11.296

a) Las reacciones se llevaron a cabo en CH_2Cl_2 como disolvente ([monómero]$_o$ = 1.2 M), a 25 ºC, 24 h, bajo N_2, proporción molar monómero/Pd = 500:1. b) Rendimientos referidos a la masa total de monómero. c) M_n y M_w determinados por GPC en $CHCl_3$ usando estándares de poliestireno y dado en Daltons.

Se desarrolló un nuevo sistema catalítico para la polimerización por adicción vinílica de alquenil norbornenos y en particular de vinil norborneno (NBV). Se encontró que la combinación del complejo dímero **1**, con PCy_3 y $NaBAr_4^f$ generaba resultados excelentes en la polimerización de NBV con rendimientos de hasta el 92% incluso cuando la cantidad de catalizador es de 10 mol ppm (Ecuación IV). El estudio de la etapa de iniciación en la polimerización de NB y VNB con el catalizador **4e** mostró que la iniciación de la reacción transcurre prioritariamente con inserción del norborneno en el enlace Pd-CHPh$CH_2C_6F_5$. Por otro lado, en el sistema catalítico **1**/PCy_3/$NaBAr_4^f$ se encontró que la única ruta de iniciación se producía a través del enlace Pd-H del intermedio $PdHL_n$ generado por β-eliminación de hidrogeno en el complejo bencíclico de Pd(II).

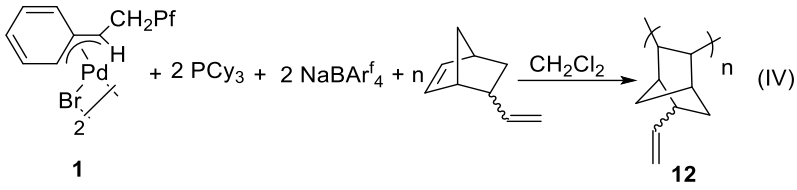

Los copolímeros VA-Co-PNB-NBV (**15**) y VA-Co-PNB-NBB (**16**) fueron empleados como productos de partida en reacciones de funcionalización post-polimerización para introducir grupos polares. Este tipo de alternativa para funcionalizar polímeros es importante dado que la polimerización de norbornenos funcionalizados con grupos como CH_2OH o COOH o su copolimerización de norborneno no es posible de forma eficaz. Se empleó una ruta de hidroboración sobre el copolímero **15** para funcionalizar el polímero con grupos OH y, a partir de este, grupos fosfito obteniéndose buenos resultados en ambos casos. Por otro lado, el copolímero **16** se empleó para incorporar grupos silicio al polímero por medio de una reacción de hidrosililación con $HSiMe_2Cl$ y el catalizador de Karstedt. El enlace Si-Cl se empleó como nuevo punto de partida para formar enlaces Si-H y Si-alilo.

Capítulo 3: Estudio Mecanístico en la Polimerización por Adicción Vinílica de Norborneno: Un Nuevo Camino de Propagación Mediante β-Eliminación de Carbono

Como hemos comentado con anterioridad en el *Capítulo 2*, el esqueleto de los polímeros por adicción vinílica (VA-PNBs) es completamente alifático. Sin embargo, durante el estudio en la copolimerización de norborneno y carbonato de norbornenilo realizado con anterioridad en nuestro grupo de investigación, se encontró la presencia de señales adicionales en el espectro de ^{1}H NMR en torno a 5.8-5.6 ppm. Por algunas similitudes con trabajos anteriores, se dedujo que estas señales pertenecían a la apertura del anillo de norborneno (RO) por una β-eliminación de carbono formándose un anillo de ciclohexeno.[VI] Nos pareció interesante estudiar este proceso con complejos arílicos de Ni(II) y como el mecanismo de polimerización-VA puede verse afectado por distintos factores.

Primero se estudió la polimerización-VA de norborneno con complejos del tipo [Ni(C_6F_5)L_2] donde L = $SbPh_3$ (**27**), $AsPh_3$ (**28**) y PPh_3 (**29**). Se encontró que el factor principal que permite el cambio de un mecanismo exclusivamente por VA a una combinación de VA-apertura del anillo (RO) está relacionado directamente con la constante de propagación en la polimerización: disminuir la constante de propagación (coordinación/inserción de norborneno) supone un incremento de la apertura del anillo por β-eliminación de carbono. Se encontraron tres factores principales que afectan a la constante de propagación: i) la concentración inicial de NB (al disminuir la concentración, se disminuye la constante de propagación y el número de unidades de apertura de anillo NB_{RO} presentes en el esqueleto aumenta), ii) los ligandos coordinados al níquel (mejor capacidad coordinante del ligando, menor velocidad de propagación) y iii) la presencia adicional de disolventes coordinantes. En relación a la presencia de disolventes coordinantes se encontraron dos factores que se traducen en un aumento de las unidades NB_{RO}: la capacidad coordinante del disolvente de modo que al aumentar esta, aumenta el número de NB_{RO} en el esqueleto (DMA > PhCOMe > MeCOMe) y la cantidad de disolvente pues al aumentar la relación NB:disolvente, la coordinación del

[VI] a) Kandanarachchi, P.; Chang, C.; Simth, S.; Bradley, P.; Rhodes, L. F.; Lattimer, R. P.; Benedikt, G. M. *J. Photopolym. Sci. Thecnol*. **2013**, *26*, 431-439. b) McDermott, J.; Chang, C.; L. Martín, F.; Rhodes, L. F. *Macromolecules* **2008**, *41*, 2984-2986.

norborneno es menos favorable y por lo tanto la propagación de la polimerización-VA se hace más lenta. Esto se traduce en un aumento de las unidades NB_{RO} con la cantidad de disolvente.

Se estudio además la estructura de los VA/RO-PNB generados confirmando la presencia de estos errores estructurales dentro del esqueleto del polímero. La etapa de iniciación de la polimerización es claramente visible en el espectro de ^{19}F con la presencia de grupos C_6F_5 anclados en el esqueleto del polímero. En cuanto a la distribución de las unidades NB_{RO}, se encontró que no era homogénea en todo el polímero. Al principio el número de unidades de NB_{RO} era baja debido a que la concentración de norborneno es alta y por lo tanto la constante de propagación también es alta. En cambio, a medida que avanza la reacción el número de unidades de NB_{RO} aumenta con la disminución de la concentración de norborneno y por ende la constante de propagación. Finalmente, la terminación en estos polímeros no tiene un mecanismo claro, pero la β-eliminación de hidrogeno después de la apertura es visible en un polímero corto sintetizado de la misma forma. La estructura del polímero se representa en la Figura II.

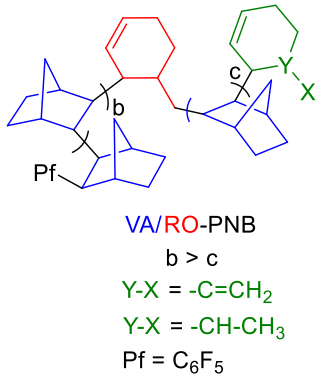

Figura II. Representación de la estructura del polímero VA/RO-PNB.

También se estudió la formación de estos errores estructurales con sistemas catiónicos de niquel(II) del tipo ([Ni(Ar)(MeCOCH$_2$C(XR)Me$_2$)(PPh$_3$)](BF$_4$) donde Ar = *o*-CF$_3$-C$_6$H$_4$ o *o*-CH$_3$-C$_6$H$_4$; y XR = OH, **34**; OMe, **37**; o SMe, **38**) y complejos neutros del tipo [Ni(Ar)(L-X)PPh$_3$] donde L-X = acac y Ar = *o*-CF$_3$-C$_6$H$_4$ (**36**).

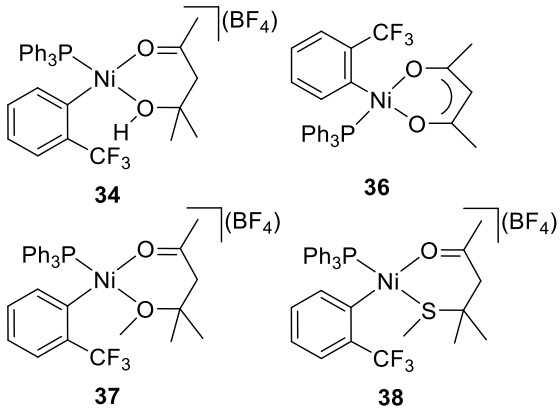

Figura III. Complejos empleados en el estudio de la formación del polímero VA/RO-PNB.

El complejo neutro **36** no mostro buenos resultados para la polimerización del norborneno y solo generó oligómeros. Por otro lado, los complejos **34**, **37** y **38** mostraron resultados en la polimerización de norborneno que dependía de la capacidad coordinante del grupo XR. El complejo **38** aislado, que presenta el átomo dador más difícil de desplazar, solo generó dímeros en la polimerización por adición vinílica de norborneno. Por otro lado, los complejos generados in situ **34** y **37** mostraron buenos resultados para la formación de los polímeros VA/RO-PNB con rendimientos entre buenos y modestos y polímeros con pesos moleculares bajos. El número de unidades NB_{RO} puede ser controlada por medio de la cantidad de catalizador en los complejos de tipo **34**: disminuyendo la cantidad de catalizador, se disminuye la cantidad de unidades de NB_{RO} en el esqueleto y se obtienen polímero con pesos moleculares más altos. La estructura del esqueleto también fue estudiada como en el caso anterior mostrando muchas similitudes con los polímeros generados con el sistema $[Ni(C_6F_5)L_2]$/disolvente coordinante pero una diferencia principal: la terminación por β-eliminación de hidrogeno después de la apertura del anillo en estos casos es clara con la presencia de unidades de terminación (NB_{ROterm}) caracterizadas por la formación de un doble enlace terminal.

Este tipo de esqueleto, VA/RO-PNB, no tiene precedente en las reacciones de polimerización de norborneno. Aunque la apertura del anillo de norborneno se había observado con anterioridad, este es el primer caso en que, tras dicha apertura, la polimerización continúa y los grupos metil-ciclohexenil quedan incorporados en el polímero final dando lugar a un nuevo esqueleto.

Capítulo 4: Síntesis de Complejos Trispirazolilboratos de Cobre(I) en VA-PNBs

Los trispirazolilboratos (Tp^x) son una clase de ligandos tridentados que han sido ampliamente empleados en combinación con numerosos metales de transición. Son ligandos nitrógeno-dadores que presentan una estructura similar a los ligandos Cp, pero a diferencia de estos, los trispirazolilboratos ofrecen una mayor riqueza para modular las características electrónicas o estéricas de los mismos. El uso de estos ligandos en catálisis es importante.[VII]

Es de especial interés anclar complejos metálicos, en matrices poliméricas para usarlos como catalizadores con las ventajas que ofrece un soporte sólido como el fácil reciclaje del catalizador por una simple filtración.

En el *Capítulo 4* se describe la ruta sintética diseñada para el anclaje de complejos trispirazolilborato de cobre(I) en los polinorbornenos de adicción vinílica (VA-PNBs). Se empleó como sustratos de partida para el anclaje los copolímeros de norborneno y alquenil norbornenos **15** y **16**, sintetizados en este caso empleando el catalizador $[Ni(C_6F_5)_2(SbPh_3)_2]$ (**27**). A través de una ruta de hidroboración con $HBBr_2{\cdot}SMe$, sustitución de los átomos de Br en presencia de distintos pirazoles y deprotonación utilizando LDA como base, se pudieron sintetizar complejos trispirazolilborato de litio (Tp^xLi) anclados al esqueleto de VA-PNB tal y como se refleja en el Esquema II. Cuando el polímero Tp^xLi se puso en contacto con una disolución de CuI en MeCN se obtuvieron los correspondientes complejos $Tp^xCu(NCMe)$. Los polímeros fueron caracterizados por RMN de sólidos, IR e ICP-MS. El RMN de ^{11}B de todos los polímeros presentaba señales entre 0-2 ppm típica de boratos. El análisis por ICP-MS mostraba contenidos de cobre en torno a 40-90 mg de Cu por gramo de polímero. Además, el entorno tetraédrico del cobre se pudo determinar mediante la síntesis del correspondiente polímero VA-PNB-Tp^xCuCO. La banda de absorción de CO en el espectro IR del polímero

[VII] a) Díaz-Requejo, M. M.; Pérez, P. J. *Chem. Rev.* **2008**, *108*, 3379-3394. b) Caballero, A.; Pérez, P. J.; *J. Organomet. Chem.* **2015**, *793*, 108-113. c) Caballero, A.; Díaz-Requejo, M. M.; M. R. Fructos, J. Urbano, Pérez P. J. Ligand Design in Metal Chemistry. In *Modern Applications of Trispyrazolylborate Ligands in Coinage Metal Catalysis.* Eds. Stradiotto, M.; Lundgren R. J. John Wiley & Sons, 2016, pp. 308-329. d) Caballero, A.; Díaz-Requejo, M. M.; Fructos, M. R.; Olmos, A.; Urbano, J.; Pérez, P. J. *Dalton Trans.* **2015**, *44*, 20295-20307. e) McKeown, B. A.; Lee, J. P.; Mei, J.; Cundari, T. R.; Gunnoe, T. B. Eur. J. *Inorg. Chem.* **2016**, 2296-2311.

mostraba números de onda muy similares a los complejos discretos Tp^xCuCO descritos con anterioridad.

Los VA-PNB-$Tp^xCu(NCMe)$ fueron probados en reacciones catalíticas por el grupo del Profesor Pedro Pérez en la Universidad de Huelva mostrando similares resultados que sus homólogos homogéneos y pudiéndose reciclar hasta en 5 ciclos.

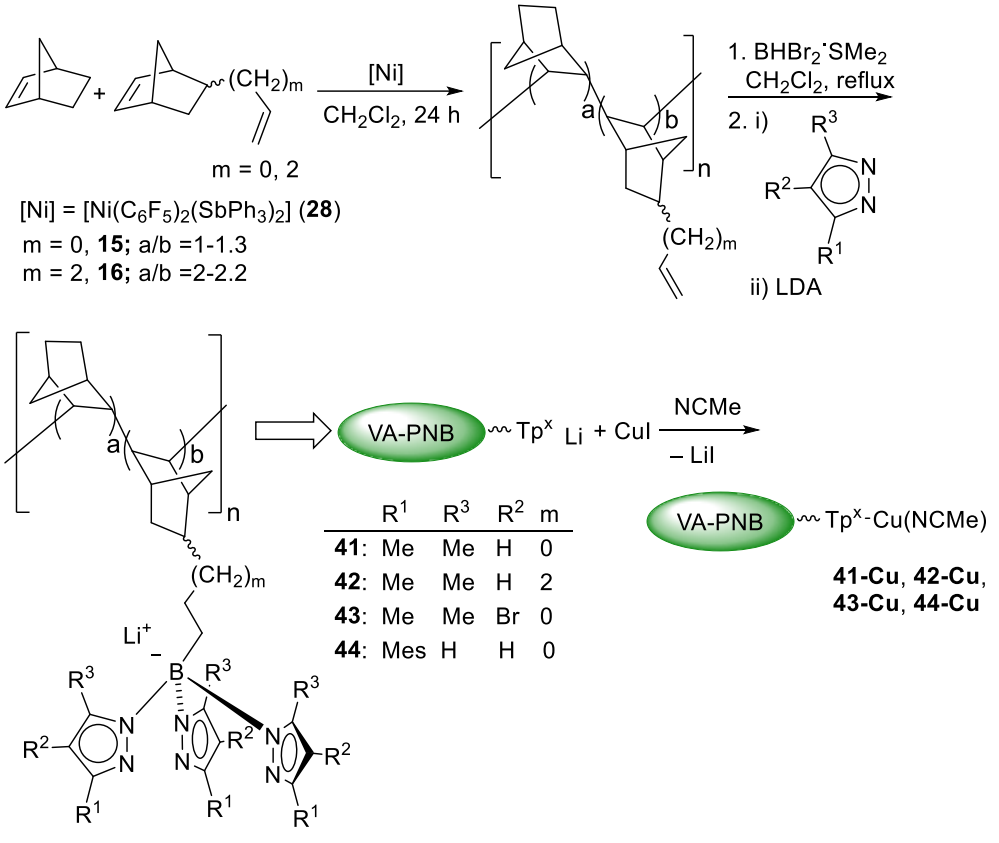

Esquema II. Ruta de síntesis para el anclaje de Tp^x de cobre(I) al esqueleto de VA-PNBs.

Conclusiones Generales

Se han caracterizado una variedad de complejos η^3-bencílicos de paladio(II) con diferentes ligandos que presentan un grupo α-pentafluorofenilmetil. La presencia del isómero *syn* o *anti* fue determinada mediante experimentos de ROESY de RMN donde se observó la presencia del isómero *syn* en los complejos **1** y **4b** y el isómero *anti* en los complejos **4d-f**. Las evidencias experimentales fueron apoyadas por cálculos DFT donde se determinó la preferencia del isómero *anti* en el complejo **4d**. Un aliviamiento del impedimento estéreo por pentacoordinación se propuse para los complejos η^3-bencílicos neutros **6d-f** generados in situ mezclando **1** y dos equivalentes de los ligandos $AsPh_3$, PPh_3 y dppf por paladio. Las evidencias experimentales fueron apoyadas por cálculos DFT donde se confirmó la mayor estabilidad de dos geometrías pentacoordinadas piramidal cuadradas (**6d**-spy-apiBr y **6d**-spy-apiPPh_3) con respecto a la forma σ-bencílica.

Todos los complejos η^3-bencílicos se descomponen, a distintos tiempos, por β-eliminación de hidrógeno para dar **2** y un intermedio ``$PdHL_n$´´ El hidruro intermedio de paladio puede ser transferido a un fragmento bencilo-paladio para dar el producto de reducción **3**. O bien, el intermedio ``$PdHL_n$´´. puede ser atrapado en presencia de dienos como R-(+)-limoneno para generar alilos como **7** y **8**. Un proceso de descomposición especial se encontró para el hidruro generado a partir del complejo **4d** donde se observó la formación del clúster $[Pd_3(PPh_3)_4](BF_4)_2$ (**9**).

Se probaron los complejos η^3-bencílicos de paladio(II) en la polimerización por adicción vinílica (VA) de norborneno y derivados del mismo. El catalizador que dio mejores resultados para la síntesis de VA-PNBs fue el complejo $[Pd(\eta^3\text{-}CHPhCH_2Pf)(AsPh_3)_2](BF_4)$ (**4e**), un complejo catiónico con ligandos lábiles. Por otro lado, este catalizador mostraba baja actividad para la polimerización-VA de alquenil norbornenos, pero fue eficiente en la copolimerización de norborneno y alquenil norbornenos generando polímeros con buenos rendimientos. Además, se desarrolló un catalizador altamente activo para la polimerización por adicción vinílica de NBV por combinación del dímero neutro η^3-bencílico **1**, PCy_3 y el contraión BAr_4^{f-} que es crucial en la estabilización de la especie activa. La homopolimerización de 5-vinil-2-norborneno puede llevarse a cabo de forma cuantitativa usando cantidades molares de paladio tan bajas como 0.01 mol% (10 ppm).

El estudio de la etapa de iniciación con el catalizador **4e** mostro una inserción preferente del norborneno y del NBV a través del enlace Pd-$CHPhCH_2C_6F_5$. Por otro lado, en la polimerización-VA con el sistema precatalítico **1**/PCy_3/$NaBAr_4^f$ la iniciación ocurre exclusivamente a través del enlace Pd-H generado in situ por β-eliminación de hidrógeno. Los copolímeros VA-Co-PNB-NBV (**15**) y VA-Co-PNB-NBB (**16**) se emplearon como materiales de partida para la introducción de nuevos grupos funcionales por un proceso de funcionalización post-polimerización de los grupos colgantes alquenilo mediante reacciones conocidas como la hidroboración o la hidrosililación.

Un nuevo tipo de esqueleto VA/RO-PNB se encontró por combinación de dos procesos distintos empleando el mismo catalizador: la polimerización por adicción vinílica (VA) y la apertura del anillo del norborneno por β-C eliminación (RO). La estructura de estos VA/RO-PNBs concuerda con la presencia de dos unidades distintas dentro del esqueleto: estructuras de biciclo norbornenilo como resultado de la polimerización por adicción vinílica de norborneno (NB_{VA}), y grupos metil-ciclohexenil formados por la apertura del anillo de norborneno por β-C eliminación (NB_{RO}). La formación de este tipo de polinorbornenos-VA/RO se puede conseguir mediante el efecto que producen distintos factores en la disminución de la velocidad de la etapa de propagación pero asegurando el crecimiento de la cadena polimérica.

De la variedad de catalizadores empelados del tipo [$Ni(C_6F_5)_2L_2$] donde L = PPh_3 (**29**), $AsPh_3$ (**28**) y $SbPh_3$ (**27**), el complejo **28** es el más conveniente para generar el esqueleto VA/RO-PNB. El número de unidades abiertas de NB puede ser modificado cambiando las condiciones de la reacción cuando se emplea el complejo **28**. Un incremento en el número de unidades de NB_{RO} se puede lograr cuando se reduce la concentración inicial de monómero o la relación NB:Ni. Una combinación entre el complejo [$Ni(C_6F_5)_2(AsPh_3)_2$] (**28**) y cantidades controladas de disolventes coordinantes es un sistema catalítico útil para la síntesis de VA/RO-PNBs. La capacidad coordinante de los disolventes está directamente correlacionada con la cantidad de apertura del anillo en el esqueleto de VA/RO-PNB, siguiendo la siguiente tendencia: MeCN > DMA > PhCOMe > MeCOMe.

También se descubrió un nuevo tipo de complejos catiónicos de niquel(II) que poseían ligandos quelato [Ni(*o*-CF_3-C_6H_4)($MeCOCH_2C(XR)Me_2$)(PPh_3)] (XR = OH, **34**; OMe, **37**; o SMe, **38**) con una aplicación directa en la formación del esqueleto VA/RO-PNB. La capacidad

coordinante del ligando es crucial en la formación de las unidades de NB_{RO} y solo dímeros se formaron con el ligando SMe. Sin embargo, con los ligandos O,O-dadores se obtuvieron los esqueletos VA/RO-PNBs con una mayor cantidad de estructuras de NB_{RO} con el ligando OR = OMe que con el ligando OR = OH. La terminación de la polimerización por β-eliminación de hidrógeno es clara en estos sistemas. Después de la β-γ-C-C ruptura del norborneno se observó una cantidad máxima de terminación del 25%. Es importante recalcar que la terminación por β-eliminación de hidrógeno es más importante en los polímeros VA/RO-PNBs obtenidos con los complejos **34** y **37** que con la combinación de $[Ni(C_6F_5)_2(AsPh_3)_2]$ (**28**)/co-disolvente.

Finalmente, hemos desarrollado una nueva ruta sintética para el anclaje de ligandos del tipo trispirazolilboratos (Tp^xLi) en el esqueleto de los polinorbornenos-VA (VA-PNB-Tp^xLi), por funcionalización de los alquenil copolímeros **15** y **16**. El anclaje de cobre sobre los polímeros VA-PNB-Tp^xLi permitió sintetizar los polímeros VA-PNB-Tp^xCu con buenos rendimientos e incorporaciones entre 40-90 mg de cobre por gramo de polímero. El entorno tetraédrico de Cu(I) fue demostrado por comparación de las absorciones del CO en el polímero VA-PNB-Tp^xCuCO con las de sus homólogos complejos discretos Tp^xCuCO. La actividad catalítica de estos complejos fue probada en el grupo del Profesor Pedro Pérez de la Universidad de Huelva mostrando una actividad similar a la encontrada para las condiciones en catálisis homogénea. Además, el catalizador polimérico puede ser reciclado.

Appendix

Abbreviations and Acronyms

Abbreviations

General Abbreviations

acac	acetylacetonate
BNB	5-(but-1-en-4-yl)-2-norbornene
DMA	Dimethylacetamide
ENB	5-ethylidene-2-norbornene
EDA	Ethyldiazoacetate
ROMP	Ring Opening Metathesis Polymerization
NB	Norbornene
NBCOOH	2-carboxylic acid-5-norbornene
$NBCH_2OH$	2-methanol-5-norbornene
M_w	Weight Average Molecular Weight
M_n	Number Average Molecular Weight
MeCN	Acetonitrile
MeCOMe	Acetone
Mes	Mesityl
$NaBAr_4^f$	Sodium tetrakis[3,5-bis(trifluoromethyl)phenyl]borate
NB_{VA} units	Vinylic Addition units
NB_{RO} units	Ring Opening units

NB_{ROint} units	Internal Ring Opening units
NB_{ROterm} units	Terminal Ring Opening units
PDI	Polydispersity Index
PhI=NTs	N-tosyliminobenzyliodinane
PhCOMe	Acetophenone
Pf	Pentafluorophenyl
ROMP	Ring Opening Metathesis Polymerization
Tp^x	Trispyrazolylborate
VA	Vinylic Addition
VA-PNB	Vinylic addition polynorbornene
VA-Co-PNB-	Copolymer of norbornene and a substituted norbornene
VA-PNB-Tp^xCu	Trispyrazolylborate of copper(I) supported on VA-PNB
VNB	5-vinyl-2-norbornene
VA/RO-PNBs	Vinylic Addition/Ring Opening Polynorbornene

Abbreviations for NMR spectroscopy

b	broad
bd	broad doublet
bs	broad singlet
COSY	Correlation Spectroscopy
HMBC	Heteronuclear Multiple Bond Correlation
HOESY	Heteronuclear Overhauser Effect Spectroscopy
HSQC	Heteronuclear Simple Quantum Correlation
NOE	Nuclear Overhauser Effect

ROESY	Rotating-frame Overhauser Spectroscopy
d	doublet
t	triplet
q	quartet
m	multiplet
CP-MAS NMR	Cross Polarization/Magic Angle Spinning Nuclear Magnetic Resonance

Abbreviations used in IR spectroscopy

FT-IR	Fourier Transform Infrared
ν	stretching
ν-CH sym.	Symmetric stretching for the C-H bond
ν-CH asym.	Asymmetric stretching for the C-H bond
δ	bending out of the plane

Abbreviations used in MS

EI	Electronic Impact
ICP-MS	Inductively Coupled Plasma Mass Spectrometry

Abbreviations used in X-Ray diffraction

CCD	Charge Coupled Device
ORTEP	Oak Ridge Thermal-Ellipsoid

Abbreviations used in theorical calculation

DFT	Density Functional Theory
SMD	Solvation Model based on Density

References

1. a) Mintz, E. A.; Moloy, K. G.; Marks, T. J.Actinide Tris(hydrocarbyls). Synthesis, Properties, Structure, and Molecular Dynamics of Thorium and Uranium Pentamethylcyclopentadienyl Tris(η^n-benzyls) *J. Am. Chem. Soc*. **1982**, *104*, 4692-4695. b) Edwards, P. G.; Andersen, R. A.; Zalkin, A. Preparation of Tetraalkyl Phosphine Complexes of the f-Block Metals. Crystal Structure of $Th(CH_2Ph)_4$($Me_2PCH_2CH_2PMe_2$) and $U(CH_2Ph)_3Me(Me_2PCH_2CH_2PMe_2)$ *Organometallics* **1984**, *3*, 293-298. c) Gwyneth, R. D.; Jarvis, A. J. Kilbour, B. T. The Crystal and Molecular Structures (at -40 ºC) of the Tetrabenzyls of Titanium, Hafnium, and Tin *J. Chem. Soc. D: Chem. Comm.* **1971**, 1511-1512.

2. a) Burch, R. R.; Muetterties, E. L.; Day, V. W. Dehydrogenation of 1,3-Cyclohexadiene by $\{HRh[P(O\text{-}\mathit{I}\text{-}C_3H_7)_3]_2\}_2$. Preparation, Dynamic NMR, and X-ray Crystal Structure of $[\eta^3\text{-}CH_2C_6(CH_3)_5]Rh[P(O\text{-}\mathit{l}\text{-}C_3H_7)_3]_2$ *Organometallics* **1982**, *1*, 188-197. b) Hamon, J. -H.; Astruc, D.; Roman, E. η^5-Benzyl: Crystal Structure, Nucleophilic Properties, and Electron-Transfer Reactions of $CpFe(\eta^5\text{-}C_6Me_5CH_2)$, an Intermediate in C-H Activation by $O_2^{-\cdot}$ via O2 *J. Am. Chem. Soc*. **1981**, *103*, 2431-2433.

3. Trost, B. M.; Czabaniuk, L. C. Structure and Reactivity of Late Transition Metal η^3-Benzyl Complexes. *Angew. Chem., Int. Ed*. **2014**, *53*, 2826-2851.

4. Jacob, V. K.; Thiele, K. -H.; Keilberg, Ch. Niebuhr, R. Zur Existenz und Darstellung von Benzylnickelverbindungen Z. *Anorg. Allg. Chem*. **1975**, *415*, 109-1144.

5. Carmona, E.; Marin, J. M.; Paneque, M.; Poveda, M. L. New nickel o-methylbenzyl complexes. Crystal and molecular structures of $Ni(\eta^3\text{-}CH_2C_6H_4\text{-}\mathit{o}\text{-}Me)Cl(PMe_3)$ and $Ni_3(\eta^1\text{-}CH_2C_6H_4\text{-}\mathit{o}\text{-}Me)_4(PMe_3)_2(\mu^3\text{-}OH)_2$ *Organometallics* **1987**, *6*, 1757-1765.

6. Komon, Z. J. A.; Bu, X.; Bazan, G. C. Synthesis, Characterization, and Ethylene Oligomerization Action of $[(C_6H_5)_2PC_6H_4C(O\text{-}B(C_6F_5)_3)O\text{-}\kappa^2P,O]Ni(\eta^3\text{-}CH_2C_6H_5)$ *J. Am. Chem. Soc*. **2000**, *122*, 12379-12380.

7. Shim, C. B.; Kim, Y. H.; Lee, B. Y.; Dong, Y.; Yun, H. [2-(Alkylideneamino)benzoato]nickel(II) Complexes: Active Catalysts for Ethylene Polymerization *Organometallics* **2003**, *22*, 4272-4280.

8. a) Kim, Y. H.; Kim, T. H.; Lee, B. Y. α-Iminoenamido Ligands: A Novel Structure for Transition-Metal Activation *Organometallics* **2002**, *21*, 3082-3084, b) Kwon, H. Y.; Lee, S. Y.; Lee, B. Y.; Shin, D. M.; Chung, Y. K. Synthesis, characterization and ethylene reactivity of 2-diphenylphosphanylbenzamido nickel complexes *Dalton Trans.* **2004**, 921-928. c) Albers, I. Eleuterio, A.; Cámpora, J.; Maya, C. M.; Palma, P.; Sánchez, L. J.; Passaglia, E. Cationic η^3-benzyl nickel compounds with diphosphine ligands as catalyst precursors for ethylene oligomerization/polymerization: influence of the diphosphine bite angle *J. Organomet. Chem*. **2004**, *689*, 833-839. d) Sujith, S.; Noh, E. K.; Yeoul, B. L.; Han, J. W. Synthesis, characterization, and norbornene polymerization of η^3-benzylnickel(II) complexes of N-heterocyclic carbenes *J. Organomet. Chem.* **2008**, *693*, 2171-2176.

9. Crascall, L. E.; Lister, S. A.; Redhouse, A. D.; Spencer, J. L. Synthesis of Pt(II)-η^3-benzyl complexes: crystal structure of $[Pt(Bu_2^tP(CH_2)_3PBu_2^t)(\eta^3$-*anti*-1-$MeCHC_6H_4Br$-4)$][BF_4]$ *J. Organomet. Chem.* **1990**, *394*, C35 -C38.

10. Crascall, L. E.; Spencer, J. L. Preparation and Fluxional Behaviour of η^3-Methylbenzyl Platinum and Palladium Complexes *J. Chem. Soc. Dalton Trans*. **1992**, 3445-3452.

11. a) Hesp, K. D.; McDonald, R.; Ferguson, M. J.; Schattec, G. Stradiotto, M. (κ^2-P,S)Pt(benzyl) complexes derived from 1/3-P^i-Pr^2-2-S^tBu-indene: facile synthesis of carbanion- and borate-containing zwitterionsw *Chem. Commun.* **2008**, 5645-5647. b) Marx, T.; Wesemann, L.; Dehnen, S. A Zwitterionic Transition-Metal Complex: Platinum-closo-Borate Coordination Synthesis, Structure, and DFT Calculations *Organometallics* **2000**, *19*, 4653-4656.

12. Stevens, R. R.; Shier, G. D. π-benzylbis(triethylphosphine)palladium(II) Tetrafluoroborate *J. Organomet. Chem*. **1970**, *21*, 495-499.

13. Calvin; G.; Coates, G. E. Organopalladium Compounds *J. Chem. Soc*. **1960**, 2008-2016.

14. Roberts, J. S.; Klabunde, K. The Direct Synthesis of η^3-$ArCH_2PdCl$ Compounds by the Oxidative Addition of $ArCH_2$-Chlorine Bonds to Palladium Atoms *J. Am. Chem. Soc*. **1977**, *99*, 2509-2515.

15. Sonoda, A.; Bailey, P. M.; Maitlis, P. M. Crystal and Molecular Structures of Pentane-2,4-dionato-(α,l,2-η-triphenylmethy1)-palladium and -platinum *J. Chem. Soc. Dalton Trans*. **1979**, 346-350.

16. Gatti, G.; Lopez, J. A.; Mealli, C.; Musco, A. Structural and NMR spectroscopic characterization of η^3-Benzyl palladium(II) complexes *J. Organomet. Chem.* **1994**, *483*, 77-89.

17. Brookhart, M.; Rix, F. C.; DeSimone, J. M. Palladium(II) Catalysts for Living Alternating Copolymerization of Olefins and Carbon Monoxide *J. Am Chem. Soc*. **1992**, *114*, 5894-5895.

18. a) Oitsuka, K.; Yamamoto, M.; Suzuki, S.; Takahashi, S. Structure and Reactivity of (η^3-Indolylmethyl)palladium Complexes Generated by the Reaction of Organopalladium Complexes with o-Alkenylphenyl Isocyanide *Organometallics* **2002**, *21*, 581-583. b) Dewhurst, R. D.; Müller, R.; Kaupp, M.; Radacki, K.; Götz, K. The η^3-Furfuryl Ligand: Plausible Catalytic Intermediates and Heterocyclic η^3-Benzyl Analogues with Superior Binding Ability *Organometallics*, **2010**, *29*, 4431-4433.

19. a) Becker, Y.; Stille, J. K. The Dynamic η^1- and η^3 -Benzylbis(triethylphosphine)palladium(II) Cations. Mechanisms of Interconversion *J. Am. Chem. Soc.* **1978**, *100*, 845-850. b) Brookhart, M.; Buck, R. C.; Danielson III, E. Synthesis, spectroscopic characterization, dynamics, and phosphine trapping of Cp(CO)Fe[.eta.3-CH(R)C_6H_5] complexes (R = H, OCH_3) *J. Am. Chem. Soc*. **1989**, *111*, 567-574. c) Rix, F. C.; Brookhart, M.; White, P. S. Electronic Effects on the β-Alkyl Migratory Insertion Reaction of para-Substituted Styrene Methyl Palladium Complexes *J. Am. Chem. Soc.* **1996**, *118*, 2436-2448.

20. a) Stühler, H.-O. (1,2,5,6-η-1,5-Cyclooctadiene)- (1,2,7,-η-7-methylbenzyl)(7,8-η-styrene)rhodium(I)-Antarafacial Fluctuation of the Benzyl Ligand and Temperature-Dependent Coordination of Styrene *Angew. Chem. Int. Ed. Engl.* **1980**, *19*, 468-469. b) Su, S.-C. H.; Wojcicki, A. Stereochemical studies on thermal and photochemical reactions of (.eta.^{5}-C_5H_5)$W(CO)_3(CH_2CH_2Ph)$ containing deuterium-labeled phenethyl ligands

Organometalics **1983**, *2*, 1296-1301. c) Carmona, E.; Paneque, M.; Poveda, M. L. Synthesis and characterization of some new organometallic complexes of nickel(II) containing trimethylphosphine *Polyhedron* **1989**, *8*, 285-291. d) Campora, J.; Gutierrez, E.; Poveda, M. L.; Ruiz, C.; Carmona, E. Binuclear σ- and η^3-Benzylic Derivatives of Nickel *J. Chem. Soc. Dalton Trans*. **1992**, 1769-1774.

21. Recent review: a) Liégault, B.; Renaud, J.-L.; Bruneau, Activation and functionalization of benzylic derivatives by palladium catalysts *C. Chem. Soc. Rev*. **2008**, *37*, 290-299. Recent examples: c) Hikawa, H.; Koike, T.; Izumi, K.; Kikkawa, S.; Azumaya, I. Borrowing Hydrogen Methodology for N-Benzylation using a π-Benzylpalladium System in Water *Adv. Synth. Catal*. **2016**, *358*, 784-791; d) Yang, M. -H.; Hunt, J. R.; Sharifi, N.; Altman, R. A. Palladium Catalysis Enables Benzylation of α,α-Difluoroketone Enolates *Angew. Chem. Int. Ed*. **2016**, *55*, 9080-9083. e) Najib, A.; Hirano, K.; Miura, M. Palladium-Catalyzed Asymmetric Benzylic Substitution of Secondary Benzyl Carbonates with Nitrogen and Oxygen Nucleophiles *Org. Lett.* **2017**, *19*, 2438-2441.

22. a) LaPointe, A. M.; Rix, F. C.; Brookhart, M. Mechanistic Studies of Palladium(II)-Catalyzed Hydrosilation and Dehydrogenative Silation Reactions *J. Am. Chem. Soc*. **1997**, *119*, 906-917. b) Trzeciak, A. M.; Ciunik, Z.; Ziólkowski, J. J. Synthesis of Palladium Benzyl Complexes from the Reaction of $PdCl_2[P(OPh)_3]_2$ with Benzyl Bromide and Triethylamine: Important Intermediates in Catalytic Carbonylation *Organometallics* **2002**, *21*, 132-137. c) Johns, A. M.; Utsunomiya, M.; Incarvito, C. D.; Hartwig, J. F. A Highly Active Palladium Catalyst for Intermolecular Hydroamination. Factors that Control Reactivity and Additions of Functionalized Anilines to Dienes and Vinylarenes *J. Am. Chem. Soc*. **2006**, *128*, 1828-1839. d) Narahashi, H.; Shimizu, I.; Yamamoto, A. Synthesis of benzylpalladium complexes through C-O bond cleavage of benzylic carboxylates: Development of a novel palladium-catalyzed benzylation of olefins *J. Organomet. Chem*. **2008**, *693*, 283-296.

23. Heck, R. F.; Nolley, J. P. Palladium-Catalyzed Vinylic Hydrogen Substitution Reactions with Aryl, Benzyl, and Styryl Halides *J. Org. Chem*. **1972**, *37*, 2320-2322.

24. a) Wu, G.-Z.; Lamaty, F.; Negishi, E.-I. Metal-promoted cyclization. 26. Palladium-catalyzed cyclization of benzyl halides and related electrophiles containing alkenes and

alkynes as a novel route to carbocycles *J. Org. Chem.*, **1989**, *54*, 2507-2508. b) Grigg, R.; Sukirthalingham, S.; Sridharan, V. Palladium catalysed tandem cyclisation-anion capture processes initiated by alkyl- and π-allyl-palladium species *Tetrahedron Lett.***1991**, *32*, 2545-2548.

25. Yang, Z.; Zhou, J. S. Palladium-Catalyzed, Asymmetric Mizoroki-Heck Reaction of Benzylic Electrophiles Using Phosphoramidites as Chiral Ligands *J. Am. Chem. Soc*. **2012**, *134*, 11833-11835.

26. Suzuki-Miyaura Coupling of Diarylmethyl Carbonates with Arylboronic Acids: A New Access to Triarylmethanes *Org. Lett*., **2008**, *10*, 973-976.

27. Shimizu, M.; Tomioka, Y.; Nagao, I.; Hiyama, T. Palladium-Catalyzed Double Cross-Coupling Reaction of vic-Diborylalkenes and -arenes with vic-Bromo(bromomethyl)arenes *Synlett* **2009**, 3147-3150.

28. Legros, J. -Y.; Fiaud, J. -C. Palladium-Catalyzed Nucleophilic Substitution of Naphthylmethyl and 1-Naphthylethyl Esters *Tetrahedron Lett.* **1992**, *33*, 2509-2510.

29. Legros, J.-Y.; Primault, G.; Toffano, M.; Riviere, M.-A.; Fiaud, J.-C. Reactivity of Quinoline- and Isoquinoline-Based Heteroaromatic Substrates in Palladium(0)-Catalyzed Benzylic Nucleophilic Substitution *Org. Lett*. **2000**, *2*, 433-436.

30. Urkalan, K. B.; Sigman, M. S. Palladium-Catalyzed Oxidative Intermolecular Difunctionalization of Terminal Alkenes with Organostannanes and Molecular Oxygen *Angew. Chem. Int. Ed*. **2009**, *48*, 3146-3149.

31. Albéniz, A. C.; Espinet, P.; Lin, Y. -S. Involvement of Intramolecular Hydride Transfer in the Formation of Alkanes from Palladium Alkyls *Organometallics*, **1997**, *16*, 4030-4032

32. Albéniz, A. C.; Espinet, P.; López-Fernández, R.; Sen, A. Warning on the Use of Radical Traps as a Test for Radical Mechanisms: They React with Palladium Hydrido Complexes *J. Am. Chem. Soc*. **2002**, *124*, 11278-11279.

33. Albéniz, A. C.; Espinet, P.; Lin, Y.-S.; Martín-Ruiz, B. Gated Migration" for Enantioselective Synthesis of Palladium Allyls Using a "PdHBr" Synthon. *Organometallics* **1999**, *18*, 3359-3363.

34. a) Martín-Ruiz, B.; Pérez-Ortega, I.; Albéniz, A. C. Benzylic Complexes of Palladium(II): Bonding and Pentacoordination for Steric Relief *Organometallics* **2018**, *37*, 1074-1085.

35. As it was mentioned in the text, suitable crystals for a high quality X-ray crystal structural determination could not be obtained for **4f**. However, a disordered molecular structure (the disorder affecting mainly but not only to the anion and solvent molecules of crystallization) was obtained which could not be completely refined (R = 12%). It shows the structure of an *anti*-η^3-benzylic complex. A CIF file for this structure is included just for easier inspection of the basic structure, but it does not comply with the requirements of the IUCr.

36. Geometries were calculated for two different relative locations of the cation and anion, labeled up and down relative to the C^{ipso} benzylic carbon. There is no significant energy difference for the up or down BF_4^- structures for each isomer (less than 1 kcal/mol), the down location being always more stable. Thus, the energy differences between the syn and *anti* isomers are given in Figure 1.11 for the down BF_4^- location.

37. Pentacoordinated palladium(II) complexes are not common but representative examples have been long known: Albéniz, A. C.; Espinet, P. In Encyclopedia of Inorganic Chemistry, King, R. B. Ed.; England; 1994, *6*, 3018.

38. Selected examples of trigonal bipyramidal Pd(II) compounds (other than those with specially designed tripod ligands): a) Konietzny, A.; Bailey, P. M.; Maitlis, P. M. The cyclotetramerisation of dimethyl acetylenedicarboxylate and the x-ray structure of [Pd{h(C_8(CO_2Me)$_8$)}cl(pyridine)$_2$], an unusual five-co-ordinate palladium(II) complex *J. Chem. Soc. Chem. Commun*. **1975**, 78-79. b) Albano, V. G.; Castellar, C.; Cucciolino, M. E.; Panunzi, A.; Vitagliano, A. Synthesis and characterization of five-coordinate olefin complexes of palladium(II). Molecular structure of the acetone solvate of (2,9-dimethyl-1,10-phenanthroline)(maleic anhydride)methylchloropalladium *Organometallics*, **1990**, *9*, 1269-

1276. c) Burger, P. Baumeister, J. M. Transition metal complexes with sterically demanding ligands. I. Synthesis and X-ray crystal structure of 1,5-cyclooctadiene palladium methyl triflate, (COD)Pd(Me)(OTf) and its cationic penta-coordinate adducts with sterically demanding 2,9-diaryl-substituted 1,10-phenanthroline ligands *J. Organomet. Chem.* **1999**, *575*, 214-222. d) López-Torres, M.; Fernández, A.; Fernández, J. J.; Suárez, A.; Pereira, M. T.; Ortigueira, J. M.; Adams, H. Mono- and Dinuclear Five-coordinate Cyclometalated Palladium(II) Compounds *Inorg. Chem.* **2001**, *40*, 4583-4587. e) Binotti, B.; Bellachioma, G.; Cardaci, G.; Macchioni, A.; Zuccaccia C.; Foresti, E.; Sabatino, P. Intramolecular and Interionic Structural Studies of Novel Olefin Palladium(II) and Platinum(II) Complexes Containing Poly(pyrazol-1-yl)borate and -methane Ligands. X-ray Structures of Palladium Five-Coordinate Complexes *Organometallics* **2002**, *21*, 346-354. f) Bedford, R. B.; Betham, M.; Butts, C. P.; Coles, S. J.; Cutajar, M.; Gelbrich, T.; Hursthouse, M. B.; Scully, P. N.; Wimperis, S. Five-coordinate Pd(II) orthometallated triarylphosphite complexes *Dalton Trans*. **2007**, 459-466. g) Kirai, N.; Ta-kaya, J.; Iwasawa, N. Two Reversible σ-Bond Metathesis Pathways for Boron–Palladium Bond Formation: Selective Synthesis of Isomeric Five-Coordinate Borylpalladium Complexes *J. Am. Chem. Soc*. **2013**, *135*, 2493-2496.

39. Square pyramidal Pd(II) derivatives: a) Collier, J. W.; Mann, F. G.; Watson, D. G.; Watson, H. R. 351. The constitution of complex metallic salts. Part XIX. The 2-phenylisophosphindoline derivatives of platinum (II), palladium (II), and nickel(II) *J. Chem. Soc*. **1964**, 1803-1814. b) Chui, K. M.; Powell, H. M. Crystal and molecular structure of tetracarbonyl-(7,7-dimethoxynorborn-2-ene)chromium(0) *J. Chem. Soc. Dalton Trans.* **1974**, 1879-1889. c) Chui, K. M.; Powell, H. M. Comparison of stereochemistry in racemic and optically resolved forms of a five-co-ordinate compound. Crystal and molecular structures of dibromotris-(2-phenylisophosphindoline)palladium(II)–acetone (orange) and dibromotris-(2-phenylisophosphindoline)palladium(II)(red) *J. Chem. Soc. Dalton Trans.* **1974**, 2117-2122. d) Louw, W. J.; de Waal, D. J. A. Preparation of the five-co-ordinate complexes $[PdX_2(PMe_2Ph)_3]$(X = Cl, Br, or I) and the crystal and molecular structure of dichlorotris-[dimethylphenylphosphine]palladium *J. Chem. Soc Dalton Trans.***1976**, 2364-2368. e) Hansson, S.; Norrby, P.-O.; Sjögren, M. P. T.; Åkermark, B.; Cucciolito, M. E.; Giordano, F.; Vitagliano, A. Effects of phenanthroline type ligands on the dynamic processes of (.eta.3-allyl)palladium complexes. Molecular structure of (2,9-dimethyl-1,10-phenanthroline)[(1,2,3-.eta.)-3-methyl-2-butenyl]chloropalladium *Organometallics*, **1993**,

12, 4940-4948. f) Bröring, M.; Brandt, C. D. A five coordinate PdII complex stable in solution and in the solid state Synthesis of tetra- and pentacoordinate palladium complexes of functionalized N-heterocyclic carbenes and a comparative study of their catalytic activities *Chem. Commun*. **2003**. 2156-2157. g) Zhang, X.; Xia, Q.; Chen, W. Synthesis of tetra- and pentacoordinate palladium complexes of functionalized N-heterocyclic carbenes and a comparative study of their catalytic activities *Dalton Trans.* **2009**, 7045-7054.

40. Rülke, R. E.; Ernsting, J. M.; Spek, A. L.; Elsevier, C. J.; Van Leeuwen, P. W. N. M.; Vrieze, K. NMR study on the coordination behavior of dissymmetric terdentate trinitrogen ligands on methylpalladium(II) compounds *Inorg. Chem.* **1993**, *32*, 5769-5778.

41. Cambridge Structural Database System (CSD System, version 5.38, **2016**). Cambridge Crystallographic Data Centre, 12 Union Road, Cambridge CB2 1EZ, UK.

42. Kemmitt, R. D. W.; McKenna, P.; Russell, D. R.; Sherry, L. J. S. Chemistry of metallacyclobutanones. Part 2. Synthesis and ring inversion of some highly puckered metallacyclobutan-3-one (slipped oxodimethylenemethane) complexes of palladium; crystal structures of 2,4-bis(methoxycarbonyl)-1,1-bis(triphenylphosphine)palladacyclobutan-3-one, 2,4-bis(methoxycarbonyl)-1,1-bis(triphenylarsine)palladacyclobutan-3-one, and 1,1-(2′,2″-bipyridyl)-2,4-bis(methoxycarbonyl)palladacyclobutan-3-on *J. Chem. Soc. Dalton Trans.* **1985**, 259-268.

43. Van Haaren, R. J.; Goubitz, K.; Fraanje, J.; van Strijdonck, G. P. F.; Oevering, H.; Coussens, B.; Reek, J. N. H.; Kamer, P. C. J.; van Leeuwen P. W. N. M. An X-ray Study of the Effect of the Bite Angle of Chelating Ligands on the Geometry of Palladium(allyl) Complexes: Implications for the Regioselectivity in the Allylic Alkylation *Inorg. Chem*. **2001**, ***40***, 3363-3372.

44. Martín-Ruiz, B; Pérez-Ortega, I; Albéniz, A. C. α-Substituted Benzylic Complexes of Palladium(II) as Precursors of Palladium Hydrides *Organometallics* **2018**, *37*, 1665-1670.

45. Heaton, B. T.; Hébert, S. P. A.; Iggo, J. A.; Metz, F.; Whyman, R. Characterisation of Hydridopalladium Complexes. *J. Chem. Soc., Dalton Trans.* **1993**, 3081-3084.

46. Casado, A. L.; Casares, J.; Espinet, P. An Aryl Exchange Reaction with Full Retention of Configuration of the Complexes: Mechanism of the Aryl Exchange between [PdR2L2] Complexes in Chloroform (R = Pentahalophenyl, L = Thioether) *Organometallics* **1997**, *16*, 5730-5736.

47. a) Cacchi, S; Arcadi, A. Palladium-catalyzed conjugate addition reaction of aryl iodides with .alpha.,.beta.-unsaturated ketones *J. Org. Chem*. **1983**, *48*, 4236-4240. b) Friestad, G. K.; Branchaud, B. P. Intramolecular Pd-catalyzed aryl-enone conjugate additions. Control of reductive vs non-reductive cyclization *Tetrahedron Lett.* **1995**, *36*, 7047-7050. c) Gligorich, K. M.; Cummins, S. A.; Sigman, M. S. Palladium-Catalyzed Reductive Coupling of Styrenes and Organostannanes under Aerobic Conditions *J. Am. Chem. Soc*. **2007**, *129*, 14193-14195. d) Gottumukkala, A. L.; de Vries, J. G.; Minnaard, A. J. Pd-NHC Catalyzed Conjugate Addition versus the Mizoroki-Heck Reaction *Chem. Eur. J*. **2011**, *17*, 3091-3095. d) Raoufmoghaddam, S.; Mannathan, S.; Minnaard, A. J.; de Vries, J. G.; Reek, J. N. H. Palladium-Catalyzed Asymmetric Reductive Heck Reaction of Aryl Halides *Chem. Eur. J.* **2015**, *21*, 18811-18820. e) Yue, G.; Lei, K.; Hirao, H.; Zhou, J. *Angew. Chem. Int. Ed.* **2015**, *54*, 6531-6535. f) Kong, W.; Wang, Q.; Zhu, J. Water as a Hydride Source in Palladium-Catalyzed Enantioselective Reductive Heck Reactions *Angew. Chem. Int. Ed.* **2017**, *56*, 3987-3991.

48. a) Kannan, S.; James, A. J.; Sharp, P. R. $[Pd_3(PPh_3)_4]^{2+}$, a New Palladium Triphenylphosphine Complex *J. Am. Chem. Soc.* **1998**, *120*, 215-216. b) Omondi, B.; Shawb, M. L.; Holzapfel, C. W. Synthesis and crystal structures of new palladium catalysts for the hydromethoxycarbonylation of alkenes *J. Organomet. Chem.* **2011**, *696*, 3091-3096.

49. Zudin, V. N.; Chinakov, V. D.; Nekipelov, V. M.; Likholobov, V.A. Yermakov, Y. L. formation and reactivity of palladium hydride complexes, $[(PPh_3)_3PdH]^+$ and $[(PPh_3)_3Pd(\mu\text{-}H)(\mu\text{-}CO)Pd(PPh_3)_2]^+$, in aqueous trifluoroacetic acid solutions *J. Organomet. Chem.* **1985**, *289*, 425-430.

50. Urriolabeitia, E. P. Coordination chemistry of Pd(II) complexes with P-donor ligands. An Introduction to synthesis and structural characterization in coordination chemistry *J. Chem. Edu.* **1997**, *74*, 325-327.

51. Becke, A. D. Density-functional thermochemistry. III. The role of exact exchange *J. Chem. Phys.* **1993**, *98*, 5648-5652.

52. Grimme, S.; Antony, J.; Ehrlich, S.; Krieg, H. A consistent and accurate ab initio parametrization of density functional dispersion correction (DFT-D) for the 94 elements H-Pu *J. Chem. Phys.* **2010**, *132*, 154104.

53. Gaussian 09, Revision D.01. Frisch, M. J.; Trucks, G. W.; Schlegel, H. B.; Scuseria, G. E.; Robb, M. A.; Cheeseman, J. R.; Scalmani, G.; Barone, V.; Mennucci, B.; Petersson, G. A.; Nakatsuji, H.; Caricato, M.; Li, X.; Hratchian, H. P.; Izmaylov, A. F.; Bloino, J.; Zheng, G.; Sonnenberg, J. L.; Hada, M.; Ehara, M.; Toyota, K.; Fukuda, R.; Hasegawa, J.; Ishida, M.; Nakajima, T.; Honda, Y.; Kitao, O.; Nakai, H.; Vreven, T.; Montgomery, Jr., J. A.; Peralta, J. E.; Ogliaro, F.; Bearpark, M.; Heyd, J. J.; Brothers, E.; Kudin, K. N.; Staroverov, V. N.; Keith, T.; Kobayashi, R.; Normand, J.; Raghavachari, K.; Rendell, A.; Burant, J. C.; Iyengar, S. S.; Tomasi, J.; Cossi, M.; Rega, N.; Millam, J. M.; Klene, M.; Knox, J. E.; Cross, J. B.; Bakken, V.; Adamo, C.; Jaramillo, J.; Gomperts, R.; Stratmann, R. E.; Yazyev, O.; Austin, A. J.; Cammi, R.; Pomelli, C.; Ochterski, J. W.; Martin, R. L.; Morokuma, K.; Zakrzewski, V. G.; Voth, G. A.; Salvador, P.; Dannenberg, J. J.; Dapprich, S.; Daniels, A. D.; Farkas, O.; Foresman, J. B.; Ortiz, J. V.; Cioslowski, J.; Fox, D. J. Gaussian, Inc., Wallingford CT, **2013**.

54. Francl, M. M.; Petro, W. J.; Hehre, W. J.; Binkley, J. S.; Gordon, M. S.; DeFrees, D. J.; Pople, J. A. Self-consistent molecular orbital methods. XXIII. A polarization-type basis set for second-row elements *J. Chem. Phys.* **1982**, *77*, 3654-3665.

55. Clark, T.; Chandrasekhar, J.; Schleyer, P. V. R. Efficient diffuse function-augmented basis sets for anion calculations. III.† The 3-21+G basis set for first-row elements, Li-F *J. Comput. Chem.* **1983**, *4*, 294-301.

56. Ehlers, A. W.; Böhme, M.; Dapprich, S.; Gobbi, A.; Höllwarth, A.; Jonas, V.; Köhler, K. F.; Stegmann, R.; Veldkamp, A.; Frenking, G. A set of f-polarization functions for pseudo-potential basis sets of the transition metals Sc□Cu, Y□Ag and La□Au *Chem. Phys. Lett.* **1993**, *208*, 111-114.

57. Roy, L. E.; Hay, P. J.; Martin, R. L. Revised Basis Sets for the LANL Effective Core Potentials *J. Chem. Theory Comput*. **2008**, *4*, 1029-1031.

58. Bauld, L. N. Cation radical cycloadditions and related sigmatropic reactions *Tetrahedron* **1989**, *45*, 5307-5363.

59. Wynne, J. H.; Lloyd, C. T.; Cozzens, R. F. Facile synthetic approach to functionalized 4,5-disubstituted norbornene monomers *Chem. Lett.* **2002**, *31*, 926-927.

60. Liaw, D. J.; Huang, C. C.; Hong, S. M.; Chen, W. H.; Lee, K. R.; Lai, J. Y. Molecular architecture effect on reactivity of polynorbornenes with pendant alpha,beta-unsaturated amide or ester bridged chains via ring-opening metathesis polymerization *Polymer* **2006**, *47*, 4613-4621.

61. Rudin, A.; Choi, P. The Elements of Polymer Science & Engineering. *In Free-Radical Polymerization;* Academic Press*;* 2013; pp. 341-389.

62. Gaylord, N. G; Mandal, B. M.; Martan, M. Peroxide-induced polymerization of norbornene *J. Polym. Sci. Polym. Lett. Ed.* **1976**, *14*, 555-559.

63. Yeh, A. -C. Free Radical-Induced and Pd(II) Complexes-Catalyzed Poly(norbornene) Formation *J. Chin. Chem. Soc.* **2003**, *50*, 959-964.

64. Graham, P. J.; Buhle, E. L.; Pappas, N. Transannular Polymerization of 2-Carbethoxybicyclo[2.2.1]-2,5-heptadiene *J. Org. Chem.* **1961**, *26*, 4658-4662.

65. Niu, Q. J.; Frechet, J. M. Polymers for 193-nm Microlithography: Regioregular 2-Alkoxycarbonylnortricyclene Polymers by Controlled Cyclopolymerization of Bulky Ester Derivatives of Norbornadiene *Angew. Chem., Int. Ed.* **1998**, *37*, 667-670.

66. Shiotsuki, M.; Kai, H.; Endo, T. Radical Polymerization of 2,5-Norbornadienes Containing Ester Groups by AIBN and Oxygen Gas *J. of Polym. Sci., Part A: Polym. Chem.* **2014**, *52*, 2528-2536.

67. Pasquale, A. J.; Allen, R. D.; Long, T. E. Fundamental Investigations of the Free Radical Copolymerization and Terpolymerization of Maleic Anhydride, Norbornene, and Norbornene tert-Butyl Ester: In-Situ Mid-Infrared Spectroscopic Analysis *Macromolecules* **2001**, *34*, 8064-8071.

68. Kanao, M.; Otake, A.; Tsuchiya, K.; Ogino, K. Stereo-Selective Synthesis of *exo*-Norbornene Derivatives for Resist Materials *J. Photopolym. Sci. Tec.* **2009**, *22*, 365-370.

69. a) Kennedy J. P., Hinlicky, J. A. Cationic Transannular Polymerization of Norbornadiene *Polymer* **1965**, *6*, 133-141. b) Kennedy, I. P.; Makowski, H. S. Reactivities and Structural Aspects in the Cationic Polymerization of Mono- and Diolefinic Norbornanes. *J. Polym. Sci., Part C* **1968**, *22*, 247-265. c) Gaylord, N. G.; Deshpande, A. B.; Mandal, B. M.; Martan, M. Poly-2,3- and 2,7-Bicyclo[2.2.1]hept-2-enes: Preparation and Structures of Polynorbornenes *J. Macromol. Sci. Chem. A* **1977**, 11/5, 1053-1070. d) Bermeshev, M. V.; Bulgakov, B. A; Genaev, A. M.; Kostina, J. V.; Bondarenko, G. N.; Finkelshtein, E. S. Cationic Polymerization of Norbornene Derivatives in the Presence of Boranes *Macromolecules* **2014**, *47*, 5470-5483.

70. a) Grubbs, R. H.; Tumas, W. Polymer Synthesis and Organotransition Metal Chemistry *Science*, **1989**, 243, 90-915. b) Bielawski, C. W.; Hillmyer, M. A. Handbook of Metathesis. *In Synthesis of Ruthenium Carbene Complexes;* Eds. Grubbs, R. H.; Wiley-VCH: Winham, Germany 2003; pp 86-94. c) Sutthasupa, R.; Masashi, S. Sanda, F. Recent advances in ring-opening metathesis polymerization, and application to synthesis of functional material *Polymer Journal* **2010**, *42*, 905-915. c) Choinopoulos, I. Grubbs' and Schrock's Catalysts, Ring Opening Metathesis Polymerization and Molecular Brushes-Synthesis, Characterization, Properties and Applications *Polymers* **2019**, *11*, 298-329.

71. Hérisson, P. J. -L.; Chauvin, Y. Y. Catalyse de transformation des oléfines par les complexes du tungsténe. II. Télomérisation des oléfines cycliques en présence d'léfines acycliques. *Makromol. Chem*. **1970**, *141*, 161-176.

72. a) Gilliom, L. R.; Grubbs, R. H. Titanacyclobutanes derived from strained, cyclic olefins: the living polymerization of norbornene. J. *Am. Chem. Soc*. **1986**, *108*, 733-742. b) Cannizzo,

L. F.; Grubbs, R. H. Block copolymers containing monodisperse segments produced by ring-opening metathesis of cyclic olefins *Macromolecules* **1988**, *21*, 1961-1967.

73. a) Schrock, R. R.; Feldman, J.; Cannizzo, L. F; Grubbs, R. H. Ring-opening polymerization of norbornene by a living tungsten alkylidene complex *Macromolecules* **1987**, *20*, 1169-1172. b) Ivin, K. J.; Kress, J; Osborn, J. A. 1H NMR study of the kinetics of metathesis polymerization of 5- and 5,6-methoxycarbonyl derivatives of bicyclo[2.2.1]hept-2-ene, initiated by $W[=C(CH_2)_3CH_2](OCH_2CMe_3)_2Br_2$ *Makromol. Chem.* **1992**, *193*, 1695-1707.

74. Porri, L.; Diversi, P.; Lucherimi, A.; Rossi, R. Catalysts derived from ruthenium and iridium for the ring-opening polymerization of cycloolefins *Makromol. Chem.* **1975**, *176*, 3121-3125.

75. Nguyen, S. T.; Johnson, L. K.; Grubbs, R. H; Ziller, J. W. Ring-opening metathesis polymerization (ROMP) of norbornene by a group VIII carbine complex in protic media *J. Am. Chem. Soc.* **1992**, *114*, 3974-3975.

76. a) Scholl, M.; Ding, S.; Lee, C. W.; Grubbs, R. H. Synthesis and activity of a new generation of ruthenium-based olefin metathesis catalysts coordinated with 1,3- dimesityl-4,5-dihydroimidazol-2-ylidene ligands. *Org. Lett.* **1999**, *1*, 953-956. b) Love, J. A.; Morgan, J. P.; Trnka, T. M.; Grubbs, R. H. A practical and highly active ruthenium-based catalyst that effects the cross metathesis of acrylonitrile. *Angew. Chem. Int. Ed*. **2002**, *4*1, 4035-4037. c) Garber, S. B.; Kingsbury, J. S.; Gray, B. L.; Hoveyda, A. H. Efficient and recyclable monomeric and dendritic Ru-based metathesis catalysts. *J. Am. Chem. Soc*. **2000**, *12*, 8168-8179.

77. a) Hou, X.; Nomura, K. Ring-Opening Metathesis Polymerization of Cyclic Olefins by (Arylimido)vanadium(V)-Alkylidenes: Highly Active, Thermally Robust Cis Specific Polymerization *J. Am. Chem. Soc.* **2016**, *138*, 11840-11849. b) Wised, K.; Nomura, K Cis-Specific Chain Transfer Ring-Opening Metathesis Polymerization Using a Vanadium(V) Alkylidene Catalyst for Efficient Synthesis of End-Functionalized Polymers *Organometallics*, **2017**, *36*, 4103-4106. c) Ring Opening Metathesis Polymerization of Norbornene and Tetracyclododecene with Cyclooctene by Using (Arylimido)vanadium(V)-Alkylidene Catalyst *J. Polym. Sci., A: Polym. Chem.* **2017**, *55*, 3067-3074.

78. Wised, K.; Nomura, K. Synthesis of (Imido)niobium(V)-Alkylidene Complexes That Exhibit High Catalytic Activities for Metathesis Polymerization of Cyclic Olefins and Internal Alkynes *Organometallics*, **2016**, *35*, 2773-2777.

79. Górski, M.; Szymánska-Buzar, T. Tungsten(II)-initiated ring-opening metathesis polymerization and other C-C bond forming reactions of 5-vinyl-2-norbornene *J. Mol. Catal. A: Chem.* **2006**, *257*, 41-47.

80. García-Loma, R.; Albéniz, A. C. Poly(u-bromoalkylnorbornenes-co-norbornene) by ROMP-hydrogenation: a robust support amenable to post-polymerization functionalization *RSC Adv.* **2015**, *5*, 70244-70254.

81. Park, K. H.; Twieg, R. J.; Ravikiran, R.; Rhodes, L. F.; Shick, R. A. Yankelevich, D.; Knoesen, A. Synthesis and Nonlinear-Optical Properties of Vinyl-Addition Poly(norbornene)s *Macromolecules* **2004**, *37*, *14*, 5163-5178.

82. Varanasi, P. R.; Mewherter, A. M.; Lawson, M. C.; Jordhamo, G.; Allen, R.; Optiz, J.; Ito, H.; Wallow, T.; Hofer, D. IBM 193nm Semiconductor Resist: Material Properties, Resist Characteristics and Lithographic Performance *J. Photopolym. Sci. Technol.* **1999**, *12*, 493-500.

83. Grave, N. R.; Kohl, P. A.; Bidstrup-Allen, S. A.; Jayaraman, S.; Shick, R. A. Functionalized polynorbornene dielectric polymers: Adhesion and mechanical properties*J. Polym. Sci., Part B: Polym. Phys.* **1999**, *37*, 3003-3010.

84. Kohl, P. A.; Zhao, Q.; Patel, K.; Schmidt, D.; Bidstrup-Allen, S. A.; Shick, R. A.; Jayaraman, S. Air-Gaps for Electrical Interconnections *Electrochem. Solid-State Lett.* **1998**, *1*, 49-51.

85. a) Brumbaugh, J. S.; Whittle, R. R.; Parvez, M.; Sen, A. Insertion of Olefins into Palladium(II)-Acyl Bonds. Mechanistic and Structural Studies *Organometallics* **1990**, *9*, 1735-1747. b) Markies, B. A.; Kruis, J. D.; Marco, J.; Rietveld, H. P.; Kai, J.; Verkerk, A. N.; Boersma, J.; Kooijman, H.; Lakin, M. T.; Spek, A. L.; van Koten, G. Alkene and Carbon

Monoxide Insertion Reactions of Nitrogen-Coordinated Monoorganopalladium(II) Complexes: The Stepwise Construction of Alternating Copolymers of CO and Alkenes on a Palladium(II) Center *J. Am. Chem. Soc.* **1995**, *117*, 5263-5274.

86. Wilks, B R; Chung, W. J.; Ludovice, P. J.; Rezac, M. R.; Meakin, Hill, P. A. J. Impact of Average Free-Volume Element Size on Transport in Stereoisomers of Polynorbornene. I. Properties at 35 °C *J. Polym. Sci: Part B* **2003**, *41*, 2185-2199.

87. Arndt, M.; Engehausen, R.; Kaminsky, W.; Konstantin, Z. Hydrooligomerization of cycloolefins a view of the microstructure of polynorbomene *J. Mol. Cat. A: Chem.* **1995**, *101* 171-178.

88. a) Boggioni, L.; Losio, S.; Tritto, I. Microstructure of Copolymers of Norbornene Based on Assignments of ^{13}C NMR Spectra: Evolution of a Methodology *Polymers* **2018**, *10*, 647-671. b) Ahmed, S.; Ludovice. P. J.; Kohl, P. Microstructure of 2,3 erythro di-isotactic polynorbornene from atomistic simulation *Comput. Theor. Polym. Sci.* **2000**, *10*, 221-233.

89. Finkelshtein, E. S.; Bermeshev, M. V.; Gringolts, M. L.; Starannikova, L. E.; Yampolskii, Y. P Substituted polynorbornenes as promising materials for gas separation membranes *Russ. Chem. Rev*. **2011**, *80*, 341-361

90. Hasan, T.; Nishii, K.; Shiono, T.; Ikeda, T. Living polymerization of norbornene via vinyl addition with ansa-fluorenylamidodimethyltitanium complex *Macromolecules* **2002**, *35*, 8933-8935.

91. a) Yoshida, Y.; Mohri, J. -I.; Ishii S. -I.; Mitani, M.; Saito, J.; Matsui, S.; Makio, H.; Nakano, T.; Tanaka, H.; Onda, M.; Yamamoto, Y.; Mizuno, A.; Fujita, T. Living Copolymerization of Ethylene with Norbornene Catalyzed by Bis(PyrrolideImine) Titanium Complexes with MAO *J. Am. Chem. Soc.* **2004**, *126*, 12023-12032. b) Tang, L. -M.; Hu, T.; Bo, Y. -J.; Li, Y. -S.; Hu, N. -H Titanium complexes bearing aromatic-substituted b-enaminoketonato ligands: Syntheses, structure and olefin polymerization behavior *J. Organomet. Chem.* **2005**, *690*, 3125-3133. c) Ravasio, A.; Boggioni, L.; Scalcione, G.; Bertini, F.; Piovani, D.; Tritto, I.Living Copolymerization of Ethylene with Norbornene by Fluorinated Enolato-imine Titanium Catalyst *J. Polym. Sci. A: Polym. Chem.* **2012**, 50, 3867-3874. d) Ochedzan-Siodłak, W.; Siodłak, D.; Piontek, A.; Doležal, K. Titanium and Vanadium Catalysts with 2-

Hydroxyphenyloxazoline and Oxazine Ligands for Ethylene-Norbornene (co)Polymerization *Catalysts* **2019**, *9*, 1041-1052.

92. a) Kaminsky, W.; Bark, A.; Arndt, M. New polymers by homogenous zirconocene/aluminoxane catalysts *Makromol. Chem., Macromol. Symp.* **1991**, *47*, 83-93. b) Lasarov, H.; Mönkkönen, K.; Pakkanen, T. T. Influence of batch reaction conditions on norbornene/ethylene copolymers made using C_2v- and C_s- symmetric metallocene/MAO catalysts *Macromol. Chem. Phys.* **1998**, *199*, 1939-1942. c) Tschage, M.; Jung, S.; Spaniol, T. P.; Okuda, J. Polymerization of Norbornene Using Chiral Bis(phenolate) Zirconium Catalysts *Macromol. Rapid Commun.* **2015**, *36*, 219-223.

93. Endo, K.; Fuji, K.; Otsu, T. Monomer-isomerization copolymerizations of branched 1-alkenes and 2-butene with a Ziegler-Natta catalyst *Makromol. Chem. Rapid Commun.* **1991**, *12*, 409-412. b) Endo, K.; Fuji, K.; Otsu, T. Polymerization of 5-vinyl-2-norbornene with $TiCl_3$ and alkylaluminium catalysts *Macromol. Chem. Phys.* **1996**, *197*, 97-104.

94. Lohse, D. J.; Datta, S.; Kresge, E. N. Graft Copolymer Compatibilizers for Blends of Polypropylene and Ethylene-Propylene Copolymers *Macromolecules* **1991**, *24*, 561-566. b) Marathe, S.; Sivaram, S. Regioselective Copolymerization of 5-Vinyl-2-norbornene with Ethylene Using Zirconocene Methylaluminoxane Catalysts: A Facile Route to Functional Polyolefins *Macromolecules* **1994**, *27*, 1083-1086. c) Lasarov, H.; Pakkanen, T. T. Copolymerization of ethylene with 5-vinyl-2-norbornene in the presence of the $Ph_2C(Flu)(Cp)ZrCl_2$/MAO catalyst *Macromol. Chem. Phys.* **2000**, *201*, 1780-1786. d) Lasarov, H.; Pakkanen, T. T. Ethylene-Norbornene Terpolymerization with 5-Vinyl-2-norbornene Using Single-Site Catalysts *Macromol. Rapid Commun.* **2001**, *22*, 434-438.

95. a) Sato, Y.; Nakayama, Y.; Yasuda, H. Controlled vinyl-addition-type polymerization of norbornene initiated by several cobalt complexes having substituted terpyridine ligands *J. Organomet. Chem.* **2004**, *689* 744-750. b) Leone, G.; Boglia, A.; Boccia, A. C.; Scafati, S. T.; Bertini, F.; Ricci, G. Vinyl-Type Addition Polymerization of Norbornene and Synthesis of Norbornene Macromonomers in the Presence of Ethylene Catalyzed by Cobalt(II)-Phosphine Complexes *Macromolecules* **2009**, *42*, 9231-9237.

96. a) Lassahn, P.-G.; Lozan, V.; Timco, G. A.; Christian, P.; Janiak, C.: Winpenny, R. E. P. Homo- and heterometallic carboxylate cage complexes as precatalysts for olefin polymerization-Activity enhancement through "inert metals" *J. Catal.* **2004**, *222*, 260-267. b) Chen, Y. J.; Huang, Z. L.; Zhang, C. Z.; Wie, T.; Zhang, L. W. Syntheses of iron, cobalt, chromium, copper and zinc complexes with bulky bis(imino)pyridyl ligands and their catalytic behaviors in ethylene polymerization and vinyl polymerization of norbornene *J. Mol. Catal. A: Chem.* **2006**, *259*, 133-141. c) Benade, L. L.; Ojwach, S. O.; Obuah, C.; Guzei, I. A.; Darkwa. J. Vinyl-addition polymerization of norbornene catalyzed by (pyrazol-1-ylmethyl)pyridine divalent iron, cobalt and nickel complexes *Polyhedron*, **2011**, *30*, 2878-2883.

97. a) Carlini, C.; Giaiacopi, S.; Marchetti, F.; Pinzino, C.; Galletti, A. M. R.; Sbrana, G. Vinyl Polymerization of Norbornene by Bis(salicylaldiminate)copper(II)/Methylalumoxane Catalysts *Organometallics* **2006**, *25*, 3659-3664. b) Pei, L.; Gao, H. Bis(-ketoamino) copper complexes for vinyl polymerization of norbornene: Correlation between precursor structure and catalytic activity *J. Mol. Cat. A: Chem.* **2011**,*336*, 94-99. c) Tian, J.; He, X.; Liu, J.; Denga, X.; Chen, D. Palladium(II) and copper(II) chloride complexes bearing bulky a-diimine ligands as catalysts for norbornene vinyl-addition (co)polymerization *RSC Adv*. **2016**, *6*, 22908-22916.

98. a) Blank, F.; Janiak, C. Metal catalysts for the vinyl/addition polymerization of norbornene *Coord. Chem. Rev*. **2009**, *253*, 827-861. b) Finkelshtein, E. S.; Gringolts, M.; Bermeshev, M. V.; Chapala, P.; Yulia, R. Membrane Materials for Gas and Vapor Separation: Synthesis and Application of Silicon-Containing Polymers. *In Polynorbornenes***.** John Wiley & Sons Ltd. 2017; pp 143-221. c) García-Loma, R.; Albéniz, A. C. Vinylic Addition Polynorbornene in Catalysis *Asian J. Org. Chem.* **2019**, *8*, 304-315.

99. a) Zhao, C. T.; Ribeiro, M. D.; Portela; M. F.; Pereira, S.; Homo- and copolymerisation of norbornene and styrene with nickel bis(acetyl acetonate)/methylaluminoxane system *Eur. Polym. J.* **2001**, *37*, 45-54. b) Sachse, A.; Demeshko, S.; Dechert, S. Daebel, V.; Langeb, A.; Meyer. F. Highly preorganized pyrazolate-bridged palladium(II) and nickel(II) complexes in bimetallic norbornene polymerization *Dalton Trans.* **2010**, 39, 3903-3914. c) Blank, F.; Scherer, H.; Ruiz, J.; Rodríguez, V.; Janiak, C. Palladium(II) complexes with

pentafluorophenyl ligands: structures, C_6F_5 fluxionality by 2D-NMR studies and pre-catalysts for the vinyl addition polymerization of norbornene *Dalton Trans.* **2010**, *39*, 3609-3619. d) Blank, F.; Vieth, J. K.; Ruiz, J.; Rodríguez, R.; Janiak, C. η^5-Cyclopentadienylpalladium(II) complexes: Synthesis, characterization and use for the vinyl addition polymerization of norbornene and the copolymerization with 5-vinyl-2-norbornene or 5-ethylidene-2-norbornene *J. Organomet. Chem.*, **2011**, *696*, 473-487. e) Qiao, Y. -L.; Jin. G. -X. Nickel(II) and Palladium(II) Complexes with Tridentate [C,N,S] and [C,N,P] Ligands: Syntheses, Characterization, and Catalytic Norbornene Polymerization *Organometallics* **2013**, *32*, 1932-1937. f) Hao, Z.; Yang, N.; Gao, W.; Xin, L.; Luo, X.; Mu, Y. Nickel complexes bearing N,N,N-tridentate quinolinyl anilido-imine ligands: Synthesis, characterization and catalysis on norbornene addition polymerization *J. Organomet. Chem.* **2014**, *749*, 350-355. g) Zhuang, R.; Liu, H.; Guo, J.; Dong, B.; Zhao, W.; Hu, Y.; Zhang, X.; Highly Active Nickel(II) and Palladium(II) Complexes Bearing N,N,P Tridentate Ligand for Vinyl Addition Polymerization of Norbornene *Eur. Polym. J.* **2017**, *93*, 358-367. h) Youa, F.; Liua, H.; Luo, G.; Shi, X. Tridentate Diarylamido-based Pincer Complexes of Nickel and Palladium: Sidearm Effects in Polymerization of Norbornene *Dalton Trans.* **2019**, *48*, 12219-12227. f) Liu, H.; Yuan, H.; Shi, X. Synthesis of nickel and palladium complexes with diarylamido-based unsymmetrical pincer ligands and application for norbornene polymerization *Dalton Trans*. **2019**, *48*, 609-617.

100. a) Barnes, D. A.; Benedikt, G. M.; Goodall, B. L.; Huang, S.S.; Kalamarides, H. A.; Lenhard, S.; McIntosh, L. H.; Selvy, K. T.; Shick, R. A.; Rhodes, L. F. Addition Polymerization of Norbornene-Type Monomers Using Neutral Nickel Complexes Containing Fluorinated Aryl Ligands *Macromolecules* **2003**, *36*, 2623-2632. b) Saito, T.; Wakatsuki, Y. Addition polymerization of norbornene, 5-vinyl-2-norbornene and 2-methoxycarbonyl-5-norbornene with a catalyst based on a palladium(0) precursor complex *Polymer*, **2012**, *53*, 308-315. c) He, X.; Liu, Y.; Chen, L; Yiwang, C.; Chen, D. Ni(II) and Pd(II) Complexes Bearing Benzocyclohexane-Ketoarylimine for Copolymerization of Norbornene with 5-Norbornene-2-Carboxylic Ester *J. Pol. Sci. Part A: Pol. Chem.* **2012**, *50*, 4695-4704. d) Tiana, J.; Zhua, H.; Liua, J.; Chenb, D.; Hea, X. Pd(II) complexes bearing di- and monochelate fluorinated β-ketonaphthyliminato ligand and their catalytic properties towards vinyladdition polymerization and copolymerization of norbornene and ester-functionalized norbornene derivative *Appl. Organometal. Chem.* **2014**, *28*, 702-711.

101. a) Sen, A.; Lal, T. -W. Catalytic Polymerization of Acetylenes and Olefins by Tetrakis(acetonitrile)palladium(II) Bis(tetrafluoroborate) *Organometallics* **1982**, *1*, 415-418. b) Mehler, C.; Risse, W. The Pd^{2+}-catalyzed polymerization of norbornene *Makromol. Chem., Rapid Commun.* **1991**, *12*, 255-259. c) Mehler, C.; Risse, W. Addition polymerization of norbornene catalyzed by palladium(2+) compounds. A polymerization reaction with rare chain transfer and chain termination *Macromolecules* **1992**, *25*, 4226-4228. d) Safir, A. L.; Novak, B. M. Living 1,2-Olefin-Insertion Polymerizations Initiated by Palladium(II) Alkyl Complexes: Block Copolymers and a Route to Polyacetylene-Hydrocarbon Diblocks *Macromolecules* **1995**, *28*, 5396-5398. e) Hennis, A. D.; Polley, J. D.; Long, G. S.; Yandulov, A. S.; D.; Lipian, J.; Benedikt, G. M.; Rhodes L. F. Novel, Efficient, Palladium-Based System for the Polymerization of Norbornene Derivatives: Scope and Mechanism *Organometallics* **2001**, *20*, 2802-2812. f) Lipian, J.; Mimna, R. A.; Fondran, J. C.; Yandulov, D.; Shick, R. A.; Goodall, B. L.; Rhodes, L. F.; Huffman, J. C. Addition Polymerization of Norbornene-Type Monomers. High Activity Cationic Allyl Palladium Catalysts *Macromolecules* **2002**, *35*, 8969-8977. g) Casares, J. A.; Espinet, E.; Martín-Alvarez, J. M.; Martínez-Ilarduya, J. M.; Gorka, S. Stable Nickel Catalysts for Fast Norbornene Polymerization: Tuning Reactivity *Eur. J. Inorg. Chem.* **2005**, 3825-3831. h) Casares, J. A.; Espinet, E.; Gorka, S. Palladium Catalysts for Norbornene Polymerization. A Study by NMR and Calorimetric Methods *Organometallics* **2008**, *27*, 3761-3769. i) Walter, M. D.; Moorhouse, R. A.; Urbin, S. A.; White, P. S.; Brookhart, M. γ-Agostic Species as Key Intermediates in the Vinyl Addition Polymerization of Norbornene with Cationic (allyl)Pd Catalysts: Synthesis and Mechanistic Insights *J. Am. Chem. Soc.* **2009**, *131*, 9055-9069. j) Walter, M. C.; Moorhouse, R. A.; White, P. S.; Brookhart, M. Vinyl Addition Polymerization of Norbornene with Cationic (allyl)Ni Catalysts: Mechanistic Insights and Characterization of First Insertion Products *J. Pol. Sci. Part A: Pol. Chem.* **2009**, *47*, 2560-2573.

102. Cowie, J. M. G.; Arrighi, V. Polymers: Chemistry and Physics of Modern Materials. *In Polymer for the Electronic Industry*; 3rd edition; Chapman & Hall: New York, 1991, pp. 455-487.

103. Stannylates reagents: a) Carrera, N.; Gutiérrez, E.; Benavente, R.; Villavieja, M. M.; Albéniz, A. C.; Espinet, P. Stannylated Polynorbornenes as New Reagents for a Clean Stille Reaction *Chem. Eur. J.* **2008**, *14*, 10141-10148. b) Meana, I.; Albéniz, A. C.; Espinet, P.

Selective Green Coupling of Alkynyltins and Allylic Halides to Trienynes via a Tandem Double Stille Reaction *Adv. Synth. Catal*. **2010**, *352*, 2887-2891. c) Martínez-Arranz, S.; Carrera, N.; Albéniz, A. C.; Espinet, P.; Vidal-Moya, A. Batch Stille Coupling with Insoluble and Recyclable Stannylated Polynorbornenes *Adv. Synth. Catal*. **2012**, *354*, 3551-3560. NHCs: d) Molina de la Torre, J. A.; Albéniz, A. C. N-Heterocyclic Carbenes Supported on Vinylic Addition Polynorbornene: A Recyclable and Recoverable Organocatalyst *ChemCatChem* **2014**, *6*, 3547-3552. e) Molina de la Torre, J. A.; Albéniz, A. C. Vinylic Addition Polynorbornene as Support for N-Heterocyclic Carbene Palladium Complexes: Use as Reservoir of Active Homogeneous Catalytic Species in C-C Cross-Coupling Reactions *ChemCatChem* **2016**, *8*, 2241-2248. Organocatalysis: f). Sagamanova, I. K.; Sayalero, S.; Martínez-Arranz, S.; Albéniz, A. C.; Pericàs, M. A. Asymmetric organocatalysts supported on vinyl addition polynorbornenes for work in aqueous media *Catal. Sci. Technol*. **2015**, *5*, 754-764. Diimines: g) Molina de la Torre, J. A.; Albéniz, A. C. α-Diimine-Palladium Complexes Incorporated in Vinylic-Addition Polynorbornenes: Synthesis and Catalytic Activity *Eur. J. Inorg. Chem*. **2017**, 2911-2919. Radical reactions: h) García-Loma, R.; Albéniz, A. C. Stannylated Vinylic Addition Polynorbornene: Probing a Reagent for Friendly Tin-Mediated Radical Processes *Eur. J. Org. Chem*. **2017**, 4247-4254.

104. a) Kang, M.; Sen, A. Reaction of Palladium 1,5-Cyclooctadiene Alkyl Chloride with Norbornene Derivatives: Relevance to Metal-Catalyzed Addition Polymerization of Functionalized Norbornenes *Organometallics* **2004**, *23*, 5396-5398. b) Funk, J. K.; Andes, C. E.; Sen, A. Addition Polymerization of Functionalized Norbornenes: The Effect of Size, Stereochemistry, and Coordinating Ability of the Substituent *Organometallics* **2004**, *23*, 1680-1683. c) Potier, J.; Commarieu, B.; Soldera, A.; Claverie, J. P. Thermodynamic Control in the Catalytic Insertion Polymerization of Norbornenes as Rationale for the Lack of Reactivity of Endo- Substituted Norbornenes *ACS Catal*. **2018**, *8*, 6047-6054.

105. Blank, F.; Scherer, H.; Janiak, C. Oligomers and soluble polymers from the vinyl polymerization of norbornene and 5-vinyl-2-norbornene with cationic palladium catalysts *J. Mol. Cat. A: Chem.* **2010**, *330*, 1-9.

106. a) Farquhar, A. H.; Brookhart, M.; Miller, A. J. M. Oligomerization and polymerization of 5-ethylidene-2-norbornene by cationic palladium and nickel catalysts *Polym. Chem*. **2020**, *11*, 2576-2484. b) Bermesheva, E. V.; Wozniak, A. I.; Fedor A. Andreyanov, F. A.; Karpov, G. O.; Nechaev, M. S.; Asachenko, A. F.; Topchiy, M. A.; Melnikova, E. K.; Nelyubina, Y. V.;

Gribanov, P. S.; Bermeshev, M. V. Polymerization of 5-Alkylidene-2-norbornenes with Highly Active Pd-N-Heterocyclic Carbene Complex Catalysts: Catalyst Structure-Activity Relationships *ACS Catal*. **2020**, *10*, 1663-1678.

107. a) Strohmeier, W.; Müller, F. -J. Klassifizierung phosphorhaltiger Liganden in Metallcarbonyl-Derivaten nach der π-Acceptorstärke *Chem. Ber*. **1967**, 2812-2821. b) Tolman, C. A.; Seidel, W. C.; Gosser, L. W. Formation of three-coordinate nickel(0) complexes by phosphorus ligand dissociation from NiL_4 *J. Am. Chem. Soc.* **1974**, 96, 53-60. c) Tolman, C. A. Steric Effects of Phosphorus Ligands in Organometallic Chemistry and Homogeneous Catalysis **1977**, *3*, 313-347.

108. Breunig, S.; Risse, W. Transition-metal-catalyzed vinyl addition polymerizations of norbornene derivatives with ester groups *Makromol. Chem.* **1992**, *193*, 2915-2927.

109. a) Torraca, K. E.; Huang, X. H.; Parrish, C. A.; Buchwald, S. L. An Efficient Intermolecular Palladium-Catalyzed Synthesis of Aryl Ethers *J. Am. Chem. Soc*. **2001**, *123*, 10770-10771. b) Lee, S.; Beare, N. A.; Hartwig, J. F. Palladium-Catalyzed α-Arylation of Esters and Protected Amino Acids *J. Am. Chem. Soc.* **2001**, *123*, 8410-8411. c) Littke, A. F.; Schwarz, L.; Fu, G. C. Pd/P(t-Bu)3: A Mild and General Catalyst for Stille Reactions of Aryl Chlorides and Aryl Bromides *J. Am. Chem. Soc*. **2002**, *124*, 6343-6348. d) Littke, A. F.; Fu, G. C. Palladium-Catalyzed Coupling Reactions of Aryl Chlorides *Angew. Chem., Int. Ed*. **2002**, *41*, 4176-4121. e) Strieter, E. R.; Blackmond, D. G.; Buchwald, S. L. Insights into the Origin of High Activity and Stability of Catalysts Derived from Bulky, Electron-Rich Monophosphinobiaryl Ligands in the Pd-Catalyzed C-N Bond Formation *J. Am. Chem. Soc*. **2003**, *125*, 13978-13980. f) Anderson, K. W.; Buchwald, S. L. General Catalysts for the Suzuki-Miyaura and Sonogashira Coupling Reactions of Aryl Chlorides and for the Coupling of Challenging Substrate Combinations in Water *Angew. Chem., Int. Ed*. **2005**, *44*, 6173-6177.

110. a) Yamashita, M.; Takamiya, I.; Jin, K.; Nozaki, K. Syntheses and Structures of Bulky Monophosphine-Ligated Methylpalladium Complexes: Application to Homo- and Copolymerization of Norbornene and/or Methoxycarbonylnorbornene *Organometallics* **2006**, *25*, 4588-4595. b) Yamashita, M.; Takamiya, I.; Jin, K.; Nozaki, K. Syntheses of Ester-Substituted Norbornyl Palladium Complexes Ligated with $^tBu_3P$: Studies on the Insertion of exo- and endo-Monomers in the Ester-Substituted Norbornene Polymerization *Organometallics* **2008**, *27*, 5347-5352 c) Kim, D. -G.; Bell, A.; Register,

R. A. Living Vinyl Addition Polymerization of Substituted Norbornenes by a *t*-Bu_3P-Ligated Methylpalladium Complex *ACS Macro Lett*. **2015**, *4*, 327-330.

111. Wendt, A. R.; Fink, G. Homogeneous metallocene/MAO-catalyzed polymerizations of polar norbornene derivatives: copolymerizations using ethene, and terpolymerizations using ethene and norbornene *Macromol. Chem. Phys.* **2000**, *201*, 1365-1373.

112. Martínez-Arranz, S.; Albéniz, A. C.; Espinet, P. Versatile Route to Functionalized Vinylic Addition Polynorbornenes. *Macromolecules* **2010**, *43*, 7482-7487.

113. Park, K. H.; Twieg, R. J.; Ravikiran, R.; Rhodes, L. F.; Shick, R. A.; Yankelevich, D.; Knoesen, A. Synthesis and Nonlinear-Optical Properties of Vinyl-Addition Poly(norbornene)s *Macromolecules* **2004**, *37*, 5163-5178.

114. Nomura, K.; Liu, J.; Fujiki, M.;Takemoto, A. Facile, Efficient Functionalization of Polyolefins via Controlled Incorporation of Terminal Olefins by Repeated 1,7-Octadiene Insertion. *J. Am. Chem. Soc.* **2007**, *129*, 14170-14171.

115. Commarieu, B.; Potier, J.; Compaore, M.; Dessureault, S.; Goodall, B. L.; Li, X.; Claverie, J. P. Ultrahigh Tg Epoxy Thermosets Based on Insertion Polynorbornenes. *Macromolecules*, **2016**, *49*, 920-925.

116. Nozaki, K.; Komaki, H.; Kawashima, Y.; Hiyama, T.; Matsubara, T. Predominant 1,2-Insertion of Styrene in the Pd-Catalyzed Alternating Copolymerization with Carbon Monoxide *J. Am. Chem. Soc.* **2001**, *123*, 534-544.

117. Sen, A.; Lai, T. W.; Thomas, R. R. Reactions of electrophilic transition metal cations with olefins and small ring compounds. Rearrangements and polymerizations *J. Organomet. Chem.* **1988**, *358*, 567-588.

118. Sen, A. Organometallic Chemistry of Electrophilic Transition and Lanthanide Metal Ions. The Dominant Pathways for Reactions Involving C=C, C-C, and C-H Bonds *Acc. Chem. Res.* **1988**, *21*, 421-428.

119. Fineman, R.; Ross, S. D. Linear Method for Determining Monomer Reactivity Ratios Copolymerization *J. Polym. Sci*. **1950**, *5*, 259-269.

120. Rudin, A.; Choi, P. The Elements of Polymer Science & Engineering. *In Copolymerization*; Academic Press; 2013; pp. 391-425.

121. a) Krossing, I. Raabe, I. Noncoordinating Anions-Fact or Fiction? A Survey of Likely Candidates *Angew. Chem. Int. Ed*. **2004**, *43*, 2066-2090. b) BÖing, C.; Franciò, G.; Leitner, W. Cationic Nickel Complexes with WeaklyCoordinating Counterions and Their Application in the Asymmetric Cycloisomerisation of 1,6-Dienes *Adv. Synth. Catal*. **2005**, *347*, 1537-1541. c). Brownie, J. H.; Baird, M. C. Formation and Properties of a Novel Dinuclear, Cationic α-Diimine Palladium-Based Ethylene Polymerization Catalyst Containing a Pd-Pd Bond and Bridging Methylene and Methyl Groups *Organometallics* **2003**, *22*, 33-41.

122. Goel A. B.; Goel S.; Formation of Unusual Palladium(II) Complexes Containing Metalated Tri-t-Butylphosphine and Bidentate Ligands *Inorg. Chim. Acta* **1985**, *98*, 67-70.

123. Chu, P. P.; Huang, W.-J.; Chang, F.-C.; Fan, S. Y. Conformational conversion and chain ordering in cyclo olefin copolymer (COC) *Polymer* **2000**, *41*, 401-404

124. a) Raducan, M.; Rodríguez-Escrich, C.; Cambeiro, X. C.; Escudero-Adán, E. C: Pericás, E. C.; Echavarren, A. M. A multipurpose gold(I) precatalyst. *Chem. Commun*., **2011**, *47*, 4893-4895. b) Swennenhuis, B. H. G.; Chen, R.; Van Leeuwen, P. W. N. M.; Vries, J. G.; Kamer, P. C. J. Supported Chiral Monodentate Ligands in Rhodium-Catalysed Asymmetric Hydrogenation and Palladium-Catalysed Asymmetric Allylic Alkylation. *Eur. J. Org. Chem*. **2009**, 5796-5803.

125. Williams, B. D. G.; Netshiozwi, T. E. Synthesis and characterisation of severely hindered P-OR compounds *Tetrahedron*, **2009**, *65*, 9973-9982.

126. a) Pandarus, V.; Ciriminna, R.; Gingras, G.; Béland, F.; Kaliaguine, S., Pagliaro, M. Waste-free and efficient hydrosilylation of olefins *Green Chem.* **2019**, *21*, 129-140. b) Nakajimaa, Y.; Shimada, S. Hydrosilylation Reaction of Olefins: Recent Advances and

Perspective *RSC advances* **2015**, 20603-20616. c) Chungkyun, K., Kyungmi, A. Preparation and termination of carbosilane dendrimers based on a siloxane tetramer as a core molecule: silane arborols, part VIII *J. Orgrnomet. Chem.* **1997**, *547*, 55-63. d) Sommer, L. H.; Pietrusza, E. W.; Whitmore, F. C. Peroxide-Catalyzed Addition Of Trichlorosilane To 1-Octene *J. Am. Chem. Soc*. **1947**, *69*, 188-188. e) Speier, J. L. Webster, J. A. G.: Barnes, H. The Addition of Silicon Hydrides to Olefinic Double Bonds. Part II. The Use of Group VIII Metal Catalysts *J. Am. Chem. Soc*. **1957**, *79*, 974-979.

127. Niemiec, W.; Szczygiel, P.; Jelén, P.; Handke, M. IR investigation on silicon oxycarbide structure obtained from precursors with 1:1 silicon to carbon atoms ratio and various carbon atoms distribution *J. Mol. Struct.* **2018**, *1164*, 217-226.

128. H. G. G. Dekking, Synthesis and polymerization of an alkene-substituted norbornylene *J. Pol. Sci.* **1961**, *55*, 525-530.

129. A. Zwierzak, Cyclic organophosphorus compounds. I. Synthesis and infrared spectral studies of cyclic hydrogen phosphites and thiophosphites *Can. J. Chem.* **1967**, *45*, 2501-2512.

130. a) Salari, A.; Young, R. E. Application of attenuated total reflectance FTIR spectroscopy to the analysis of mixtures of pharmaceutical polymorphs *Int. J. Pharm* **1998**, *163*, 157-166. b) Hua, Y.; Erxlebena, A.; Rydera, A. G.; McArdle, P. Quantitative analysis of sulfathiazole polymorphs in ternary mixtures by attenuated total reflectance infrared, near-infrared and Raman spectroscopy *J. Pharm. Biomed. Anal.* **2010**, *53*, 412-420. c) Mallah, M. A.; Sherazi, S. T. H.; Bhanger, M. I.; Sarfaraz Ahmed Mahesar, Bajeer, M. A. A rapid Fourier-transform infrared (FTIR) spectroscopic method for direct quantification of paracetamol content in solid pharmaceutical *Spectrochim. Acta A Mol. Biomol. Spectrosc* **2015**, *141*, 64-70.

131. Mayo, F. R.; Lewis, F. M. Copolymerization. I. A Basis for Comparing the Behavior of Monomers in Copolymerization; The Copolymerization of Styrene and Methyl Methacrylate *J. Am. Chem. Soc.* **1944**, *66*, 1594-1601.

132. a) Karafilidis, C.; Hermann, H.; Rufínska, A.; Gabor, B.; Mynott, R. J.; Breitenbruch, G.; Weidenthaler, C.; Rust, J.; Joppek, W.; Brookhart, M. S.; Thiel, W.; Fink, G. Metallocene-Catalyzed C7-Linkage in the Hydrooligomerization of Norbornene by σ-Bond Metathesis:

Insight into the Microstructure of Polynorbornene *Angew. Chem. Int. Ed*. **2004**, *43*, 2444-2446. b) Karafilidis, C.; Angermund, K.; Gabor, B.; Rufínska, A.; Mynott, R. J.; Breitenbruch, G.; Thiel, W.; Fink, G. Helical Microstructure of Polynorbornene *Angew. Chem. Int. Ed*. **2007**, *46*, 3745-3749.

133. Deng, J.; Gao, H.; Zhu, F.; Wu, Q. Synthesis and Structure of Imine-N-Heterocyclic Carbene Palladium Complexes and Their Catalytic Behavior in Norbornene Polymerization *Organometallics* **2013**, *32*, 4507-4515.

134. a) Dall'asta, G.; Motroni, G. Polymerization of Cyclobutene Rings. VII. Polymerization of Bicyclo[4,2,0]octa-7-ene and Bicyclo[3,2,0]hepta-2,6-diene with Ziegler-Natta Catalysts and with Group VIII Metal Halides *J. Polym. Sci. A: Pol. Chem* **1968**, *6*, 2405-2413. b) Dall'asta, G.Polymerization of cyclobutene rings. VI. Influence of the organometallic compound of the Ziegler-Natta catalysts on the mechanism of polymerization of cyclobutene and 3-methylcyclobutene *J. Polym. Sci. A: Pol. Chem* **1968**, *6*, 2397-2404.

135. Johnston, J. A.; Tokles, M.; Hatvany, G. S.; Rinaldi, P. L.; Farona, M. F. Polymerization of norbornene by olefin metathesis catalysts: insertion and ring opening in the same chain *Macromolecules* **1991**, *24*, 5532-5534.

136. a) Hartner, F. M.; Schwartz, J.; Clift, S. M. Synthesis of carbene complexes of Group IV metals from alkylidene-bridged heterobimetallic precursors *J. Am. Chem. Soc.* **1983**, *105*, 640-641. b) Tritto, I.; Sacchi, M. C.; Grubbs, R. H. From ring-opening metathesis polymerization to Ziegler-Natta polymerization: A method for obtaining polynorbornene-polyethylene block copolymers *J. Mol. Catal.* **1993**, *82*, 103-111. c) Manivannan, R.; Sundararajan, G.; Kaminsky, W. Switching the mechanism of polymerisation from vinyl addition to metathesis using single-site catalysts *Macromol. Rapid Commun.* **2000**, *21*, 968-972. d) Manivannan, R.; Sundararajan, G.; Kaminsky, W. Studies in switching the mechanism of polymerisation by single-site catalysts-from vinyl addition to metathesis *J. Mol. Catal. A: Chem.* **2000**, *160*, 85-95.

137. a) Zou, Y.; Wang, D.; Wurst, K.; Kühnel, C.; Reinhardt, I.; Decker, U.; Gurram, V.; Camadanli, S.; Buchmeiser, M. R. Group 4 Dimethylsilylenebisamido Complexes Bearing the 6-[2-(Diethylboryl)phenyl]pyrid-2-yl Motif: Synthesis and Use in Tandem Ring- Opening

Metathesis/Vinyl-Insertion Copolymerization of Cyclic Olefins with Ethylene *Chem. Eur. J.* **2011**, *17*, 13832-13846. b) Buchmeiser, M. R.; Camadanli, S.; Wang, D.; Zou, Y.; Decker, U.; Kühnel, C.; Reinhardt, I. A Catalyst for the Simultaneous Ring-Opening Metathesis Polymerization/ Vinyl Insertion Polymerization *Angew. Chem. Int. Ed.* **2011**, *50*, 3566-3571.

138. Gold, L. Statistics of Polymer Molecular Size Distribution for an Invariant Number of Propagating Chains*J. Chem. Phys.* **1958**, *28*, 91-99.

139. Woo, T. K.; Fan, L.; Ziegler, T. A Density Functional Study of Chain Growing and Chain Terminating Steps in Olefin Polymerization by Metallocene and Constrained Geometry Catalysts *Organometallics* **1994**, 13, 2252-2261.

140. Lohrenz, J. C. W.; Woo, T. K.; Fan, L.; Ziegler, T. A density functional study on the insertion mechanism and chain termination in Kaminsky-type catalysts; comparison of frontside and backside attack *J. Organomet. Chem.* **1995**, *497*, 91-104.

141. Margl, P.; Deng, L.; Ziegler, T.; A Unified View of Ethylene Polymerization by d^0 and d^0f^n Transition Metals. 3. Termination of the Growing Polymer Chain *J. Am. Chem. Soc*. **1999**, *121*, 154-162.

142. O'Connor, K. S.; Lamb, J. R.; Vaidya, T.; Keresztes, I.; Klimovica, K.; LaPointe, A. M.; Daugulis, O.; Coates, G. W. Understanding the Insertion Pathways and Chain Walking Mechanisms of α-Diimine Nickel Catalysts for α-Olefin Polymerization: A 13C NMR Spectroscopic Investigation *Macromolecules* **2017**, *50*, 7010-7027.

143. Benedikt, G. M.; Elce, E.; Goodall, B. L.; Kalamarides, H. A.; McIntosh, L. H.; Rhodes, L. F.; Selvy, K. T.; Andes, C.; Oyler, K.; Sen, A. Copolymerization of Ethene with Norbornene Derivatives Using Neutral Nickel Catalysts *Macromolecules* **2002**, *35*, 8978-8988.

144. Kandanarachchi, P.; Chang, C.; Simth, S.; Bradley, P.; Rhodes, L. F.; Lattimer, R. P.; Benedikt, G. M. Palladium catalyzed vinyl addition Poly(norbornenes): Formic Acid as a Chain Transfer Agent. Mechanism and Polymer Optical Properties *J. Photopolym. Sci. Thecnol*. **2013**, *26*, 431-439.

145. McDermott, J.; Chang, C.; L. Martín, F.; Rhodes, L. F. β-γ-Carbon-Carbon Bond Cleavage as a Prelude to Chain Transfer in Ester-Functionalized Norbornene Polymerization *Macromolecules* **2008**, *41*, 2984-2986.

146. a) Noyori, R.; Takaya, H. Reaction of Methylenecyclopropanes with Palladium Chloride *J. Chem. Soc. D*, **1969**, 525-525. b) Miller, R. G.; Golden, H. J.; Baker, D. J.; Stauffer, R. D. Homogeneous Catalysis of Diene Rearrangements via a Carbon-Metal β Elimination *J. Am. Chem. Soc.* **1971**, *93*, 6308-6309. c) Calvo, C.; Hosokawa, T.; Reinheimer, H.; Maitlis, P. M. A Model System for Acid and Base Reactions, Carbonylation, and β-Hydride Elimination in Organopalladium Chemistry *J. Am. Chem. Soc.* **1972**, *94*, 3238-3240. d) Nishimura, T.; Uemura, S. Palladium(0)-Catalyzed Ring Cleavage of Cyclobutanone Oximes Leading to Nitriles via β-Carbon Elimination *J. Am. Chem. Soc.* **2000**, 122, 12049-12050. e) Zhang, Z.; Lu, X.; Xu, Z.; Zhang, Q.; Han, X. Role of Halide Ions in Divalent Palladium-Mediated Reactions: Competition between β-Heteroatom Elimination and β-Hydride Elimination of a Carbon-Palladium Bond *Organometallics* **2001,** *20*, 3724-3728. f) Satoh, T.; Miura, M.; Catalytic Processes Involving b-Carbon Elimination *Top Organomet. Chem.* **2005**, *14*, 1-20. g) Matsuda, T.; Ashida, S.; Murakami, M. Eight-Membered Ring Construction by [4 + 2 + 2] Annulation Involving β-Carbon Elimination *J. Am. Chem. Soc.* **2006**, *128*, 2166-2167. h) O'Reilly, M. E.; Dutta, S.; Veige A. S. β-Alkyl Elimination: Fundamental Principles and Some Applications *Chem. Rev.* **2016**, *116*, 8105-8145. i) Fumagalli, G.; Stanton, S.; Bower, J. F. Recent Methodologies That Exploit C-C Single-Bond Cleavage of Strained Ring Systems by Transition Metal Complexes *Chem. Rev.* **2017**, *117*, 9404-9432. j) Song, F.; T Gou, T.; Wanga, B. -Q.; Shi, Z. -J. Catalytic activations of unstrained C-C bond involving organometallic intermediates *Chem. Soc. Rev.* **2018**,*47*, 7078-7115. k) Cao, J.; Chen, J.; Sun, F. -N.; Sun, Y. -L.; Jiang, K. -Z.; Yang, K. -F.; Xu, Z.; Xu, L.-W. Pd-Catalyzed Enantioselective Ring Opening/Cross-Coupling and Cyclopropanation of Cyclobutanones *Angew. Chem. Int. Ed.* **2019**, *58*, 897-901.

147. Albéniz, A. C.; Espinet, P.; Lin, Y. -S. Cyclization versus Pd-H Elimination-Readdition: Skeletal Rearrangement of the Products of Pd-C_6F_5 Addition to 1,4-Pentadienes *J. Am. Chem. Soc.* **1996**, *118*, 7145-7152

148. a) Green, M.; Hughes, R. P. Reactions of co-ordinated ligands. Part XI. The ring opening of methylenecyclopropanes by palladium(II)-nucleophile systems: formation of substituted η^3-but-3-enyl complexes of palladium(II) *J. Chem. Soc., Dalton Trans*. **1976**, 1880-1889. b) Larock, R. C.; Varaprath, S. Mercury in organic chemistry. 30. Synthesis of (.pi.-allyl)palladium compounds via organopalladium additions to alkenyl- and

methylenecyclopropanes and alkenyl- and methylenecyclobutanes *J. Org. Chem*. **1984**, *49*, 3432-3435 c) Fischetti, W.; Heck, R. F. The mechanism of reactions of organopalladium salts with vinylcyclopropanes *J. Organomet. Chem.* **1985**, *293*, 391-405. d) Owczarczyk, Z.; Lamaty, F.; Vawter, E. J.; Negishi, E. Apparent Endo-Mode Cyclic Carbopalladation with Inversion of Alkene Configuration via Exo-Mode Cyclization-Cyclopropanation-Rearrangement *J. Am. Chem. Soc.* **1992**, *114*, 10091-10092.

149. Campora, J.; Gutierrez-Puebla, E.; Lopez, J. A.; Monge, A.; Palma, P.; del Rio, D.; Carmona, E. Cleavage of the C-Alkyl-C-Aryl Bond of [Pd-CH_2CMe_2Ph] Complexes. *Angew. Chem., Int. Ed*. **2001**, *40*, 3641.

150. a) Catellani, M.; Chiusoli, G. P. Catalytic Activation of Aromatic C-H Bonds. *J. Organomet. Chem.* **1982**, *239*, C35-C37. b) Catellani, M.; Chiusoli, G. P. Palladium-Catalyzed Synthesis of 1,2,3,4,4a,12b-Hexahydro-1,4-Methanotriphenylenes. *J. Organomet. Chem*. **1985**, *286*, C13-C16. c) Catellani, M.; Chiusoli, G. P.; Ricotti, S. A New Palladium-Catalyzed Synthesis of 1,2,3,4,4a,8b-Hexahydro-1,4-methanobipheny- lenes and 2-Phenylbicyclo[2.2.1]hept-2-enes. *J. Organomet. Chem.* **1985**, *296*, C11-C15.

151. a) Wang, J.; Dong, G. Palladium/Norbornene Cooperative Catalysis *Chem. Rev*. **2019**, *119*, 7478-7528. b) Della Ca', N.; Fontana, M.; Motti, E.; Catellani, M. Pd/ Norbornene: A Winning Combination for Selective Aromatic Functionalization via C-H Bond Activation. *Acc. Chem. Res*. **2016**, *49*, 1389-1400.

152. a) Catellani, M.; Chiusoli, G. P.; Sgarabotto, P. Palladium-Catalyzed Syntheses of Condensed Cyclopentanes. The Crystal and Molecular Structure of 3-benzylidenpentacyclo[9.2.l.^{5,8}.1$^{1.11}$.0 $^{2.10}$.0.$^{4.9}$]-pentadecane *J. Organomet. Chem.* **1982**, *240*, 311-319. b) Catellani, M.; Chiusoli, G. Palladium-catalyzed sequential insertion of double bonds followed by β,γ-cleavage of a C-C bond *J. Organomet. Chem.* **1983**, 247, C59-C62. c) Bocelli, G.; Catellani, M.; Chiusoli, G. P. Palladium-catalyzed c-c bond formation involving aromatic c-h activation III *. aspects of aromatic substitution and structure of 1-bromo-3-[3-(2-methylenecyclohex-5-en-1-yl)bicyclo[2.2.1)hept-2-yl-]4-bicyclo[2.2.1)hept-2 ylbenzene** *J. Organomet. Chem.* **1984**, *219*, 225-232. d) Catellani, M. Catalytic Multistep Reactions via Palladacycles *Synlett* **2003**, *3*, 298-313.

153. Dzhemilev, U. M.; Khusnutdinov, R. I.; Galeev, D. K.; Tolstikov, G. A. Homodimerization of bicyclo[2.2.1]-2-heptene in Presence of Complex Nickel Catalysts *Izvestiya Akademii Nauk SSSR*, **1979**, *28*, 854-856.

154. Tenaglia, A.; Terranova, A.; Waegell, B. Nickel-catalyzed dimerization of norbornene *J. Mol. Cat.* **1987**, *40*, 281-287

155. Portnoy, M.; Ben-David, Y.; Rousso, I.; Milstein, D. Reactions of Electron-Rich Arylpalladium Complexes with Olefins. Origin of the Chelate Effect in Vinylation Catalysis *Organometallics* **1994**, *13*, 3465-3479.

156. Standley, E. A.; Smith, S. J.; Müller, P.; Jamison, T. F. Broadly Applicable Strategy for Entry into Homogeneous Nickel(0) Catalysts from Air-Stable Nickel(II) Complexes *Organometallics* **2014**, 33, 2012-2018.

157. SennŌ, M.; Tsuchiya, S.; Hidai, M.; Uchida, Y. X-Ray Photoelectron Spectra of Aryl-Nickel Complexes *Bull. Chem. Soc. Japan*, **1976**, *49*, 1184-1186.

158. 8 is the number of protons of the cyclohexene ring of NB_{ROint}; 5 are the protons of the cyclohexene ring of NB_{ROterm};10 are the protons of the norbornene.

159. Muetterties, E. L.; Alegranti, C. W. Solution Structure and Kinetic Study of Metal-Phosphine and-Phosphite Complexes. I. The Silver (I) System *J. Am. Chem. Soc.* **1972**, 94, 6386-6391.

160. Bachman, R. E.; Andretta, D. F. Metal-Ligand Bonding in Coinage Metal-Phosphine Complexes: The Synthesis and Structure of Some Low-Coordinate Silver(I)-Phosphine Complexes *Inorg. Chem.* **1998**, *37*, 5657-5663.

161 a) Aalyea, E. C.; Dia, S. A. Stevens, S. Two coordinate Silver(I) Complexes of Trimesitylphosphine and Trimesitylarsine *Inorganica Chim. Acta* **1980**, 44, L203-L204. b) Camalli, M.; Caruso, F.Correlation Between ^{31}P NMR Data and Structural Parameters on $Ag(PPh_3)_3X$ Series. Crystal and

Molecular Structure of Tris(triphenylphosphine)silver(I)tetrafluoroborate and Tris(triphenylphosphine)silver(I)iodide *Inorganica Chim. Acta* **1987**, *127*, 209-213.

162. Barron, P. F.; Dyason, J. C.; Healy, P. C.; Engelhardt, L. M.; Skelton, B. W.; White, A. H. Lewis Base Adducts of Group 11 Metal Compounds. Part 24. Co-ordination of Triphenylphosphine with Silver Nitrate. A Solid-state Cross-polarization Magic Angle Spinning ^{31}P Nuclear Magnetic Resonance, Crystal Structure, and Infrared Spectroscopic Study of $Ag(PPh_3)_nNO_3$ (n = 1-4) *J. Chem. Soc., Dalton Trans.* **1986**, 1965-1970.

163. a) Klein, H. F.; Karsch, H. K. Methyl(trimethy1phosphin)nickel-hydroxid und verwandte Verbindungen *Chem. Rer.* **1973**, *106*, 1433-1452. b) Christian, A. H.; Müller, P.; Monfette, S. Nickel Hydroxo Complexes as Intermediates in Nickel-Catalyzed Suzuki-Miyaura Cross-Coupling *Organometallics* **2014**, *33*, 2134-2137. c) Carmona, E.; Pilar Palma, J. M. M; Paneque, M.; Poveda, M. L. Pyrrolyl, Hydroxo, and Carbonate Organometallic Derivatives of Nickel(II). Crystal and Molecular Structure of $[Ni(CH_2C_6H_4$-*o*-$Me)(PMe_3)(\mu\text{-}OH)]_2 \cdot 2,5\text{-}HNC_4H_2Me_2$ *Inor. Chem.*, **1989**, *28*, 1895-1900.

164. Cotton, A. F.; Frenz, B. A.; Hunter, D. L. Structure of (2,4-Pentanedionato) (triphenylphosphine)ethylnickel(II) in the Crystalline State and in Solution *J. Am. Chem. Soc* **1974**, *96*, 4820-4825.

165. Horváthm, I. T.; Anastas, P. T. Innovations and Green Chemistry *Chem. Rev.* **2007**, *107*, 2169-2173.

166. Li, C. J. Organic Reactions in Aqueous Media with a Focus on Carbon−Carbon Bond Formations: A Decade Update *Chem. Rev.* **2005**, *105*, 3095-3165.

167. Trost, B. On Inventing Reactions for Atom Economy *Acc. Chem. Res.* **2002**, *35*, 695-705.

168. Hodge, P. Polymer-supported organic reactions: what takes place in the beads? *Chem. Soc. Rev*. **1997**, *26*, 417-423.

169. Yu, H.; Zheng, X.; Lin, Z.; Hu, Q.; Huang, W.; Pu, L. Asymmetric Epoxidation of α,β-Unsaturated Ketones Catalyzed by Chiral Polybinaphthyl Zinc Complexes: Greatly Enhanced Enantioselectivity by a Cooperation of the Catalytic Sites in a Polymer Chain *J. Org. Chem.* **1999**, *64*, 8149-8155.

170. Harrison, C. R.; Hodge, P.; Hunt, B. J.; Khoshdel, E.; Richardson, G. Preparation of alkyl chlorides, acid chlorides, and amides using polymer-supported phosphines and carbon tetrachloride: mechanism of these reactions *J. Org. Chem.* **1983**, *48*, 3721-3728.

171. Egorova, K. S.; Ananikov, V. P. Toxicity of Metal Compounds: Knowledge and Myths *Organometallics* **2017**, *36*, 4071-4090.

172. For reviews about polymer-supported catalysts, see: a) Clark, J. H.; Mcquarrie, D. Handbook of Green Chemistry & Technology; Blackwell Publ., London, 2002. b) Leadbeater, N. E.; Marco, M. Preparation of Polymer-Supported Ligands and Metal Complexes for Use in Catalysis *Chem. Rev*. **2002**, *102*, 3217-3274. c) McNamara, C. A.; Dixon, M. J.; Bradley, M. Recoverable Catalysts and Reagents Using Recyclable Polystyrene-Based Supports *Chem. Rev*. **2002**, 102, 3275-3300. d) Buchmeiser, M. R. Polymeric materials in organic synthesis and catalysis, Wiley-VCH, Weinheim, 2003. e) Benaglia, M.; Puglisi A.; Cozzi, F. Polymer-Supported Organic Catalysts *Chem. Rev.* **2003**, *103*, 3401-3430. f) Dioos, B. M. L.; Vankelecom, I. F. J.; Jacobs, P. A. Aspects of Immobilisation of Catalysts on Polymeric Supports *Adv. Synth. Catal*. **2006**, *348*, 1413-1446. g) Itsuno, S.; Haraguchi, N. Handbook of Asymmetric Heterogeneous Catalysis. *In Heterogeneous Enantioselective Catalysis Using Organic Polymeric Supports* eds. Ding K.; Uozumi, Y.; WileyVCH, Weinheim, 2008, pp. 73-129. h) Benaglia, M Recoverable and Recyclable Catalysts; John Wiley & Sons, Chichester, 2009.

173. a) Orlandi, S.; Mandoli, A.; Pini, D.; Salvadori, P. An Insoluble Polymer-Bound Bis-Oxazoline Copper(II) Complex: A Highly Efficient Heterogeneous Catalyst for the Enantioselective Mukaiyama Aldol Reaction *Angew. Chem., Int. Ed.*, **2001**, *40*, 2519-2521. b) Mandoli, A.; Orlandi, S.; Pini, D.; Salvadori, P. A reusable, insoluble polymer-bound bis(oxazoline) (IPB-box) for highly enantioselective heterogeneous cyclopropanation reactions. *Chem. Commun*. **2003,** 2466-2467. c) Valodkar, V. B.; Tembeb, G. L.;

Ravindranathan, M.; Rama, R. N; Ramaa H. S. Catalytic oxidation by polymer-supported copper(II)-L-valine complexes *J. Mol. Cat. A: Chem*. **2004**, *208*, 21-32. d) Chiang, G. C. H.; Olsson, T. Polymer-Supported Copper Complex for C-N and C-O Cross-Coupling *Org. Lett.* **2004**, *6*, 3080-3082. e) Werner, H.; Herrerías, C. I.; Glos, M.; Gissibl, A.; Fraile, J. M.; Péres, I.; Mayoral, J. A.; Reiser, O. Synthesis of polymer bound azabis(oxazoline) ligands and their application in asymmetric cyclopropanations *Adv. Synth. Catal.* **2006**, *348*, 125-132. f) Drabina, P.; Svoboda, J.; Sedlák, M. Recent Advances in C-C and C-N Bond Forming Reactions Catalysed by Polystyrene-Supported Copper Complexes *Molecules* **2017**, *22*, 865-883. g) Yan, S.; Pan, S.; Osako, T.; Uozumi, Y. Solvent-Free A3 and KA2 Coupling Reactions with mol ppm Level Loadings of a Polymer-Supported Copper(II)-Bipyridine Complex for Green Synthesis of Propargylamines *ACS Sustainable Chem. Eng.* **2019**, *7*, 9097-9102.

174. a) Chtchigrovsky, M.; Primo, A.; Gonzalez, P.; Molvinger, K.; Robitzer, M.; Quignard, F.; Taran, F. Functionalized Chitosan as a Green, Recyclable, Biopolymer-Supported Catalyst for the [3+2] Huisgen Cycloaddition *Angew. Chem. Int. Ed.* **2009**, *48*, 5916-5920. b) Pourjavadi, A.; Habibi, Z. Cellulose-Immobilized NHC-Cu(I) Complex: An Efficient and Reusable catalyst for Multicomponent Synthesis of 1,2,3-Triazoles *RSC Adv*. **2015**, 99498-99501. c) Mandala, B. H.; Rahman, L.; Hasbi, Rahim M. H.; Sarkar, S.M. Highly Active Kenaf Bio-Cellulose Based Poly(hydroxamic acid) Copper Catalyst for Aza-Michael Addition and Click Reactions *ChemistrySelect* **2016**, *1*, 2750-2756. d) Mandala, B. H.; Rahman, L. Yusoffa, M. M.; Chonga, K. F.; Sarkara, S. M. Bio-waste corn-cob cellulose supported poly(hydroxamic acid)copper complex for Huisgen reaction: Waste to wealth approach *ChemistrySelect* **2016**, *1*, 2750-2756. e) Sarkar, S. M.; Rahman, L. Cellulose supported poly(amidoxime) copper complex for Click reaction *J. Clean. Prod.* **2017**, *141*, 683-692.

175. a) Sun, Z.; Unruean, P.; Aoki, H.; Kitiyanan, B.; Nomura, K. Phenoxide-Modified Half-Titanocenes Supported on Star-Shaped ROMP Polymers as Catalyst Precursors for Ethylene Copolymerization *Organometallics 2020*, **39**, *16*, 2998-3009. b) Vidal, F.; McQuade, J.; Lalancette, R.; Jäkle, F. ROMP-Boranes as Moisture-Tolerant and Recyclable Lewis Acid Organocatalysts *J. Am. Chem. Soc*. **2020**, *142*, 14427-14431. c) Kröll, R. M.; Schuler, N.; Lubbad, S.; Buchmeiser, M. R. A ROMP-derived, polymer-supported chiral Schrock catalyst for enantioselective ring-closing olefin metathesis *Chem. Commun*., **2003**, 2742-2743.

176. a) Trofimenko, S. Boron-Pyrazole Chemistry. *J. Am. Chem. Soc*. **1966**, *88*, 1842-1844. b) Trofimenko, S. Recent Advances in Poly(pyrazoly1) borate (Scorpionate) Chemistry. *Chem. Rev*. **1993**, *93*, 943-980. c) S. Trofimenko Scorpionates: The Coordination Chemistry of Polypyrazolylborate Ligands, Imperial College Press, London, 1999. d) C. Pettinari, Scorpionates II: Chelating Borate Ligands, Imperial College Press, London, 2008. e) Pettinari, C.; Santini, C. Comprehensive Coordination Chemistry II, Vol. 1. *In Polypyrazolylborate and Scorpionate Ligands*. Eds.: Mc Claverty J. A.; Meyer T. J. Elsevier, Oxford, 2004, pp. 159-210.

177. Trofimenko, S. Poly(1-pyrazolyl)borates, Their Transition-Metal Complexes, and Pyrazaboles *Inorg. Synth.* **1970**, *12*, 99-109.

178. Janiak, C.; Esser, L.; Teil B, The Bishydridobis(tetrazol-l-yl)borate Anion, $[H_2B(CHN_4)_2]$-: Synthesis and Structure of the First Tetrazolylborate *Z. Naturforsch.***1993**, *48*, 394-396.

179. a) S. Trofimenko, Boron-pyrazole chemistry. II. Poly(1-pyrazolyl)-borates *J. Am. Chem. Soc*. **1967**, *89*, 3170-3177. b) Kitamura, M.; Takenaka, Y.; Okuno, T.; Holl, R.; Wünsch, B. New, Efficient and Direct Preparation of TlTp and Related Complexes with $TlBH_4$ *Eur. J. Inorg. Chem.* **2008**, 1188-1192.

180. a) Cotton, F. A.; Murillo, C. A.; Stults, B. R. Preparation of Several Polypyrazolylborato Compounds. Structures of Two Phenyltrispyrazolylborato Complexes *Inorg. Chim. Acta* **1977**, 22, 75-80. b) White, D. L.; Falle, J. W. Covalently Bound Paramagnetic Shift Reagents. 1. A Versatile Lithium Reagent Derived from Bis[(4-bromophenyl)tris(1-pyrazolyl)borato]cobalt(II) *J. Am. Chem. Soc*. **1982**, *104*, 1548-1552. c) Jäkle, F.; Polborn, K.; Wagner, M. Novel Ferrocene-Based Mono- and Bifunctional Tri-1-pyrazolylborate Ligands *Chem. Ber.* **1996**, *129*, 603-606. d) Biani, F. F.; Jäkle, F.; Spiegler, M.; Wagner, M.; Zanello, P. Ferrocene-Based Tris(1-pyrazolyl)borates: A New Approach to Heterooligometallic Complexes and Organometallic Polymers Containing Transition Metal Atoms in the Backbone *Inorg. Chem.* **1997**, *36*, 2103-2111. e) Kisko, J. L.; Hascall, T.; Kimblin, C.; Parkin, G. Phenyl tris(3-*tert*-butylpyrazolyl)borato complexes of lithium and thallium, $[PhTp^{But}]M$ (M= Li, Tl): a novel structure for a monomeric tris(pyrazolyl)boratothallium complex and a study of its stereochemical nonrigidity by ^1H and

^{205}Tl NMR spectroscopy *J. Chem. Soc., Dalton Trans.* **1999**, 1929-1935. f) Zhang, F.; Bolte, M.; Lerner, H. -W.; Wagner, M. Tl(I)-, Cu(I)-, and Ag(I) Complexes of the Ditopic 1,3-Phenylene-Bridged Heteroscorpionate Ligand $[1,3\text{-}C_6H_4(tBuBpz_2)_2]^{2-}$ *Organometallics* **2004**, *23*, 5075-5080. g) Reger, D. L.; Gardinier, J. R.; Smith, M. D.; Shahin, A. M.; Long, G. J.; Rebbouh, L.; Grandjean, F. Polymorphism in $Fe[(p\text{-}IC_6H_4)B(3\text{-}Mepz)_3]_2$ (pz = Pyrazolyl): Impact of Supramolecular Structure on an Iron(II) Electronic Spin-State Crossover *Inorg. Chem.* **2005**, *44*, 1852-1866. h) Reger, D. L.; Gardinier, J. R.; Gemmill, W. R.; Smith, M. D.; Shahin, A. M.; Long, G. J.; Rebbouh, L.; Grandjean, F Formation of Third Generation Poly(pyrazolyl)borate Ligands from Alkyne Coupling Reactions of $Fe[(p\text{-}IC_6H_4)B(3\text{-}Rpz)_3]_2$ (R) H, Me; pz) Pyrazolyl): Pathways toward Controlling an Iron(II) Electronic Spin-State Crossover.. *J. Am. Chem. Soc*. **2005**, *127*, 2303-2316. i) Graziani, O.; Hamon, P.; Thépot, J. -Y.; Toupet, L.; Szilágyi, P. A.; Molnár, G.; Bousseksou, A.; Tilset, M.; Hamon, J. -R. Novel tert-Butyl-tris(3-hydrocarbylpyrazol-1-yl)borate Ligands: Synthesis, Spectroscopic Studies, and Coordination Chemistry *Inorg. Chem*. **2006**, *45*, 5661-5674.

181. a) Reger, D. L.; Tarquini, M. E. Poly(pyrazolyl)borate complexes of zirconium(IV) *Inorg. Chem.* **1982**, *21*, 840-842. b) Janiak, C.; Braun, L.; Girgsdies, F. A new route to tris(pyrazolyl)borate ligands and new structural variations in TlTp complexes *J. Chem. Soc., Dalton Trans.* **1999**, 3133-3136.

182. a) Díaz-Requejo, M. M.; Pérez, P. J. Coinage Metal Catalyzed C-H Bond Functionalization of Hydrocarbons *Chem. Rev*. **2008**, *108*, 3379-3394. b) Caballero, A.; Pérez, P. J.; *J. Organomet. Chem.* **2015**, *793*, 108-113. C) Caballero, A.; Díaz-Requejo, M. M.; M. R. Fructos, J. Urbano, Pérez P. J. Ligand Design in Metal Chemistry. *In Modern Applications of Trispyrazolylborate Ligands in Coinage Metal Catalysis*. Eds. Stradiotto, M.; Lundgren R. J. John Wiley & Sons, 2016, pp. 308-329.

183. a) Caballero, A.; Díaz-Requejo, M. M.; Fructos, M. R.; Olmos, A.; Urbano, J.; Pérez, P. J. Catalytic functionalization of low reactive $C(sp^3)$-H and $C(sp^2)$-H bonds of alkanes and arenes by carbene transfer from diazo compounds *Dalton Trans.* **2015**, *44*, 20295-20307. b) McKeown, B. A.; Lee, J. P.; Mei, J.; Cundari, T. R.; Gunnoe, T. B. Transition Metal Mediated C-H Activation and Functionalization: The Role of Poly(pyrazolyl)borate and Poly(pyrazolyl)alkane Ligands *Eur. J. Inorg. Chem*. **2016**, 2296-2311.

184. Sallmann, M.; Limberg, C. Utilizing the Trispyrazolyl Borate Ligand for the Mimicking of O2-Activating Mononuclear Nonheme Iron Enzymes *Acc. Chem. Res*. **2015**, *48*, 2734-2743.

185. Hamon, P.; Thépot, J. -Y.; Le Floch, M.; Boulon, M. -E.; Cador, O.; Golhen, S.; Ouahab, L.; Fadel, L.; Saillard, J. -Y.;. Hamon, J.-R Dramatic Remote Substitutent Effects on the Electronic Spin State of Bis(scorpionate) Iron(II) Complexes† *Angew. Chem. Int. Ed*. **2008**, *47*, 8687-8691.

186. M. M. Díaz-Requejo, T. R. Belderrain, M. C. Nicasio, P. J. Pérez From Homogeneous to Heterogeneous Catalysis: Novel Anchoring of Polypyrazolylborate Copper(I) Complexes on Silica Gel through Classical and Nonclassical Hydrogen Bonds. Use as Catalysts of the Olefin Cyclopropanation Reaction *Organometallics* **2000**, *19*, 285-289.

187. Camerano, J. A.; Casado, M. A.; Ciriano, M. A.; Oro, L. A. Tris(pyrazolyl)borate carbosilane dendrimers and metallodendrimers *Dalton Trans*. **2006**, 5287-5293.

188. a) Kuchta, M. C.; Gross, A.; Pinto, A.; Metzler-Nolte, N. Labeling of the Neuropeptide Enkephalin with Functionalized Tris(pyrazolyl)borate Complexes: Solid-Phase Synthesis and Characterization of *p*-[Enk-OH]$COC_6H_4TpPtMe_3$ and *p*-[Enk-OH]$COC_6H_4TpMeRe(CO)_3$ *Inorg. Chem.* **2007**, *46*, 9400-9404. b) Desrochers, P. J.; Pearce, A. J.; Rogers, T. R.; Rodman, J. S.; Rapid Synthesis of a Functional Resin-Supported Scorpionate and Its Copper(I, II), Rhodium(I), and Chromium(III) Complexes *Eur. J. Inorg. Chem*. **2016**, 2465-2473. c) Desrochers, P. J.; Corken, A. L.; Tarkka, R. M.; Besel, B. M.; Mangum, E. E.; Linz, T. N. A Simple Route to Single-Scorpionate Nickel(II) Complexes with Minimum Steric Requirements *Inorg. Chem.* **2009**, *48*, 3535-3541.

189. a) Qin, Y.; Cui, C.; Jäkle, F. Tris(1-pyrazolyl)borate (Scorpionate) Functionalized Polymers as Scaffolds for Metallopolymers *Macromolecules* **2008**, *41*, 2972-2974. b) Qin, Y.; Shipman, P. O.; Jäkle, F. Self-Assembly of Borane End-Functionalized Polystyrene Through Tris(1-pyrazolyl)borate (Tp) Iron(II) Linkages *Macromol. Rapid Commun.* **2012**, *33*, 562-567.

190. Shipman, P. O.; Cui, C.; Lupinska, P.; Lalancette, R. A.; Sheridan, J. B.; Jäkle, F. Nitroxide-Mediated Controlled Free Radical Polymerization of the Chelate Monomer 4-Styryl-tris(2-pyridyl)borate (StTpyb) and Supramolecular Assembly via Metal Complexation *ACS Macro Lett.* **2013**, *2*, 1056-1060.

191. Desrochers, P. J.; Besel, B. M.; Corken, A. L.; Evanov, J. R.; Hamilton, A. L.; Nutt, D. L.; Tarkka, R. M. Immobilized Boron-Centered Heteroscorpionates: Heterocycle Metathesis and Coordination Chemistry *Inorg. Chem.* **2011**, *50*, 1931-1941.

192. We cannot discard the formation of pyrazabole units in this process. Spectroscopic data would not differentiate between pyrazaboles and the targeted pyrazolylborates, albeit the former would not be useful toward the formation of pyrazolyl-bonded metal complexes.

193. a) Caballero, A.; Pérez, P. J. Catalyst design in the alkane C-H bond functionalization of alkanes by carbene insertion with Tp^xM complexes (Tp^x = hydrotrispyrazolylborate ligand; M = Cu, Ag) *J. Organomet. Chem.* **2015**, *793*, 108-113. b) Mairena, M. A.; Urbano, J.; Carbajo, J.; Maraver, J. J.; Álvarez, E.; Díaz-Requejo, M. M.; Pérez, P. J. Effects of the Substituents in the Tp^xCu Activation of Dioxygen: An Experimental Study *Inorg. Chem.* **2007**, *46*, 7428-7435.

194. Morgan, G. T.; Ackerman, I. CLII.-Substitution in the pyrazole series. Halogen derivatives of 3: 5-dimethylpyrazole *J. Chem. Soc. Trans* **1923**, *123*, 1308-1318.

195. Rheingold, A. L.; White, C. B.; Trofimenko, S. Hydrotris(3-mesitylpyrazol-1-yl)borate and hydrobis(3-mesitylpyrazol-1-yl)(5-mesitylpyrazol-1-yl)borate: symmetric and asymmetric ligands with rotationally restricted aryl substituents *Inorg. Chem.* **1993**, 32, 3471-3477.

196. Yamada, Y.; Yamamoto, T.; Okawara, M. Synthesis and Reaction of New Type I-N ylide, N-Tosyliminoiodinane *Chem. Lett.* **1975**, *4*, 361-362.

197. Weiss, J. W. E.; Bryce, D. L. A Solid-State 11B NMR and Computational Study of Boron Electric Field Gradient and Chemical Shift Tensors in Boronic Acids and Boronic Esters *J. Phys. Chem. A* **2010**, *114*, 5119-5131.

198. The alkene content of the polymer **15** (z = mmol $CH=CH_2$/g) and the polymer composition given as a ratio of monomers incorporated (a/b = NB/NB-$CH=CH_2$) are related by the equation: z = 1000/(94.16(x/y) + 120.194), where 94.16 and 120.194 are the molecular weights of norbornene and 5-vinyl-2-norbornene respectively.

199. Acetonitrile is visible in the spectrum but due to the expected small chemical shift difference, it is not possible to tell if it is coordinated to the metal or it is free solvent embedded in the polymer.

Chapter 1

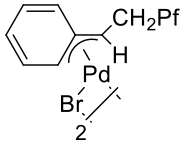

1

Pf = C_6F_5

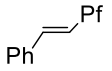

2

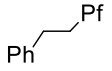

3

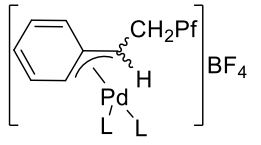

4

L = PMe_3, **4a**
L = 1/2 dppe, **4b**
L = 1/2 $(PhSCH_2)_2$, **4c**
L = PPh_3, **4d**
L= $AsPh_3$, **4e**
L = dppf, **4f**

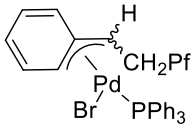

5

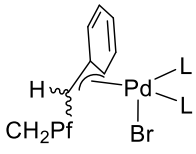

6

L = PPh_3, **6d**
L= $AsPh_3$, **6e**
L = dppf, **6f**

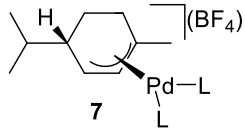

7

L = PPh_3, **7d**
L = $AsPh_3$, **7e**

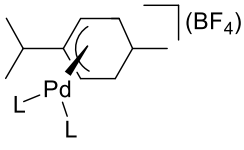

8

L = PPh_3, **8d**
L = $AsPh_3$, **8e**

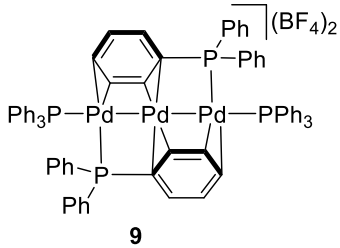

9

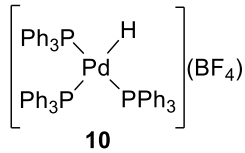

10

Chapter 2

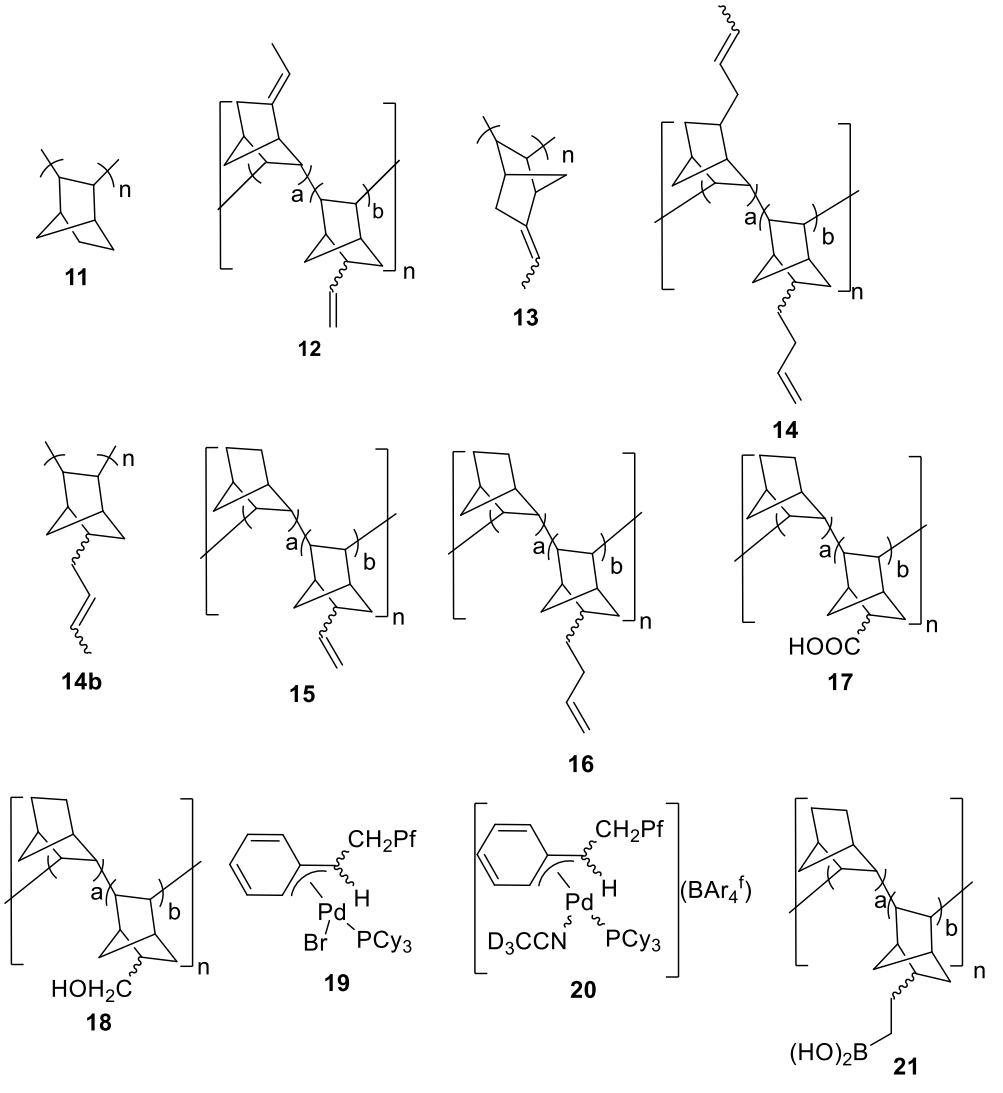
n
11
a
b
n
12
n
13
a
b
n
14
n
14b
a
b
n
15
a
b
n
16
a
b
n
HOOC
17
a
b
n
HOH2C
18
CH2Pf
Pd
H
Br
PCy3
19
CH2Pf
Pd
H
D3CCN
PCy3
(BAr4f)
20
a
b
n
(HO)2B
21

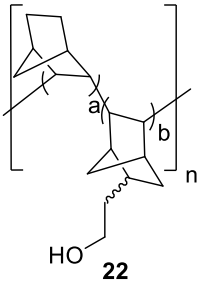

22

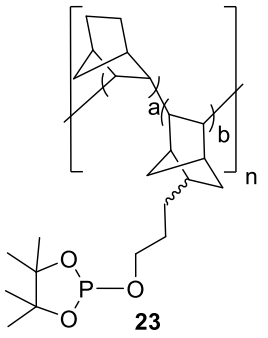

23

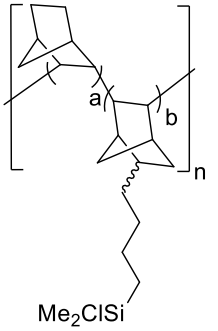

24

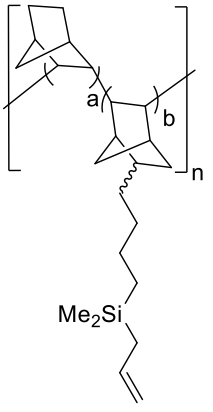

25

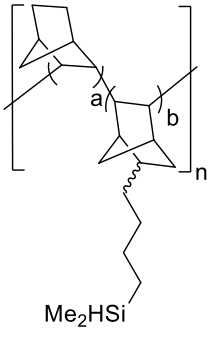

26

Chapter 3

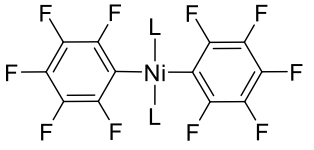

L = $SbPh_3$ **27**
L = $AsPh_3$ **28**
L = PPh_3 **29**

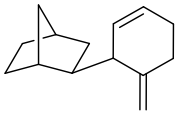

30

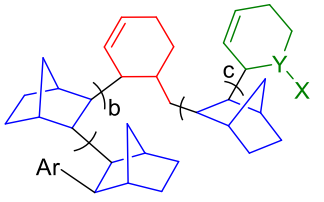

Y-X = -CH=CH_2 Ar = C_6F_5, *o*-CF_3-C_6H_4,
Y-X = -CH_2-CH_3 *o*-CH_3-C_6H_4

VA/RO-PNB

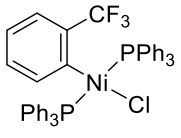

31

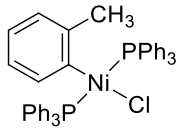

32

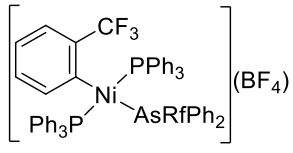

33

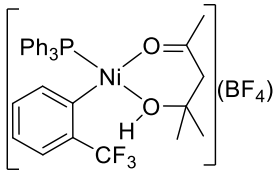

34

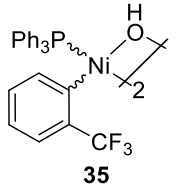

35

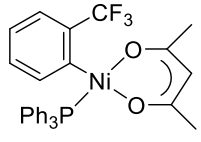

36

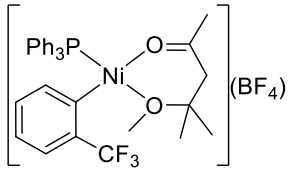

37

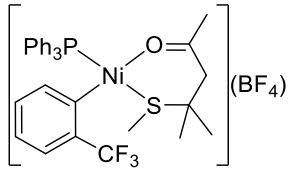

38

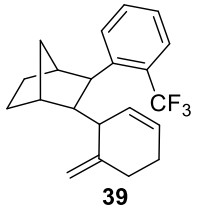

39

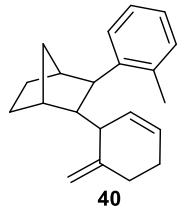

40

Chapter 4

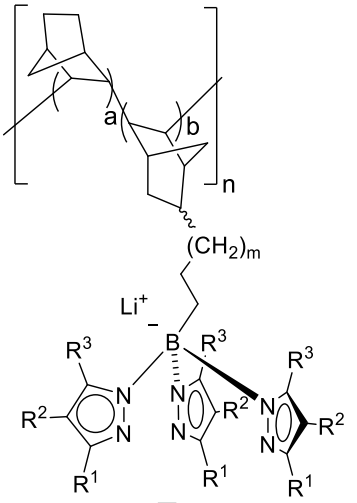

VA-PNB ~~ Tp^x Li

VA-PNB ~~ Tp^x-Cu(NCMe) **41-Cu**, **42-Cu**, **43-Cu**, **44-Cu**

VA-PNB ~~ Tp^x-CuCO **41-CuCO**, **42-CuCO**, **43-CuCO**, **44-CuCO**

	R^1	R^3	R^2	m
41:	Me	Me	H	0
42:	Me	Me	H	2
43:	Me	Me	Br	0
44:	Mes	H	H	0